Diels–Alder Reactions in Multi-Ring Forming Processes

A thesis submitted in fulfillment of the requirements for admission to the degree of

Doctor of Philosophy

Natalie Shadwell

Research School of Chemistry

The Australian National University

December 2020

Declaration

Except where specific acknowledgements of others are made, the work described in this thesis was carried out by the author during the period of February 2016 to December 2020 in the Research School of Chemistry of the Australian National University, Australia, under the supervision of Professor Michael S. Sherburn. The material presented has not been submitted for any other degree and is less than 100,000 words in length.

Natalie Shadwell

December 2020

"*The structure known, but not yet accessible by synthesis, is to the chemist what the unclimbed mountain, the uncharted sea, the untilled field, the unreached planet, are to other men…"* – R. B. Woodward (1963)

Acknowledgements

Firstly, I would like to thank my supervisor Professor Mick Sherburn, without whom I would not have pursued further study in organic chemistry. I am grateful to have had the opportunity to work on such interesting research. Thank you for challenging me in so many different ways and for always insisting on the pursuit of perfection.

Secondly, I would like to thank both the past and present members of the Sherburn Group - Dr Joshua Boyle, Dr Nicholas Green, Dr Samuel Drew, Dr Imants Kreituss, Dr Josemon George, Dr Cecile Elgindy, Eliza Tarcoveanu, Dr Maddie Sowden, Dr Nicholas Magann, Yi-Min Fan, Chloe Larcombe, Dr Mathieu Morin, Dr Kim Roper, Dr Emily Mackay, Joseph Wang, Dr Siu Min (Margaret) Tan, Dr Supanimit Chiampanichayakul and Dr Ross Harvey. Thank you for your kindness, for teaching and inspiring me, and for sharing this journey with me.

Thirdly, I'm grateful to the RSC technical and support staff - Dr Nicholas Kanizaj, Dr Hideki Onagi, Anitha Jeyasingham, Dr Michael Gardiner, Dr Brett Schwartz, Codi De Veau, Chris Blake, Paul Car, and Dr Tony Willis. Thank you not only for your invaluable assistance, but also for your unfailing patience and understanding.

Finally, I would like to thank my family - Mum, Dad, Matt and Alistair. Your support means the world to me and without you this would not have been possible.

Presentations

This thesis is submitted in standard format.

The following list details the presentations that have resulted from the author's research during her candidature for the Degree of Doctor of Philosophy:

Joshua Boyle, **Natalie Shadwell**, Samuel L. Drew, Nicholas Green, Michael S. Sherburn. *Enantioselective Total Synthesis of Xestoquinone*. Poster Presentation: Royal Australian Chemical Institute, 38th Annual One-Day Symposium, University of Sydney, 2017, Sydney, New South Wales, Australia.

Joshua Boyle, **Natalie Shadwell**, Samuel L. Drew, Nicholas Green, Michael S. Sherburn. *Enantioselective Total Synthesis of Xestoquinone*. Poster Presentation: Royal Australian Chemical Institute, Organic18, 24th Organic Division National Conference, University of Western Australia, 2018, Perth, Western Australia, Australia.

Joshua Boyle, **Natalie Shadwell**, Samuel L. Drew, Nicholas Green, Michael S. Sherburn. *Enantioselective Total Synthesis of Xestoquinone*. Oral Presentation: Royal Australian Chemical Institute, Organic18, 24th Organic Division National Conference, University of Western Australia, 2018, Perth, Western Australia, Australia.

Abbreviations

$[\alpha]_D$	optical rotation
%	percentage yield
°C	degree(s) Celsius
δ	chemical shift
Ac	acetyl
AcO	acetoxy
AIBN	azobisisobutyronitrile
aq.	aqueous
Ar	aryl/argon
b.p.	boiling point
BHT	2,6-di-*tert*-butyl-4-methylphenol
BINAP	2,2'-bis(diphenylphosphino)-1,1'-binaphthyl
BINOL	1,1'-bi-2-naphthol
Bn	benzyl
Boc	*tert*-butoxycarbonyl
BOM	benzyloxymethyl
bpy	2,2'-bipyridine
br	broad
Bz	benzoyl
c	concentration (g/100mL)
ca	*circa* (approximately)
calc.	calculated
CAN	ceric ammonium nitrate
cat.	catalyst/catalytic
cm^{-1}	wave number
CMPI	2-chloro-1-methylpyridinium iodide
COD	1,5-cyclooctadiene
COSY	correlated spectroscopy
CSA	camphorsulfonic acid
d	day(s)/doublet(s)
d.r.	diastereomeric ratio
DA	Diels–Alder

DABCO	1,4-diazabicyclo[2.2.2]octane
dba	dibenzylideneacetone
DBU	1,8-diazabicyclo[5.4.0]undec-7-ene
DCB	dichlorobenzene
DCC	dicyclohexylcarbodiimide
DCM	dichloromethane
dd	doublet of doublets
DDQ	2,3-dichloro-5,6-dicyano-1,4-benzoquinone
DFT	density functional theory
DIBAL-H	diisobutylaluminium hydride
DIP	diisopinocampheylborane
DIPA	diisopropylamine
DMAD	dimethyl acetylenedicarboxylate
DMAP	4-dimethylaminopyridine
DME	dimethoxyethane
DMF	dimethylformamide
DMHH	N,O-dimethylhydroxylamine hydrochloride
DMP	Dess-Martin periodinane
DMSO	dimethylsulfoxide
dppb	1,4-bis(diphenylphosphino)butane
dppf	1,1'-bis(diphenylphosphino)ferrocene
dppp	1,3-bis(diphenylphosphino)propane
DTDA	diene transmissive Diels–Alder
e.e.	enantiomeric excess
e.r.	enantiomeric ratio
EDC	N-(3-dimethylaminopropyl)-N′-ethylcarbodiimide
EI	electron impact
Enz	enzyme
equiv.	equivalent(s)
ESI	electrospray ionisation
Et	ethyl
FMO	frontier molecular orbital
FTIR	Fourier Transform Infrared
GC	gas chromatography

h	hour(s)
HDA	hetero Diels–Alder
HFIP	hexafluoroisopropanol
HG-II	Hoveyda Grubbs II catalyst
HMBC	heteronuclear multiple bond coherence
HMDS	hexamethyldisilazane
HMPA	hexamethylphosphoramide
HMPT	hexamethylphosphorous triamide
HOMO	highest occupied molecular orbital
HP	high pressure
HPLC	high performance liquid chromatography
HRMS	high resolution mass spectrometry
HSQC	heteronuclear single quantum coherence
Hz	Hertz
i-Pr	isopropyl
IBX	2-iodoxybenzoic acid
IMDA	intramolecular Diels–Alder
IMDAF	intramolecular Diels–Alder (furan diene/dienophile)
IMHDA	intramolecular hetero Diels–Alder
IPA	isopropanol
IR	infrared
J	coupling constant
LA	Lewis acid
LDA	lithium diisopropylamide
lit.	literature
LUMO	lowest unoccupied molecular orbital
M	molar
m	multiplet/*meta*
m-CPBA	*meta*-chloroperoxybenzoic acid
m.p.	melting point
m/z	mass to charge ratio
M^+	molecular ion
Me	methyl
MHAT	metal-hydride H atom transfer

MHz	megahertz
min	minute(s)
MMC	methoxymagnesium methyl carbonate
mol	mole/molar
MOM	methoxymethyl
MS	mass spectrometry
MV	methyl viologen
n-BuLi	*n*-butyl lithium
NBS	*N*-bromosuccinimide
NMM	*N*-methylmaleimide
NMO	*N*-methylmorpholine *N*-oxide
NMP	*N*-methyl-2-pyrrolidone
NMR	nuclear magnetic resonance
nOe	nuclear Overhauser effect
NOESY	nuclear Overhauser and exchange spectroscopy
o	ortho
OTf	triflate
p	*para*
p-TsOH	*para*-toluenesulfonic acid
PCC	pyridinium chlorochromate
PDA	photodiode array
PDC	pyridinium dichromate
Ph	phenyl
PHOX	phosphinooxazoline
PIFA	[bis(trifluoroacetoxy)iodo]benzene
PMB	*para*-methoxylbenzyl
PMP	1,2,2,6,6-pentamethylpiperidine
ppm	parts per million
PPTS	pyridinium *para*-toluenesulfonate
Pr	propyl
PS	petroleum spirits
PTAD	4-phenyl-1,2,4-triazoline-3,5-dione
Py	pyridine
PYBOX	pyridine-2,6-bis(oxazolines)

q	quartet
quant.	quantitative
r.t.	room temperature
R_f	retention factor
s	singlet
sat.	saturated
SEM	trimethylsilylethoxymethyl
SFC	supercritical fluid chromatography
SM	starting material
SOI	secondary orbital interaction
sp.	species
t	time/triplet
t-Bu	*tert*-butyl
T1	type 1
T2	type 2
TADA	transannular Diels–Alder
TBAB	tetra-*n*-butylammonium bromide
TBAF	tetra-*n*-butylammonium fluoride
TBDPS	*tert*-butyldiphenylsilyl
TBS	*tert*-butyldimethylsilyl
TCB	trichlorobenzene
TCNE	tetracyanoethylene
TDAM	tris(dimethylamino)methane
TEA	triethylamine
temp.	temperature
TEMPO	(2,2,6,6-tetramethylpiperidin-1-yl)oxyl
TES	triethylsilyl
Tf	trifyl
TFA	trifluoroacetic acid
TFAA	trifluoroacetic anhydride
TFP	tri(2-furyl)phosphine
THF	tetrahydrofuran
THP	tetrahydropyran
TIPS	triisopropylsilyl

TLC	thin layer chromatography
TMP	2,2,6,6-tetramethylpiperidine
TMS	trimethylsilyl
TOF	time of flight
TPAP	tetrapropylammonium perruthenate
t_R	retention time
Troc	2,2,2-trichloroethoxycarbonyl
TS	transition structure/state
UPC2	ultra-performance convergence chromatography
UHP	ultra-high pressure
ν	absorption maxima (IR)

Abstract

The Diels–Alder reaction is one of the most powerful reactions available to the synthetic organic chemist. Its greatest strength is its ability to generate the most prevalent cyclic system, namely the six-membered ring, in one synthetic operation from a versatile array of substrates. This thesis explores the application of the Diels–Alder reaction to multi-ring forming processes.

Chapter 1 – By way of introduction, the first chapter provides a brief commentary on the pursuit of efficiency in synthetic organic chemistry and, as a matter of course, the power of the Diels–Alder reaction as a multi-bond forming process. As a preamble, it signposts these important themes, which have driven the investigations conducted in this thesis.

Chapter 2 – The second chapter encapsulates two separate pieces of synthetic work. Firstly, the diene-transmissive twofold Diels–Alder reaction sequence of [3]dendralene with relatively un-activated cyclic dienophiles is developed. This methodology permits access to a diverse array of polycyclic structures, with twenty structurally distinct tetracyclic frameworks prepared. Secondly, Chapter 2 reports the application of this methodology to the concise enantioselective synthesis of the popular synthetic target and biologically-important marine natural product, (+)-xestoquinone. Notably, this work a) constitutes the first application of the parent [3]dendralene in total synthesis; and b) constructs three out of the four carbocyclic rings of the natural product *via* a Diels–Alder reaction, resulting in the shortest preparation of the molecule to date. This work is presented as a journal article draft for submission to *Science*.

Chapter 3 – In the third chapter, the pentacyclic marine natural products, (+)-xestoquinone and (+)-halenaquinone are introduced in detail. Previous syntheses of these natural products as well as structurally similar compounds are comprehensively and systematically reviewed to place the preceding synthetic work (Chapter 2) in context.

Chapter 4 – In Chapter Four, the diene-transmissive Diels–Alder reaction sequence of parent and substituted [3]dendralenes is developed to use enantiomerically pure, readily available, cyclic dienophiles for the first time. This methodology builds upon the key Diels–Alder reaction sequence reported in the synthesis of (+)-xestoquinone (Chapter 2) and enables the rapid synthesis of a range of chiral polycyclic frameworks in enantiopure form.

Chapter 5 – Chapter Five reviews the development and application of the intramolecular Diels–Alder reaction to total synthesis and takes the form of an invited journal article drafted for publication in *Angewandte Chemie.* The application of the Diels–Alder reaction to multi-ring forming events is explored from a different perspective to that examined throughout the rest of this thesis.

Table of Contents

1

Preamble

This preamble seeks to set the scene for the following chapters and to draw together the themes which underpin the work described in this thesis. It does not present a comprehensive literature review. Surveys of both the natural products, (+)-xestoquinone and (+)-halenaquinone, and of the intramolecular Diels–Alder reaction are presented in Chapters 3 and 5, respectively. Rather, it provides a brief commentary on the motivations which have inspired this work.

1.1 Efficiency in Synthetic Organic Chemistry

It has been said that *"As a community, we have become quite adept at being able to make anything with enough resources, but we are still decades or perhaps even centuries away from making everything well."*[1] Wender's 'ideal synthesis' presents this ambition succinctly as the production of a target molecule using readily available starting materials in one simple, safe, environmentally-acceptable, and resource-effective operation that proceeds quickly and in quantitative yield.[2] While this ultimate ideal itself remains elusive, the concept of efficiency may be used in target molecule synthesis to measure our progress towards it. There are many nuanced views of efficiency,[i] but for the purposes of this discussion focus is placed on step count. The ability to generate target relevant molecular complexity using the minimum number

[i] It is acknowledged that the definition of efficiency can be subjective. In addition to step count, efficiency may also be measured by factors such as by-product minimisation and yield. Step count efficiency broadly encompasses aspects such as the use of protecting groups and redox economy.

of steps improves access to important target structures, and often reduces time, resource use, environmental effects and cost. Minimisation of step count can be achieved through either strategic application of known reactions or the development of new methodology. Thus, the pursuit of efficiency drives progress in synthetic organic chemistry.

1.2 Multi-bond Forming Processes in Efficient Synthesis

In the construction of target molecules, synthetic chemistry on the most basic level focuses on the formation of new chemical bonds. Consequently, perhaps one of the most powerful techniques for efficient synthesis is the multi-bond forming process. In such a transformation two or more covalent bonds are formed in a single synthetic operation, without intermediate work up or purification procedures. Broadly, multi-bond forming processes may be classified into four main categories.[3]

The first of these is the domino or cascade reaction sequence,[ii] which is defined as '*a transformation of two or more bond- forming reactions under identical reaction conditions, in which the latter transformations take place at the functionalities obtained in the former bond forming reactions*'.[4] This is exemplified by Robinson's landmark synthesis of tropinone (Scheme 1.1).[5] Inter- followed by intramolecular nucleophilic addition of methylamine (**1**) to succinaldehyde (**2**) affords the intermediate **4**, which, under the same reaction conditions, then undergoes dehydration and double alkylation to yield bridged bicycle **6** *en route* to tropinone.

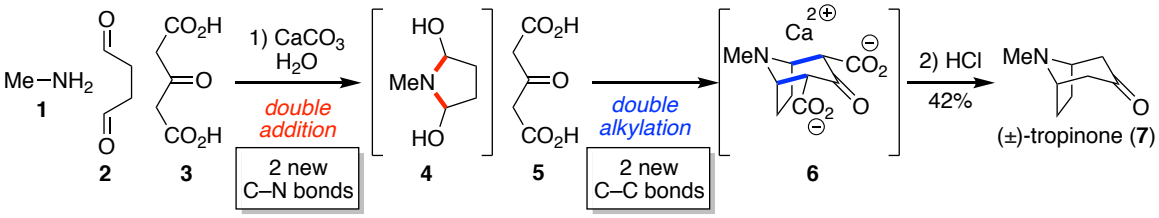

Scheme 1.1 Application of a domino reaction sequence to the synthesis of (±)-tropinone (**7**) by Robinson and co-workers[5]

In contrast to domino reaction sequences, consecutive reaction sequences require a change in conditions to complete the reaction sequence. Such alterations can include an increase in

[ii] These are also referred to as 'domino reactions' or 'cascade reactions'. In this thesis, a reaction sequence is defined as a series of two or more reactions, with a reaction being a chemical transformation whose intermediates generally are not isolable.

temperature or the introduction of additional reagents to the reaction mixture. This type of transformation is aptly illustrated in Sherburn's synthesis of selaginpulvilin D (Scheme 1.2).[6] Intramolecular aromatic substitution of bicycle **8** forms fluorenone **9**. The addition of anisole (**10**) to the reaction mixture then enables a two-fold intermolecular aromatic substitution involving the newly formed ketone of **9** to yield pentacycle **11** *en route* to selaginpulvilin D.

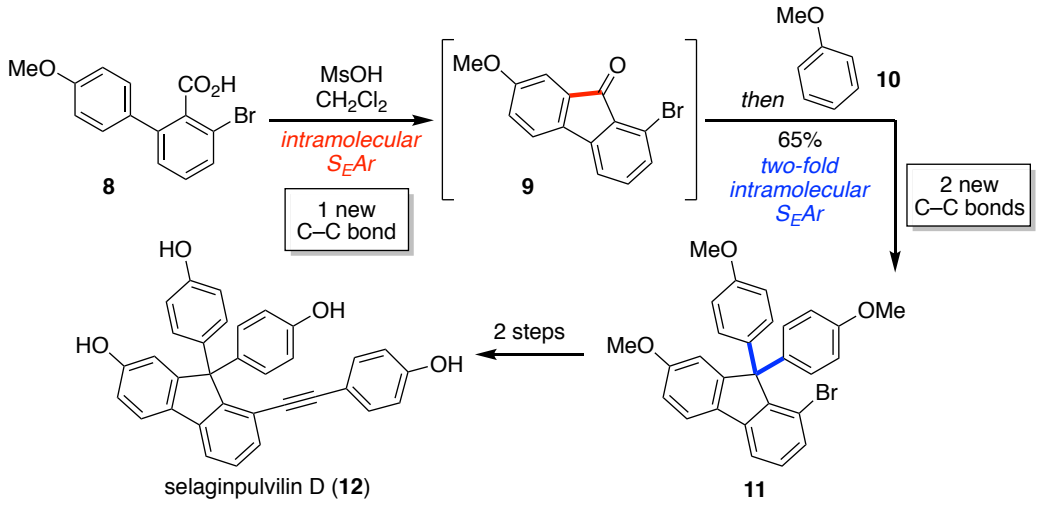

Scheme 1.2 Application of a consecutive reaction sequence to the synthesis of selaginpulvilin D (**12**) by Sherburn and Sowden[6]

The third class of multi-bond forming processes, independent reactions, occur wherein unconnected reactions take place at two or more distinct sites on a molecule, under the same reaction conditions, to form multiple new bonds in one synthetic transformation. Independent reactions are distinct from both domino and consecutive reactions in that one bond forming event is not reliant on the previous one. This process is demonstrated by Johnson's skillful two-directional synthesis of squalene, in which two independent reactions are employed in each step (Scheme 1.3).[7] Organolithium addition to both aldehydes of succinaldehyde (**2**) forms diol **14**, which undergoes Johnson Claisen rearrangement of both allylic alcohols to afford **15**. The two resulting esters are then reduced to the corresponding primary alcohols and oxidized back to the aldehyde to afford **16**. This process is iteratively repeated to build the framework of the molecule, with each reaction occurring at both ends of the molecule in the same step. Finally, Wittig reaction of both aldehydes of **19** yields squalene (**21**).

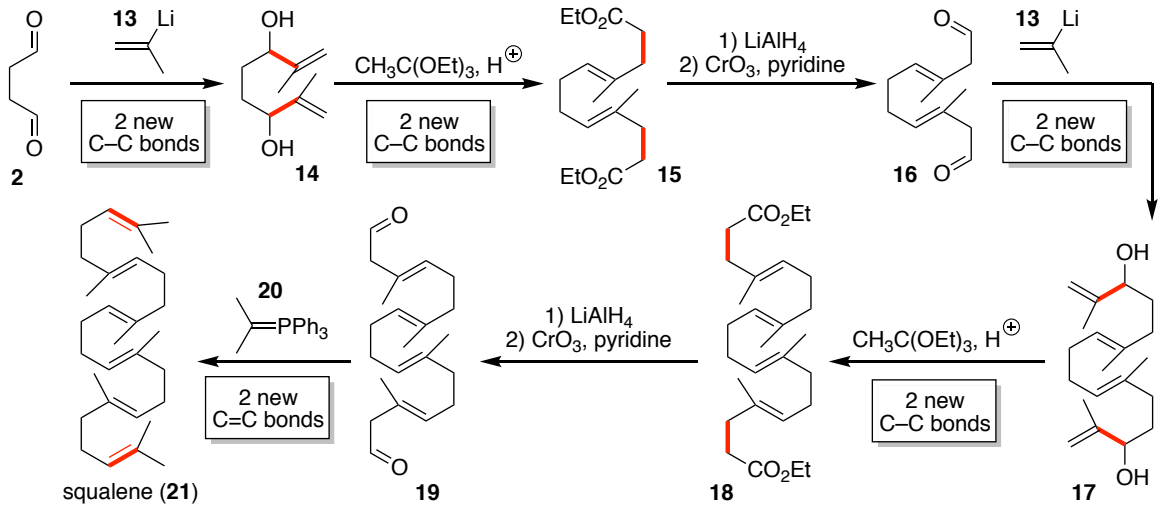

Scheme 1.3 Application of independent reactions to the synthesis of squalene (**21**) by Johnson and co-workers[7]

The last class of multi-bond forming processes is the multi-bond forming *reaction*, in which two or more bonds are formed, in a concerted manner, as part of a single reaction. This privileged class of reactions includes pericyclic reactions such as dipolar [3+2] cycloadditions, the Diels–Alder reaction (or [4+2] cycloaddition) and the Pauson–Khand reaction (a formal [2+2+1] cycloaddition). It is the Diels–Alder reaction which is the focus of this thesis.

1.3 The Diels-Alder Reaction in Efficient Synthesis

The Diels–Alder reaction (Scheme 1.4) was first described by Otto Diels and Kurt Alder in 1928,[8] a contribution for which they were awarded a Nobel Prize in 1950. Almost 100 years after its discovery, the reaction continues to be deployed in total synthesis and is the subject of numerous studies for reactivity and selectivity.[iii] Undoubtedly the popularity of this reaction[iv] stems from its utility to form the most prevalent cyclic system, the 6-membered ring, in just one step, in the process generating two new C–C (or C–X) σ-bonds, and up to four new stereocentres.

[iii] A research topic search on the "Diels–Alder reaction" in SciFinder Scholar returned ~50 000 references as of March 2020.
[iv] By way of comparison, equivalent searches for "metathesis" gave 44 000, "Suzuki" gave 34 000, "aldol" gave 32 000, "Wittig" gave 27 000, "Friedel-Crafts" gave 26 000, "organocatalysis" gave 19 000, "Heck" gave 15 000, "Claisen" gave 14 000 and "photoredox" gave 7000 references.

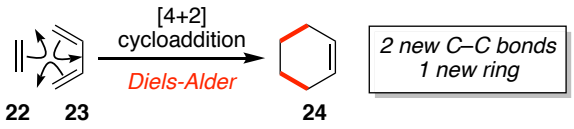

Scheme 1.4 The simplest Diels–Alder reaction involving ethylene (**22**) and 1,3-butadiene (**23**)

This thesis examines the extension of this already powerful process to the diene transmissive Diels–Alder (DTDA) reaction sequence, as well as to the intramolecular Diels–Alder (IMDA) reaction.

1.3.1 DTDA Reaction Sequences in Efficient Synthesis

The DTDA reaction sequence combines the power of a multi-bond forming reaction, the Diels–Alder reaction, with that of domino or consecutive reaction sequences, in a sequence of two successive [4+2] cycloadditions; a process enabled by unique cross-conjugated hydrocarbon building blocks called dendralenes.

Dendralenes are a fundamental class of oligoalkenic hydrocarbons, which are acyclic systems characterized by branched, cross-conjugated alkene units (Figure 1.1).[9] Previously thought to be too unstable and difficult to handle,[10] the dendralene family of compounds have since succumbed to synthesis,[11] allowing an investigation of their physical properties and chemical reactivity.

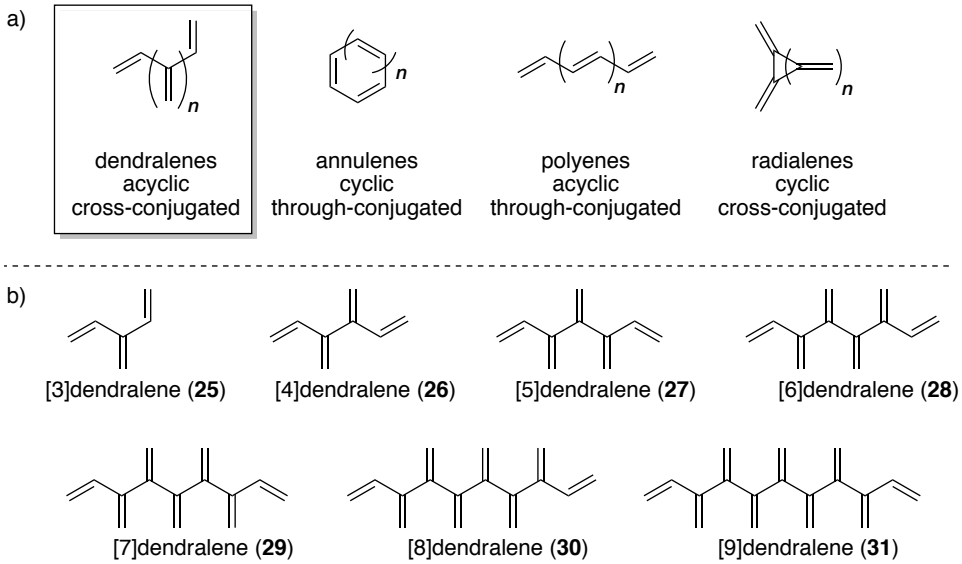

Figure 1.1 a) The four fundamental classes of conjugated polyalkenic hydrocarbons;[12] b) The first seven [n]dendralenes

Arguably, dendralenes are of most interest due to their singular ability to participate in DTDA reaction sequences. In this process, taking the parent [3]dendralene (**25**) as the simplest example, the molecule is able to act as a diene in a Diels–Alder reaction with the dienophile *N*-phenylmaleimide (**32**) to form monoadduct **33**, in which one C=C unit is transmitted to form a second diene (Scheme 1.5). This then undergoes a second Diels–Alder reaction with *N*-phenylmaleimide to form bisadduct **34** with high selectivity.[13] Notably, from the perspective of efficiency, this sequence not only forms four new C–C σ-bonds in one step, but also constructs two new rings, to very rapidly assemble complex multi-cyclic systems.

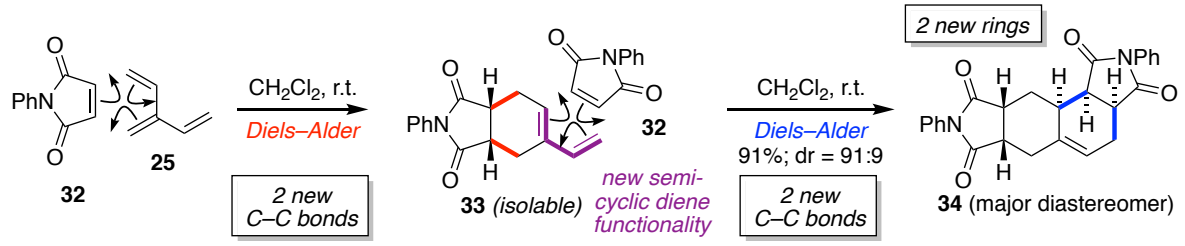

Scheme 1.5 DTDA reaction sequence between [3]dendralene (**25**) and *N*-phenylmaleimide (**32**)[13]

The synthetic value of this sequence is illustrated by the application of a substituted [3]dendralene (**35**) to achieve the shortest synthesis of the natural product, (–)-triptolide (**42**) (Scheme 1.6).[14]

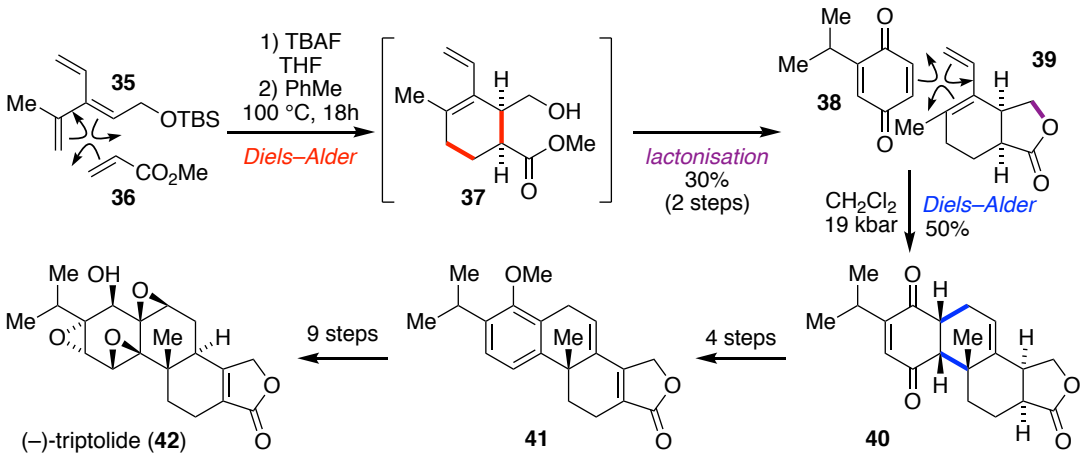

Scheme 1.6 Application of the DTDA reaction sequence to the synthesis of (–)-triptolide (**42**) using a substituted [3]dendralene[14]

1.3.2 IMDA Reactions in Efficient Synthesis

Complementary to the DTDA reaction sequence, the IMDA reaction provides a different yet still powerful variation to the fundamental Diels–Alder reaction. This intramolecular variant occurs when the diene and dienophile are tethered as part of the same molecule and results in the formation of two new rings from a single [4+2] cycloaddition reaction, thus surpassing the intermolecular process in terms of rapid structural complexity generation (Scheme 1.7 a).

Unlike the relatively limited use of the DTDA reaction sequence to date, the IMDA reaction has numerous applications in total synthesis, with one such notable example being MacMillan's synthesis of (–)-solanapyrone D (**47**) (Scheme 1.7 b).[15]

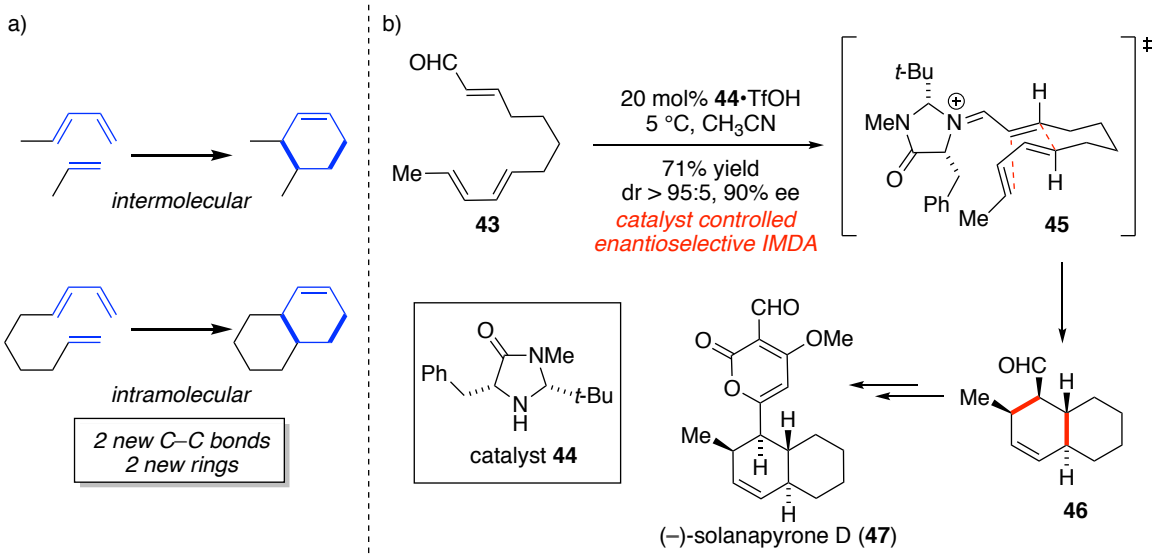

Scheme 1.7 a) A comparison of structural complexity generation between intermolecular and intramolecular Diels–Alder reactions; b) The IMDA reaction employed as a key step in the synthesis of (–)-solanapyrone D (**47**) by MacMillan and co-workers[15]

1.4 Conclusions

Undoubtedly, what ties together both the DTDA reaction sequence and the IMDA reaction is their shared ability to generate not only multiple bonds, but also multiple rings. In both processes a bicyclic framework is formed from acyclic precursors in a single synthetic operation, with ideal atom economy. Inspired by the concept of efficiency, the following chapters of this thesis explore the power and potential of these two related transformations in chemical synthesis.

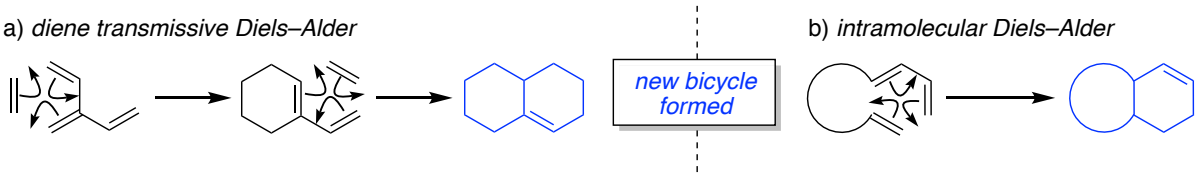

Figure 1.2 The formation of a bicyclic system from acyclic precursors in a single synthetic sequence by a) a DTDA reaction sequence and b) an IMDA reaction

2

Diverse polycycles from the simplest cross-conjugated molecule

2.1 Context

This chapter describes the use of [3]dendralene and the DTDA reaction sequence to rapidly generate molecular complexity. It is comprised of two sections: the development of new synthetic methodology and its application to total synthesis.

The methodological section outlines the development of the DTDA reaction sequence of the parent [3]dendralene with target relevant cycloalkenone dienophiles for the first time. The twofold DA sequence allows the synthesis of a diverse array of polycyclic structures. The merits of this work include a) the large range of carbocyclic dienophiles tolerated; and b) the generation of target relevant molecular complexity in just two bond forming events, with ideal atom economy and high selectivity.

In the total synthesis section, the value of this methodology is demonstrated by the shortest total synthesis of the marine natural product and popular synthetic target, (+)-xestoquinone. Previous syntheses of xestoquinone and structurally similar molecules are discussed in detail

in Chapter 3 to place this work in context. Notably, this work a) constitutes the first use of the parent [3]dendralene in total synthesis; and b) constructs 3 out of the 4 carbocyclic rings of the natural product *via* a Diels–Alder reaction, resulting in the shortest preparation of (+)-xestoquinone to date.

This chapter is formatted for publication in the journal *Science*, but, at the time of completion of this thesis, is yet to be submitted. As such, compound numbering and references in the following manuscript are distinct from those in other chapters of this thesis. Experimental and references for this work are provided in Chapters 6 and 7, respectively.

The other authors listed in the manuscript are Professor Michael S. Sherburn, Dr Joshua Boyle, Dr Samuel Drew, and Dr Nicholas Green. The project was conceived and evolved in collaboration between Professor Michael S. Sherburn, Dr Joshua Boyle and myself. Crystallographic data was obtained, solved and refined by Dr Anthony C. Willis and Dr Michael Gardiner.

Experimental work was conducted by myself in conjunction with Dr Joshua Boyle, Dr Samuel Drew and Dr Nicholas Green.

Dr Joshua Boyle performed preliminary methodological experiments, developed a one-step synthesis of [3]dendralene, and accessed a tetracyclic naphthalene intermediate *en route* to xestoquinone. Dr Samuel Drew assisted in optimisation of the Clemmensen reduction to reduce zinc powder aggregation, the first-generation development of the dihydroxylation-over oxidation and a two-step furan formation (supporting information). Dr Nicholas Green performed preliminary experiments towards the synthesis of a chiral dienophile using organocatalysis.

In the methodological section, all 8 monoadducts and 19 of the 20 bisadducts were synthesised by myself. In the total synthesis section, I repeated and optimised the synthesis using racemic material, then I carried out all experimental work in the enantioselective total synthesis. The specific steps of the total synthesis that I made a substantial contribution to are as follows:

a) I developed and optimised the alkene dihydroxylation/over-oxidation step;

b) I devised, developed and optimised the one-step dehydration and furan ring formation step; and

c) I developed and optimised the chiral dienophile synthesis and preparation of xestoquinone in enantio-enriched form.

My contributions to the total synthesis resulted in rendering the synthesis enantioselective, and in a 3 step reduction of the total synthesis step count (longest linear sequence).

The following manuscript describing this work was prepared by myself in collaboration with Professor Michael S. Sherburn.

Science AAAS

Submitted Manuscript: Confidential

Diverse polycycles from the simplest cross-conjugated molecule

J. W. Boyle, N. Shadwell, S. L. Drew, N. Green, M. S. Sherburn*

Research School of Chemistry, Australian National University, Canberra ACT 2601, Australia

*Correspondence to: michael.sherburn@anu.edu.au

Abstract:

In Nature's biosynthesis of multicyclic carbon-based molecules, enzymes control sequences of ionic cyclizations of an acyclic precursor. When mimicked synthetically, many reactions are needed to prepare the cyclization precursor, and the process is narrow in scope. Here, we disclose a powerful alternative strategy for polycyclic carbon framework construction, which uses significantly fewer reactions and generates a wide diversity of structures. The method deploys the smallest cross-conjugated hydrocarbon, [3]dendralene, which by cycloaddition fuses with two feedstock building blocks in a modular manner. Twenty structurally distinct polycyclic frameworks are prepared, and the effectiveness of the method is established by the shortest chemical synthesis of (+)-xestoquinone, a biologically active polycyclic marine natural product that is a popular target for chemical synthesis.

One Sentence Summary:

A general, modular method for polycycle synthesis permits the shortest synthesis of a biologically active natural product.

Science AAAS

Submitted Manuscript: Confidential

Main Text:

Nature uses a variety of chemical reactions to prepare complex polycyclic molecules. A particularly remarkable example is the tetracyclization of a single chain precursor (2,3-epoxysqualene) through four intramolecular π-cation additions (**Fig. 1A**) *(1)*. An intricate network of enzymes is required, both to assemble epoxysqualene and to mediate its cyclization into a specific polycyclic product *(2)*. Synthetic chemists have benefited immensely by emulating this process, which magnifies the power of an individual addition reaction (i.e. a single ring formation) through iteration. Here, we describe a complementary approach to polycycle synthesis, in which three separate, readily accessible building blocks are united to rapidly form *m*–6–6–*n* fused tetracyclic ring systems (where *m*, *n* = 3–8; **Fig. 1B**) through an iterative sequence involving the intermolecular Diels-Alder reaction: the most powerful chemical reaction for C–C bond formation (*3*) that is surprisingly rare in biosynthesis (*4*). Thus, two modular cyclic building blocks are combined with a C=C bond rich hydrocarbon lynchpin, [3]dendralene. The first reaction of [3]dendralene (as a diene) with a separate carbocyclic dienophile relocates a C=C π-bond, thereby creating a new diene for a second cycloaddition with a separate cyclic dienophile, in a diene-transmissive manner *(5)*. Despite the differences in execution of Nature's polycyclization and our own, the outcome in both cases is the rapid generation of a fused tetracarbocyclic framework through the transformation of four C=C π–bonds into four new C–C σ–bonds, by way of an iterative addition process.

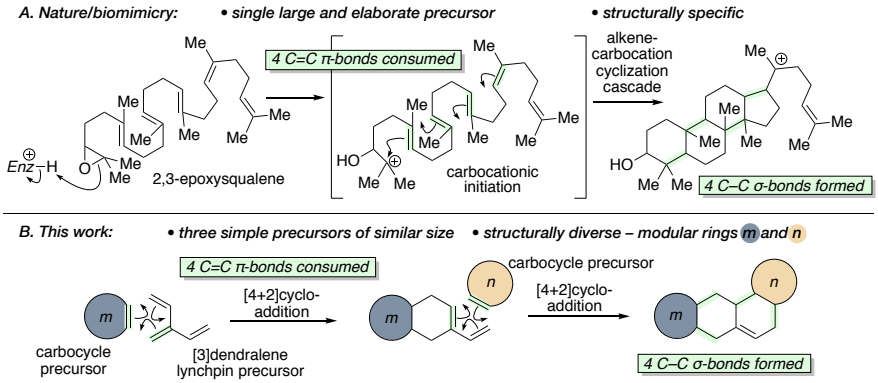

Fig. 1. *Iterative additions* in tetracarbocyclic molecule construction: **A.** Nature's enzyme-mediated cationic cyclization of 2,3-epoxysqualene en route to lanosterol, cholesterol and countless steroids; **B.** A convergent and modular method for carbon framework construction.

Table 1 lists the products of the modular double cycloaddition sequence to [3]dendralene. Cyclic dienophiles **1** with ring sizes ranging between 3 and 8 carbon atoms react with [3]dendralene and its cycloaddition products. Twenty distinct tetracyclic *m*-6-6-*n* polycyclic frameworks are generated in this manner. The strained π-bond dienophiles (3,3-dimethoxycyclopropene (**1a**), cyclobut-2-en-1-one (**1b**) and benzyne **1h** (generated *in situ*)) are the most reactive, participating

in uncatalyzed reactions with [3]dendralene at ambient temperature. Five- through eight-membered ring dienophiles react with [3]dendralene cleanly by Lewis acid catalysis at sub-ambient temperatures. The second cycloaddition of the sequence is generally best performed at ambient temperature under high pressure.(*6*) The structures of twelve of the frameworks were confirmed by single crystal X-ray analysis. Where detectible, both cycloadditions proceed with the retention of *cis*-cycloalkene geometry and exhibit *endo*-diastereoselectivity. Where stereocenters are formed by the initial cycloaddition, the second addition occurs with π-diastereofacial selectivity for the less hindered face of the diene. In cases where orientational regioisomeric products are possible, the reactions exhibit a clear preference for the product that would be expected on the basis of FMO theory (*7*). Thus, the results depicted in **Table 1** expose a highly predictable, robust and broad-spectrum process for polycycle construction.

Table 1. Synthesis of tetracyclic frameworks from [3]dendralene.

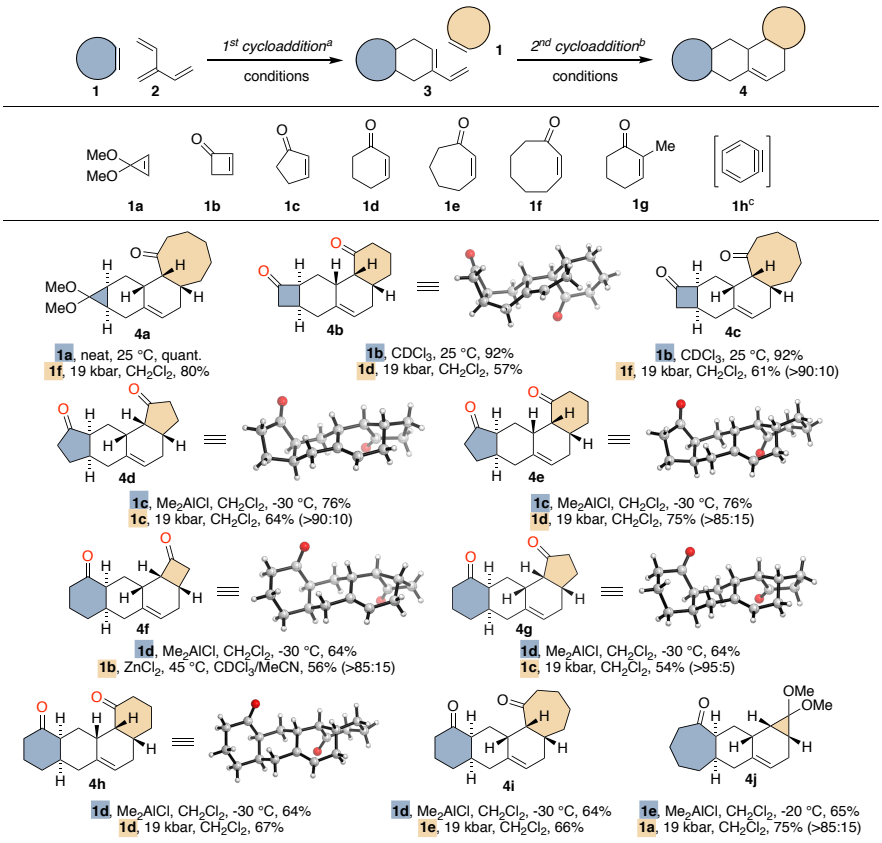

Science AAAS

Submitted Manuscript: Confidential

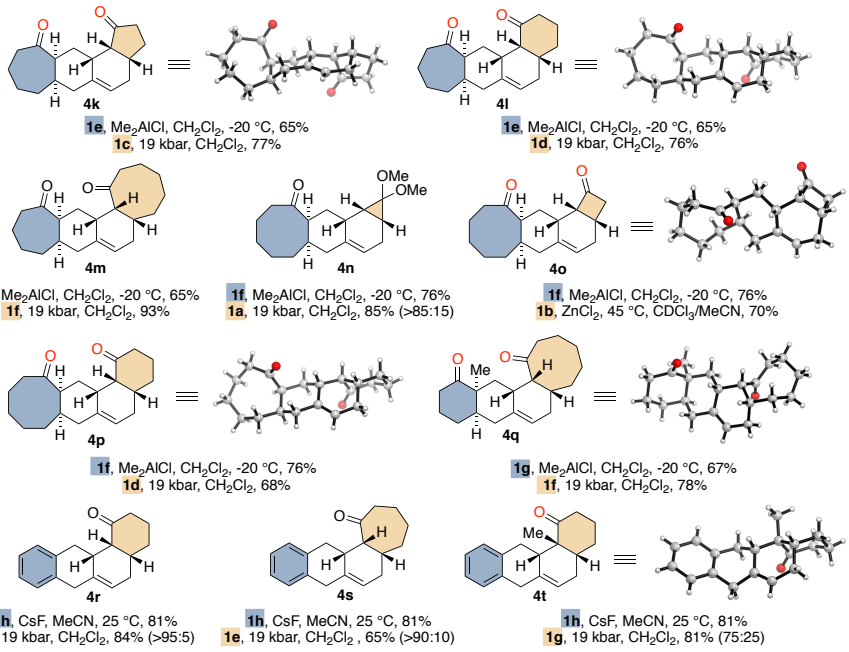

[a]Regio/diastereo-selectivity >95:5 as determined by analysis of crude ^{1}H NMR spectra; [b]Regio/diastereo-selectivity quoted in parentheses as determined by analysis of crude ^{1}H NMR spectra. Where no ratio is given, no isomers where observable by ^{1}H NMR spectroscopic analysis; [c]Benzyne dienophile **1h** generated in situ (see SI for details).

While diene-transmissive cycloaddition sequences have been previously described, the use of target-relevant cycloalkenone dienophiles is unprecedented *(8)*, as are most of the *n*-6-6-*m* tetracarbocyclic frameworks depicted in **Table 1**, which populate new regions in drug-like chemical structure space (*9*)(*10*). Moreover, the method is a valuable addition to total synthesis endeavors, as we will now demonstrate. The 6-6-6-6 tetracarbocyclic framework seen in structures **4h**, **4r** and **4t** (**Table 1**) is present in numerous bioactive polyketide and terpene natural products *(11)(12)(13)(14)(15)(16)(17)(18)(19)(20),* which should be accessible through this strategy. In addition to the 6-6-6-6 (ABCD) tetracarbocycle nucleus, the marine natural product, and our chosen synthetic target, (+)-xestoquinone **5** contains an additional fused furan (E) ring and a ring junction quaternary all-carbon stereogenic center. First isolated from tropical sponges of the genus *Xestospongia (12)*, (+)-xestoquinone exhibits cytotoxicity against human squamous cell carcinoma lines *(21)* and anti-malarial properties *(22),* has been shown to induce muscle excitation and relaxation *(23),* and is a potent cardiotonic agent (*24*). (+)-Halenaquinone (**6**), a very closely related natural product whose previous total syntheses are also used to benchmark our own, is an antifungal agent *(25)*. Owing to their challenging structures and

diverse biological activities, xestoquinone and halenaquinone have attracted considerable attention from synthetic and medicinal chemists, with no less than ten total syntheses reported to date (**Fig. 2**) *(26)(27)(28)(29)(30)(31)(32)(33)(34)(35)(36)(37)(38)*. Our synthesis of (+)-xestoquinone **5**, which features three Diels-Alder cycloadditions, namely a catalytic enantioselective reaction followed by the diene-transmissive Diels-Alder sequence developed above, enables the shortest synthesis thus far.

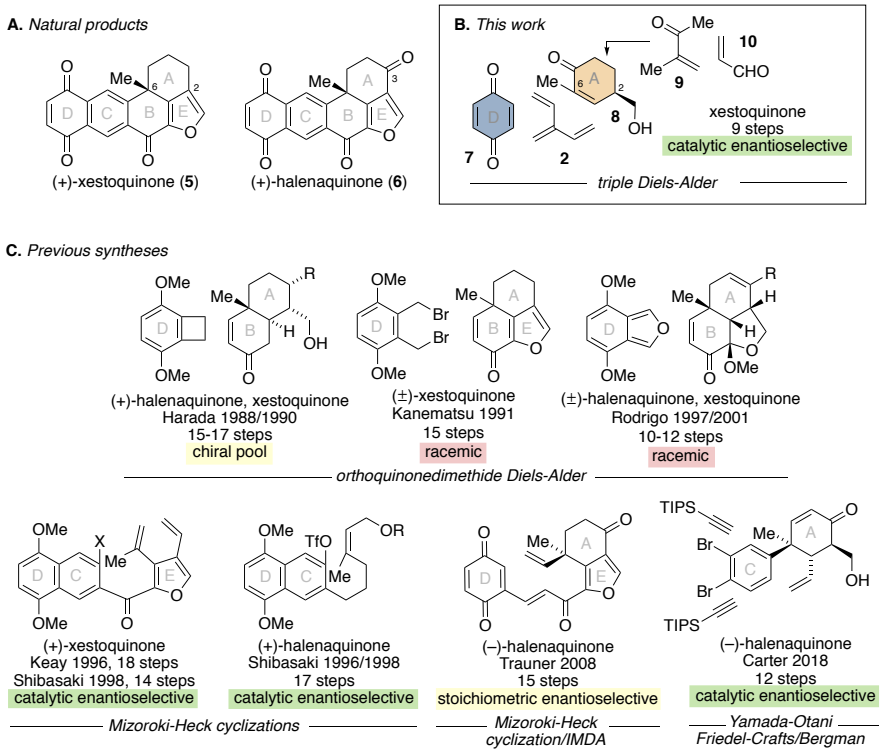

Fig. 2. A summary of the current approach to (+)-xestoquinone along with published syntheses of xestoquinone and halenaquinone. **A**. Structures of (+)-xestoquinone and (+)-halenaquinone; **B**. The new approach to (+)-xestoquinone, featuring three × [4+2] cycloadditions; **C**. Key intermediates and reactions employed in previous syntheses, the longest linear sequence (LLS) step count, and stereochemical classification of synthesis.

Science AAAS

Submitted Manuscript: Confidential

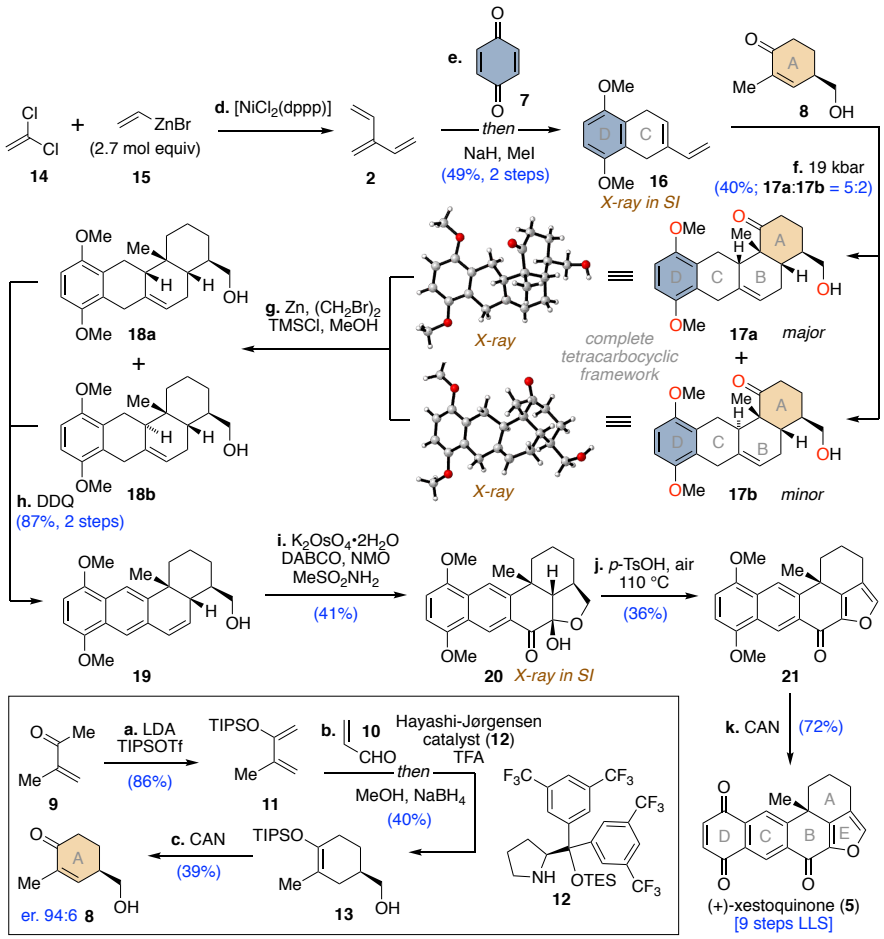

Fig. 3. A concise total synthesis of (+)-xestoquinone (**5**) featuring three Diels-Alder cycloadditions.

[a]Reagents and conditions: (a) DIPA (1.2 equiv.), *n*-BuLi (1.1 equiv.), TIPSOTf (1.1 equiv.), THF (86%); (b) Hayashi-Jørgensen catalyst (**12**) (2.5 mol %), TFA (5.0 mol %), acrolein (5.0 equiv.), PhMe, *then* MeOH, $NaBH_4$ (3.0 equiv.), (40%); (c) CAN (3.0 equiv.), THF/MeOH (39%); (d) [$NiCl_2$(dppp)] (1.0 mol%), $ZnBr_2$ (2.75 equiv.), CH_2=CH–MgBr (2.75 equiv.), THF; (e) *para*-benzoquinone (1.0 equiv.), THF, *then* NaH (5.0 equiv.), MeI (3.0 equiv.) (49%, 2 steps); (f) diene **16** (1.0 equiv.), dienophile **8** (3.0 equiv.), CH_2Cl_2, 19 kbar (40%); (g) Zn (120 equiv.), $(CH_2Br)_2$ (4.9 equiv.), TMSCl (120 equiv.), MeOH; (h) DDQ (2.2 equiv.), C_6H_6 (87%, 2 steps); (i) K_2OsO_4•$2H_2O$ (20 mol %), DABCO (14.4 mol %), $MeSO_2NH_2$ (2.08 equiv.), NMO (8.0

equiv.), acetone/H_2O (41%); (j) *p*-TsOH (1.0 equiv.), PhMe, air 110 °C (36%); (k) CAN (3.0 equiv.), MeCN/H_2O (72%). DIPA = diisopropylamine, *n*-BuLi = *n*-butyl lithium, LDA = lithium diisopropylamide, TIPSOTf = triisopropyl trifluoromethane sulfonate, TFA = trifluoroacetic acid, CAN = ceric ammonium nitrate, TMSCl = trimethylsilyl chloride, DDQ = 2,3-dichloro-5,6-dicyano-1,4-benzoquinone, NMO = *N*-methylmorpholine *N*-oxide, *p*-TsOH = *p*-toluenesulfonic acid.

We commenced the synthesis (**Fig. 3**) with a twofold Negishi cross-coupling reaction of 1,1-dichloroethylene (**14**) with vinylzinc bromide (**15**) to give [3]dendralene **2** on multi-gram scale as a THF solution *(39)*. A Diels-Alder reaction with *p*-benzoquinone (**7**) followed by twofold *O*-methylation with sodium hydride and methyl iodide furnished 1,4-dihydronaphthalene **16** on multi-gram scale in 49% yield from 1,1-dichloroethylene in a one-pot procedure *(40)*. A second Diels-Alder reaction, under high pressure (19 kbar) between **16** and dienophile **8,** furnished **17a** and **17b** in 40% yield. Pertinent to the theme of this work is the assembly of the full tetracarbocyclic framework of the target natural product in two steps, through an iterative double cycloaddition sequence. The Diels-Alder reaction of diene **16** and dienophile **8** proceeded with high regio- and π-diastereofacial selectivity to produce an inconsequential mixture of *endo*- and *exo*-isomers, **17a** and **17b**, as the two major products, both of which contain the desired structural features for the natural product. Chiral cyclohexenone **8** was synthesized in enantioenriched form by a sequence including an enantioselective Diels-Alder reaction, mediated by organocatalyst **12**, between TIPS enol ether **11** (synthesized from **9** in 86% yield) and acrolein. *In situ* reduction of the product aldehyde with sodium borohydride provided **13** in 40% yield, which was oxidized to enone **8** by ceric ammonium nitrate in 39% yield and 94:6 er.

Endgame functionalization proceeded with reductive deoxygenation of the ketone via a modified Clemmensen reduction, employing zinc powder with trimethylsilyl chloride *(41)*. Finally, four successive oxidation reactions afforded pentacycle **5**. First, oxidation with DDQ gave styrene **19**, not only aromatizing the B ring, but also introducing an alkene in conjugation with the newly formed naphthalene system. Secondly, the freshly-minted alkene underwent dihydroxylation and *in situ* 1,2-diol oxidation *(42)* to form lactol **20**, presumably through the intermediacy of the diketone. Thirdly, the furan ring was installed by *para*-toluene sulfonic acid-catalyzed dehydration and aerobic oxidation *(43)*, yielding pentacycle **21**, a known precursor to xestoquinone *(27)*. The final step of the synthesis involved oxidation of the 1,4 dimethoxynaphthalene moiety to the corresponding *para*-naphthoquinone *(27)*, to afford (+)-xestoquinone (**5**).

In summary, the diene-transmissive twofold Diels-Alder reaction sequence involving [3]dendralene is a strategy of exceptional applicability and predictability, permitting access to polycyclic frameworks of both proven and potential value. The deployment of [3]dendralene as a lynchpin for the convergent union of three small building blocks is conceptually simple but remarkably powerful. Target relevant structural complexity is generated in two cycloaddition bond-forming events, with ideal atom economy (*44*). This approach has been validated through the most concise synthesis of the bioactive natural product (+)-xestoquinone. We anticipate that the unprecedented scope and modularity of this strategy for polycycle synthesis from acyclic π-bond rich hydrocarbons will result in many further applications to realize the full potential of this nascent area. *(45)(46)(47)(48)*

Acknowledgments: We thank Min Yue (Amelia) Ng for preliminary investigations into the synthesis of **8** as a racemic mixture, Drs Hideki Onagi and Nicholas Kanizaj for assistance with the ultra-high pressure reactor and Drs Anthony Willis and Michael Gardiner (ANU) for single crystal X-ray analyses. Molecular structures from single crystal X-ray analyses are visualized using CYLview 1.0b; C. Y. Legault, Université de Sherbrooke, 2009 (http:// www.cylview.org).

Funding: This work was supported by the Australian Research Council (DP0665161).

Author contributions: J.W.B., M.S.S. and N.S. developed the project concept. J.W.B. and N.S. performed all experimental work for the methodological section. J.W.B., N.S., and S.L.D. performed all experimental work for the total synthesis section. N.G. performed preliminary experiments towards the enantioselective synthesis of **8**. N.S. and M.S.S. wrote the manuscript.

Competing interests: The authors declare no competing interests.

Data and materials availability: X-ray crystal structure data have been deposited in the Cambridge Structural Database.

Supplementary Materials:

Materials and Methods

Figures S1-S18

Tables S1-S4

X-Ray Crystallography Data

Analytical HPLC and SFC Traces

NMR Spectra

References (*49-79*)

Combined CIF File

Combined CheckCIF Report

3

(+)-Xestoquinone and (+)-Halenaquinone: A Review

3.1 Introduction

3.1.1 Isolation and Structure

(+)-Xestoquinone (**48**) and (+)-halenaquinone (**49**) (Figure 3.1a) are closely related pentacyclic polyketides produced by the tropical marine sponges *Xestospongia sapra* and *Xestospongia exigua* respectively.[16] (+)-Halenaquinone was first isolated in 1983 by Scheuer and co-workers,[16b] and (+)-xestoquinone in 1985 by Nakamura and co-workers.[16a] Subsequently, (+)-xestoquinone and a range of related adociaquinones were also isolated from an *Adocia sp*. sponge in the Truk lagoon in 1988 by Schmitz and co-workers.[17]

(+)-Xestoquinone and (+)-halenaquinone each possess a quinone moiety, an aromatic ring, a furan ring and a single ring junction quaternary all-carbon stereocentre. The two natural products share the same stereochemistry at this C6 stereocentre and differ only in the oxidation state of the A ring, with halenaquinone possessing an additional carbonyl group (C3).

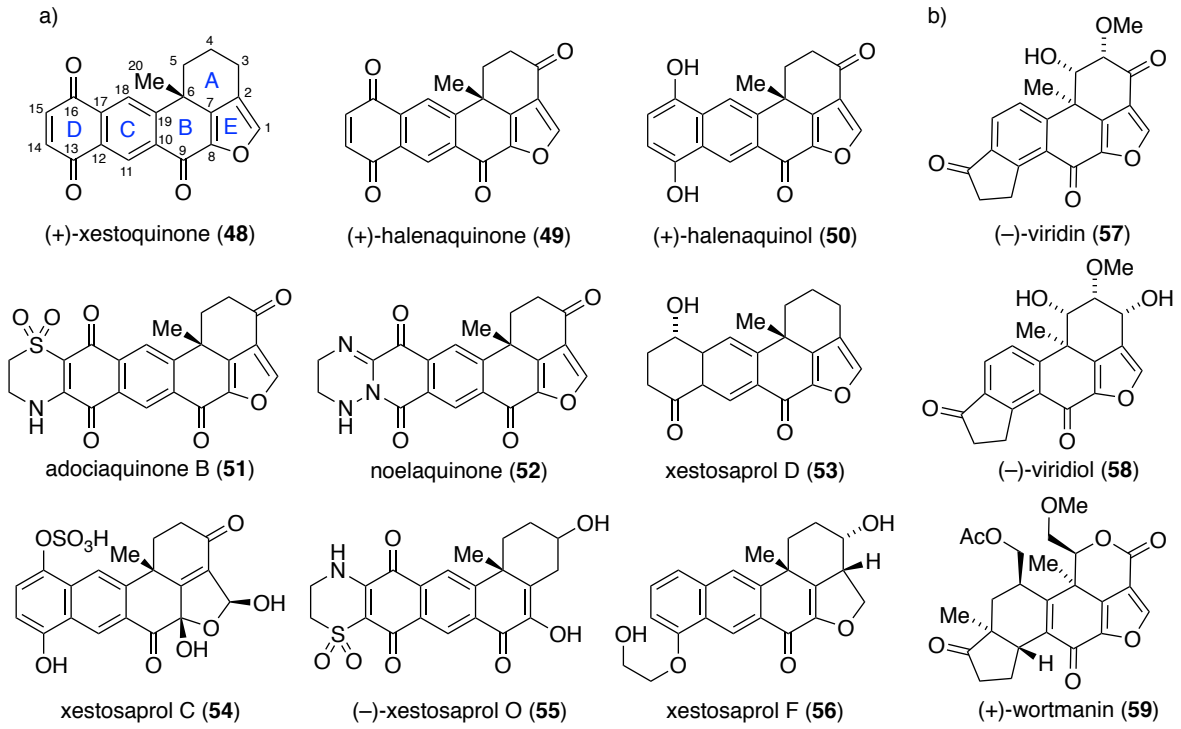

Figure 3.1 a) (+)-Xestoquinone and related marine natural products from the xestoquinone family; b) Structurally similar furanosteroid natural products

Structurally related natural products mainly vary in substitution and oxidation state of the quinone moiety and C3 functionality (e.g. halenaquinol and adociaquinone B), as well as of the fused furan ring (e.g. xestosaprols C, F and O). The fused tricyclic furan moiety including the ring junction quaternary all-carbon stereocentre and aromatic ring are also structural features shared with the more complex and highly substituted furanosteroid fungal natural products, (–)-viridin, (–)-viridiol and (+)-wortmannin (Figure. 3.1b). To date more than 40 different structural analogues of xestoquinone have been isolated, with the family of marine natural products continuing to grow.[16-18]

3.1.2 Biological Activity

(+)-Xestoquinone and (+)-halenaquinone have been shown to exhibit a wide variety of biological activities. (+)-Xestoquinone exhibits cytotoxicity against human squamous cell carcinoma lines,[19] as well as moderate anti-malarial properties, inhibiting Pfnek-1 (IC_{50} = 1 μM).[20] Moreover, it has been shown to induce muscle excitation and relaxation,[21] having applications as a biochemical probe for the study of muscle contractile machinery[22] and as a potent cardiotonic agent.[23]

By contrast, the related family member, (+)-halenaquinone, which differs only in its oxidation state at C3, has antibiotic[16b] and strong anti-fungal properties.[19] Halenaquinone also irreversibly inhibits protein tyrosine kinase $pp60^{v\text{-}src}$ (IC_{50} = 1.5 μM)[24] and phosphatidylinositol 3-kinase (IC_{50} = 3 μM).[25]

These distinct biological properties suggest that the oxidation state at C3 plays an integral role. Facile ring opening of the heterocyclic furan moiety by amines and thiols has been shown in the structurally similar furanosteroid natural product, (+)-wortmannin.[26] This mode of reactivity, similarly, appears to play a key role in the structure-function relationship of (+)-halenaquinone.[24a, 25, 27] In contrast, (+)-xestoquinone, which lacks the requisite C3 carbonyl functionality in this regard, appears to primarily undergo nucleophilic addition at the quinone moiety,[19, 28] thus rationalising the divergent biological properties observed.

3.1.3 Biosynthetic Origins

Despite their wide range of biological activities, the biosynthetic origins of xestoquinone and halenaquinone remain largely unexplored. Upon their isolation, it was suggested that the natural products were secondary metabolites of polyketide origin.[16b] Xestoquinone and halenquinone, however, are now believed to arise from a sesquiterpene-quinone mixed biosynthesis (Figure 3.2),[24a] owing to their structural similarities to viridin and wortmanin (Figure 3.1b), shown to be of steroid biosynthetic origins, and to marine sponge and algal terpene-hydroquinone metabolites such as avarone (**60**) (Figure 3.2).[29]

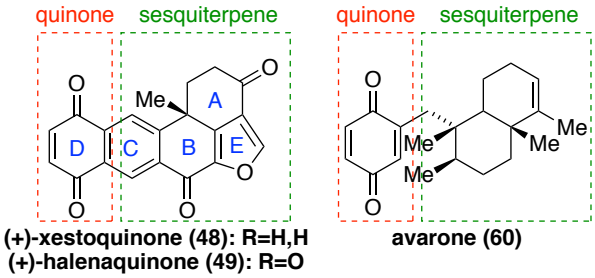

Figure 3.2 Structural similarities of (+)-xestoquinone and (+)-halenaquinone to avarone and proposed sesquiterpene-quinone mixed biosynthetic origins

Beginning from the representative metabolite, farnesylhydroquinone (**61**), a cyclisation cascade, analogous to that employed in steroid formation, may form the *trans*-decalin framework of the known marine natural product zonarol (**62**) (Scheme 3.1).[30] It is proposed by Crews and co-workers that related tautomer, isozonarol **63,** is a precursor to halenaquinone,

although the transformation of the former to the latter remains speculative.[24a, 30a] Here we hypothesise that zonarol selectively undergoes allylic oxidation to form enone **64**. The α-β-unsaturated ketone may then act as a Michael acceptor, with nucleophilic addition of the hydroquinone moiety forming the C ring of tetracycle **65**. Subsequent demethylation of tetracycle **65** to remove one of the geminal-dimethyl substituents, for example *via* oxidation and decarboxylation, would then afford hydroquinone **66**. This could plausibly be converted to the isolated marine metabolite, prehalenaquinone **67**, *via* a series of oxidation reactions to install the dihydrofuran ring, naphthoquinone moiety, and secondary alcohol functionality. Finally, prehalenaquinone may be converted to both xestoquinone (**48**) and halenaquinone (**49**), (in an analogous manner to that demonstrated synthetically by Harada and co-workers from the dimethoxynaphthalene equivalent;[31] see Section 3.3.6) *via* either an elimination-isomerisation sequence or a series of oxidation reactions, respectively.

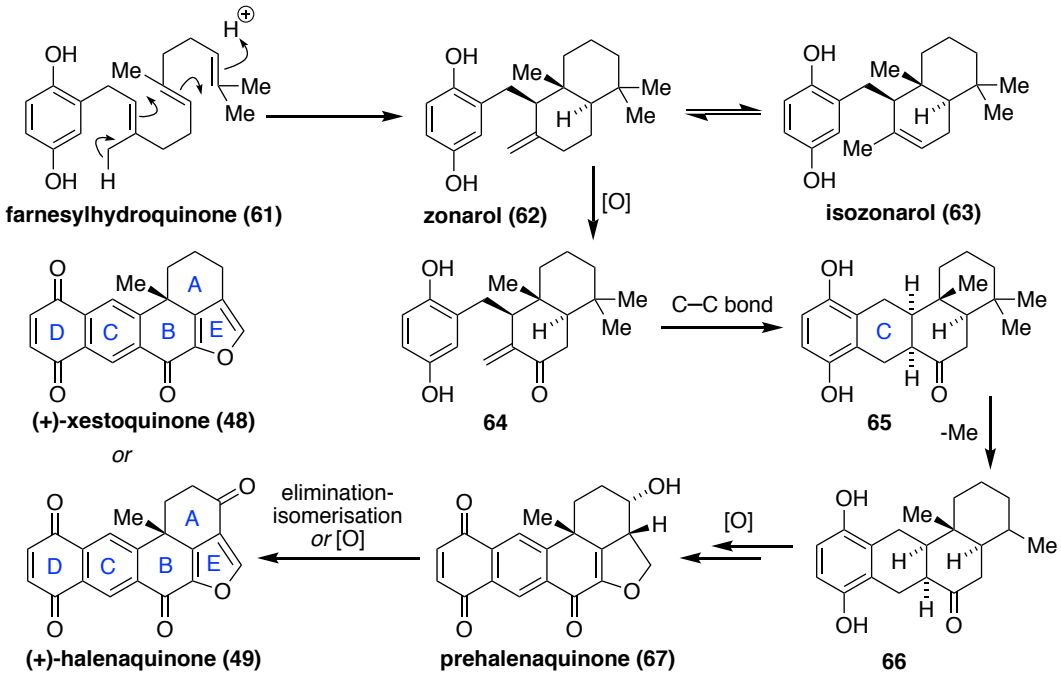

Scheme 3.1 Proposed biosynthesis of (+)-xestoquinone and (+)-halenaquinone from farneslhydroquinone

3.1.4 Review Scope and Classification of Syntheses

While xestoquinone and halenaquinone possess deceptively simple structures, in as much as their high sp^2-C content and single stereocentre, their fused tricyclic furan moiety and ring junction quaternary all-carbon stereocentre present notable and synthetically challenging moieties, respectively. These structural features, together with the wide range of exhibited

biological activities, render the two natural products attractive targets. Within the xestoquinone family of related natural products, synthetic efforts have been primarily focussed on these two compounds, and to date, 10 total or formal syntheses of xestoquinone and halenaquinone have been published, in addition to our own very recently completed synthesis of (+)-xestoquinone.

This review provides an analysis of these previous syntheses, with an emphasis on the ring forming reactions, the end-game oxidation chemistry and the overall strategies employed. To provide a holistic summary and insight into their construction, the review is also expanded to briefly cover studies on the synthesis of unnatural analogues, model systems and derivatisation of these two molecules. The reader should note that a recent review by Schwarzwalder and Vanderwal also provides an excellent and complimentary discussion of many of these total syntheses.[32]

Lastly, this review is extended to include the syntheses of several structurally similar compounds, most notably xestosaprol N and O, wortmannin, viridin, viridiol and nodulisporoviridin E. Total syntheses of these natural products are examined, as well as pertinent model studies involving the novel construction of the core-framework or functionalisation relevant across the xestoquinone family of natural products. Additional references for those synthetic studies of model systems not discussed are provided,[33] as well as for an insightful perspective piece on wortmannin by Wipf and Halter,[34] should they be of interest to the reader.

3.2 Syntheses of Xestoquinone and Halenaquinone

3.2.1 Overall Approaches Employed

While each of the 10 previous syntheses of xestoquinone and halenaquinone have provided unique contributions to the field of synthetic organic chemistry, some parallels may be drawn between the different approaches (Figure 3.3). Six syntheses have employed a Diels–Alder reaction to construct the C ring of the natural product as a key step. Beginning with the Harada group's seminal syntheses of both halenaquinone and xestoquinone from a chiral pool starting material,[35] this approach was also utilized in the formal and total syntheses of Kanematsu and co-workers[36] and Rodrigo and co-workers,[37] to deliver the natural products in racemic form. Trauner's synthesis of (–)-halenaquinone additionally also uses an intramolecular Diels–Alder reaction to form the C ring of the natural product.[38]

The second common strategic transformation is the use of a Mizoroki-Heck cyclisation reaction to install the quaternary carbon stereogenic centre and form the A and/or B ring(s) of the natural products. This approach was pioneered by the Keay group[39] and later also adapted by Shibasaki and co-workers [40] and Trauner and co-workers.[38]

More recently, Carter and co-workers have published a unique enantioselective synthesis of (–)-halenaquinone, that differs from previous syntheses in both construction of the core framework and functionalisation.[41]

Finally, our own synthesis of (+)-xestoquinone, described in Chapter 2, (and the eleventh synthesis of these two molecules) features 3 Diels–Alder reactions to rapidly assemble the tetracyclic carbon framework of the compound; namely a catalytic enantioselective Diels–Alder reaction followed by a diene-transmissive twofold Diels–Alder reaction sequence.

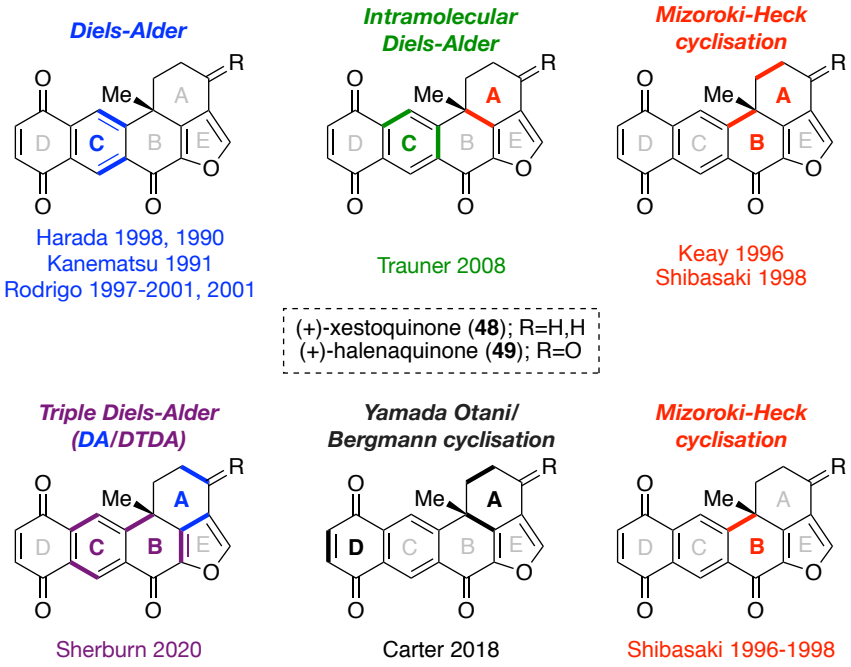

Figure 3.3 Summary of key strategic steps in the syntheses of xestoquinone and halenaquinone Common approaches to xestoquinone/halenaquinone include construction of the C ring *via* a Diels–Alder reaction and installation of the quaternary carbon stereogenic centre/formation of the A and/or B rings *via* a Mizoroki-Heck cyclisation. Key bonds/rings formed by each transformation are highlighted in bold.

3.2.2 (+)-Halenaquinone, Harada, 1988

The first total synthesis of (+)-halenaquinone was completed by Harada and co-workers in 1988, five years after its isolation (Scheme 3.2).[35a] Their synthesis began with the

commercially available Wieland-Miescher ketone (–)-**68**, which was transformed into enone **70** in 9 steps. Diels–Alder reaction of this compound with an *ortho*-quinone dimethide diene, generated *in situ* from 4π electrocyclic ring opening of benzocyclobutane **71**, afforded tetracycle **72** containing the entire carbon framework of the natural product. This key intermediate was obtained as a single stereoisomer (although the relative configurations of the newly formed stereocentres were not determined due to their inconsequential nature). A series of oxidation reactions then delivered the natural product, beginning with dehydrogenation of the C ring with DDQ to afford naphthalene **73**. This compound underwent further oxidation of the B ring using oxygen in the presence of potassium *tert*-butoxide to yield diosphenol **74**. Following treatment with acetic acid to remove the ketal protecting group, a modified Pfitzner-Moffat oxidation was then used to install the furan ring of **76** in a single sequence, involving oxidation of the unmasked 1,3-diol to the β-keto aldehyde and spontaneous cyclisation and dehydration. Finally, oxidation of the 1,4 dimethoxynaphthalene moiety to the corresponding *para*-naphthoquinone with ceric ammonium nitrate (CAN) yielded (+)-halenaquinone.

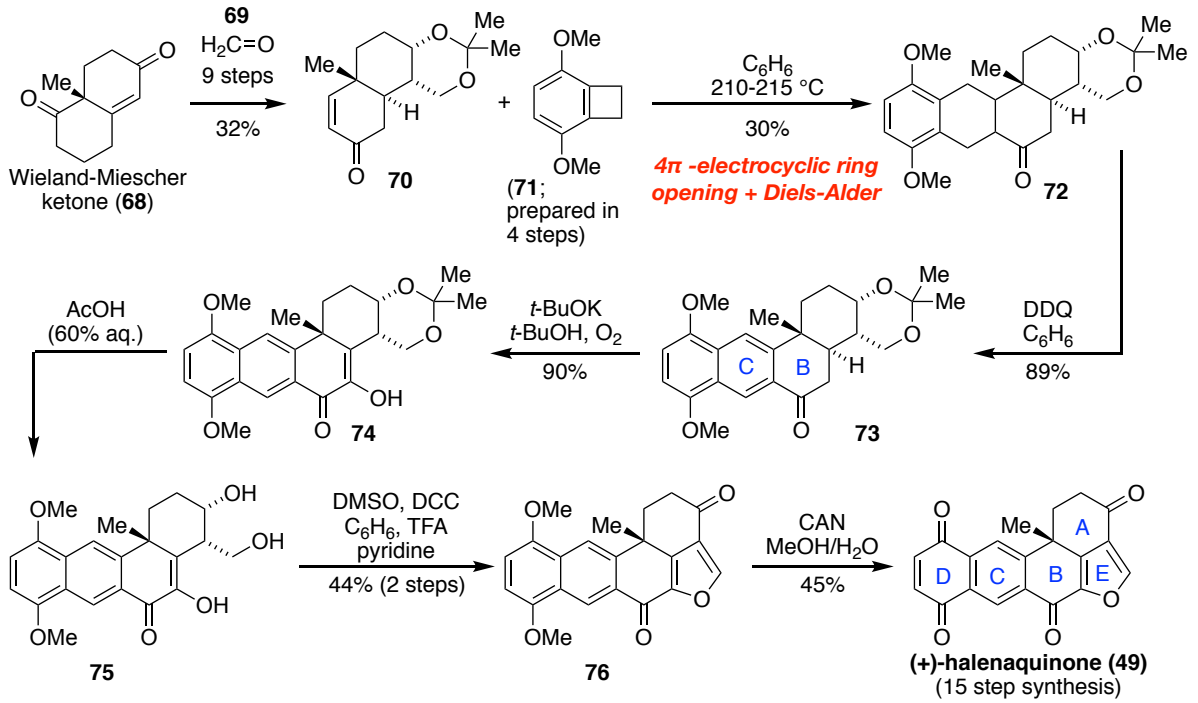

Scheme 3.2 Harada's 1988 chiral pool total synthesis of (+)-halenaquinone

Strategically, the preparation of halenaquinone from the reduced 1,4-dimethoxynaphthalene tetracycle precursor allowed for the late stage installation of the reactive *para*-quinone moiety. Moreover, it allowed the core tetracyclic carbon framework of the natural product to be assembled convergently, with formation of the C ring *via* the key Diels–Alder reaction; an

approach which would prove to be popular amongst several subsequent syntheses. The use of an enantiomerically pure starting material, namely Wieland-Miescher ketone (–)-**68**, to achieve a chiral pool synthesis remains unique to Harada's syntheses (see also (+)-xestoquinone). Overall, this combined transform-based and structure-goal driven strategy delivered the natural product in a longest linear sequence of 15 steps and a 1.7% overall yield.

3.2.3 (+)-Xestoquinone, Harada, 1990

In 1990, Harada and co-workers also published the first total synthesis of (+)-xestoquinone (Scheme 3.3), using a strategy akin to their previous synthesis of (+)-halenaquinone.[35b] Beginning from Wieland-Miescher ketone (–)-**68**, the preparation of an analogous dienophile (**77**), lacking the C3 oxygen functionality, allowed for assembly of the carbon framework. A series of oxidation and deprotection steps comparable to those previously published then delivered (+)-xestoquinone in 17 steps and a 1.0% overall yield.

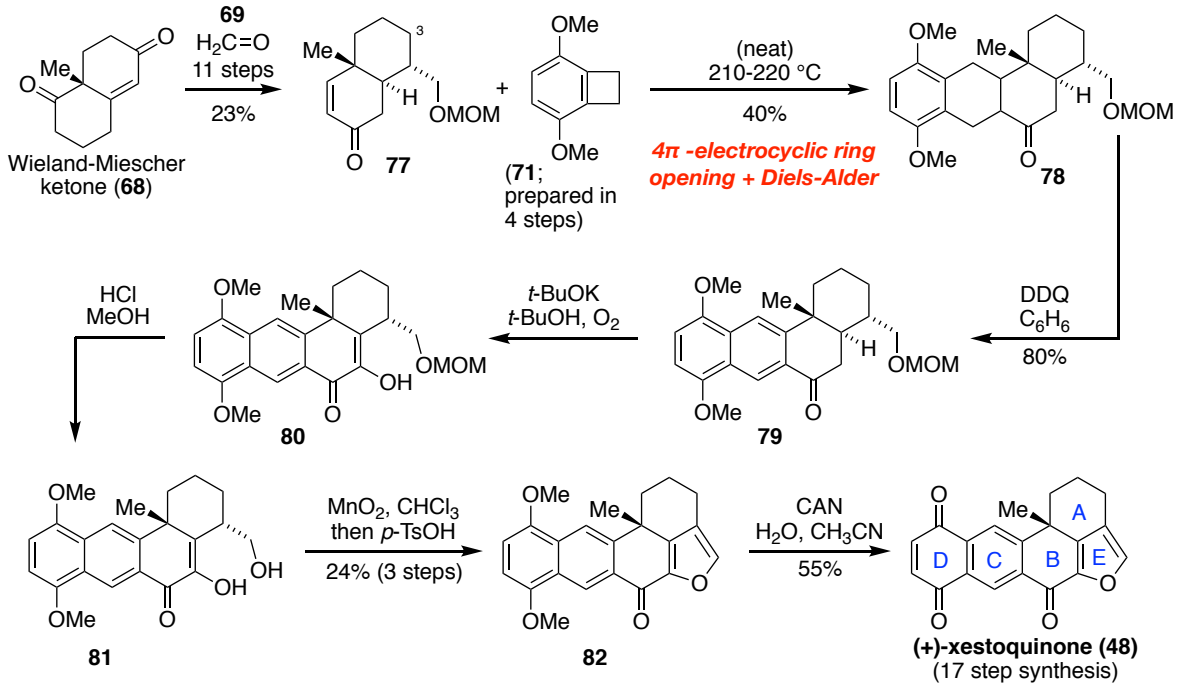

Scheme 3.3 Harada's 1990 chiral pool total synthesis of (+)-xestoquinone

3.2.4 (±)-Xestoquinone, Kanematsu, 1991

Only one year later, Kanematsu and co-workers published a formal synthesis of (±)-xestoquinone (Scheme 3.5).[36] Their approach centred around the use of a 'furan ring transfer' reaction, previously developed within their group (Scheme 3.4).[42] This reaction allows the transformation of 2-substituted furans such into 3,4-fused furans, *via* a base-

promoted cascade sequence. Beginning from representative 2-subsituted furan **83**, this process involves isomerization of the terminal alkyne to allene **84**, intramolecular Diels–Alder reaction to afford **85** and subsequent ring opening to deliver 3,4-fused furan **86**.

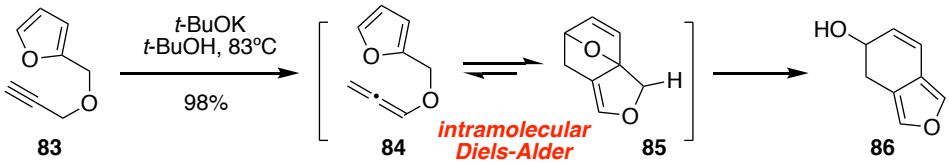

Scheme 3.4 Kanematsu's furan ring transfer reaction for the conversion of 2-substituted furans into 3,4-fused furans

Their synthesis of (±)-xestoquinone began with the application of this methodology to access furan **86** in 2 steps.[42] A further 7 steps then delivered carboxylic acid **87**. Cyclisation of this compound *via* an acyl chloride intermediate afforded tricyclic furan **88**. Subsequent α-selenylation and oxidative elimination yielded enone **90**. In a [4+2] cycloaddition reaction reminiscent of Harada's key step, enone **90** was subjected to Diels–Alder reaction with an *ortho*-quinone dimethide diene. Notably, this diene was generated *in situ via* a chromium mediated di-debromination of *o*-bis(bromo-methyl)arene **91** (an intermediate *en route* to Harada's benzocyclobutane **71**).

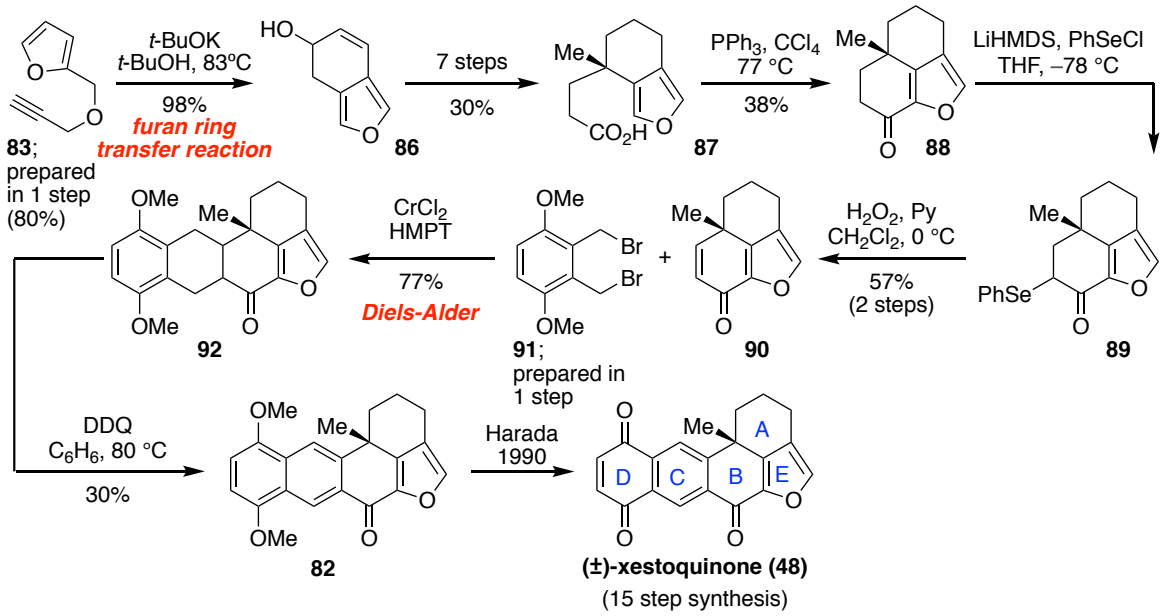

Scheme 3.5 Kanematsu's 1991 formal synthesis of (±)-xestoquinone

The novelty of Kanematsu's approach lies in the strategic generation of the complete tricyclic naphthofuranone unit in enone **90**, thereby subsequently generating pentacycle **92**, which

required little further synthetic manipulation. Borrowing from Harada's inaugural synthesis, simple installation of the naphthalene moiety using DDQ, followed by CAN oxidation of the resulting 1,4-dimethoxynaphthalene **82** yielded (±)-xestoquinone, completing Kanematsu's formal synthesis in a longest linear sequence of 15 steps and a 0.6% overall yield.

3.2.5 (±)-Xestoquinone, Rodrigo, 1997, 2001

Combining their initial efforts in 1997 with an improved sequence disclosed in 2001, Rodrigo and co-workers published a notably shorter total synthesis of (±)-xestoquinone, requiring only 10 steps (Scheme 3.6).[33e, 37] Like Harada and Kanematsu's syntheses, Rodrigo's approach also utilised the Diels–Alder reaction as a key transformation to generate the C ring and core framework of the natural product in a convergent manner. Focus was placed, however, upon the more efficient construction of a tricyclic dienophile (analogous to that used by Kanematsu and co-workers).

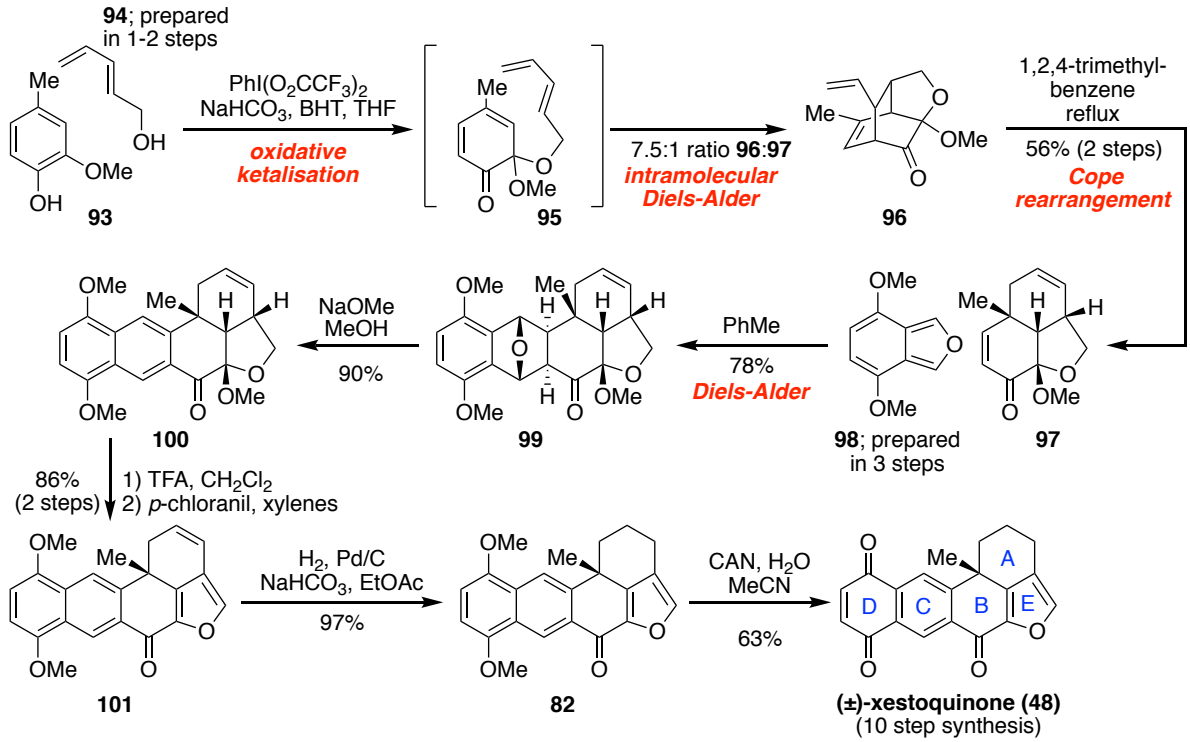

Scheme 3.6 Rodrigo's combined 1997 and 2001 total syntheses of (±)-xestoquinone

Treatment of methylguaiacol (**93**) with (*E*)-2,4-pentadienol (**94**) (accessible in 1-2 steps) in the presence of PIFA resulted in monoketalisation to afford *o*-quinone **95**. Subsequent intramolecular Diels–Alder reaction of this intermediate generated adducts **96** and **97**, resulting from the *o*-quinoid monoketal moiety reacting as a diene or dienophile, respectively. Although

the major product **96** was the undesired isomer, conversion to desired tricycle **97** could be readily achieved *via* Cope rearrangement in refluxing 1,2,4-trimethylbenzene. A second Diels–Alder reaction of this key tricyclic building block with electron rich isobenzofuran **98** (accessible in 3 steps) proceeded through an *exo* transition state with approach of the diene to the less sterically hindered face of the dienophile to generate pentacycle **99** as a single diastereomer. Treatment with sodium methoxide then afforded naphthalene **100**, which was subsequently converted into furan **82** by elimination of methanol, oxidation with *p*-chloranil and hydrogenation of the cyclic alkene. Finally, CAN oxidation to the quinone (as in Harada's inaugural synthesis) delivered the natural product in a 21% overall yield as a racemic mixture.

Strategically, the stereochemistry forming step of this synthesis, generation of *o*-quinone **95**, would be difficult to render enantioselective, likely requiring the development of new and challenging catalytic chemistry. The racemic product aside however, this 10 step total synthesis from Rodrigo was to remain the shortest synthesis of xestoquinone until our most recent contribution.

3.2.6 (±)-Halenaquinone, Rodrigo, 2001

In 2001, the Rodrigo group published their third contribution to the total synthesis of this family of natural products, applying their previously optimised approach from (±)-xestoquinone to the synthesis of (±)-halenaquinone (Scheme 3.7).[43] The synthesis employed the same rapid construction of the tricyclic ABE ring unit *via* a monoketalisation/intramolecular Diels–Alder reaction/Cope rearrangement sequence. A masked carbonyl group was included in diene **102**, however, in the form of an alkenyl sulphide to be carried through the synthesis. Subsequent introduction of the naphthalene moiety was achieved *via* Diels–Alder reaction with *iso*-benzofuran **98** and a series of functional group manipulations, analogous to those employed previously. As the penultimate step, the resulting alkenyl sulphide **108** was hydrolysed to ketone **76** by heating with titanium tetrachloride in wet acetic acid, thereby unmasking the requisite C3 carbonyl functionality. Oxidation to the quinone (as in Harada's inaugural synthesis) then completed Rodrigo's total synthesis of (±)-halenaquinone in a longest linear sequence of 12 steps and a 2.5% overall yield.

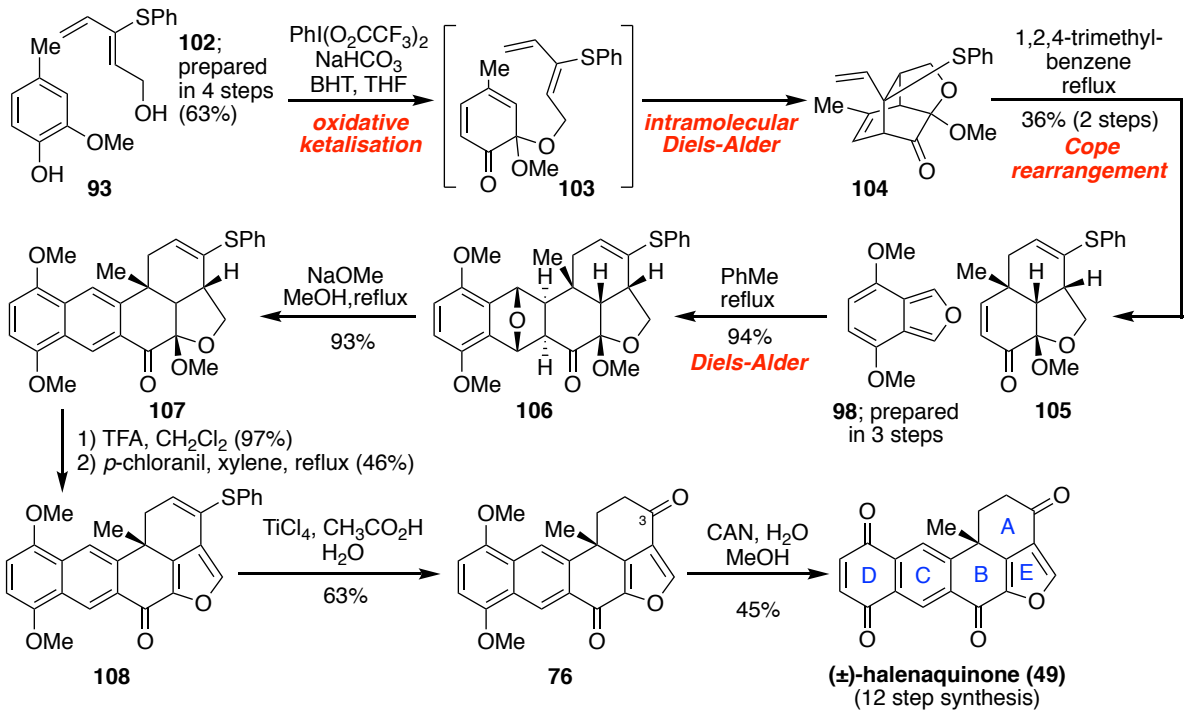

Scheme 3.7 Rodrigo's 2001 total synthesis of (±)-halenaquinone

3.2.7 (+)-Xestoquinone, Keay, 1996

The first catalytic enantioselective synthesis of (+)-xestoquinone was completed in 16 steps by Keay and co-workers in 1996 (Scheme 3.8).[39] They undertook a unique approach to assemble the pentacyclic framework of the molecule and install the quaternary stereocentre in the late stages of the synthesis *via* a catalytic Mizoroki-Heck cyclisation cascade.

Their synthesis began with the conversion of 2,5-dimethoxybenzoic acid (**109**) to benzocyclobutene **110** in 6 steps, according to the procedure developed by Wallace and co-workers.[44] Diels–Alder reaction of this compound with ethyl 3-bromopropiolate (**111**) then afforded naphthalene **112**, which could be converted to acyl chloride **113** in a further 3 steps. As the second starting point for their synthesis, tri-substituted furan **117** was prepared in 3 steps from known furan **114**. Thus, regioselective lithiation of **114** at C4 and treatment with triisopropyl borate generated the corresponding lithium triisopropyl borate *in situ*, which underwent Suzuki-Miyaura cross coupling with 2-bromopropene to afford tri-substituted furan **115**. Subsequent oxidation of the primary alcohol to the aldehyde and Wittig reaction then delivered diene **117**. Following lithiation at the unsubstituted position on the furan ring, furan **117** underwent nucleophilic acyl substitution of acyl chloride **113** to afford **118**, which could be converted to the key naphthol triflate **120** in 2 steps. As their key step, an enantioselective Mizoroki-Heck cyclisation sequence, employing $Pd_2(dba)_3$ pre-catalyst and the chiral ligand

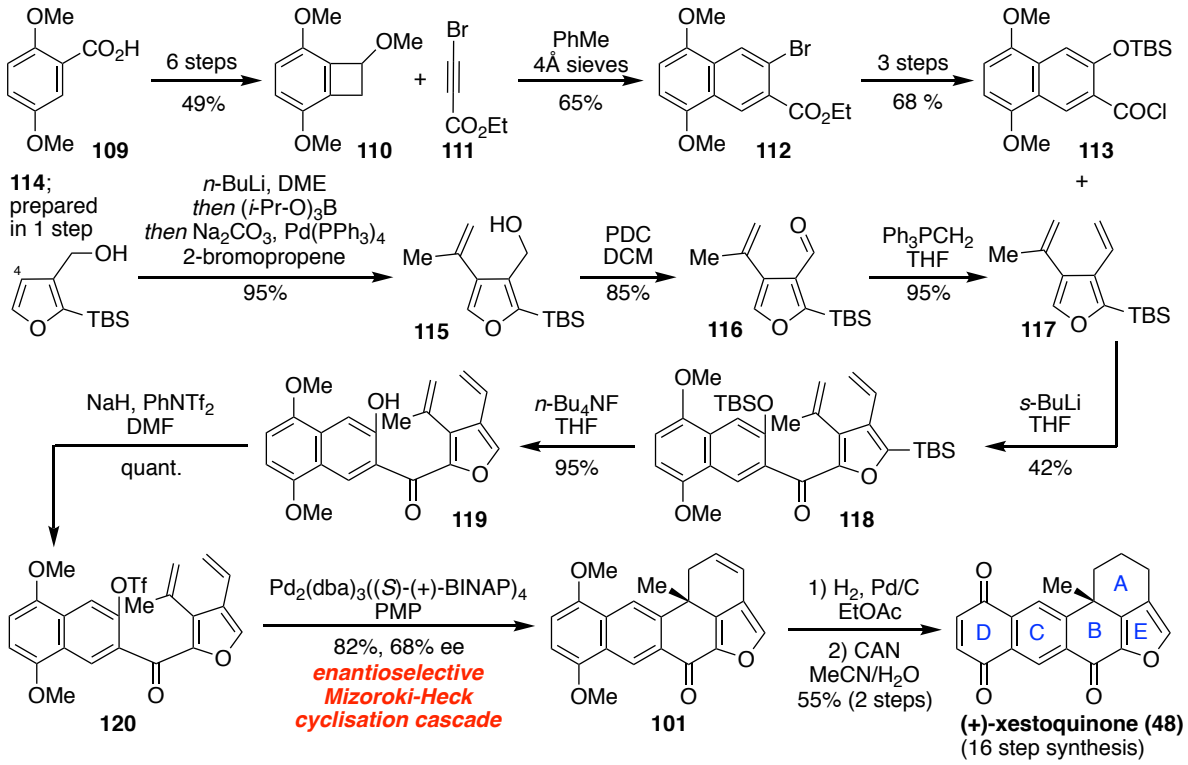

Scheme 3.8 Keay's 1996 catalytic enantioselective total synthesis of (+)-xestoquinone

(*S*)-(+)-BINAP, formed both the A and B rings along with the quaternary stereocentre of the natural product in one step, *via* a 6-*exo*-trig/6-*endo*-trig cyclisation cascade. This delivered pentacycle **101** in up to 68% ee. From here, notably, little further manipulation was required. Hydrogenation, followed by CAN oxidation delivered the natural product in a longest linear sequence of 16 steps, a 68% ee and a 4.0% overall yield.

3.2.8 (+)-Halenaquinone, Shibasaki, 1996, 1998

Shibasaki and co-workers completed the first enantioselective total synthesis of (+)-halenaquinone in 1996 (Scheme 3.9).[40b-d] They employed a novel intermolecular Suzuki-Miyaura/intramolecular Mizoroki-Heck cross coupling sequence to install the quaternary carbon stereocentre at a much earlier stage of the synthesis than in Keay's construction of (+)-xestoquinone.

Their synthesis began with commercially available tetralone **121**, which was converted to ditriflate **122**, to engage in the key cross-coupling cascade. Exposure to alkyl borane **123** (prepared in 3 steps), in the presence of $Pd(OAc)_2$ and the chiral ligand (*S*)-(+)-BINAP delivered tricycle **124** in 85% ee and 20% yield *via* a one-pot Suzuki-Miyaura

cross-coupling/enantioselective Mizoroki-Heck cyclisation cascade. Yields could be increased for this sequence *via* alternative 2 step and non-enantioselective variants.

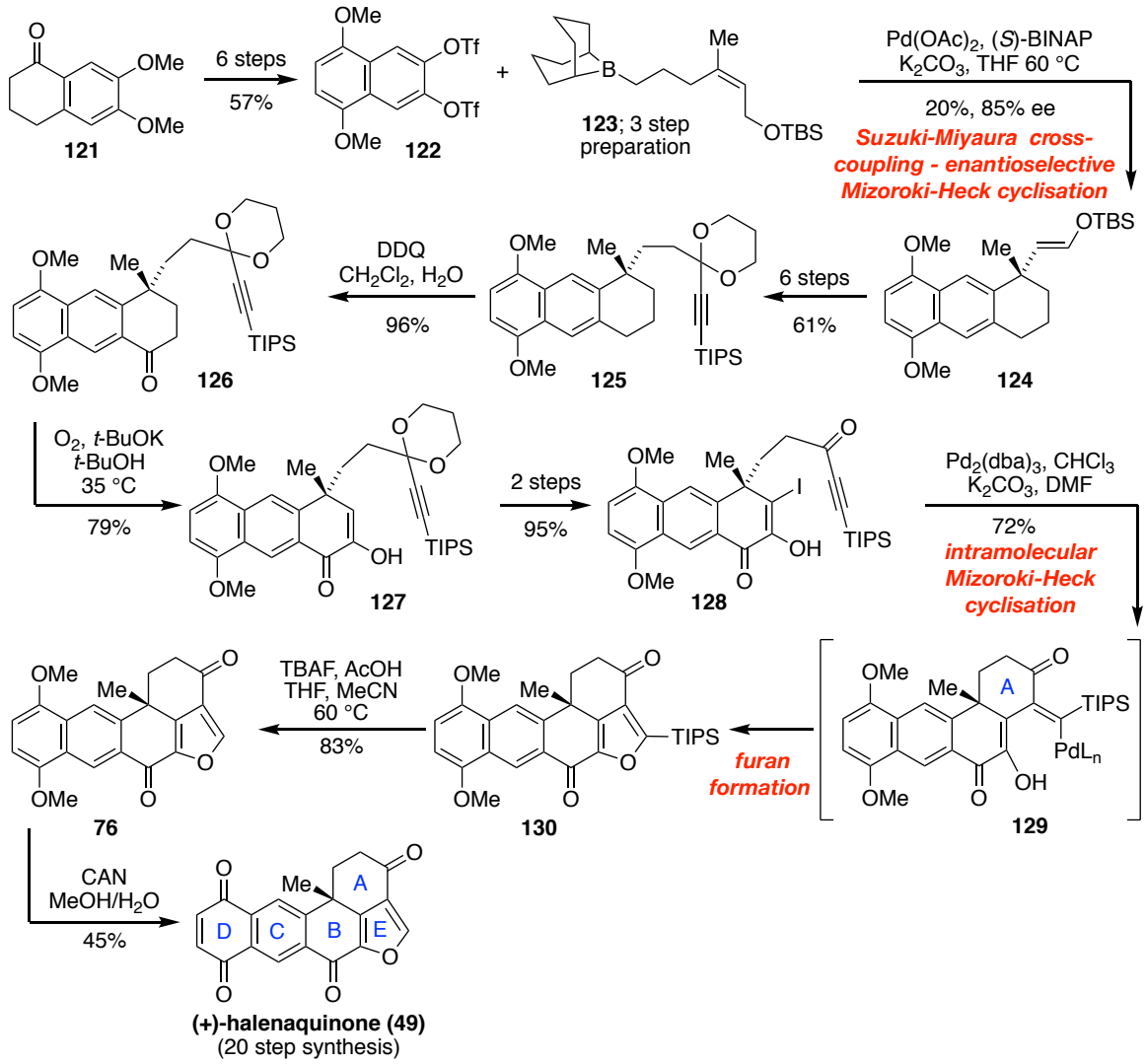

Scheme 3.9 Shibasaki's 1996 catalytic enantioselective total synthesis of (+)-halenaquinone

The conversion of tricycle **124** into alkenyl iodide **128** over a further 10 steps prepared for the second key palladium catalysed cyclisation of the synthesis. In this sequence, intramolecular Mizoroki-Heck cyclisation of iodide **128**, involving *syn*-carbopalladation of the alkyne, generated palladium intermediate **129** to form the A ring of the natural product. Intermediate **129** was then intercepted by the proximal hydroxyl functionality to forge pentacyclic furan **130**. Desilylation, followed by CAN oxidation (as in Harada's inaugural synthesis) then delivered (+)-halenaquinone in a longest linear sequence of 20 steps, a 1.5% overall yield and 85% ee.

3.2.9 (+)-Xestoquinone, Shibasaki, 1998

In 1998, Shibasaki and co-workers published a shorter enantioselective synthesis of (+)-xestoquinone, through optimisation of the enantioselective Mizoroki-Heck cyclisation cascade originally developed by Keay and co-workers (Scheme 3.10).[40a] Shibasaki and co-workers used the more readily obtained aryl bromide **131** in place of Keay's aryl triflate **120** by employing a silver salt additive. This modification delivered (+)-xestoquinone in a reduced longest linear sequence of 14 steps, 63% ee and 5.0% overall yield.

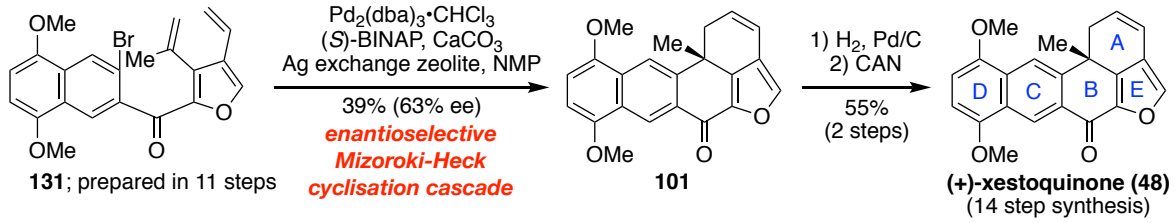

Scheme 3.10 Shibasaki's 1998 catalytic enantioselective total synthesis of (+)-xestoquinone

3.2.10 (–)-Halenaquinone, Trauner, 2008

The Trauner group employed an intramolecular inverse-demand Diels–Alder reaction of an alkenyl quinone as their key step to synthesise the non-natural enantiomer, (–)-halenaquinone, in 2008 (Scheme 3.11).[38] Lithiation and nucleophilic addition of diiodofuran **133** to aldehyde **132** (prepared in 2 steps and 4 steps, respectively), afforded the corresponding secondary alcohol, whose subsequent oxidation and supra-stoichiometric enantioselective reduction with (–)-DIP-Cl delivered alcohol **136** in 94% ee.[45] In a further 2 steps, this compound was converted to 2-furaldehyde **137**, which underwent intramolecular Mizoroki-Heck cyclisation with good diastereoselectivity to afford bicycle **138** as the major isomer (dr = 7:1), thereby selectively installing the quaternary stereocentre of the natural product.

Nucleophilic addition of lithiated alkenyl stannane **139** (prepared in 3 steps) to bicycle **138** delivered enol **140** as an inconsequential mixture of diastereomers. Subsequent deprotection and Ley-Griffith oxidation of both secondary alcohols then afforded diketone **141**, which underwent oxidative demethylation with silver (II) oxide and nitric acid to deliver the key alkenyl quinone **142**. As their second key step, **142** underwent intramolecular inverse-electron demand Diels–Alder under high pressure conditions to afford pentacycle **143**, which rapidly tautomerised to alkenyl hydroquinone **144** *in situ*. While the diastereoselectivity of the Diels–Alder reaction therefore could not be determined, DFT calculations suggested the reaction proceeds *via* an *exo* transition state. As the final step of their synthesis, aromatisation

and oxidation of **144** yielded *ent*-(–)-halenaquinone. Notably, the key intramolecular Diels–Alder reaction could also be performed thermally as part of a one pot intramolecular Diels–Alder-oxidation sequence employing DDQ, albeit in low yield, to complete Trauner's supra-stoichiometric enantioselective synthesis in a longest linear sequence of 15-16 steps, a 0.36% overall yield and 94% ee.

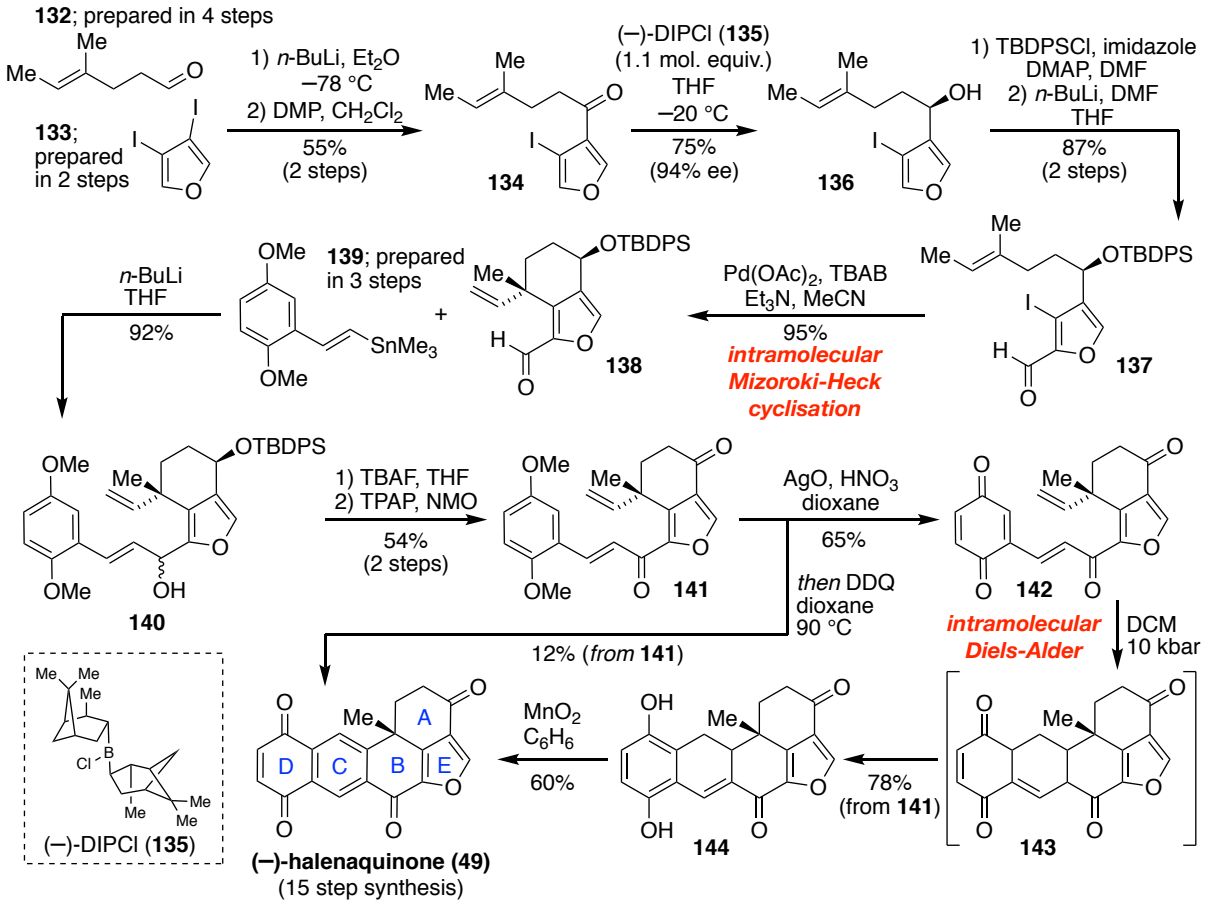

Scheme 3.11 Trauner's 2008 supra-stoichiometric enantioselective synthesis of (–)-halenaquinone

3.2.11 (–)-Halenaquinone, Carter, 2018

More recently, in 2018, Carter and co-workers completed a catalytic enantioselective synthesis of the non-natural enantiomer, (–)-halenaquinone, using a unique approach to build the functionalized pentacyclic framework (Scheme 3.12).[41]

Starting from commercially available methyl ketone **145**, olefination and deprotection delivered benzylic aldehyde **146**. As the first key step of the synthesis, this compound was subjected to a proline sulfonamide catalysed Yamada-Otani reaction to install the quaternary stereocentre of the natural product enantioselectively (90.5:9.5 er on sulfide intermediate),

before *in situ* oxidation with H_2O_2 and HFIP yielded sulfoxide **149**. Thermal elimination of the sulfoxide then afforded the corresponding alkene, and diastereoselective formylation of the cyclohexenone moiety was achieved using LiHMDS and the formaldehyde equivalent, benztriazole **150**, to yield **151**. As their second key step, the furan ring (and requisite aldehyde functionality), were then introduced *via* a novel one-step palladium catalysed oxidation cascade using $Pd(OTFA)_2$ in the presence of DMSO, O_2 and 4Å mol sieves. Pinnick oxidation of the resulting aldehyde **152** and selective hydrogenation of the cyclohexenone alkene, yielded carboxylic acid **153**. Following conversion of the carboxylic acid to the corresponding acid chloride *in situ*, Friedel-Crafts acylation proceeded with complete regioselectivity to deliver tetracycle **155**. Finally, the quinone moiety of the natural product was appended, beginning with two-fold Sonogashira cross-coupling of dibromide **155** with TIPS-acetylene, followed by deprotection. On small scale (<5 mg), as the third key step of the synthesis, thermolysis in the presence of TEMPO, achieved Bergman cyclisation and *in situ* oxidation to yield (–)-halenaquinone. Alternatively, selective reduction of the C3 carbonyl to the secondary alcohol, oxidative Bergman cyclisation and DMP oxidation back the carbonyl, allowed scalable access to the natural product. Overall, Carter's contribution achieved (–)-halenaquinone in a longest linear sequence of 12-14 steps, a 1.2% overall yield and 90.5% ee.

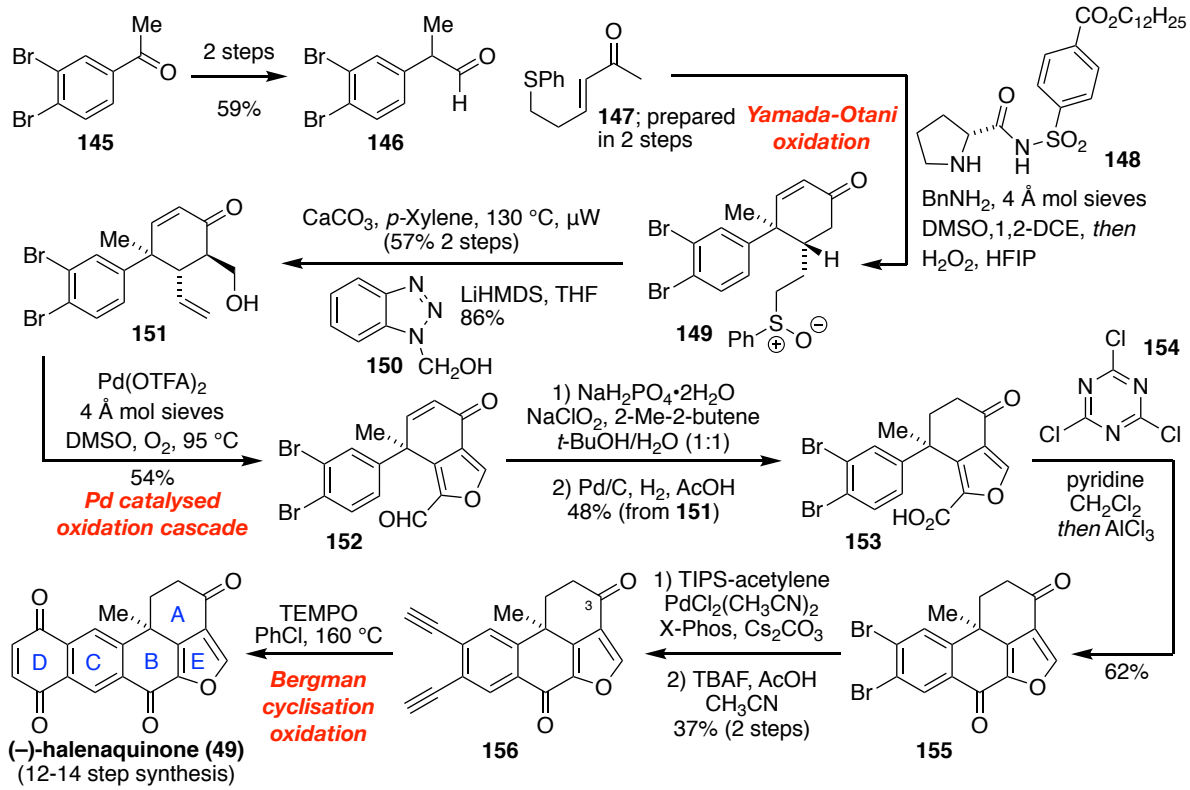

Scheme 3.12 Carter's 2018 catalytic enantioselective total synthesis of (–)-halenaquinone

3.2.12 (+)-Xestoquinone, Sherburn, 2020

While described at length in Chapter 2, a summary of our enantioselective synthesis of (+)-xestoquinone is given here to provide a complete picture to the reader (Scheme 3.13).

Our synthesis employed a novel approach to assemble the core tetracyclic carbon framework of the molecule in a convergent manner, namely a diene-transmissive two-fold Diels–Alder reaction sequence, enabled by the first use of the cross-conjugated hydrocarbon, [3]dendralene, in total synthesis.

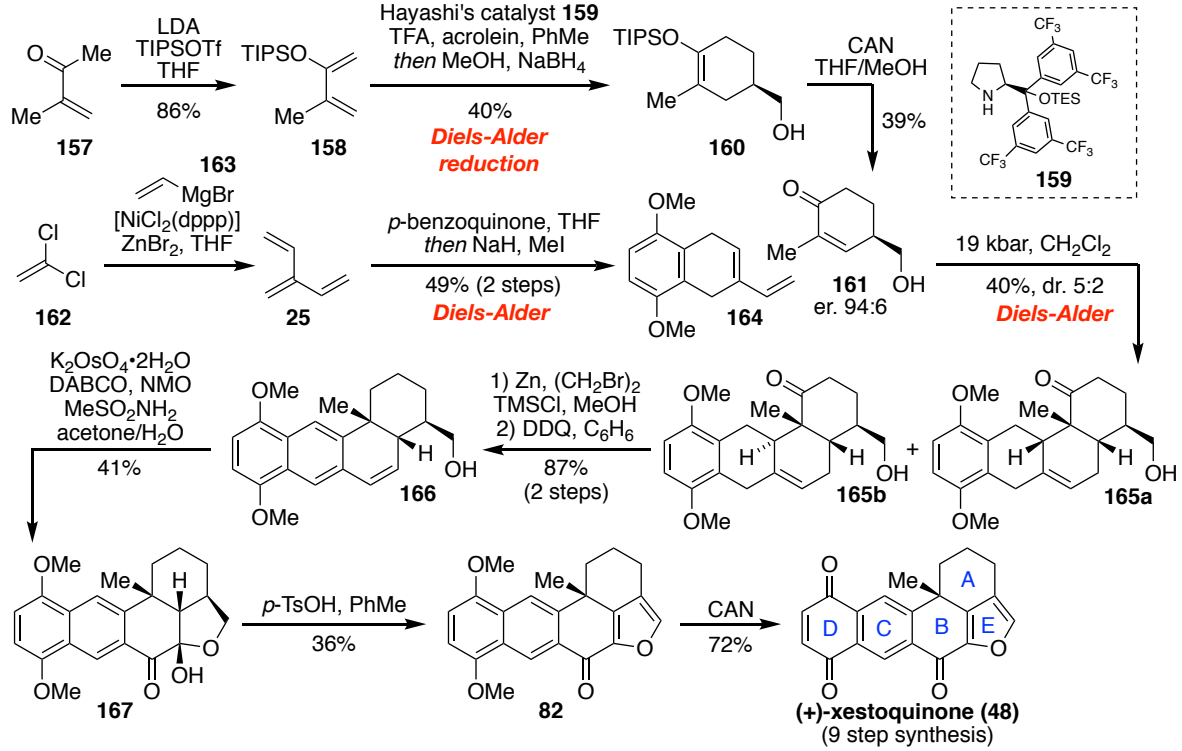

Scheme 3.13 Sherburn's 2020 catalytic enantioselective total synthesis of (+)-xestoquinone

Our synthesis began with the 3-step preparation of chiral cyclohexenone **161**. Thus, formation of silyl enol ether **158**, subsequent organocatalysed enantioselective Diels–Alder reaction and *in situ* reduction to yield cyclohexene **160,** and lastly, oxidation, afforded dienophile **161** in high enantioselectivity (94:6 er).

As the second starting point for our convergent synthesis, a one-step preparation of [3]dendralene (**25**) was developed, involving two-fold Negishi cross-coupling of 1,1-dichloroethylene (**162**) with vinyl magnesium bromide (**163**). One-pot Diels–Alder reaction of [3]dendralene with *p*-benzoquinone, followed by two-fold deprotonation/methylation, afforded diene **164**. This compound then underwent a

diastereoselective Diels–Alder reaction with chiral cyclohexenone dienophile **161** to afford tetracycles **165a** and **165b** as an inconsequential mixture of diastereomers. Importantly, as the key phase of the synthesis, this DTDA reaction sequence both assembled the entire carbon framework and installed the quaternary carbon stereocentre of the natural product in just two steps.

Deoxygenation *via* a Clemmensen reduction, followed by oxidation with DDQ delivered naphthalene **166**. Subsequent oxidation under Sharpless dihydroxylation conditions afforded lactol **167**, which could be dehydrated using *p*-toluene sulfonic acid to deliver the requisite furan functionality of **82**. Lastly, CAN oxidation to the quinone (as in Harada's seminal synthesis), afforded (+)-xestoquinone in a longest linear sequence of 9 steps, a 0.48% overall yield and an er of 98:2. Of note strategically, 3 of the 4 six-membered rings of (+)-xestoquinone are formed *via* Diels–Alder reactions and our synthesis is the shortest synthesis of the natural product to date.

3.2.13 Summary

In total, 11 total and formal syntheses of xestoquinone and halenaquinone are described (summarised in Figure 3.4). These syntheses range from 9 to 18 steps in length (longest linear sequence) and use a broad variety of strategies. Notably, no published syntheses are biomimetic (see Section 3.1.3 Biosynthetic Origins).

As outlined in Section 3.2.1 (Overall Approaches Employed), Mizoroki-Heck and Diels–Alder reactions are predominantly used to construct the core ring system of the molecules, presumably favoured due to their ability to enantio/diastereo-selectively introduce the quaternary carbon stereocentre and/or their high efficiency and step economy.

In all 11 syntheses, the reactive quinone moiety is installed last, *via* oxidation of a dimethoxynahpthalene, with the exception of Carter and co-workers who employ a Bergmann cyclisation and oxidation to introduce this moiety in their final step. In contrast, a diverse array of approaches are used to address the furan ring, ranging from early to late stage introduction.

Of note, a chiral pool approach is only employed by Harada and co-workers. There are also 5 enantioselective syntheses. Of these, 3 employ Mizoroki-Heck reactions to form the quaternary stereocentre, 2 employ enantioselective organocatalysed reactions to introduce stereocentres, 1 employs an enantioselective reduction and 2 use a diastereoselective reaction to introduce the quaternary stereocentre of the natural product.

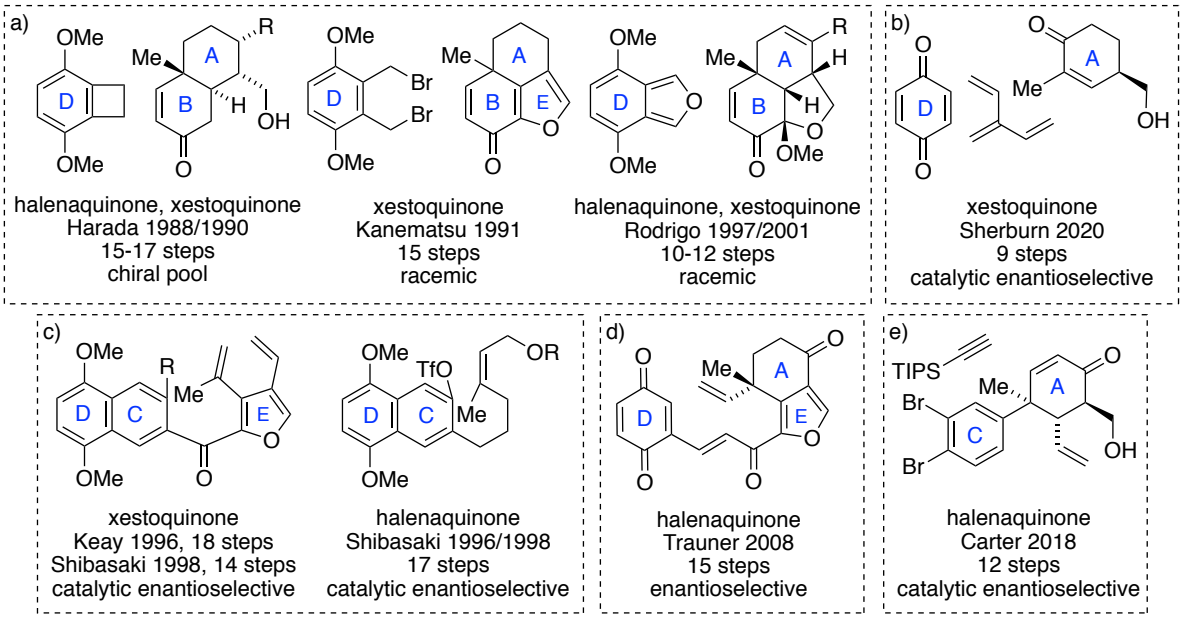

Figure 3.4 Summary of key strategic steps in the syntheses of xestoquinone and halenaquinone; syntheses are grouped according to key step: a) orthoquinonedimethide Diels–Alder reaction (C ring); b) DTDA reaction sequence (B/C rings); c) Mizoroki-Heck cyclisation (A/B ring); d) Mizoroki-Heck cyclisation/IMDA reaction (A/B/C rings); e) Yamada-Otani/ /Bergman cyclisation (A/D rings).

Strategic approaches to construct and functionalise the core framework also vary. Distinct construction and functionalisation phases are present in the syntheses of Harada and Rodrigo, as well as in our own work, wherein the core carbon framework is constructed in the early stages of the synthesis. In contrast, Keay, Kanematsu, Shibasaki, Trauner and Carter employ a more gradual approach, wherein functionalisation is interspersed with C–C bond formation.

3.3 Analogues, Model Studies and Manipulations of Xestoquinone and Halenaquinone

Beyond the natural products themselves, synthetic studies have also explored the construction of natural and unnatural analogues, model compounds and the derivatisation of xestoquinone and halenaquinone into related natural products.

Analogues have been made primarily to probe their biological activity, focussing mainly on modifications to the furan ring. While these synthetic endeavours are important medicinally, they can also drive the development of new strategies and approaches to allow for different substitution patterns and structural changes, or alternatively, demonstrate the versatility of known routes. In contrast, the function of model studies is primarily to allow novel approaches and often new methodologies to be tested. Lastly, semi-syntheses involving the manipulation of xestoquinone and halenaquinone provide insight not only into their relationship with different natural products, but also a better understanding of their stability and chemical reactivity.

3.3.1 Analogue, (±)-Xestoquinone and (±)-Halenaquinone, Crews, 1993

In 1993, Crews and co-workers prepared a variety of analogues of (±)-xestoquinone and (±)-halenaquinone for biological testing, with those of most relevance being tetracycle **171** lacking the furan ring and pentacycles **176** and **177** in which the furan moiety is replaced with a benzene ring (Scheme 3.14).[24a] They employed an approach reminiscent of Harada's inaugural synthesis. Diels–Alder reaction of an *ortho*-quinodimethide diene, generated *in situ via* thermal

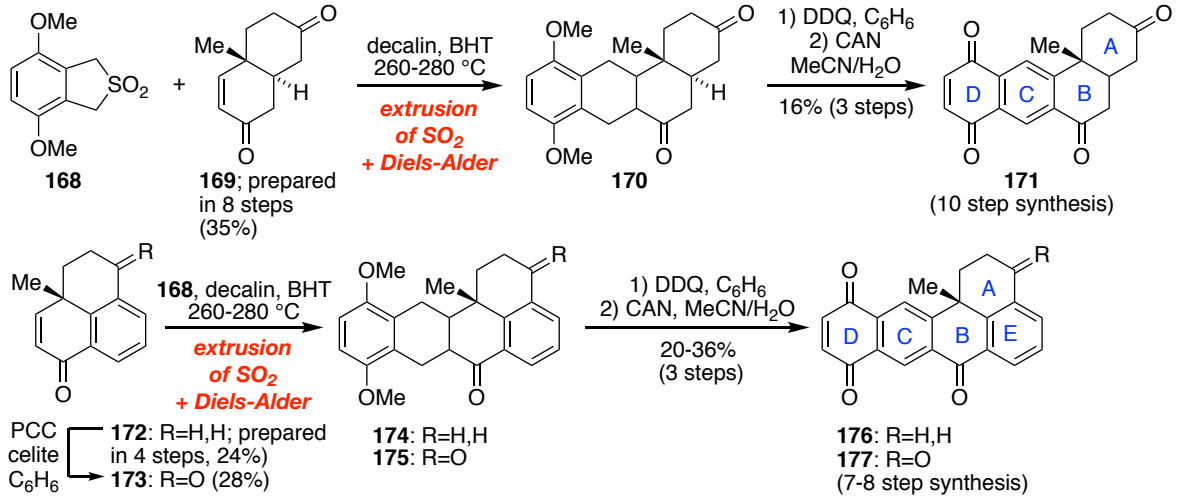

Scheme 3.14 Crew's 1993 syntheses of (±)-xestoquinone and (±)-halenaquinone analogues

cheletropic extrusion of sulphur dioxide from **168**, with substituted enones **169**, **172** and **173**[46] assembled the core carbon framework of the molecules. Subsequent dehydrogenation with DDQ and oxidation to the naphthoquinone with ceric ammonium nitrate delivered the final targets in a longest linear sequence of 7-10 steps and an overall yield of 2.4% to 5.6%.

3.3.2 Analogue, (±)-9-Methoxyxestoquinone and (±)-10-Methoxyxestoquinone, Rodrigo, 2001

In 2001 Rodrigo and co-workers completed the first total syntheses of the analogues (±)-9-methoxyxestoquinone and (±)-10-methoxyxestoquinone (Scheme 3.15), using a strategy akin to their previous synthesis of (±)-xestoquinone.[37] Notably, their synthesis provided the first pure samples of these two compounds, which are themselves natural products, isolated as an inseparable mixture from a *Xestospongia* sp. Sponge in the Philippines.[18g]

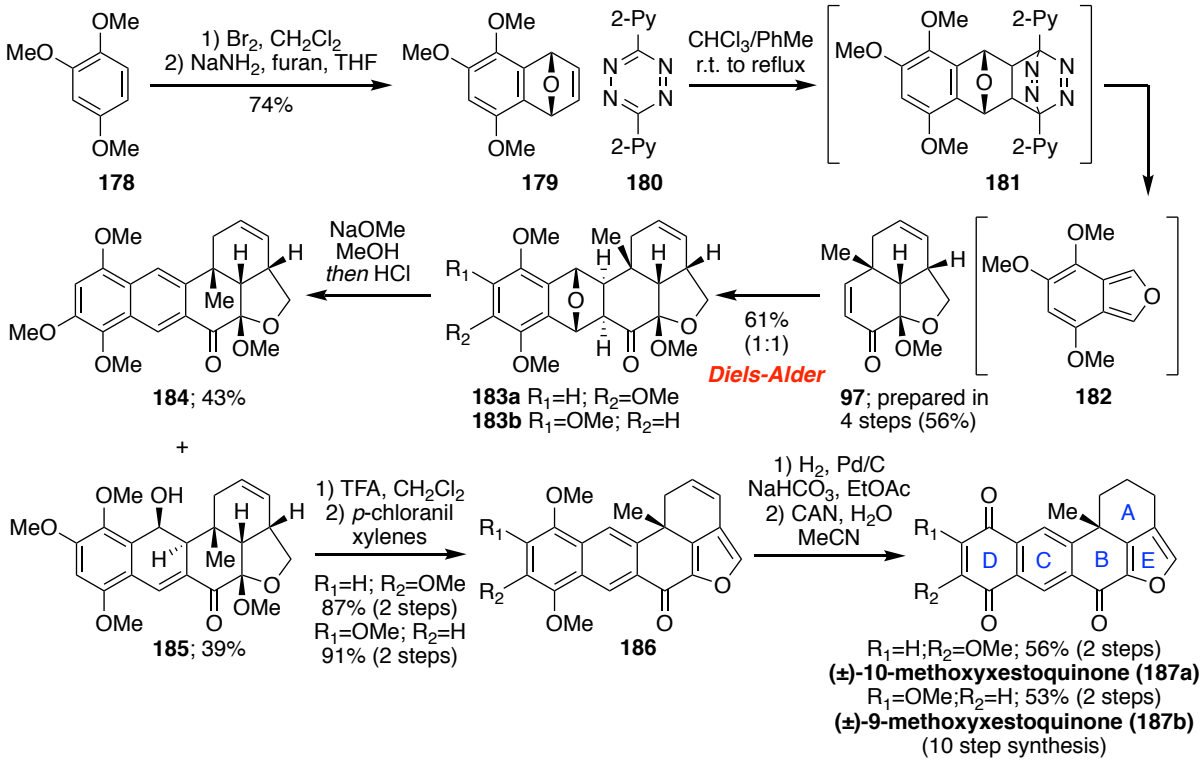

Scheme 3.15 Rodrigo's 2001 synthesis of (±)-9-methoxyxestoquinone and (±)-10-methoxyxestoquinone

Beginning from 1,2,4-trimethoxybenzene **178**, the preparation of an analogous diene with the additional methoxy functionality allowed for assembly of the carbon framework, delivering the adducts **183a** and **183b** in a 1:1 ratio as an inseparable mixture of isomers. Base catalysed retro-oxa-Michael addition and dehydration was used to differentiate between these two compounds;

dehydration of the alcohol resulting from **183a** was assisted by the methoxy group to afford naphthalene **184**, while alcohol **185** remained. These two compounds were easily separated by column chromatography, and were then converted to the natural products using a series of functionalisation steps comparable to those published previously, thus affording (±)-9-methoxyxestoquinone and (±)-10-methoxyxestoquinone in a longest linear sequence of 10 steps and a 6.4% to 7.2% overall yield.

3.3.3 Analogue, (±)-Thiohalenaquinone, Wipf, 2007

In 2007, Wipf and co-workers completed a synthesis of the unnatural thiophene analogue of halenaquinone, (±)-thiohalenaquinone, to probe the importance of the fused furan functionality to the compound's biological activity and cytotoxicity (Scheme 3.16).[47]

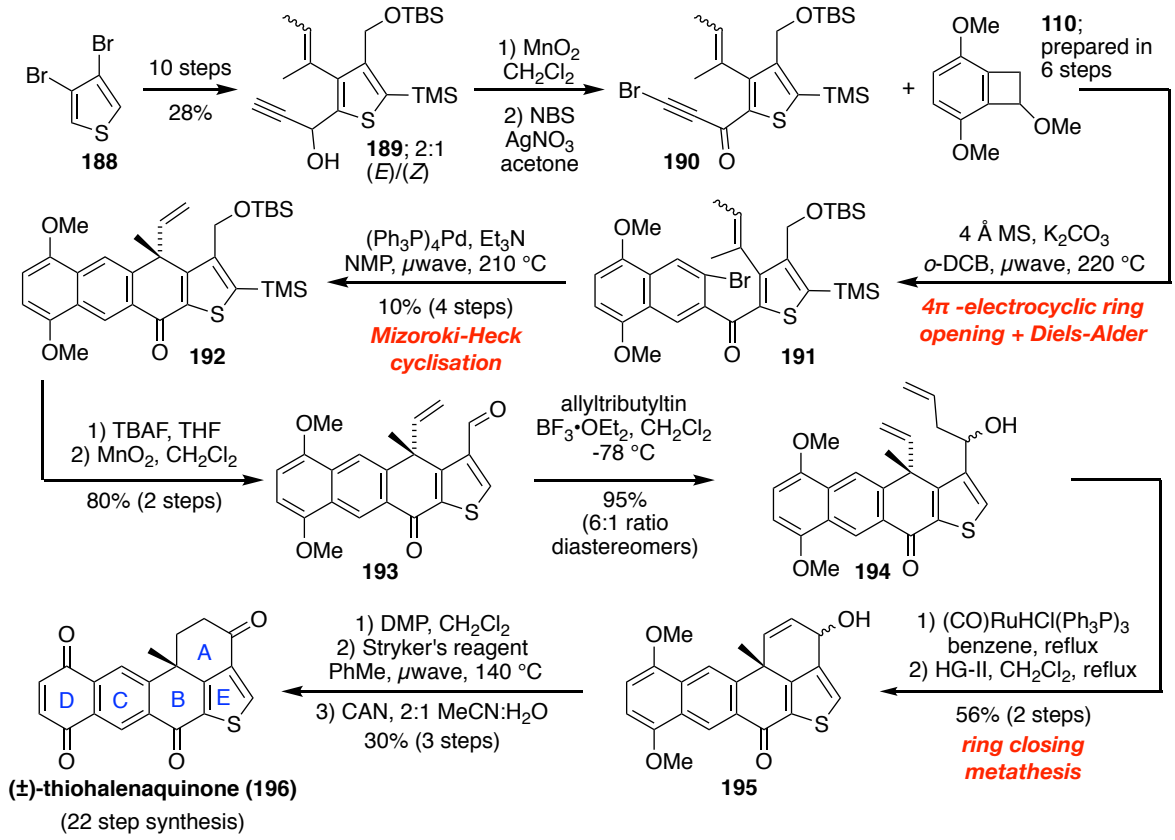

Scheme 3.16 Wipf's 2007 synthesis of (±)-thiohalenaquinone

Their synthesis began with the functionalization of thiophene **188** to afford alkyne **190** in 12 steps. In a key step reminiscent of Harada's seminal approach to (+)-halenaquinone, and of Keay's pioneering enantioselective synthesis of (+)-xestoquinone, Diels–Alder reaction of this compound with an *ortho*-quinone dimethide diene, generated *in situ* from 4 π electrocyclic ring opening of benzocyclobutane **110**, delivered tricycle **191**. Subsequent palladium catalysed

Mizoroki-Heck reaction of aryl bromide **191** *via* a 6-*exo-trig* cyclisation afforded tetracycle **192**. Deprotection, oxidation, addition of allyltributyl tin and finally isomerization of the newly introduced alkene, then set the scene for a late stage ring closing metathesis, to afford **195** and complete the pentacyclic framework of the molecule. Lastly, DMP oxidation of the allylic alcohol in pentacycle **195**, selective reduction of the cyclic alkene and oxidation to the quinone (according to Harada and co-workers seminal work), afforded (±)-thiohalenaquinone. Overall, Wipf and co-workers accessed the unnatural analogue in a longest linear sequence of 22 steps and a 0.4% overall yield.

3.3.4 Model Study, Halenaquinone Core, Nemoto, 2001 / 2002

In 2001and 2002, Nemoto and co-workers reported a synthesis of the ABCE fused tetracyclic core framework of (±)-halenaquinone (Scheme 3.17).[48] As their key step, they employed a 4π electrocyclic ring opening of substituted benzocyclobutane **199**, followed by intramolecular Diels–Alder reaction of the tethered furan ring to assemble the tetracyclic framework. Oxidation to re-instate the furan ring was then achieved over a further 3 steps, to afford tetracycle **202** in a longest linear sequence of 10 steps and a 4.8% overall yield.

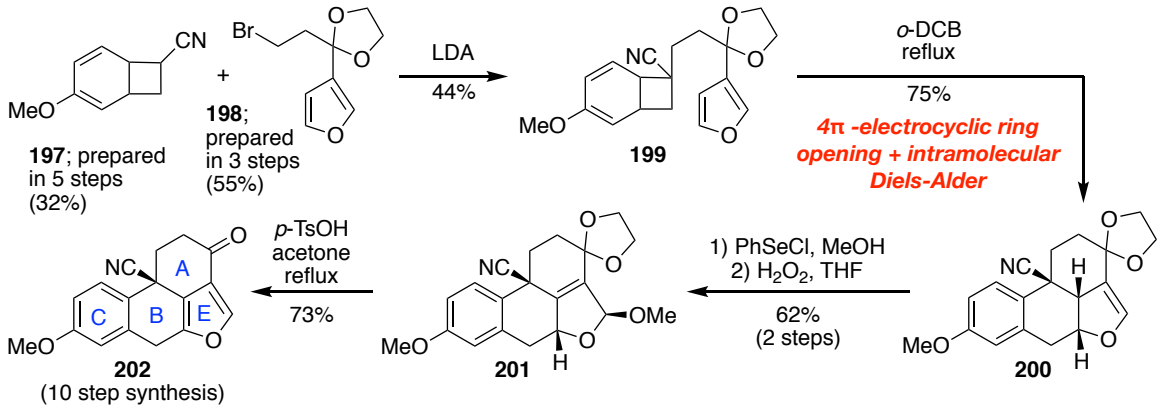

Scheme 3.17 Nemoto's 2001/2002 synthesis of the ABCE (±)-halenaquinone core

3.3.5 Model Study, Xestoquinone Core, Ahn, 2003

In 2003, the Ahn group published a synthesis of the ABCE fused tetracyclic core ring system of (±)-xestoquinone (Scheme 3.18).[49] They employed a unique approach to form the 6-5 (A-E) fused ring system in one step. Ynal **203** (prepared in 12 steps) was subjected to the key cascade reaction, involving tetra-dehydro Diels–Alder reaction, followed by rearrangement to afford furan **205**, forming two new rings in one step, albeit in low yield. A one-pot

demethylation and intramolecular Friedel-Crafts reaction of furan **205** afforded fused tetracycle **206** in a longest linear sequence of 14 steps and 0.17% overall yield.

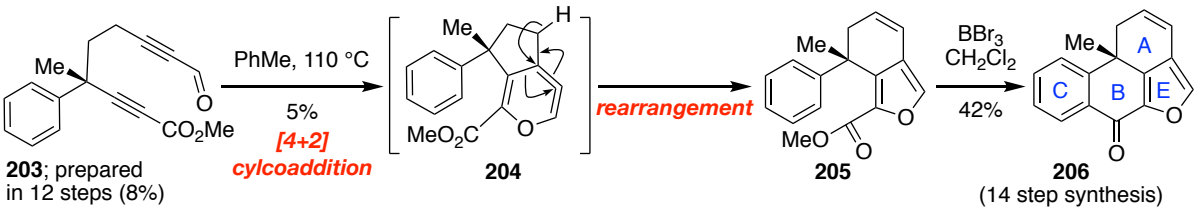

Scheme 3.18 Ahn's 2003 synthesis of the ABCE (±)-xestoquinone core

3.3.6 Manipulation, (+)-Xestoquinone and (+)-Halenaquinone, Harada, 1994

In 1994, Harada and co-workers demonstrated the synthesis of (+)-xestoquinone and (+)-halenaquinone from a common synthetic precursor (Scheme 3.19).[31] The core tetracyclic framework of **75** was formed *via* the same strategy as in their original synthesis of (+)-halenaquinone.

Mild oxidation of triol **75** yielded dihydrofuran **207**, successfully halting before oxidation to the furan ring. Known reduced precursor to xestoquinone, **82**, could then be accessed by dehydration of this compound with *p*-toluene sulfonic acid. Alternatively, further oxidation of dihydrofuran **207** forged the furan and A ring carbonyl functionality, to yield known reduced precursor to halenaquinone **76**, thereby completing a formal synthesis of the two natural products. Significantly, this is the only divergent synthesis these two compounds reported.

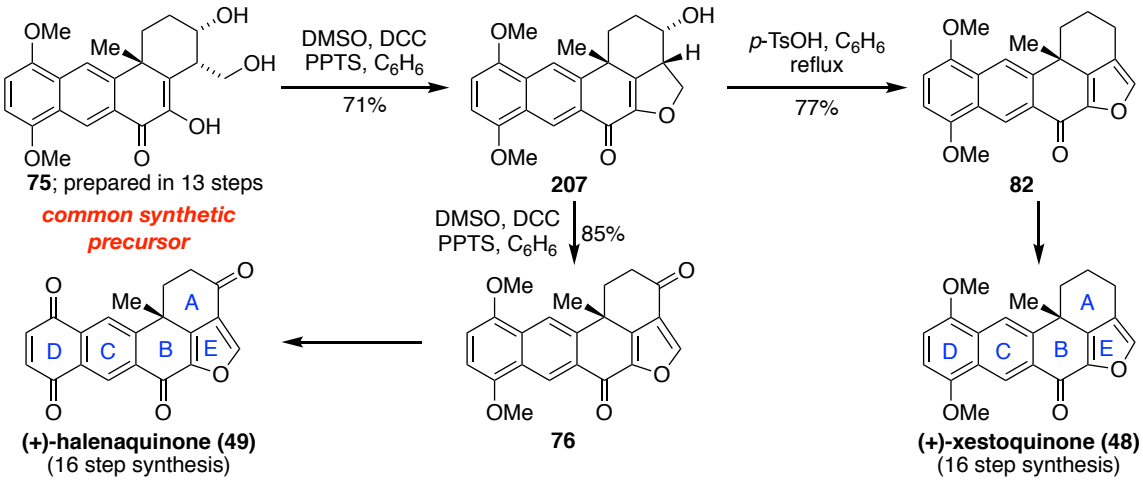

Scheme 3.19 Harada's 1994 divergent synthesis of (+)-xestoquinone and (+)-halenaquinone

3.3.7 Manipulation, (–)-Prehalenaquinone, Harada, 1994

In 1994, Harada and co-workers also published the synthesis (and isolation) of (–)-prehalenaquinone, a putative biosynthetic precursor to (+)-xestoquinone and (+)-halenaquinone (Scheme 3.20).[31] They employed the same common synthetic precursor as in their divergent synthesis of (+)-xestoquinone and (+)-halenaquinone. Thus treatment of dimethyl ether **75** with ceric ammonium nitrate introduced the quinone and dihydrofuran functionalities, to afford the natural product (**67**).

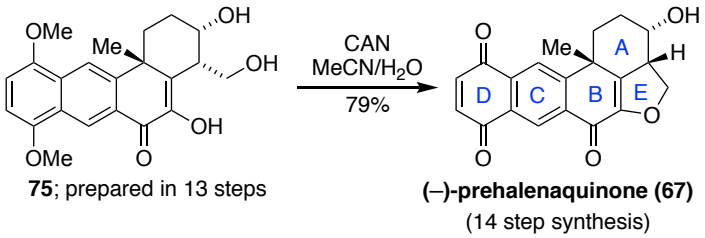

Scheme 3.20 Harada's 1994 synthesis of (–)-prehalenaquinone

3.3.8 Manipulation, (+)-Halenaquinol, Harada, 1988

In conjunction with their 1988 synthesis of (+)-halenaquinone, Harada and co-workers accessed the related natural product (+)-halenaquinol *via* reduction with aqueous sodium hydrosulfite (Scheme 3.21).[35a] This transformation has also been replicated by Shibasaki and co-workers.[40b]

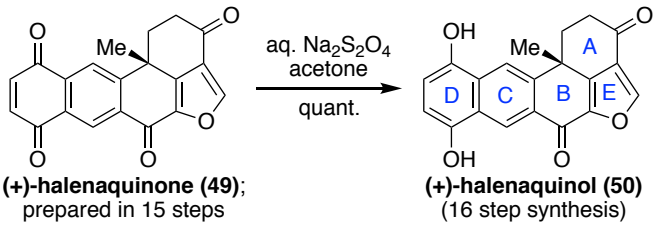

Scheme 3.21 Harada's 1988 conversion of (+)-halenaquinone to (+)-halenaquinol

3.3.9 Manipulation, Xestoquinol, Harada, 1990

In an analogous manner to their synthesis of (+)-halenaquinol, Harada and co-workers generated xestoquinol by reduction of synthetic (+)-xestoquinone, although this compound is yet to be confirmed as a natural product (Scheme 3.22).[35b]

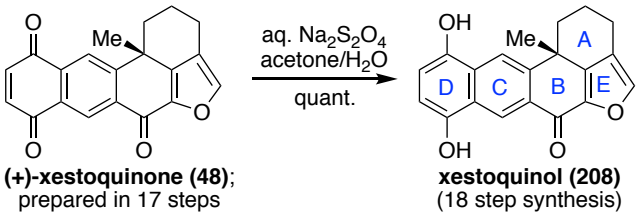

Scheme 3.22 Harada's 1990 conversion of (+)-xestoquinone to xestoquinol

3.3.10 Manipulation, (+)-Adociaquinones A and B, Schmitz, 1988; Harada, 1995

Schmitz and co-workers synthesised (+)-adociaquinones A and B in one pot from isolated (+)-xestoquinone *via* treatment with hypotaurine and heating (steam bath, 1 min) (Scheme 3.23). [17] This procedure was later adapted by Harada and co-workers using synthetic (+)-xestoquinone, the addition of water, and heating at 40 °C for a longer reaction time to obtain the natural products in higher yield.[50]

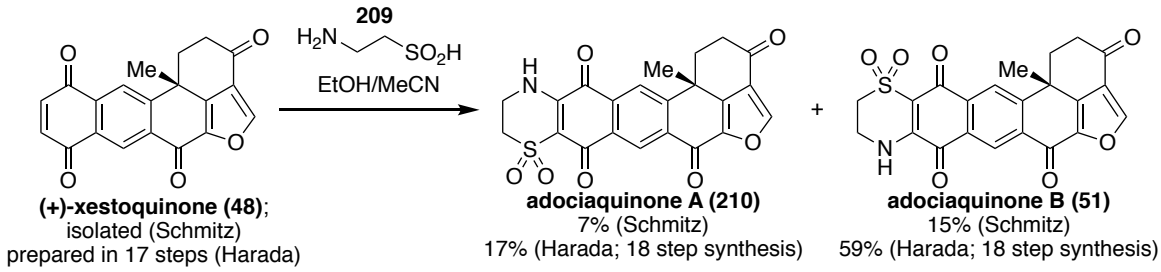

Scheme 3.23 Schmitz's 1988 and Harada's 1995 conversion of (+)-xestoquinone to (+)-adociaquinone A and (+)-adociaquinone B

3.3.11 Summary

This section has outlined the synthesis of analogues and models of, and manipulations involving, xestoquinone and halenaquinone (Figure 3.5). Three synthetic studies of analogues are discussed, focusing on modifications to the furan and quinone rings. The synthetic routes employed are reminiscent of syntheses of the natural products themselves, engaging both similar strategic disconnections and tactics to arrive at the target structures.

In contrast, both model studies outlined contribute very different approaches to those taken previously. Nemoto's 4π-electrocyclic ring opening – intramolecular Diels–Alder sequence provides a powerful and novel way to construct the AB rings fused to the furan E ring. Similarly, Ahn's intricate [4+2] cycloaddition – rearrangement to forge the fused AE rings has been not applied to this class of molecules before.

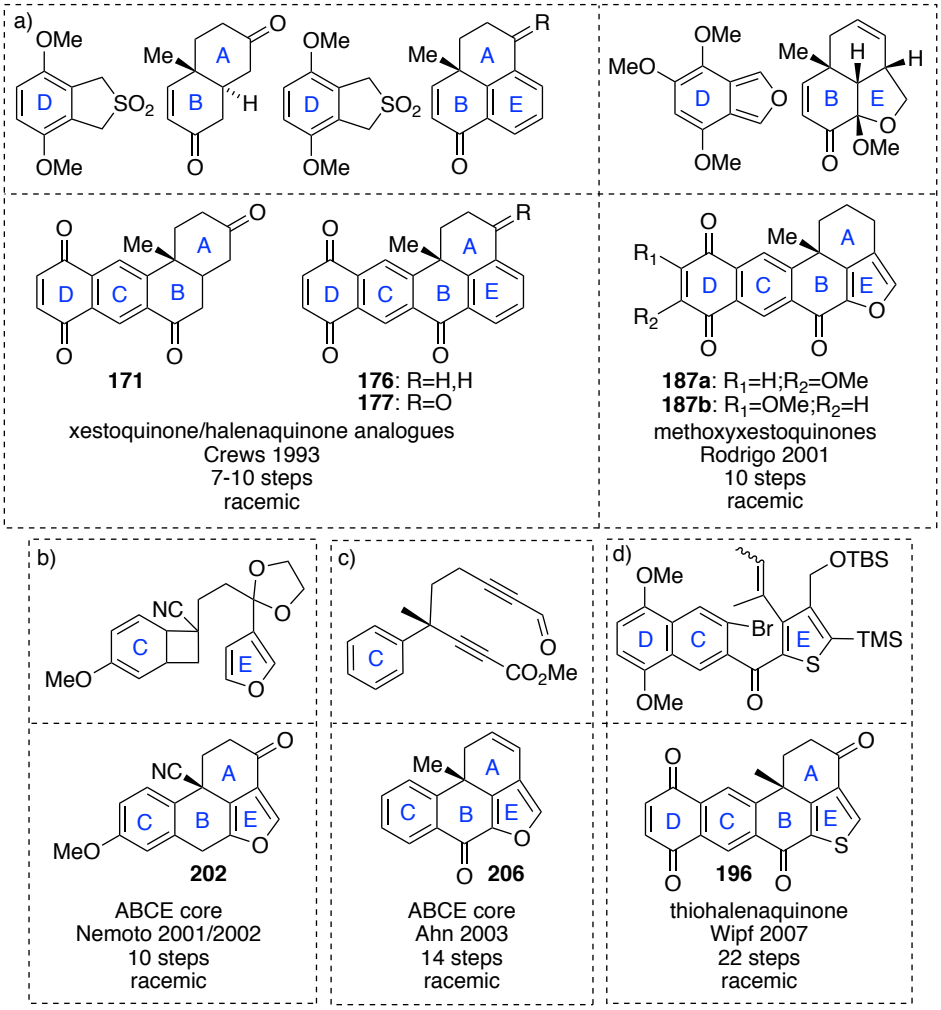

Figure 3.5 Summary of key strategic steps in the syntheses of xestoquinone and halenaquinone analogues and models. Top: key intermediates; Bottom: target structures. Syntheses are grouped according to key step: a) Diels–Alder reaction (C ring); b) 4π-electrocyclic ring opening – intramolecular Diels–Alder (A/B rings); c) [4+2] cycloaddition – rearrangement (A/E rings); d) Mizoroki-Heck cyclisation (B ring).

Despite the many manipulations to access compounds such as halenquinol, xestoquinol, and adociaquinones A and B, conversion of (+)-xestoquinone to (+)-halenaquinone (or *vice versa*) appears to remain unexplored. Notably, Harada's work is the only divergent approach to (+)-xestoquinone and (+)-halenaquinone, and it employs the elimination or oxidation of functionality from a common alcohol precursor, rather than the introduction or removal of the additional carbonyl functionality itself. To this end, the benzylic oxidation to introduce ketone functionality in the synthesis of analogues by Crews and co-workers is interesting, although admittedly the potential challenges imposed by the furan ring are in that case removed.

3.4 Syntheses of Other Structurally Related Natural Products

In addition to the numerous synthetic contributions towards xestoquinone and halenaquinone, several published syntheses of structurally similar natural products are also of note (Figure 3.6). Completed syntheses as well as pertinent model studies towards xestosaprol N, xestoaprol O, wortmannin, viridin, viridiol and nodulisporoviridin E are discussed.

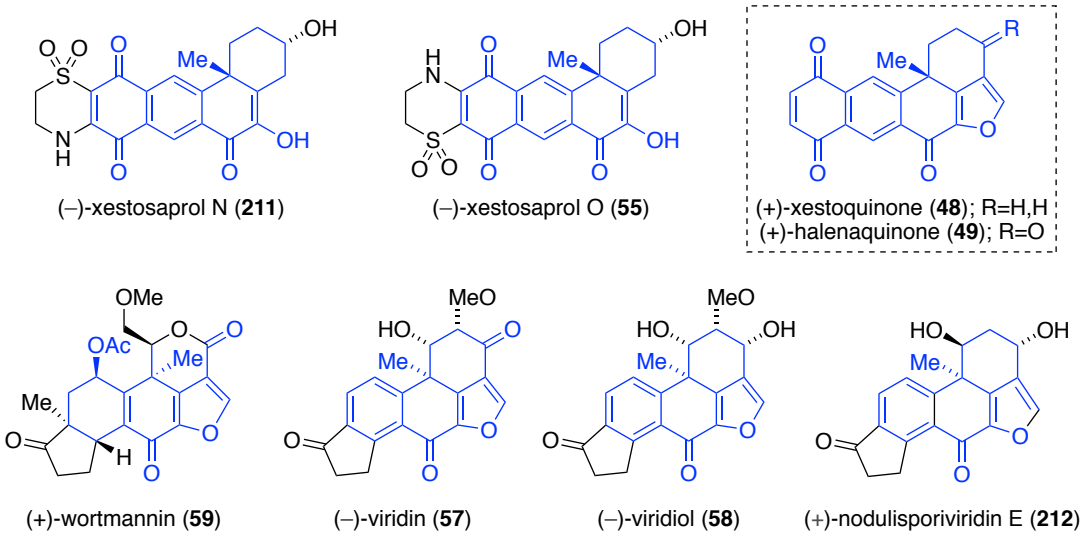

Figure 3.6 Structurally related natural products to (+)-xestoquinone and (+)-halenaquinone, which have succumbed to chemical synthesis. Shared structural motifs are highlighted in blue and (+)-xestoquinone and (+)-halenaquinone are shown for comparison.

3.4.1 (±)-Deoxy-xestosaprol O and N, Andersen, 2014

The first reported syntheses within the xestosaprol sub group of natural products, are Andersen and co-workers' 2014 syntheses of the deoxy analogues of (±)-xestosaprol O and (±)-xestosaprol N (lacking a hydroxyl group at the C3 position) (Scheme 3.24).[18f] Their short, divergent synthesis began with the bromination of commercially available ketone **213** to afford **214**. As their key step, bromide **214** and alkene **215** were subjected to a silver (I) catalysed photochemical annulation, using conditions developed by Sato and co-workers,[51] to afford tetracycle **216**. In this process, silver (I) acts to weaken the C–Br bond of **214**, which undergoes homolysis under irradiation with UV light to generate the corresponding carbon radical. Intermolecular radical addition to **215**, single electron transfer to generate the radical cation and subsequently intramolecular Friedel-Crafts alkylation then achieve the successive formation of 2 C–C σ-bonds to afford tetracycle **216**. Benzylic oxidation of tetracycle **216** with $KMnO_4$ gave rise to a 1:1 mixture of regioisomers **217a** and **217b**. Separate oxidation of these two regioisomers afforded diosphenols **218a** and **2180b** respectively, before finally condensation with hypotaurine (as in Schmitz's synthesis of adociaquinones A and B) delivered (±)-deoxy-xestosaprol O and (±)-deoxy-xestosaprol N, in a longest linear sequence of 5 steps and an overall yield of 1.2% and 1.3%, respectively.

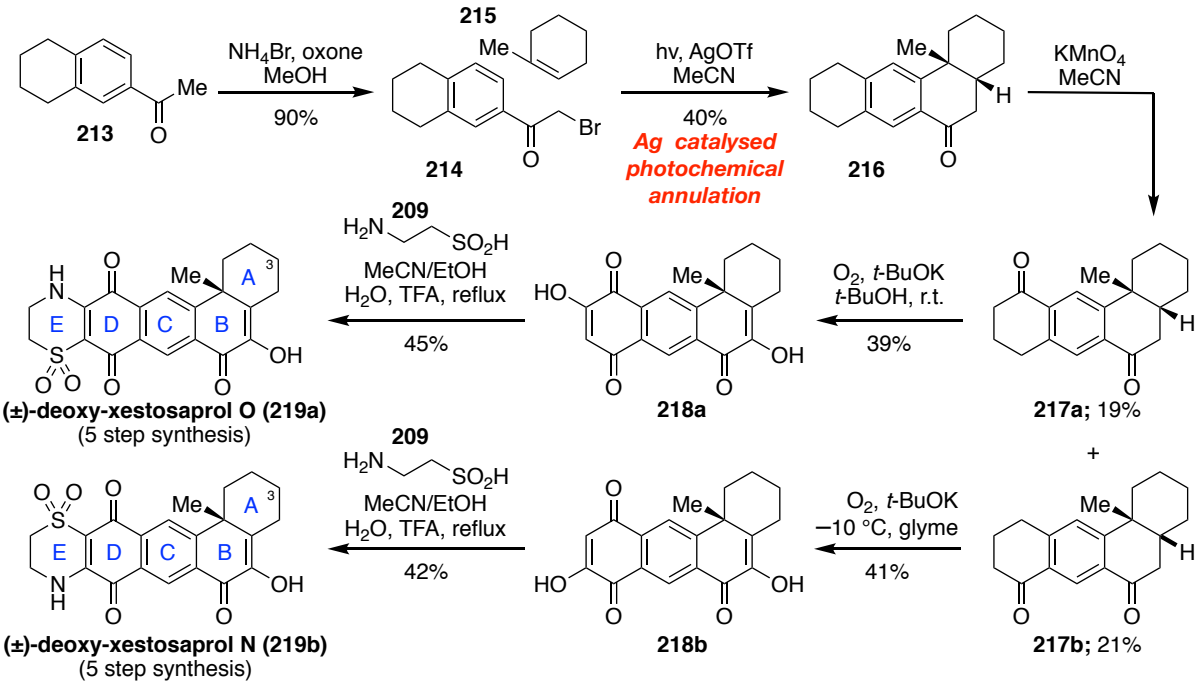

Scheme 3.24 Andersen's 2014 total synthesis of (±)-deoxy-xestosaprol O and (±)-deoxy-xestosaprol N

3.4.2 (–)-Xestosaprol N and O, Gao, 2018

In 2018, Gao and co-workers employed a convergent, chiral pool approach to achieve the first total syntheses of (–)-xestosaprol N and (–)-xestosaprol O (Scheme 3.25).[52] Their synthesis began with the preparation of chiral alcohol **226** from (–)-quinic acid (**225**) in 7 steps according to the work of Wind and co-workers.[53] A further 6 steps then delivered chiral iodide **227**. As their second starting point for their convergent synthesis, bromide **220**[54] and (bis)trimethylsilyl enol ether **221**[55] (each prepared in 2 steps respectively), were submitted to a Hauser-Heck-type coupling reaction using conditions developed by Koert and co-workers to yield ester **222**.[55] Subsequent intramolecular condensation then afforded naphthalene **223**, which was converted to aldehyde **224** in a further 3 steps. Lithium-halogen exchange of **227** and nucleophilic addition to **224**, then united these two key building blocks, followed by oxidation of the resulting secondary alcohol to afford ketone **228**.

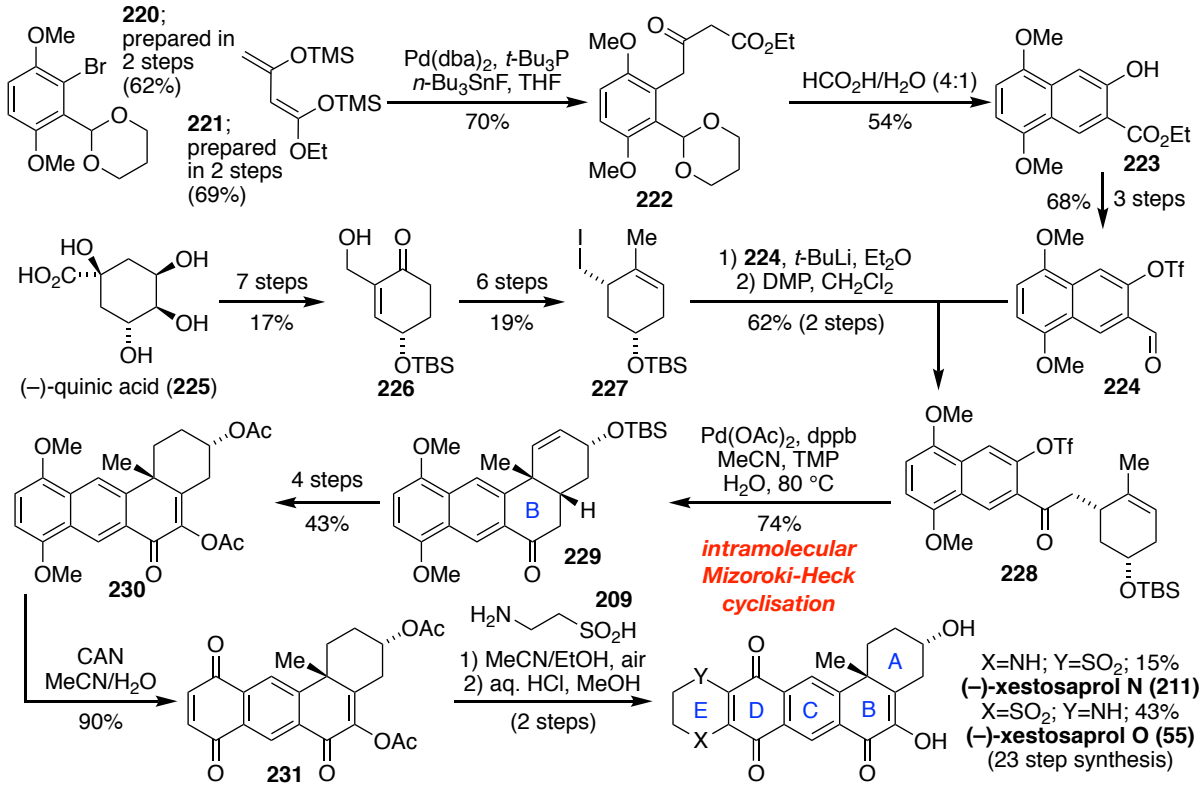

Scheme 3.25 Gao's 2018 chiral pool total synthesis of (–)-xestosaprol O and (–)-xestosaprol N

In a key step reminiscent of Keay's synthesis of (+)-xestoquinone, diastereoselective intramolecular Mizoroki-Heck cyclisation of **228** formed the B ring and installed the quaternary carbon stereocentre of the natural products to afford tetracycle **229**. Functionalisation of the A and B rings was then achieved in 4 steps to yield **230** before

oxidation to quinone **231**, using ceric ammonium nitrate as in Harada's inaugural synthesis of (+)-halenaquinone and installation of the taurine moiety (E ring) akin to the work of Schmitz and co-workers. Finally, deprotection delivered (–)-xestosaprol N and (–)-xestosaprol O in a longest linear sequence of 23 steps and a 0.086% to 0.25% overall yield.

3.4.3 (+)-Wortmannin, Shibasaki, 1996

Shibasaki and co-workers first synthesised (+)-wortmannin in 1996 *via* a semi-synthetic approach from hydrocortisone (**232**) (Scheme 3.26).[56]

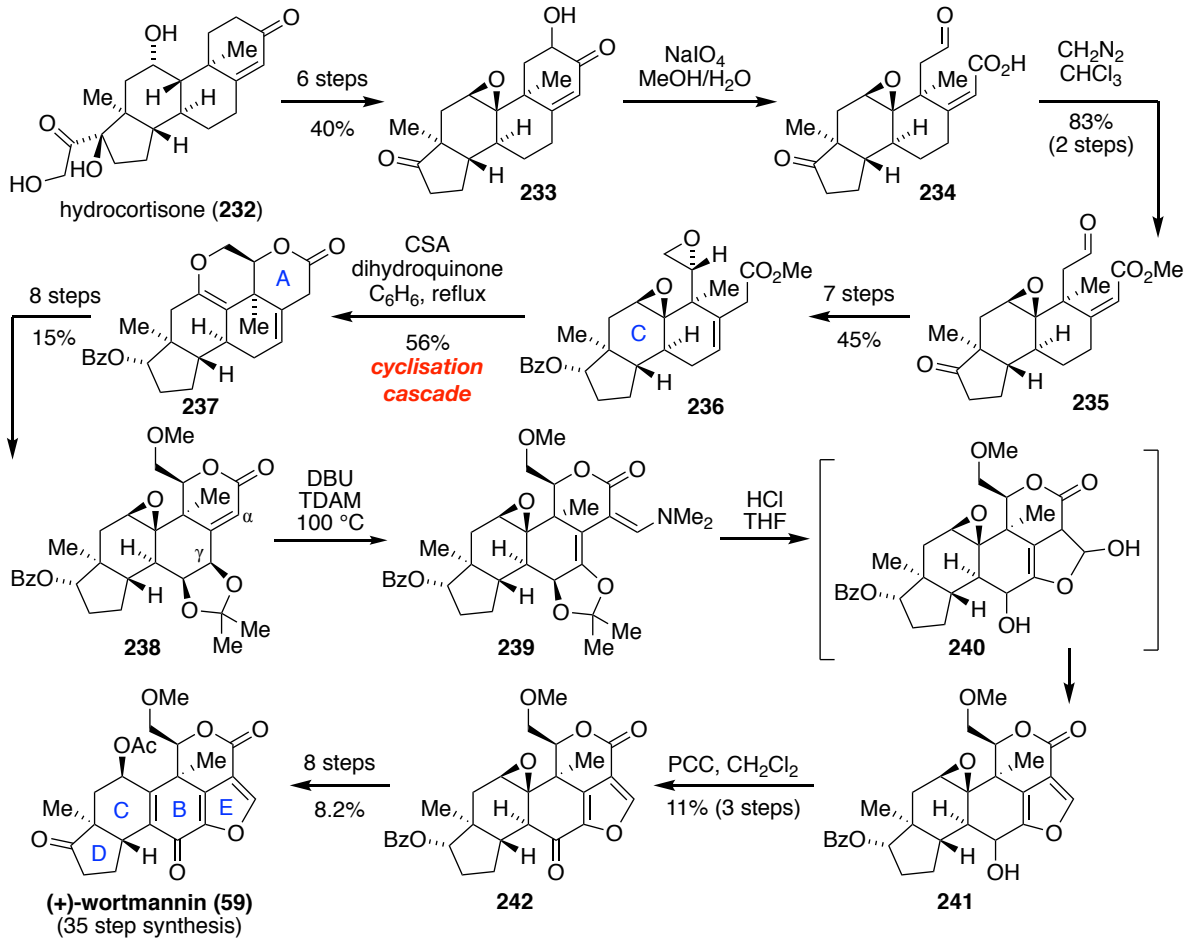

Scheme 3.26 Shibasaki's 1996 semi-synthesis of (+)-wortmannin from hydrocortisone

They were able to install the necessary A ring lactone functionality *via* ring opening of tetracycle **233** (accessed in 6 steps) and subsequent CSA catalysed cyclisation of tricycle **236** (accessed in a further 8 steps). Thus, oxidative cleavage of the α-hydroxyl ketone of **233**, *via* formation of a periodate ester and its subsequent decomposition by a cyclic mechanism, afforded carboxylic acid **234**. Esterification of acid **234** with diazomethane yielded methyl ester **235**. A further 7 steps then set up **236** for the key step of their synthesis, proposed to

involve hydrolysis of the methyl ester by H_2O, protonation of the C ring epoxide oxygen, subsequent cyclisation cascade to form the ether and lactone rings and finally dehydration of the resulting tertiary alcohol to deliver lactone **237**. A further 8 steps then afforded intermediate **238**. Installation of the furan ring was achieved in 2 steps, beginning with deprotonation of **238** *gamma* to the lactone carbonyl using DBU to form an extended enolate, which reacted with TDAM at the position alpha to the carbonyl to afford aminomethylene-lactone **239**. In a second step, hydrolysis of the resulting enamine to the aldehyde and of the acetal to the corresponding diol resulted in cyclisation to form the dihydrofuran lactol ring **240**, which, following dehydration, afforded furan **241**. Oxidation of the secondary alcohol yielded ketone **242**. Wortmannin was then accessed in a further 9 steps, to afford the natural product in a longest linear sequence of 35 steps and a 0.11% overall yield.

3.4.4 (±)-Wortmannin, Shibasaki, 2002

In 2002, Shibasaki and co-workers published the first total synthesis of (±)-wortmannin (Scheme 3.27).[57] Beginning from methyl vinyl ketone **244** and cyclopentadiene **243**, they constructed known bicycle **250** according to the work of Stork and Guthikonda, Nomine and co-workers, and Stone and co-workers.[33h, 58] Thus, Diels–Alder reaction of **244** and **243** gave a mixture of *endo* and *exo* isomers of cycloadduct **245**, which underwent deprotonation to the kinetic enolate and nucleophilic addition to dimethyl carbonate to afford β-keto-ester **246**. Retro-Diels–Alder reaction under vacuum pyrolysis then afforded alkenyl β-keto-ester **247**. Finally, Robinson annulation with 2-methylcyclopentane-1,3-dione (**248**) afforded bicycle **249**, which underwent enol-keto-tautomerisation and hydrogenation of the remaining alkene to yield bicycle **250**. This building block was functionalised to yield the key precursor **251** over a further 10 steps. Reminiscent of their approaches to xestoquinone and halenaquinone, stereoselective introduction of the allylic quaternary carbon stereocentre was achieved *via* Mizoroki-Heck cyclisation of **251** which also constructed the B ring of the natural product. As their second key step, Claisen rearrangement of *o*-allyl diosphenol **253** (accessed in a further 12 steps) afforded **254** to set the stage for formation of the A ring. Reduction of the α-diketone to the diol and protection then gave cyclic orthoester **255**, before a further 10 steps afforded lactone **256**. Finally, in the penultimate sequence, the furan ring was introduced *via* acid promoted hydrolysis of enamine **257** to the aldehyde, cyclisation to form the dihydrofuran lactol ring and dehydration to deliver **258**, as in their previous semi-synthesis. Deprotection and acetylation then delivered (±)-wortmannin, in a longest linear sequence of 45 steps and a 0.0025% overall yield.

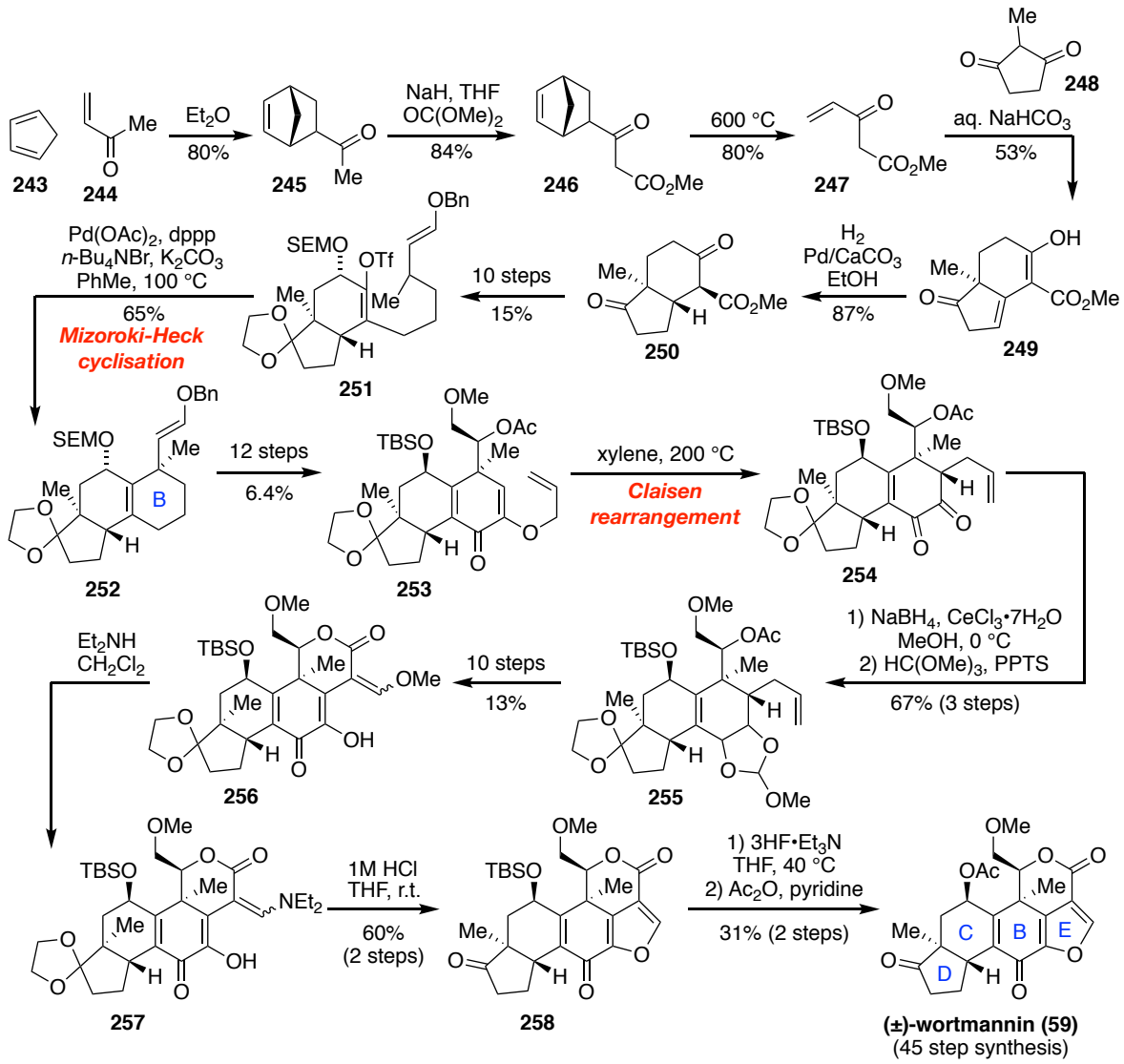

Scheme 3.27 Shibasaki's 2002 total synthesis of (±)-wortmannin

3.4.5 (+)-Wortmannin, Luo, 2017

Luo and co-workers published a notably shorter synthesis of (+)-wortmannin requiring only 20 steps in 2017, utilising a chiral pool approach (Scheme 3.28).[59]

Beginning from the Hajos-Parish ketone (**259**), known carboxylic acid **260** was prepared in 3 steps according to the work of Sorensen and co-workers.[60] As their first key step, installation of the furan moiety was achieved *via* a Pd-catalysed cascade reaction with alkyne **261**, proposed to proceed *via* formation of a Pd-allenyl complex, subsequent cyclisation to the dihydrofuran, nucleophilic addition of the enol derived from **260**, and lastly decarboxylation and dehydration to the furan ring. This reaction cascade afforded coupled product **263** in 42% yield, alongside decarboxylated starting material **262** (33%), which could be reconverted to

acid **260** in one step.[60] A further 6 steps afforded epoxide **264** which, as their second key step, underwent Friedel-Crafts alkylation to form the B ring of the natural product, yielding tetracycle **265**. This reaction was catalysed by a combination of HFIP/Ph_4PBF_4, which has been used previously to promote 'epoxide-initiated' cyclisations and is proposed to act as both a Brønsted acid and to provide stabilisation of cationic intermediates.[61] Subsequent selective TBS deprotection then afforded primary alcohol **266**. Selective oxidation of the primary alcohol of **266** in the presence of the secondary alcohol delivered the corresponding aldehyde, which was converted to carboxylic acid **267** *via* Pinnick oxidation. Formation of the A ring to complete the pentacyclic framework of the natural product was achieved by lactonisation of the carboxylic acid to deliver **269** using Mukaiyama's reagent (CMPI) **268;** a process wherein deprotonation of the carboxylic acid and subsequent nucleophilic substitution of the chloride of CMPI provides a good leaving group to promote lactonisation.

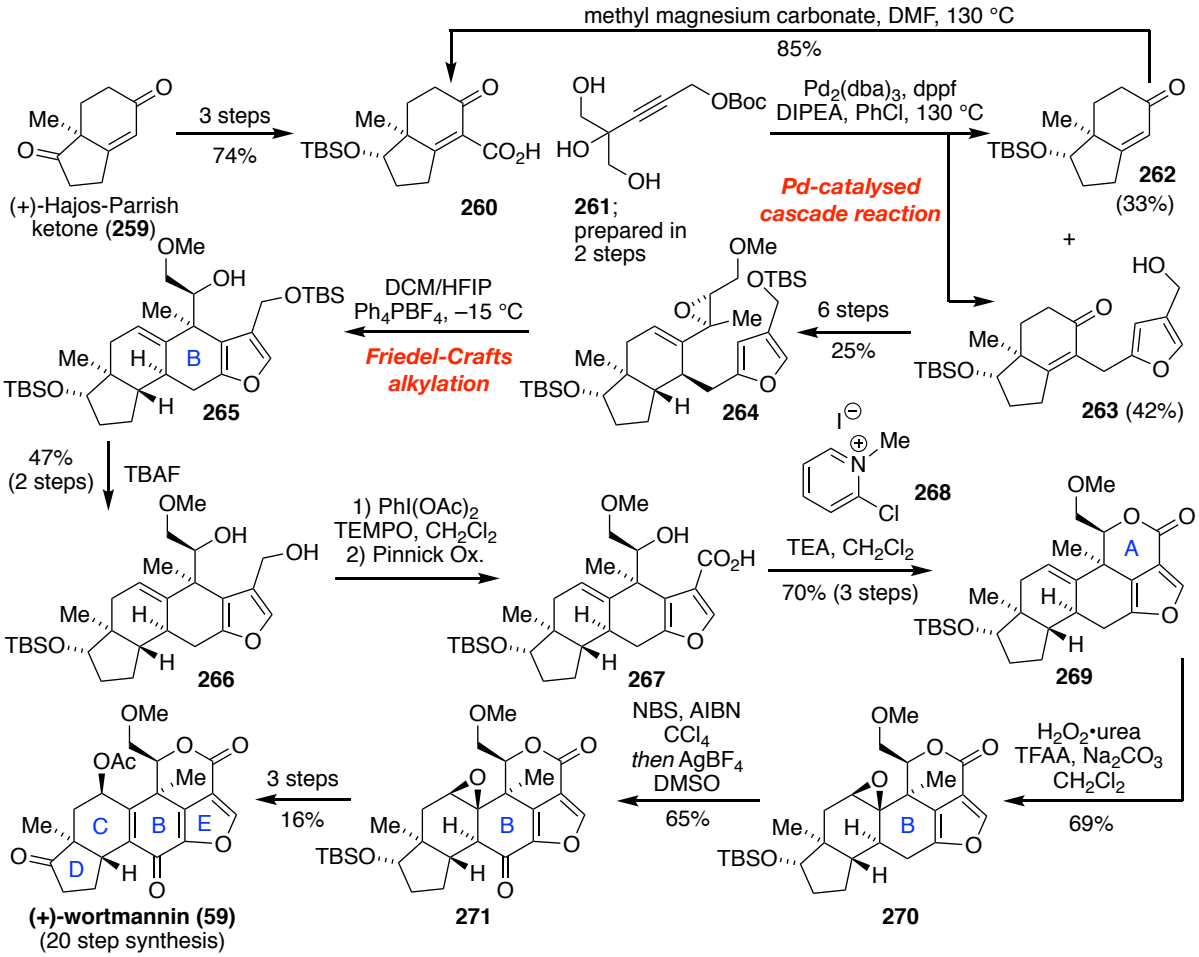

Scheme 3.28 Luo's 2017 chiral pool total synthesis of (+)-wortmannin

Following epoxidation of the alkene to afford hexacycle **270**, the B ring carbonyl group was introduced by radical bromination, and subsequent Kornblum oxidation (akin to Jacobi's 2014 model study;[62] see Section 3.4.12) to yield pentacycle **271**. Finally, a further 3 steps afforded (+)-wortmannin, in a longest linear sequence of 20 steps and a 0.18% overall yield.

3.4.6 (±)-Viridin, Sorensen, 2004

The first total synthesis of (±)-viridin was completed by Sorensen and co-workers in 2004 (Scheme 3.29).[63] Their synthesis began with the preparation of triyne **273** in 6 steps from pent-4-yn-1-ol (**272**) as an inconsequential mixture of four diastereomers. Subjection of this key intermediate to [$RhCl(PPh_3)_3$] achieved alkyne cyclotrimerisation, to afford benzocyclobutane **274**. Swern oxidation of the secondary alcohol then delivered benzocyclobutanone **275**. Following conversion of 2-trimethylsilyl-3-vinylfuran (**276**; prepared in 2 steps) to the corresponding organolithium species, nucleophilic addition to **275** occurred selectively from the less sterically hindered face, to form tetracycle **277**. Triethylsilyl protection of the newly formed tertiary alcohol then delivered tetracycle **278**.

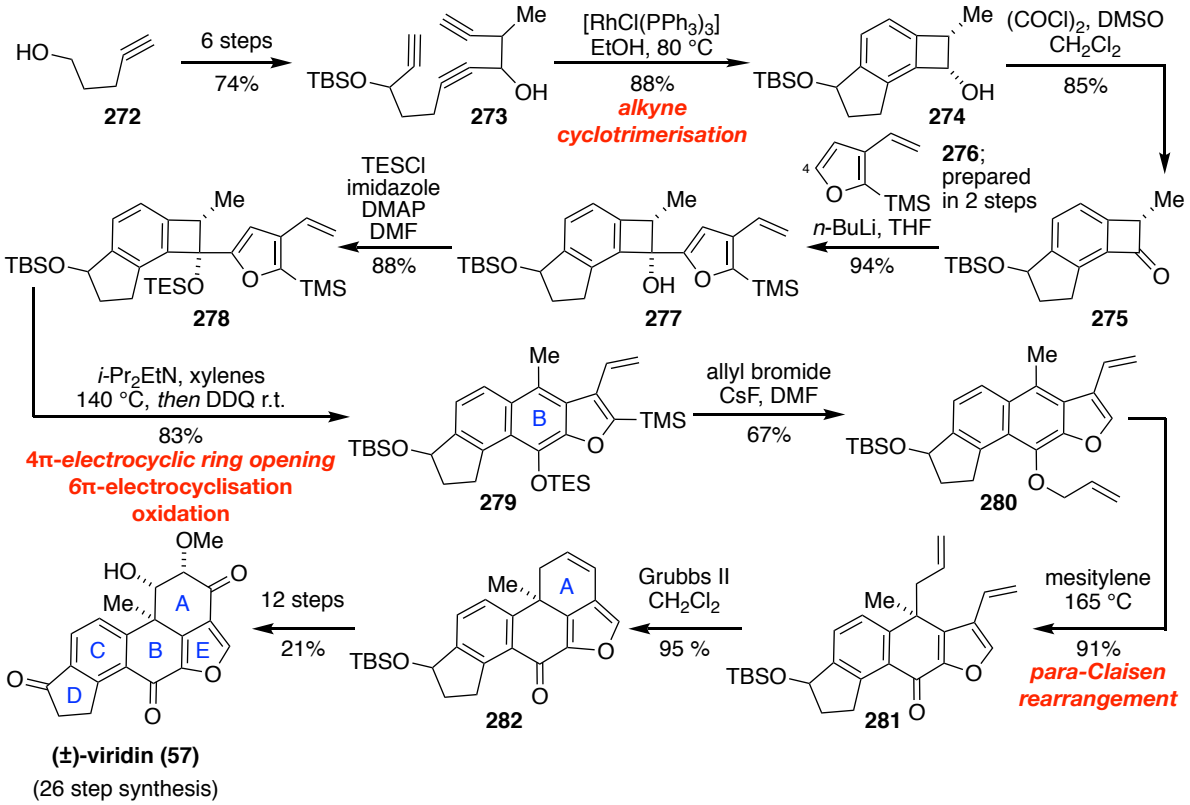

Scheme 3.29 Sorensen's 2004 total synthesis of (±)-viridin

As their second key step the B ring was introduced, *via* 4π electrocyclic ring opening of the benzocyclobutane to generate an *ortho*-quinone dimethide in *situ*, followed by 6π electrocyclisation and oxidation with DDQ, to afford naphthofuran **279**. The A ring was then installed *via* a 3-step sequence, beginning with selective removal of the TMS and TES groups and allylation of the newly formed phenol to generate allyl ether **280**. In their third key step, *para*-Claisen rearrangement generated the quaternary carbon stereocentre resulting in diene **281**, which was subjected to ring closing metathesis to yield pentacycle **282**. Finally, oxidative functionalization of the A ring was achieved in a further 12 steps, to yield (±)-viridin in a longest linear sequence of 26 steps and a 4.6% overall yield.

3.4.7 (–)-Viridin and (–)-Viridiol, Guerrero, 2017

In 2017, Guerrero and co-workers published the first enantioselective total syntheses of (–)-viridin and (–)-viridiol (Scheme 3.30).[64] They employed a convergent approach involving the coupling of two achiral fragments of similar complexity, to allow for the future synthesis of analogues with C and D ring modifications for medicinal testing.

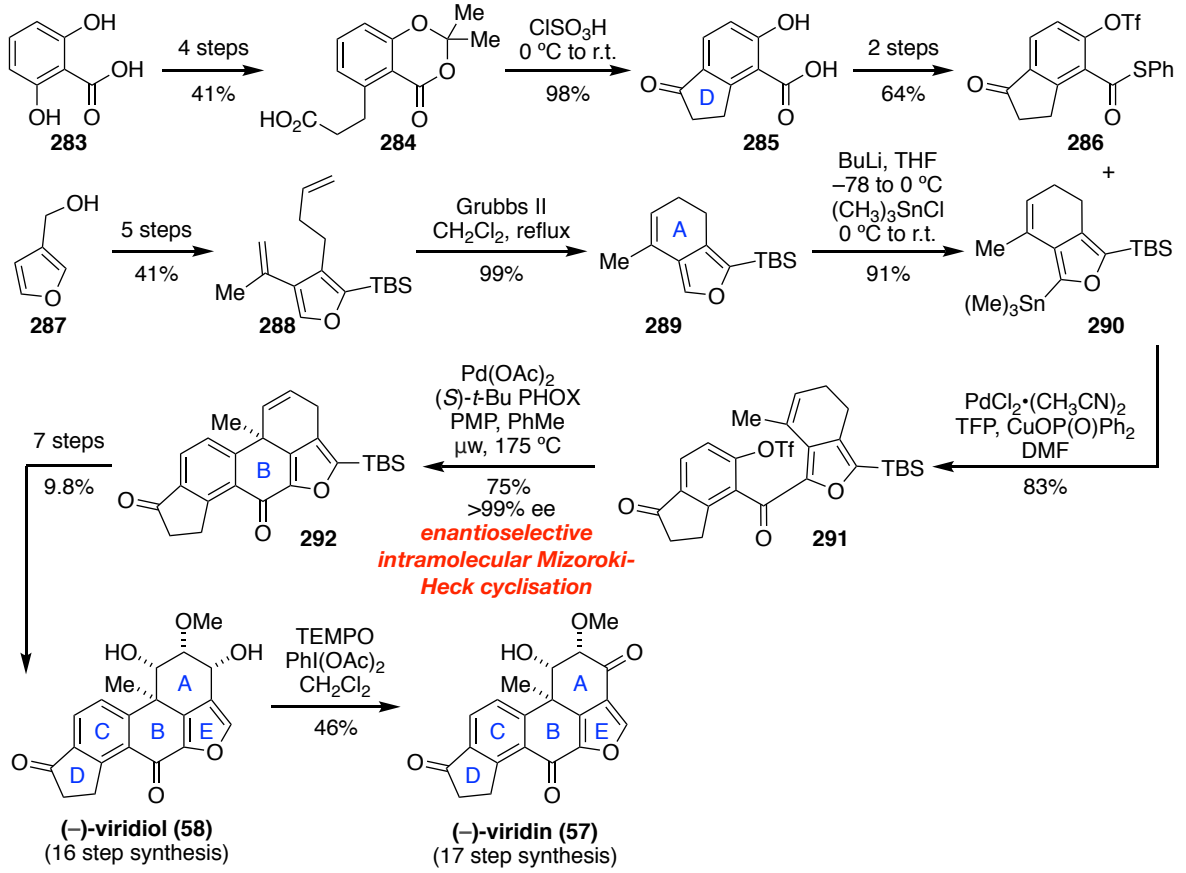

Scheme 3.30 Guerrero's 2017 enantioselective total synthesis of (–)-viridiol and (–)-viridin

Their synthesis began with a 7 step preparation of indanone **286**, involving the acid promoted cylisation of dihydrocinnamic acid **284** to form the D ring of the natural product. The second starting point for their convergent synthesis was furan **287**, previously employed in model studies by Keay and co-workers towards viridin.[65] This compound was converted to diene **288** in 5 steps, to undergo ring closing metathesis to form the A ring. Conversion to stannane **290**, enabled the two fragments **286** and **290** to be combined *via* Liebeskind stannane-thioester coupling to generate tetracycle **291**. As their key step, an enantioselective intramolecular Mizoroki-Heck cyclisation, reminiscent of that used by Keay and Shibasaki, was used to form the B ring and introduce the quaternary carbon stereocentre, forming pentacycle **292** in high ee (>99%). A series of site-and diastereo-selective oxidations were then used to access the natural product, (–)-viridiol, as well as (–)-epi-viridiol. Both these compounds could in turn be converted to (–)-viridin by chemoselective oxidation with TEMPO and palladium acetate. Overall, Guerrero and co-workers accessed the natural products in a longest linear sequence of 16 to 17 steps and a 1.6% to 0.72% overall yield.

3.4.8 (–)-Viridin and (–)-Viridiol, Gao, 2019

More recently, in 2019, Gao and co-workers applied a convergent chiral pool approach to the total synthesis of (–)-viridin and (–)-viridiol (Scheme 3.31).[66]

Recognising the challenges posed by late stage stereoselective functionalisation of the D ring, Gao and co-workers elected to instead introduce the chiral *cis*-diol moiety at the beginning of the synthesis. Thus known derivative **294** was generated in 3 steps from the readily available chiral building block *L*-ribose (**293**) according to the work of Pal and co-workers.[67] A further 4 steps, including [3+2] cycloaddition, then delivered cyclohexane **295**. Subsequent conversion of ester **295** to the corresponding Weinreb amide enabled nucleophilic substitution by the organolithium species derived from dihydroindenol **296**, to produce tricyclic ketone **297**. As their first key step, **297** underwent Co-catalysed metal-hydride H atom transfer (MHAT) radical cyclisation to form the B ring and quaternary carbon stereocentre of the natural products, generating tetracycle **299**. *In situ* selective removal of the triethylsilyl group then afforded secondary alcohol **300**, which was oxidised to yield ketone **301**. Installation of an exocyclic alkene to the A ring was achieved by aldol condensation with formaldehyde, before bis TBS deprotection furnished pentacycle **302**. In a novel approach, the requisite furan ring was introduced by epoxidation of the exocyclic alkene to generate **303** and oxidative cyclisation to afford lactol **304**; the latter process involving oxidation of the secondary alcohol

to afford the β-diketone, tautomerisation to the enol, nucleophilic ring opening of the epoxide by the enol and lastly dehydration. Following removal of the acetal protecting group to afford *cis*-diol **305**, conversion to the furan ring was achieved concurrently with selective etherification of the α-hydroxyl group to the ketone to afford (–)-viridin. Subsequent reduction with sodium borohydride delivered (–)-viridiol, thus providing access to both natural products in a longest linear sequence of 17-18 steps and a 1.5% to 1.0% overall yield.

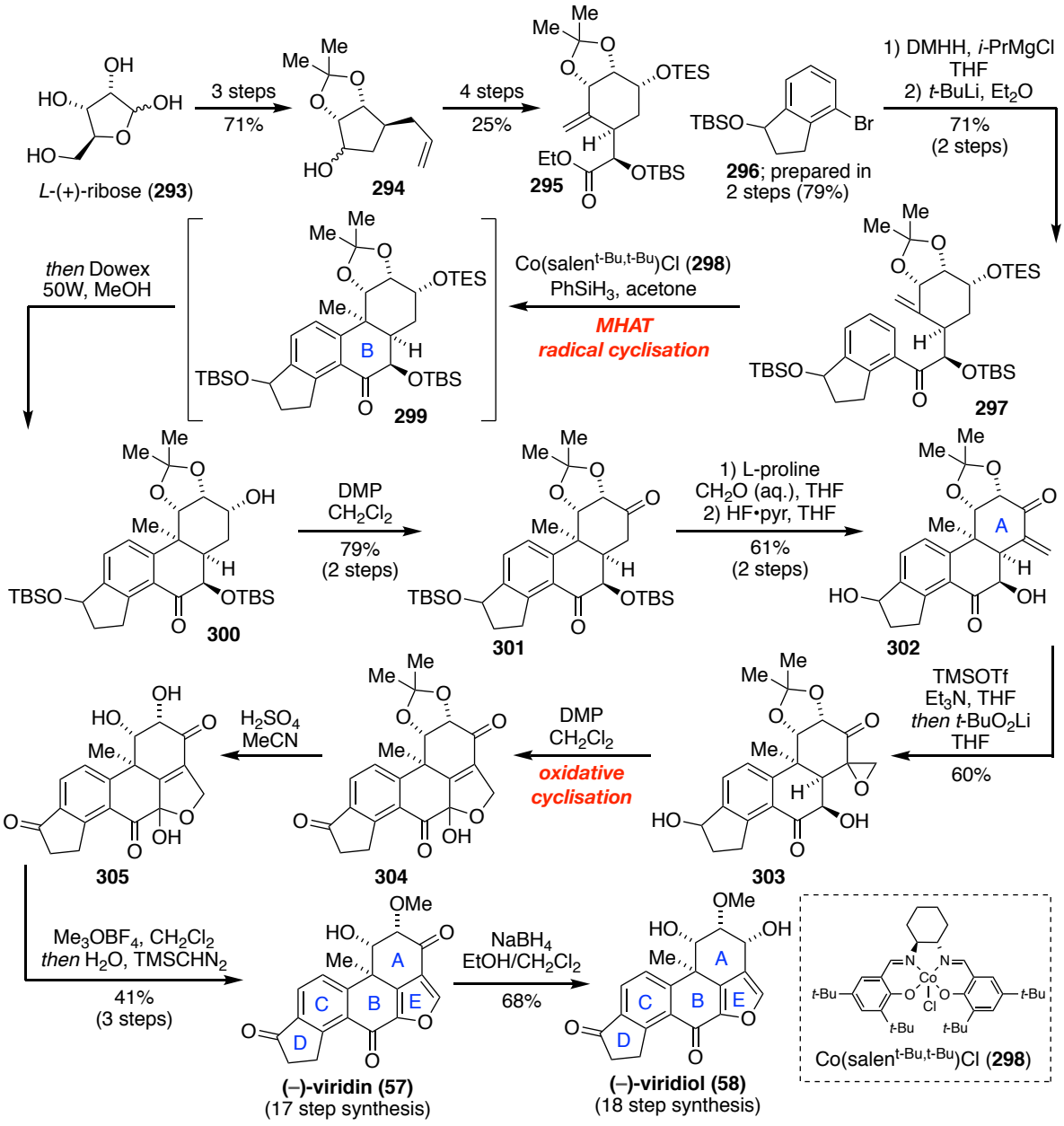

Scheme 3.31 Gao's 2019 chiral pool total synthesis of (–)-viridin and (–)-viridiol

3.4.9 (+)-Nodulisporiviridin E, Gao, 2020

Less than a year later Gao and co-workers completed the first synthesis of (+)-nodulisporoviridin E (Scheme 3.32).[68] They employed the same strategic approach as in their syntheses of (–)-xestosaprol N, (–)-xestosaprol O, (–)-viridin and (–)-viridiol; namely synthesis of the A ring from a chiral pool starting material, convergent preparation of the C-D ring moiety, and following linkage of these two fragments, cyclisation to form the B ring.

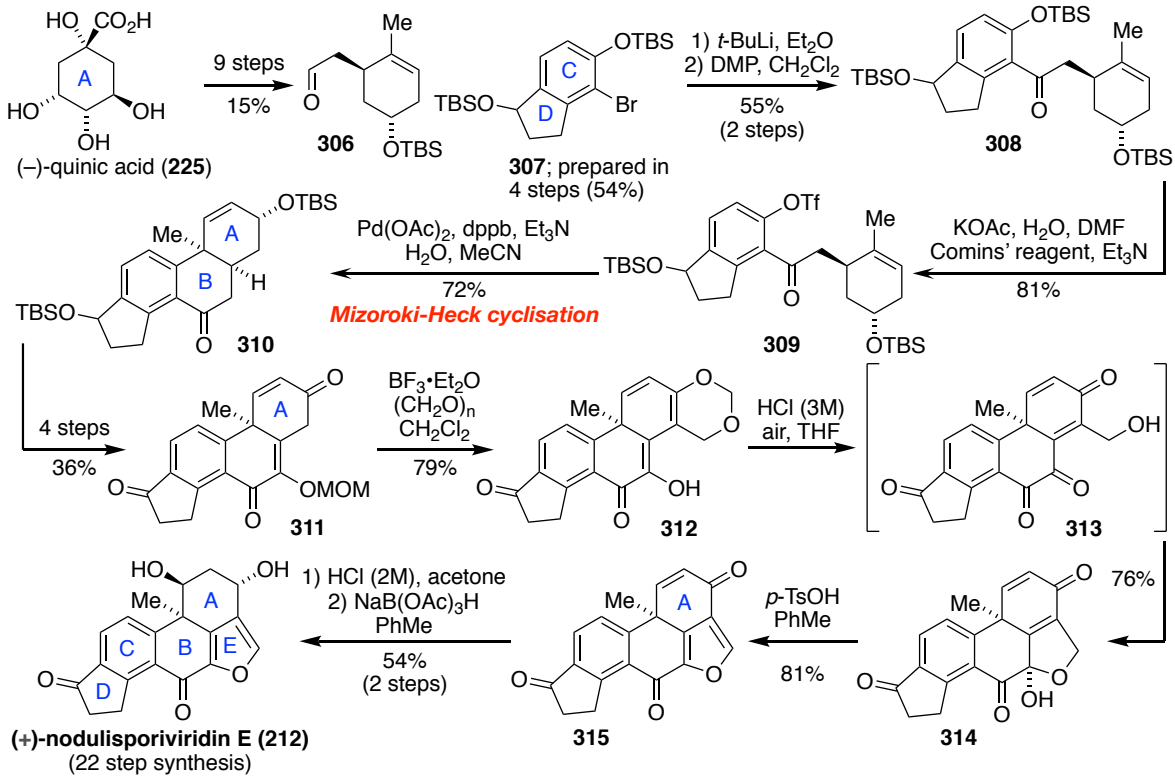

Scheme 3.32 Gao's 2020 chiral pool total synthesis of (+)-nodulisporoviridin E

Thus beginning from (–)-quinic acid (**225**),[53, 69] as in their synthesis of xestosaprols N and O, aldehyde **306** was prepared in 9 steps. Reminiscent of their synthesis of viridin and viridiol, lithium halogen exchange of dihydroindenol **307**, nucleophilic addition of the resulting organolithium species to aldehyde **306** and subsequent oxidation of the resulting secondary alcohol delivered tricyclic ketone **308**, which was converted to triflate **309**. As their key step, the B ring was forged *via* intramolecular Mizoroki-Heck cyclisation of **309** to complete the core tetracyclic framework of the molecule, again akin to their synthesis of xestosaprols N and O. Oxidation of the A and B rings of tetracycle **310** was then achieved across 4 steps to afford triketone **311**. As in their synthesis of viridin, installation of the furan ring employed formaldehyde as the source of the additional carbon atom required. Thus, enolisation of the A

ring carbonyl and aldol reaction with formaldehyde formed the α-hydroxy ketone, which underwent reaction with a second molecule of formaldehyde to form the acetal and finally dehydration to afford dioxane **312**. Sequential treatment with acids then induced hydrolysis of the acetal to the diol, rearrangement to tetraketone **313**, cyclisation to form lactol **314** and dehydration to furan **315**. Finally, oxa-Michael addition to the A ring enone and chemo- and diastereo-selective reduction of the A ring carbonyl completed their total synthesis of (+)-nodulisporoviridin E, in a longest linear sequence of 22 steps and a 0.56% overall yield.

3.4.10 Model Study, Viridin, Jacobi, 2006/2012

Combining their initial efforts in 2006 with a more comprehensive sequence disclosed in 2012, Jacobi and co-workers published a synthesis of the ABCDE core pentacyclic framework of viridin (Scheme 3.33).[70]

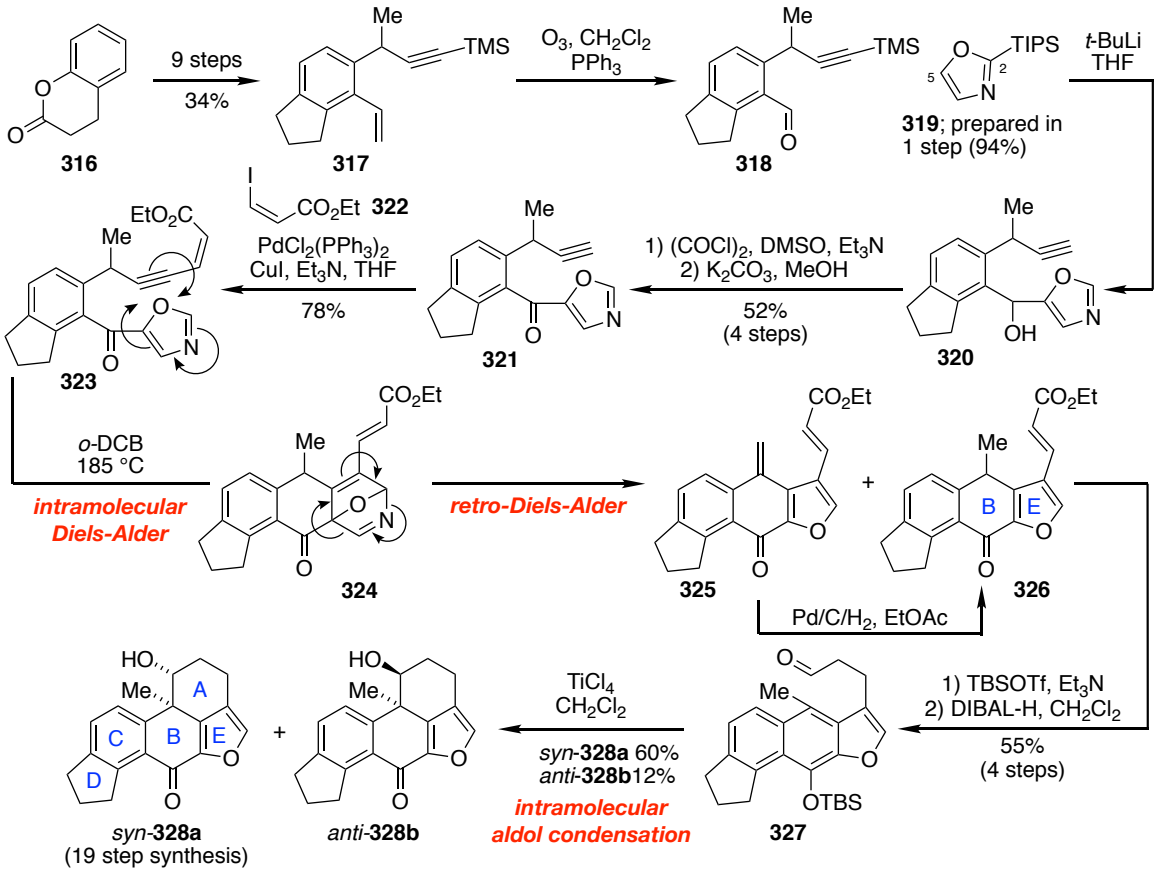

Scheme 3.33 Jacobi's 2012 synthesis of the ABCDE (±)-viridin core

Their synthesis began with the preparation of styrene **317** from dihydrocumarin **316** in 9 steps. Chemoselective ozonolysis of alkene **317** then afforded the corresponding aldehyde, **318**. Known TIPS protected oxazole **319**[71] was selectively lithiated at the C5 position and the

resulting organolithium species underwent nucleophilic addition to aldehyde **318** to deliver secondary alcohol **320**. The secondary alcohol was then oxidised back to the ketone under Swern conditions, and the silyl protecting groups removed, to deliver terminal alkyne oxazole **321**. Ensuing Sonogashira cross coupling afforded enyne **323**. As their key step, this compound underwent an intramolecular Diels–Alder-retro-Diels–Alder reaction sequence to install the B ring and furan ring (E) of viridin, delivering tetracycle **326**, as well as the quinone methide oxidation product **325**. Quinone methide **325** could be converted to desired product **326** *via* hydrogenation of the terminal alkene. Subsequent silylation and DIBAL reduction then afforded aldehyde **327**. Finally, formation of the A ring was achieved *via* an intramolecular phenol-dienone-aldol condensation to afford *syn* isomer **328a** as the major product, thereby constructing the core ABCDE framework in a longest linear sequence of 19 steps and a 4.6 % overall yield.

3.4.11 Model Study, Viridin, Jacobi, 2012

In 2012, Jacobi and co-workers published a new approach to the core skeleton of viridin,[72] differing in their use of a CB ring starting material (Scheme 3.34). Aryloxylketone **330**, prepared in 4 steps, underwent acid promoted cyclodehydration to form benzofuran **331**; a process involving an intramolecular Friedel-Crafts type reaction, with addition to the ketone, followed by subsequent dehydration to efficiently install the furan ring. A further 3 steps afforded aldehyde **332**, permitting construction of the A ring *via* an intramolecular aldol condensation, as in previous model studies.[70a] Following extensive optimisation, this cyclisation proceeded to afford the desired *syn* isomer **333a** as the major product, delivering 4 of the 5 rings of viridin in a longest linear sequence of 9 steps and a 18% overall yield.

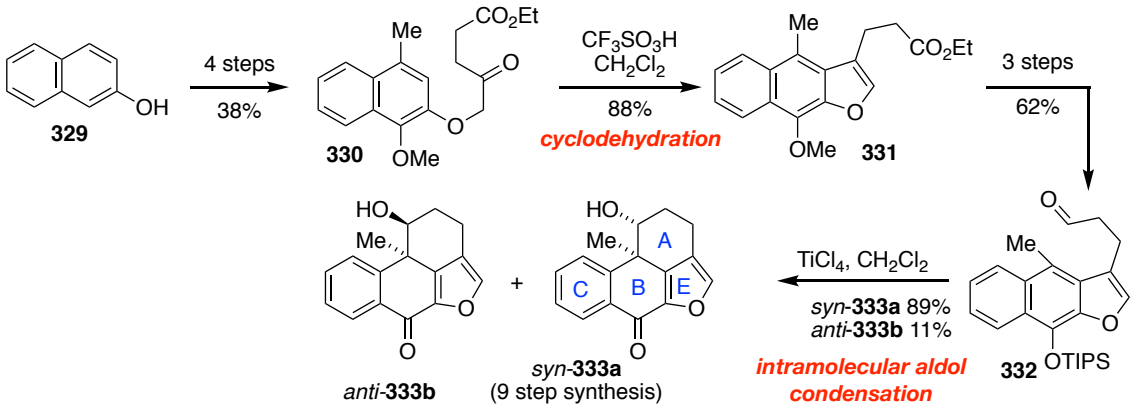

Scheme 3.34 Jacobi's 2012 synthesis of the ABCE (±)-viridin core

3.4.12 Model Study, Viridin, Jacobi, 2014

In 2014, Jacobi and co-workers reported synthetic studies on elaboration of the requisite A ring functionality of viridin (Scheme 3.35).[62] Utilising the truncated ABCE viridin core skeleton **333a**, synthesised in their previous model studies,[70a] they achieved late stage introduction of the A ring carbonyl group. Furan **333a** underwent radical bromination with *N*-bromosuccinimide and AIBN to yield bromide **334**. Subsequent Kornblum oxidation then delivered carbonyl containing **335**. Notably, this is the only benzylic-type oxidation reported to install the A ring ketone functionality adjacent to the furan ring.

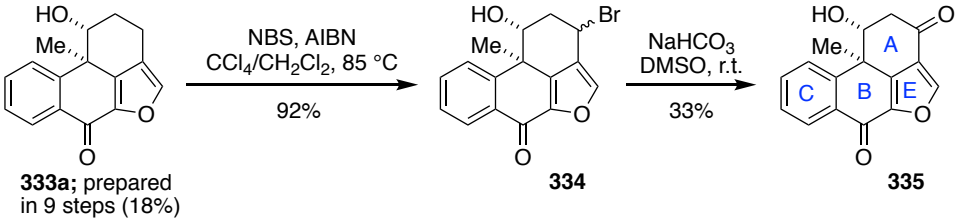

Scheme 3.35 Jacobi's 2014 late-stage installation of the A ring carbonyl functionality on a (±)-viridin ABCE skeleton

3.4.13 Summary

In this section, 9 syntheses of structurally similar products to (+)-xestoquinone and (+)-halenaquinone are summarised, targeting xestosaprols N and O, wortmannin, viridin, vidiriol and nodulisporoviridin E, and ranging in step count (longest linear sequence) from 5 to 45 steps (Figure 3.7).

Several notable distinctions due to differences in the compounds' structures may be observed. Syntheses of viridin and wortmannin are in general longer, due to the highly oxidised intricate A ring which complicates construction, while the synthesis of deoxyxestasaprols N and O, lacking the challenging fused furan ring, is significantly shorter.

Strategically, chiral pool building blocks are employed by Gao and co-workers, by Luo and co-workers and in Shibasaki's semi-synthesis from hydrocortisone. Unfortunately, with the exception of Luo and co-workers' study, lengthy manipulation of the chiral building blocks is required, however, to make the desired chiral 'starting materials'. These stand alongside Harada's syntheses of (+)-xestoquinone and (+)-halenaquinone as the only chiral pool approaches employed.

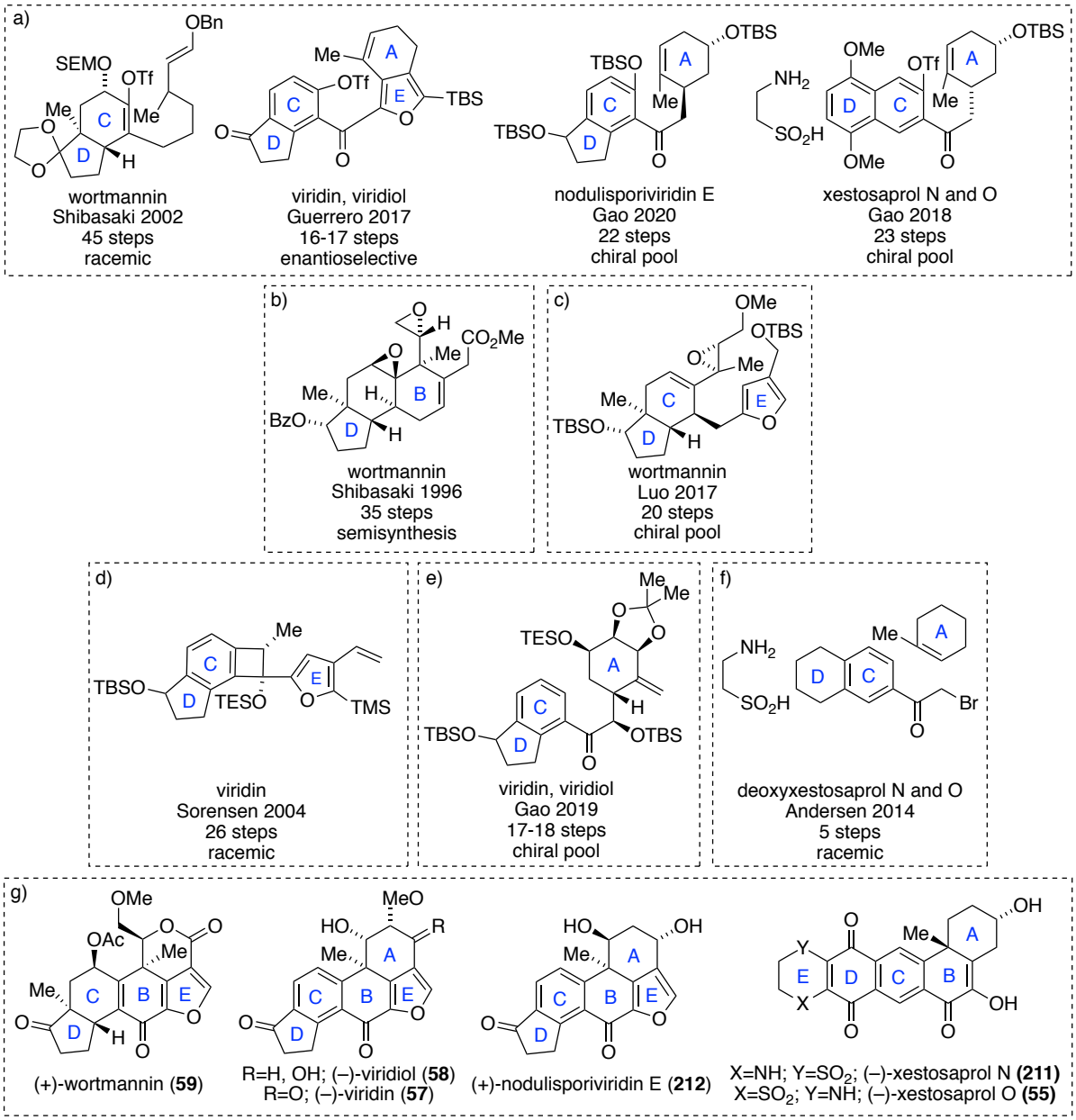

Figure 3.7 Summary of key strategic steps and intermediates in the syntheses of structurally related natural products to (+)-xestoquinone and (+)-halenaquinone. Syntheses are grouped according to key step: a) Mizoroki-Heck cyclisation (B ring); b) cyclisation cascade (A ring); c) Friedel-Crafts alkylation (B ring); d) 4π electrocyclic ring opening- 6π electrocyclisation (B ring); e) MHAT radical cyclisation (B ring); f) Ag catalysed photochemical annulation (B ring). Structures of target natural products are shown in g).

As in the synthesis of xestoquinone and halenaquinone, the use of an intramolecular Mizoroki-Heck reaction has proved popular to construct the B ring of the natural products, present in the work of Shibasaki, Guerrero and Gao (Figure 3.7 a). With the exception of Shibasaki's semi-synthesis, the formation of the B ring is penultimate in assembly of the core pentacyclic

framework in the other syntheses to enable a convergent route to the skeleton of the molecule, although very different tactics were used; namely, a Friedel-Crafts cyclisation by Luo, a 4π electrocyclic ring opening- 6π electrocyclisation by Sorensen, Andersen's silver (I) catalysed photochemical annulation and MHAT radical cyclisation by Gao. Key precursors to these steps are summarised in the second and third rows of Figure 3.7 (b, d-f). Notably, these are different tactics to those used in the synthesis of xestoquinone and halenaquinone, and, although other pericyclic reactions are present, the Diels–Alder reaction does not feature. Only Jacobi's 2006/2012 model study towards viridin employed an intramolecular Diel–Alder-retro-Diels–Alder sequence to form the B ring and furan ring of the target structure.

Only Guerrero's synthesis of (–)-viridiol and (–)-viridin is enantioselective, which employs the aforementioned catalytic enantioselective Mizoroki-Heck cyclisation to introduce the quaternary carbon stereocentre, as in syntheses of xestoquinone and halenaquinone.

A variety of different tactics are used across the 7 relevant syntheses to incorporate the furan ring, including distinct approaches by Shibasaki, Luo and Gao. Of note, model studies by Jacobi also contribute two innovative ways to introduce this functionality.

Significantly, Jacobi's final model study introduces a ketone adjacent to the furan ring of a (±)-viridin ABCE core skeleton; a tactic which was also later utilised to functionalise the B ring in Luo's synthesis of (+)-wortmannin. This selective oxidation has possible future applications to the conversion of (+)-xestoquinone to (+)-halenaquinone.

3.5 Conclusions and Outlook

The syntheses of xestoquinone and halenaquinone, as well as structurally similar compounds, wortmannin, viridin, viridiol, nodulisporoviridin E and xestosaprols N and O, like the molecules' bioactivities, are rich and varied. Many of these significant accomplishments have displayed careful design to deploy reactions in an innovative and discerning manner in the pursuit of efficiency. Equally, many of these outstanding synthetic contributions have also involved the development or showcase of new synthetic methodologies, further highlighting these structures as an ideal instrument for the advancement of organic synthesis.

In this way, our own synthesis of (+)-xestoquinone fittingly joins them, to demonstrate the pioneering use of the parent [3]dendralene in total synthesis. The successful strategy deploys a DTDA reaction sequence to rapidly assemble the tetracyclic carbon framework of the molecule, permitting the shortest total synthesis of (+)-xestoquinone to date.

Certainly, as the vast amass of work described here shows, this class of molecules will continue to both inspire the development of new methodology and prove as a means for its rigorous validation. Indeed, in addition to our own work on (+)-xestoquinone, recent publications from Gao, Carter, Guerrero and Luo describing syntheses of halenaquinone, viridin, viridiol, wortmannin, nodulisporoviridin E and xestosaprols N and O, reflect the continued interest that there is in this important field.

4

Rapid Synthesis of Enantiopure Polycycles

4.1 Introduction

4.1.1 Chiral Pool Building Blocks in Synthesis

Chiral pool building blocks are secondary metabolites, which occur in high natural abundance and in enantio-enriched form. Owing to their ready availability and low cost (e.g. Figure 4.1), they present an excellent starting material in organic synthesis. The efficient incorporation of chiral pool starting materials allows effective introduction of stereocentres with defined absolute configurations (as well as other functionality), which otherwise may be difficult to obtain.

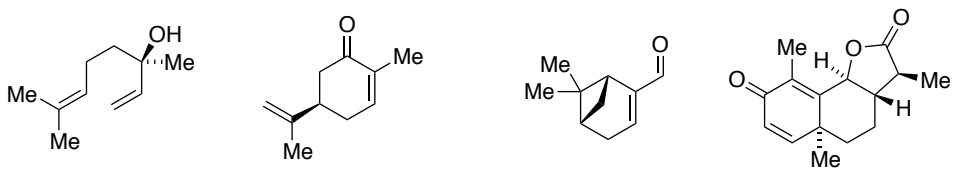

(*R*)-(–)-linalool (**336**) $0.18/gram

(*R*)-(–)-carvone (**337a**) $0.65/gram

(*R*)-(–)-myrtenal (**338**) $0.82/gram

(–)-α-santonin (**339**) $9.34/gram

Figure 4.1 Selected examples of commercially available chiral building blocks. (Prices in AUD from Sigma Aldrich as at 18/07/2020)

Despite significant advances in the field of enantioselective synthesis,[73] chiral building blocks remain a privileged and fundamentally important synthetic resource. Recent applications of chiral pool starting materials to enantiospecific step economic total syntheses include Reisman's synthesis of (+)-pleuromutilin from (+)-*trans*-dihydrocarvone[74] and Sarpong's synthesis of (–)-xishacorene B from (*R*)-carvone (Figure 4.2).[75]

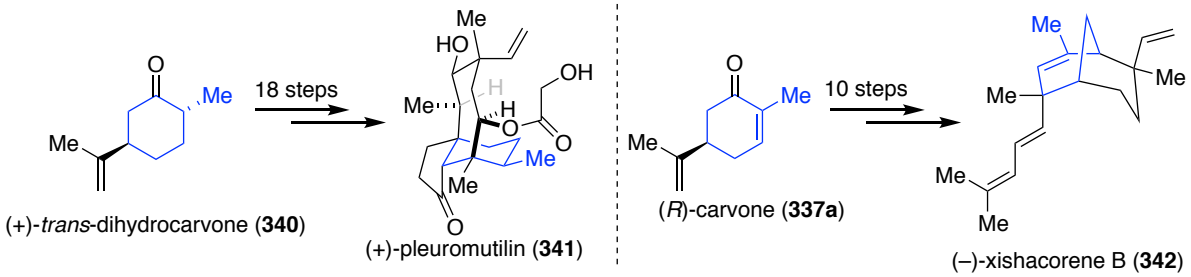

Figure 4.2 Recent step economic, chiral pool approaches to natural product total synthesis.[74-75] Atoms incorporated into the natural product from chiral pool starting materials are highlighted in blue.

Central to the success of these syntheses is the method by which the chiral building block is integrated into the skeleton of the molecule. The deployment of chiral building blocks in Diels–Alder reactions was of particular interest to us. This approach not only incorporates the chiral starting material, but in the same process also forms two new C–C σ-bonds, one new ring, and up to four new stereocentres (Scheme 4.1).

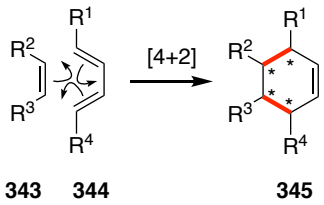

Scheme 4.1 Generalised Diels–Alder reaction showing the potential generation of two new carbon-carbon bonds and up to four new stereocentres (*)

We envisaged that this tactic may be extended to the DTDA reaction sequence as a powerful synthetic technique to rapidly construct enantiopure polycyclic frameworks.

4.1.2 Application of DTDA Reaction Sequences to Chiral Polycyclic Frameworks

Enantioenriched polycyclic frameworks can be generated from the DTDA reaction sequence *via* three methods; either through enantioselective Diels–Alder reaction of achiral precursors, via Diels–Alder-based kinetic resolution of racemic precursors, or by diastereoselective Diels–Alder reaction of enantioenriched precursors.

Despite the power of the DTDA reaction sequence, there exist in the literature only four separate reports of enantioselective Diels–Alder reactions or DTDA reaction sequences of dendralenes. The first comes from Fallis and co-workers, who employed trimethylaluminium and (*S*)-BINOL to provide a temporary tether to control the Diels–Alder reaction of substituted [3]dendralene **346** with methyl acrylate (**36**) (Scheme 4.2a).[76] Later, enantioselective cycloaddition of [3]dendralene (**25**) with the same dienophile was achieved within the Sherburn group in high yield and good e.r., using a modified Corey oxazaborolidinium catalyst (Scheme 4.2b).[13]

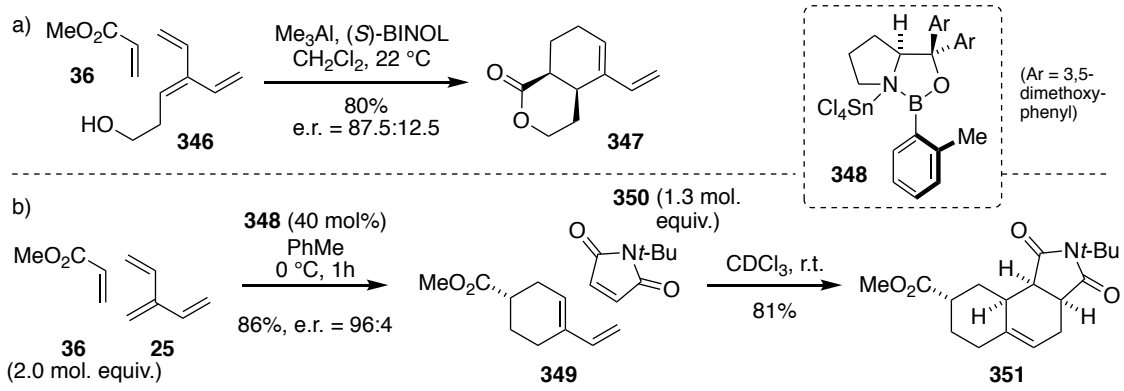

Scheme 4.2 Enantioselective Lewis acid catalysed Diels–Alder reactions of [3]dendralene[13, 76]

The other two reports of enantioselective Diels–Alder reactions of dendralenes come from organocatalysed reactions performed within the Sherburn group (Scheme 4.3). Diels–Alder reaction of [3]dendralene with β-substituted acrolein dienophiles, promoted by MacMillan's imidazolidinone catalyst, afforded, after *in situ* reduction of the formyl group, enantioenriched mono-cycloadducts **354**.[77] This method also proved successful for reaction of a range of substituted [3]dendralenes in DTDA reaction sequences.[78]

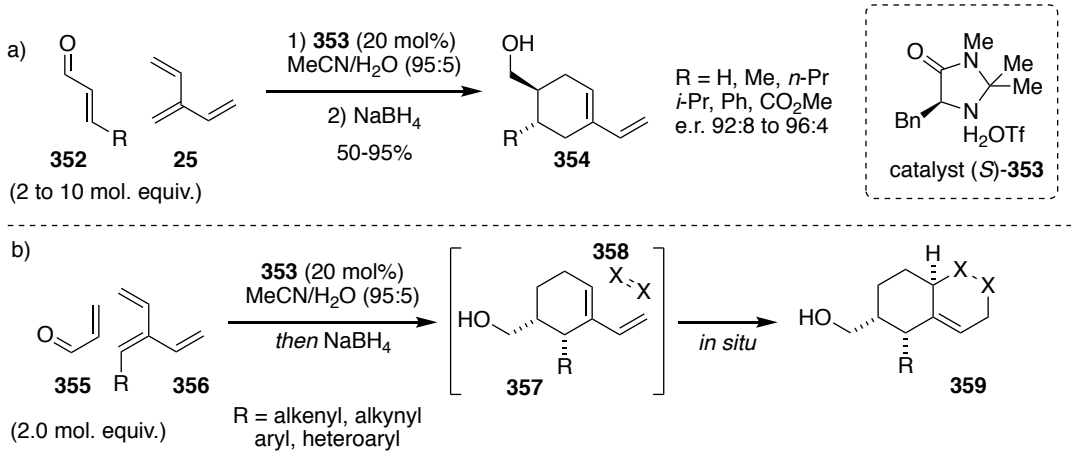

Scheme 4.3 Enantioselective organocatalysed Diels–Alder reactions of [3]dendralene[77-78]

Perhaps due to its inherent inefficiency,[i] to the best of our knowledge there exist in the literature no examples of kinetic resolution effected by DTDA reaction sequences of dendralenes for the synthesis of enantioenriched polycyclic frameworks from racemic precursors. Other chiral polycyclic frameworks forged through DTDA reaction sequences stem from diastereoselective processes employing enantioenriched precursors. Again, these are limited to a small selection of examples. In 1999, Fallis and co-workers employed a chiral precursor in a diene–transmissive IMDA–DA sequence to construct pentacycle **362**, utilising stereochemistry borne by the diene-dienophile tether (Scheme 4.4).[79]

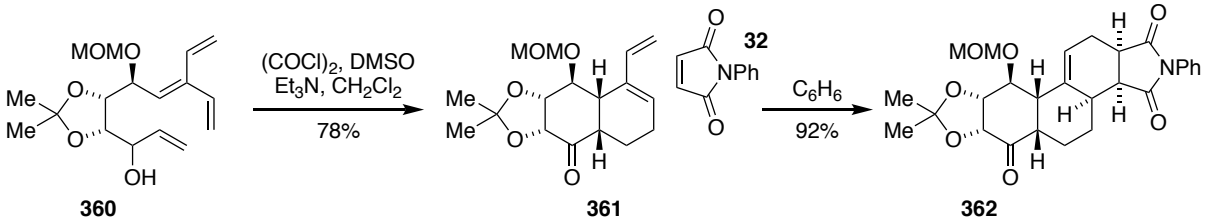

Scheme 4.4 A diastereoselective DTDA reaction sequence employing stereochemistry borne by the diene-dienophile tether[79]

The use of dendralenes themselves bearing stereocentres with defined absolute configurations has also been explored. Within the Sherburn group, chiral substituted [3]dendralene **364** permitted the formation of 12 new stereocenters and 6 new rings in a series of three Diels–Alder reactions to construct a novel, enantiomerically pure, multicyclic system (Scheme

[i] The maximum theoretical yield from kinetic resolution of a racemic precursor is 50%. While enantioconvergent synthetic pathways have the potential to convert racemic starting material into an enantioenriched product with a maximum theoretical yield of 100%, two distinct synthetic sequences are required.

4.5a).[80] Moreover, the deployment of a chiral "allenic dendralene" or 1,1-divinylallene in a sequence of three Diels–Alder reactions was used to achieve the shortest enantioselective total synthesis of a pseudopterosin aglycone, demonstrating the power of this synthetic sequence (Scheme 4.5b).[81]

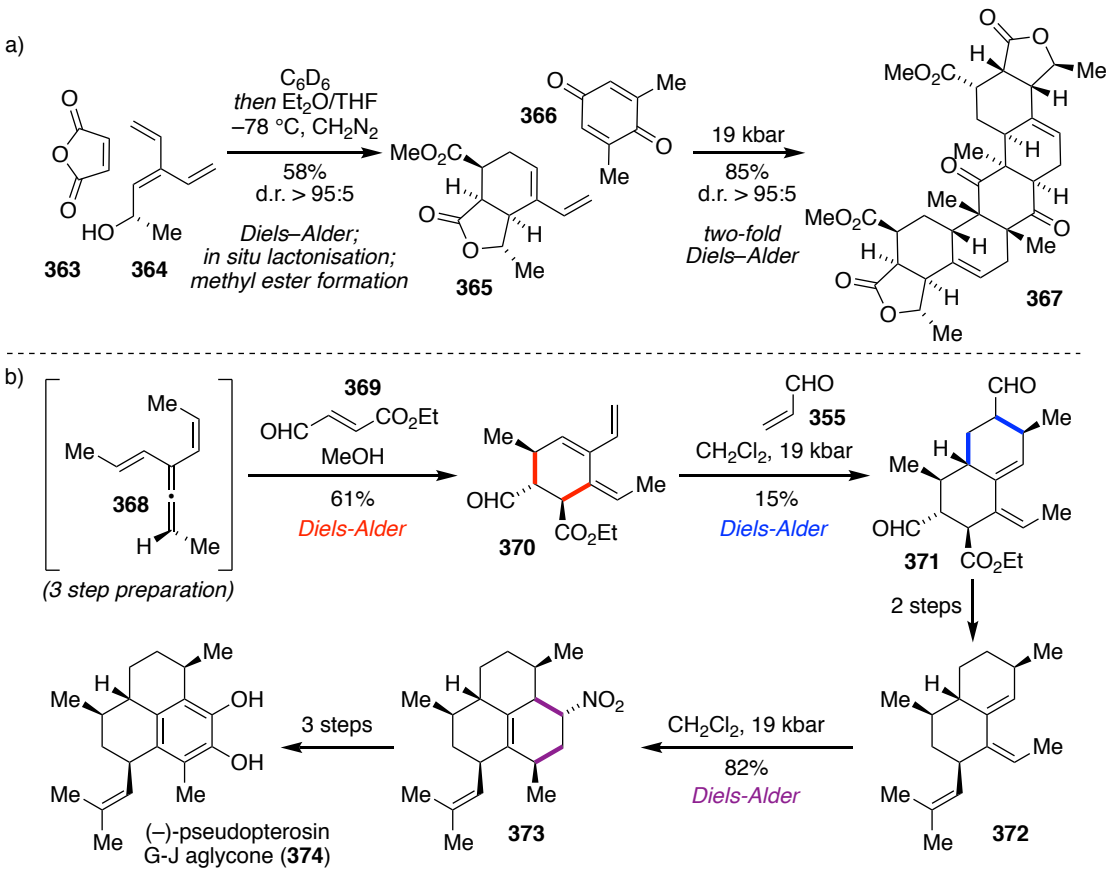

Scheme 4.5 a) DTDA reaction sequence with a mono-substituted chiral dendralene;[80] b) Total synthesis of a pseudopterosin aglycone from a chiral allenic dendralene[81]

In contrast, there is a lack of knowledge regarding the deployment of chiral dienophiles in cycloaddition sequences with [3]dendralenes, despite the obvious advantages they present; namely, the ready availability of many enantiomerically pure chiral building blocks with potential to be used as dienophiles (in contrast to chiral dendralenes which require preparation) and the potential ease with which different dienophiles could be incorporated into the skeleton of a molecule in a convergent, 'mix and match' manner.

To the best of our knowledge, the only example of a chiral dienophile employed in a DTDA reaction sequence comes from our synthesis of (+)-xestoquinone (Scheme 4.6; see also Chapter 2). Cycloaddition between [3]dendralene and *p*-benzoquinone, followed by deprotonation and etherification forms an achiral monoadduct, which then undergoes a second cycloaddition

reaction with enantio-enriched dienophile **161** to introduce the quaternary stereocentre of the natural product.

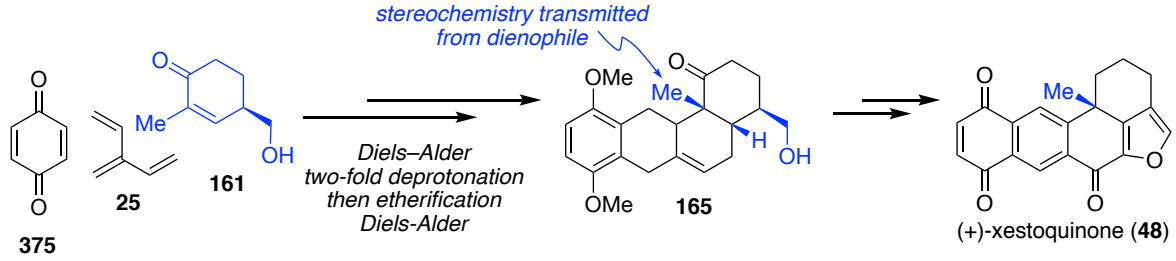

Scheme 4.6 The DTDA reaction sequence *en route* to (+)-xestoquinone, employing a chiral dienophile.

We envisaged that the chiral dienophile could be deployed in the first, rather than the second, cycloaddition reaction (Scheme 4.7c). This approach would permit a second, substrate-controlled diastereoselective Diels–Alder reaction and thus the stereochemical control exhibited by the dienophile could be parlayed throughout the polycyclic framework formed.

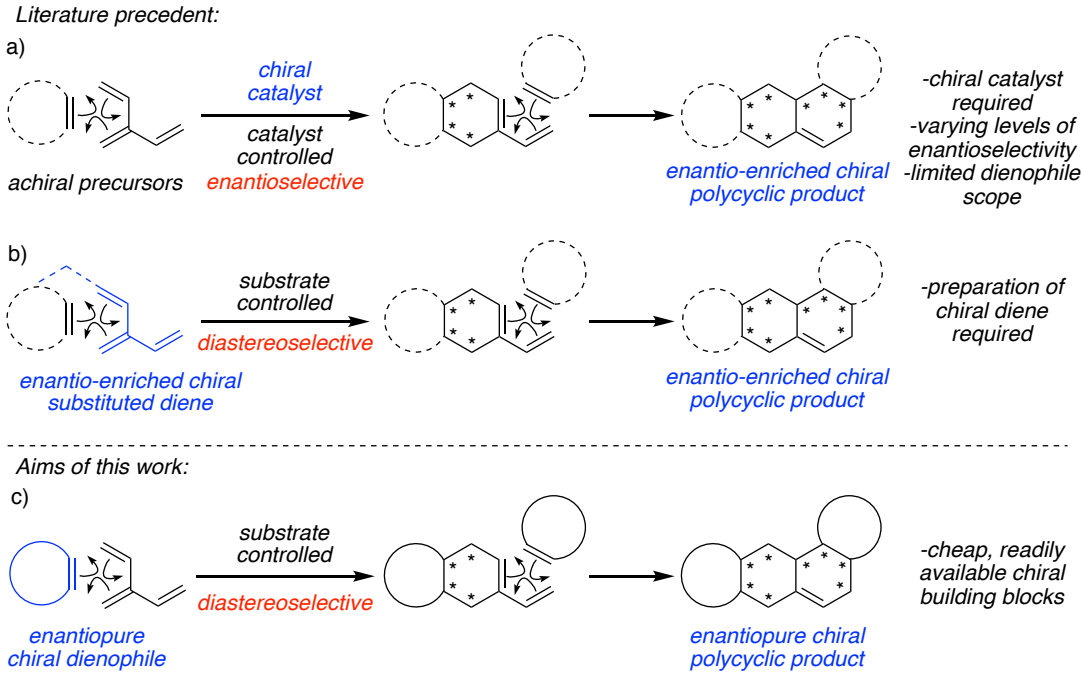

Scheme 4.7 The use of DTDA reaction sequences to construct chiral polycyclic frameworks. Asterisks (*) denote potential new stereocentres with defined absolute configuration (dependent on substitution pattern). Literature precedent: a) chiral catalyst, catalyst controlled, enantioselective; b) chiral diene (or tether bearing stereochemistry with defined absolute

configuration), substrate controlled, diastereoselective. This work: c) chiral dienophile, substrate controlled, diastereoselective.

Presented in this chapter is an investigation of DTDA reaction sequences of [3]dendralenes with readily available chiral building blocks, with the aim of exploring the generality and synthetic utility of this powerful strategy to rapidly access enantiopure polycyclic products.

4.2 Synthesis of Enantiopure Polycycles

4.2.1 Precursors and Precedents

4.2.1.1 Synthesis of [3]Dendralenes

In order to facilitate an investigation of the DTDA reaction sequence, the parent [3]dendralene (**25**) and a range of substituted [3]dendralenes were prepared according to known methods. Thus [3]dendralene was synthesised in 5 steps from 1,2-dichlorobutene **376** (Scheme 4.8). Elimination using calcium hydroxide generated chloroprene **377**,[82] which was converted to the corresponding Grignard reagent.[83] Subsequent nucleophilic ring opening of ethylene oxide,[84] followed by bromination of the resulting primary alcohol,[13] and lastly elimination using DBU[13] then afforded the parent [3]dendralene.

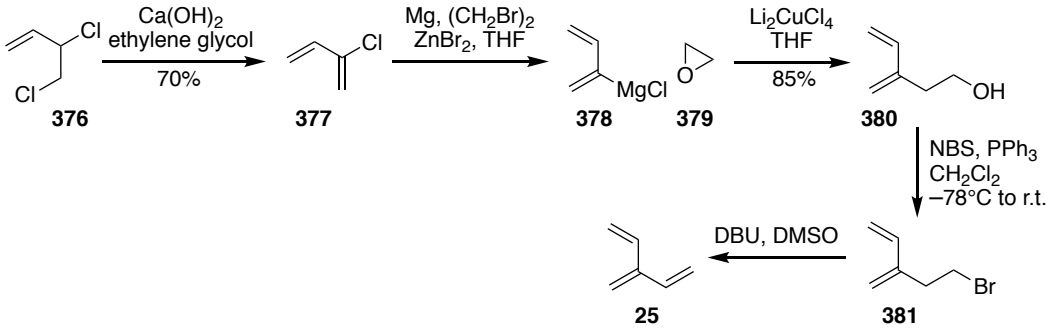

Scheme 4.8 Preparation of [3]dendralene (**25**)

Table 4.1 Synthesis of substituted [3]dendralenes **384-387**

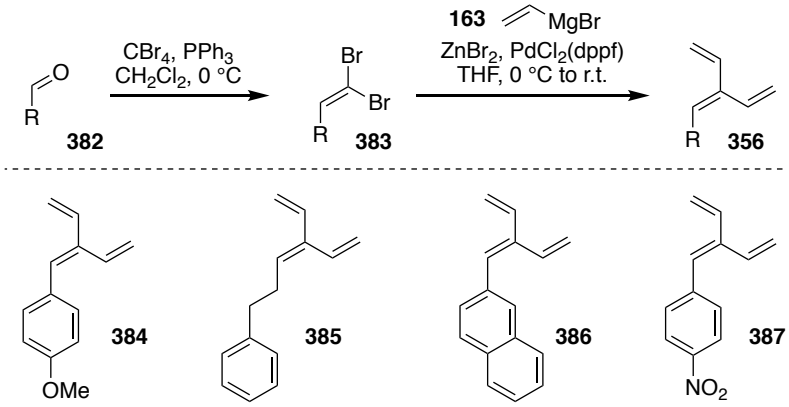

3'-Monosubstituted [3]dendralenes were prepared in two steps[85] *via* dibromoolefination of the aldehyde, and double cross-coupling with vinyl magnesium bromide (Table 4.1).[ii]

4.2.1.2 DTDA Reaction Sequence Dienophile Scope

With dienes **25**, **384**, **385**, **386** and **387** in hand, we next turned our attention to the identification of suitable dienophiles. Of particular interest to us were cyclic dienophiles, due to their greater ability to rapidly construct polycyclic systems. Typically, only highly activated, reactive and symmetrical cyclic dienophiles have been employed in DTDA reaction sequences, such as quinones (6-membered rings), and maleimides and maleic anhydride (5-membered rings) (Figure 4.3a). Deviation from these dienophiles poses challenges not only in reactivity, but also in regio- and diastereo-selectivity.

Our confidence was bolstered, however, by our previous investigations. In Chapter 2, 3- through to 8-membered ring carbocycles were shown to be successful dienophiles with the parent [3]dendralene (Figure 4.3b). Furthermore, these dienophiles ranged from being highly activated (e.g. benzyne, cyclobutenone), through to relatively un-activated (e.g. cyclohexenone). High levels of regioselectivity were also obtained with a range of unsymmetrical structures.

[ii] Dendralenes **386** and **387** prepared *via* this route were available in-house, thanks to Yi-Min Fan.

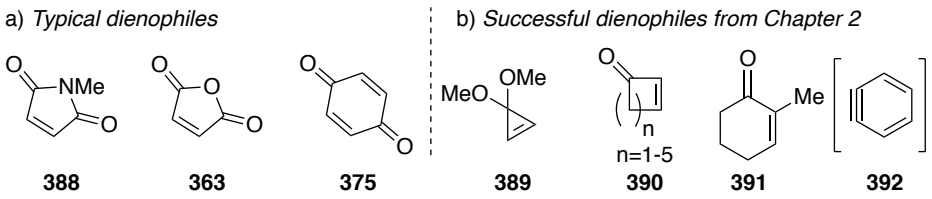

Figure 4.3 Current carbocyclic dienophile scope of the DTDA reaction sequence

As such, we were optimistic about the deployment of readily available chiral building blocks,[iii] containing an enone moiety, as dienophiles. The similarity between such molecules and parent cyclenones, cyclohexenone and cycloheptenone, can be appreciated in Figure 4.4.

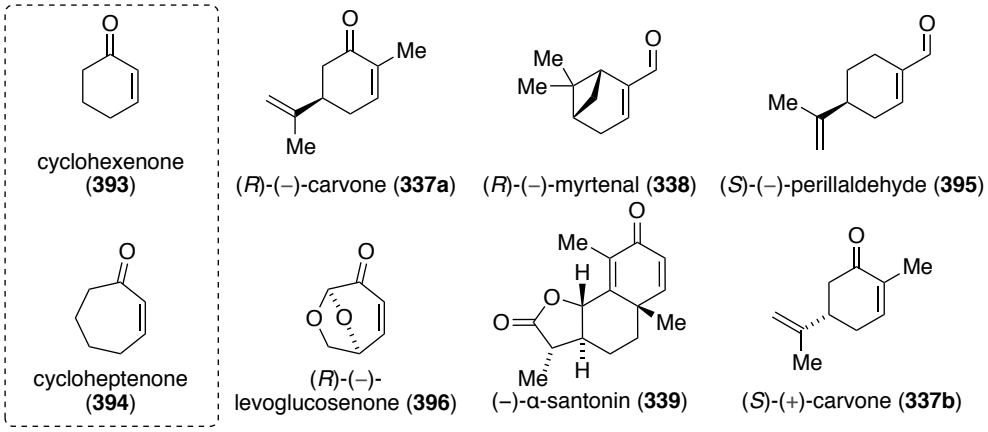

Figure 4.4 Proposed readily available chiral dienophiles and comparison to parent cyclenones, cyclohexenone and cycloheptenone

By way of brief introduction, the chiral building block carvone is terpene derived, with both enantiomers (**337a** and **337b**) occurring naturally. (*R*)-carvone is a major component in spearmint oil and has been found in *Mentha spicata*, *M. viridis* var. *crispa*, *M. longifolia*, *Eucalyptus globulas*, and several other mint species.[86] In addition, it is also prepared commercially from (*R*)-(+)-limonene.[86a] In contrast, (*S*)-carvone is a major component in caraway and dill oils and has also been found in *Anethum sowa*, *Lippia carviodora*, and *Mentha arvensis*.[86b, 86c] Notably, (*R*)- and (*S*)-carvone have distinctly different odours, of spearmint and caraway, respectively.[87]

[iii] (*R*)-Levoglucosenone received free of charge from Circa Group. All other chemicals sourced from Sigma Aldrich. Prices in AUD as at 18/07/2020: (*R*)-carvone $0.65/g; (*S*)-carvone $0.20/g; (*R*)-myrtenal $0.82/g; (*S*)-perillaldehyde $1.75/g; α-santonin $9.34/g.

The chiral building block (*R*)-myrtenal (**338**) is also terpene derived. It has been found in a range of plants including *Blepharocalyx tweedii*, *Renealmia speciosa*, Sri Lankan ginger, *Xylopia longifolia*, and *Amomum testaceum*.[88] Although currently less commercially available, the other enantiomer, (*S*)-myrtenal is also naturally occurring, most notably in *Astartea leptophylla* and *Astartea* sp. nov. endemic to Western Australia.[89]

The chiral building block (*S*)-perillaldehyde (**395**) is again terpene derived and is isolated from the leaves of the herb *Perilla frutescens*, which is used extensively in Chinese medicine.[90] In contrast, (–)-levoglucosenone (**396**) is of carbohydrate origin and is produced by pyrolysis of cellulose,[91] thus presenting an attractive building block due to its abundant, biorenewable source.[92] Lastly, the natural product α-Santonin (**339**) is isolated from flower heads of the *Artemisia* sp and has had medicinal use as an anthelmintic for treatment of parasitic worms.[93]

4.2.2 Monoadducts

4.2.2.1 Viability of Chiral Building Block Dienophiles

The successful deployment of two different dienophiles in the first and second cycloadditions of a DTDA reaction sequence requires, of the first dienophile, mono-selective addition. Consequently, monoadducts were targeted in the first instance, with the dual purpose of, firstly, investigating the viability of the selected chiral building blocks as dienophiles with [3]dendralenes, and of secondly, assessing the potential for a different second dienophile in the DTDA reaction sequence.

In Chapter 2, general conditions for the Diels–Alder reaction of carbocyclic dienophiles with [3]dendralene were established using Me_2AlCl catalysis. Noting the structural similarities between examples such as cyclohexenone, 2-methylcyclohexenone and the chiral dienophile, carvone, reaction of (*R*)-carvone with [3]dendralene was trialled by the same method. A review of Diels–Alder reactions of carvone in the literature[94] also indicated several examples using aluminium-based Lewis acid catalysis,[94a, 94d, 94h, 94k, 94m] supporting the viability of this approach (Scheme 4.9a).

Gratifyingly, Diels–Alder reaction proceeded to selectively afford monoadduct **399a**, with no bisadduct observed by ^{1}H NMR spectroscopic analysis. Furthermore, with both (*R*)- and (*S*)-carvone being commercially available, both enantiomers of bicycle **399** could be generated, albeit in a modest yield of 35-36% (Scheme 4.9b). The structure of **399** was unambiguously

confirmed by single crystal X-ray analysis of a bisadduct (**497**; see Scheme 4.30) derived from **399a**.

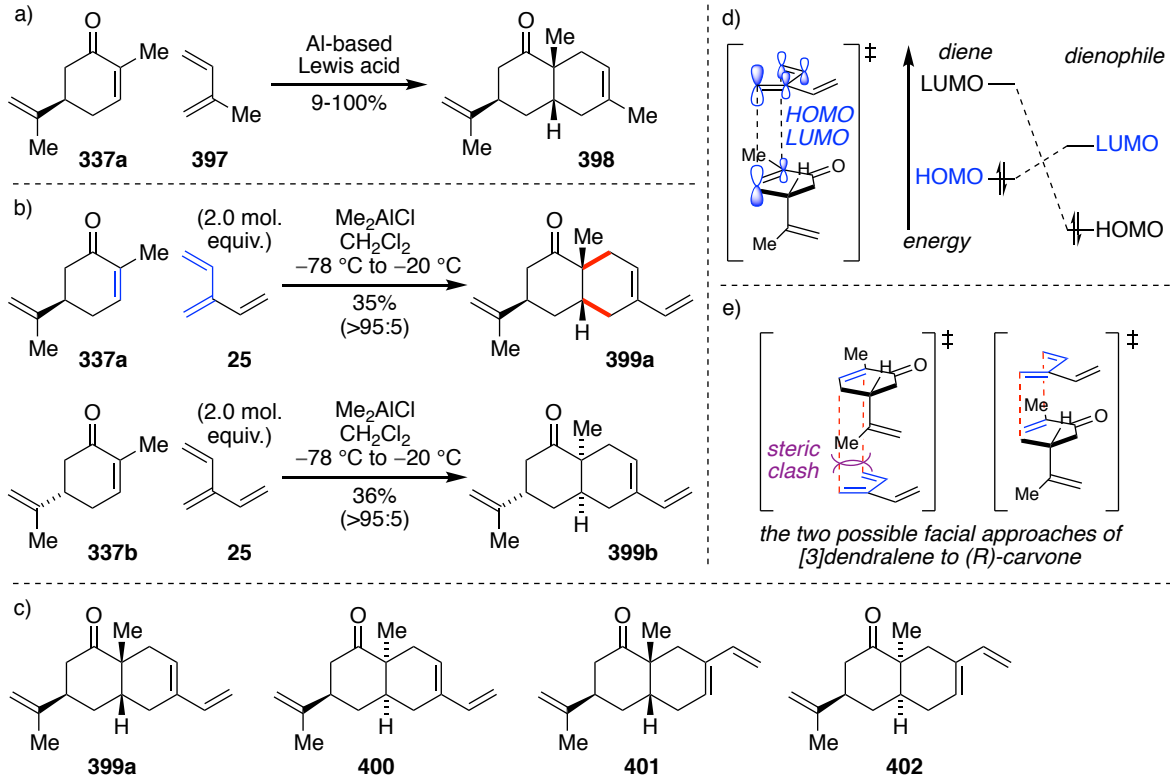

Scheme 4.9 a) Literature precedent: Diels–Alder reaction of (*R*)-carvone with isoprene using aluminium-based Lewis acid catalysis;[94a, 94d, 94h] b) Mono-selective Diels–Alder reaction of (*R*)- and (*S*)-carvone with [3]dendralene; regio/diastereo-selectivities are quoted in parentheses as determined by analysis of crude ^{1}H NMR spectra; c) Possible regioisomeric and diastereomeric products from monocycloaddition of (*R*)-carvone to [3]dendralene; d) Diene-dienophile HOMO-LUMO overlap in reaction of (*R*)-carvone with [3]dendralene; e) Approach of [3]dendralene from either face of (*R*)-carvone

Pleasingly, the reaction proceeded with high levels of regio- and diastereoselectivity. Taking the reaction of (*R*)-carvone with [3]dendralene, there are two possible regioisomers that may be formed, **399a** (or its corresponding diastereomer **400**) in which the ketone of carvone is *para* to the vinyl substituent of the diene in the newly formed ring and **401** (or its corresponding diastereomer **402**) in which the ketone of carvone is *meta* to the vinyl substituent in the newly formed ring (Scheme 4.9c). Consistent with the reaction of 2-methylcylohexenone (**391**) in Chapter 2, effectively only **399a** was observed. This is consistent with the '*ortho-para*' rule predicted by frontier molecular orbital (FMO) theory, wherein the activating substituent of the dienophile is *para* to the activating 2-substituent of the diene in the newly formed ring.[95] It is

believed that carvone preferentially approaches [3]dendralene in this orientation as a result of the electron-withdrawing substituent on the dienophile (ketone), and of the electron-donating group on the diene (vinyl substituent), to maximise diene-dienophile HOMO-LUMO overlap in the transition state (Scheme 4.9d).

In terms of diastereoselectivity, there are two possible (non-regioisomeric) monoadducts that can arise. Due to the lack of terminal diene substituents on the parent [3]dendralene (C1 and C4 of the 1,3-butadiene subunits), an *endo*- or *exo*-mode of addition gives rise to the same diastereomeric product and thus, it is not possible to determine whether the reaction proceeded via an *endo*- or *exo*-transition state. An *endo*-arrangement is predicted however, due to the benefit of secondary orbital interactions. The two possible diastereomers that can arise from the reaction instead result from π-diastereofacial selectivity, wherein the ring junction proton and methyl substituents are on the same face as the isopropenyl subsitutent as in **399** or on the opposite face as in **400**. These diastereomers arise from approach of [3]dendralene from the bottom or top face of carvone, respectively. The selective formation of **399** is rationalised as the bottom face of (*R*)-carvone, opposite to that of the isopropenyl substituent, is expected to be less sterically encumbered (Scheme 4.9e). It is acknowledged that the simplified representation of carvone in this explanation (Scheme 4.9e) however, does not take into account the conformation of the cyclohexenone ring.

Considering the lowest energy conformation of (*R*)-carvone, **337a-c1** (Figure 4.5), the isopropenyl substituent is *quasi*-equatorial, while in its ring flipped form, **337a-c2**, the isopropenyl substituent is *quasi*-axial. In **337a-c1** approach of the diene to the C=C bond from the top face in an *endo* arrangement is blocked, while approach from the bottom face is relatively unhindered. In contrast, in **337a-c2** approach of the diene to the C=C bond from the bottom face in an *endo* arrangement is blocked, while approach from the top face is relatively unhindered.

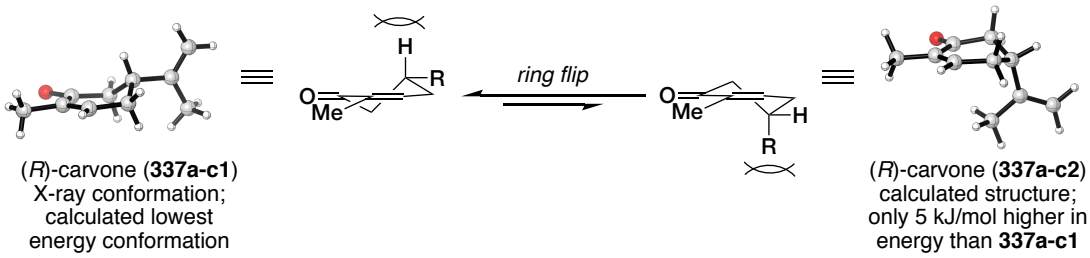

Figure 4.5 The lowest energy conformation of (*R*)-carvone[96] and its ring-flipped form

It is reasoned that the product resulting from approach to the top face as depicted in Figure 4.5 is formed due to a) the small energy difference between the two conformations, resulting in rapid interchange between the two ring-flipped forms and b) the greater steric encumbrance caused by the *quasi*-axial isopropenyl substituent in **337a-c2** as compared to the *quasi*-axial proton in **337a-c1**.

The second readily available chiral dienophile investigated was (*R*)-myrtenal. There exist no reports in the literature of Diels–Alder reaction of myrtenal as a C=C dienophile, although it has been used as a diene in Diels–Alder reactions, following Wittig methylenation to form (+)-nopadiene (**403**) (Scheme 4.10).[97]

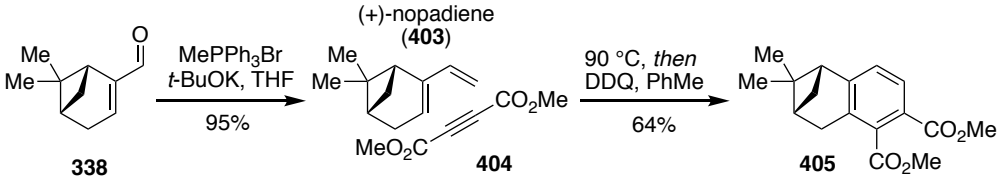

Scheme 4.10 Conversion of (*R*)-myrtenal (**338**) to (+)-nopadiene and subsequent use as a Diels–Alder diene[97]

The closest literature example of a C=C dienophile to (*R*)-myrtenal comes from Chapius and co-workers who report [4+2] cycloaddition of 1-cyclohexene-1-carboxaldehyde (**406**) with cyclopentadiene (**243**) using $AlCl_3$ catalysis (Scheme 4.11a).[98] In this reaction, there is no orientational regioselectivity issue due to the symmetric nature of the diene, and with both precursors being achiral, a racemic product is formed. The reaction proceeds with reasonable diastereoselectivity (80:20), favouring formation of the *exo* product. Based on this precedent, and the broad scope of carbocyclic dienophiles tolerated in Chapter 2, we were optimistic in the deployment of a dienophile bearing an exocyclic electron-withdrawing group. Furthermore, while there exists no X-ray crystal structure of (*R*)-myrtenal in the literature, the calculated lowest energy conformation **338-c1** (Scheme 4.11b) shows the top face of the C=C bond is less sterically hindered than the bottom face, suggesting approach of the diene should be facially selective.

Pleasingly, reaction of [3]dendralene (**25**) with (*R*)-myrtenal proceeded more rapidly[iv] and in significantly higher yield (71%), than with carvone under the same conditions (Scheme 4.11c).

[iv] Reaction completion achieved in less than one third of the time required for (*R*)-carvone.

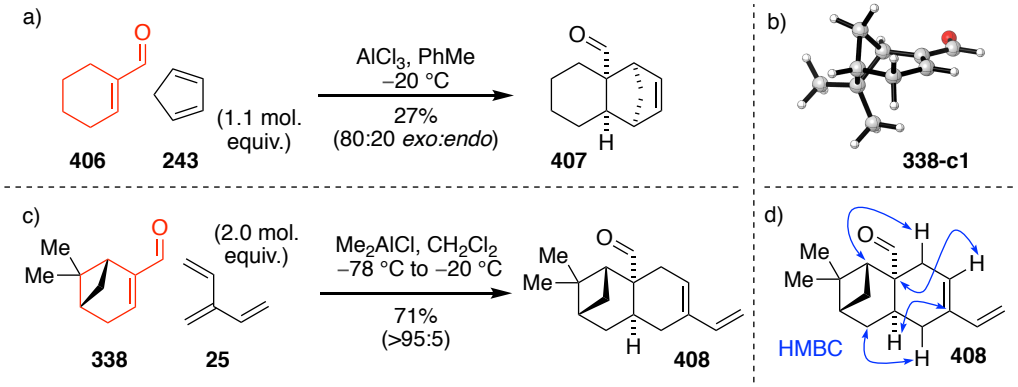

Scheme 4.11 a) Literature precedent: Diels–Alder reaction of 1-cyclohexene-1-carboxaldehyde;[98] similarity to (*R*)-myrtenal is highlighted in red; b) Calculated lowest energy conformation of (*R*)-myrtenal; c) Mono-selective Diels–Alder reaction of (*R*)-myrtenal with [3]dendralene; regio/diastereo-selectivity is quoted in parentheses as determined by analysis of crude ^{1}H NMR spectra; d) Double headed arrows depict key HMBC NMR correlations in blue

The relatively sluggish reaction of carvone is consistent with that of 2-methyl-cyclohexen-1-one (**391**) in Chapter 2, when compared to the unsubstituted cyclohexenone dienophile (**393**). It is proposed that steric hindrance introduced by the methyl substituent, combined with inductive electron donation, render the Lewis acid complexes of 2-methyl-cyclohexen-1-one (and carvone) less reactive dienophiles. In this regard, the greater success of (*R*)-myrtenal, also bearing an alkyl substituent α- to the carbonyl, is then perhaps somewhat surprising. It may be reasoned that the alkene of (*R*)-myrtenal, however, is still more electron deficient due to the conjugated aldehyde functionality and therefore is a more activated dienophile. Furthermore, the enone of (*R*)-myrtenal can adopt the more reactive[95] *s-cis* conformation, to maximise secondary orbital interactions in the Diels–Alder transition state,[95] with the *s-cis* conformation calculated to be only 6 kJ/mol higher in energy than the *s-trans* conformation. In contrast, cyclic enones such as carvone are locked in the less reactive[95] *s-trans* conformation (Figure 4.6).

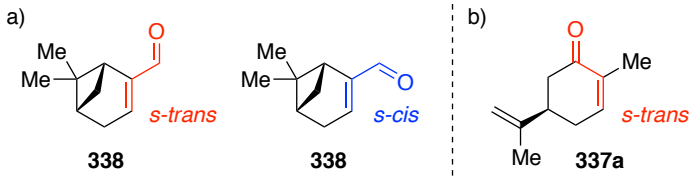

Figure 4.6 Possible enone conformations for a) (*R*)-myrtenal (**338**) and b) (*R*)-carvone (**337a**)

High levels of regio- and diastereoselectivity were observed in the formation of **408** from (*R*)-myrtenal, as predicted by the *ortho-para* rule[95] and by approach of the diene from the top, less sterically hindered face of the chiral dienophile as depicted in calculated lowest energy conformation **338-c1** (Scheme 4.11b). The structural assignment of monoadduct **408** was supported by HMBC NMR correlations (Scheme 4.11d) and by nOe NMR experiments performed on bisadducts (**499**, **500** and **502**; see Scheme 4.31 and Figure 4.18) derived from **408**.

Given this positive result with (*R*)-myrtenal, we proceeded to probe the reactivity of the related chiral dienophile, (*S*)-perillaldehyde (**395**), also bearing an exocyclic aldehyde. While there again is no X-ray crystal structure of (*S*)-perillaldehyde in the literature, the calculated lowest energy structures of the molecule suggest approach of the diene should be facially selective (Figure 4.7). The enone moiety of (*S*)-perillaldehyde bears similarity to that of myrtenal, while the cyclohexene ring has a similar conformation to that of carvone. In the lowest energy conformation, **395-c1**, the isopropenyl substituent is *quasi*-equatorial, while in its ring flipped form, **395-c2**, the isopropenyl substituent is *quasi*-axial. There is only a small energy difference between the two conformations, and so it is expected that approach of the diene from the top face of (*S*)-perillaldehyde (as depicted in Figure 4.7) will be hindered.

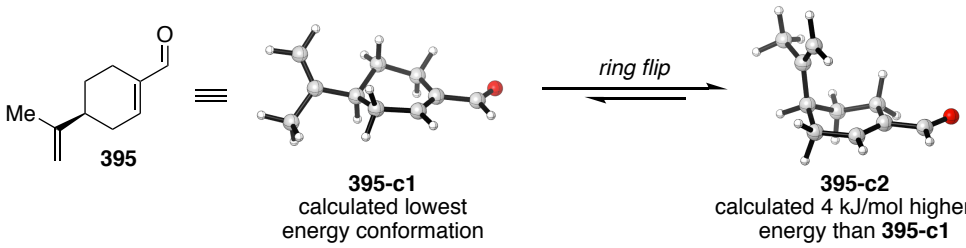

Figure 4.7 The lowest energy conformation of (*S*)-perillaldehyde and its ring-flipped form

(*S*)-Perillaldeyde has limited use as a C=C dienophile in the literature, with its Diels–Alder reaction only reported with two different dienes (Scheme 4.12). In 2008 Mulzer and co-workers utilised (*S*)-perillaldehyde to achieve a notably shorter formal synthesis of the natural product platencin (**414**).[99] Thus, Diels–Alder reaction of (*S*)-perillaldehyde with reactive Rawal diene **409** under thermal conditions afforded monoadduct **410**, which was subjected to acidic hydrolysis *in situ* to yield dicarbonyl **411**. The cycloaddition reaction proceeded with high regio- and diastereoselectivity, with approach of the diene to the less sterically hindered, bottom face of (*S*)-perillaldehyde as predicted from Figure 4.7. In the same year, Rutjes and co-workers reported Diels–Alder reaction of (*S*)-perillaldehyde with Danishefsky diene **412** *en*

route to the same natural product.[100] Reaction with this less reactive diene required high pressure conditions (regioisomeric/diastereomeric ratio not reported). Conversion to dicarbonyl **411** was then achieved *in situ* using a Lewis acidic workup. These two cycloaddition-deprotection-elimination sequences have subsequently been deployed in several other total and formal syntheses.[101]

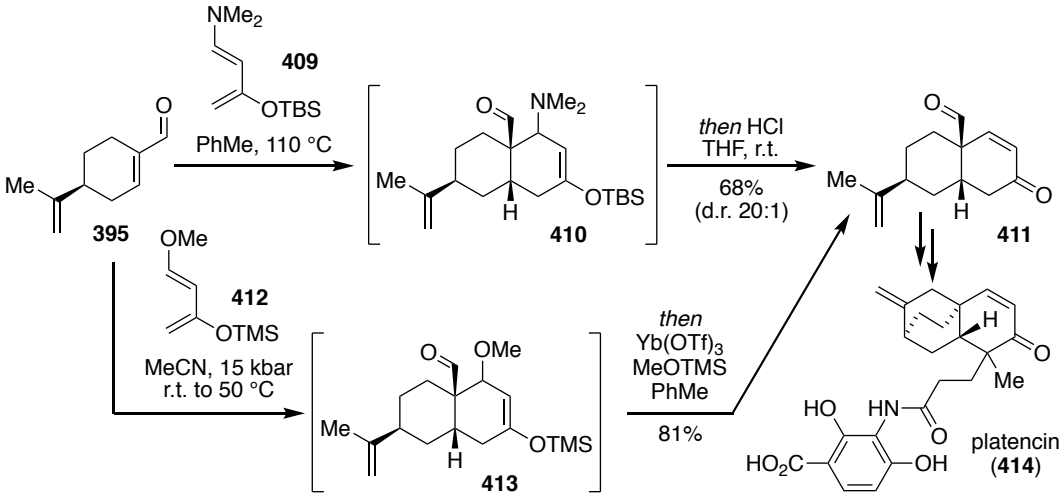

Scheme 4.12 Literature precedent: Diels–Alder reaction of (*S*)-perillaldehyde (**395**) as a C=C dienophile

Gratifyingly, in our hands Diels–Alder reaction of (*S*)-perillaldehyde with [3]dendralene under Me_2AlCl catalysis proved to be successful (Scheme 4.13). However, expected monoadduct **415** was not observed. Bridged cyclic systems **416a** and **416b** were instead isolated, proposed to be from Diels–Alder reaction of (*S*)-perillaldehyde, followed by subsequent transannular ene cyclisation of Diels–Alder adduct **415**.

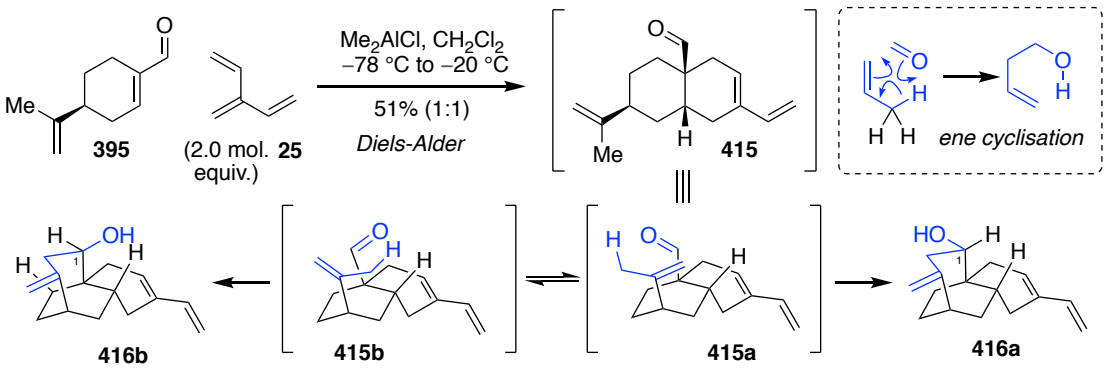

Scheme 4.13 Diels–Alder-ene reaction sequence of (*S*)-perillaldehyde with [3]dendralene

To the best of our knowledge, the only literature report of a possible ene cyclisation involving (*S*)-perillaldehyde comes from Rutjes and co-workers, who report conversion of (*S*)-perillaldehyde Diels–Alder derived **411** to bridged cyclic system **422** (Scheme 4.14a).[101b] It is proposed by the authors that aldehyde **411** undergoes an acid mediated Prins cyclisation to form alcohol **419**. Subsequent dehydration then affords triene **422**. It is equally acknowledged however, that a carbonyl ene cyclisation pathway to **419** would also be possible. More broadly, there are several examples of Me_2AlCl catalysed carbonyl-ene reactions to form seven-membered rings in the literature (Scheme 4.14b).[102]

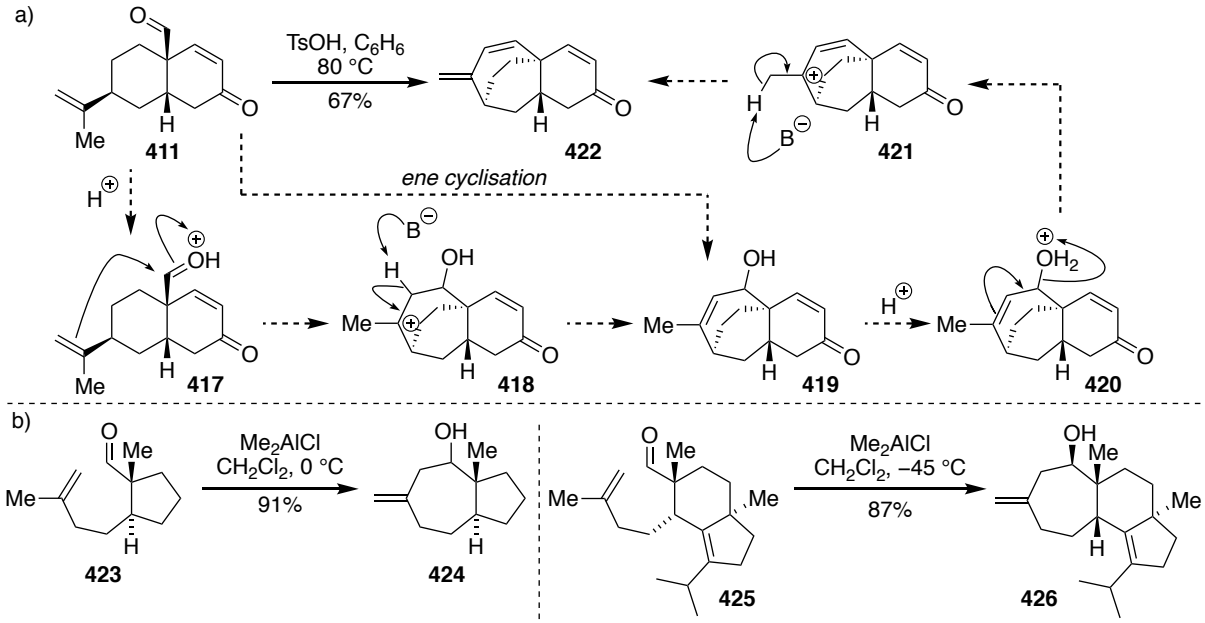

Scheme 4.14 Literature precedent for a) possible ene cyclisation of an (*S*)-perillaldehyde Diels–Alder adduct[101b] and b) seven-membered ring formation *via* a Me_2AlCl catalysed carbonyl-ene reaction[102b, 102c] (stereochemistry at the secondary alcohol of **424** not reported).

High levels of regio- and diastereoselectivity were observed from the Diels–Alder reaction of (*S*)-perillaldehyde with [3]dendralene, again as predicted by the *ortho-para* rule and by approach of the diene from the less sterically hindered face of the chiral dienophile (see Figure 4.7). Subsequent ene reaction of intermediate **415** however produced a 1:1 mixture of diastereomers. This may be rationalised by ene reaction of the two possible conformations of intermediate **415** (**415a** and **415b**), resulting in opposite absolute configurations at the newly formed C1 stereocentre of **416a** and **416b**. This assignment was based upon HMBC and nOe NMR experiments performed on both **416a** and **416b**, which were separated chromatographically (Figure 4.8).

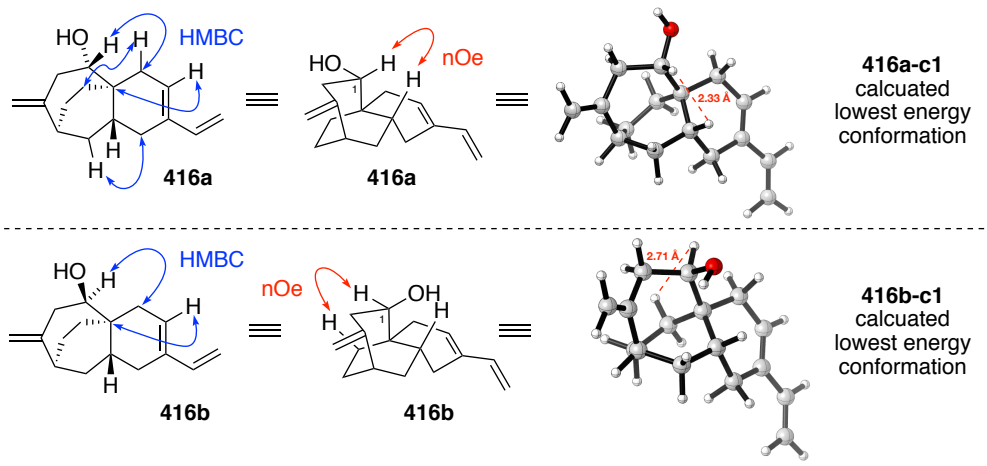

Figure 4.8 Double headed arrows depict key HMBC (blue) and nOe (red) NMR correlations. Calculated lowest energy conformations are depicted, with distances between protons for corresponding nOe correlations shown in red.

Despite the lack of diastereoselectivity arising from the ene reaction, the Diels–Alder-ene pericyclic reaction sequence discovered still presents a powerful synthetic technique, especially when considered in the context of a potential further Diels–Alder reaction of dienes **416a** and **416b**. The two diastereomers could presumably be combined by oxidation of the secondary alcohol back to the ketone. It is proposed that the stereoisomeric alcohol could then be re-generated selectively, if desired, *via* a stereoselective reduction.[103]

Recognising that the dienophiles, (*R*)- and (*S*)-carvone, (*R*)-myrtenal and (*S*)-perillaldehyde are all structurally similar, terpenoid-derived molecules, we expanded our investigation to include the chiral building block (–)-levoglucosenone (**396**) (Scheme 4.15). This molecule, like myrtenal, has a bridged structure. It differs however, in the presence of two ether moieties. While there is no X-ray crystal structure of (–)-levoglucosenone available in the literature, calculations of the lowest energy conformation of the molecule, **396-c1**, show the lower –O– bridged face to be less sterically hindered than the top –CH_2O– bridged face (Scheme 4.15c), suggesting selective approach of the diene to the lower face of the molecule should occur.

Initially, we attempted Me_2AlCl catalysed Diels–Alder reaction of (–)-levoglucosenone with [3]dendralene. Perhaps not surprisingly however, in this instance, (–)-levoglucosenone proved to be incompatible with Lewis acid catalysis. Dienophile decomposition was observed and we could find no examples of Al-based Lewis acid catalysed Diels–Alder reactions of (–)-levoglucosenone in the literature.

Despite this setback, our confidence was bolstered however by several reports in the literature of thermal Diels–Alder reaction of (–)-levoglucosenone with dienes such as 1,3-butadiene and cyclopentadiene.[104] In reaction of (–)-levoglucosenone with cyclopentadiene (**243**), Diels–Alder adduct **427** is formed in high selectivity at room temperature (Scheme 4.15a). There is no orientational regioselectivity issue due to the symmetric nature of the diene and the reaction proceeds with high diastereoselectivity, favouring formation of the *endo* product and approach of the diene to the less sterically hindered –O– bridged face of (–)-levoglucosenone, as predicted from **396-c1**.

Thus based on literature precedent, and the knowledge that [3]dendralenes are reactive dienes,[9, 105] thermal reaction was instead pursued. Gratifyingly, (–)-levoglucosenone was found to be a sufficiently active dienophile to undergo Diels–Alder reaction with [3]dendralene neat at room temperature (Scheme 4.15b).

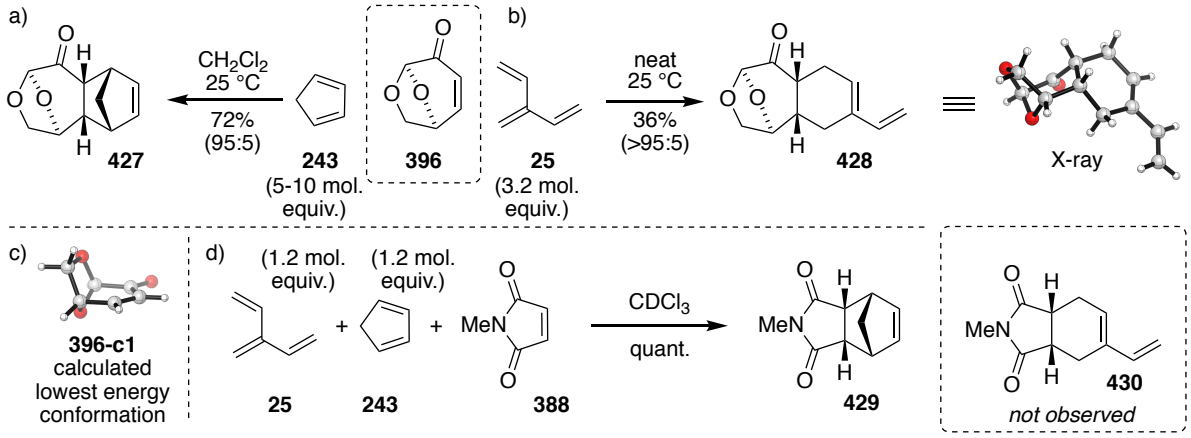

Scheme 4.15 a) Literature precedent[104b] for thermal reaction of (–)-levoglucosenone and cyclopentadiene; b) Mono-selective Diels–Alder reaction of (–)-levoglucosenone with [3]dendralene; regio/diastereo-selectivity is quoted in parentheses as determined by analysis of crude ^{1}H NMR spectra; c) Calculated lowest energy conformation of (–)-levoglucosenone; d) Competition reaction between [3]dendralene (**25**) and cyclopentadiene (**243**) with NMM

Of interest as a side note, is the comparison in reactivity of [3]dendralene and cyclopentadiene. Both are reactive dienes with (–)-levoglucosenone at room temperature, and neat at room temperature the major decomposition pathway of both molecules is Diels–Alder dimerisation. In a competition reaction between [3]dendralene and cyclopentadiene with 0.83 molar equivalents of NMM, cyclopentadiene-derived Diels–Alder monoadduct **429** was found to be generated exclusively, with dendralene-derived monoadduct **430** not observed (Scheme 4.15d).

Both cyclopentadiene and [3]dendralene also remained in the reaction mixture, thus suggesting the propensity of cyclopentadiene to act as a better diene than [3]dendralene. Indeed, this is in accordance with computational studies which predict the relative rate constant for the Diels–Alder dimerisation of cyclopentadiene to be 7 times greater than that for [3]dendralene.[106]

The assignment of structure and relative stereochemistry of product **428** from (–)-levoglucosenone was confirmed by single crystal X-ray analysis, and may be explained by approach of [3]dendralene from the less sterically encumbered face of the dienophile and by the *ortho-para* rule.[95]

The final chiral building block investigated was α-santonin (**339**) (Scheme 4.16a). While there is no literature precedent for Diels–Alder reaction of this molecule, we were hopeful that it may be an effective dienophile due its structural similarity (cyclohexenone moiety) to the other chiral molecules employed. α-Santonin possesses two possible dienophile reaction sites; a tetra-substituted alkene (red) and a di-substituted alkene (blue). Examples of intermolecular Diels–Alder reactions of tetra-substituted dienophiles in the literature are largely limited to highly strained dienophiles and those bearing strong electron withdrawing groups such as TCNE and substituted quinones,[107] with less activated β-alkyl substituted cyclenones, such as 3-methylcyclohexenone, being unreactive Diels–Alder dienophiles.[108] Thus, it was hypothesised that Diels–Alder reaction of α-santonin would instead occur at the less substituted alkene, lacking both the α-methyl and β-alkyl substituents, as depicted in blue (Scheme 4.16a).

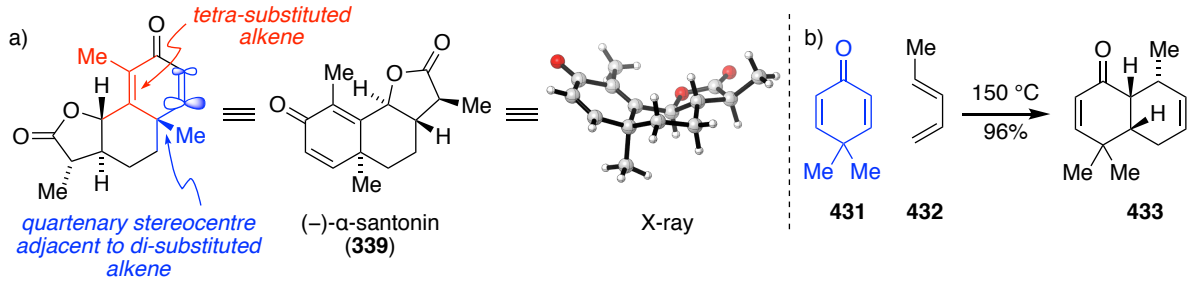

Scheme 4.16 a) X-ray crystal structure of α-santonin[109] and potential sites of α-santonin Diels–Alder dienophile reactivity; b) Literature precedent: Diels–Alder reaction of *gem*-dimethyl substituted cyclohexadienone **431** (regioisomeric/diastereomeric ratio not reported)[108]

Encouragingly, Liotta and co-workers have reported Diels–Alder reaction of a cyclohexadienone dienophile similarly possessing *geminal* C4 substitution (Scheme 4.16b).[108]

Reaction of cyclohexadienone **431** with 1,3-pentadiene (**432**) under thermal conditions proceeds in high yield, favouring formation of the *endo* product.

Reaction of α-santonin with the parent [3]dendralene was first attempted using Lewis acid (Me_2AlCl) catalysis as employed previously (Scheme 4.17). Neither mono- nor bisadducts (or their regio-/diastereo-isomers) however, were observed, and increasing the number of molar equivalents of Lewis acid (3.0 mol. equivs.) gave no improvement. Given the successful Diels–Alder reactions of cyclohexenone, as well as 2-methylcyclohexenone and (*R*)- and (*S*)-carvone, it was reasoned that the lactone was perhaps a contributing factor in this process. As the ester functional group is more Lewis basic than the ketone, it is expected to preferentially form a LA-LB complex. It is hypothesised that the complexation of a second equivalent of Lewis acid (to the ketone) may then be inhibited by Coulombic repulsion.

In light of these results, thermally promoted reaction of α-santonin was instead targeted. Our confidence in this approach, admittedly, was low, due to the relatively unreactive nature of parent cyclenones as dienophiles[110] and the propensity of [3]dendralene to undergo dimerisation.[111] Indeed, attempted thermal Diels–Alder reaction at 25 °C through to 40 °C, resulted in consumption of [3]dendralene with no target material observed by ^{1}H NMR spectroscopic analysis.

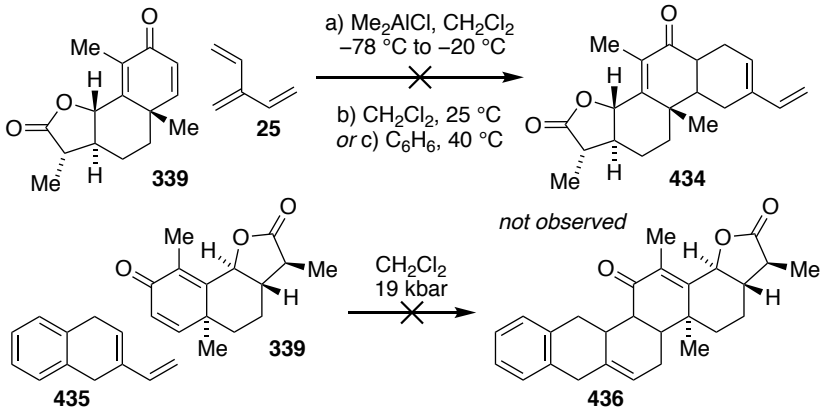

Scheme 4.17 Attempted Diels–Alder reactions of α-santonin

[3]Dendralenes, similarly, are known to polymerise under high pressure conditions,[112] which otherwise may be used to promote Diels–Alder reaction. It was envisaged however, that an alternative, potentially more robust, diene could be employed. The use of an achiral diene, as in the synthesis of (+)-xestoquinone, would still allow the generation of an enantiomerically pure polycyclic structure resulting from Diels–Alder reaction of α-santonin in the second

cycloaddition of the DTDA reaction sequence, rather than the first. Consequently, an attempt was made to react α-santonin under ultra-high pressure conditions, with achiral diene **435**, generated from reaction of [3]dendralene with benzyne.

However, once again the reaction provided no positive results, with bisadduct **436** not observable by ^{1}H NMR spectroscopic analysis of the crude reaction mixture, or in attempted purification. Instead, consumption of diene **435** was observed as in the previously attempted thermal reaction, presumably due to radical polymerisation or cationic polymerisation, initiated through adventitious oxygen or acid, respectively. It is hypothesised that Diels–Alder reaction of α-santonin may be precluded due to steric hindrance. In the asynchronous, but concerted Diels–Alder transition state for reaction at the di-substituted alkene of α-santonin, the shorter forming bond is expected at the more electron deficient carbon (β-carbonyl position) according to FMO theory (Scheme 4.16a). It is theorised however that the quaternary stereocentre directly adjacent to the β-position hinders approach of the diene to this site, thus diminishing the rate of the Diels–Alder reaction and permitting other processes (i.e. diene polymerisation) to compete. This hypothesis is supported by a comparison of Diels–Alder reactions of *geminal* C4 substituted cyclohexenone dienophiles,[108] wherein more forcing reaction conditions are required as the steric bulk of the smaller of the two *geminal* substituents increases (Scheme 4.18).

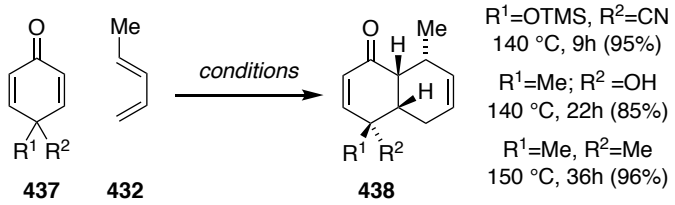

Scheme 4.18 Differing Diels–Alder reactivity of C4 *geminal* substituted cyclohexadienones[108]

In summary, 5 of the 6 readily available chiral building blocks investigated were found to undergo mono-selective Diels–Alder reaction with the parent [3]dendralene, with all Diels–Alder reactions exhibiting high levels of regio- and diastereoselectivity.

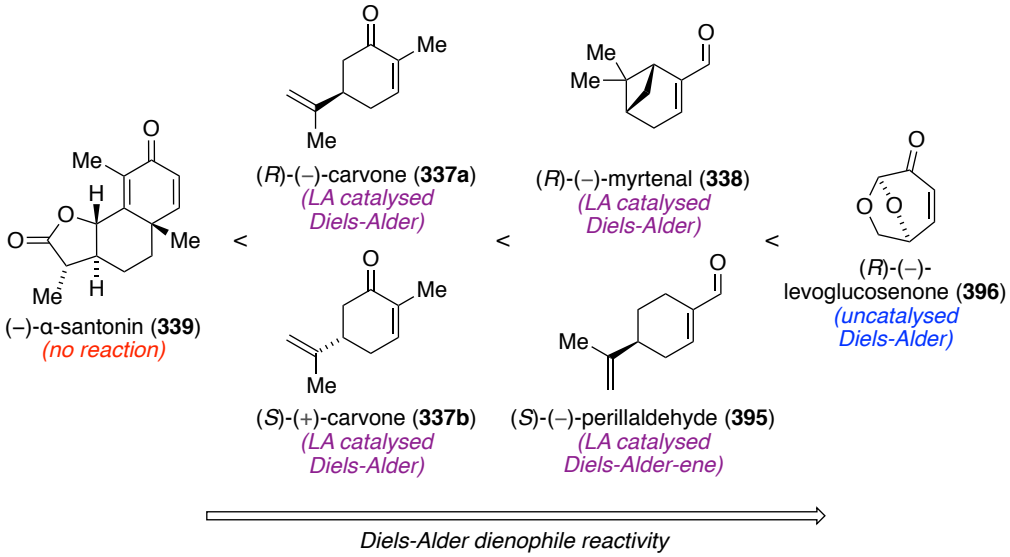

Figure 4.9 Summary of chiral building blocks examined. Diels–Alder dienophile reactivity with the parent [3]dendralene increases from left to right.

4.2.2.2 Substituted [3]Dendralene Scope

Having identified several chiral building blocks suitable as dienophiles in the first cycloaddition of the DTDA reaction sequence, we next sought to examine the scope of this reaction with respect to dendralene substitution.

Taking into account the symmetry of the molecule, there are four possible positions for mono-substitution of [3]dendralene (Figure 4.10). Of these, there is limited information regarding cycloaddition of 1-*E*- and 1-*Z*-substituted dendralenes in the literature, in contrast to 2-subsituted and, to a much greater extent, 3-substituted dendralenes, for which numerous applications in DTDA reaction sequences are reported.[113]

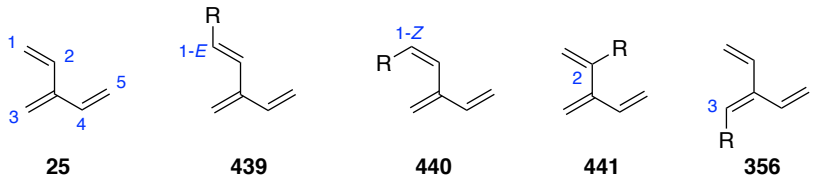

Figure 4.10 Numbering of [3]dendralene and possible mono-substituted [3]dendralenes

Of note, where the substituent is conjugating, such as a phenyl group, substitution at the 1-*Z*, 2- and 3-positions has been found to increase the stability of the molecule relative to the parent [3]dendralene. In contrast, 1-*E*-phenyl-substituted [3]dendralene, is significantly de-stabilised, with Diels–Alder dimerisation occurring at a significantly greater rate than that of the parent

[3]dendralene (Scheme 4.19),[113b] thus making it a less attractive diene for handling and deployment in DTDA reaction sequences.

With respect to 1-*Z*-monosubstituted dendralenes, there is a dearth of information regarding Diels–Alder reaction, presumably due to the steric hindrance imparted by the 1-*Z*-substituent, which would block approach of the dienophile to the substituted diene site in both the first and second cycloadditions of the DTDA reaction sequence.

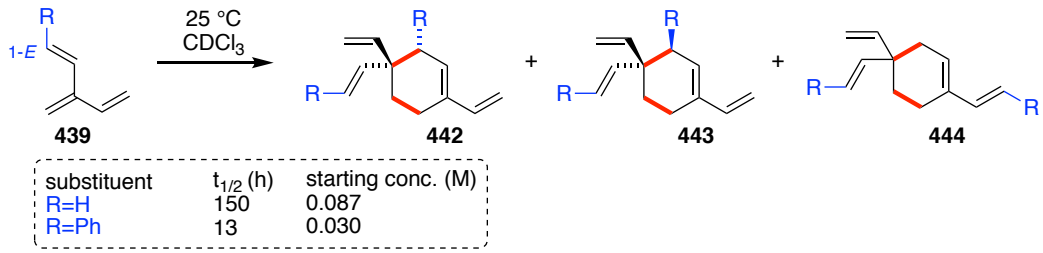

substituent	$t_{1/2}$ (h)	starting conc. (M)
R=H	150	0.087
R=Ph	13	0.030

Scheme 4.19 Experimental half-life measurements for Diels–Alder dimerisation of [3]dendralene and 1*E*-phenyl-substituted [3]dendralene[113b]

2-Substitution of [3]dendralene, similarly, is less attractive, as the substituent generally does not impart good Diels–Alder site or stereo-selectivity.[113a] This is exemplified by reaction of 2-*para*-methoxyphenyl and 2-phenyl substituted dendralenes **441** with NMM (**388**) under uncatalysed conditions (Scheme 4.20). In these reactions, there is no orientational regioselectivity issue due to the symmetric nature of the dienophile, however the first cycloaddition reaction can occur at two possible non-equivalent diene sites, A or B, on [3]dendralene **441**. Bisadducts **446** and **447** arise from initial cycloaddition of NMM to diene site A, followed by subsequent cycloaddition of NMM in an *endo* arrangement to either the top or bottom face of monoadduct **445**, respectively. Reaction of NMM at diene site B in the first Diels–Alder reaction results in monoadduct **448**. Notably, the "transmitted" diene of monoadduct **448** bears a 1-*Z*-methyl substituent, which hinders approach of the dienophile in the second Diels–Alder reaction. Ultra-high pressure conditions are instead required to promote this second cycloaddition, resulting in a 70:30 mixture of bisadducts **449** and **450**, again proposed to arise from an *endo* transition state and approach of NMM to either the top or bottom face of the monoadduct. Although Diels–Alder diene site selectivity for this reaction can be improved through the use of Lewis acid catalysis to exclusively generate bisadducts **446** and **447** arising from initial cycloaddition at diene site A, poor π-diastereofacial selectivity is observed in the second cycloaddition reaction (d.r. 33:66).

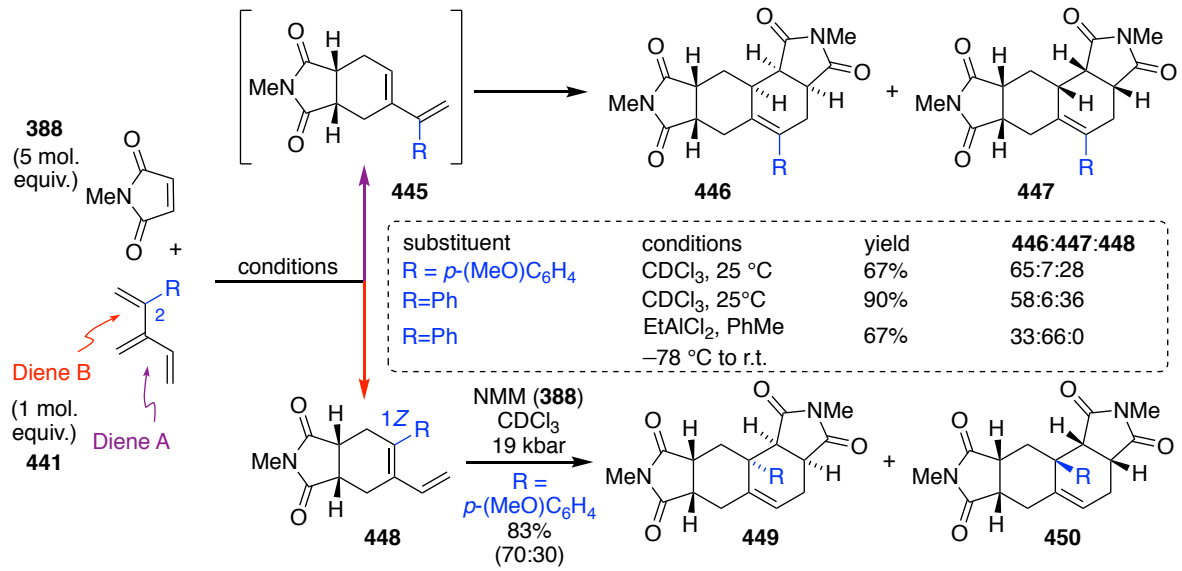

Scheme 4.20 Diene transmissive Diels–Alder reaction sequence of 2-*para*-methoxyphenyl and 2-phenyl substituted dendralenes **441** with NMM (**388**)[113a]

In contrast, 3-substitution of [3]dendralene results in high site selectivity in the first cycloaddition, and generally high π-diastereofacial selectivity in the second cycloaddition of the DTDA reaction sequence. This is exemplified by reaction of 3-phenyl-substituted [3]dendralene **452** with *N*-ethylmaleimide (**451**) to form Diels–Alder bisadduct **454** (Scheme 4.21).[114] The first cycloaddition reaction occurs exclusively at 1*E*-substituted diene site A over the more sterically hindered 1-*Z*-substituted diene site B. The transmitted diene of monoadduct **453** bears only the 1-*E*- and 2-substituents which comprise the cyclohexene ring and undergoes a second Diels–Alder reaction with *N*-ethylmaleimide under ambient conditions. This second cycloaddition proceeds with high selectivity, proposed to arise from an *endo* transition state and approach of *N*-ethylmaleimide from the less sterically hindered, top face of monoadduct **453**. Thus, due to both their stability and their Diels–Alder diene reactivity and selectivity, we elected to focus on 3-substituted [3]dendralenes in this work.

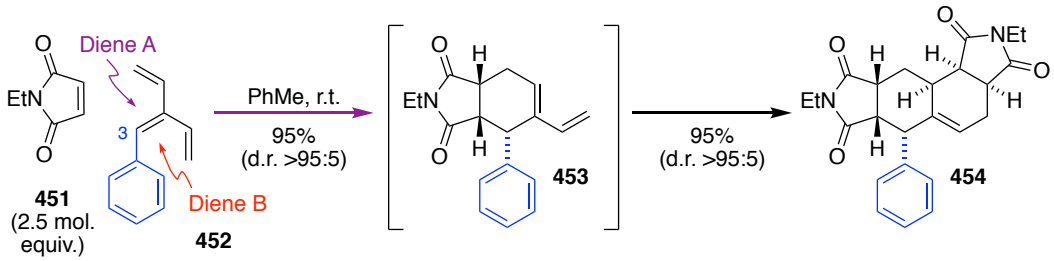

Scheme 4.21 Diene transmissive Diels–Alder reaction sequence of 3-phenyl-substituted [3]dendralene **452** with *N*-ethylmaleimide (**451**)[114]

In the event, Diels–Alder reaction of (*R*)-myrtenal with *para*-methoxyphenyl 3-substituted [3]dendralene **384**, afforded monoadduct **455** in good yield (Scheme 4.22a).

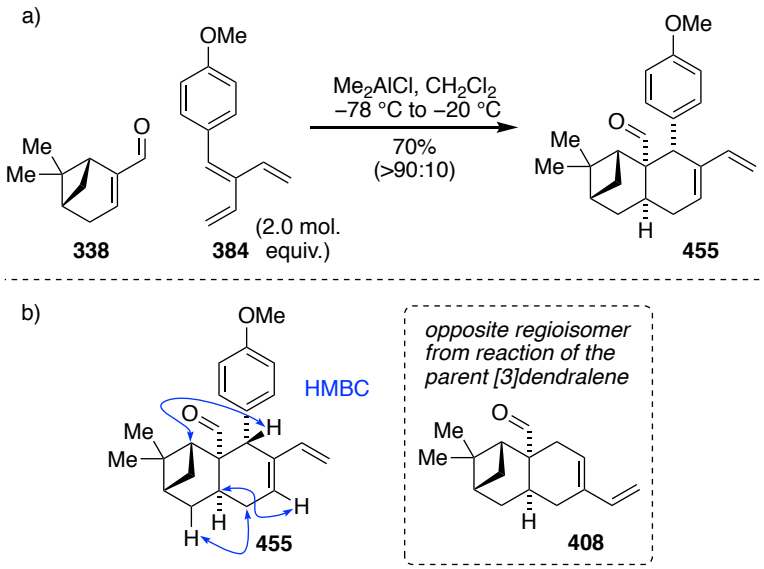

Scheme 4.22 a) Mono-selective Diels–Alder reaction of (*R*)-myrtenal (**338**) with substituted [3]dendralene **384**; regio/diastereo-selectivity is quoted in parentheses as determined by analysis of crude ^{1}H NMR spectra; b) Double headed arrows depict key HMBC NMR correlations in blue

The reaction proceeded with high diastereoselectivity, proposed to arise from an *endo* transition state and approach of the diene from the less sterically hindered face of the chiral dienophile. Notably, the opposite regioisomer was observed to that formed from reaction of (*R*)-myrtenal with the parent, unsubstituted [3]dendralene (**25**), thus providing access to a complimentary molecular framework. This assignment was based upon HMBC and nOe NMR experiments performed on **455** and on a bisadduct (**504**; see Scheme 4.32 and Figure 4.20) derived from **455**.

The regiochemical outcome of the reaction is consistent with recent research within the Sherburn group[78] (see Scheme 4.3b), wherein dendralenes substituted at the internal C=C π-bond underwent enantioselective organocatalysed Diels–Alder reactions with acrolein to selectively form monoadducts with the opposite regioselectivity to those generated from the parent [3]dendralene.

The observed switch in regioselectivity may be explained by approximation of the highly polarised, asynchronous, but concerted, Diels–Alder transition states to discrete cationic

intermediates.[78] Considering Figure 4.11, in which (*R*)-myrtenal is truncated to the simplest enone dienophile, approach of the dienophile to [3]dendralene can occur in two different orientations (Figure 4.11a). In both orientations, the transition state is asynchronous, with the shorter bond forming at the more electron deficient carbon of the alkene of the dienophile. Monoadduct, **408** from reaction of myrtenal with the parent [3]dendralene may be mapped onto favoured product **458**. This product arises from Diels–Alder transition state **456**-*int*, which possesses pentadienyl cation character (**457**-*int*), and thus is preferred over transition state **456**-*term* with less stable allyl cation character (**457**-*term*).

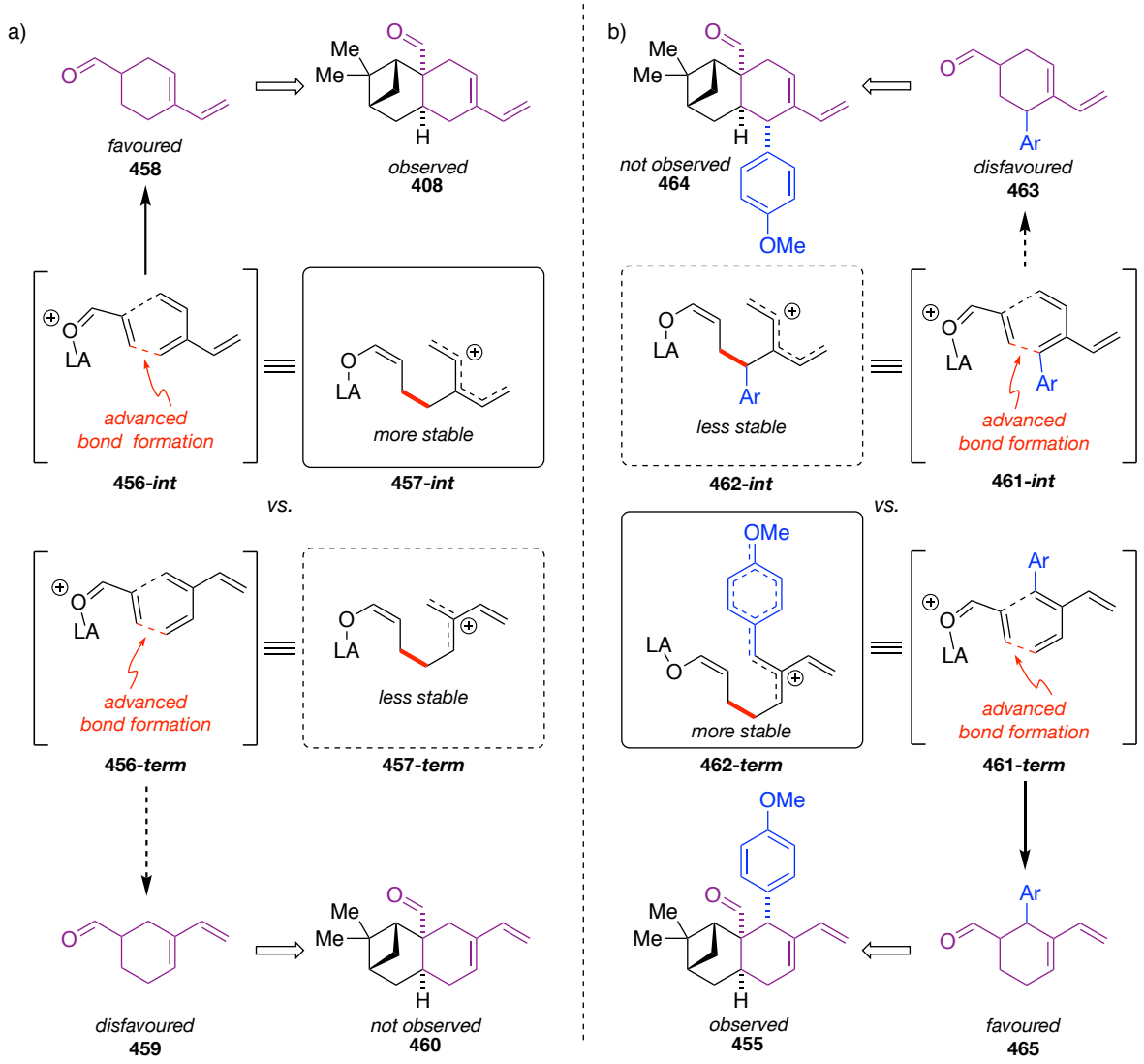

Figure 4.11 Rationalisation of regioisomeric outcomes of the Lewis acid catalysed Diels–Alder reactions involving a) [3]dendralene and b) *para*-methoxyphenyl 3-substituted [3]dendralene **384**

The opposite regioselectivity in reaction of dendralenes substituted at the internal C=C π-bond can then be justified by two reasons (Figure 4.11b). Firstly, if the substituent on the dendralene is electron rich and conjugating, as in the case of *para*-methoxyphenyl substituted dendralene **384**, the Diels–Alder transition state **461**-*term* is provided with greater stabilisation and is therefore preferred over transition state **461**-*int* with pentadienyl cation character. Secondly, steric hindrance of the dendralene substituent may impede advanced bond formation in **461**-*int*, wherein the substituent is attached to the site of the diene with a short developing bond. Consequently, product **465** is expected to be favoured. This may be mapped onto monoadduct **455** from reaction of (*R*)-myrtenal with substituted [3]dendralene **384**.

In light of the mediocre yields obtained upon reaction of (*R*)-carvone with the parent [3]dendralene (see Scheme 4.9), we elected to re-optimise reaction conditions for this dienophile while investigating reaction with substituted [3]dendralene **384**.

It was reasoned that the slow rate of reaction may be improved by increasing the reaction temperature from –20 °C to room temperature. While low temperatures proved vital in controlling the regioselectivity of Diels–Alder reaction between cyclohexenone and the parent [3]dendralene (see Chapter 2, optimisation data), we were optimistic that in this case high levels of selectivity could still be obtained at warmer temperatures due to the influence of the α-methyl substituent on the dienophile and the electron-donating aromatic substituent on the diene.

It was theorised that an increase in reaction rate and yield may also be achieved by increasing the Lewis acidity of the catalyst employed, compared to Me_2AlCl. As a result, a range of aluminium-based Lewis acids were selected for screening (Table 4.2). A broader survey of the literature also suggested several other Lewis acid catalysts could be of use, including $BF_3 \bullet Et_2O$[115] and TMSOTf.[116]

Table 4.2 Optimisation of conditions[a] for reaction of (*R*)-carvone with substituted [3]dendralene **384**

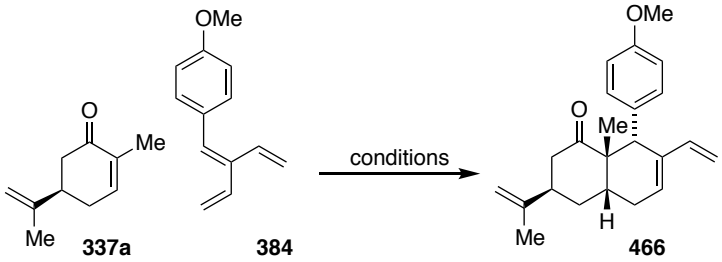

entry	catalyst (mol. equiv.)	mol. equiv. dendralene	mol. equiv. (*R*)-carvone	temperature (°C)	yield (%)[b]
1	Et_2AlCl (0.6)	1.0	1.0	r.t.	0%
2	$MeAlCl_2$ (0.6)	1.0	1.0	r.t.	22%
3	$EtAlCl_2$ (0.6)	1.0	1.0	r.t.	54%
4	$AlCl_3$ (0.6)	1.0	1.0	r.t.	0%
5	TMSOTf (10 mol%) 1,2-bis(TMS)-ethane (1.06)	1.0	1.0	–78 °C	<10%
6	BF_3•Et_2O (1.0)	1.0	1.0	–40 °C	0%
7	$EtAlCl_2$ (0.6)	2.0	1.0	r.t.	34%
8[c]	$EtAlCl_2$ (1.1)	1.0	2.0	r.t.	43%
9	$EtAlCl_2$ (0.1)	1.0	1.0	r.t.	0%
10	$EtAlCl_2$ (0.3)	1.0	1.0	r.t.	<10%
11	$EtAlCl_2$ (0.8)	1.0	1.0	r.t.	53%
12	$EtAlCl_2$ (0.9)	1.0	1.0	r.t.	59%
13	$EtAlCl_2$ (1.0)	1.0	1.0	r.t.	61%
14	$EtAlCl_2$ (0.6) pyridine (0.06)	1.0	1.0	r.t.	0%
15[c]	$EtAlCl_2$ (1.1) 2,6-lutidine (1.1)	1.0	2.0	r.t.	0%

[a] Unless otherwise specified reactions were performed in CH_2Cl_2; [b] Yield determined by internal standard and analysis of crude ^{1}H NMR spectra; [c]Reaction performed in PhMe.

Entries 1-6 of Table 4.2 describe the results from screening of different Lewis acids. In the event, deployment of Et_2AlCl (Entry 1) proved unsuccessful, with no reaction occurring (both starting materials remaining). Pleasingly, however, the more Lewis acidic catalysts, $MeAlCl_2$ and $EtAlCl_2$ (Entries 2-3) afforded the desired monoadduct, albeit with some starting material decomposition observed. Nonetheless, in the case of the latter a 54% yield was obtained; an increase in yield relative to the reaction of (*R*)-carvone with the parent [3]dendralene under Me_2AlCl catalysis. Further increasing Lewis acidity, with the use of $AlCl_3$, resulted in complete decomposition of dendralene **384**, with no target material observable by ^{1}H NMR spectroscopic

analysis (Entry 4). Alternative non-aluminium based catalysts (Entries 5-6) were similarly ineffective, resulting in decomposition of dendralene **384**.

Again, as in the case of (*R*)-myrtenal discussed above (Scheme 4.22), the regioisomeric outcome of this reaction is the opposite to that from reaction of (*R*)-carvone with the parent [3]dendralene. This outcome is consistent with literature precedent for the reaction of (*R*)-carvone with phenyl substituted diene **467**[94b] (Scheme 4.16) and supports the generality of this regioselectivity, governed by the aromatic substituent of dendralene **384**.

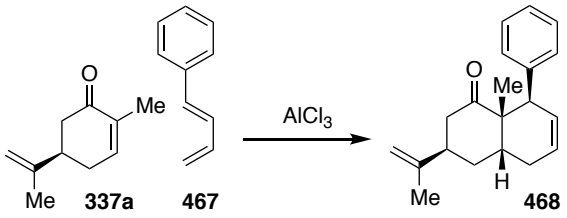

Scheme 4.23 Literature precedent for the regioisomeric outcome of the LA catalysed Diels–Alder reaction of (*R*)-carvone (**337a**) with 4-methoxyphenyl substituted [3]dendralene **384** (yield and regioisomeric/diastereomeric ratio not specified)[94b]

The reaction also proceeded with high levels of diastereoselectivity proposed to arise from an *endo* transition state and approach of the diene from the less sterically hindered face of the chiral dienophile. The structure of monoadduct **466** was unambiguously confirmed by single crystal X-ray analysis of a bisadduct (**498**; see Scheme 4.30) derived from **466**.

Given the success of $EtAlCl_2$, focus was placed on further optimisation of reaction conditions using this catalyst (Table 4.2, Entries 7-15). Increasing the relative ratio of either [3]dendralene or (*R*)-carvone did not lead to an increase in reaction yield (Entries 7-8). Decreasing the catalyst loading significantly decreased the yield of monoadduct **466**, while increasing the catalyst loading led to a small improvement in the reaction yield (Entries 9-13).

It was hypothesised that the presence of Brønsted acid, generated by quenching of $EtAlCl_2$ by adventitious moisture, may be causing dendralene decomposition. A potential solution to this problem was the addition of a sterically hindered base to the reaction mixture, with some limited literature precedent suggesting the compatibility of amines such as pyridine with aluminium-based Lewis acids.[117] In our hands, both pyridine and the more sterically encumbered 2,6-lutidine, however, inhibited reaction progress (Table 4.2, Entries 14-15).

It is acknowledged that further optimisation of conditions for this reaction could be performed in the future such as increasing catalyst loadings or screening further alternative catalysts. However, noting that fully optimised conditions may depend upon the substituted dendralene deployed, as well as the chiral dienophile employed in each individual example, we elected to proceed with the improved reaction conditions identified for carvone ($EtAlCl_2$ catalysis; Table 4.2, Entry 13) to continue our broader investigations.

Application of $EtAlCl_2$ to reaction of (*R*)- and (*S*)-carvone with the parent [3]dendralene proved successful, with an increase in yield from 35-36% to 50-52% (Scheme 4.24).

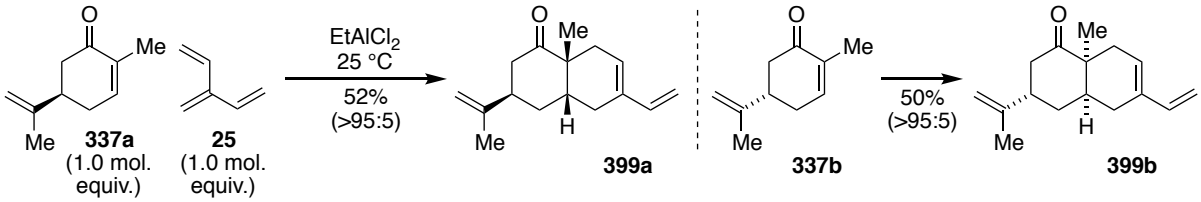

Scheme 4.24 Mono-selective Diels–Alder reactions of (*R*)- and (*S*)-carvone with [3]dendralene (**25**) under $EtAlCl_2$ catalysis; regio/diastereo-selectivities are quoted in parentheses as determined by analysis of crude ^1H NMR spectra

Interestingly however, application of these more forcing conditions, employing $EtAlCl_2$ at room temperature, to the Diels–Alder reaction of (*R*)-myrtenal was unsuccessful, resulting in decomposition of dendralene **384** (Scheme 4.25). Given this differing outcome between attempted reactions of (*R*)-carvone (Table 4.2, Entry 13) and (*R*)-myrtenal (Scheme 4.25) under the same conditions, the Lewis acid catalyst and reaction conditions for following investigations were selected based upon the dienophile employed; namely, $EtAlCl_2$ for carvone and Me_2AlCl for (*R*)-myrtenal.

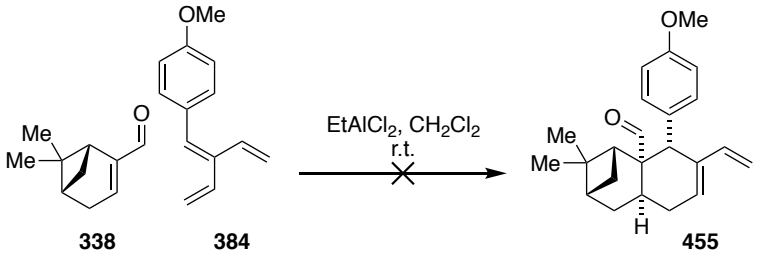

Scheme 4.25 Attempted Diels–Alder reaction of (*R*)-myrtenal with substituted [3]dendralene **384** under $EtAlCl_2$ catalysis

With suitable reaction conditions now identified, several other alternative substituted [3]dendralenes were investigated. Thus, Me_2AlCl catalysed Diels–Alder reaction of (*R*)-myrtenal with naphthyl-substituted [3]dendralene **386** afforded monoadduct **469** albeit in low yield (Scheme 4.26a). Reasonable levels of regio- and diastereoselectivity were observed from the reaction, with the regiochemical outcome of the reaction being consistent with monoadduct **455** formed from reaction of *para*-methoxyphenyl substituted dendralene **384** (Scheme 4.15). The major isomer is proposed to arise from an *endo* transition state and approach of the diene from the less sterically hindered face of the chiral dienophile. This assignment was based upon HMBC and nOe NMR experiments performed on monoadduct **469** (Scheme 4.26b).

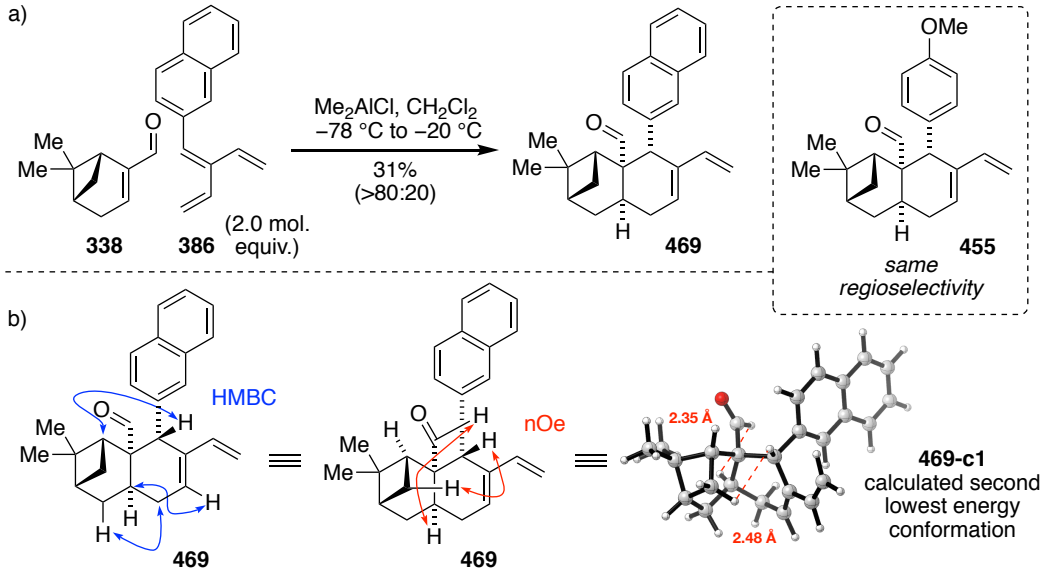

Scheme 4.26 a) Mono-selective Diels–Alder reaction of (*R*)-myrtenal (**338**) with substituted [3]dendralene **386**; regio/diastereo-selectivity is quoted in parentheses as determined by analysis of crude ^{1}H NMR spectra; b) Double headed arrows depict key HMBC (blue) and nOe (red) NMR correlations. Distances between protons for corresponding nOe correlations are shown in red on calculated second lowest energy conformation **469-c1** (+0.04 kJ/mol relative to an *endo* carbonyl –CHO rotated form).

In contrast, attempted Diels–Alder reaction of substituted [3]dendralene **387** with (*R*)-myrtenal proved unsuccessful, with no mono- or bisadduct observable by ^{1}H NMR analysis (Scheme 4.27). Given the persisting presence of both starting materials in the reaction mixture, it was theorised that coordination of Me_2AlCl to the nitro group of the diene may be preventing activation of (*R*)-myrtenal and thus promotion of Diels–Alder reaction. Increasing the Lewis acid up to 3.0 molar equivalents, however, did not improve the reaction outcome.

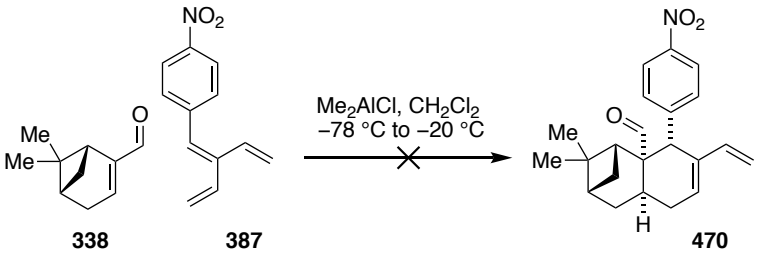

Scheme 4.27 Attempted Diels–Alder reaction of (*R*)-myrtenal with substituted dendralene **387**

This result may be rationalised by again considering the simplified Diels–Alder transition states for this reaction (Figure 4.12). The presence of an electron-withdrawing conjugating substituent, in this case the nitro moiety, would de-stabilise transition state **471**-*term* (exacerbated further by the coordination of a Lewis acid to the nitro moiety), while advanced bond formation in **471**-*int* would be also be impeded by steric hindrance of the dendralene substituent.

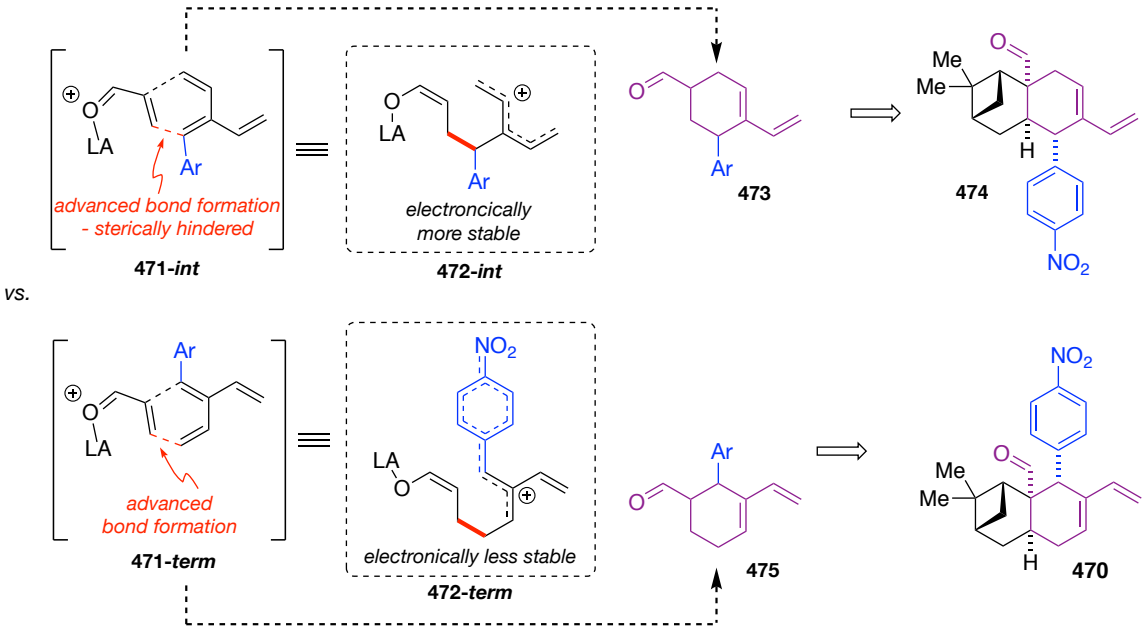

Figure 4.12 Rationalisation of the prohibitively slow Lewis acid catalysed Diels–Alder reaction of substituted [3]dendralene **387** by consideration of the two possible regioisomeric outcomes

Interestingly, mono-selective reaction with phenethyl-substituted [3]dendralene **385** to afford monoadduct **476** also could not be achieved. Only bisadduct **477** was observed upon reaction with (*R*)-carvone even when using dendralene **385** in excess (Scheme 4.28). Notably, the rate of reaction was also slow when compared to the same reaction of (*R*)-carvone with

para-methoxyphenyl substituted dendralene **384**. This is consistent with recent research within the Sherburn Group, wherein organocatalysed Diels–Alder reaction of dendralene **384** was found to be prohibitively slow.[78] While generally the rate of the second Diels–Alder reaction is slower than that of the first in a DTDA reaction sequence,[9, 13, 105] surprisingly, in this case, it is believed that the inverse is true, i.e. the rate of the first Diels–Alder reaction is slower than that of the second. Limited literature precedent for this stems from Schrieber and co-workers' library of DTDA reaction sequence bisadducts generated from Diels–Alder reaction of solid-supported 3'-substituted [3]dendralenes with maleimide and benzoquinone dienophiles.[114] Formation of a mixture of monoadduct **453** and bisadduct **454** was observed on reaction of phenyl-substituted dendralene **452** with 1.0 molar equivalent of *N*-ethylmaleimide (**451**).

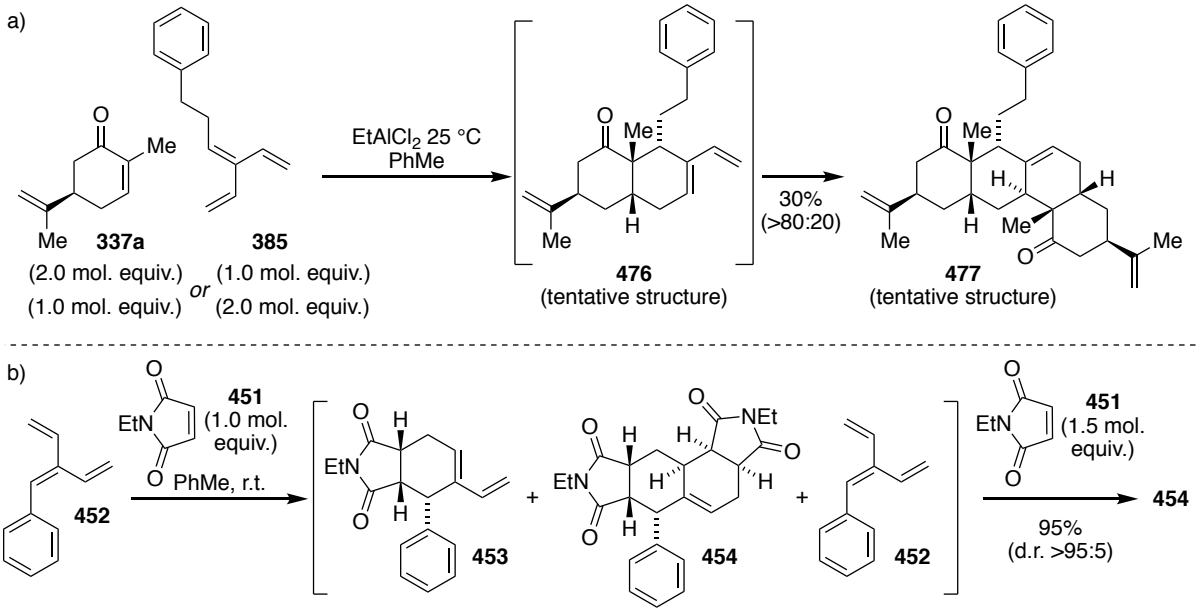

Scheme 4.28 a) Diels–Alder reaction of (*R*)-carvone with substituted [3]dendralene **385**. Regio/diastereo-selectivity is quoted in parentheses as determined by analysis of crude ^{1}H NMR spectra; b) Literature precedent for non-monoselective Diels–Alder reaction of a 3-substituted [3]dendralene[114]

The theory that the rate of the first Diels–Alder reaction of dendralene **385** is slower than that of the second, was supported by reaction of substituted dendralene **385** with 0.95 molar equivalents of NMM (Scheme 4.29). In the event, monoadduct **478** and bisadduct **479** were obtained in yields of 33% and 29% respectively, thus indicating a propensity of the second Diels–Alder reaction in the cycloaddition sequence to occur faster than the first.

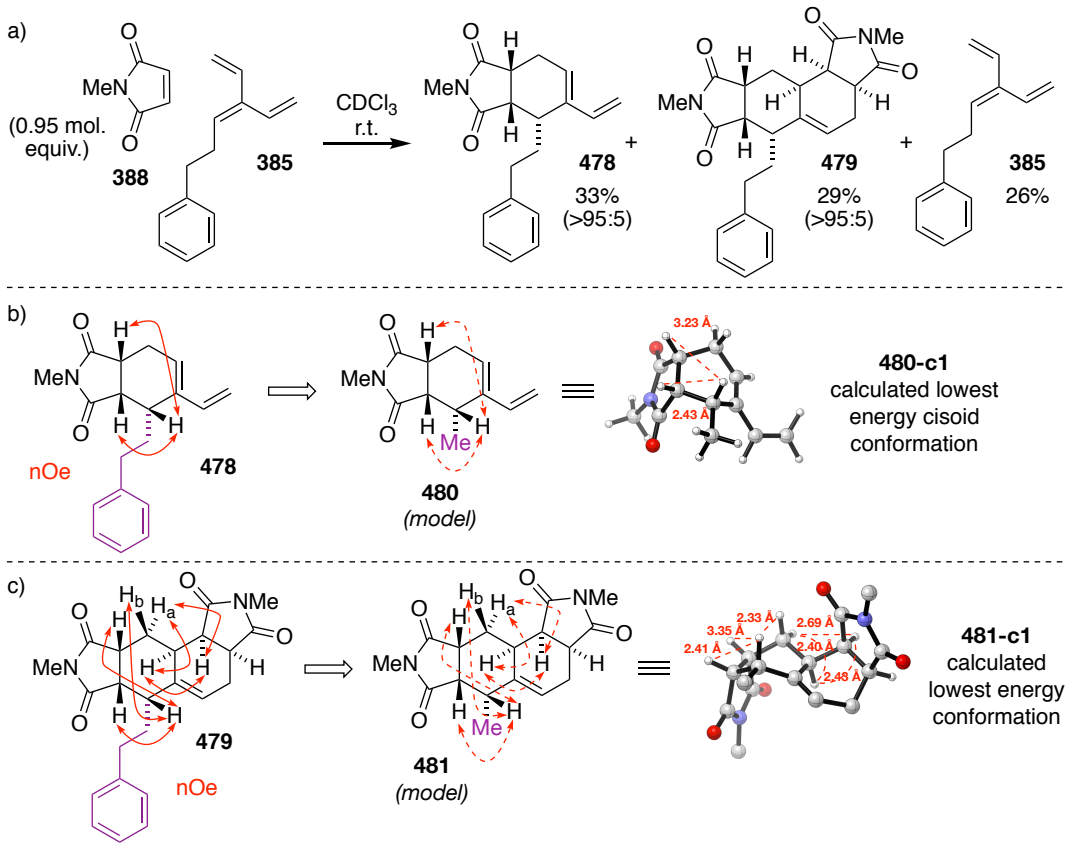

Scheme 4.29 a) Diels–Alder reaction of substituted [3]dendralene **385** with NMM (**388**). Regio/diastereo-selectivities are quoted in parentheses as determined by analysis of crude ^{1}H NMR spectra; stereochemical assignments are based upon nOe NMR experiments performed on **478** and **479**; b) and c) Double headed arrows depict key nOe NMR correlations for **478** and **479** in red. Calculated lowest energy conformations of Me-substituted models **480** (lowest energy *cisoid* diene; second lowest energy conformation overall (+6.52 kJ/mol)) and **481** are depicted, with distances between protons for corresponding nOe correlations shown in red. Some hydrogens are omitted for clarity.

The slow rate of the first Diels–Alder reaction may be rationalised by considering the simplified Diels–Alder transition states in Figure 4.13. In the case of reaction of substituted [3]dendralene **385** with (*R*)-carvone, in the absence of an electron-donating conjugating substituent, the transition state **482**-*term* would not receive significant stabilisation, while advanced bond formation in **481**-*int*, which possesses pentadienyl cation character (**483**-*int*) and is therefore more stable, would be impeded by steric hindrance of the alkyl chain.

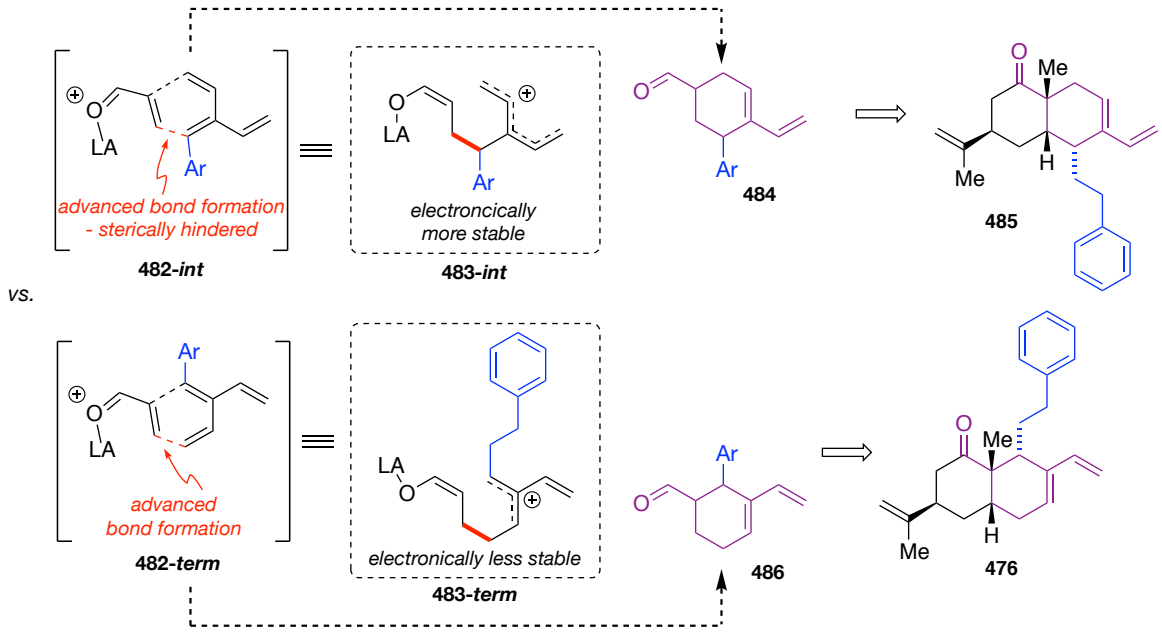

Figure 4.13 Rationalisation of the slow Lewis acid catalysed Diels–Alder reaction of substituted [3]dendralene **385** by consideration of the two possible regioisomeric outcomes

Similarly, therefore, in reaction of substituted dendralene **385** with the symmetrical dienophile NMM, advanced bond formation at both termini of the diene would be disfavoured, thus raising the barrier for the first Diels–Alder reaction to occur.

The faster rate of the subsequent second Diels–Alder reaction (relative to reaction of semicyclic dienes derived from the parent [3]dendralene) can be understood by considering the conformational preferences of the monoadducts derived from both substituted dendralene **385** and the parent [3]dendralene (**25**). While the location of Diels–Alder transition states, and hence the computational modelling of each Diels–Alder reaction, is currently under investigation in the Sherburn group, calculations are complicated by the existence of many different conformations of the diene. Thus, initial analysis is presented herein based upon diene (and dienophile) ground state conformations.

For monoadduct **399a** derived from the parent [3]dendralene, there are 9 conformers calculated to be within 15 kJ/mol of the minimum energy conformation. The three lowest energy structures have an *s-trans* diene, a chair cyclohexanone and a half-chair cyclohexene, and differ only in the orientation about the isopropenyl substituent relative to the cyclohexanone ring. Of the remaining 6 conformers, 4 have *cisoid* dienes (with the vinyl group twisted above the cyclohexene ring in 3 cases) and all have the same chair cyclohexanone and half-chair cyclohexene. The final two structures have boat cyclohexanones and *s-trans* dienes. The lowest

energy *cisoid* diene conformation, **399a-c1**, lies 11.69 kJ/mol above the global minimum *s-trans* conformation, and differs only in the diene conformation, with a C=C–C=C dihedral angle of 36.3° (Figure 4.14).

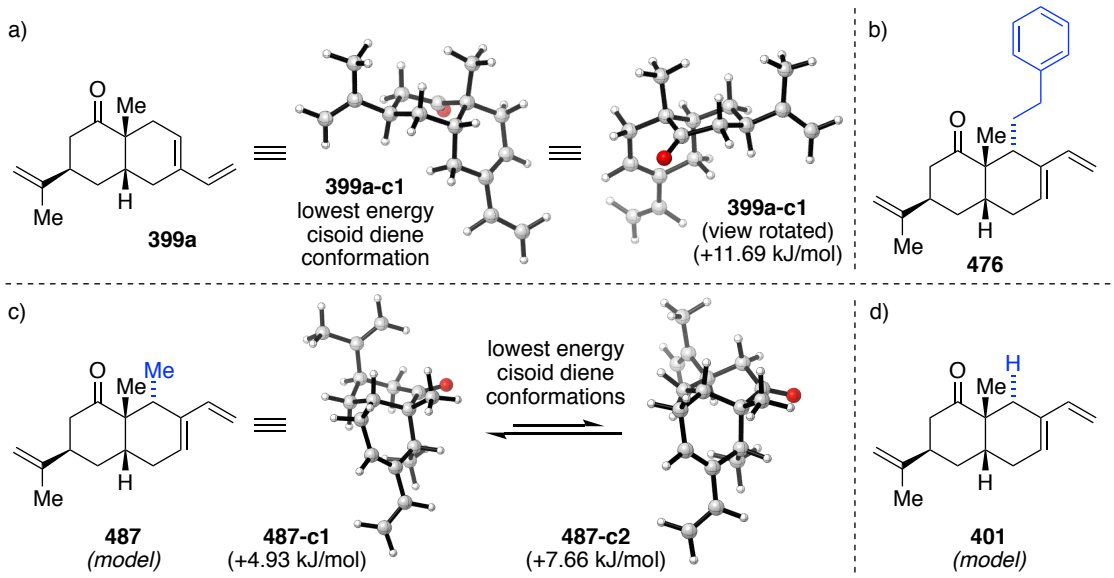

Figure 4.14 a) Calculated lowest energy *cisoid* diene conformation of **399a**; b) Monoadduct **476**; c) Calculated lowest energy *cisoid* diene conformation of Me-substituted model diene **487** for **476**; d) Unsubstituted mono-adduct **401**. Energy differences from calculated structures to the global energy minimum conformation are quoted in parentheses.

Due to the conformational flexibility of the phenethyl group, Me-substituted analogue **487** was selected as a truncated model for monoadduct **476** derived from substituted [3]dendralene **385**. Calculations were also performed for non-Me substituted compound **401** to investigate whether conformational preferences were due to the substituent or the diene location, and thus probe the validity of **487** as a model for **476**. Me-substituted model **487** has two cyclohexanone conformers that are close in energy; a) a chair conformation cyclohexanone with an axial isopropenyl substituent, and b) a boat conformation cyclohexanone with a *quasi*-equatorial isopropenyl substituent. The energy difference between the two *cisoid* diene conformers is only 2.73 kJ/mol, and the lower energy (chair) form (**487-c1**) is only 4.93 kJ/mol higher in energy than the global minimum energy conformer. The skew angle of the *cisoid* diene is 39.3° in boat form **487-c2** and 41.2° in the chair form (**487-c1).** Non-Me substituted compound **401** was found to also have the same boat/chair conformation mix, suggesting that the change in conformation is not due to the substituent, but instead the location of the semicyclic diene.

Of note, the energy difference between the *s-trans* and *cisoid* conformers is lower for **487** than for **399a** derived from the parent [3]dendralene. It is reasoned therefore that the substituent of **487** (and **476**) and the location of the semicyclic diene, destabilises the *s-trans* diene conformation relative to the *cisoid* diene conformation through steric strain, thus making the *cisoid* diene conformation more accessible and the barrier to the second Diels–Alder reaction lower.

Interestingly, reaction of bicyclic diene **476** with (*R*)-carvone is also an example of double stereodifferentiation.[118] In reaction of [3]dendralene with (*R*)-carvone for example (Scheme 4.9), there is only one chiral reactant present and the reaction proceeds with high diastereoselectivity. The π-diastereofacial selectivity of the reaction is controlled solely by the chiral dienophile and thus is an example of 'single stereodifferentiation'.[118] In contrast, the reaction of bicyclic diene **476** with (*R*)-carvone involves two chiral reactants that can both influence the stereochemical outcome of the reaction. The diene and dienophile may be a 'matched' pair and both favour the same docking mode and formation of the same stereoisomer leading to high levels of stereoselectivity, or the diene and dienophile may prefer differing docking modes and formation of differing stereoisomers in a 'mismatched' pair, which may result in low selectivity.

As discussed previously in its reaction with the parent [3]dendralene (Scheme 4.9; Figure 4.5), addition of a diene to carvone occurs preferentially on the π-diastereoface of the cyclic C=C bond that avoids the isopropenyl substituent (Figure 4.15). Addition of a dienophile to bicyclic diene **430** is expected to occur from the top, less sterically hindered face (Figure 4.15). As can be appreciated from model **487-c1**, approach of the dienophile to the lower diene face would be blocked by both the fused cyclohexanone ring and the (Me/phenethyl) substituent (Figure 4.14).

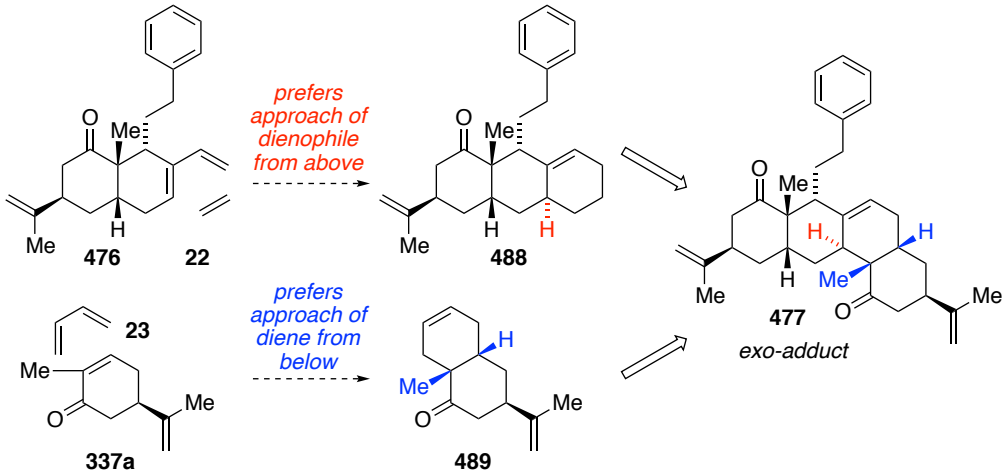

Figure 4.15 π-diastereofacial preferences of chiral diene **476** and (*R*)-carvone (**337a**)

In terms of regioselectivity, the activating (carbonyl) substituent of the dienophile is expected to be *ortho* to the activating 1-subsituent on the diene in the newly formed ring, as predicted by the *ortho-para* rule, wherein the 1-subsituent on the diene is expected to have a greater influence than the 2-substituent on the basis of FMO theory.[95] Therefore considering the Diels–Alder reaction between chiral bicyclic diene **476** and (*R*)-carvone *via* an *endo* transition state which benefits from favourable secondary orbital interactions (Figure 4.15; Figure 4.16a), the diene and dienophile are mismatched, with the dienophile favouring approach from the bottom face of the diene leading to **491** and the diene favouring approach of the dienophile from the top face leading to **490**. This concept of matched and mismatched reactants may be further appreciated by comparison to reaction of the same bicyclic diene **476** with (*S*)-carvone (Figure 4.16b). In contrast to reaction with (*R*)-carvone, reaction with (*S*)-carvone is expected to be matched; in an *endo* transition state both the diene and dienophile favour the formation of the same isomer (**494**).

Due to the mismatched nature of chiral bicyclic diene **476** and (*R*)-carvone, it is hypothesised that Diels–Alder reaction instead proceeds *via* an *exo* transition state, with approach of the dienophile from the top face of the diene (Figure 4.16a). While lacking secondary orbital interactions, this docking mode allows approach between the less sterically hindered faces of both the diene and dienophile. More work is needed however to confirm the proposed stereochemistry of **477**, whose assignment by single crystal X-ray analysis and HMBC and nOe NMR experiments was precluded due to its non-crystalline nature and congested NMR spectrum. To this end, computational studies are currently underway within the Sherburn group to predict and understand the outcome of this as well as related reactions.

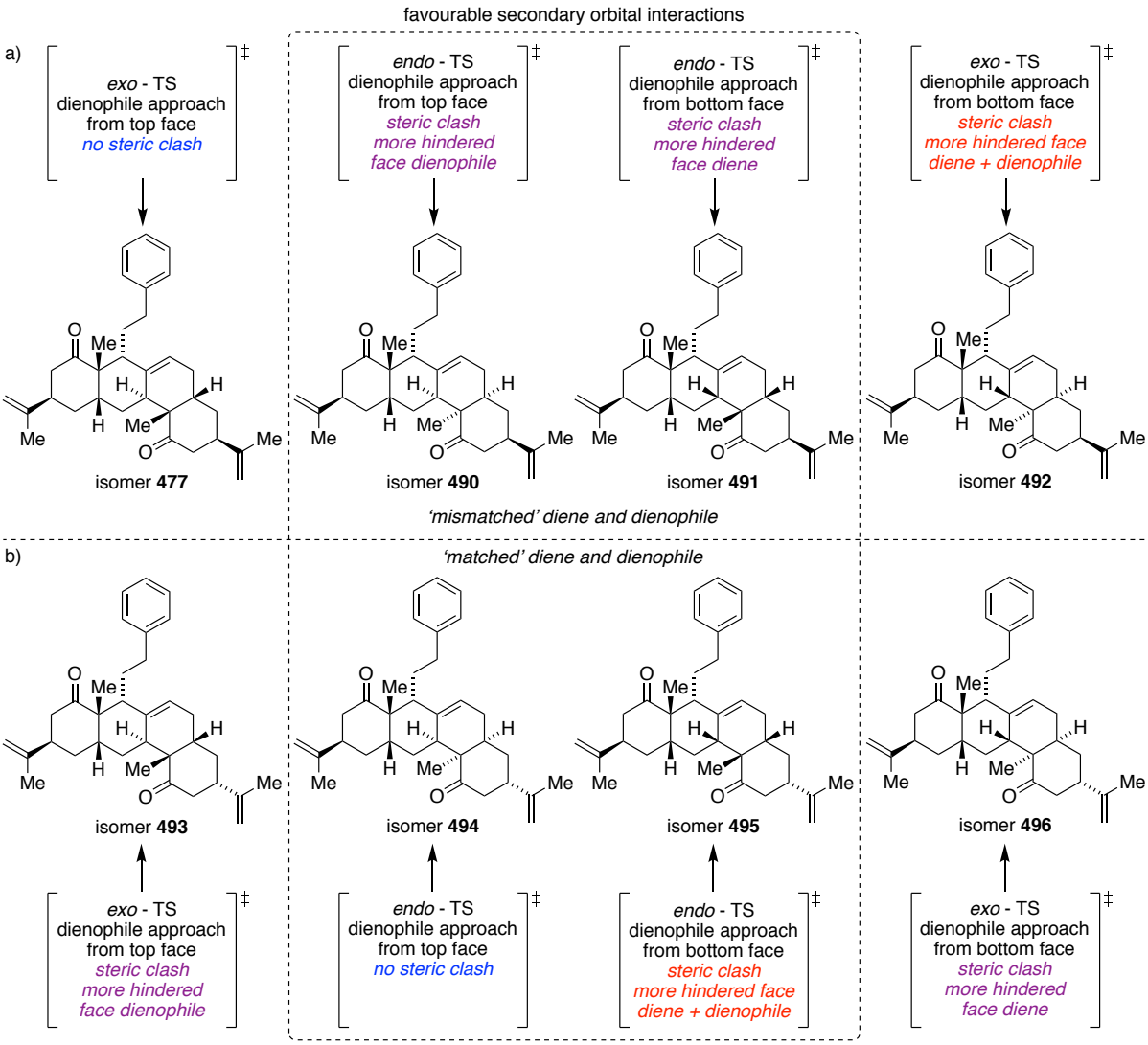

Figure 4.16 Possible diastereoisomeric outcomes from Diels–Alder reaction of bicyclic diene **476** with a) (*R*)-carvone or b) (*S*)-carvone. Stereoisomers arise from reaction through either an *endo* or *exo* transition state and approach of the dienophile from either the top or bottom face of the diene. Comparison between *endo* transition states for reactions involving (*R*)- and (*S*)-carvone highlight differences arising from double stereodifferentiation.

4.2.3 Bisadducts

We next turned our attention to the deliberate generation of Diels–Alder bisadducts, to generate tri- and tetracyclic products.

Adaptation of the previously developed Lewis acid catalysed (Me_2AlCl or $EtAlCl_2$) Diels–Alder reaction conditions for selective mono-cycloaddition to a multi-dienophile, one-pot DTDA reaction sequence was achieved conveniently *via* quenching of the Lewis acid with saturated aqueous sodium bicarbonate solution and treatment with an excess of a second,

more reactive, dienophile. Thus, cycloaddition reaction of both the parent and substituted [3]dendralenes **25** and **384**, with dienophiles (*R*)-carvone and NMM, proceeded well to afford Diels–Alder bisadducts (Scheme 4.30).

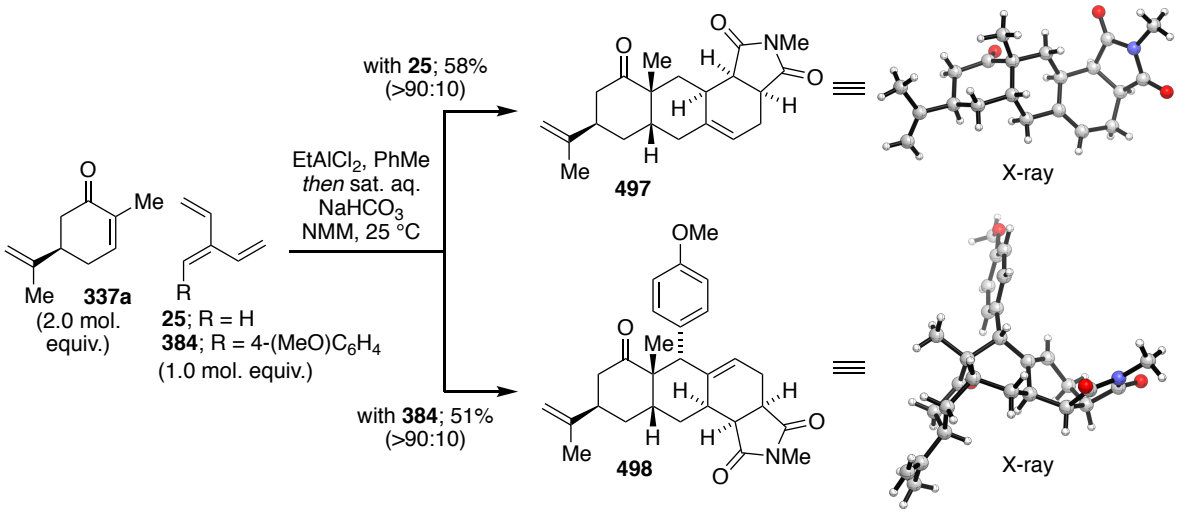

Scheme 4.30 One pot double Diels–Alder reaction sequences using (*R*)-carvone as the first dienophile; regio/diastereo-selectivity is quoted in parentheses as determined by analysis of crude ^{1}H NMR spectra

Gratifyingly, high levels of diastereoselectivity were exhibited in the second Diels–Alder reaction, arising from an *endo* transition state and selective approach of the dienophile from the less sterically hindered face of the diene. As depicted previously in calculated lowest energy conformations **399a-c1** and **487-c1** (Figure 4.14), approach of the dienophile to the bottom face of the diene would suffer steric clashes with the fused cyclohexanone ring, in particular the carbonyl group, and also with the substituent (Me/*para*-methoxyphenyl group) in the case of *para*-methoxyphenyl substituted diene **466** (modelled by Me-substituted diene **487**). The structures of bisadducts **497** and **498** were unequivocally confirmed by single crystal X-ray analysis.

These one-pot reaction conditions could also be employed utilising (*R*)-myrtenal as the first dienophile in the DTDA reaction sequence, with a variety of different dienophiles deployed in the second cycloaddition. Thus, reaction of the parent [3]dendralene with (*R*)-myrtenal, followed by DMAD (**404**), NMM (**388**), or PTAD (**501**) all afforded bisadducts in high yields and with good diastereoselectivity (Scheme 4.31).

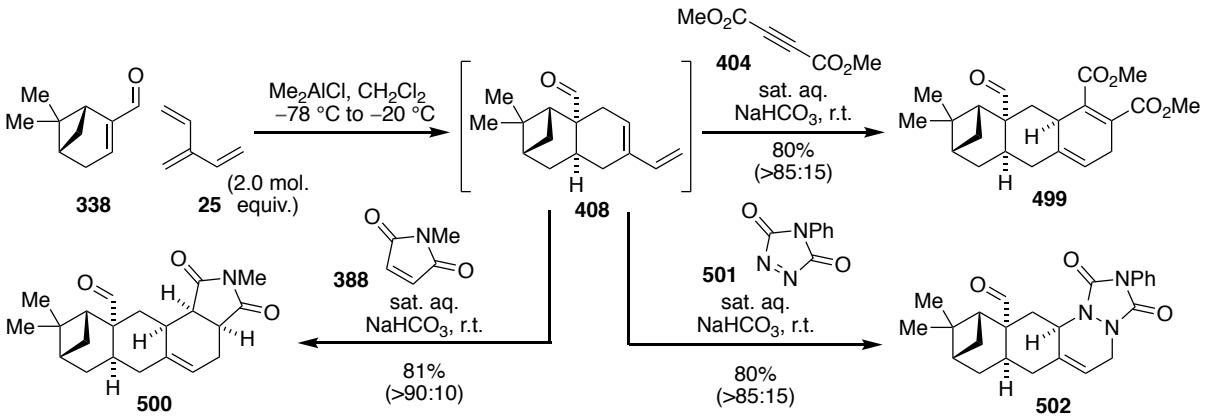

Scheme 4.31 One-pot DTDA reaction sequences of [3]dendralene (**25**) with (*R*)-myrtenal as the first dienophile. Regio/diastereo-selectivities are quoted in parentheses as determined by analysis of crude ^{1}H NMR spectra

In the case of bisadduct **499**, the major diastereomer is proposed to arise from selective approach of DMAD (**404**) from the top face of monoadduct **408**. Computationally, eight conformers were located within 15 kJ/mol of the minimum energy conformation for monoadduct **408**. These conformers differ in structure in a) the orientation of the formyl group (orientation about the C–CHO bond); b) the orientation of the diene (*s-trans* and *cisoid*) and c) the conformation of the cyclohexene ring (two distinct boat conformers, giving a more open S-shaped structure or a more compact U-shaped structure). The global energy minimum conformer has an *endo*-oriented formyl oxygen, an *s-trans* diene, and a U-shaped structure. The second lowest energy conformation (+1.55 kJ/mol) is the same as the lowest energy conformer, but with an *exo*-formyl group. The lowest energy *cisoid* diene, **408-c1** depicted in Figure 4.17, is the third lowest energy conformation overall (+6.03 kJ/mol), and has an *exo*-formyl group, a C=C–C=C dihedral of 34.3° and an S-shape. The fifth lowest energy conformation (**408-c2** (+8.95 kJ/mol) has an *endo* formyl group, a *cisoid* diene (dihedral 34.9°) and a U-shape. In the lower energy S-shaped conformation of *cisoid* diene **408-c1**, the lower face of the diene is blocked by the formyl group, while in the higher energy U-shaped conformation of *cisoid* diene **408-c2**, the top face of the diene is hindered by the bridging methylene of the cyclobutane ring. It is therefore theorised that approach of DMAD preferentially occurs to the less sterically hindered upper face of lower energy conformer **408-c1**, to produce observed isomer **499**.

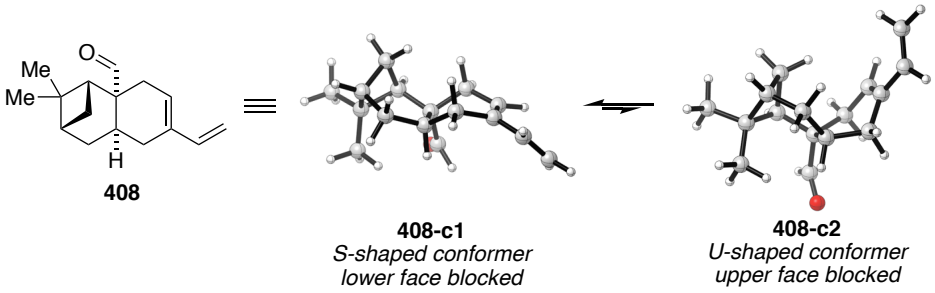

Figure 4.17 Calculated lowest energy *cisoid* diene conformations of chiral monoadduct **408**

Reaction of monoadduct **408** with PTAD (**501**) was observed to proceed with the same π-diastereofacial selectivity to form bisadduct **502**. In the case of bisadduct **500**, the major isomer is proposed to arise from an *endo* transition state and approach of NMM (**388**) again from the less sterically hindered, top face of chiral monoadduct **408**. These assignments are based upon HMBC and nOe NMR experiments performed on bisadducts **499**, **500** and **502** (Figure 4.18).

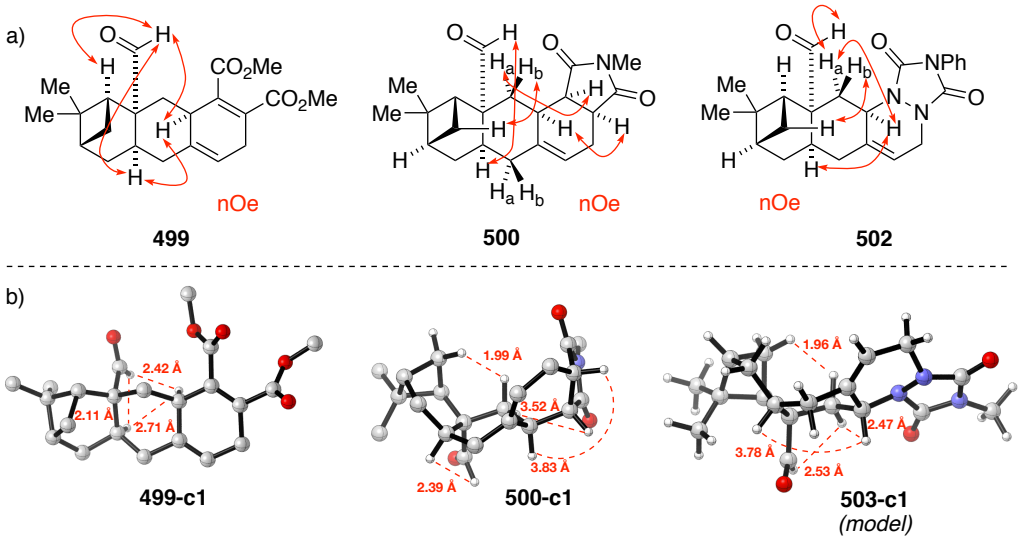

Figure 4.18 a) Double headed arrows depict key nOe NMR correlations in red; b) Calculated conformations with distances between protons for corresponding nOe correlations shown in red; **499-c1** lowest energy conformer; **500-c1** third lowest energy conformer (+9.98 kJ/mol); **503-c1** (N-Me model) lowest energy conformer. Some hydrogens are omitted for clarity.

Application of the one-pot reaction conditions with (*R*)-myrtenal to substituted [3]dendralene **384** was equally successful. In order to demonstrate the synthetic utility of this methodology, reaction with (*R*)-myrtenal and NMM (**388**) was performed to generate bisadduct **504** on multi-gram scale (Scheme 4.32).

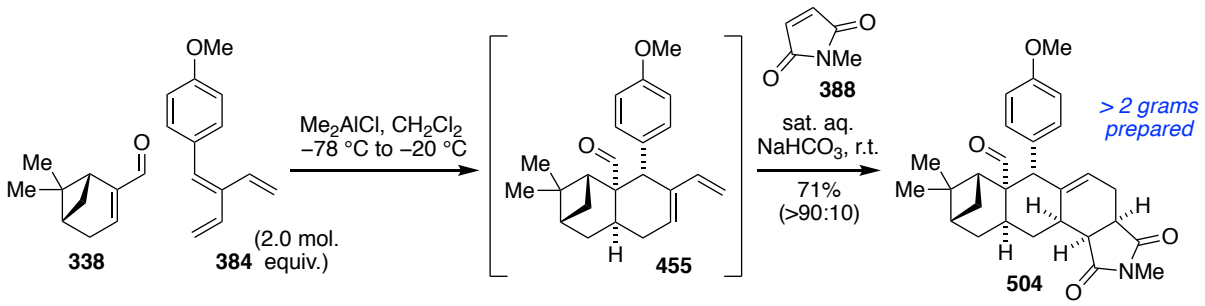

Scheme 4.32 Scalability of the one-pot diene-transmissive Diels–Alder reaction sequence: reaction of substituted dendralene **384** with (*R*)-myrtenal and NMM to yield bisadduct **504** on multi-gram scale. Regio/diastereo-selectivity is quoted in parentheses as determined by analysis of crude ^{1}H NMR spectra

The second cycloaddition reaction proceeded with high levels of diastereoselectivity, proposed to arise from an *endo* transition state and selective approach of NMM to the less sterically hindered face of the monoadduct, as predicted by calculated lowest energy conformations of methyl substituted diene model **505** (Figure 4.19). Computationally, nine conformers were located within 15 kJ/mol of the lowest energy conformation. As in the case of non-substituted diene **408**, the conformers differ in structure in a) the orientation of the formyl group (orientation about the C–CHO bond); b) the orientation of the diene (*s-trans* and *cisoid*); and c) the conformation of the cyclohexene ring (two distinct boat conformers). Regarding the orientation of the formyl group, the oxygen of the C=O bond points away from the tricyclic ring system in 5 conformers, and is located under the tricyclic portion in the remaining 4 cases. Regarding the orientation of the diene, 7 out of the 9 conformers have a *cisoid* conformation, with the C=C–C=C dihedrals ranging from 36.8-40.0°. The remaining two conformers have *s-trans* dienes (within 2° of an in-plane conformation). Regarding the conformation of the cyclohexene ring, 3 molecules have the diene portion flipped down (giving a more open, S-shaped structure) and 6 have the diene portion flipped up, towards the methylene bridge of the cyclobutane ring, giving a more compact U-shaped structure).

The global energy minimum conformer has an *endo*-oriented formyl oxygen, an *s-trans* diene, and a U-shaped structure. The second lowest energy conformation (+3.19 kJ/mol) is the same as the lowest energy one, but with an *exo*-formyl group. The lowest energy *cisoid* diene, **505-c1** (Figure 4.19), is the third lowest energy conformation overall (+6.23 kJ/mol), and has an *exo*-formyl group, a C=C–C=C dihedral of 39.8° and an S-shape. The fourth lowest energy

conformation, **505-c2**, (+9.52 kJ/mol) has an *endo* formyl group, a *cisoid* diene (37.0°) and a U-shape.

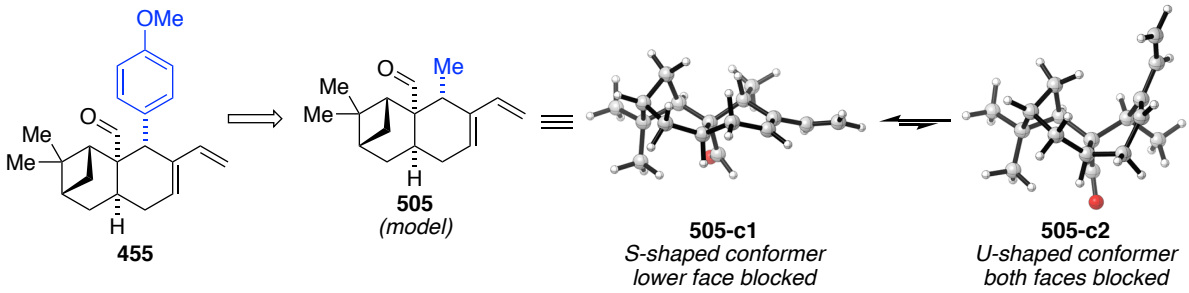

Figure 4.19 Calculated lowest energy *cisoid* diene conformations of Me-substituted model **505**

Both faces of the diene are blocked in the U-shaped conformation; the top face is hindered by the bridging methylene of the cyclobutane ring and the lower face by the (Me) substituent. In contrast, the upper face of the diene is more exposed in the S-shaped conformation, with the lower face blocked by the formyl group. Approach of NMM is therefore expected to occur to the less sterically hindered upper face of the monoadduct, as observed. This stereochemical assignment of was based upon HMBC and nOe NMR experiments performed on bisadduct **504** (Figure 4.20).

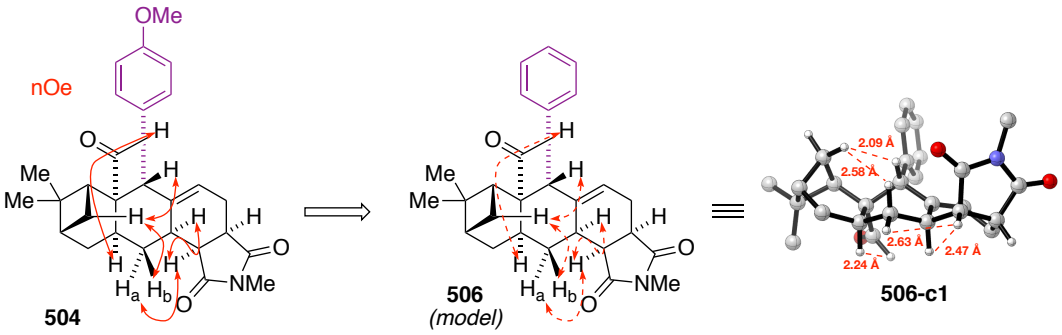

Figure 4.20 Double headed arrows depict key nOe NMR correlations for **504** in red. Calculated second lowest energy conformation of Ph-substituted model **506** is shown (+8.07 kJ/mol relative to an *endo* carbonyl –CHO rotated form), with distances between protons for corresponding nOe correlations shown in red. Some hydrogens are omitted for clarity.

The second cycloaddition of the DTDA reaction sequence could also be performed using relatively unactivated dienophiles under high pressure conditions (Scheme 4.33). Reaction of monoadduct **399b**, derived from (*S*)-carvone, with cyclohexenone afforded tetracycle **507** in 55% yield. Similarly, tetracycle **508** could also be generated from monoadduct **399a**, by

reaction with (*R*)-carvone. In these reactions, high levels of diastereoselectivity were exhibited in the second cycloaddition, proposed to arise from selective approach of the dienophile from the less sterically hindered, convex face of the chiral diene, as predicted (Figure 4.14a) and observed (Scheme 4.30) previously. Notably, in the latter case, in which the second dienophile is also chiral, the depicted stereoisomer is expected from double stereodifferentiation of a matched diene-dienophile pair; in an *endo* transition state, both the diene and dienophile favour the formation of the same isomer, which arises from approach between the less sterically hindered faces of both the diene and dienophile. High levels of regioselectivity were also observed in these reactions, as predicted by the *ortho-para* rule, with the 1-subsituent on the diene having a greater influence than the 2-subsituent, as expected on the basis of FMO theory.[95]

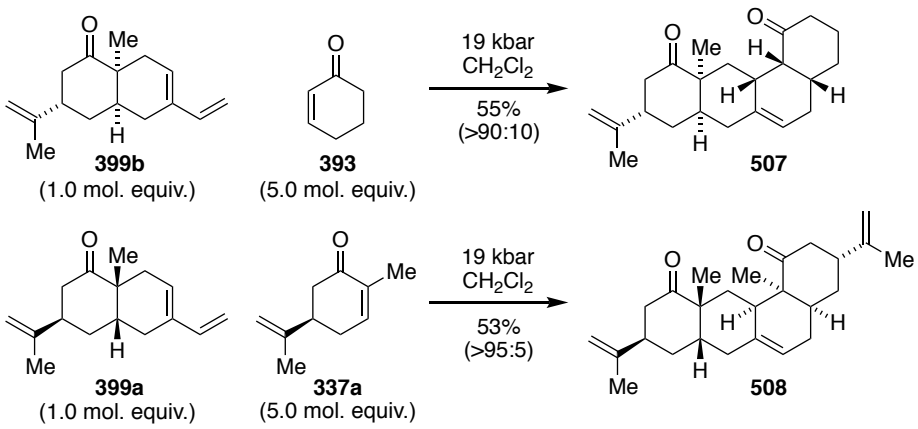

Scheme 4.33 Ultra-high pressure Diels–Alder reactions of chiral bicycles **399** with cyclohexenone and (*R*)-carvone. Regio/diastereo-selectivities are quoted in parentheses as determined by analysis of crude ^{1}H NMR spectra

Unfortunately, overlapping signals in the ^{1}H NMR spectrum and the non-crystalline nature of **507** and **508** precluded full assignment of regio- and stereochemistry for these bisadducts by single crystal X-ray analysis or HMBC and nOe NMR experiments. Instead assignment of regio- and stereochemistry arising from the second cycloaddition is based upon analogy to structurally similar Diels–Alder bisadducts **509**, **510** and **497** (Figure 4.21; see also Scheme 4.30 and Chapter 2), whose structures were unequivocally confirmed by single crystal X-ray analysis.

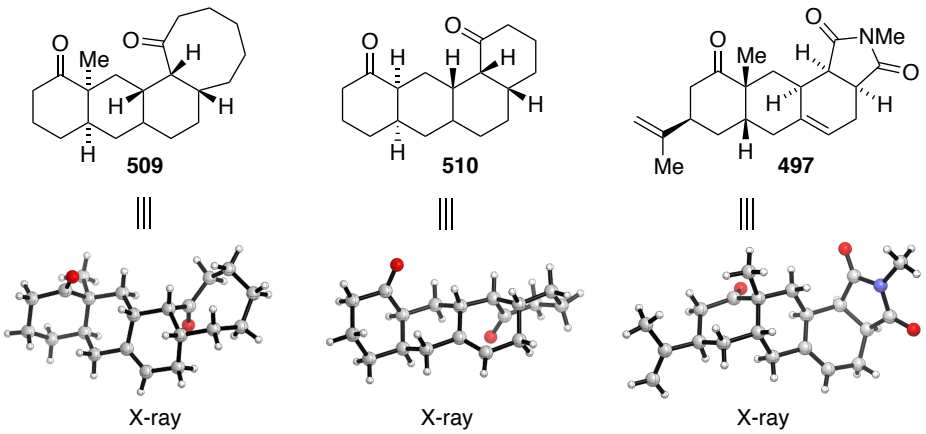

Figure 4.21 Diels–Alder bisadducts structurally similar to **507** and **508**

Lastly, a one-pot DTDA reaction sequence using (*R*)-carvone as both the first and second dienophile was developed using promotion by $EtAlCl_2$ (Scheme 4.34). Significantly, this achieved the second Diels–Alder reaction with (*R*)-carvone without the need for ultra-high pressure conditions, albeit in moderate yield.

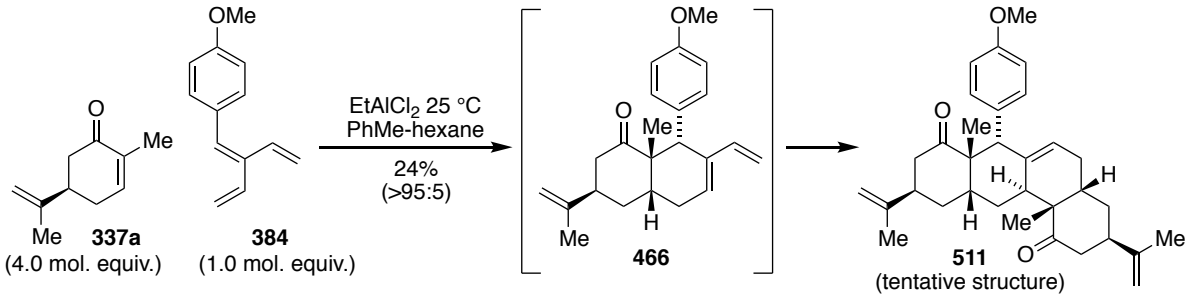

Scheme 4.34 Lewis acid catalysed DTDA reaction sequence of substituted [3]dendralene **384** and (*R*)-carvone. Regio/diastereo-selectivity is quoted in parentheses as determined by analysis of crude ^{1}H NMR spectra; assignment of stereochemistry arising from the second Diels–Alder reaction is tentative

High levels of regioselectivity were observed in the second cycloaddition reaction, as predicted by the *ortho-para* rule, wherein the 1-subsituent on the diene is expected to have a greater influence, on the basis of FMO theory.[95] As in the formation of **477** (Scheme 4.28; Figures 4.15 and 4.16), the second cycloaddition of this reaction sequence is also an example of double stereodifferentiation in which the diene and dienophile are mismatched. As discussed previously in its reaction with the parent [3]dendralene (Scheme 4.9; Figure 4.5), addition of a diene to carvone occurs preferentially on the π-diastereoface of the cyclic C=C bond that avoids

the isopropenyl substituent, while dienophile approach to the less sterically hindered, convex top face of chiral diene **466** is expected, as predicted (Figure 4.14) and observed (Scheme 4.30) previously. Thus, in an *endo* transition state the dienophile favours approach from the bottom face of the diene, while the diene favours approach of the dienophile from the top face. Consequently, the reaction is proposed to proceed *via* an *exo* rather than *endo* transition state, to enable approach between the less sterically encumbered faces of both the diene and dienophile. While overlapping signals in the ^{1}H NMR spectrum and the non-crystalline nature of **511** precluded full assignment of regio- and stereochemistry from the second cycloaddition reaction by single crystal X-ray analysis or HMBC and nOe NMR experiments, recent studies within the Sherburn group which build upon the work described in this chapter provide some precedent for this predicted stereoselectivity.[119] Thermal reaction of (–)-levoglucosenone with phenethyl-substituted dendralene **385** afforded bisadduct **513** (Scheme 4.35).

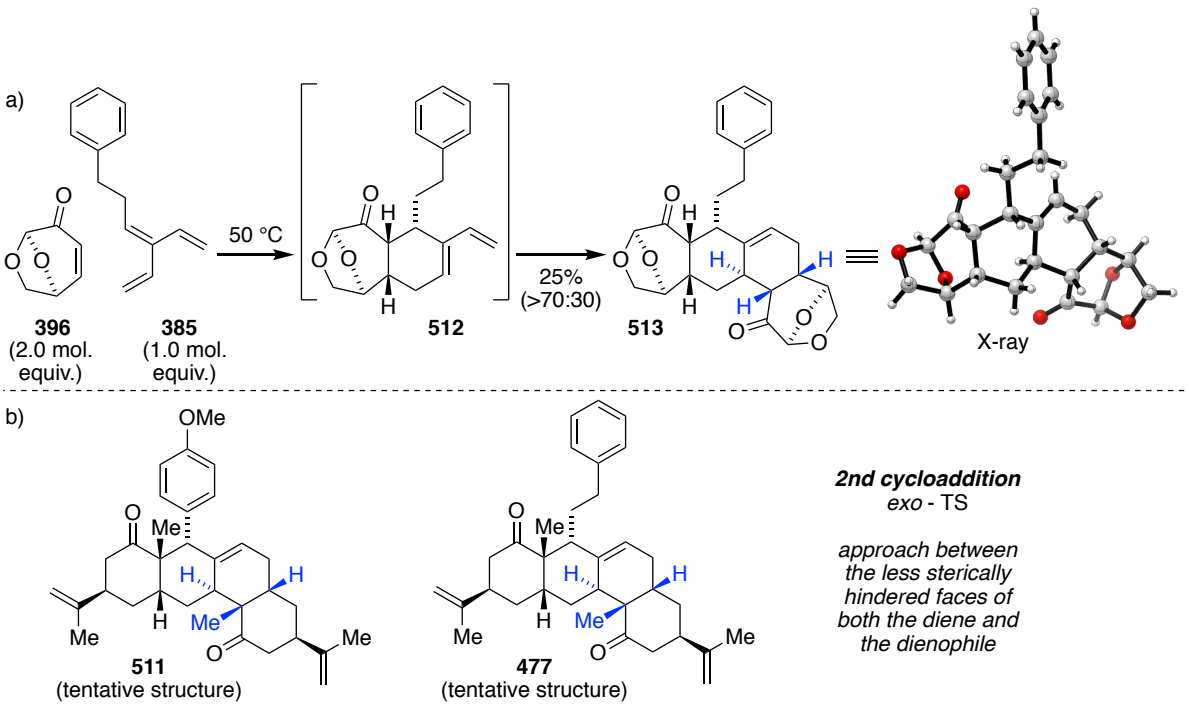

Scheme 4.35 a) DTDA reaction sequence of substituted [3]dendralene **385** and (–)-levoglucosenone (**396**).[119] Regio/diastereo-selectivity is quoted in parentheses as determined by analysis of crude ^{1}H NMR spectra; b) Predicted stereochemistry of bisadducts **511** and **477**. Stereochemistry arising from the second Diels–Alder cycloaddition is highlighted in blue.

In the second cycloaddition reaction of this sequence, chiral diene **512** and (–)-levoglucosenone are a mismatched pair. As discussed previously in its reaction with the parent [3]dendralene

(Scheme 4.15), addition of a diene to (–)-levoglucosenone occurs preferentially to the less sterically hindered –O– bridged face of the molecule, away from the $–CH_2O–$ bridge face, while dienophile approach to the less sterically hindered, convex top face of chiral diene **512** is expected to be favoured. This can be appreciated in the calculated lowest energy conformations for Me-substituted model diene **514** (truncated for calculation purposes due to the conformational flexibility of the phenethyl substituent) in which the top face of the diene appears to be significantly more accessible than the bottom face (Figure 4.22).

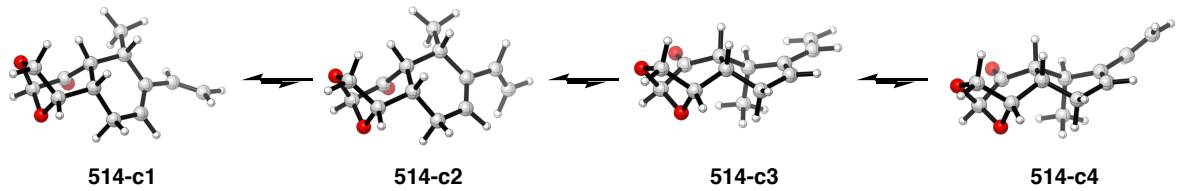

Figure 4.22 The calculated four lowest energy conformations of chiral diene **514**. Left to right, lowest to highest energy.

Thus, in an *endo* transition state the diene and dienophile are expected to prefer approach from opposite faces. Indeed, the observed stereochemistry of **513**, whose structure was unequivocally confirmed by single crystal X-ray analysis, is consistent with an *exo* rather than *endo* transition state, allowing approach between the less sterically encumbered faces of both the diene and dienophile. As can be appreciated in Scheme 4.35, this is consistent with the stereochemistry proposed for bisadducts **511** and **477.**

Of interest, as discussed previously in its reaction with dienophiles (*R*)-carvone and NMM (Schemes 4.28a and 4.29a), Diels–Alder reaction of phenethyl substituted dendralene **385** with (–)-levoglucosenone also exhibited a propensity of the second Diels–Alder reaction in the DTDA reaction sequence to occur faster than the first, further supporting the generality of these results.

In the case of levoglucosenone-derived diene **512**, the faster rate of the second Diels–Alder reaction can be rationalised by closer examination of the calculated lowest energy conformations of Me-substituted model **514** (Figure 4.22). The levoglucosenone-derived portion of the molecule is conformationally rigid, adopting the same shape in each conformation. When the annulated cyclohexane ring sits in the (preferred) half chair conformation, the (Me) substituent is *quasi*-equatorial. With the (Me) substituent in this orientation, the adjacent vinyl group cannot adopt the (usually more favoured) *s-trans*

conformation, due to steric repulsion, and the *cisoid* diene conformation is preferred. A less skewed *cisoid* diene would also suffer steric repulsion, as evidenced by the larger C=C–C=C dihedrals of 46.1° and 45.8° in the two lowest energy conformations, **514-c1** and **514-c2**. These two lowest energy conformers differ only in the orientation of the vinyl group relative to the cyclohexene ring, being twisted either up or down respectively, and differ only in 0.71 kJ/mol. When the cyclohexene ring adopts the boat conformation, the (Me) substituent is *quasi*-axial and the diene is free to adopt the *s-trans* conformation, as seen in the 3rd lowest energy conformation, **514-c3**, which lies 2.72 kJ/mol above the minimum energy conformation. The final conformer located within 15 kJ/mol of the minimum energy conformation, **514-c4** (+13.10 kJ/mol), has a boat cyclohexene, akin to the third lowest energy conformation, but possesses a *cisoid* diene. Free of the steric repulsion from the adjacent (Me) substituent, this *cisoid* diene exhibits a significantly less skewed conformation (C=C–C=C dihedral = 33.8°).

The preference of this molecule to adopt the *cisoid* diene conformation explains its heightened reactivity as a Diels–Alder diene relative to the precursor 3-substituted-[3]dendralene and thus the increased rate of the second Diels–Alder reaction. This is congruent with predictions based on computational ground states for reaction of phenethyl-substituted dendralene **385** with (*R*)-carvone discussed previously (Figure 4.14).

4.3 Future Work

4.3.1 Conclusions and Future Prospects

This chapter described the development of the first DTDA reaction sequences employing enantio-enriched dienophiles in the leading Diels–Alder reaction of the double cycloaddition sequence. The first Diels–Alder reactions of [3]dendralenes with enantio-enriched dienophiles were developed, including novel use of the chiral building block (*R*)-myrtenal as a C=C dienophile (Figure 4.23).

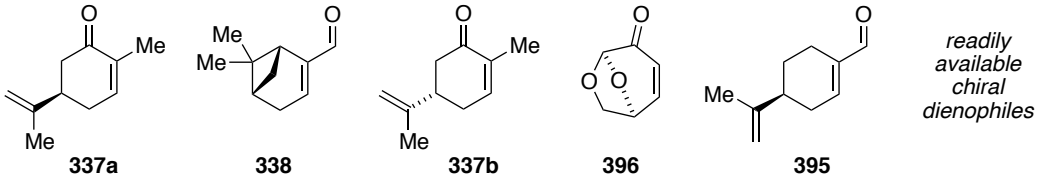

Figure 4.23 Readily available chiral building blocks employed in DTDA reaction sequences

It was demonstrated that substitution of the [3]dendralenes can influence both their selectivity and reactivity in DTDA reaction sequences. Notably, opposite regioisomeric outcomes were

observed from reaction of the parent [3]dendralene (**25**) and internally substituted dendralenes **384**, **386** and **385**. Diels–Alder reaction of internally substituted [3]dendralenes bearing electron rich substituents proceeded more rapidly than their electron poor counter parts (Figure 4.24). This may be rationalised by the greater energy gap experienced between the HOMO of the diene and LUMO of the dienophile when the HOMO of the diene is more electron deficient and thus lower in energy.

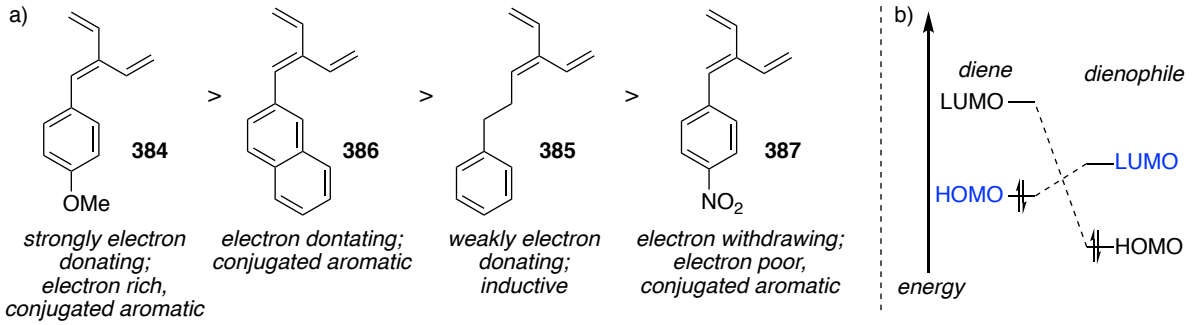

Figure 4.24 a) Relative reactivity of internally substituted [3]dendralenes in the initial Diels–Alder reaction; b) Diene-dienophile HOMO-LUMO overlap

The methods developed allow the rapid generation of enantiomerically pure polycyclic structures, using commercially available chiral building blocks in diene-transmissive Diels–Alder (DTDA) reaction sequences of dendralenes. A summary of mono- and bisadducts synthesised is given in Tables 4.3 and 4.4.

Table 4.3 Monoadducts synthesised from Diels–Alder reaction of [3]dendralenes with readily available chiral dienophiles

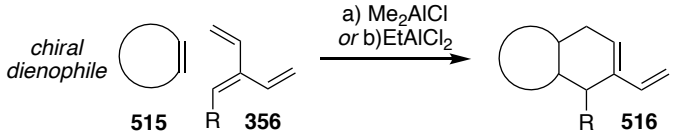

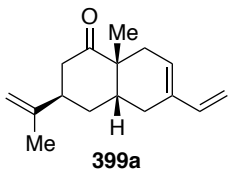

399a

35%[a]; 52%[b] (>95:5)

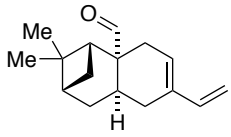

408

71%[a] (>95:5)

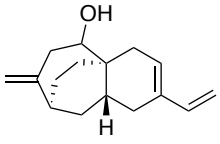

416

51%[a] (1:1)

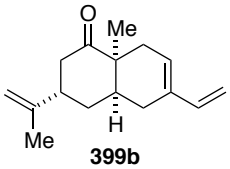

399b

36%[a]; 50%[b] (>95:5)

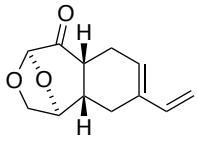

428

36%[c] (>95:5)

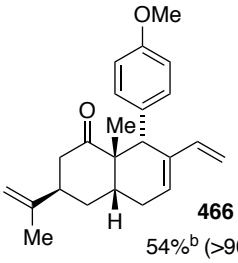

466

54%[b] (>90:10)

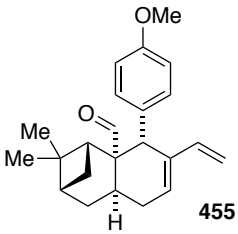

455

60%[a] (>90:10)

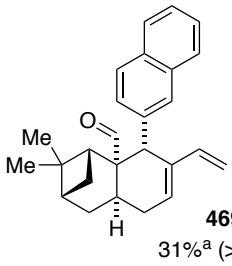

469

31%[a] (>80:20)

Regio/diastereo-selectivities are quoted in parentheses as determined by analysis of crude ^{1}H NMR spectra. [a] Me_2AlCl catalysed; [b] $EtAlCl_2$ catalysed; [c] neat room temperature.

Table 4.4 Bisadducts synthesised from Diels–Alder reaction of [3]dendralenes with readily available chiral dienophiles[a]

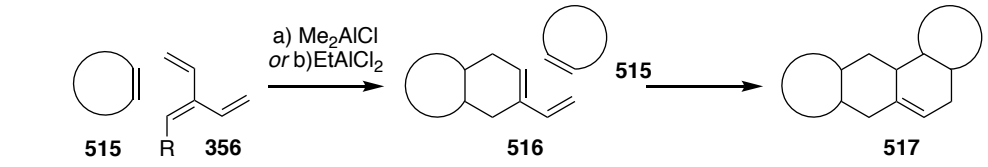

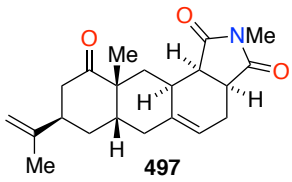

497
58% (>90:10)

≡

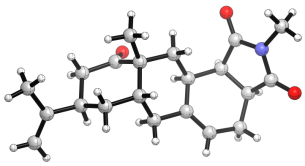

X-ray

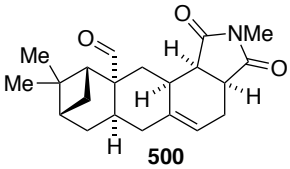

500
81% (>90:10)

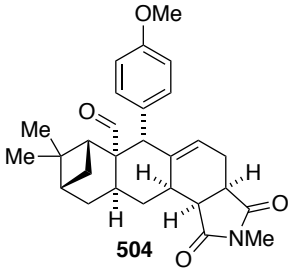

504
71% (>90:10)

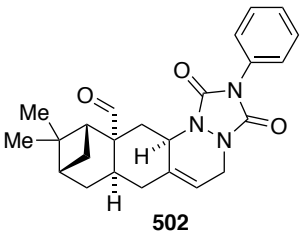

502
80% (>85:15)

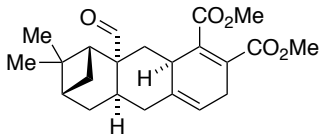

499
80% (>85:15)

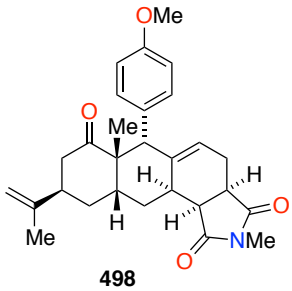

498
51% (>90:10)

≡

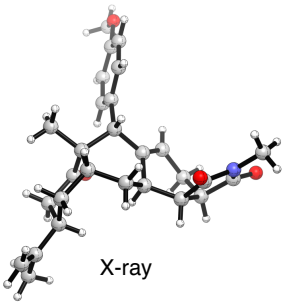

X-ray

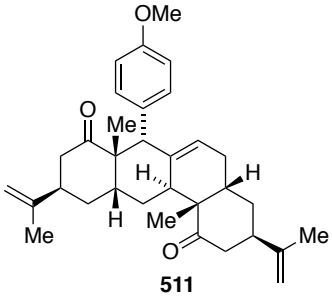

511
24%[b] (>95:5)

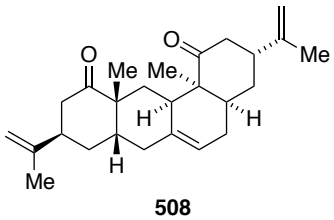

508
53%[c] (>95:5)

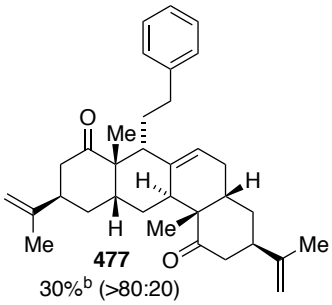

477
30%[b] (>80:20)

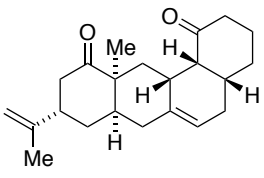

507
55%[c] (>90:10)

[a] Unless otherwise specified, yields refer to products from one-pot double Diels–Alder reaction sequences, involving a first Lewis acid catalysed Diels–Alder reaction, followed by quenching with sat. aq. $NaHCO_3$ and a second uncatalysed Diels–Alder reaction at room temperature. Regio/diastereo-selectivities are quoted in parentheses as determined by analysis of crude ^{1}H NMR spectra; [b] Double Lewis acid catalysed Diels–Alder reaction; [c] Yield from monoadduct as starting material, ultra-high pressure Diels–Alder reaction.

The results of this work have aided in the application of chiral building blocks in other Diels–Alder reactions within the Sherburn group and work is currently being undertaken to expand the library of bisadducts synthesised, as well as to further probe the scope and effects of substituted [3]dendralenes on this sequence.

We envisage this methodology will be amenable to extension to higher order dendralenes, such as [4]dendralenes, as well as to other π-bond rich hydrocarbons such as allenic dendralenes. Notably, these molecules are also compatible with Lewis acid catalysis.

To this end, it is of note that Diels–Alder reaction site selectivity of [4]dendralenes may be directed by different patterns of substitution on the dendralene (Scheme 4.36a).[120] As an interesting aside, preliminary investigations into the Diels–Alder reaction of allenic dendralene **521** using $MeAlCl_2$ catalysis have also revealed useful selectivity (Scheme 4.36b). Varying molar equivalents of Lewis acid were found to give rise to complementary diastereomeric products with the dienophile NMM, an outcome which, if general, may find useful application with reaction of allenic dendralenes and chiral dienophile building blocks.

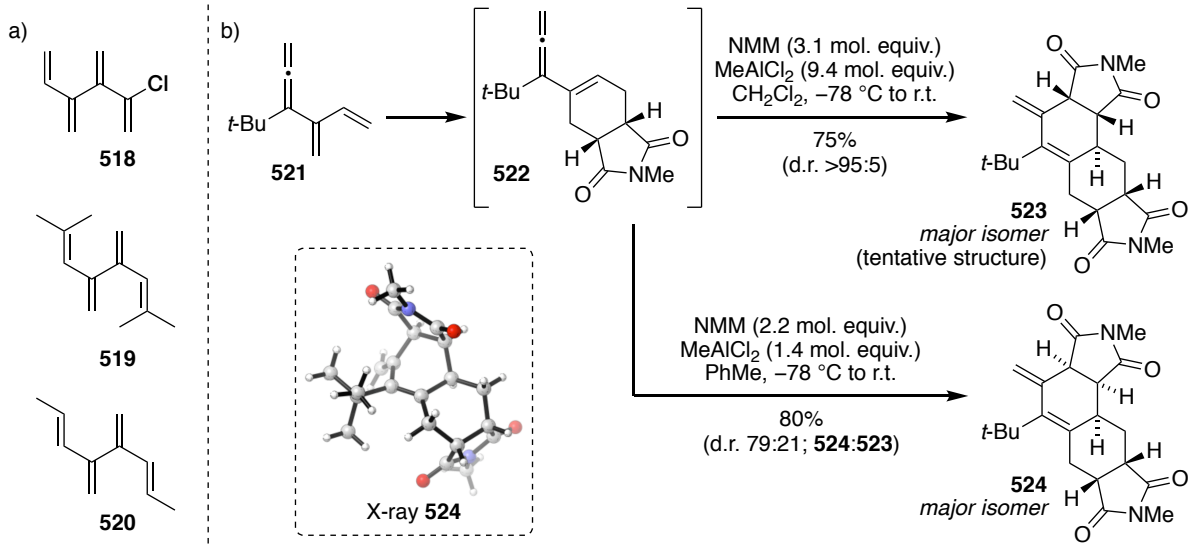

Scheme 4.36 a) Potential application to Diels–Alder reaction of [4]dendralenes, especially where dendralene substituents guide site selectivity; b) Lewis acid catalysed, diastereoselective Diels–Alder reaction of allenic dendralene **521**. Diastereo-selectivities are quoted in parentheses; stereochemical assignment of **523** is tentative.

The work described in this chapter has also set the scene to examine other chiral dienophiles, including both naturally occurring chiral building blocks[121] and those which are readily synthesised[74, 122] (Figure 4.25).

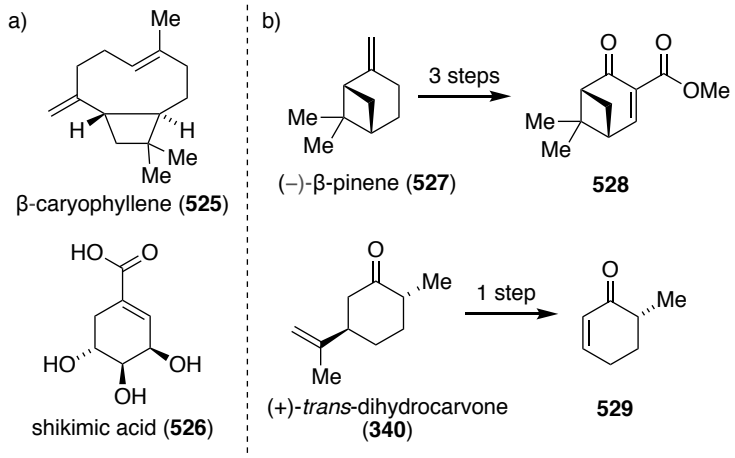

Figure 4.25 Examples of other potential dienophiles; a) Naturally occurring, commercially available chiral building blocks; b) Readily derived chiral building blocks.[74, 122a] [122b]

Furthermore, we predict the potential for not only pre- but also post Diels–Alder modification of the chiral building blocks employed. To this end, recent work reported by Kwon and co-workers,[123] which describes the hydrodealkenylative cleavage of $C(sp^3)$–$C(sp^2)$ bonds (Scheme 4.37), presents an interesting possibility. While the isopropenyl substituent of carvone is required for transmission of chirality in the DTDA reaction sequence, this technique may allow for later convenient removal of this directing moiety; a strategy that would be particularly powerful, given that both enantiomers of carvone are readily available. The similarity between Diels–Alder bisadduct **497** and substrate **530**, reported by Kwon and co-workers, can be appreciated in Scheme 4.37.

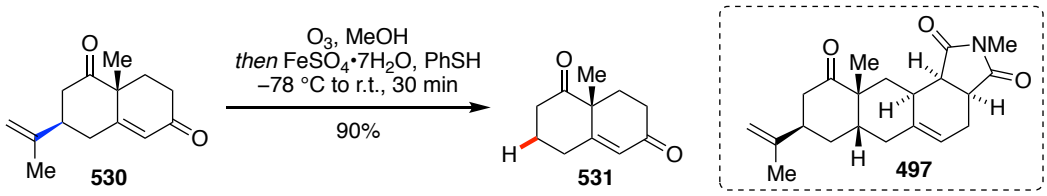

Scheme 4.37 Hydrodealkenylative $C(sp^3)$-$C(sp^2)$ bond fragmentation;[123] C–C σ-bond cleaved highlighted in blue; new C–H bond highlighted in red.

Finally, we anticipate the developed methodology may be expanded to a DTDA-cyclopropanation sequence (Scheme 4.38). This triple cycloaddition sequence would exhaustively elaborate all C=C π-bonds originating from [3]dendralene, thus taking advantage of its full potential to introduce molecular complexity.

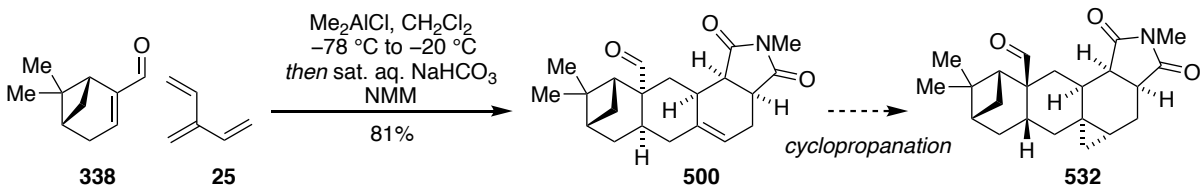

Scheme 4.38 Potential exhaustive pericyclic sequence of [3]dendralene

We believe this work as a whole will provide access to many synthetically useful structures by not only rapidly generating molecular complexity, but by doing so in enantiopure form.

5

Strategic Applications of Intramolecular Diels-Alder Reactions in Target Synthesis

5.1 Context

This chapter provides a review of the intramolecular Diels–Alder (IMDA) reaction. The IMDA reaction is a powerful synthetic technique and has enjoyed extensive use in the construction of complex molecular targets.

The last attempts to exhaustively review the IMDA reaction were published in 1984,[124] perhaps because its prevalence has since prevented a comprehensive review of the field, with more than 5000 publications focussed on the IMDA reaction at the time of writing of this thesis.[i]

[i] A research topic search on the "Intramolecular Diels–Alder Reaction" in SciFinder Scholar returned ~5000 references as of August 2020.

Nevertheless, the following review aims to highlight the most original and significant total synthesis applications of the IMDA reaction to date, and to discuss and critique their selectivity and strategic implications. It also endeavours to identify underdeveloped areas and predict likely future work in this important field.

This chapter has been written and formatted for publication as an invited review by the journal *Angewandte Chemie*, but at the time of completion of this thesis, has not yet been submitted. As such, compound numbering and references are distinct from those in other chapters of this thesis. References for this Chapter are provided in Chapter 7.

The other authors listed on the manuscript are Professor Michael S. Sherburn, Dr Imants Kreituss, Dr Supanimit Chiampanichayakul and Mr Nicholas Magann. All authors collaborated in the conception, development and writing of the manuscript.

WILEY-VCH

REVIEW

Strategic Applications of Intramolecular Diels-Alder Reactions in Target Synthesis

Supanimit Chiampanichayakul, Natalie Shadwell, Imants Kreituss, Nicholas Magann and Michael S. Sherburn*

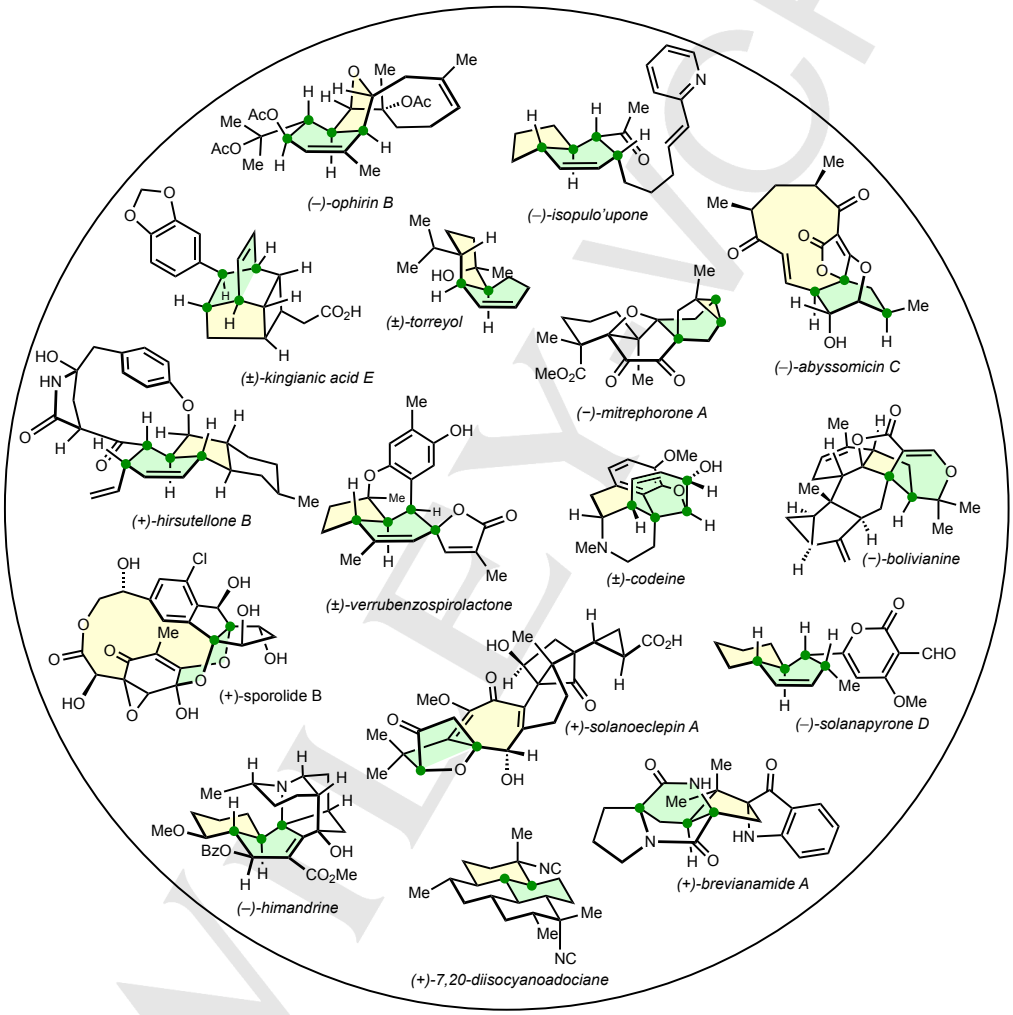

WILEY-VCH

REVIEW

[a] Dr S. Chiampanichayakul, N. Shadwell, Dr I. Kreituss, N. Magann, Prof M. S. Sherburn
Research School of Chemistry
Australian National University
Canberra, ACT 2601 (Australia)
E-mail: michael.sherburn@anu.edu.au

Abstract: The intramolecular Diels-Alder (IMDA) cycloaddition is more than a reaction: instead, it is a strategic maneuver and defining feature of every target synthesis in which it is deployed. The immense synthetic power of the process is evidenced by its creation of a substantial, bicyclic portion of a target structure in a single, concerted two-bond-forming event. The deceptive simplicity of the unimolecular Diels-Alder process is revealed, upon closer inspection, to be both mechanistically complex and of extremely broad scope. In this Review, we highlight important recent target synthesis contributions involving the IMDA reaction, and frame them within the context of earlier, groundbreaking contributions.

1. Introduction

The Diels-Alder (DA) reaction[1] is the most powerful single-step process in synthetic chemistry. Its most potent asset is the generation of the most prevalent cyclic system, namely the six-membered ring, in the most direct manner, over an impressively broad range of structural variations. The concerted [4+2] cycloaddition proceeds with the generation of a six-membered ring and two covalent bonds through the union of two components, namely a diene and a dienophile. The "diene" is a conjugated 4π electron fragment, commonly a 1,3-butadiene unit, and the dienophile is a 2π electron component, frequently a C=C double bond. The process is, however, by no means limited to these functionalities. In fact, a plethora of 2π and 4π units incorporating elements other than carbon and systems involving triple bonds have been reported.

In terms of rapid structural complexity generation, the **i**ntra**m**olecular **D**iels-**A**lder (IMDA) reaction outshines the intermolecular process. The generalized (but by no means comprehensive set of) equations depicted in **Scheme 1** demonstrate that the covalent tethering of a diene to a dienophile *always* creates a cycloaddition product with an additional ring, irrespective of either diene/dienophile substitution or the number of pre-existing rings. **Scheme 1** also introduces a convention of ring fill colorization that is used throughout this review to facilitate understanding, specifically: (a) green for the ring formed directly in the cycloaddition; (b) yellow for the ring formed by the tether connecting the diene and dienophile, and (c) blue for pre-existing rings.[2]

A comprehensive survey of the DA reaction has not been published for over 50 years and for good reason: at the time of completion of this manuscript (December 2020), approximately 50,000 publications on the topic exist.[3] A conservative estimate of the proportion describing the intramolecular variant is 5,000,[3] a number that precludes an exhaustive treatment of the field.

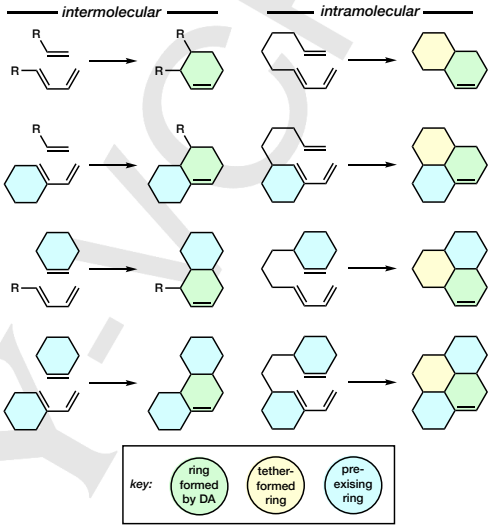

Scheme 1. A comparison of structural complexity generation from (left) intermolecular and (right) intramolecular DA reactions between (top) acyclic dienes and dienophiles through to (bottom) cyclic ones.

The earliest comprehensive reviews of the IMDA reaction were by Oppolzer in 1977,[4] Brieger and Bennett in 1980,[5] Taber in 1984,[6] Ciganek in 1984,[7] and Fallis in 1984.[8] These first five reviews serve important roles in documenting and categorizing the earliest work in the field. The subsequent reviews by Craig in 1987[9] and Roush in 1990[10] and 1991[11] represent the first attempts to provide detailed explanations of the influence of substrate structure upon IMDA stereoselectivity. A review of the DA reaction in total synthesis by Nicolaou and coworkers was published in 2002, which contains a substantial number of IMDA examples.[12] In the previous year, Shea reviewed the Type 2 IMDA reaction[13] and Deslongchamps reviewed the transannular DA reaction.[14] Reviews summarizing recent aspects of the IMDA reaction in total synthesis were published in 2005,[15] 2009[16] and 2015.[17] In 2014, Tanner and Ascic published a broader review as an update to Roush's 1991 work.[18] Other reviews have generally been selective, either focusing on specific subgroups of IMDA reactions, such as those involving furans as dienes or imines as dienophiles, or those involved in the total synthesis of specific groups of natural products.[19] These reviews are an excellent source of information. We neither reproduce the format of these important contributions here, nor their treatment of the primary literature.

In the present review, we bring together, discuss and critique the most significant primary literature involving IMDA reactions in total synthesis. Our review differs significantly from previous ones in both the selection of examples and their treatment.

In terms of content, the main focus is on IMDA reactions in total synthesis: we specifically identify what each IMDA process contributes to a synthesis, in terms of molecular complexity creation. While the focus is on the most recent contributions, we also include important work from the earlier literature, with new insights made possible due to the current, better understanding of the IMDA process. In terms of breadth of coverage, we survey the most prevalent sub-classes of IMDA reactions from the literature. A major consideration in the majority of total synthesis applications of IMDA processes is stereoselection. Consequently, throughout the review, we discuss instructive aspects of stereoselectivity. In many cases, the discussion provided here is our own interpretation.

We also cover some of the many methodological contributions that represent the most general, powerful and enabling synthetic technologies involving IMDA processes. Synthetic methods are not included in a separate section but instead are integrated into the discussion of total syntheses, to provide a more engaging narrative to this lengthy survey.

A significant difference from previous reviews is our chosen style of graphical representation. We provide a perspective sketch of each transition state structure (TS) to assist an understanding of the stereoselectivity of every IMDA reaction, and in most cases a perspective representation of the IMDA product and target molecule. Often, these TSs were neither provided nor discussed in the original research article. Many structures have been reoriented for consistency of presentation, specifically to assist in the recognition of repeated patterns of substrate behavior. These sketches are derived from X-ray crystal structures, where these are available, or DFT computed conformations where they are not. We take full responsibility for the inevitable (hopefully minor) errors that result from these changes in orientation, and our own interpretation.

In addition to the color fill identifiers for rings in structures (see **Scheme 1** and associated text), we also identify stereocenter carbons with colorized bullets. Stereocenters generated directly by the [4+2] cycloaddition process are green, pre-existing stereocenters from substrates are blue, and stereocenters in the target molecule formed *after* the IMDA event are grey. We introduce this method to facilitate the mapping of IMDA precursors, TSs, IMDA products and target molecules, and, in combination with ring color fills, to draw attention to the significant target-relevant complexity introduced during the IMDA process. We are aware that the so-called "H-Dot representation" for a *β*-face hydrogen attached to a stereocenter is still applied by some researchers, although IUPAC recommends against its use.[20] We hope that the reader finds this inclusion neither confusing nor controversial.

1.1. Classes of IMDA Reactions

The IMDA reaction exhibits extraordinarily broad scope. Nevertheless, a relatively small number of sub-categories can be identified, through the systematic analysis of IMDA precursor structure. To state the obvious, every precursor of an IMDA reaction contains a 4*π* portion, a 2*π* portion, and a tether that connects them. One of the most fundamental sub-categorizations of IMDA reactions spotlights the point of attachment of the tether to the diene (**Scheme 2**).

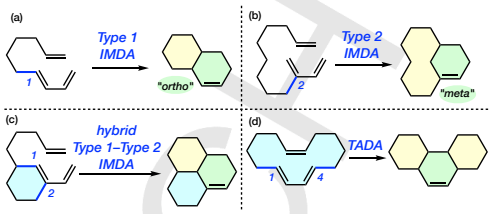

Scheme 2. Classes of IMDA reactions: (a) Type 1 IMDA reactions involve a single connection of the tether to C1 of the diene, whereas (b) Type 2 IMDA reactions involve a single connection of the tether to C2 of the diene (right). With two connecting points, either (c) Type 1-Type 2 hybrid or TADA processes are feasible. (IMDA = intramolecular Diels-Alder; TADA = transannular Diels-Alder.)

With a single point of connection of the dienophile to the diene, there are two possibilities: connection at C1 of the diene, which gives a fused bicycle through a Type 1 IMDA reaction (**Scheme 2a**), or connection at C2 of the diene, which leads to a bridged ring system by way of a Type 2 IMDA process (**Scheme 2b**). IMDA reactions are dominated by examples involving *proximal* regioselection, meaning they proceed with bond formation between the pairs of atoms on the ends of the diene and dienophile that are closest to the tether, leading to "*ortho*" and "*meta*" cyclohexenes, respectively. It should be noted, particularly when dealing with longer tethers, that the opposite (i.e. *distal*) diene-dienophile orientational regioselectivity may also be feasible. Indeed, such an outcome might be preferred, if the tether conformation or diene/dienophile substituents steer the reaction this way. By a very wide margin, the most studied category of these four IMDA sub-types is the one that leads to fused- (rather than bridged) ring systems.

Several permutations exist for a diene-dienophile pair with two points of connection, but all fit into two categories: either the two points of connection to the diene unite *en route* to the dienophile, for which we introduce the *hybrid Type 1-Type 2 IMDA* descriptor (**Scheme 2c**), or alternatively, in substrates carrying *two discrete* diene–dienophile connections, cycloadditions can occur in a transannular manner (**Scheme 2d**). An acronym that evokes the sound of a fanfare, TADA (**t**rans**a**nnular **D**iels-**A**lder) is widely used to indicate this latter category. Hybrid Type 1-Type 2 IMDA reactions are generally identified in the literature by the shorter tether connection, i.e. the reaction involving the semicyclic diene substrate shown in **Scheme 2c** would be referred to as a Type 1 IMDA process.

The present introduction section (**Section 1**) describes general features of the major sub-categories of IMDA processes. The majority of the review (**Sections 2-4**), covering the IMDA reaction in target synthesis, is divided into three sections, each describing sub-types of IMDA processes. Literature searching[21] reveals that Type 1 IMDA reactions are the focus of the majority of publications. Type 1 IMDA reactions of 1,3,9-decatrienes (**Scheme 3**) are the most prevalent sub-type, hence are the focus of **Section 2**. Type 1 IMDA reactions of 1,3,8-nonatrienes

(**Scheme 3**) account for the second highest proportion of papers, and are covered in **Section 3**. Publications describing other Type 1 IMDA reactions (i.e. either smaller or larger than 3 or 4 connecting atoms), Type 2 IMDA reactions, and transannular Diels-Alder reactions are significantly fewer in number, accounting for around 5% of reported IMDA processes. **Section 4** covers these sub-categories.

The IMDA substrate descriptors 1,3,9-decatriene and 1,3,8-nonatriene (**Scheme 3**) are generally used, irrespective of the presence of substituents and heteroatoms. Specific modifiers (e.g. 1,3,9-decatrien-8-one) are occasionally employed to describe a subtype that exhibits specific behavior. 1,3,9-Decatrienes and 1,3,8-nonatrienes dominate IMDA chemistry because they generate the most prevalent bicyclic ring systems, namely (hydro)naphthalenes,[22] (hydro)indenes and their corresponding O- and N-containing systems.

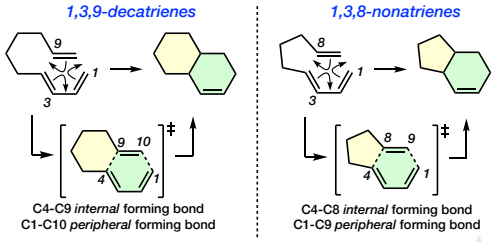

Scheme 3. The two most common sub-classes of IMDA reactions, and identification of *internal* and *peripheral* forming bonds in IMDA TSs. The names nonatrienes and decatrienes are used for heteroatom-containing systems and substituted systems.

As a concerted Diels-Alder reaction progresses, two σ-bonds are generated at the expense of two π-bonds. The concerted nature of the reaction means that the two σ-bonds start to form and complete their formation at the same time. Concertedness is not, however, synonymous with *synchroneity*. In fact, bond formation in DA TSs is commonly asynchronous, meaning that the two developing σ-bonds are of differing lengths in the DA TS. Several factors contribute to the structure of an IMDA TS and hence to which of the two forming σ-bonds is longer and which is shorter. The two developing σ-bonds in an IMDA TS are referred to as the *internal* and *peripheral* bonds.

The main issue confronting those new to the IMDA reaction is the challenge of coming to terms with the relationship between IMDA precursor structure, reactivity and stereoselectivity. Both the ease of reaction and the stereochemical outcome of a concerted, pericyclic IMDA reaction can be controlled by the substrate (hence influenced by the tether, diene and dienophile compositions and associated substituents) and/or by an external catalyst. Some general guiding principles are described in the following section.

1.2 Introduction to Reactivity and Stereoselectivity in Type 1 IMDA Reactions

The descriptions of IMDA stereoselectivities by Craig[9] and Roush[11] in their reviews provided detailed analyses of substituent effects upon TS conformations and TS asynchronicities. A particular emphasis was placed upon whether the TS *internal* or *peripheral* bond formation is advanced, hence whether the TS of a 1,3,9-decatriene IMDA reaction is more 6 membered ring like, or 10 membered ring like. The accuracy of many of these early qualitative analyses is remarkable, considering the limited methods available.

Since the 1980s, computational methods have developed considerably and quantitative accuracy is now the goal of such studies. Many transition structures (TSs) for IMDA reactions have now been located computationally, and our understanding has been refined. For kinetically-controlled IMDA reactions (which represent the majority of cases studied), calculated free energies of the lowest energy TSs have been used to construct Boltzmann distributions that allow stereoselectivities to be calculated. If computed values match experimentally-determined product ratios, then the outcomes can be explained by interpretation of the located TSs. Specifically, destabilizing contributions from torsional and steric strain, for example, can be identified and theories about stereoselectivities can be proposed.

Many researchers have contributed to a better understanding of IMDA reactions, and stereoselectivity in particular, through computational modelling. The Houk group has played a leading role.[23] Paddon-Row, in an extended computational-experimental collaboration with the senior author of the present review, has also made substantial contributions.[24] A review of these extensive investigations, while overdue, is not the focus of the present summary, which instead aims to provide a perspective on total synthesis applications of IMDA reactions by way of a case study-driven narrative.

To serve as a brief introduction, simple examples of 1,3,9-decatriene and 1,3,8-nonatriene systems are presented here. These examples are provided to facilitate the visualization of the subsequent TSs. In each case, we will start with the simplest possible precursor and consider a couple of simple substituted examples that are representative of the many possible synthetically useful transformations.

Whereas 1,3-butadienes are generally reactive participants in concerted DA reactions irrespective of substitution, C=C dienophiles generally need substitution with conjugating, electron-withdrawing groups to participate, at least under mild conditions. As might be expected, the connection of a 1,3-butadiene to a C=C dienophile through a tether permits IMDA reactions that are much more challenging in an intermolecular setting. So-called *unactivated IMDA reactions* (meaning those involving C=C dienophiles that lack conjugating, electron-withdrawing substituents such as C=O, C≡N, etc.) are widely used. The absence of a dienophile activating group means that *endo*-stereoselection is not feasible, hence other stereocontrolling influences must be at play for synthetically-useful processes.

Experimentally, the IMDA reaction of 1,3,9-decatriene **1** (**Scheme 4**) proceeds at a useful rate above around 160 °C but is essentially non-stereoselective, giving roughly equal amounts of *cis* and *trans*-octalin products **4** and **5**.[25] Calculated TSs for the IMDA reaction, **2** and **3**, were most recently reported by Krenske and Houk[26] but explanations were originally provided by Brown and Houk in 1985.[23]

The *boatlike* conformation of the DA TS (i.e. the diene and dienophile) is most apparent from the views of the *trans*-TS **2**. The

chairlike conformation of the tether is clearly visible in both TSs **2** and **3**, with the butadiene and vinyl "substituents" about the *chairlike* tether adopting pseudoequatorial orientations in three out of four cases. The exception is the butadiene substituent in the *cis*-TS **3**, which is pseudoaxial, thereby engendering 1,3-allylic strain. This energetic penalty is counterbalanced, however, by destabilizing 1,3-diaxial strain in the *chairlike-trans* TS **2**, which is exacerbated by the tilting of C4-H towards C8.

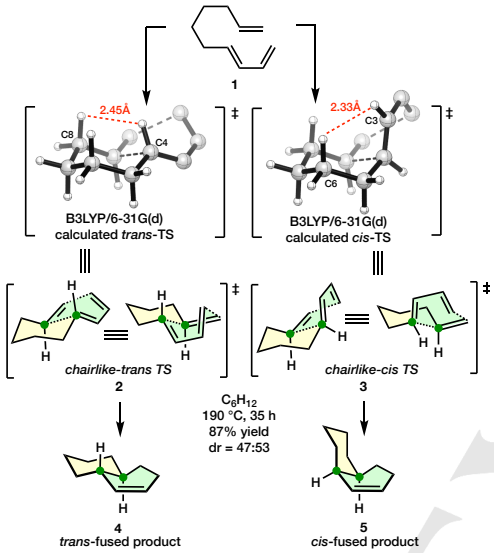

Scheme 4. The parent 1,3,9-decatriene IMDA reaction, the two lowest energy diastereomeric TSs with their destabilizing close contacts, and IMDA products. (Green atom bullets indicate stereocenters formed by the IMDA reaction.)

The closely matched TS energies of **2** and **3** means that a swing in preference towards either product **4** or **5** is possible by substrate modification. Removal of one of the hydrogens involved in the two different TS destabilizing interactions described above would eliminate that steric effect, hence favor the pathway. Alternatively, replacement of one of the Hs involved in either the 1,3-allylic or 1,3-diaxial strain with a larger substituent would enhance the destabilization of that TS relative to the other. As we will see in Section 2, whereas several different factors influence the outcome of unactivated 1,3,9-decatriene IMDA reactions, the *chairlike-trans* pathway is more commonly seen.

Whereas the tether in the parent 1,3,9-decatriene series adopts a *chairlike*-conformation in the lowest energy TSs, the shorter tether of the parent 1,3,8-nonatriene system adopts a more flattened shape reminiscent of the cyclopentane envelope conformer.

Scheme **5** depicts experimental results with the unsubstituted, parent 1,3,8-nonatriene **6**. As shown by Houk, the thermal IMDA reaction proceeds with *cis*-selectivity[27] (*trans*:*cis* = 25:75) and the most recently computed product ratio from Paddon-Row is in very good agreement (*trans*:*cis* = 24:76).[28] The computed *trans* TS is destabilized by the same transannular steric interaction between C4-H and one of the hydrogens of the allylic C7 methylene group as was seen in the 1,3,9-decatriene system. In addition, torsional strain exists between the eclipsing C5 and C6 methylene groups. Finally, 1,3-allylic strain involving the diene is discernible. Destabilizing eclipsing interactions are also visible in the *cis*-TS, along with 1,3-allylic strain involving the diene. Once again, the system is finely balanced and here the *cis*-fused product prevails.

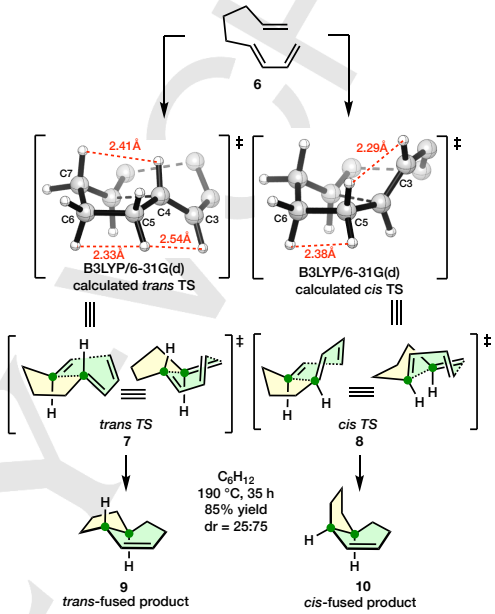

Scheme 5. The parent 1,3,8-nonatriene IMDA reaction, the two lowest energy diastereomeric TSs with destabilizing close contacts, and IMDA products.

As previously mentioned, no stabilizing secondary orbital interactions (SOIs) are possible in the TSs depicted in **Schemes 4** and **5**, since the dienophile lacks activating (conjugating, electron-withdrawing) substituents that can adopt *endo*-dispositions. As we will see, the judicious incorporation of a dienophile activating group can cause a significant swing towards the product formed through an *endo*-mode cycloaddition by selective TS stabilization, especially under Brønsted or Lewis acid activation. But this is not the only stereocontrolling influence that results from dienophile polarization. A second factor relates *twist mode asynchronicity*, a type of developing *σ*-bond asynchronicity in IMDA TSs that was introduced and explained by Houk and Brown[23] with later refinements with *Z*-dienophiles by Paddon-Row.[29]

One effect of dienophile polarization is the shortening of a developing *σ*-bond at the *β*-position to the activating substituent. This bond shortening is the result of an increase in the size of the LUMO coefficient at this dienophile position. It is enhanced by further LUMO energy lowering, brought about by, for example Lewis acid catalysts, Brønsted acid catalysts and iminium organocatalysts. In asynchronous IMDA TSs, the dienophile bond

is twisted about a pivot defined by the shorter developing σ-bond. This twisting can either move the other dienophile atom further under the diene (*endo*-twist) or away from the diene (*exo*-twist).

The effect of twist mode asynchronicity is most pronounced with terminal activating substituents (i.e. a substituent attached to the peripheral dienophile atom), which causes a twisting about the developing *internal* (ring fusion) bond. In 1,3,9-decatrienes and 1,3,8-nonatrienes carrying *E*-terminal activating groups, the effects of twist mode asynchronicity and SOIs pull in the same direction, favouring *trans*-fused cycloadducts. In contrast, the effects in the corresponding *Z*-activated trienes are opposing, which often leads to less stereoselective reactions.

Instructive reactions involving terminally- and internally-activated 1,3,9-decatrienes and 1,3,8-nonatrienes are provided in **Schemes 6** and **7**, respectively. Considering 1,3,9-decatrienes first, octalins with either *trans*- or *cis*-ring junction stereochemistry can be obtained with synthetically useful diastereoselectivity through terminal *E*-activation as in enal **11**[30] or tether-based activation as in 1,3,9-decatrien-8-one **12**,[31] respectively.

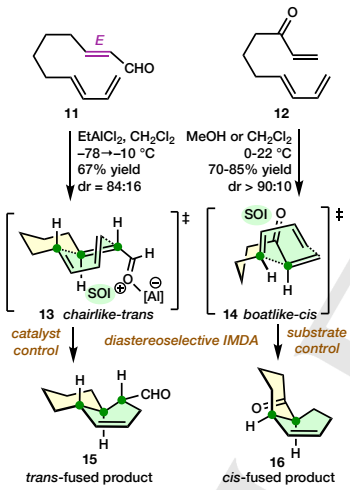

Scheme 6. Representative dienophile-activated precursors in 1,3,9-decatriene IMDA reactions.

Terminally *E*-activated 1,3,9-decatrienes such as **11** are poorly stereoselective in their thermally-promoted IMDA reactions. Under catalysis with Lewis acids, Brønsted acids or iminium organocatalysts, however, they generally undergo IMDA reactions preferentially through the *chairlike-trans* TS, **13**, which is favoured due to enhanced stabilizing SOIs with the *endo*-oriented dienophile activating group and favourable twist-mode asynchronicity. (The corresponding *cis*-TS has the dienophile activating group *exo*.)

1,3,9-Decatrien-8-one **12** undergoes IMDA reaction at below room temperature and with strong *cis*-diastereoselectivity, without catalysts. Interestingly, the lowest energy TSs in the 1,3,9-decatrien-8-one series are usually those with a *boatlike* tether conformation, which has been attributed to destabilizing gauche interactions involving the carbonyl group in the *chairlike* tether conformation.

In the 1,3,8-nonatriene series, terminally-*E*-activated substrates such as **17** show high levels of *trans*-diastereoselectivity under LUMO-lowering catalysis (**Scheme 7**).[32] IMDA cyclisation through *trans*-TS **19** again is favored through stabilizing SOIs of the *endo*-oriented dienophile activating group and twist asynchronicity. It is notable that the preference for *trans*-fused hexahydroindene **21** is a reversal of that seen in the unactivated IMDA reaction (**Scheme 5**).

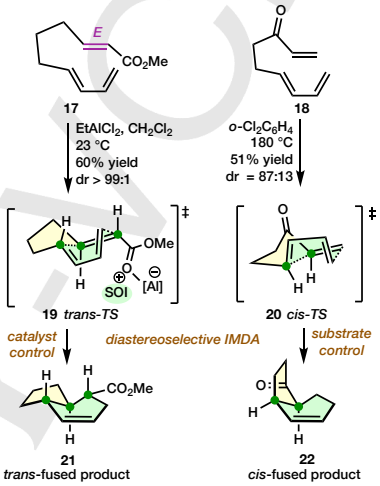

Scheme 7. Representative dienophile-activated precursors in 1,3,8-nonatriene IMDA reactions.

Interestingly, the reactivity of 1,3,8-nonatrien-7-one **18** is manifestly distinct from the corresponding 1,3,9-decatrien-8-one **12** (**Scheme 6**), in that the thermal reaction does not occur at ambient temperature. The IMDA reaction of **18** is not accelerated by LUMO-lowering catalysts, and requires heating to 180 °C to proceed at a reasonable rate, i.e. essentially the same temperature regime as the unactivated 1,3,8-nonatriene IMDA reaction.[33] A slightly enhanced preference for the *cis*-fused product **22** is seen relative to the unactivated IMDA reaction (**Scheme 5**), for reasons that are not clear. It appears that due to geometrical constraints, enone conjugation is decreased through out-of-plane twisting during the IMDA TS **20**, thereby minimizing the LUMO-lowering effect of the C=O group upon the dienophile C=C bond.

A detailed explanation of the stereochemical outcomes of all possible IMDA reactions is outside the scope of this review. Nonetheless, this brief introduction to the most common types of IMDA reactions will hopefully serve as useful background information pertaining to the more complex examples shown in **Sections 2** and **3**, where additional rings, substituents, heteroatoms, and π-diastereofacial selectivity are extra factors for consideration in each IMDA TS.

2. 1,3,9-Decatriene IMDA Reactions

Instructive examples of 1,3,9-decatriene IMDA reactions are presented in this section, commencing with the simplest precursors and gradually building in substrate complexity through additional substitution and ring annulation.

2.1. Solanapyrone D (MacMillan, 2005)

The simplest precursors for IMDA reactions are achiral and acyclic, with minimal functional group content beyond the diene and dienophile. Such substrates are ideal candidates for enantioselective catalysis, if the requisite catalyst binding point is present.

The first enantioselective organocatalytic IMDA reactions were reported by the MacMillan group in 2005.[34] Various enal dienophile-containing 1,3,9-decatriene and 1,3,8-nonatriene Type 1 substrates and one Type 2 substrate were shown to undergo IMDA reactions in generally excellent diastereo- and enantioselectivities. The application of the method to the total synthesis of (–)-solanapyrone D **27**, a natural product from phytopathogenic fungi, was also reported (**Scheme D1**).

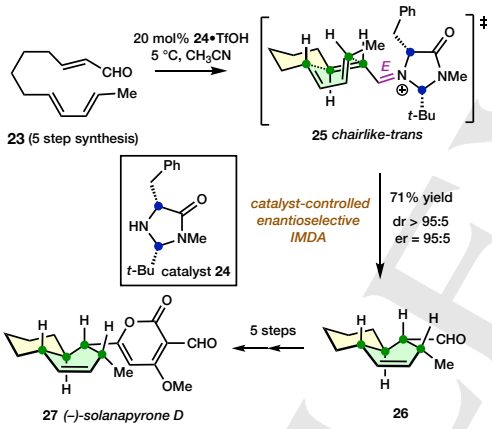

Scheme D1. MacMillan's 11 step total synthesis of (–)-solanapyrone D (2005) features an IMDA reaction at the half way point of the synthetic journey, but an early stage in the structural complexity generation.

In the presence of 20 mol % of **24**•TfOH,[35,36] cycloaddition of trienal **23** afforded *trans*-fused octalin **26**, which was converted into the natural product in a five-step sequence. Thus, in addition to the generation of a bicyclic ring system and the forging of two C–C bonds, the IMDA reaction installed all four stereocenters of the natural product with near complete control of relative and absolute stereochemistry. The stereoselectivity of this reaction may be attributed to several factors. The imidazolidinone catalyst **24** condenses reversibly with the formyl group of precursor **23** to generate chiral iminium ion **25**, with the more sterically demanding *tert*-butyl group controlling the formation of the *E*-iminium geometry. With the in-plane, *s-trans* C=C–C=N moiety activating the C=C dienophile through LUMO-lowering relative to the precursor aldehyde, the IMDA process now ensues. With the imidazolidinone lower face (as drawn in **Scheme D1**) substituted, folding of the IMDA chain brings the diene from the upper face, thereby suffering less steric repulsion. The IMDA reaction is proposed to proceed preferentially through *chairlike-trans* TS **25**, with both the diene and dienophile moieties occupying more favorable pseudoequatorial orientations about the tether-forming (i.e. yellow) cyclohexane ring, which places the dienophile in an *endo*-orientation with respect to the diene, hence permitting stabilizing SOIs in the TS. This arrangement gives rise to the *trans*-fused octalin **26**, with the methyl and formyl substituents *syn*- to one another. The formyl group is of central importance in this synthesis: following its use as a catalyst binding point, the formyl group of cycloadduct **26** is elaborated into the pyrone substituent of the natural product **27**.

As studied extensively by Oikawa, Ichihara and coworkers, the diastereomeric solanapyrones A and D, **30** and **27**, respectively, are produced naturally in enantiomerically pure form through biological, enzyme-catalyzed IMDA reactions of prosolanapyrone III **28** (**Scheme D2**).[37] Solanapyrone synthase was claimed as the first Diels-Alderase in 1995,[38] although an understanding of how it brings about catalytic enantioselecitve IMDA reactions remains elusive.[39] Solanapyrone D **27** is the product of a *chairlike-trans* IMDA TS, whereas its diastereomer solanapyrone A **30** is the result of a *boatlike-cis* IMDA TS from the same precursor.[40] It would be remarkable if it is ultimately proven that a single enzyme catalyzes the highly enantioselective conversion of the same precursor **28** into two diastereomeric products **30** and **27**.

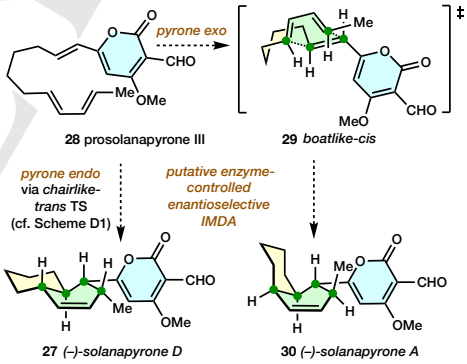

Scheme D2. Proposed biosynthesis of solanapyrone natural products, featuring enzyme-catalyzed *endo*- and *exo*-selective IMDA reactions of "prosolanapyrone" precursors.

Returning to the MacMillan synthesis of solanapyrone D: The same IMDA reaction was used by Westwood and coworkers ten years later in the first total synthesis of the protein-protein interaction inhibitor JBIR-22.[41] In order to ascertain the absolute configuration of the natural product, both enantiomers were prepared separately, by deploying both enantiomers of imidazolidinone catalyst **24** in the IMDA reaction.[42]

Whilst MacMillan's imidazolidinone catalyst is restricted to specific enal dienophiles, it remains one of a limited number of catalysts to bring about high levels of enantiocontrol in IMDA

reactions.[43] It is also one of a very small number of organocatalysts to achieve this feat.[44,45]

Only a tiny percentage of total syntheses deploy catalyst-controlled enantioselective IMDA processes. The vast majority of target molecule-focused applications of IMDA reactions instead use chiral substrates, and the pre-existing stereocenters influence the outcome of the IMDA process. This is demonstrated clearly by our next selected synthesis.

2.2. Equisetin (Dixon and Ley, 2000)

In 2000, Dixon, Ley and co-workers reported the first synthesis of (–)-equisetin. This enantiospecific synthesis employs citronellol as a chiral terpene precursor, and employs a late-stage, diastereoselective IMDA reaction to prepare the *trans*-octalin core.[46] The synthesis illustrates how a single, small tether substituent in an IMDA precursor (i.e. **31**, **Scheme D3**) can control the generation of up to four new target-relevant stereocenters. Thus, subjection of β-keto thioester **31** to a 5 M ethereal solution of lithium perchlorate resulted in the formation of bicycle **33** in 70% yield with excellent diastereoselectivity (dr > 95:5). The IMDA reaction proceeds through *chairlike-trans* TS **32**, with the diene, dienophile and tether methyl substituent all adopting pseudoequatorial orientations.

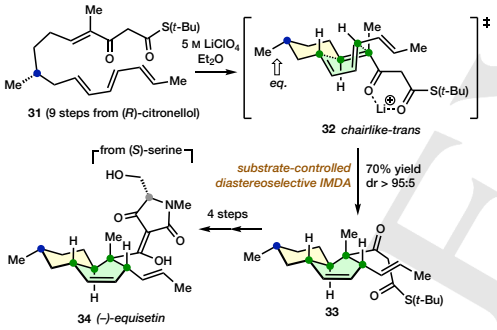

Scheme D3. Dixon and Ley's 14 step total synthesis of (–)-equisetin (2000) features a late-stage IMDA reaction.

The use of a 5 M ethereal solution of lithium perchlorate to accelerate Diels-Alder cycloadditions was originally introduced by the Grieco group.[47] In addition to the coordination of the lithium cation to the 1,3-dicarbonyl moiety to activate the dienophile, this particular medium (5 M $LiClO_4$ in Et_2O) is proposed to restrict solute movement and effectively compress the diene-dienophile system. This is thought to promote the cycloaddition reaction by bringing the reacting functionalities in close proximity, in an analogous manner to the application of elevated external pressure.[48,49]

Following the Dixon-Ley synthesis, several related diastereoselective IMDA approaches to equisetin and closely-related natural products including fusarisetin A and epi-trichosetin were reported.[50]

Solanaquinone and equisetin belong to a growing family of octalin-containing natural products produced by microorganisms that are biosynthesized through an IMDA reaction.[51] The enzymes involved in biosynthetic pericyclic processes, termed "pericyclases", have recently been reviewed.[52]

The use of a tether substituent is one of the most popular methods to control the stereochemical outcome of an IMDA reaction.[53] This approach was used in one of the first IMDA reaction-based natural product total syntheses, which was reported by Taber and Gunn in 1979.[54] This is both an interesting and instructive synthesis because it features a sub-class of 1,3,9-decatriene IMDA reactions that proceed preferentially through a TS with a *boatlike* tether conformation.

2.3. Torreyol (Taber and Gunn, 1979)

Taber and Gunn's seven step total synthesis of racemic torreyol **38** is summarized in **Scheme D4**. Oxidation of allylic alcohol **35**, prepared in 6 steps from isovaleraldehyde, generated the substituted 1,3,9-decatrien-8-one, which underwent IMDA reaction *in situ* at 0 °C within 25 min through *boatlike-cis* TS **36** to form the *cis, anti*-diastereomeric octalinone **37**. The total synthesis was completed by methyl addition to the ketone functionality on the concave face of the bicycle, through equatorial approach of the cuprate-derived nucleophile.

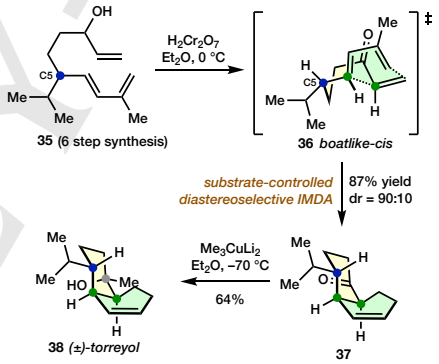

Scheme D4 One of the earliest uses of an IMDA reaction in a total synthesis: Taber and Gunn's 8 step total synthesis of (±)-torreyol (1979).

To benefit from stabilizing SOIs, the tether dienophile activating group adopts an *endo*-orientation with respect to the diene in the IMDA TS, hence favoring the *cis*-ring junction geometry. Roush and Coe demonstrated in 1989 that most decatrienones preferentially cyclize through *boatlike-cis* TSs.[55] The C5 allylic isopropyl group adopts a pseudoequatorial conformation, again to minimize allylic strain, resulting in an *anti*-relationship with the adjacent C4 ring junction stereocenter.

Taber and Gunn's ground-breaking study also introduced the idea that the analysis of destabilizing interactions in IMDA TSs might have predictive power on stereoselectivities. The concluding statement of their paper: "*this reaction should find widespread application in complex natural product synthesis*" proved to be prophetic: The IMDA process has since become one of the most important reactions in total synthesis. In particular,

1,3,9-decatrien-8-one IMDA reactions are abundant in the total synthesis literature.[56]

The very best total synthesis applications of the IMDA reaction bring about its seamless integration in a reaction sequence, setting up the requisite functionality for the next step. A striking example, which also involves an expansion of an initially-formed tether ring, was invented by the Aube laboratory.

2.4. Stenine (Aube, 2002)

In 2002, Golden and Aube reported an ingenious 1,3,9-decatrien-8-one IMDA/intramolecular Schmidt sequence to prepare a tricyclic intermediate that had been previously used in the total synthesis of (±)-stenine (**Scheme D5**).[57] The two-step sequence commenced with acyclic 1,3,9-decatrien-8-one precursor **39**, delivering the desired 5,6,7-azatricyclic core **43** in a 43% yield as the major diastereomeric product. The Lewis acid Me_2AlCl was identified as a suitable mediator of both processes. The major pathway for the cycloaddition is the familiar *endo*-carbonyl *boatlike-cis* TS **40**, which generates *cis*-octalin **41**.

Even though substrate **39** carries both ketone and azide functional groups, it cannot undergo the intramolecular Schmidt reaction prior to the cycloaddition due to the geometrical constraints imposed by the *E*-configured C=C bond. The IMDA reaction brings these reactive functionalities into sufficiently close proximity, enabling equatorial addition of the azido-nucleophile to the cyclohexanone carbonyl (**41**→**42**). and the subsequent rearrangement-elimination (**42**→**43**). During this concerted process, the migrating C–C bond must be aligned antiperiplanar to the N_2 leaving group. Thus, only the equatorial N_2 intermediate **42** gives rise to the desired tricycle **43**.

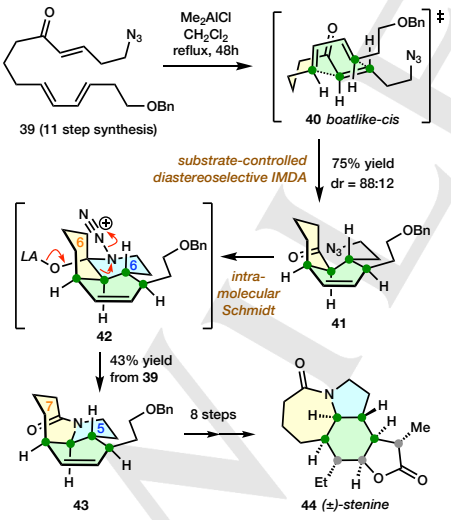

Scheme D5. Aube's 20 step formal total synthesis of (±)-stenine (2002) features a decatrienone IMDA-intramolecular Schmidt sequence.

Azatricycle **43** contains four of the seven stereocenters and three of the four rings of stenine. This compound was converted to a late stage intermediate previously used by Hart and co-workers for the total synthesis of (±)-stenine.[58] The direct generation of tricycle **43** by way of an IMDA reaction would be extremely challenging. Aube's strategic use of the Schmidt reaction expands the scope of the IMDA process. More generally, efficient synthetic methods based upon post-IMDA cyclizations and rearrangements are poorly studied. They represent a worthwhile area of future investigation, which should permit the rapid assembly of a much broader diversity of structures than those accessible directly through IMDA processes.

Analysis of Taber and Gunn's synthesis of torreyol (**Scheme D4**) reveals an alternative way to integrate an IMDA reaction into a synthetic sequence, by carrying out the IMDA process *in situ*, as the triene precursor is generated. In 2011, the White group capitalized on the mild reaction conditions required for IMDA cyclization of the parent 1,3,9-decatrien-8-one **12** by demonstrating the value of their dehydrogenative method for diene synthesis (**Scheme D6**).[59] This *in situ* diene synthesis/IMDA reaction sequence nicely complements the existing methods of dienophile activation (cf. Taber and Gunn) and masked diene unveiling, for example through thermolysis of 3-sulfolenes.[60] Although used primarily to facilitate the dehydrogenation reaction, the Brønsted acid might also catalyze the IMDA reaction in this instance.

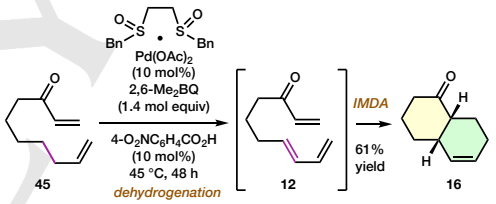

Scheme D6 *In situ* IMDA reaction of 1,3,9-decatrien-8-one **12** generated by dehydrogenation by White and coworkers (2011).

The first examples of this commonly-deployed subclass of IMDA reaction were reported separately by Oppolzer[61] and Gras,[62] and were conducted at ambient temperature. The ease by which a 1,3,9-decatrien-8-one undergoes IMDA reaction is interesting, particularly in light of the need for the precursor to adopt a *boatlike*-TS, which might be otherwise considered to be energetically unfavorable. Presumably, both stabilizing SOIs and (apart from the *boatlike* tether conformation) an otherwise strain-free TS contribute to the low activation barrier. Another synthetically useful result from this early work on decatrienones is the facile epimerization from the *cis*-ring junction stereochemistry, generated from the kinetically-controlled IMDA reaction, to the more thermodynamically favored *trans*-diastereomer.[63] To access the *trans*-fused ring system from a decatrienone precursor directly, we could envisage ways of removing stabilizing SOIs from the IMDA TS, thereby favoring the *trans*-diastereomer as the kinetic product. Corey and Magriotis introduced a substrate-based stereocontrol method to achieve this outcome in 1987.[64]

2.5 7,20-Diisocyanoadociane (Corey 1987)

Corey and Magriotis used the IMDA reaction of an acetal-protected 1,3,9-decatrien-8-one **46** in their total synthesis of 7,20-diisocyanoadociane **49** in 1987 (**Scheme D7**). Protection of the ketone has a profound effect upon the reactivity of the dienophile: heating to 150 °C is required to bring about cycloaddition. Processes that deploy a C=C dienophile that lacks an electron-withdrawing substituent are generally referred to as "unactivated" cases. Without SOIs to stabilize TSs with an *endo*-disposed carbonyl group, the substrate adopts the *chairlike-trans* TS **2** (cf. **Schemes D1, D3**), in which the side chain substituent, diene and dienophile adopt pseudoequatorial orientations with respect to the tether-forming (yellow) ring. The process leads to *anti, trans*-octalin **48**, installing two of the four rings, and two of the ten stereocenters of the natural product. Another IMDA reaction later in the synthesis forged the remaining two rings and three more stereocenters.

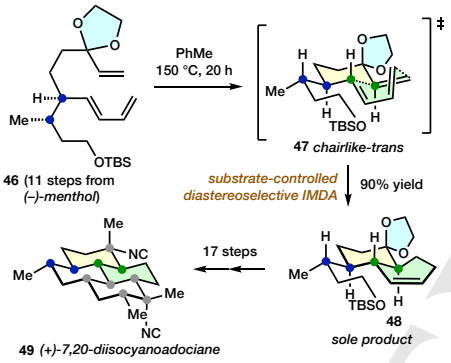

Scheme D7 The first IMDA reaction used by Corey and Magriotis in their 29 step total synthesis of (+)-7,20-diisocyanoadociane (1987).

In a footnote, the authors report that the enone corresponding to **47** underwent IMDA reaction at 23 °C but generated the *cis*-fused product. Acid or base-mediated epimerization of this compound, presumably the *anti, cis*-diastereomer, should have furnished the desired *anti, trans*-compound **48**, albeit in unprotected ketone form. Presumably this approach was not taken since subsequent transformations ran more smoothly with the ketone protected.

One of the most significant contributions in Diels-Alder chemistry – indeed in catalysis more generally – was Yates and Eaton's 1960 demonstration that stoichiometric amounts of $AlCl_3$ enhances the rate of Diels-Alder reactions.[65] Fray and Robinson reported Lewis acid *catalysis* of Diels-Alder reactions in 1961.[66] Reports of enhancements in diene-dienophile orientational regioselectivity[67] and *endo*- (vs. *exo*) stereoselectivity[68] followed shortly thereafter. The rate enhancement and improved regio- and stereoselectivities are due to the lowering of the LUMO energy of the dienophile C=C–C=O system upon binding with an oxophilic Lewis acid.

Many different Lewis acids have since been used to promote IMDA reactions, but one, reported by Yamamoto and coworkers in 1994, has the remarkable effect of favoring *exo*-selectivity with certain substrates. The 2-methyl-1,3,7-decatrien-6-one **50** substrate is the case in point (**Scheme D8**). In independent studies reported in 1994, both Grieco[69] and Yamamoto[70] showed that simple Lewis acids (5M $LiClO_4/Et_2O$ and Me_3Al, respectively) elicit a preference for the *cis*-fused product **54** (formed through *boatlike*-TS **52** with an *endo*-oriented tether ketone group). With the very sterically bulky Lewis acid ATPH (aluminium tris(2,6-diphenylphenoxide)), however, a strong preference was seen for the *trans*-fused product **53**. The stereochemical switch was rationalised through destabilisation of the tether *endo*-TS by the sterically demanding ATPH promoter, whose aluminum center is located deep inside a tight binding pocket that can only accommodate the less sterically demanding *chairlike-trans*-TS **51**, with an *exo*-carbonyl group.

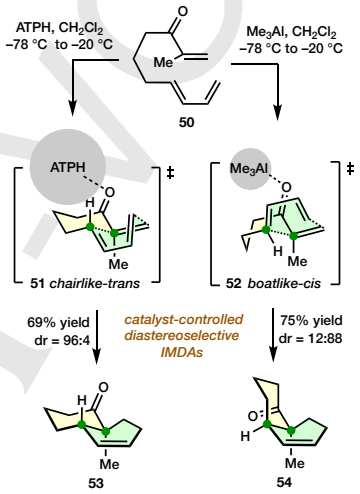

Scheme D8 Influence of Lewis acid size upon IMDA reaction stereoselectivity by Yamamoto (1994). Grey shading indicates qualitatively that ATPH is a much more sizeable Lewis acid.

Note the shrewd choice of the IMDA substrate for this reaction: the methyl group of triene **50** not only puts the brakes on the uncatalyzed IMDA reaction,[71] thereby allowing catalysts to be useful, but also precludes the epimerization mechanism for the generation of the *trans*-octalone. Thus far, only one total synthesis exploiting this astonishing reversal of diastereoselectivity has been disclosed.[72] ATPH is a catalyst that deserves wider application in IMDA reactions. It would be extremely valuable if the principles behind the function of ATPH would permit an extension to enantioselective catalysis.

Whereas achiral, terminally-activated trienes of many different types have been successfully cyclized through highly enantioselective IMDA processes,[43] the development of a highly catalytic enantioselective process for IMDA reactions involving trienes with "tether-activated" dienophiles remains an unsolved problem.[73]

Returning to terminally-activated 1,3,9-decatrienes, some of the most remarkable alkaloid total syntheses of recent times use early stage IMDA reactions to establish bicyclic frameworks upon

which multicyclic systems are built. While the target structures of these multicyclic alkaloids are vastly different from those covered thus far, the conformations of IMDA TSs of these key steps should by now appear reassuringly familiar.

2.6. Galbulimima Alkaloids GB 13 (Movassaghi, 2006) and Himandrine (Movassaghi, 2009)

The Movassaghi group reported the first synthesis of complex galbulimima alkaloid GB 13, **58**, in 2006 (**Scheme D9**).[74] A heat-promoted IMDA reaction was used to construct the octalinone bicyclic ring system of the natural product in the first phase of ring closures *en route* to the natural product. Thus, tetraenal **55** underwent IMDA reaction at 90 °C to afford *trans*-octalin **57** in high yield and high diastereoselectivity. The major product of the reaction is proposed to arise from *chairlike-trans* TS **56**, in which both diene and dienophile adopt favorable pseudoequatorial positions, and the C10 formyl substituent is in an *endo*-disposition, permitting stabilizing SOIs. The racemic cycloadduct **57** was resolved by combination with an enantiopure building block to give a pair of diastereomeric intermediates, which were readily separated *via* column chromatography. Thus, only one of the two enantiomers from the IMDA reaction ended up in the product (–)-GB 13 **58**. This achiral substrate appears well suited to enantioselective catalysis, for example by one of MacMillan's organocatalysts (cf. **Scheme D1**).

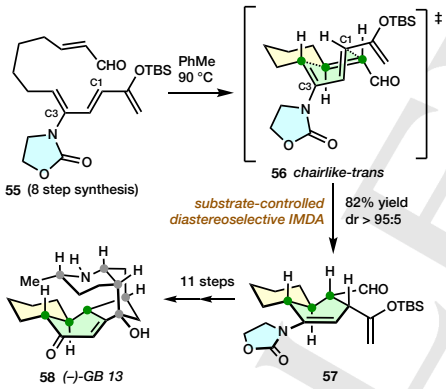

Scheme D9. Movassaghi's 20 step total synthesis of (–)-GB 13 (2006) features a relatively early-stage IMDA reaction.

The C3 (1,3,9-decatriene numbering) oxazolidinonyl substituent served as a masked ketone in the GB 13 synthesis, with the C1 (1-silyloxy)vinyl substituent as a masked methyl ketone. The subsequent synthesis of the more complex target (–)-himandrine **62** deployed a similar IMDA strategy but with a couple of notable differences (**Scheme D10**).[75]

First, the C3 oxazolidinonyl group was replaced by a more labile 2-azetidinonyl substituent, and secondly, the IMDA precursor carried a C5 (1,3,9-decatriene numbering) methoxy group, which was required for the natural product but would be deployed to control the π-diastereofacial selectivity of the IMDA reaction. Thus, uncatalyzed IMDA reaction of the highly enantioenriched tetraene **59** at 95 °C afforded the *trans*-octalin **61** as the major product. IMDA reaction is proposed to proceed *via chairlike-trans* TS **60**, with the aforementioned methoxy substituent adopting a pseudoequatorial position, along with the diene and dienophile, about the tether-forming cyclohexane ring. As the authors intimate, perhaps the C3-heterocycle substituents favour *cisoid* 1,3-butadiene conformations of the IMDA reaction precursors, thereby facilitating their IMDA reaction.

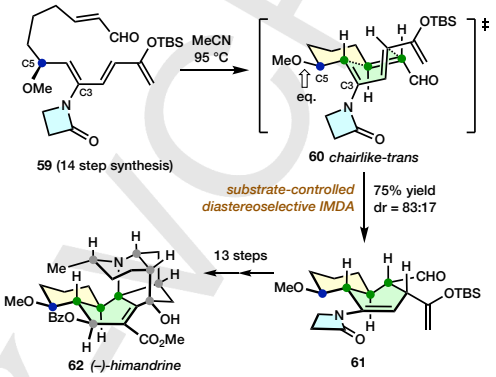

Scheme D10. Movassaghi's 28 step total synthesis of (–)-himandrine (2009).

All examples thus far have featured acyclic precursors. (Cyclic substituents attached to an acyclic triene and spiro-annulated rings behave like acyclic trienes, hence are counted as such.) We now move on to ring-containing precursors. Rings can be present in the diene, the dienophile, the tether component of an IMDA precursor, or can span two or more of these. Our first example of an IMDA reaction involving a cyclic triene precursor contains a ring exclusively in the tether.

2.7. Salvinorin A (Forsyth, 2008-2016)

Forsyth and co-workers reported the enantioselective total synthesis of the diterpenoid (–)-salvinorin A **66** featuring an IMDA reaction to prepare the *trans*-fused decalin ring system (**Scheme D11**).[76] The IMDA reaction bears some similarities with the one used by Corey in his 7,20-diisocyanoadociane synthesis (**Scheme D7**), in that it is of the acetal-protected 1,3,9-decatrien-8-one type. Nonetheless, this example also features an interesting method for tether ring-based stereocontrol.

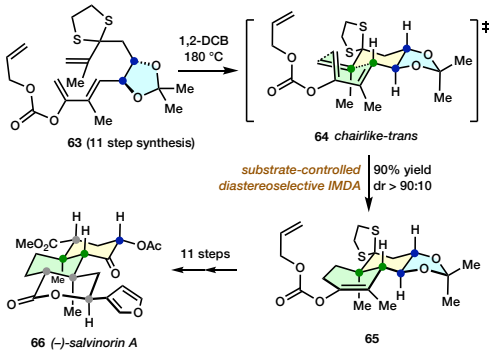

Scheme D11. Forsyth's 23 step total synthesis of (–)-salvinorin A (2008-2016), featuring an unactivated IMDA reaction with tether ring-based stereocontrol. (DCB = dichlorobenzene)

Thus heating of triene **63** in 1,2-dichlorobenzene selectively afforded *trans*-octalin **65** in 90% yield, forging both carbocyclic rings of the natural product and two stereocenters, one of which is a challenging all-carbon quaternary center. (The corresponding enone cyclised in refluxing toluene but gave an unsatisfactory 50:50 mixture of *cis* and *trans* diastereomers.)

The cyclic isopropylidene acetal is not required for the target molecule but it is used here as a stereocontrolling feature: The diene and dienophile in precursor **63** are 1,2-*trans*-oriented substituents upon the dioxolane ring, and must adopt pseudoequatorial dispositions for cyclization. This, in turn, imposes limitations upon the developing IMDA tether ring and the DA TS. Specifically, it precludes the *boatlike-cis* and *trans* TSs.

The observed product **65**, possessing the required stereochemistry for the natural product at the two new stereocenters, arises from *chairlike-trans* TS **64**. The potential *chairlike-cis* TS is disfavoured due to steric repulsion, as are most 1,3,9-decatriene IMDA TSs (see above). The controlling influence of the cyclic isopropylidene acetal group was shown through replacement of the dithiane ring with a single triene substituent and methine stereocenter: irrespective of need for a substituent to adopt an equatorial or axial disposition, the same TS was followed.

Section 2.1 described a natural product that is proposed to form by way of a biological IMDA reaction. There are many superb examples of biomimetic IMDA-based total syntheses. Possibly the first reported example is the key phase of Chapman's classic total synthesis of carpanone,[77] which involves a 1,3,8-decatriene IMDA reaction. The Chapman IMDA reaction is of the inverse electron demand type, featuring an electron rich dienophile and electron poor orthoquinone methide diene. The next synthesis involves the biomimetic IMDA reaction of a cyclic dienophile with a fascinating, internal mode of activation.

2.8. Symbioimine (Snider 2006)

The Snider group[78] reported the synthesis of (±)-symbioimine in 2006 (**Scheme D12**). Their approach involved an imine formation/IMDA/epimerization sequence, inspired by Uemura's proposed[79] biosynthetic pathway.

Treatment of precursor **67** with $BF_3{\bullet}OEt_2$ brought about elimination of the hydroxyl group (a vinylogous aminal) to generate a 5,6-dihydropyridinium cation, which underwent an IMDA reaction, presumably through *boatlike-cis* TS **68** to form an unstable *cis*-cycloadduct, which finally loses a ring junction proton to form tricyclic enamine **69**. The *π*-diastereofacial selectivity of the IMDA reaction is controlled by the one stereocenter carried by the direct (i.e. dehydroxylated) IMDA precursor, with the diene approaching from the opposite face of the dihydropyridinium ring to the methyl substituent, to avoid steric repulsion from the diene and its aromatic substituent.

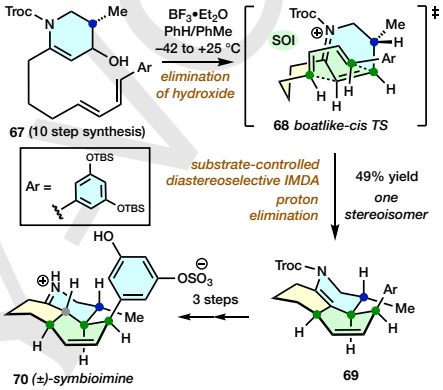

Scheme D12. The Snider group's 14 step total synthesis of (±)-symbioimine (2006).

The synthetic utility of the IMDA reaction for the synthesis of symbioimine and related natural products is further illustrated in the work of Varseeve and Maier,[80] Thomson[81] and others.[82] A related IMDA reaction of a cyclic oxocarbenium ion was also developed by Sammakia and co-workers for the synthesis of (–)-dihydrocompactin.[83] The tactic of substrate-based iminium activation was advanced further in Thomson's outstanding total syntheses of two structurally dissimilar alkaloids by divergent modes of cyclization of a pair of almost identical precursors.

2.9. Himandravine and GB17 (Thomson 2015)

The Thomson group's synthesis of himandravine **77** and GB17 **78** is a significant achievement in biomimetic synthesis.[84] The two natural products are structurally distinct but biosynthetically related. They are proposed to originate from bicyclic tetraene iminium precursors akin to **71** and **72**, which undergo divergent IMDA processes in which the diene and dienophile components are reversed (**Scheme D13**). The synthetic work was supported by intriguing computational findings by the Tantillo group, who, while locating discrete TSs for the separate IMDA processes, describe them as exhibiting significant ambimodal pericyclic character. (Ambimodal processes are discussed further at the end of **Section 4**.)

Iminium precursors **71** and **72** differ in the absence or presence of a third stereocenter in the tether which connects the two dienes. In the himandravine series, the dienophile is the C=C bond with vinylogous iminium activation, which reacts with the semicyclic diene through *chairlike-trans* TS **73** to give adduct **75**, following iminium reduction and carbamate formation. The *π*-diastereofacial selectivity of this IMDA process is controlled by the remote allylic stereocenter on the lactone ring, with the dienophile approaching the diene away from the lactone's methyl group. The vinylamine substituent is also *endo*-disposed in TS **73** and may benefit from SOIs. Himandravine **77** was prepared in short order from adduct **75**.

In the GB17 series, iminium substrate **72** carries a benzyloxy substitutent, and cyclizes predominantly through *chairlike-trans* TS **74** to give adduct **76** after iminium reduction and allylic (C2=C3 to C1=C2) tautomerization. In this case, the diene in conjugation with the iminium is the 4π component and the dienophile is the unactivated C=C bond of the 2-vinylbutenolide. This latter case is an inverse electron demand IMDA reaction. The synthesis of GB17 was completed through lactam formation, debenzylation and oxidation.

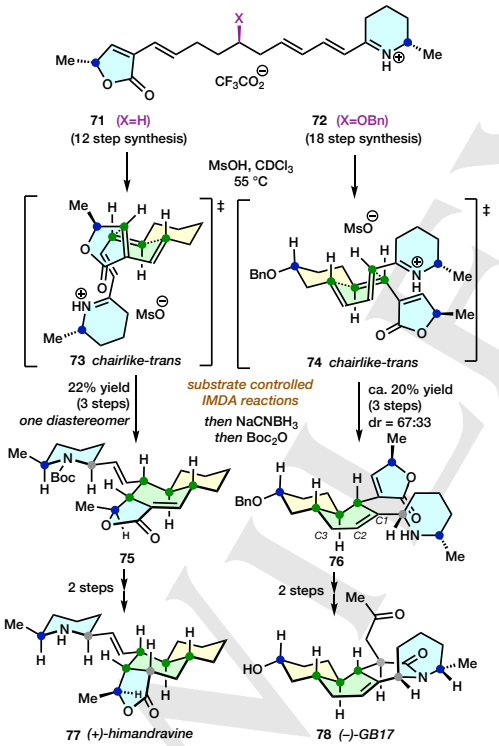

Scheme D13. The Thomson group's 17-23 step total syntheses of (+)-himandravine and (–)-GB17 (2015).

Each of the substrates **71** and **72** gives some of the product of the alternate pathway. In addition, the *π*-diastereofacial selectivity of IMDA reaction leading to GB17 is modest: while TS **74** where the –OBn group is pseudoequatorial is favored, the corresponding pseudoaxial –OBn TS is also accessible. Perhaps in nature, enzyme assistance is provided, or maybe these other products are used as building blocks for other metabolites. Irrespective, this superb contribution to IMDA based total synthesis significantly extends earlier contributions and adds important new information to the growing body of work with the fascinating *Galbulimima* alkaloids.

IMDA tether-located rings can be of various sizes and compositions, although the majority of examples in the total synthesis literature involve six-membered carbocyclic rings. These pre-existing carbocyclic rings don't always find their way into the target molecule, and their presence introduces new structural features that impact upon IMDA stereoselectivity. The next target molecule is instructive from this perspective. It also shows the versatility of the IMDA reaction in cutting edge synthesis: here it is applied to one of the most challenging targets, through two conceptually distinct and unrelated 1,3,9-decatriene IMDA approaches.

2.9. Norzoanthamine (Miyashita, 2004; Kobayashi, 2009)

Short step count total syntheses of molecules of the complexity of norzoanthamine are beyond what is currently possible. The Herculean efforts of Miyashita and Kobayashi, whose groups independently completed total syntheses of this target in 42 and 49 steps (LLS), provide much useful information for anyone with sufficient courage to attempt a practical synthesis. While the two approaches are entirely different, both deploy IMDA reactions relatively early in the synthesis to forge the ABC tri-carbocyclic portion of the molecule, upon which the heterocyclic ring systems are subsequently assembled.

Miyashita and co-workers reported the first stereoselective synthesis of (–)-norzoanthamine **82** in 2004 (**Scheme D14**).[85] Whilst by no means a biomimetic synthesis, this approach was inspired by the proposed biogenetic pathway for the zoanthamine alkaloids.[86] Thus, an IMDA reaction was used to construct the BC ring system of the natural product, including two all carbon quaternary stereocentres. The ability of the DA reaction to forge these, the most challenging of stereocenters, has been emphasized in recent reviews.[87] IMDA reaction was brought about by the dropwise addition of a solution of precursor **79** into 1,2,4-tricholorobenzene at 240 °C. Subsequent treatment with HF-pyridine afforded the major product **81**. The reaction is proposed to proceed predominantly *via chairlike-trans* TS **80**, with the familiar arrangement of the diene and dienophile adopting pseudoequatorial positions.

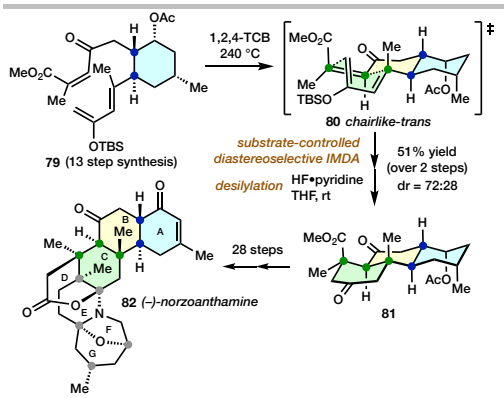

Scheme D14. Miyashita's 43 step total synthesis of (–)-norzoanthamine (2004) features a decatrienone-type IMDA reaction to simultaneously fuse the B and C rings onto an A ring precursor. (TCB = trichlorobenzene)

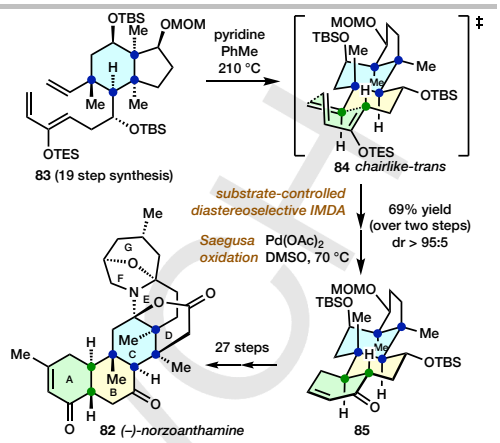

Scheme D15. Kobayashi's 48 step total synthesis of (–)-norzoanthamine (2009) deploys an unactivated 1,3,9-decatriene IMDA reaction to annelate the B and C rings onto an existing A-ring precursor.

Closer inspection reveals a decatrienone-type precursor **79**, which generally undergo IMDA reactions at ambient temperature and with a preference for the *cis*-fused product through a *boatlike*-tether conformation, which permits stabilizing SOIs between the diene and tether carbonyl group. Substrate **79**, however, bears three significant structural differences from a simple 1,3,9-decatrien-8-one precursor. Firstly, the pre-existing cyclohexane ring carries the diene and dienophile substituents in a 1,2-*trans*-arrangement, which must sit in (pseudo)equatorial orientations to permit IMDA cyclization. This requirement essentially precludes the *boatlike*-tether conformation. Secondly, the dienophile has a carbomethoxy group *cis*- to the tether ketone, which has a disruptive influence, in that only one of the two carbonyl groups can be fully conjugated (i.e. coplanar) with the C=C bond at any given time, with the non-coplanar group causing steric repulsion on approach of the dienophile to the diene. Thirdly, the diene carries an "inside" methyl substituent at C4, which greatly diminishes its DA reactivity by destabilizing the required *cisoid*-diene conformation. In summary, we interpret the unusually high temperature required for this IMDA reaction to an energetically unfavourable IMDA TS which does not benefit from stabilizing SOIs.

Kobayashi's synthesis of norzoanthamine **82** featured a stereoselective IMDA reaction to construct the AB *trans*-octalin ring system of the natural product (**Scheme D15**).[88] The IMDA reaction of triene **83** was carried out at 210 °C in toluene in the presence of pyridine as an acid scavenger, to afford an acid-labile cycloadduct, which was directly subjected to modified Saegusa oxidation conditions to obtain enone **85** as a single diastereomer. The IMDA reaction is proposed to proceed through the familiar *chairlike-trans* TS **84**, with the –OTBS group of the tether, the diene and the dienophile occupying favorable pseudoequatorial positions.

The diene and dienophile in precursor **83** can be seen as a pair of 1,2-*trans*-oriented substituents attached to the cyclohexane of a pre-existing hexahydroindane ring system. The dienophile is not activated in this IMDA reaction, hence no stabilizing SOIs are possible. Nonetheless, the barrier for this IMDA reaction (**83**→**85**) still appears to be of lower energy than that of the apparently activated precursor **79** depicted in **Scheme D14**.

So far, we have considered 1,3,9-decatriene IMDA reactions of either acyclic precursors or those with a ring exclusively within the diene-dienophile interconnecting tether. We will next consider examples where either the diene or the dienophile contain rings. Cyclic dienes are available in several structural permutations. One of the very earliest examples of IMDA reactions in total synthesis featured a late stage IMDA reaction of a *semicyclic* diene.

2.10. Gibberellic Acid (Corey, 1978)

The Corey group synthesis of gibberellic acid **89** published in 1978 features two [4+2] cycloadditions, the second of which is of the 1,3,9-decatrien-8-one IMDA type (**Scheme D16**). The following quotation from the manuscript demonstrates the level of challenge presented by this target: *"the combination of overall molecular complexity, centers of high sensitivity toward many reagents, and a singularly diabolical placement and density of functionality serves to thwart all but the most sophisticated of approaches".*[89] The group deployed the IMDA reaction in a manner that was ground-breaking, to simultaneously install the cyclohexene A-ring of the target, with the requisite configuration at the C4 stereocenter (1,3,9-decatriene numbering; the C5 center would be corrected later), while also incorporating functionality to permit elaboration to the natural product **89**.

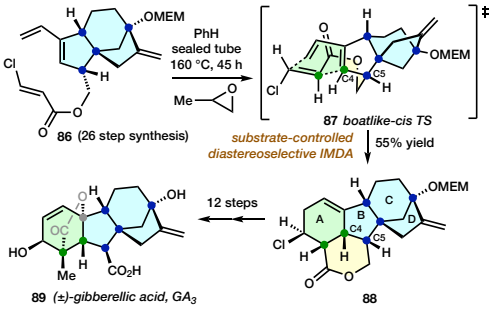

Scheme D16 One of the earliest uses of an IMDA reaction in a total synthesis: 39 step (±)-gibberellic acid total synthesis by Corey and coworkers (1978) featuring a late stage 1,3,9-decatrien-8-one-type IMDA reaction.

Ester-tethered (1,3,9-decatrien-8-one type) IMDA precursor **86** underwent IMDA reaction at 160 °C, presumably through *boatlike-cis* TS **87**, to give cycloadduct **88**. More than 40 years after its publication, the Corey group's use of the IMDA reaction still feels fresh.

Esters and amides are convenient tethers for IMDA reactions due to their ease of synthesis. Their IMDA reactions in non-polar organic solvents often need significantly higher temperatures than the corresponding all-carbon tethers (e.g. **Scheme D14**). The Jung group explained the high activation barrier for ester-linked precursors in terms of the reactive rotamer effect: specifically, the need for the *cisoid* ester conformation (i.e. a low C–O–C(O)–C torsion angle), which is energetically unfavorable relative to the *transoid* form.[90] IMDA reactions of ester-linked precursors can be carried out at significantly lower temperatures in more polar solvents such as DMSO, which are thought to preferentially stabilize the more polar *cisoid* ester conformation.[90] More recently, Lewis acids capable of binding both ester oxygens, thereby favoring the *cisoid* ester conformation, have been introduced.[91] Jung's work builds upon the seminal studies by Gschwend and co-workers with amide tethered IMDA reactions, who demonstrated that a non-participating, bulky *N*-substituent can accelerate the reaction rate by favoring the reactive conformation.[92] Perhaps the IMDA reaction depicted in **Scheme D16** could be performed at a significantly lower temperature by performing the reaction in DMSO.

A decatrienone-type IMDA reaction related to one described by the Corey group (Scheme D16) was reported by the Stork group a few years later. Instead of a plant hormone, the application was in the synthesis of a mammalian hormone.

2.11. Adrenosterone and Related Steroids (Stork, 1981-1987)

Stork and Saccomano's 1987 total synthesis of adrenosterone showcases a powerful synthetic maneuver involving a 1,3,9-decatrien-8-one-type IMDA reaction (**Scheme D17**).[93] The cyclohexene ring generated through the intramolecular cycloaddition does not find its way into the final product. Instead, it is used to simultaneously install both the challenging C11 (steroid numbering) ketone functionality and the functionality required for A-ring closure.

The IMDA reaction of decatrienone **90** was brought about by trifluoroacetic acid (which brings about concomitant deprotection of the acetal), providing tetracycle **92** in good yield. The internal bond formed in the IMDA reaction closes the B-ring of the natural product but the cyclohexene ring is destined to become the greater part of the steroid A-ring. The *π*-diastereofacial selectivity of this reaction is controlled by the configuration of the stereocenter at C8 in precursor **90**, which places the chain carrying the dienophile on the lower face of the diene. The major, *cis*-fused product **92** forms by way of *boatlike-cis* TS **91**, fashioning the required configuration at the all-carbon quaternary C10 (steroid numbering) stereocenter. Ozonolysis of the freshly generated cyclohexene ring installs the C11 ketone, then an intramolecular aldol reaction annulates the A-ring of the natural product, with epimerization at C9 to the more thermodynamically stable *anti, trans*-diastereomer completing the total synthesis.

The Stork group initially prepared 11-keto progesterone using this type of sequence,[94] based upon work originally reported in 1981,[95] before refining it in the adrenosterone synthesis shown here. Nakamura and Kuwajima adopted Stork's approach for total syntheses of cortisone and several related corticosteroids in 1986-1989.[96]

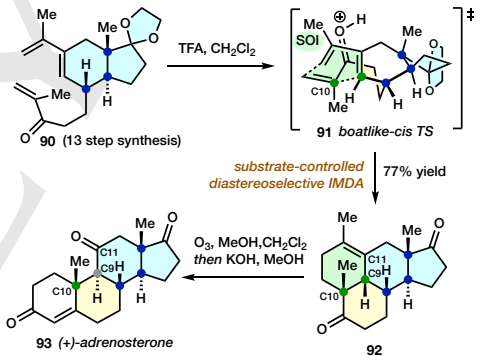

Scheme D17. The 16 step total synthesis of (+)-adrenosterone by Stork and Saccomano (1987), featuring a late stage decatrienone-type IMDA reaction, as the first step of a beautifully orchestrated DA-ozonolysis-aldol endgame. (TFA = trifluoroacetic acid)

Those who choose to carry out total syntheses commencing with precursors that are significantly simpler than the target molecule have the daunting task of forming many C–C bonds, many stereocenters and many rings. Some of the most impressive recent syntheses somehow achieve this feat in a step economic manner.

2.12. Antimalarial Amphilectanes and Cycloamphilectanes (Shenvi, 2012-2016)

In 2012, Shenvi and Pronin disclosed a concise synthesis of 7-isocyano-11(20),14-epiamphilectadiene **98**, a highly potent antimalarial compound (**Scheme D18**).[97] The authors united

cross-conjugated triene **94** containing a 1,3-dioxygenation pattern–dubbed a Danishefsky-type dendralene–with bis-dienophile **95** in a sequence comprising an intermolecular DA reaction followed later by an IMDA reaction. For decades, dendralenes and related C=C-bond rich acyclic cross-conjugated hydrocarbons have been seen as molecular outcasts, due to the false belief that they are unmanageable.[98] Their value as multi-dienes in so-called diene-transmissive Diels-Alder sequences is becoming more widely appreciated. In only the second application of a diene-transmissive Diels-Alder sequence in total synthesis,[99] Shenvi and Pronin build upon seminal work by Tsuge[100] to bring about a breathtakingly short synthesis of racemic natural product **98**.

The more electron-rich diene component of dendralene **94** reacted with the more electron-poor C=C dienophile of reaction partner **95** in an intermolecular DA reaction at room temperature, with excellent control of orientational regioselectivity. Upon addition of catalytic $Yb(OTf)_3$, the initial cycloadduct underwent silyl enol ether hydrolysis and methanol elimination to give rise to a cross-conjugated dienone, which underwent IMDA reaction presumably through *chairlike-trans* TS **96**. The unactivated IMDA cycloaddition of this semicyclic diene precursor was performed by microwave heating in 1,2-dichlorobenzene at 210 °C. Subsequent Krapcho demethylation-decarboxylation gave tricycle **97**, which was converted into the natural product **98** in short order.

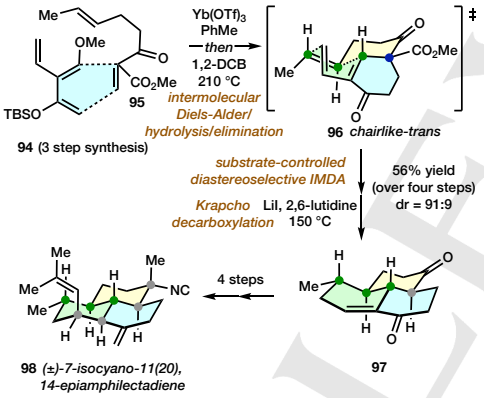

Scheme D18. Shenvi and Pronin's 10 step total synthesis of (±)-7-isocyano-11(20),14-epiamphilectadiene (2012) featuring an unactivated IMDA reaction.

The *chairlike-trans* TS **96** orients the diene and dienophile pseudoequatorially about the developing tether ring, and the dienophile approaches the semicyclic diene from below due to its attachment to the existing cyclohexenone ring. The short step count of this synthesis stems from its masterful design. Specifically, the DA-IMDA cycloaddition sequence installs both the isolated ketone and enone functionalities in tricycle **97** to permit the introduction of the remaining methyl, isobutenyl and exocyclic methylene groups, the first under substrate-stereocontrol.

In 2016, the Shenvi group built upon these results, reporting the enantioselective total synthesis of (+)-7,20-diisocyanoadociane **49** deploying an interesting variation of their earlier diene transmissive Diels-Alder sequence (**Scheme D19**).[101] We have previously seen a summary of Corey's total synthesis of this molecule (**Scheme D7**). In the Shenvi approach, intermolecular DA product **99** was generated in a similar manner to their earlier synthesis. This molecule has a stereocenter that is a spectator in the IMDA reaction but will become the C5 center (1,3,9-decatriene numbering) in the final product. The 8-phenylmenthyl ester auxiliary was used to set up the C5 stereocenter during the intermolecular DA reaction and this, in turn, now controls the configurations of the three new stereocenters formed in the IMDA reaction, which is brought about through heating a 1,2-dichlorobenzene solution of enone **99** to 180 °C for 24 h. The 8-phenylmenthyl ester chiral auxiliary undergoes thermal syn-elimination followed by decarboxylation under the reaction conditions. The resulting enol tautomerizes, perhaps under equilibrating conditions, to give the required *anti*-relative stereochemistry at the carbons α- and β- to the ketone. This impressive synthesis sets a very high standard for those wishing to further optimize the total synthesis of cycloamphilectane natural products.[102]

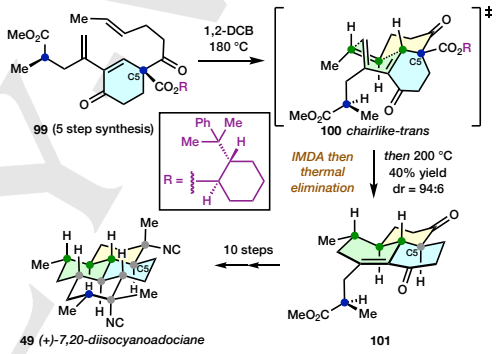

Scheme D19. The Shenvi group's 16 step total synthesis of (+)-7,20-diisocyanoadociane (2016).

Reiher and Shenvi subsequently used a 2-formyl-1,3-butadiene (an oxadendralene) in a double DA approach to kahlinol C.[103]

2.13. Vinigrol (Baran, 2009)

In 2009, the Baran group reported the first total synthesis of the terpenoid natural product vinigrol **105** (**Scheme D20**).[104] Vinigrol was isolated in 1987, and numerous unsuccessful attempts to complete the total synthesis of this particularly challenging diterpene had been made.[105] The successful synthesis by Baran and coworkers was a major achievement in total synthesis. The group utilized an IMDA reaction to assemble the key tetracyclic intermediate, which was set-up for a subsequent Grob fragmentation/ring expansion. The direct IMDA cyclization approach to vinigrol, i.e. without the need for the Grob fragmentation, had previously been reported by the Barriault laboratory.[106] The Barriault approach was ultimately successful, through a total synthesis which drew upon the Baran group synthesis endgame.[107,108]

The Baran synthesis contains a remarkable IMDA process, in that triene **102** underwent IMDA reaction *at ambient temperature* over 2 weeks to afford product **104** in quantitative yield as a single diastereomer. [109] The IMDA TS exhibits a *chairlike-cis* conformation **103**, thereby setting up two stereocentres and two rings of the natural product, after the subsequent Grob fragmentation clears the superfluous C–C bond.

The unusually mild conditions for this unactivated IMDA cycloaddition prompted a computational investigation by Krenske, Houk and coworkers.[26] Calculated barriers for the vinigrol IMDA system were 5.4 kcal/mol lower than the parent deca-1,3,9-triene, which is consistent with experimental observations. The unexpected ease of this "proximity induced" IMDA reaction was found to be only partly due to substrate preorganization. While the rigidity of the framework and an internal H-bond[110] were involved, strain release in the diene, specifically the endocyclic bicyclo[2.2.2]octene C=C bond, was also an important factor.

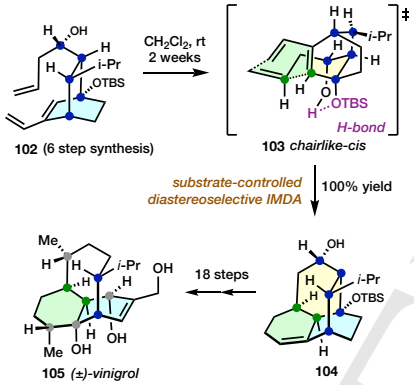

Scheme D20. An unusually facile unactivated IMDA reaction in the Baran group's 25 step total synthesis of (±)-vinigrol (2009).

The IMDA process is arguably at its most impressive when it is used to its full capacity: specifically, to directly form two new rings and four new stereocenters of a target molecule. Such is the case with the next synthesis.

2.14. Codeine (Stork, 2009)

The first use of an IMDA process for the synthesis of codeine **109** was reported by Stork and co-workers in 2009 (**Scheme D21**). [111] Their approach involved a [4+2] cycloaddition of a tethered, electron-rich diene onto a benzofuran dienophile. Benzofurans are electron-rich dienophiles and their use has been limited.[112,113] Nonetheless, the key cycloaddition was successfully carried out with racemic precursor **106** at 230 °C in a sealed tube to afford tetracycle **108** as the major product, carrying the requisite relative configuration at the four newly formed stereocenters generated in the IMDA reaction.

The authors speculated that the formation of the major diastereomer **108** might be the result of attractions between the ester carbonyl and the –OTES group (The minor diastereomer was the epimer at C5 (1,3,9-decatriene numbering), with a less sterically demanding pseudoequatorial –OTES substituent). We hypothesize that the product is formed through *boatlike-cis* TS **107**, which is perhaps necessary due to the conformational restrictions (three rotatable bonds) imposed by this very unusual tether. The two epimers were not separated, since the formation of the piperidine ring present in the natural product relied on the oxidation of the secondary alcohol (arising from the TES deprotection) to the ketone.

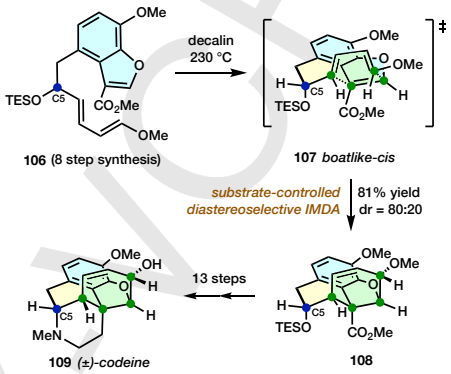

Scheme D21. The Stork group's 22 step total synthesis of (±)-codeine featuring an unusual benzofuran dienophile IMDA reaction (2009).

The IMDA reaction subsequently featured in other syntheses of morphinans.[114] Our next example of a 1,3,9-decatriene IMDA reaction in total synthesis involves the creation of two rings in the middle of a pentacyclic framework. Such an approach naturally lends itself to a convergent synthesis. The IMDA reaction is also strategically fascinating for another reason: it uses a 1,3-butadiene and a C=C dienophile, yet constructs an aromatic ring in the target molecule.

2.15. Halenaquinone (Trauner, 2008)

In 2008, Trauner and co-workers reported a synthesis of the polyketide natural product (–)-halenaquinone **113** (**Scheme D22**).[115] An IMDA reaction between a vinyl *para*-quinone as a diene [116] and an unactivated vinyl group as dienophile was implemented at a late stage of the synthesis. Various conditions were screened to optimize this reaction including elevated temperatures and Lewis acidic additives. The best yields were obtained, however, using ultra high-pressure. The cycloaddition was carried out in dichloromethane at room temperature under 10 kbar of pressure to afford the pentacycle **112** in 78% yield. The anticipated product from the IMDA step could not be isolated, as it underwent tautomerization under the reaction conditions to furnish product **112**. An MnO_2 oxidation completed the total synthesis.

This IMDA precursor is intriguing since it only carries one sp^3 carbon in the tether, which leads to a flattened conformation of the tether-forming ring in the preferred TS **111**. The authors used DFT calculations to locate TS **111**, which leads to the observed product **112**, along with an isomeric TS leading to the *cis*-ring junction isomer. TS **111** was found to be approximately 3 kcal/mol

lower in energy than the alternative, most likely due to the development of greater steric repulsion between the methyl and vinyl quinone moieties in the latter.

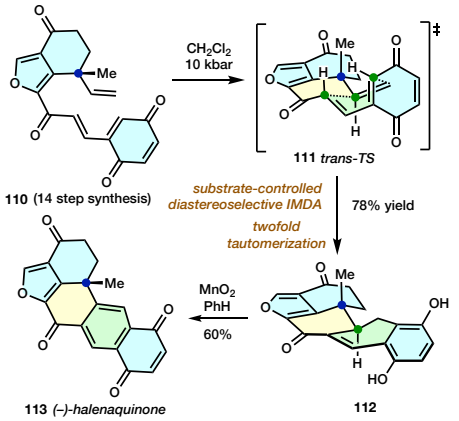

Scheme D22. The Trauner group's 16 step total synthesis of (–)-halenaquinone (2008).

The Trauner synthesis of halenaquinone generates two rings embedded within a multicyclic framework. The next synthesis achieves the same result but through a different IMDA tactic, and one with a long and distinguished history. The method generates a highly reactive diene through a temporary disruption in aromaticity. The IMDA reaction brings about re-aromatization.

2.16. Chelidonine (Hsung, 2012; Oppolzer, 1971)

The Hsung group reported the total synthesis of the alkaloid chelidonine **117** in 2012 (**Scheme D23**).[117] An ingenious enamide-benzyne [2+2] cycloaddition generated benzocyclobutane **114** in a step economic manner, which on heating in xylene at 120 °C underwent electrocyclic ring opening to an *ortho*-quinonedimethide (oQDM). An IMDA reaction of the *in situ* generated oQDM with the tethered, unactivated alkyne through TS **115** furnished 1,4-dihydronaphthalene **116**. Redox manipulations gave the natural product **117** (along with its desmethyl analogue, which is also a natural product) in short order.

Since the oQDM IMDA precursor is achiral and the dienophile is an alkyne, the product 1,4-dihydronaphthalene **116** is generated as a racemic mixture, resulting from alkyne approach to both π-enantiofaces of the diene in equal measure. (There are no *endo/exo*-diastereoselectivity attributes in DA reactions of alkyne dienophiles.)

The Hsung group's work followed in the footsteps of Opplozer and Keller's ground-breaking total synthesis of chelidonine **117** from 1971,[118] improving upon it with a better precursor synthesis. As was the case in the Trauner halenoquinone synthesis, the tether contains only a single sp^3 center, and the IMDA process simultaneously forges the central two rings of the natural product.

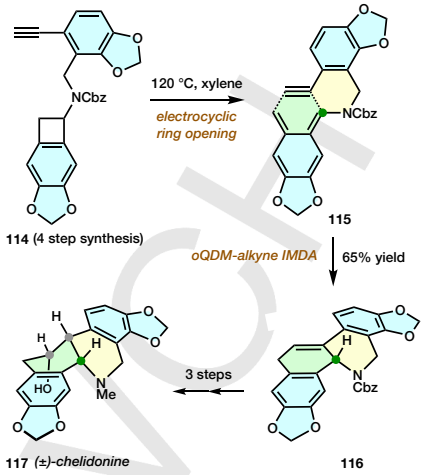

Scheme D23. The Hsung group's 8 step total synthesis of (±)-chelidonine (2012).

Due to their enhanced reactivity, oQDMs are generally not isolated and instead are generated and reacted *in situ.*[119] Oppolzer made many other important contributions in oQDM IMDA chemistry,[4] as did Vollhardt[120] and Kametani,[121] particularly in the synthesis of steroids.[122] The Kametani[123] and Vollhardt[124] total syntheses of estrone in 1976 and 1980, respectively, were a high point for the discipline.

Aromatic rings have been deployed as precursors to dienes in a number of creative ways. With oQDMs, aromaticity is broken then repaired in the electrocyclic ring opening/IMDA sequence, with new bonds being forged at adjacent benzylic sites. The situation is different with oxidative dearomatization, which is commonly used to generate 1,3-cyclohexadienes that react with dienophiles to form sp^3 carbon-rich bicyclo[2.2.2]octane frameworks. The next synthesis exemplifies the power of this sequence in a decatriene IMDA setting.

2.17. Platencin (Chen/Nicolaou, 2008-2009)

Inspired by earlier methodological contributions by the Liao group,[125] the Chen/Nicolaou group reported a formal synthesis of platencin **121** which used, as a centrepiece, an early stage IMDA reaction of an orthoquinonemethide monoacetal (**Scheme D24**).[126] The synthesis of the tricyclic core of the natural product **120** is exceptional, rapidly creating complexity from a structurally much simpler precursor. An enantioselective ketone reduction delivered precursor **118** in a step economic manner. Exposure to buffered $PhI(OAc)_2$ gave the requisite orthoquinonemethide monoacetal, which cyclized in refluxing toluene through *chairlike cis*-TS **119** to give tricycle **120**. The vinyl group dienophile is unactivated in this process, but the diene is electron poor. Perhaps this process is best categorized as an inverse electron demand Diels-Alder reaction.

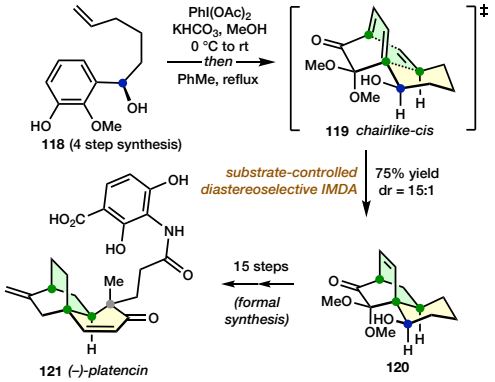

Scheme D24. The Nicolaou group's 20 step total synthesis of (–)-platencin (2008).

The hydroxyl group, vinyl group dienophile and more sterically demanding portion of the cyclic diene all adopt pseudoequatorial orientations in *chairlike cis*-TS **119**. A little work (8 steps) was then needed to manipulate cycloadduct **120** into an intermediate that had previously been converted into platencin **121**. The stereocenter carrying the hydroxyl group in substrate **118** is ablated later in the synthesis, having served its role to steer the creation of 3 target-relevant stereocenters in the IMDA event.

Cyclization of precursor **118** through *chairlike-cis* TS **119** is noteworthy. Roush and coworkers developed important methods for the stereocontrol of 1,3,8-decatriene IMDA reactions through a C5 (tether-based) stereocenter that is located adjacent to the diene. [127] High *trans*-diastereoselectivity in such IMDA processes was achieved through the incorporation of Br (a removable, bulky group) at C3 of the 1,3,8-decatriene. The process works through a combination of two effects: the preference of the C5 substituent to adopt an equatorial disposition in the IMDA TS, and the avoidance of 1,3-allylic strain between the C5 substituent and the C3 bromine. The Roush group coined the term "steric directing group strategy" to describe this method, which has significant synthetic value.

While 1,3,8-decatriene IMDA reactions are the most commonly reported subtype in the literature, they are by no means representative of the proven and potential scope of the process in target synthesis. Section 3 will describe the next most well-populated subtype of IMDA process, namely 1,3,8-nonatrienes, where different types of dienes, dienophiles, tethers and strategic maneuvers will be revealed, and powerful new variations on tactics introduced in Section 2 will be described.

3. 1,3,8-Nonatriene IMDA Reactions

IMDA reactions involving 1,3,8-nonatriene precursors are incredibly well represented in the literature, being only marginally fewer in number than those involving 1,3,9-decatrienes. As was the case with the previous section, catalyst-controlled enantioselective IMDA reactions in total synthesis are discussed first, since these processes involve some of the simplest substrates. Several catalytic enantioselective IMDA reactions of 1,3,8-nonatrienes have been reported[128] but its use in natural product synthesis is extremely rare. The first example was described in the late 1990s.

3.1. Isopulo'upone (Evans, 1997)

The 1997 total synthesis of isopulo'upone **126** by Evans and Johnson was a pivotal contribution, being the first example of a catalytic enantioselective IMDA reaction in total synthesis.[129] The development of the Cu(II) bis-oxazoline (BOX) catalyst **123** was reported earlier, being initially used for the intermolecular variant of the cycloaddition.[130] The total synthesis (**Scheme N1**) is dominated by the IMDA reaction (**122**→**125**), which creates the fused bicyclic system and all four stereocenters of the target. The IMDA reaction was performed on a precursor with an acyloxazolidinone-activated dienophile. Two point binding of this group to the Cu(II) center of C_2-symmetric chiral Cu(II)(BOX) catalyst **123** forms a square planar complex, which controls enantioselectivity by blocking the rear face of the dienophile C=C bond, as depicted in TS **124**. The *trans*-diastereoselectivity of IMDA reactions of 1,3,8-nonatrienes with terminal *E*-activated dienophiles such as this comes about from SOIs and favorable twist mode asynchronicity (see Introduction, **Scheme 7**).

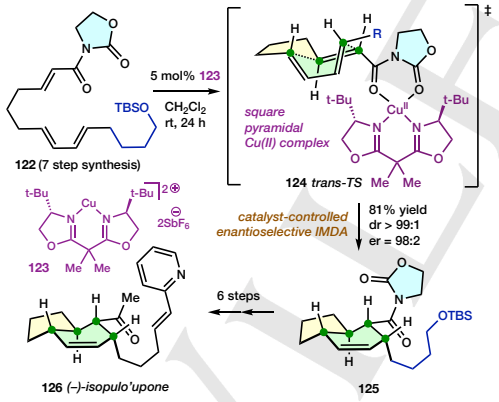

Scheme N1. Evans and Johnson's 14 step total synthesis of (–)-isopulo'upone (1997).

The deployment of this catalyst comes at a cost to the step count of the synthesis. Ideally, the IMDA reaction would be performed as the final step of the synthesis, on a fully armed precursor. Presumably, it is both the incompatibility of the pyridyl substituent with the catalyst and the requirement for a two-point binding mode of the dienophile activating substituent that preclude this.

In IMDA reactions–indeed synthesis more generally–we most often rely upon the influence of existing stereocenters in a molecule to control the configurations of new ones. Occasionally, however, existing stereocenters are too distant to exert an influence. The next example describes a rare case of a catalyst-controlled IMDA reaction of an enantiopure chiral precursor.

3.2. Muironolide A (Zakarian, 2015)

In 2015, Zakarian and co-workers reported an enantioselective total synthesis of the marine polyketide (+)-muironolide A **132** (**Scheme N2**).[131] The synthesis led to a reassignment of the relative stereochemistry of the natural product. A 1,3,8-nonatriene IMDA reaction was used to assemble the bicyclic isoindolinone ring system of the natural product roughly mid-way through the synthetic campaign. The IMDA reaction is unusual in that the diene was generated *in situ* from *β*-ketoamide **127** through a soft enolization method. A combination of La(OTf)$_3$, a chiral C_2-symmetric bis-oxazolinylpyridine (PYBOX) ligand[132] and Et$_3$N were deployed to generate the enolate and bring about a stereoselective IMDA process,[133] which proceeds with a 3:1 preference through TS **129** over its pseudoenantiomer.

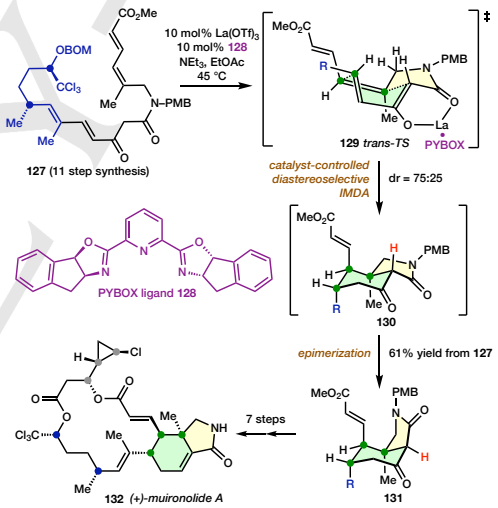

Scheme N2. The Zakarian group's 19 step total synthesis of (+)-muironolide A (2015).

The conformational restriction imposed upon the tether by chelation precludes a *cis*-TS, hence instigating *trans*-diastereoselectivity. Both the enolate derived from precursor **127** and the PYBOX ligand chelate to the La(III) ion. More structural information on this complex is needed, however, in order to explain, and perhaps improve upon, the modest *π*-facial stereoselectivity of the IMDA process. The initial *trans*-fused IMDA product **130** equilibrates to the more thermodynamically stable *cis*-isomer **131** under the reaction conditions. This epimerization does not impact upon the total synthesis, since this stereocenter is eliminated *en route* to the natural product. The

incorporation of the C=C bond at the correct location in the cyclohexene ring of muirinolide A **132** caused problems in an earlier approach by Molinski.[134] The use of ketoamide precursor **127** by Zakarian is an inspired solution to this issue, since it also permits catalyst-based IMDA stereocontrol.

In model systems, the IMDA reaction also proceeds with high kinetic *trans*-diastereoselectivity through an internally H-bonded enol structure related to *trans*-TS **129**. The lack of acceleration of the process with added base, in addition to other observations, led to the authors discounting the alternative, stepwise double Michael addition mechanism.[135]

Prototropic shifts of products and precursors feature in the following two examples of early stage IMDA reactions in natural product total syntheses.

3.3. Harringtonolide (Zhai, 2016)

In 2016, Zhai and co-workers reported the catalytic enantioselective synthesis of the diterpenoid (+)-harringtonolide **137**, deploying a diastereoselective IMDA reaction at an early stage of the synthesis (**Scheme N3**).[136] Target molecule **137** carries seven stereocenters, six of which are contiguous and located on one cyclohexane ring of the molecule. The IMDA reaction generates three of these, by parlaying stereogenicity from a pre-existing stereocenter in **133**, which is generated through enantioselective ketone reduction.

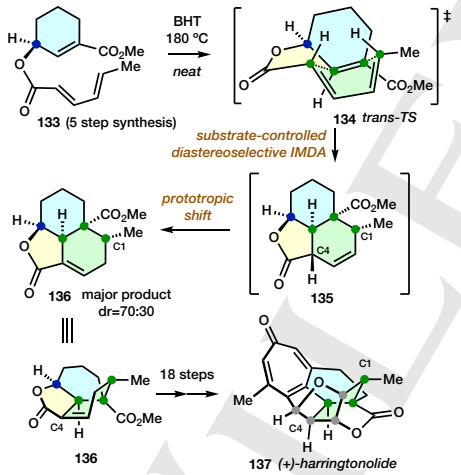

Scheme N3. The Zhai group's 24 step total synthesis of (+)-harringtonolide (2016).

The IMDA process (**133**→**135**) was promoted by heating the neat starting material at 180 °C in the presence of 10 mol% of the radical chain inhibitor BHT.[137] The forcing conditions required for the IMDA reaction, which was carried out on a batch of over 50 g of precursor **133**, was accompanied by tautomerization to the conjugated enoate **136**. The *cis*-fused C4 epimer of **135** was generated though deprotonation and kinetic protonation of conjugated enoate **136**, to set up the required configuration at this site for the natural product. The direct generation of this diastereomer, with the C1-Me and C4-H *cis*- to one another, would have mandated the IMDA cyclization of a challenging *E,Z*-diene.

Only two diastereomeric IMDA adducts are accessible from substrate **133**, since approach to the top *π*-diastereoface of the dienophile (as drawn) is mandated by the configuration of the pre-existing stereocenter on the cyclohexene ring. In TS **134**, which leads to the major product, the C9-CO_2Me group is *endo;* the minor product (the C1 epimer of **136**) arises from the corresponding *exo*-CO_2Me TS. The tether carbonyl is likely to be substantially twisted from the plane of the diene in TS **134**, thereby raising the diene HOMO relative to the ground state, hence promoting a normal electron demand DA process. Perhaps a higher preference for the *trans*-pathway would result by replacing the –CO_2Me group with a more electron withdrawing (and smaller) –CHO group.

Tactically, this synthesis deploys the ester link between the diene and dienophile as a temporary connection, a concept first articulated by Stork.[138] The reactivity of the functionalized carbons of **136** and the latent reactivity of methylene groups adjacent to them was exploited to elaborate the natural product.

The next synthesis features an IMDA reaction of a 1,3,8-nonatriene precursor that is generated *in situ*, by way of a catalyst-controlled enantioselective tautomerization.

3.4. Himalensine A (Dixon, 2017)

The Dixon group's total synthesis of himalensine A **142** features enantioselective catalysis of a proton transfer event that immediately precedes an IMDAF (intramolecular Diels-Alder with a furan diene) reaction (**Scheme N4**).[139] The substrate is designed such that the proton transfer causes: (a) a C=C bond shift into conjugation, hence bringing about its LUMO-lowering activation as a dienophile, while simultaneously (b) extending the diene-dienophile tether from 2 to 3 atoms, replacing a much less reactive 1,3,7-octatriene with a 1,3,8-nonatriene, hence setting up the IMDAF event, and (c) converting an achiral precursor into a chiral one, which can bring about a substrate-controlled IMDAF event. Thus, five new stereocenters are created during this spectacular transformation. While only three of these find their way into the final target, the functionality originating from the amidofuran precursor is instrumental in the elaboration of the natural product from the IMDAF adduct. The IMDAF event also creates two of the five rings of the natural product.

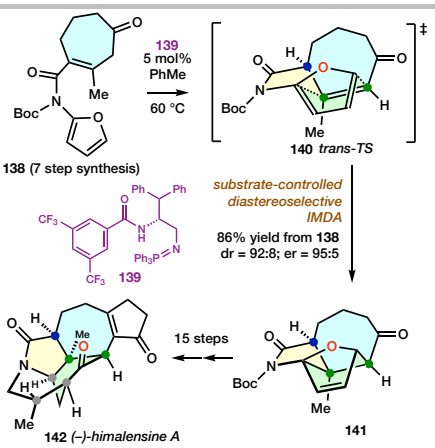

Scheme N4. The Dixon group's 23 step total synthesis of (–)-himalensine A (2017).

An optimized bifunctional iminophosphorane (BIMP) catalyst **139** was used to bring about the enantioselective tautomerization on multigram scale. Constrained by the short three atom diene-dienophile tether, the furan diene is required to approach from the lower face of the cycloheptenone dienophile in the ensuing IMDAF event. The *endo/exo*-selectivity of the IMDAF reaction is inconsequential for the total synthesis, since the relevant stereocenters are removed in subsequent steps. Nonetheless, the reaction is highly *exo*-selective, a result ascribed to destabilizing steric clashes involving the quaternary Me group in the *endo*-TS.

IMDAF reactions involving amidofuran dienes feature prominently in alkaloid total synthesis, largely thanks to the efforts of the Padwa group, who have made many important contributions in the field. The total synthesis of dendrobine is representative, highlighting the key sequence of these processes, a powerful IMDAF-oxabridge ring opening sequence.

3.3. Dendrobine (Padwa, 2000)

Padwa and co-workers reported the synthesis of the alkaloid dendrobine **148** in racemic form in 2000 (**Scheme N5**).[140] The assembly of the tricyclic core **147** relied on an IMDAF reaction between an amidofuran and a cyclopentene dienophile, the intrinsically poor Diels-Alder reactivity of which was overcome through tethering. The cycloaddition was induced by heating a toluene solution of the IMDA precursor at 165 °C in a sealed vessel. Under the reaction conditions, the resulting oxanorbornene product **145** underwent cleavage of the oxa-bridge to give putative zwitterionic intermediate **146**, which furnished tricyclic product **147** through hydride shift. The cycloaddition is proposed to proceed *via trans*-TS **144**, which was noted in earlier nonatriene-type IMDAF studies.[141] The adoption of the alternative *cis*-TS would presumably be met with steric repulsion between the furan and cyclopentene rings.

In a related study using a model substrate lacking the isopropyl group, the corresponding ring opened product was obtained as a single diastereomer.[142] Presumably, the 1,2-hydride shift is constrained to occur through a suprafacial mechanism, and epimerization takes place thereafter, to give a mixture of epimers **147**. This epimeric mixture is inconsequential, since this stereocenter is ablated then regenerated stereoselectively later in the synthesis. The IMDAF reaction and concomitant bridge scission represents the key phase of the synthesis, creating the bicyclic hexahydroindole segment of the natural product and two stereocenters. While the reported synthesis involves a racemic IMDAF precursor **143**, it could be rendered enantioselective through preparation of the same precursor in nonracemic form.

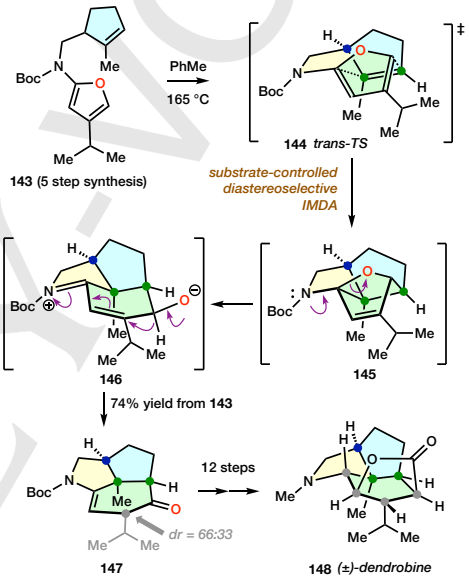

Scheme N5. The Padwa group's 18 step total synthesis of (±)-dendrobine (2000).

While IMDAF substrate **143** needs high temperatures to cyclize, the incorporation of a carbonyl group in the tether can lead to a dramatic rate enhancement through conformational control, in a situation where the C=O bond is *not* in conjugation with a C=C dienophile.[143] The room temperature IMDAF reaction of such an unactivated dienophile-furan diene combination was exploited in Padwa's subsequent synthesis of the alkaloid *epi*-zephyranthine.[144]

The Boger group have also made many important and creative contributions in alkaloid synthesis. Arguably, the pinnacle of these contributions[145] involves a domino sequence of three pericyclic reactions initiated by an IMDA process of a close relative of a furan, namely a 1,3,4-oxadiazole.

3.4. Vindoline (Boger, 2010)

The Boger group's synthesis of vindoline **154** deploys precursor **149**, which contains only two of the five rings of the natural product; the remaining three rings are created in the key phase of the synthesis, which is depicted in **Scheme N6**.

Upon heating to 140 °C, an inverse electron demand IMDA reaction occurs between the carbomethoxy-substituted 1,3,4-oxadiazole ring diene and the trisubstituted enol ether C=C dienophile of precursor **149**, to generate oxabridged heterocycle **151**. This initial 1,3,8-nonatriene IMDA process proceeds by way of either *trans*-TS **150** –or its *cis*-congener– in which the π-diastereofacial stereoselectivity is controlled by the preference for a pseudoequatorial orientation of the $–CH_2OMOM$ substituent in the developing pyrrolidine ring. The *cis/trans*-stereoselectivity of this initial IMDA process is inconsequential for the completion of the total synthesis, since both initial IMDA adducts, i.e. *trans*-isomer **151** and its *cis*-diastereomer, unite through the following step, a retro-[3+2] cycloaddition to expel a molecule of dinitrogen. This process generates an oxonium ylide, which undergoes an intramolecular [3+2] cycloaddition through TS **152** to form oxabridged hexacycle **153**. Cleavage of the oxabridge and several additional manipulations, including an ingenious one carbon ring expansion of the IMDA tether-generated pyrrolidine ring, afforded the target natural product **154**.

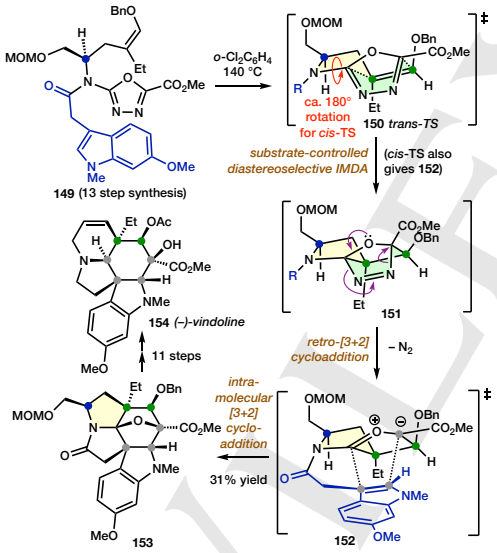

Scheme N6. The Boger group's 25 step total synthesis of (–)-vindoline (2010).

The IMDA reaction **149**→**151** generates two of the six stereocenters of the natural product, and creates the setting for the *in situ* generation of three more, in the ensuing [3+2] cycloaddition. The final stereocenter is installed through reductive cleavage of the oxabridge. It is noteworthy that the ring expansion proceeds with deletion of the pre-existing stereocenter, which controlled the initial IMDA event. This synthesis is intriguing from a strategic perspective, since neither of the two rings formed in the IMDA reaction find their way into the natural product. Hence, there are no direct clues in the target molecule which hint at the retrosynthetic application of the IMDA process.

Another impressive synthesis of a very different type is Wipf's cycloclavine synthesis, which features no less than two 1,3,8-nonatriene IMDA reactions. The second in the sequence is an IMDAF process and the first, which will be discussed in detail, uses an unusual methylenecyclopropane dienophile.

3.7. Cycloclavine (Wipf, 2011-2017)

The Wipf group reported the enantioselective total synthesis of the alkaloid (–)-cycloclavine **158** in 2017, following the disclosure of a closely related route to the racemic natural product in 2011.[146] The concise 11 step sequence (**Scheme N7**) involved two separate 1,3,8-nonatriene IMDA cycloadditions, the first of which was assisted by strain-release of an unusual methylenecyclopropane dienophile.[147] Thus, vinylogous imide **155** was converted into its corresponding silyl enol ether and the resulting 1,3,8-nonatriene underwent IMDA reaction upon microwave irradiation, predominantly through *trans*-TS **156**. Tricycle **157** was isolated as the major product, along with a small amount of its C4 epimer (1,3,8-nonatriene numbering), resulting from the corresponding *cis*-TS. The total synthesis was completed though annulation of a bicyclic indole system onto the cyclohexanone ring of adduct **157**, which was achieved *via* an IMDAF–aromatization sequence.[148]

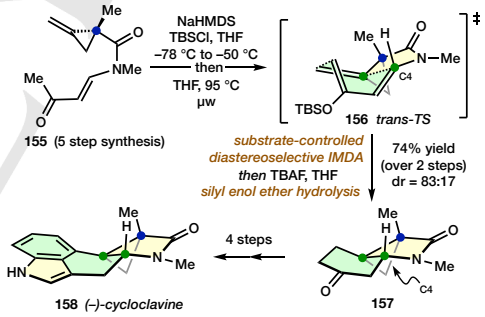

Scheme N7. The Wipf group's 11 step total synthesis of (–)-cycloclavine (2011-2017).

The IMDA reaction depicted in **Scheme N7** represents the most significant step of the synthesis, since it creates two of the five rings of the natural product and two of its three stereocenters. Both the developing γ-lactam ring in TS **156** and the one in product **157** are closer to planarity than those in a typical 1,3,8-nonatriene IMDA process, due to the presence of the cyclopropane ring and the amide group. Only two diastereomeric cycloaddition pathways are feasible, since the diene is constrained to approach the dienophile from the front face, as shown in TS **156**. (The tethered diene projects forward from its point of attachment to the cyclopropane ring in TS **156**.) The diene is an electron rich, Rawal-type[149] system. The strain in methylenecyclopropane presumably causes LUMO lowering,[150]

which may be a contributing factor to the low barrier of this IMDA reaction.

Experimentally determined product compositions were mirrored by computational studies, which indicate that TS **156** leading to *trans* product **157** is favored over the *cis*-TS since the latter has a steric clash between the diene and the methyl group attached to the cyclopropane ring.

One of the most intricate and unusual tethers in a type 1 IMDA reaction was described by the Crimmins group.

3.8. Eunicellin diterpenes (Crimmins, 2004-6)

Crimmins and co-workers reported the total synthesis of the eunicellin diterpenes (–)-astrogorgin and (–)-ophirin B in 2004-6.[151] The synthesis of (–)-ophirin B **162** is summarized in **Scheme N8**. 1,3,8-Nonatriene **159**, with a nine-membered ring bridging C5 and C7 (1,3,8-nonatriene numbering), underwent IMDA reaction at room temperature. The low barrier for this IMDA process is a manifestation of the presence of a diene and dienophile that are both electronically activated for a normal electron demand cycloaddition to proceed with the correct orientational regioselectivity. The diastereoselectivity of the IMDA reaction of **159** was 75:25 with a free tertiary alcohol but >98:2 with a TES protecting group (as shown in **Scheme N8**). Adduct **161** was converted into the target molecule by functional group manipulations.

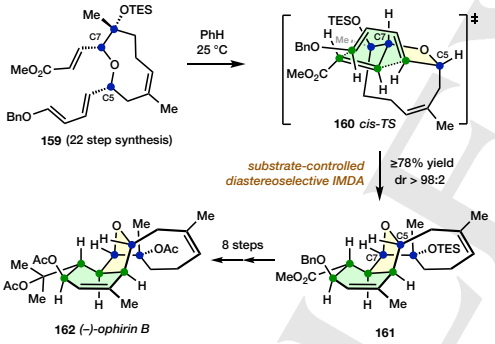

Scheme N8. The Crimmins group's 31 step total synthesis of (–)-ophirin B (2004-6).

Product **161** is proposed to arise from *cis*-TS **160**, with an *exo*-disposed dienophile $-CO_2Me$ group. In light of subsequent computational modeling of related systems by Hooper, Houk and coworkers,[152] the bridge between C5 and C7 is most likely accommodated about the developing five membered (tetrahydrofuran) ring through one pseudoaxial and one pseudoequatorial substituent. The three alternative modes of addition, which would lead to diastereomeric products, would all place the diene or dienophile (or both) closer to the bridging carbon chain, hence suffering destabilizing steric interactions.

The Kim[153] and Holmes[154] groups reported similar results from IMDA reactions of related precursors. The study by Hooper, Houk and co-workers[152] reported the effect of bridging ring size on IMDA stereoselectivity. Whereas 7 and 8 membered bridges favor *trans*-TSs through C5,C7-diaxial bridge conformations, 9 membered rings prefer a *trans*-TS with a C5,C7-axial/equatorial bridge conformation.

In **Section 2.16**, we highlighted the synthetic power of orthoquinone dimethide generation and *in situ* IMDA reaction in the decatriene series. Benzocyclobutane precursors are also commonly deployed as precursors to orthoquinone dimethides in nonatriene IMDA reactions. Magnus' total synthesis of vindoline and 8-oxotabersonine deploy such processes involving indole-based orthoquinone dimethides.[155] An alternative method for the generation of orthoquinone dimethides is photoenolization. The Nicolaou group's synthesis of the hamigerans is an instructive illustration of the value of this relatively underutilized method.

3.9. Hamigerans (Nicolaou, 2001-2004)

The syntheses of several hamigeran natural products were reported by the Nicolaou group in the early 2000s.[156] The preparation of hamigeran B **166** (**Scheme N9**) is representative. Irradiation of substituted benzaldehyde **163** in deoxygenated benzene promoted a 1,5-sigmatropic hydrogen shift from the benzylic methylene to the formyl oxygen, to generate the reactive enolic orthoquinone dimethide depicted in TS **164**. An *in situ* IMDA reaction with the tethered enoate C=C dienophile afforded the tricyclic system **165** in 92% yield.

The cycloaddition is proposed to proceed *via trans*-TS **164**, with the *π*-diastereofacial stereoselectivity controlled by the preference of the tether –OMOM substituent to adopt a familiar pseudoequatorial orientation, and the *endo*-oriented $-CO_2Me$ group of the *E*-dienophile dictating the *trans*-preference of the process.

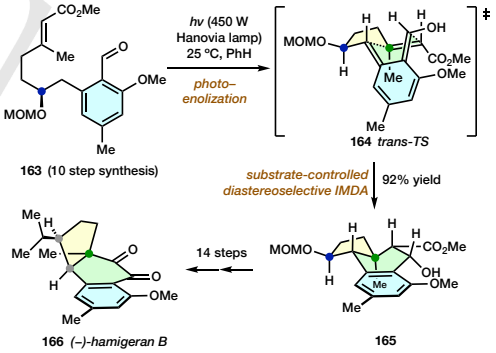

Scheme N9. The Nicolaou group's 25 step total synthesis of (–)-hamigeran B (2001-2004).

The IMDA reaction generates two of the three rings of the product but only one of its three stereocenters, despite four being created in the IMDA reaction. Two of the four stereocenters generated in the IMDA reaction are eliminated *en route* to the natural product and a third, at the ring junction, is inverted to generate the *cis*-geometry of the natural product.

The photoenolization and *in situ* intermolecular Diels-Alder trapping of *o*-methylbenzophenone was originally reported by Yang and Rivas in 1961.[157] Relatively few photoenolization/Diels-Alder sequences have been reported since.[158] While the Nicolaou group study is an important contribution, we feel that the definitive, short step count application of this process in total synthesis has yet to be reported.

Dearomatization-IMDA sequences are by no means limited to orthoquinone dimethides. IMDA reactions of *in situ*-generated orthoquinone monoacetals have also been deployed to great effect, with many notable reports featuring nonatriene-type precursors, including Rodrigo's total synthesis of xestoquinone and halenoquinone [159] and Hudlicky's hydromorphone synthesis.[160] The process highlights the impressive synthetic efficiency gains that can be achieved by conducting an IMDA reaction *in situ*, immediately following precursor generation. The next example hints at the broad applicability of this tactic.

3.10. Gibberellins GA_{12}, GA_{111} and GA_{112} (Toyota, 2000)

The use of a decatriene IMDA reaction for A-ring creation in Corey's approach to the most prevalent C_{19} gibberellin, gibberellic acid (GA_3) was presented in **Section 2.10**. In 2000, Toyota and co-workers reported the use of a 1,3,8-nonatriene IMDA reaction to concurrently annulate the A and B rings onto a pre-existing CD-ring unit *en route* to the rare C_{20} gibberellins, GA_{12} **170**, GA_{111} **171** and GA_{112}, **172** (**Scheme N11**).[161]

In a one-pot sequence, bromoenoate **167** was subjected to Stille cross coupling with vinyltributylstannane to generate a diene, which underwent IMDA reaction *in situ* through *trans*-TS **168** to selectively form adduct **169**, introducing two rings and two stereocenters of the target molecule. Completion of the total synthesis required functional group manipulations and the introduction of one more carbon, for which the cyclohexene π-bond was employed.

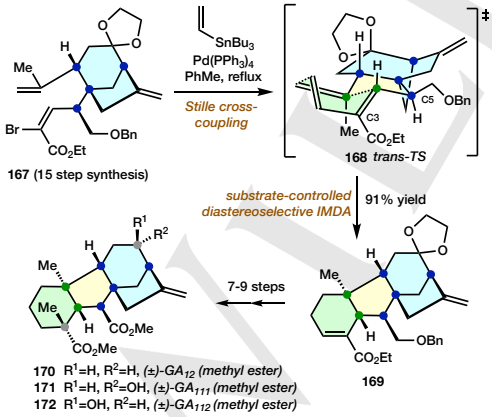

Scheme N11. The Toyota group's 23-25 step total synthesis of C_{20} gibberellins (2000).

The authors attribute the high stereoselectivity of the cycloaddition to unfavourable steric interactions between the diene's carboethoxy group and the $-CH_2OBn$ substituent at C5 in the alternative, *cis*-TS. These repulsive interactions are absent in *trans*-TS **168**, which gives rise to the desired cycloadduct **169**.

The mildness of the reaction conditions (110 °C) is notable for an IMDA reaction of an unactivated dienophile. The CD-ring system of precursor **167** is conformationally rigid, hence the diene and dienophile are constrained to be within proximity. A similar explanation was later put forward to explain a facile unactivated IMDA process in a vinigrol total synthesis (**Section 2.13).** Perhaps this IMDA reaction can be viewed as an inverse electron demand cycloaddition, perhaps with diene LUMO-lowering activation by Lewis acid complexation by the Stille reaction byproduct, Bu_3SnBr. An argument against this proposal comes in the form of the known reactivity of cross-conjugated 1-carboethoxy-1,3-butadienes, which are prone to DA dimerization involving the enoate C=C bond.[162]

Undergraduate students of chemistry are well aware of the high Diels-Alder diene reactivity of cyclopentadiene. It is perhaps surprising, therefore, that cyclopentadienes are so rarely encountered in Diels-Alder reaction-based total syntheses. Cyclopentadienes are also prone to DA dimerization, hence are also best deployed by generation *in situ*.

3.11. Illisimonin A (Rychnovsky, 2019)

The IMDA reaction deployed in Burns and Rychnovsky's recent total synthesis of illisimonin A **176** is depicted in **Scheme N12**.[163] The sequence involving the generation of the diene and its *in situ* intramolecular cycloaddition is realized beautifully. Thus, the 2-cyclopenten-1-one unit of precursor **173** is deprotonated to the dienolate, which is then trapped as a six-membered ring silyl acetal on reaction with Me_2SiCl_2. An IMDA reaction then ensues, through *trans*-TS **174**, to furnish adduct **175** after cleavage of the silyl acetal. The cycloadduct contains functionality that is well suited for elaboration into the natural product.

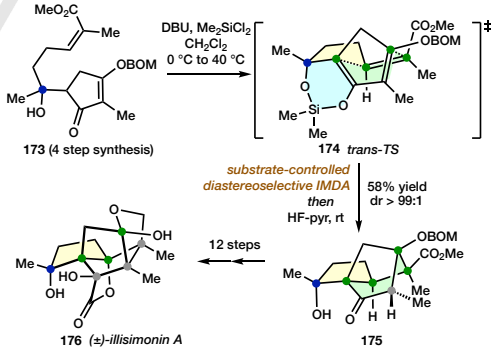

Scheme N12. Burns and Rychnovsky's 17 step total synthesis of (±)-illisimonin A (2019).

The cycloaddition is highly diastereoselective, since the presence of the silyl acetal imposes constraints upon the system, not only to react through a *trans*-TS but also for the dienophile to approach a specific π-diastereoface of the diene. Three of the

seven stereocenters of the target are installed in this process, but only the tether ring is maintained from cycloadduct **175** into target molecule **176**.

Cases have been covered thus far which show the *in situ* generation of dienes by elimination, C–C cross-coupling, and hydrogen shifts. The next example is an interesting case of a tether contraction to create a nonatriene IMDA precursor.

3.12. Hirsutellone B (Nicolaou, 2009)

The 2009 total synthesis of hirsutellone B **180** by the Nicolaou group (**Scheme N13**) features a sophisticated, one flask tricyclization process, which forms no less than three C–C bonds and six stereocenters of the target molecule.[164] This cleverly-orchestrated sequence involves an initial Sakurai-type, *6-exo-tet* epoxide scission by the 2,4,6-heptatrienyl-1-trimethylsilyl moiety of substrate **177**, which creates the 1,3,8-nonatriene precursor. This species undergoes IMDA reaction through *trans*-TS **178**–activated by the same Lewis acid as the epoxide ring opening–to furnish tricycle **179**, with *trans-anti-trans* stereochemistry. The hydroxy- and carbomethoxy-substituents of adduct **179** are ideally situated for elaboration to the bridging paracyclophane ring system of natural product **180**.

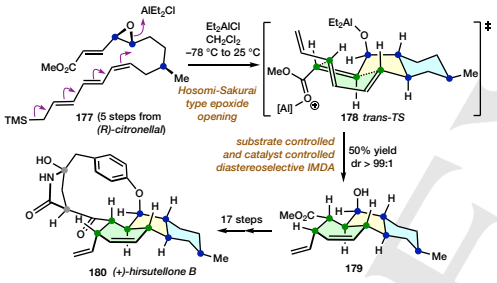

Scheme N13. The Nicolaou group's 23 step total synthesis of (+)-hirsutellone B (2009).

The initial Sakurai-type cyclization proceeds preferentially through a developing cyclohexane ring tether conformation with an equatorially-disposed methyl group. In the subsequent IMDA TS **178**, the freshly minted cyclohexane adopts a chair conformation and the diene and dienophile substituents sit in pseudoequatorial orientations relative to the developing five membered ring. The two diene C=C bonds migrate into position in the initial cyclohexane ring formation, resulting in a smooth and satisfying tricyclization event.

The Nicolaou synthesis of the tricyclic portion of hirsutellone B has an almost biomimetic feel to it, such is its elegance of composition. Domino sequences involving IMDA reactions are indeed known by Nature. The next example is an impressive biomimetic synthesis, in which a 1,3,8-nonatriene is generated *in situ* through an intermolecular Diels-Alder process.

3.13. Bolivianine (Liu, 2013)

The 2013 synthesis of (–)-bolivianine **185** by Liu and co-workers represents a validation of a proposal for a revised biosynthesis.[165] The synthesis intersected the natural product (+)-onoseriolide, which was rapidly converted into (–)-bolivianine **185** in only two synthetic steps, namely oxidation followed by an ambitious late stage domino intermolecular Diels-Alder–IMHDA sequence (**Scheme N14**). This spectacular endgame phase of the synthesis, involving heating of oxidation product **181** and monoterpene **182** in toluene at 150 °C, installed three new rings, four new C–C bonds and five stereocenters of the natural product. This impressive synthetic work, which represents the first intermolecular DA-IMHDA cascade in natural product total synthesis, is somewhat reminiscent of the biomimetic total synthesis of (–)-FR182877, which features a carbo- followed by a hetero-DA process but in a transannular setting (**Section 4.22**).

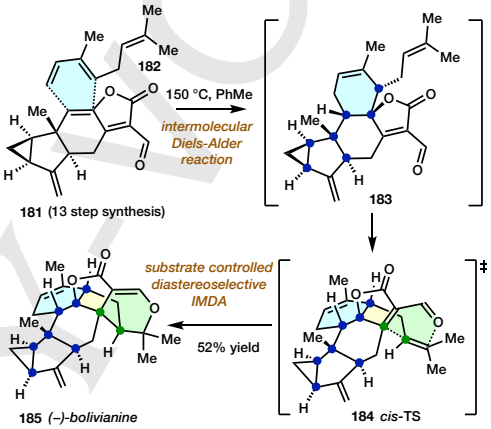

Scheme N14. The Liu group's 14 step total synthesis of (–)-bolivianine (2013).

The requirement for heating is related to the first DA reaction only, since the IMHDA reaction of intermediate **183** (prepared separately) was found to proceed at room temperature upon storage in ethyl acetate (70% yield over 2 days). The *exo*-mode intermolecular cycloaddition proceeds with diene **182** approach to dienophile **181** from the bottom face, as drawn. Thus, the trisubstituted C=C dienophile is constrained to approach the 1-oxadiene from the lower face, too, as shown in *cis*-TS **184**.

1,3,8-Nonatriene IMDA reactions feature prominently in total syntheses that result from astute biosynthetic speculation. The rather taciturn descriptor "biomimetic" does not fully acknowledge the significant intellectual contribution made in the lead up to the experimental work associated with such syntheses.

The most step economic biomimetic syntheses generate the immediate precursor to the IMDA reaction *in situ*. In Nicolaou's masterful gambogin synthesis, an aromatic Claisen rearrangement brings about a dearomatization to set up a nonatriene IMDA event.[166, 167] Trauner's pinnatal synthesis involves the oxidation of an allylic alcohol to an enal, which participates as a C=C dienophile in an IMDA reaction at ambient temperature. A 6π electrocyclization establishes the cyclic diene in the previous step of the synthesis.[168]

Another of Trauner's instructive contributions involves a tautomerization to create a nonatriene precursor for a biomimetic IMDA reaction.

3.15. Rubioncolin B (Trauner, 2008)

It is often the case in biomimetic syntheses involving IMDA reactions that the cycloaddition is deployed at a very late stage of the synthesis. Trauner's rubioncolin B synthesis[169] is a case in point, with the IMDA reaction (**186**→**188, Scheme N15**) generating a monomethyl ether of the natural product **189**. The IMDA process simultaneously generates two of the three heterocyclic rings at the center of the fused heptacyclic framework of the natural product. The strategic advantage of the process is unmistakable, with precursor **186** carrying an ester linkage: an obvious location for convergent disconnection.

The IMDA reaction involved an *ortho*-quinonemethide (as a 1-oxa-1,3-butadiene) and a benzofuran C=C dienophile, which unite as depicted in TS **187** to regenerate a naphthalene ring, along with fused dihydropyran and butyrolactone rings. TASF brings about desilylation of precursor **186**, which was oxidized *in situ* with $PhI(OAc)_2$ to the 1,4-naphthoquinone. In turn, this undergoes a (presumably reversible) 1,5-prototropic shift to the (unisolated) IMDA precursor, which cyclizes to **188** at ambient temperature.

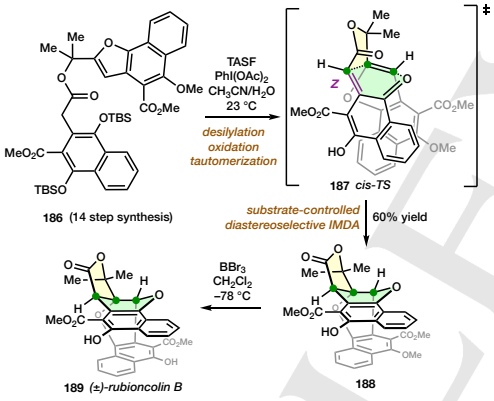

Scheme N15. The Trauner group's 16 step total synthesis of (±)-rubioncolin B (2008).

This IMDA reaction converts an achiral precursor into a racemic product carrying three contiguous stereocenters. The authors report that the TS leading to the observed *cis*-fused (lactone/dihydropyran ring junction) product was only 15 kcal/mol higher in energy than the *ortho*-quinonemethide IMDA precursor, which in turn was very similar in energy to its 1,4-naphthoquinone tautomer (DFT geometry optimizations at B3LYP/6-31G** level of theory). The *Z*-configured C=C bond of the 1-oxa-1,3-butadiene (as highlighted in TS **187**) precludes the adoption of a *trans*-TS. Both *E*- and *Z*-C=C geometries are presumably formed in this reaction but reversibly, with the *Z*-diastereomer enjoying a lower IMDA TS barrier. Perhaps *π•••π* stacking interactions stabilize TS **187**.

Evidently, this IMDA process is one of inverse electron demand, and hence is under $HOMO_{dienophile}$–$LUMO_{diene}$ FMO control. The ease by which the IMDA reaction proceeds (i.e. at ambient temperature), coupled with the fact that the natural product was isolated in racemic form, adds weight to the contention that the process is biomimetic.

3.16. Verrubenzospirolactone (George, 2017)

The total synthesis of racemic verrubenzospirolactone **192** by the George group[170] is representative of a broader, recent trend of extremely concise biomimetic total syntheses. The key step (**Scheme N16**) involved a 1,3,8-nonatriene IMDA reaction of precursor **(*Z*)-190**, which was prepared in a longest linear sequence of only five steps from 2-methylhydroquinone and citral. The IMDA reaction, which was conducted "on water", forged the *trans*-fused tetrahydroindane core in the final step of the total synthesis. Four of the five stereocenters were also installed in this IMDA reaction, which also proceeds – albeit slowly – at 30 °C. The natural product is optically active, hence appears to be nonracemic. An enantiocontrolled route to the natural product, therefore, simply requires access to precursor **(*Z*)-190** in enantioenriched form.

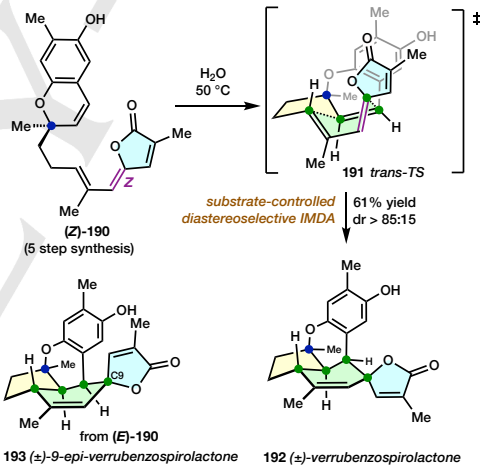

Scheme N16. The George group's 6 step total synthesis of (±)-verrubenzospirolactone (2017).

The IMDA reaction proceeds through *trans*-TS **191**, irrespective of the enol ester C=C bond geometry. Thus, the natural product is generated from precursor **(*Z*)-190** and the C9-epimer of the natural product **193** is produced from its (*E*)-isomer (and in one step fewer). Perhaps *trans*-TS **191** is stabilized by *π•••π* stacking between the electron-rich aromatic ring and electron-poor butenolide ring.

This IMDA reaction is unusual since it involves a relatively unactivated dienophile (a 2*H*-chromene) and a diene whose reactive *cisoid* conformation would likely suffer from significant steric repulsion, irrespective of C=C bond geometry. As was the case with the previous synthesis, this reaction can also be

regarded as an example of an inverse electron-demand Diels-Alder process.

Some biomimetic IMDA processes are easier to uncover than others. The presence of a cyclohexene ring in a natural product is perhaps the most obvious piece of evidence. The next example of a biomimetic IMDA reaction involves an alkaloid synthesis, wherein the Diels-Alder retron is hidden in the target structure by tautomerization.

3.17. Brevianamide A (Lawrence, 2020)

The brevianamide A synthesis by the Lawrence group is a masterclass in IMDA-based biomimetic total synthesis.[171] The IMDA reaction is the key step of an extended domino sequence, which commences with fused pentacycle **194** (**Scheme N17**). Treatment with LiOH in water at ambient temperature brings about conversion into bridged hexacycle **199**, brevianamide A. The sequence starts with a base-induced 1,2-elimination of the monoacylated aminal group of precursor **194**. The resulting 3-hydroxy-3*H*-indole **195** then undergoes a suprafacial 1,2-alkyl shift to 2,2-dialkylated-3-indolone **196**, which tautomerizes to generate the 2-aza-1,3-butadiene. IMDA reaction proceeds through TS **197** to furnish cycloadduct **198**, which finally tautomerizes to natural product **199**, along with a small amount of the diastereomeric natural product, brevianamide B, which has the opposite absolute configuration at the three newly-formed stereocenters.

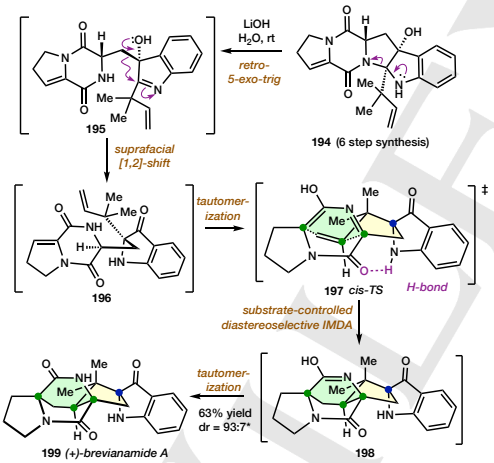

Scheme N17. The Lawrence group's 7 step total synthesis of (+)-brevianamide A (2020) (* minor diastereomer = brevianamide B)

This remarkable sequence came about through a reinterpretation of earlier work: Other groups had previously speculated on the possible biosynthetic origin of this and related natural products but experimental work did not quite fit the hypothesis.[172] The nonenzymatic synthesis of both **199** and its diastereomer in water at ambient temperature, in roughly the same relative proportions as isolated from the natural source, makes for a compelling argument for biomimicry.

The stereoselectivity of the key IMDA reaction is interesting, since both diastereomeric products result from *cis*-TSs. Domingo performed a DFT study into this reaction in 1997.[173] Brevianamide A is preferred over brevianamide B since only the TS leading to the former has the potential for a stabilizing H-bond (see TS **197**). The *π*-diastereofacial preference is, therefore, understandable but the preference for the *cis*-TSs over the *trans*-TSs has not been explained. Perhaps the *trans*-TSs are disfavored due to a steric clash between the same amide carbonyl O and the pseudoaxial methyl of the *gem*-dimethyl group.

On first inspection, it would appear that this IMDA reaction should need high temperature to proceed, since it involves an unactivated vinyl group dienophile and a 2-aza-1,3-butadiene that seems neither strongly electron poor nor rich, and might have a degree of aromatic stabilization. Perhaps the two quaternary carbons in the tether induce a rate acceleration through the Thorpe-Ingold effect.

The Lawrence synthesis owes much to earlier work by the Williams group, who made seminal contributions in synthetic and biosynthetic investigations into bicyclo[2.2.2]diazaoctane natural products,[174] and biological Diels-Alder reactions more broadly.[175]

In addition to the dienophile LUMO-lowering activation that is brought about either by: (a) complexation with a Lewis acid; or (b) through protonation with a Brønsted acid, or (c) iminium organocatalysis, there exists another mode by which a concerted pericyclic [4+2] cycloaddition reaction can be catalyzed. The next case study describes perhaps the only reported instances of this process in an IMDA reaction-based biomimetic total synthesis.

3.18. Kingianic acid E (Lawrence, Sherburn, 2015)

It was first demonstrated in the 1960s that [4+2] cycloadditions of electronically mismatched diene-dienophile systems can be promoted by photosensitized electron transfer.[176] Bauld and co-workers[177] subsequently showed that the Ledwith-Weitz salt (a bench stable aminium radical cation) could serve as a chemical catalyst in light-free processes. Most recently, Yoon and co-workers introduced Ru(II)-photocatalysts in combination with visible light irradiation to bring about intermolecular [4+2] cycloadditions.[178]

In 2015, Drew, Lawrence and Sherburn utilized the Yoon and Bauld methods for a 1,3,8-nonatiene-type IMDA reaction between a 1,3-cyclohexadiene and an electron rich dienophile in their synthesis of kingianic acid E (**205**) and other members of the kingianin family (**Scheme N18**).[179] Thus, irradiation of precursor **200** in the presence of catalytic amounts of $Ru(bpy)_3^{2+}$ and methyl viologen (MV^{2+}) afforded the IMDA adduct **204** in 50% yield. The *in situ* generated $Ru(bpy)_3^{3+}$ is a sufficiently strong oxidant to convert the electron rich dienophile to the corresponding radical cation, which subsequently undergoes the concerted [4+2] cycloaddition through TS **203**. The Ledwith-Weitz salt was also effective. Such electronically mismatched diene-dienophile systems generally require high temperatures for cyclization and indeed, this process could not be induced thermally. The removal of an electron from the electron rich styrene generates a LUMO-lowered dienophile, which cyclizes at ambient temperature, perhaps mimicking the biosynthesis of the molecule.

The IMDA process generates the caged ring system of the natural product along with four of its eight stereocenters. The stereochemical outcome of this IMDA reaction is dictated by geometrical constraints in the precursor, which only permit the adoption of TS **203**.

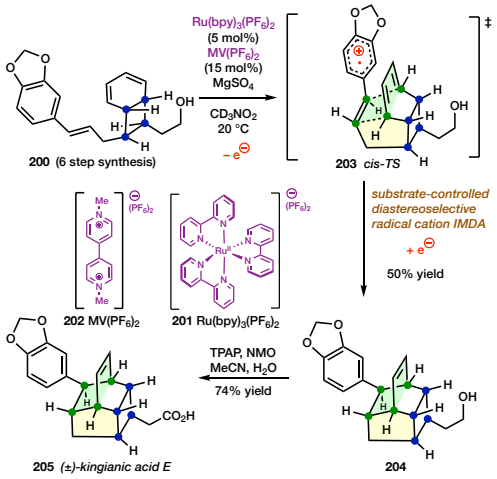

Scheme N18. Drew, Lawrence and Sherburn's 8 step total synthesis of (±)-kingianic acid E (2015).

The authors previously employed a similar approach in the total synthesis of kingianins A, D and F, which are formal 1,3-cyclohexadiene Diels-Alder dimers. In this case, the radical cation [4+2] cycloaddition was used in an intermolecular sense.[180] A contemporaneous investigation into kingianin synthesis by Lim and Parker ingeniously linked two kingianin monomers to control the mode of dimerization.[181]

So-called *dehydro*-Diels-Alder reactions are becoming increasingly more common, largely due to imaginative and high-profile contributions from the Hoye group.[182] The name *dehydro* refers to the use of triple bonds in place of the usual double bonds of the diene and dienophile.[183] Until recently, the most common examples of didehydro-IMDAs deployed alkyne dienophiles in reactions with 1,3-butadienes (*cf.* **Scheme D23**). IMDA reactions between alkyne dienophiles and styrenes as 1,3-butadienes are well known[184] and have been particularly effective for the total syntheses of arylnaphthalene lignans, with seminal work involving 1,3-nonadien-8-ynes by Klemm,[185] and important recent work by Brummond,[186] Dudley[187] and several others.

The most recent work involves *hexadehydro*-IMDA reactions of 1,3-8-nonatri*yn*es, processes that generate arynes *in situ*, which react on in domino sequences to rapidly generate complex structures. This field is presently in its early stages of development but is undoubtedly one to watch for potential future total synthesis opportunities. Thus far, contributions have focussed on synthetic method development and mechanistic studies.[188] Only one total synthesis application of a hexadehydro-IMDA reaction has been reported so far,[189] with non-IMDA-based strategies proving significantly more efficient.

The final example in this section involves a *formal* didehydro-IMDA process, in which the diene component is replaced by an enyne.

3.19. Magellanine (Barriault, 2017)

The Barriault group's total synthesis of magellanine **209** involves a stepwise, *formal* IMDA reaction of 1,8-nonadie-3-yne **206** involving Au(I)-complex **207** as catalyst (**Scheme N19**).[190] The catalyzed process (**206**→**208**) was performed on scale at ambient temperature. Regarding target-relevant complexity, it generates two new rings, two C–C bonds and a stereocenter, and represents the cornerstone of this superior total synthesis.

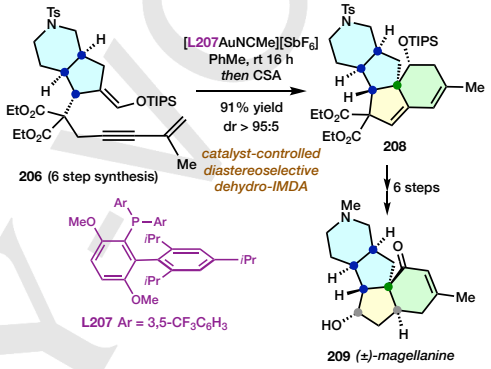

Scheme N19. The Barriault group's 13 step total synthesis of (±)-magellanine (2017).

Other formal [4+2] cycloadditions are known, which proceed through stepwise mechanisms. So far, none have seen the kind of widespread adoption in natural product total synthesis enjoyed by the concerted pericyclic reaction. There is significant scope for important new contributions in this area.

4. Beyond 1,3,8-Nonatrienes and 1,3,9-Decatrienes

Whereas type 1 IMDA reactions of 1,3,9-decatrienes and 1,3,8-nonatrienes dominate the literature, they are by no means representative of the scope of the process. This section moves on from the two most prevalent IMDA subtypes to provide a survey of the widest range of possible IMDA reactions deployed in target synthesis. Instructive examples of other type 1 IMDA processes will be covered first, followed by syntheses based upon type 2 IMDA reactions and finally, those employing transannular DA cycloadditions.

A single covalent bond connection between a putative diene and dienophile represents a through-conjugated arrangement of three formal π-bonds. Such systems do not undergo IMDA processes. Instead, alternative pericyclic reactions such as [6π] electocyclizations and [$_{\pi}4_{s}+_{\pi}2_{a}$] cycloadditions occur.[191] The shortest tether between a diene and dienophile for a type 1 IMDA reaction comprises one atom and two covalent bonds. Such processes, IMDA reactions based upon 1,3,6-heptatriene precursors, have been known since 1968.[192] The first application in total synthesis was reported by Carreira in 2018.[193]

4.1. Mitrephorone A (Carreira, 2018)

The Carreira group's synthesis of mitrephorone A **213** deploys no less than *three* Diels-Alder reactions, two of which are intramolecular. The second of these (**Scheme B1**) involves a 1,3,6-heptatriene IMDA reaction (**210**→**212**) and creates a substantial amount of the most complex subsection of the target's framework. Specifically, substituted 1,3-cyclohexadiene **210** is converted into tricyclo[3.2.1.0^{2,7}]octane **212**, which is armed with the requisite functionality for elaboration into the natural product. The IMDA reaction uses substrate-based diastereocontrol to create three new stereocenters: in the TS (**211**) the vinyl dienophile is constrained to dock exclusively to the face of the diene to which it resides, and with *cis*-stereochemistry at the fusion between the new six and three-membered rings. In the following year, the Magauer group reported the use of the same type of IMDA reaction to prepare the same natural product.[194] Carreira subsequently described studies towards trachylobane natural products deploying the same type of IMDA process.[195]

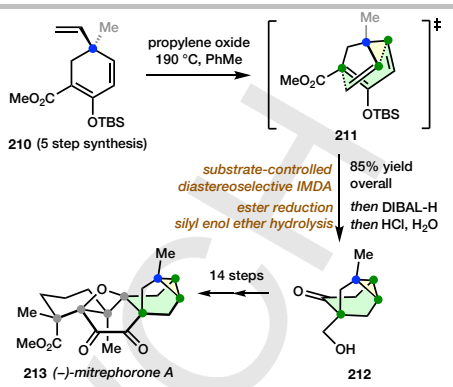

Scheme B1. The Carreira group's 21 step total synthesis of (–)-mitrephorone A (2018).

1,3,6-Heptatriene IMDA reactions are surprisingly well documented in the literature, with exploratory synthetic studies representing the majority of the published work.[196] Aside from the two syntheses of mitrephorone A, Chen has described efforts towards (+)-salvileucalin B,[197] and Miller and Trauner have predicted the existence of a natural product based upon a putative biological 1,3,6-heptatriene IMDA reaction.[143]

The majority of reported 1,3,6-heptatriene IMDA reactions involve 5-vinyl-1,3-cyclohexadiene precursors, and there is significant potential to expand the scope of this process. Reaction temperatures of around 200 °C are common for reactions of this type but there are examples of much more facile processes. Based upon synthetic work by Beaudry and Trauner, computational studies by Khuong and Houk have identified an unusual dienophile twisting in IMDA TSs of certain substituted 5-vinyl-1,3-cyclohexadienes, which can explain decreased barriers for certain processes such that the IMDA process occurs at ambient temperature.[198]

Whereas 1,3,6-heptatriene IMDA reactions are relatively well populated in the literature, very few examples of the next higher homologue, namely 1,3,7-octatriene IMDA processes, have been reported,[199] and have not located any total synthesis applications. This represents an opportunity for creative total synthesis chemists, who need a bicyclo[4.2.0]octane subunit (or heteroatom-containing equivalent) in a target molecule.

In comparison with the large volume of work done on 1,3,9-decatrienes, relatively little synthetic work has been reported on the next higher homologue, the 1,3,10-undecatriene system. Pioneering investigations in the use of IMDAF reactions of 1,3,10-undecatriene-type precursors were made by Harwood, in efforts towards daphnane diterpenes, which includes the perennial total synthesis target, phorbol.[200] More recently, this type of IMDAF process was used in a masterful total synthesis of the complex triterpenoid natural product (+)-solanoeclepin A, which stimulates potato cyst nematodes to hatch.

4.2. Solanoeclepin A (Tanino, Miyashita, 2011)

Solanoeclepin A **217** contains a unique carbon framework and represents a formidable synthetic challenge. For the total synthesis of (+)-solanoeclepin A, the Tanino and Miyashita groups deployed a late stage IMDAF to install both the oxanorbornanone and fused cycloheptane rings (**Scheme B2**).[201] The IMDAF process maps exquisitely onto the target molecule. The cycloaddition was mediated by Me_2AlCl (1 mol equiv) in diethyl ether at –78 °C to afford cycloadduct **216** "in a stereoselective manner" in 62% yield over two steps, following acid-mediated deprotection of the TMS ether of the secondary alcohol, and enol ether hydrolysis.

The use of a Lewis basic solvent is unusual, and must compete with the ketone carbonyl oxygen for the Lewis acid, thereby decreasing the effectiveness of the latter. Keay and co-workers studied the effect of Lewis acids upon IMDAF reactions in detail, after making the interesting observation that the amount of Lewis acid (i.e. 0.1 vs. 1.0 mol equiv) needed for optimal precursor conversion is sensitive to precursor (alkyl) substitution.[202] The effect was traced to differing relative basicities of carbonyl oxygens in precursors and products. We recommend to those interested in performing an IMDAF reaction to experiment with both loadings of Lewis acid.

Returning to the Tanino/Miyashita synthesis of solanoeclepin A, in principle, four diastereomeric IMDAF products are feasible from a concerted IMDA reaction of precursor **214**. The favored product stereochemistry results from TS **215**, which is presumably preferred due to the *endo*-tether carbonyl group and its associated stabilising SOIs. In addition, the *π*-diastereofacial selectivity of the process is influenced by the minimization of 1,3-allylic strain with the TMSO– substituent, which adopts a pseudoequatorial orientation in the preferred TS **215**. This controlling secondary alcohol stereocenter must be later inverted to obtain the natural product.

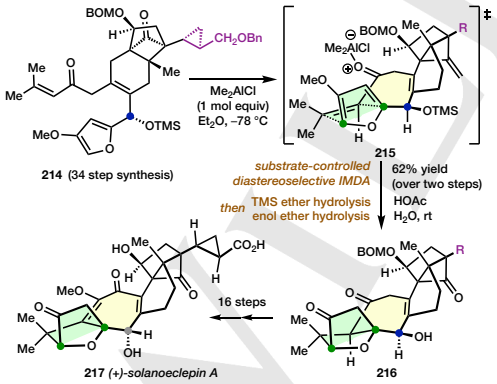

Scheme B2. The Tanino/Miyashita groups' 52 step total synthesis of (+)-solanoeclepin A (2011).

Several groups have worked towards various natural product targets using 1,3,10-undecatriene IMDA reactions [203] and a number of successful total syntheses have been completed.[204] Fukuyama's synthesis of (–)-lepenine is an interesting example, which demonstrates again (see also **Scheme B1**) that type 1 IMDA processes can generate bridged ring systems.

4.3. Lepenine (Fukuyama, 2014)

The total synthesis of the denudatine alkaloid (–)-lepenine **221**, reported by the Fukuyama group in 2014, involves two Diels-Alder cycloadditions (**Scheme B3**).[205] The IMDA reaction of the tetralone-derived 1,3,10-undecatriene **218** generated adduct **220**, with two new stereocenters required for the target molecule, one of which is of the all carbon quaternary type. The IMDA reaction installs the A ring of the natural product, with the IMDA tether-generated lactone in adduct **220** being ring opened and elaborated into the final target in a further 16 steps.

The thermal IMDA reaction (carried out at 190 °C in benzonitrile) is *endo*-selective, generating the *cis*-ring fusion geometry, with the dienophile approaching the diene from the lower *π*-diastereoface as drawn in TS **219**, controlled by the configuration at the sole pre-existing stereocenter. Sixteen steps were needed to complete the synthesis, with two key phases. The lactone and C=C bonds of adduct **220** permitted the use of a Mannich reaction to install the tertiary amine and associated bridging ring system on the left side of the molecule. Oxidative dearomatization of the right side of adduct **220** to a cyclohexadienone, and *π*-diastereoface-selective intermolecular Diels-Alder reaction with ethylene (approach from the lower face) completed the assembly of the multicyclic framework.

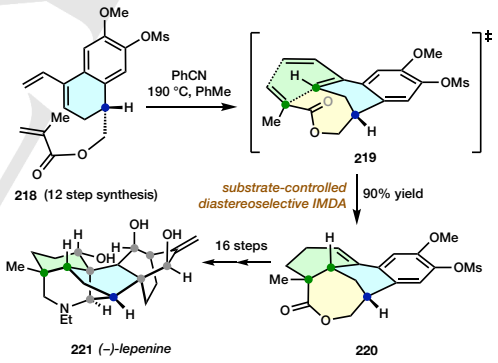

Scheme B3. The Fukuyama group's 29 step total synthesis of (–)-lepenine (2014).

Multicyclic alkaloids are common targets for IMDA reactions, particularly when the natural product contains a complete IMDA retron. The next example demonstrates such a case, while also exemplifying a rarer type of internal dienophile activation, along with an interesting case of diene site selectivity.

4.4. Andranginine (Takayama, 2017)

In 2017, the Takayama group reported a total synthesis of the alkaloid (+)-andranginine **225** (**Scheme B4**).[206] This synthesis can be considered bio-inspired, because the natural product had been proposed to arise from a non-enzymatic IMDA reaction of a

dendralenic amine precursor. The 1,3,10-undecatriene IMDA precursor **222** has a 5-vinylpyridone diene, which in principle could react with the tethered dienophile at either the endocyclic diene site or the semicyclic diene site.

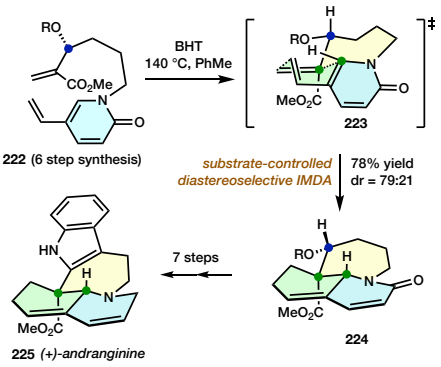

Scheme B4. The Takayama group's 14 step total synthesis of (+)-andranginine (2017). (R = 4-nitrobenzoyl)

A substrate-controlled diastereoselective IMDA reaction simultaneously generated two of the five rings of the natural product, and both of its stereocenters. A pre-existing stereocenter in the IMDA substrate controls the absolute configurations at the two new stereocenters, before it is eliminated *en route* to the natural product.

The cycloaddition was performed in toluene at 140 °C in the presence of 1 molar equivalent of BHT as a polymerization inhibitor. The semicyclic diene site of substrate **222** reacts exclusively, presumably since it is both less electronically deactivated and, upon approaching the TS, results in the development of less steric repulsion.

The dienophile activating group, namely the carbomethoxy group, is attached to the internal position–but as a substituent instead of a part of the tether, as is more frequently seen. The major diastereomeric product **224** (62% yield) is suggested to arise from TS **223**, with the dienophile activating group *endo*-oriented and the substituted benzoyloxy substitutent in the preferred pseudoequatorial position. The minor product is the other possible *trans*-fused diastereomer, which has a TS with a less favourable orientation of the tether substituent. Cycloheptane has several similar energy conformations, hence the seven-membered *chairlike* tether conformation shown in **Scheme B4** is presumably only weakly preferred. There are no computational studies into 1,3,10-undecatriene IMDA reactions that can assist this analysis. Opportunities exist for computational-theoretical studies into many of the less commonly encountered IMDA processes described in this section.

Evidently, 1,3,10-undecatriene IMDA reactions are favourable processes that can be implemented with confidence in synthetic endeavours, in a similar manner to 1,3,8-nonatrienes and 1,3,9-decatrienes. Our final example of this type illustrates the effective use of IMDA reactions to generate aromatic rings.

4.5. Vineomycinone B_2 Methyl Ester (Martin, 2006)

The Martin group introduced a disposable silyl tether approach for intramolecular benzyne-furan additions in 2003,[207] and deployed the tactic in beautiful syntheses of *C*-aryl glycosides.[208] Perhaps the most extraordinary example involves a twofold IMDA sequence, which engages a 1,2,4,5-tetrabromobenzene as a latent *tetradehydrobenzene* equivalent in the total synthesis of vineomycinone B_2 methyl ester **229** (**Scheme B5**).[209]

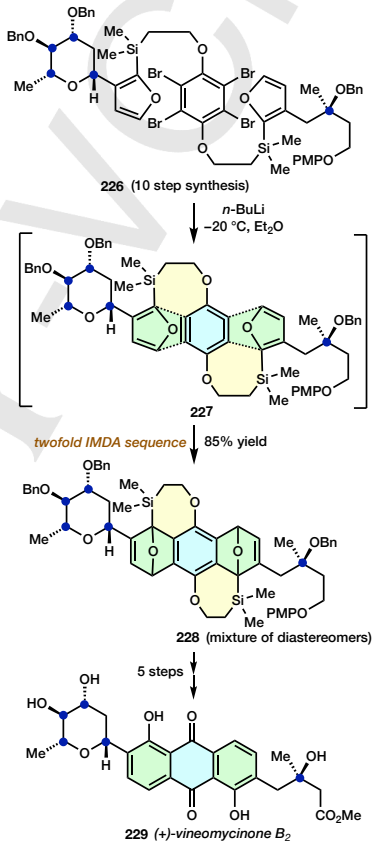

Scheme B5. The Martin group's 16 step total synthesis of (+)-vineomycinone B_2 methyl ester (2006).

The dropwise addition of *n*-BuLi (3 mol equiv) to a solution of tetrabromide **226** in diethyl ether afforded the double adduct **228** as a mixture of diastereomers, which was elaborated into the methyl ester of the natural product **229** over 5 steps. Presumably, the two benzyne-furan IMDA additions (depicted schematically in **227**) proceed separately. Desilylative aromatization of the two oxanorbornadiene rings generates the requisite phenolic functional groups of the target molecule.

The first use of an intramolecular benzyne-furan cycloaddition in total synthesis is Best and Wege's preparation of mansonone E and related natural products in 1981-1986.[210] Intramolecular benzyne cycloadditions to other dienes have also been engaged in total synthesis, albeit rarely. Castedo and co-workers described the synthesis of aristolactam and phenanthrene alkaloids by intramolecular addition of a benzyne to a styrenic diene,[211] and Buzek prepared the pseudopterosin A/E aglycone in 1995 by IMDA reaction of a benzyne to a 1,3-cyclohexadiene.[212] Superb reviews on the use of benzynes in total synthesis have appeared in the past few years.[213] The paucity of total syntheses deploying benzyne IMDA reactions indicates that the full potential of this process remains to be shown. Reported reactions are selective and high yielding. Perhaps the more recent development of mild methods for benzyne generation will promote more work in this area.

Moving up the homologous series of type 1 IMDA precursors, after 1,3,10-undecatrienes we come to the 1,3,11-dodecatrienes, examples of which are significantly less common. We have been unable to locate completed total syntheses involving IMDA reactions of precursors carrying eight membered ring tethers, with existing publications focusing on exploratory investigations.[214] In contrast, as we move yet further up the homologous series, type 1 IMDA reactions involving diene-dienophile tethers that become nine-membered rings and greater are well represented in the literature. Our selected case studies represent examples of both substrate-controlled and catalyst-controlled stereoselectivity in type 1 IMDA macrocyclizations.

4.6. Periconiasins (Liu, Tang, 2016)

A type 1 IMDA cyclization of a 1,3,12-tridecatriene was reported by Liu, Tang and co-workers in 2016, who described its use in the construction of a bicyclo[7.4.0]tridecadiene system during the total synthesis of the polyketide natural products, periconiasins A-C (**233**-**235**, **Scheme B6**).[215] Due to its instability, IMDA precursor **230** was generated *in situ via* Grieco-type selenide oxidation-elimination and directly engaged in the IMDA reaction. The cycloaddition was performed in $CHCl_3$ at 90 °C, to afford the major diastereomer **232** in a 38% overall yield. The relatively low temperature needed to bring about this IMDA process is due to the highly polarized nature of the dienophile. The dienophile bond is presumably also a very potent Michael acceptor, which explains its instability. The *N*-2-methylbenzoyl group gave a better yield than the *N*-benzoyl derivative, presumably due to the bulkier substituent engendering a slightly decreased propensity to undergo nucleophilic addition-polymerization.

The reaction proceeds through putative TS **231**, with the lactam carbonyl group *endo*, and *π*-diastereofacial selectivity controlled by the α-amido isobutyl-substituent. IMDA adduct **232** was taken on to prepare several related periconiasin natural products.

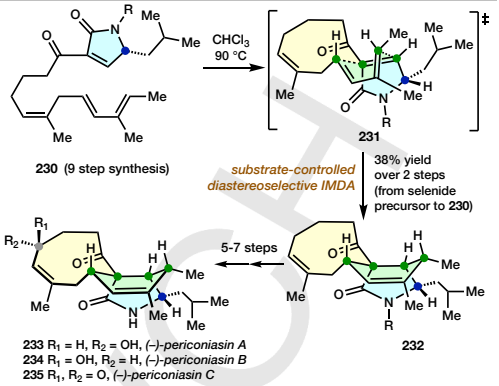

Scheme B6. Liu, Tang and co-workers' 15-17 step total syntheses of (–)-periconiasins A-C (2016). (R = 2-methylbenzoyl)

A similar IMDA strategy was employed by Nay and co-workers in 2016 to assemble the smallest cytochalasin, (+)-periconiasin G, with a seven membered ring tether.[216] These syntheses can be considered biomimetic, with their final stage IMDA reaction mimicking the way that the alkaloids are formed in Nature. Cytochalasins are fungal metabolites that inhibit actin polymerization. Their large ring domains of varying sizes have rendered the cytochalasins attractive as total synthesis targets for many years. The first total synthesis of a cytochalasin by way of a macrocyclic IMDA reaction of the general type depicted in **Scheme B6** was reported by Stork and Nakamura in 1983,[217] whose approach to cytochalasin B involved the formation of a 14 membered macrolide. A macrocyclization IMDA model study towards this natural product was, however, reported five years earlier by Thomas,[218] who went on to complete total syntheses of proxiphomin (containing a 13 membered ring), and cytochalasins H and G (12 membered ring) and D and O (11 membered ring).[219]

Whereas the *π*-diastereofacial stereoselectivity of the process depicted in **Scheme B6** was controlled by a substituent attached to the terminus of the dienophile, the outcome of the next example is steered by macrocyclic tether substituents.

4.7. Abyssomicin C (Sorensen, 2005)

In 2005, the Sorensen group reported the first total synthesis of the marine natural product (–)-abyssomicin C **239**.[220] A highly regio- and diastereoselective, biomimetic IMDA reaction was implemented to form the key tricyclic core, featuring an 11-membered macrocycle (**Scheme B7**).

$La(OTf)_3$ was identified as an efficient catalyst for a one pot elimination-IMDA sequence, which avoided isolation and handling of an unstable trienone intermediate (depicted in TS **237**). Thus, heating precursor **236** in toluene the presence of this catalyst afforded the tricyclic product **238** as a single diastereomer in 50% overall yield, which was converted into the natural product in short order. The formation of product **238** can be explained by TS **237**, which was located through calculations (at the HF/3-21G level of theory). The tether adopts a staggered conformation, with methyl

groups in pseudoequatorial orientations. Both the diene and dienophile site selectivities of this reaction are interesting, with substrate **237** containing two potentially reactive C=C dienophiles and two 1,3-butadienes. Regarding the *γ*-methylene-*β*-tetronate dienophile, the exocyclic C=C bond would be expected to react in preference to the endocyclic vinylogous ester C=C bond, both on steric and electronic grounds. A similar argument can be made for reaction at the terminal 1,3-butadiene moiety of the through-conjugated trienone, although the loss in conjugative stabilization in the [4+2] cycloaddition TS for addition to the internal 1,3-butadiene group might also play a contributing role.[221]

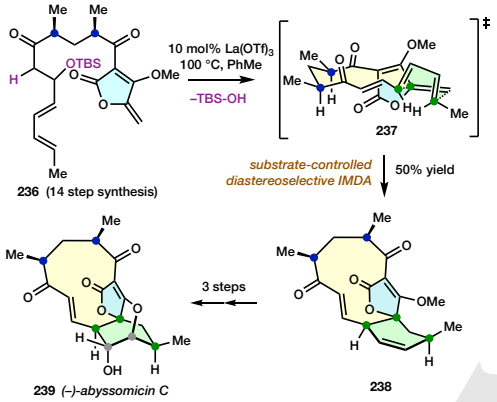

Scheme B7. The Sorensen group's 18 step total synthesis of (–)-abyssomycin C (2005).

Following investigations carried out concurrently with those of the Sorensen group, Snider and Zou reported the use of the same IMDA reaction in a separate total synthesis of the same natural product.[222] In 2012, Niu and Hoye prepared the structurally related spirotetronate (–)-okilactomycin D using a similar macrocyclic IMDA reaction.[223] The first attempt to prepare a spirotetronate natural product through a macrocyclic IMDA reaction of this type was reported by Yoshii's group in 1990, who reported an extremely courageous approach to 24-*O*-methyl chlorothricolide, involving the use of a late-stage IMDA reaction to form the 14-membered ring.[224] Perhaps the most daring use of a late-stage IMDA reaction in total synthesis, however, is Kishi's 1998 total synthesis of (–)-pinnatoxin.

4.8. Pinnatoxin (Kishi, 1998)

Kishi's total synthesis of pinnatoxin **243** involved a macrocyclic IMDA reaction to simultaneously form the cyclohexene ring and *cis*-fused 19 membered ring of the natural product (**Scheme B8**).[225] Precursor **240**, which was prepared over a sequence of 33 steps, was converted into cycloadduct **242** by way of dimerization-prone diene **241**. Three stereoisomeric cycloadducts were formed from the IMDA macrocyclization, with the desired product **242** being a major one from a reaction performed in dodecane at 70 °C. To complete the total synthesis, adduct **242** was deprotected and condensed intramolecularly to form the iminium salt.

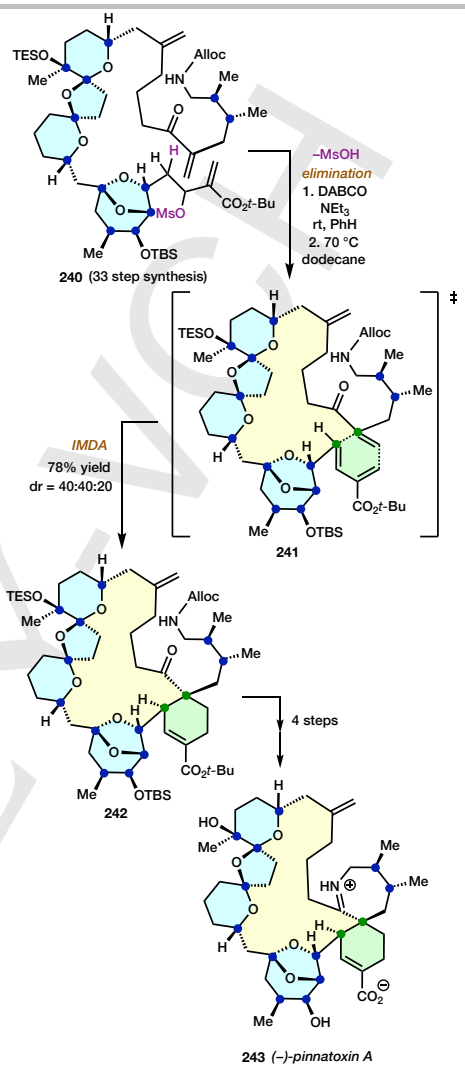

Scheme B8. The Kishi group's 39 step total synthesis of (–)-pinnatoxin (1998).

The desired diastereomer **242** is the result of an *endo*-mode IMDA process. The other possible *endo*-IMDA adduct, with the opposite configurations at the two new stereocenters (i.e. the endo-adduct of reversed *π*-diastereofacial selectivity), was formed in approximately the same amount as the desired adduct, which shows that the tether for this substrate offers little in the way of a stereocontrolling influence. Perhaps a preformed cyclic iminium dienophile could engender the requisite stereocontrol in this spectacular, biomimetic IMDA process (*cf.* Snider's synthesis of symbioimine, **Scheme D12**).

The first exploratory studies into macrocyclic IMDA reactions were reported by Corey and Petrzilka in 1975, who investigated ester-tethered precursors with diene-dienophile tethers comprising ten atoms.[226] A mixture of stereosiomeric fused and bridged products were obtained, the ratio of which correlated with the those obtained from related intermolecular DA reactions. Corey returned to this problem forty years later, to report the first catalytic enantioselective IMDA macrocyclization of an achiral, acyclic precursor.

4.9. Palominol, dolabellatrienone, β-araneosene, and isoedunol (Corey, 2006)

Corey and Snyder's collective total synthesis of the dolabellane natural products palominol, dolabellatrienone, β-araneosene, and isoedunol is unique in deploying a catalytic enantioselective IMDA reaction at a late stage in a total synthesis.[227] The IMDA reaction generates both rings and both stereocenters of the natural product palominol **248** (**Scheme B9**).

Slow addition of chiral oxazaborolidinium catalyst **245** to a stirred solution of acid-sensitive silyl enol ether **244** at low temperature resulted in the formation of bicycle **247** in 74% yield and high enantioselectivity. Remarkably, catalyst **245** was unique in its ability to effect this [4+2] cycloaddition of precursor **244**: heating led to decomposition, as did the use of standard achiral Lewis acid catalysts, such as Me_2AlCl, $MeAlCl_2$ and $EtAlCl_2$. The IMDA macrocyclization proceeds *via endo* transition state **246**. A two-point binding of the formyl group to the catalyst, a *transoid* enal conformation, and *π*-stacking between the dienophile and a phenyl group of the catalyst all contribute to an exquisitely-designed process.

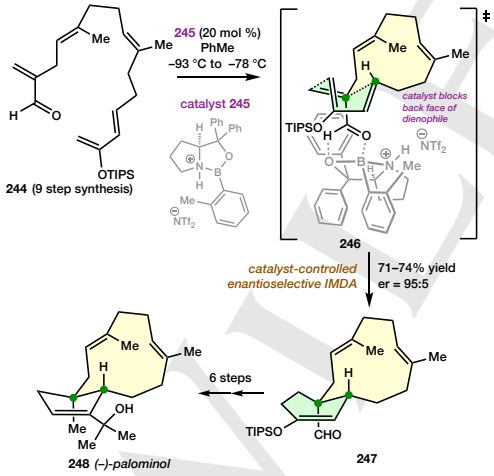

Scheme B9. Corey and Snyder's 16 step total synthesis of (–)-palominol (2006).

Following the macrocyclic IMDA reaction, a Wolff rearrangement brings about ring contraction to the desired cyclopentene ring, without disturbing the configurations at the two ring fusion positions.

The diversity of total synthesis applications that fit within the type 1 IMDA domain is extraordinary, and the creativity expressed through the work is awe-inspiring. Nonetheless, the true scope of the IMDA reaction is broader still. The remaining examples will describe some of the most impressive type 2 IMDA reactions and transannular DA cycloadditions.

We have already identified that type 2 IMDA reactions are significantly less well explored than are the corresponding type 1 processes. Total syntheses involving type 2 IMDA processes are surprisingly rare: In fact, we have located less than a dozen examples in the literature. The lack of popularity of type 2 IMDA reactions in total synthesis no doubt relates to the paucity of obviously "mappable" targets. In contrast, natural product targets containing decalin and hexahydroindane ring systems are in abundance (i.e. for the mapping of decatriene and nonatriene type 1 IMDA reactions). As our chosen examples will demonstrate, total synthesis applications of the type 2 IMDA process come in unexpected forms, and possibilities for future developments are by no means exhausted. We are convinced that many potential uses of type 2 IMDA reactions in step economic total synthesis remain to be invented.

In contrast to the small number of total syntheses deploying type 2 IMDA reactions, exploratory investigations focused on empirical findings and methods development are significantly greater in number. The Shea group were instrumental in the development of this field in the period of 1978-1994.[13]

The type 2 IMDA coverage will follow the same pattern as the first half of this section, commencing with the smallest tether size. As we have seen (**Scheme B1, Carreira**), *type 1* IMDA processes involving only a single atom (i.e. 2 bond) diene-dienophile tether are feasible. Since type 2 IMDA processes generate bridged bicyclic systems with bridgehead C=C bonds, a minimum tether length restriction holds, if kinetically stable products are required.[228] As a general guide, the shortest tethers for type 2 IMDA reactions comprise four atoms between the diene and dienophile. Basing the name of this IMDA subtype upon the simplest hydrocarbon molecule, the system is *3-methylenenona-1,8-diene*. IMDA reactions of this type are uncommon and applications in total synthesis are very rare indeed. A noteworthy 3-methylenenona-1,8-diene IMDA reaction was recently reported by Chen.

4.10. Echinopines A and B (Chen, 2011)

In 2011, Chen and co-workers reported a formal total synthesis of echinopines A and B.[229] These sesquiterpenoid natural products were first isolated in 2008 and contain an unusual [3,5,5,7] carbon framework.[230] Chen envisaged the use of an unusual type 2 IMDA reaction to intercept a tricyclic intermediate from Magauer and Tiefenbacher's 2009 total synthesis (**Scheme B10**).[231]

The acyclic precursor **249** already carries a *Z*-configured C=C dienophile but lacks the requisite 1,2-dimethylene cyclopentane diene. A Pd(0)-catalyzed ene-yne cycloisomerization at 80 °C generates this functionality, which underwent IMDA reaction, presumably through TS **250**, after increasing the reaction temperature to 160 °C. Only the *endo*-CO_2Me TS **250,** with dienophile approach from the top face, is available to the IMDA precursor. The short type 2 tether (7 membered tether ring)

imposes this constraint upon the system. Chen and co-workers incorporated the dienophile –CO_2Me substituent for the purposes of enhanced *endo*-selectivity. Nonetheless, we suspect that the alternative *exo*-mode IMDA TS is not accessible to this substrate. While the –CO_2Me group permits further elaboration of the IMDA adduct, it probably doesn't lower the IMDA reaction temperature.

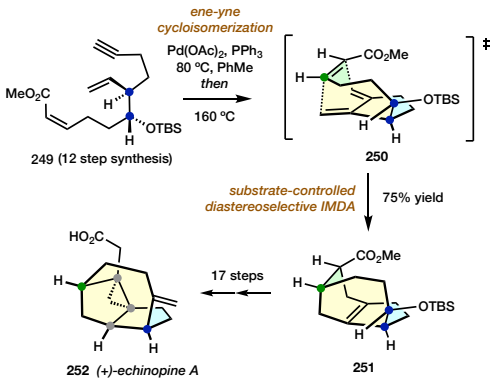

Scheme B10. The Chen group's 30 step formal total synthesis of (+)-echinopine A (2011).

The TBSO– substituent plays no part in the stereochemical outcome of the reaction, since a 70:30 ratio of diastereomeric precursors gave the same ratio of diastereomeric products.

Examples of the next higher homologous structure in the type 2 IMDA series, *3-methylenedeca-1,9-dienes*, are significantly more common. Most reports of type 2 IMDA reactions of this subclass relate to synthetic approaches to taxane diterpenes, which can be traced to original publications from two laboratories working independently: Shea and Davis in 1983 [232] and the Jenkins group in 1984.[233] The first successful synthesis of a taxane natural product using a 3-methylenenona-1,8-diene type 2 IMDA reaction was by Rubenstein and Williams, who described a 26 step synthesis of racemic taxadiene in 1995.[234] In 2012, the Baran group reported a scaleable, 12 step catalytic enantioselective synthesis of this natural product. A ketone-armed intermediate prepared *en route* to taxadiene, namely taxadienone, was subsequently taken on to prepare the most important taxane diterpene, taxol, in 2020.

4.11. Taxadiene and Taxol (Baran, 2012/2020)

The Baran group's catalytic enantioselective synthesis of (+)-taxadiene **256** in 2012 permitted the synthesis of the natural product on gram scale from feedstock precursors.[235] A Lewis acid (BF_3•OEt_2) promoted type 2 IMDA reaction of precursor **253** was used at a late stage of the synthesis to assemble enedione **255**, containing the [6-8-6] tricyclic carbon skeleton of the natural product (**Scheme B11**). A further six steps incorporate the final carbon of the target and achieve the necessary redox manipulations. The use of the IMDA reaction is instrumental to the short step count preparation of taxadiene **256**, in that it simultaneously generates two C–C bonds, two of the three carbocycles and the one remaining stereocenter. The substituents carrying the diene and dienophile are *trans*-oriented on the pre-existing cyclohexanone ring in precursor **253**, permitting the adoption of the *boat-chairlike* conformation of the 8 membered ring tether in TS **254**, with the carbonyl group of the dienophile enone *endo*-disposed.[236]

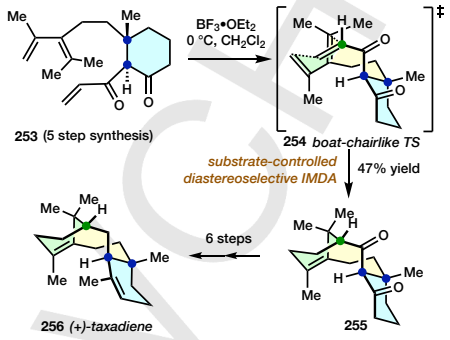

Scheme B11. The Baran group's 12 step total synthesis of (+)-taxadiene (2012).

The six-step sequence to prepare enedione **255** was subsequently optimized through process development [237] and scaled up to permit the preparation of >100 grams of this intermediate, which contains the taxane carbon skeleton. In an overall strategy dubbed *two-phase synthesis,* which mimics Nature's approach (i.e. initial carbon skeleton generation then functional group incorporation), enedione **255** was taken on to ultimately prepare taxol,[238] through a linear sequence of 19-33 steps.[239]

Other notable total synthesis triumphs involving type 2 IMDA reactions of 3-methylenedeca-1,9-dienes include Nicolaou's breakthrough synthesis of the "CP molecules" (1997-2002)[240] and Barriault's pioneering approach to vinigrol (2007-2012).[106,107] A fascinating contribution is the Shea group's total synthesis of ledol. [241] In a tactic that echoes the endgame of Stork's adrenosterone synthesis (**Scheme D17**), a type 2 IMDA adduct is ozonolyzed then engaged in an intramolecular aldol condensation. The tactic, branded a *bridged to fused ring interchange*, permits the rapid synthesis of fused [7,5]- and [8,5]-bicyclic systems, and merits wider synthetic use.

Interestingly, whereas many examples of type 2 IMDA reactions of 3-methyleneundeca-1,10-diene of an exploratory nature have been reported,[13] there appear to be no total syntheses deploying the process. The next total synthesis represents a spectacular example of the next higher homologue, which contains a 7 atom diene-dienophile tether.

4.12. Haouamine A (Baran, 2006)

Under strong heating, a Diels-Alder cycloaddition between a pyrone and an alkyne generates a bridged oxabicyclo[2.2.2]octadiene intermediate, which undergoes expulsion of CO_2 through retro-Diels-Alder reaction.[242,243] In 2006, Burns and Baran reported a late-stage, type 2 intramolecular variant of the process in the synthesis of haouamine A **261** (**Scheme B12**).[244] When subjected to microwave irradiation in

dichlorobenzene at 250 °C for 10 h, precursor **257** was converted into cyclized product **260**, which was de-acetylated to give the natural product **261** in 21% overall yield. The initial cycloaddition through TS **258** would afford putative IMDA adduct **259,** which upon retro Diels-Alder reaction with concomitant loss of CO_2 would give tetra-acetyl haouamine A, **260**.

This spectacular process involves the creation of the strained, aza-paracyclophane portion of the molecule through the simultaneous formation of both the macrocycle and the benzene ring. TS **258** contains a developing tether for the 11-membered ring of the product. The orientational regioselectivity of the IMDA reaction dictates the size of the macrocyclic ring formed and the class of cyclophane: the alternative orientational regioselectivity would give a 10 membered aza-metacyclophane. The IMDA product **260** carries the acetoxy-group of the newly created aromatic ring on the front side of the molecule as drawn, which in turn requires the pyrone carbonyl group and acetoxy substituent to be on the front side in IMDA TS **258**.

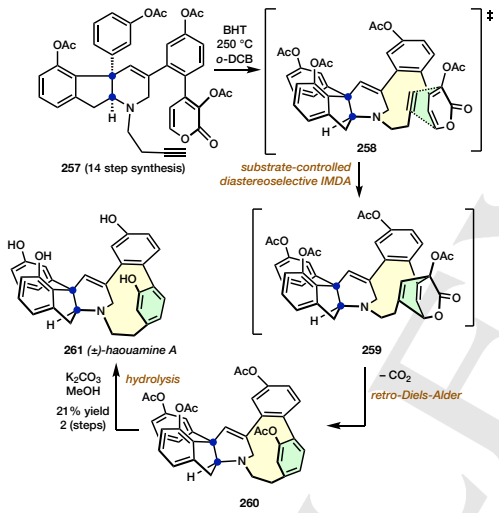

Scheme B12. The Baran group's 16 step total synthesis of (±)-haouamine A (2006).

This is an extraordinary total synthesis of a remarkable natural product: the benzene ring of haouamine A contained within the 11 membered aza-paracyclophane system is non-planar. [245] Atropisomerization of haouamine **261** (i.e. rotation of the newly-formed benzene ring through the aza-paracyclophane macrocycle) is apparently forbidden, hence the IMDA selectivity observed in the formation of atropisomer **260** was required for the successful synthesis of the natural product.[246]

The Burns and Baran synthesis of haouamine was not the first total synthesis involving a type 2 IMDA reaction of a substrate with a 7 atom tether. In 1996, the Shea group prepared the steroid adrenosterone using the same length tether, and an inventive method to overcome a stereocontrol issue.

4.13. Adrenosterone (Shea, 1996)

The synthesis of adrenosterone **93** by the Shea group involves a relatively high temperature type 2 IMDA process of precursor **262** to generate a new bridged bicyclic ring system in product **264**, containing a 10-membered ring (**Scheme B13**).[247] The diene-dienophile tether of precursor **262** contains a silyl acetal portion, a hydrobenzoin section, and an ester link. The first of these is a silyl enol ether at the diene end, and the last is an activating group on the dienophile. The type 2 IMDA reaction proceeds through TS **263**, with an *endo*-oriented tether carbonyl group attached to the dienophile C=C bond. A second, less substituted C=C bond, also carrying a conjugating ester substituent, is also present but the reaction shows high site selectivity for the C=C bond that leads to the slightly smaller (10 membered vs. 12 membered) tether ring.

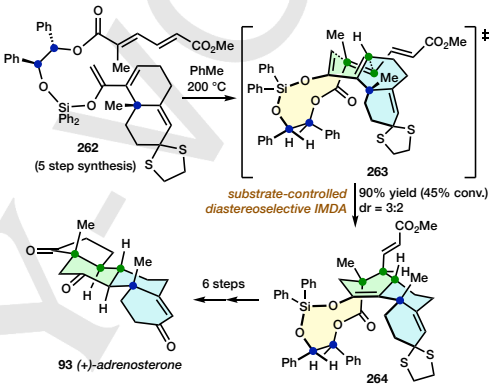

Scheme B13. The Shea group's 12 step total synthesis of (+)-adrenosterone (1996).

The *π*-diastereofacial selectivity of the cycloaddition is influenced by the hydrobenzoin tether section, which leads to the predominant formation of the desired diastereomer **264**. Interestingly, an ethylene glycol tether equivalent of **262** (i.e. lacking the two stereocenters) gave mainly (dr = 10:1) the undesired diastereomeric IMDA product. Following the IMDA reaction, the tether-generated ring of adduct **264** was cleaved and the cyclopentanone ring of natural product **93** was forged through hydrogenation of the acryloyl C=C bond then Dieckmann cyclization. The enol carbon of the silyl enol ether group of precursor **262** becomes the critical C11 ketone group in the natural product.

The last example of a type 2 IMDA reaction in total synthesis is another spectacular late-stage process, this time involving a 10 atom (shortest path) connection between a heterodiene and dienophile.

4.14. Sporolide B (Nicolaou, 2009)

The record for the largest tether used in a type 2 IMDA-based total synthesis is the Nicolaou group's total synthesis of sporolide B, **268** (**Scheme B14**).[248] This is a spectacular example of an IMDA reaction by any measure, featuring the O=C–C=O unit of an *ortho*-quinone as a heterodiene and a tetrasubstituted C=C

bond as the dienophile. The Diels-Alder reaction, the first of its class in an intramolecular setting, is one of inverse electron demand, with an electron-poor diene and electron-rich dienophile, hence $LUMO_{diene}$–$HOMO_{dienophile}$ controlled. Synthetically, catechol precursor **265** was oxidized with Ag_2O to generate the reactive *ortho*-quinone, which cyclized through TS **266** on heating to generate adduct **267**, containing both the benzannulated 1,4-dioxane ring and the macrocyclic ring of the natural product, along with two key stereocenters. While there are no issues of *endo/exo*-selectivity, two other features of this IMDA reaction are interesting: the orientational regioselectivity of the cycloaddition and its π-diastereofacial selectivity. In terms of the former, a 180° rotation about the C3–C4 bond of TS **266** gives a putative regioisomeric product, which would presumably be disfavoured due to a steric clash between the C2–OBn substituent and the C4–OMe group. Furthermore, an alternative folding of the tether could in principle permit approach of the quinone "diene" to the dienophile from their opposite π-diastereofaces, but the arrangement of oxygenated functionality about the dienophile would surely inhibit such an occurrence. Cycloadduct **267** was converted into sporolide B **268** through deprotection and oxidation, although a correction of stereochemistry at one of these three oxygenated sites was also needed.

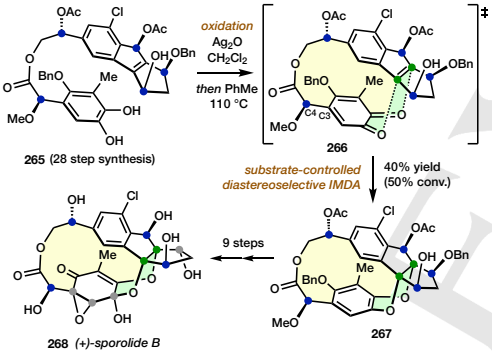

Scheme B14. The Nicolaou group's 39 step total synthesis of (+)-sporolide B (2009).

Transannular Diels-Alder (TADA) reactions are a subset of intramolecular cycloadditions that differ from type 1 and type 2 IMDA processes in that the substrates for such processes contain two distinct diene-dienophile connections. The precursor for a TADA process is, therefore, subject to greater conformational constraints than other IMDA precursors. TADA reactions are characterized by the conversion of a macrocyclic ring system into a fused and/or bridged tricyclic framework, depending upon the specific location of the diene and the dienophile with respect to the macrocycle.

Perhaps surprisingly, the number of completed total syntheses employing transannular Diels-Alder (TADA) reactions exceeds those that employ type 2 IMDA processes. As is the case with all classes of IMDA processes, the literature contains many more exploratory investigations and methodology development contributions than total synthesis applications. The Deslongchamps group was instrumental in the development of the TADA process and its stereochemical control, through systematic investigations of macrocycles of varying ring sizes containing diene and a dienophiles comprising C=C bonds of varying *E/Z* geometries.[14,249]

Consistent with previous classes of IMDA reactions already covered in this review, the simplest TADA substrates are achiral and, where stereocenters are generated during the cycloaddition, enantioselective catalysis is needed. Catalytic enantioselective TADA processes were first reported in 2007.

4.15. 11,12-Diacetoxydrimane (Jacobsen, 2007)

Balskus and Jacobsen reported the catalytic enantioselective TADA reactions of triene-containing macrocycles in 2007.[250] The study also described the first total synthesis application of the process, which involved the preparation of the sesquiterpene, 11,12-diacetoxydrimane **273**. The conversion of 15-membered ring precursor **269** into [5,6,6]-fused tricycle **272** involves not only a TADA reaction but also contraction of a–$C(=O)$–CH_2–O–$Si(Me_2)$–CH_2– tether into a –$C(=O)$–O–CH_2– group, i.e. excising a methylene and a silylene group, with stereoretention (**Scheme B15**). Unsaturated lactone **272** was converted into bicyclic target **273** in short order. Amazingly, the TADA process creates both rings of the natural product and all four stereocenters.

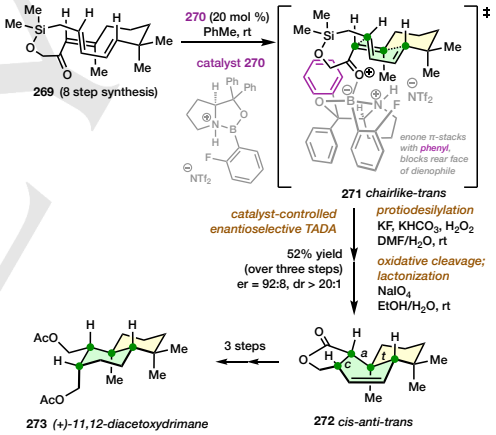

Scheme B15. The Jacobsen group's 12 step total synthesis of (+)-11,12-diacetoxydrimane (2007).

Macrocyclic trienes such as **269**, comprising all-*trans* C=C bonds, give rise to two possible *cis-anti-trans* diastereomeric products. With precursor **269**, the *cis*-fusion is generated on the longer diene-dienophile tether side. The TADA process involves a reactive conformation of the precursor (see TS **271**) in which the developing cyclohexane ring is *chairlike*, and the diene and dienophile are in pseudoequatorial orientations relative to it. The TS conformation of the second tether, containing the silyl ether group and leading to a seven membered ring, is less obvious but presumably involves an *endo*-disposed carbonyl group.

The cycloaddition was promoted by a derivative of Corey's oxazaborolidinium catalysts (cf. **Scheme B9**), and the

enantioselectivity of the reaction can be understood through application of Paddon-Row's pre-transition-state model,[251] which applies specifically to *s-cis* enone dienophiles, as shown in TS **271**. Thus, chiral Lewis acid complexation to the enone activates the dienophile through LUMO-lowering. The catalyst favours the substrate conformation TS **271** over its enantiomeric alternative (with the opposite *π*-enantiofacial selectivity of both diene and dienophile) by selectively blocking the lower *π*-enantioface of the dienophile.

The choice of the 15-membered ring substrate **269** instead of the more obvious, 13-membered macrocyclic lactone precursor to **272** was not explained fully in the paper, but macrolide formation in this case might be inhibited by destabilizing transannular interactions between methyl substituents. A 13-membered macrocyclic triene was successfully prepared by Shing in the earliest application of a TADA process in total synthesis.

4.16. Oblongolide (Shing, 1995)

Shing and Yang's 1995 synthesis of oblongolide **276** generates the natural product directly from the TADA reaction of citronellol-derived precursor **274** (**Scheme B16**).[252] This TADA process (**274**→**276**) creates the majority of the structural complexity of the natural product from a considerably simpler precursor, and is an important contribution in the field.

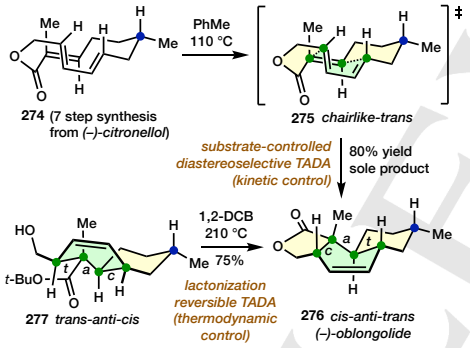

Scheme B16. The Shing group's 8 step total synthesis of (–)-oblongolide (1995).

The stereoselectivity of the TADA reaction **274**→**276** can be understood by considering the preference of the methyl substituent for an equatorial orientation about the longer, *chairlike* four carbon tether. The two possible diastereomeric TSs bearing such an arrangement are the more favoured **275**, which gives rise to the *cis-anti-trans* adduct **276**. The diene-flipped congener of TS **275** (not shown) is the *chairlike-cis* TS, which would form a stereoisomeric product with the less thermodynamically stable *trans*-fused [6,5]- and *cis*-fused [6,6]-ring junctions.

An acyclic hydroxy ester analogue of lactone **274** underwent IMDA reaction at much higher temperature (210 °C) to give a mixture of *cis*- and *trans*-fused octalins, the former **277** giving oblongolide **276** on extended heating. This demonstrates reversibility in the DA reaction. Presumably, the expulsion of *t*-BuOH and closure of the *trans*-lactone in adduct **277** introduces sufficient strain to trigger the retro-cycloaddition to triene lactone **274**, which re-cyclizes to **276**.

Nicolaou and co-workers experienced difficulties in the preparation of 13-membered triene lactones for the purposes of performing TADA reactions towards the antibiotic CJ-16,264. Their attempts to perform IMDA reactions also failed. Progress was ultimately made in an imaginative and strategically unprecedented manner.

4.17. CJ-16,264 (Nicolaou, 2015)

The initial plan made by the Nicolaou group for the synthesis of CJ-16,264 **283** involved TADA reaction of 13-membered lactone **279** (**Scheme B17**).[253] All attempts to prepare this precursor through esterification of hydroxyacid precursor **278** (or its *Z*-dienophile congener) were unsuccessful. Even more frustratingly, efforts to perform an IMDA reaction on hydroxyacid **278** were also met with failure. An opportunity to make progress with this uncooperative system came in the form of 26-membered ring cyclodimer **280**, which was isolated in 37-40% yield in one attempt to prepare lactone **279** from hydroxyacid **278**. Gratifyingly, this compound underwent a twofold TADA reaction sequence on heating in *m*-xylene at 220 °C to generate C_2-symmetric pentacycle **282**, in which each of the two DA processes have occurred with the same diastereoselectivity. Hydrolysis of the two ester groups of diolide **282** with LiOH gave a "monomeric" octalin hydroxy acid, which was converted into the natural product **283**. Thus, the TADA process creates the octalin framework and four of the nine stereocenters of the natural product.

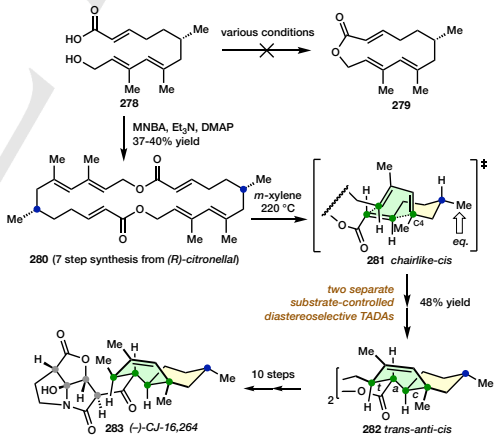

Scheme B17. The Nicolaou group's18 step total synthesis of (–)-CJ-16,264 (2015).

Each of the two TADA processes in the synthesis of CJ-16,264 involve all-*trans* trienes, hence *cis-anti-trans* diastereomeric products must be generated. In this instance (*cf.* **Schemes B15** and **B16**) a *cis*-octalin is forged, and the *trans*-ring junction is created between the octalin and the diolide rings, *viz.* **282**. The shorter, four-carbon tether sits in a *chairlike* conformation, with both the methyl group and dienophile *π*-bond

substituents adopting pseudoequatorial orientations (TS **281**). In contrast, the diene sits pseudoaxial, causing an *exo*-disposition of the dienophile activating group, resulting in the *cis*-octalin ring fusion in adduct **282**. We suspect that the presence of the C4-Me (1,3,9-decatriene numbering) is involved in this octalin *cis*-preference, through its preferential adoption of a pseudoequatorial orientation in TS **281**, although conformational requirements of the forming diolide ring presumably also play a part.

It was noted some time ago that TADA reactions can work when the equivalent single tether IMDA process fails. The Nicolaou total synthesis of CJ-16,264 extends this principle to cyclodimeric structures and their twofold TADA reactions. This general approach warrants further investigation and many potentially useful and interesting extensions can be envisaged.

Returning to the topic of TADA reactions of 13-membered triene lactones, the Nakada group reported a total synthesis of the *cis*-fused octalin (+)-phomopsin in 2004, using a macrolide precursor carrying an *E,Z*-diene.[254]

As we have just witnessed, occasionally we have the option to conduct a DA reaction either intramolecularly or in a transannular manner. The best course of action is determined by several factors, although the dominant drivers are: (a) ease of precursor synthesis; (b) (if used late stage in the synthesis) the simplicity of conversion of the DA adduct into the natural product; and (c) the likelihood of the successful generation of the correct stereoisomeric DA adduct.

Zhao and Maimone recently deliberated on the pros and cons of TADA and IMDA approaches for the synthesis of chatancin, a multicyclic diterpenoid.[255] The biosynthesis of this natural product was proposed to involve a TADA process to generate a [6,6,6]-tricycle from a 14-membered carbocyclic precursor, and the molecule had previously succumbed to total synthesis by Deslongchamps using a biomimetic TADA reaction. [256] Nonetheless, Zhao and Maimone achieved a significantly more step economic synthesis using a decatriene-type IMDA process to form an octalin, followed by a subsequent annelation of the third cyclohexane ring. The lengthy TADA route in this case was attributed to challenges surrounding precursor generation, a problem for which there remains no direct synthetic solution.

Some 13 years after publication, the Jacobsen synthesis remains the solitary example of catalyst control in a TADA reaction in total synthesis. In contrast, several substrate-controlled cases have been reported, including Deslongchamps' synthesis of maritimol in 2000 (13-membered carbocyclic precursor) [257] and momilactone in 2002 (14-membered carbocyclic precursor);[258] Tadano's synthesis of macquarimycin in 2003 (17-membered carbocyclic precursor); [259] Roush's synthesis of spinosyn A in 2004 (22-membered macrolide ring precursor) [260] and cochleamycin A in 2004 (17-membered carbocyclic precursor). [261] Deslongchamps' total synthesis of cassaine from 2008 uses an instructive example of an all carbon macrocyclic triene.

4.18. Cassaine (Deslongchamps, 2008)

The total synthesis of cassaine **287** (**Scheme B18**) was the last in an extended series of contributions in the field from the Deslongchamps group. [262] The 14-membered carbocyclic, all-*trans* triene precursor **284** cyclizes through TS **285**, which assumes a *boat-boat-chair* conformation, to give the now familiar *trans-anti-cis* product **286**. This product is one of four possible diastereomers, and a complete explanation of its formation is provided in the original publication.[262] We summarise here the main aspects of this intricate interplay of competing factors. Firstly, the *boatlike* tether conformation on the left side of TS **285** is due to the *gem*-dimethyl substitution, which destabilizes the chair conformation. A pseudoaxial orientation of the allylic silyloxy-substituent is seen in favoured TS **285** since in this position it avoids a destabilizing antiperiplanar alignment with a developing C---C bond. The alternative (diene and dienophile flipped) TS suffers destabilizing 1,3-allylic strain. To complete the total synthesis, the silyloxy group in adduct **286** was replaced by a methyl group *en route* to cassaine **287**. Inclusion of the silyloxy group in precursor **284** was by design, since the corresponding –Me for –OTBS-substituted analogue of precursor **284** underwent TADA reaction to give a mixture of diastereomers. It is remarkable that such mild conditions bring about this TADA reaction, considering that an unactivated, trisubstituted C=C dienophile is uniting with an unactivated diene. Such is the influence of constrained proximity.

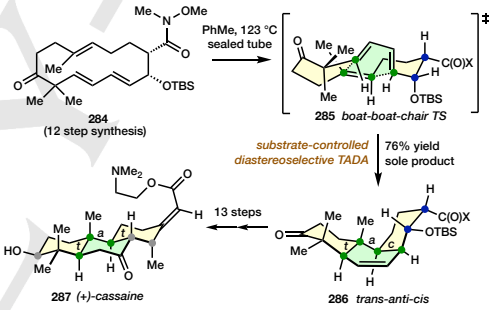

Scheme B18 The Deslongchamps group's 26 step total synthesis of (+)-cassaine (2008); X= –C(=O)NMe(OMe).

In some small measure, this example demonstrates the great depth of understanding of the factors that influence stereoselection in TADA processes that have been developed by the Deslongchamps group.

The examples of TADA reactions covered thus far involve more conventional dienes and dienophiles. The following case involves a cyclic dienone as a diene and an allene as a dienophile.

4.19. 11-*O*-Debenzoyltashironin (Danishefsky, 2006)

Dearomatization is a well-utilized method to generate reactive functionality for DA reactions, and several variations on this theme have already been shown. The Danishefsky synthesis of (±)-11-*O*-debenzoyltashironin **291** (**Scheme B19**) [263] includes a fascinating example of a TADA reaction. The synthesis is exquisitely designed such that macrocyclization occurs in concert with dearomatization, thereby generating the diene within the proximity of the pre-formed allenic dienophile. Thus, *ortho*-benzyloxyphenol precursor **288** is converted into caged structure

290, bearing the ring system of the natural product, in a one-flask operation. A PIDA-induced cyclization to an *ortho*-quinone monoacetal with a 10-membered metacyclophane-type ring system is followed by TADA reaction through TS **289**. The initial *ortho*-quinone monoacetal formation is reversible, with only one of two diastereomeric macrocycles (epimers at the acetal carbon) able to undergo TADA reaction. Throughout this process, the axial chirality of allenic precursor **288** is parlayed into that of the product **290**, firstly through the acetal stereocenter and thence to three TADA-generated stereocenters. Thus, while the natural product **291** was initially prepared in racemic form, the Danishfsky group subsequently rendered their synthesis of 11-*O*-debenzoyltashironin **291** enantioselective, through the preparation of enantioenriched precursor **288**.

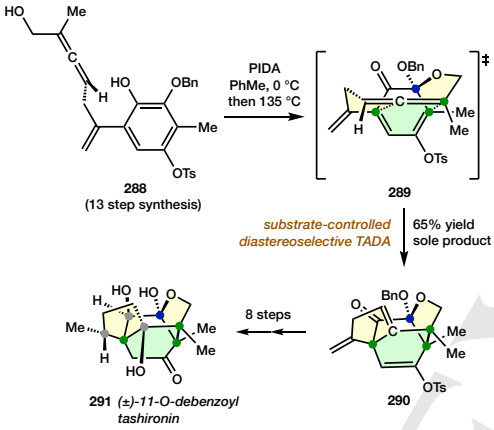

Scheme B19. The Danishefsky group's 22 step total synthesis of (±)-11-*O*-debenzoyltashironin (2006).

Cyclophane precursors for TADA reactions can be traced back to the inaugural example of such a process, reported by Cram and Knox in 1961.[264] Bodwell and Li described a striking example of the synthetic power of a paracyclophane TADA process for the synthesis of a famous alkaloid in 2002.

4.20. Strychnine (Bodwell, 2002)

The Bodwell group's formal synthesis of racemic strychnine **295** (**Scheme B20**) involved an extremely concise synthesis of a pentacyclic intermediate that had previously been used as an intermediate in Rawal's total synthesis[265] of the natural product. In essence, the Bodwell group approach replaces Rawal's 1,3,8-nonatriene IMDA reaction, and the associated lengthy precursor preparation, with a short synthesis of pyridazinophane **292** and its one step conversion into pentacycle **294**, by way of a TADA-retro DA cascade.

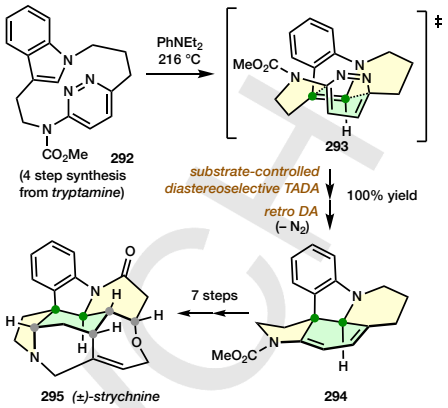

Scheme B20. Bodwell and Li's 12 step formal synthesis of (±)-strychnine (2002).

One of the two possible diastereomeric TSs for the TADA reaction is **293**, with the other being the pyridazine ring flipped analogue (i.e. with the N=N linkage pointing down, instead of up). The diastereoselectivity of the TADA reaction is immaterial, since the retro-DA reaction that immediately follows the TADA reaction expels N_2 and removes all trace of diastereoselection from the first step. Considering that two of the seven rings of strychnine **295** are present in the tryptamine starting material, the TADA step is the most important one in the synthesis, simultaneously creating three rings and two of the six stereocenters.

So far, all TADA reactions discussed involve substrates that contain an endocyclic diene and dienophile, i.e. their structures are directly related to the connectivity seen in type 1 IMDA reactions, inasmuch as the diene and dienophile are *doubly type 1 connected*, with a pair of tethers connecting each terminus of the diene and dienophile. TADA processes can also involve type 2 IMDA connections, as demonstrated by the Shair group's classic synthesis of longithorone A, which involves a precursor with one type 1 diene-dienophile tether and a second, type 2 connection.

4.21. Longithorone A (Shair, 2002)

This wonderful synthesis of a remarkable natural product involves two Diels-Alder reactions, each of which generates three of the target's six stereocenters.[266] Firstly, an intermolecular Lewis acid-process between two closely-related, 16-membered paracyclophane precursors (not shown) generates racemic pseudodimer **296** in a mildly (1.4:1) diastereoselective manner (**Scheme B21**). Desilylation gives diphenol **297**, which upon mild oxidation generates the natural product **299**, through a TADA reaction performed at the latest possible stage of the synthesis.

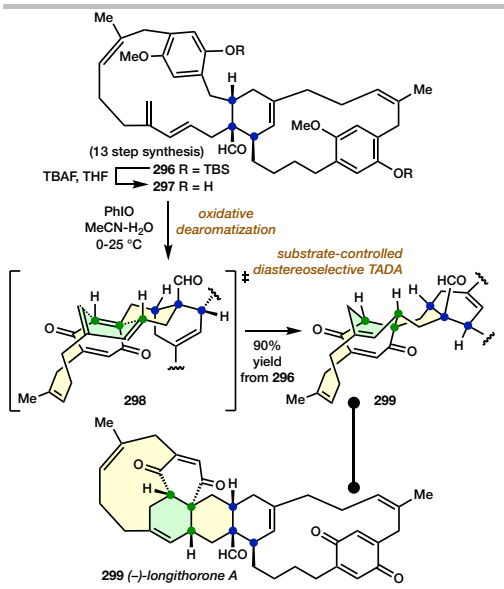

Scheme B21. The Shair group's 14 step total synthesis of (–)-longithorone A (2002)

The TADA reaction is site selective with respect to the dienophile (reaction occurs at one of four possible para-benzoquinone C=C sites) and diastereoselective. This preference can be traced back to SOIs, existing precursor stereochemistry, and conformational factors. Thus, *endo*-mode TADA reaction occurs at the most proximate dienophile C=C bond to the diene, possibly through chairlike type 1 tether conformation TS **298**. (The X-ray crystal structure of longithorone A reveals a boat conformation of the cyclohexane ring as drawn in **299**,[267] which would mandate a conformational change following the TADA reaction through TS **298**. Alternatively, the TADA process might occur through an alternative TS involving a boatlike type 1 tether, which would deliver longithorone A directly in the conformation seen in the crystal structure.) The 10 member, type 2 tether presumably also adopts a chairlike conformation within the vicinity of the diene and dienophile, as shown in TS **298**. The *π*-diastereofacial selectivity of the TADA process is controlled by the stereochemistry about the pre-existing cyclohexene ring.

TADA processes involving precursors with type 2 connections remain rare, despite being known for some time. The earliest type 2 TADA process that we can find is from the Schreiber group's efforts towards dynemicin A in 1990.[268]

The Shair synthesis of longithorone A is a biomimetic one. Another extraordinary biomimetic synthesis involving two DA processes is that of the pentacyclic natural product FR182877.

4.22. FR182877 (Evans/Sorensen, 2002)

Cascade twofold TADA-based syntheses of FR182877 **304** by Evans [269] and Sorensen [270] were reported almost simultaneously. The key phase of the two separate syntheses were similar, inasmuch as they both involved the collapse of a 19-membered macrocycle into a fused/bridged pentacyclic product containing 5, 6 and 7-membered rings and seven new stereocenters. (A separate approach involving an 1,3,8-nonatriene IMDA process before closure of the macrocycle was also successful.) In 2009, Nakada reported a twofold IMDA approach.[271] The key phase of the Sorensen synthesis is summarized in **Scheme B22**.

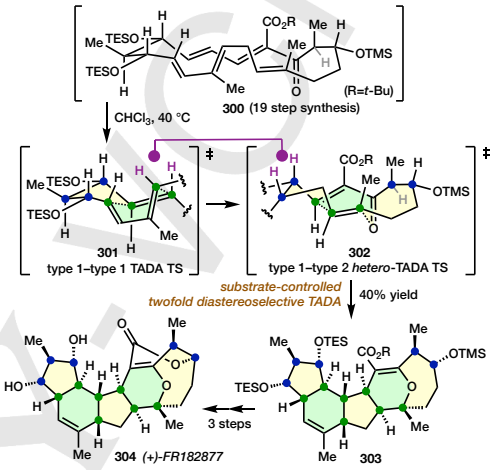

Scheme B22. The Sorensen group's 23 step synthesis of (+)-FR182877 (2002).

The putative intermediate, single TADA product was not observed, hence the order of events (carbo- vs. hetero-TADA) is not known. It seems safe to assume, however, that the first of the two TADA reactions is the type 1-type 1 carbo-process (TS **301**), with the shorter tether substituents adopting pseudoequatorial orientations, akin to a typical 1,3,8-nonatriene IMDA reaction (see **Section 3**), and extended conjugation to the ester and ketone groups causing dienophile activation. The subsequent type 1-type 2 hetero-TADA process (TS **302**) occurs within a 12-membered ring and is of the inverse electron-demand type, due to the strongly electron deficient oxadiene. Only one alternative pathway to TS **302** seems feasible, in which the diene is rotated through 180°. This approach would be disfavoured, however, by a steric clash with the newly-formed bicyclic portion of the molecule.

Exploratory/methodological studies and total synthesis pursuits are complementary. It is well known that the former provide the foundations upon which researchers can approach the latter studies with confidence but the quest of better syntheses of target molecules often provides previously unimagined theme variations. The final example of this review provides a demonstration in the TADA reaction class. The ground-breaking work of Deslongchamps focused entirely upon endocyclic, type 1 TADA trienes but eventually type 2 TADA processes were uncovered. Last year, a new class of TADA process was invented by the Luo group, by revisiting the now classic target, vinigrol.

4.23. Vinigrol (Luo, 2019)

The synthesis of vinigrol **105** by Luo and co-workers (**Scheme B23**) permits the preparation of the natural product in enantiomerically pure form on scales of up to 600 mg.[272] The ingenious route involves a pyrone diene/alkene dienophile DA reaction and *in situ* retro-DA reaction to expel CO_2. The IMDA/retro-DA process (**305**→**307**) brings about a significant structural change, generating all three rings of the natural product. This process is unique in TADA chemistry, in that only one C=C bond resides within the ring across which the DA reaction occurs; the other two C=C bonds are substituents. The diene and dienophile unite across the ten-membered ring and instigate its contraction to the eight-membered ring of the product.

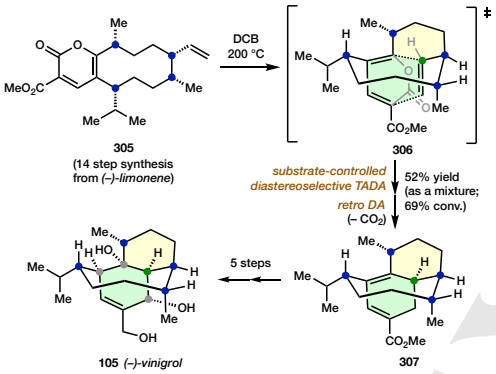

Scheme B23. The Luo group's 20 step total synthesis of (–)-vinigrol (2019).

Despite generating all three rings of vinigrol, this TADA process creates only a single stereocenter of the target, from a substrate carrying four pre-existing ones. (As an aside, three more stereocenters are installed after the cycloaddition on the ring that is generated by the [4+2] cycloaddition.) Only two diastereomeric products are, therefore, feasible, with the stereoselectivity of the TADA reaction apparently determined by the pseudoequatorial orientation of the isopropyl substituent in TS **306**, which steers the direction of folding of the macrocycle, hence diene-dienophile *π*-diastereofacial approach. The Luo synthesis of vinigrol is exceptional: it is a significant advance in the total synthesis of one of the most challenging molecules and breaks new ground in TADA reaction design.

Returning to TADA reactions in biosynthesis (Deslongchamps' biomimetic synthesis of chatancin was mentioned earlier), initial interpretations of certain biological TADA reactions have recently been re-evaluated, in light of new information on *ambimodal* pericyclic processes. Thus, macrocyclic precursors containing dienes and dienophiles bearing extended unsaturation can participate in pericyclic reactions through TSs that are, in effect, hybrids of two simpler processes. Spinosyn A, **312**, for example, is formed from macrocyclic pentaene precursor **308** by way of formal TADA product **310** (**Scheme B24**).[273]

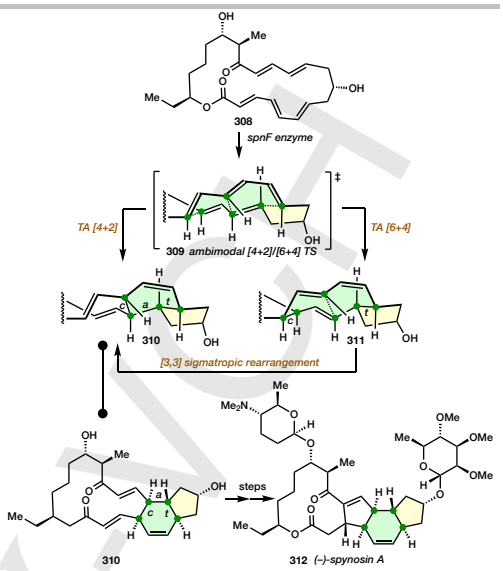

Scheme B24. The biosynthesis of spynosin A through an ambimodal transannuar pericyclic TS (2011, 2016).

Compound **310** is formed through a bifurcation on the potential energy surface, which occurs at ambimodal TS **309**. Direct transannular [4+2] cycloaddition generates **310** from TS **309**, or alternatively, transannular [6+4] cycloadduct **311** is first formed, which undergoes a rapid transannular Cope rearrangement to **310**. Both pathways generate the *cis-anti-trans* stereochemistry seen in the natural product **312**, which is formed from **310** through a further transannular ring closure and glycosylation. Related transannular ambimodal pericyclic TSs in other natural product biosyntheses are known,[274] with ambimodal (bispericyclic[275]) processes and TS bifurcations[276] growing in both number and importance.

5. Conclusions

It is hard to comprehend that a process can be at least as vital to a field more than 50 years after its first use. Nonetheless, the examples described herein demonstrate unequivocally that the IMDA process is still one of the most important reactions in total syntheses. The IMDA process remains to be bettered in both power and versatility. We predict that unprecedented variations of the reaction will continue to be seen for decades. Conceptually novel total synthesis applications will most likely involve the least well studied classes of IMDA reactions, i.e. type 1 processes other than those with 5 and 6 membered ring-forming tethers, type 2 IMDA reactions, TADA processes beyond those involving endocyclic dienes and dienophiles, and IMDA processes that don't involve C=C bonds.

IMDA reactions performed with relatively simple trienes are generally used earlier in a total synthesis. An analysis of the

examples will reveal that, while an IMDA process creates significant target-relevant complexity in a single reaction, step economy in total syntheses involving an IMDA reaction is often thwarted by substrate preparation. There is a genuine need for innovative, short routes from feedstock compounds to triene precursors. Future efforts should also be focused on a wider exploration of domino sequences involving triene preparation, IMDA reaction, and IMDA adduct transformation.

The most celebrated examples of IMDA reactions in total synthesis are those that are late-stage. Many such processes are bio-inspired, and the origin of their impressive nature can be traced to the high level of structural complexity created from an elaborate, advanced precursor. Such syntheses feel precarious since they are analogous to leaping across a chasm from a great height. We acknowledge and applaud those willing to take such risks, and encourage them to continue to be both creative and courageous in their synthetic endeavours.

WILEY-VCH

REVIEW

Entry for the Table of Contents

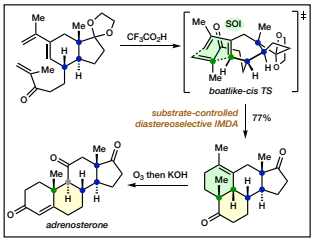

When performed in an intramolecular fashion, the Diels-Alder reaction is one of the most powerful and versatile chemical reactions. This review documents and critically analyzes the strategic deployment of the process in target synthesis. It focuses on the present scope and current limitations of the process, with an emphasis on instructive examples, landmark contributions, recent developments and future prospects.

6

Experimental

This chapter describes experimental methods and characterisation data for Chapters 2 and 4.

6.1 Experimental for Chapter 2

The following section describes experimental methods and characterisation data for Chapter 2.

Science
AAAS

Supplementary Materials for

Diverse polycycles from the simplest cross-conjugated molecule

J. W. Boyle, N. Shadwell, S. L. Drew, N. Green, M. S. Sherburn

Correspondence to: michael.sherburn@anu.edu.au

This PDF file includes:

Other Supplementary Materials for this manuscript include the following:

Combined CIF File
Combined CheckCIF Report

Table of Contents

General Methods

NMR Spectroscopy

^{1}H NMR spectra were recorded at 800 or 400 MHz using a Bruker AVANCE 400, Varian 400-MR or Bruker AVANCE 800 spectrometer, as indicated. Residual protio-solvent peaks were used as an internal reference for ^{1}H NMR spectra ($CDCl_3$ δ 7.26 ppm, toluene-d_8 7.09, C_6D_6 7.16, CD_3OD δ 3.31 ppm). Coupling constants (*J*) are quoted to the nearest 0.1 Hz. The assignment of proton signals was assisted by COSY, HSQC and HMBC experiments. ^{13}C NMR spectra were recorded at 100, 150 or 200 MHz using a Bruker AVANCE 400, Varian 400-MR or Bruker AVANCE 800 spectrometer. Solvent peaks were used as an internal reference for ^{13}C NMR spectra ($CDCl_3$ δ 77.16 ppm, toluene-d_8 137.48, C_6D_6 128.06, CD_3OD δ 49.00 ppm). Assignment of carbon signals was assisted by HSQC and HMBC experiments. The following abbreviations (or combinations thereof) are used to denote ^{1}H NMR multiplicities: s = singlet, d = doublet, dd= doublet of doublets, t = triplet, m = multiplet, br = broad.

Infrared Spectroscopy

IR spectra were recorded on a Perkin–Elmer UATR Two spectrometer as a thin film or solid, or on a Perkin–Elmer 1600 FTIR spectrometer as a thin film (NaCl plate) or solid (KBr disc).

Mass Spectrometry

Low-resolution EI mass spectra were recorded on a Finnigan Polaris Q ion trap mass spectrometer or Agilent HP 6869 series mass spectrometer using electron impact (EI+) ionization mode at 40 or 70 eV. High-resolution EI mass spectra were recorded on a VG Autospec mass spectrometer operating at 70 eV. Low resolution ESI mass spectra were recorded on a ZMD Micromass spectrometer with Waters Alliance 2690 HPLC. High resolution ESI mass spectra were recorded on a Waters LCT Premier time of flight (TOF) mass spectrometer.

Melting Points

Melting points were measured on a Stanford Research Systems Optimelt Automated Melting Point System and are uncorrected.

Optical Rotations

Optical rotations were measured on a Perkin–Elmer 341 polarimeter using a sodium lamp (589 nm) as the light source over a path length of 10 cm. $[\alpha]_D$ values are reported in units of 10^{-1}degcm^{2}g^{-1} at concentration (c) in g/100 mL.

High Performance Liquid Chromatography

Preparative HPLC was performed using an Agilent 1100 preparative binary pump, preparative automatic sampler, and diode array detector with a preparative flow cell, a Shimadzu Prominence LC-20AD chromatograph pump using SPD-M20 diode array and Shimadzu RID-10A detectors or a Waters 600E pump, a Waters 717plus autosampler, a 996 photodiode array detector and a Fraction Collector III, operated by Waters Empower 2 software. Analytical HPLC was performed using a Shimadzu Prominence LC-20AD chromatograph pump using SPD-M20 diode array and Shimadzu RID-10A detectors.

Supercritical Fluid Chromatography

Separations were performed on a Waters ACQUITY UPC2 System equipped an ACQUITY UPC2 Photodiode Array (PDA). Empower 3 FR2 Software was used for data acquisition and processing.

Ultra-High Pressure Reactor

Ultra-high pressure reactions were conducted in Telfon reaction vessels with a Psika 20 kbar ultra-high pressure reactor (see page S5, Ultra-High Pressure Reactor Setup).

Experimental Procedures, Reagents, Chromatography and Glassware

Reactions were conducted under a positive pressure of dry nitrogen in oven or heat gun-dried glassware and at room temperature, unless specified otherwise. Anhydrous solvents were either obtained from commercial sources or dried according to the procedure outlined by Grubbs and co-workers *(49)*. Commercially available chemicals were used as purchased, or where specified, purified by standard techniques *(50)*. Analytical thin-layer chromatography was conducted with aluminum-backed silica gel 60 F254 (0.2 mm) plates supplied by Merck, and visualized using UV fluorescence (λ_{max} = 254 nm), or developed using $KMnO_4$ or *p*-anisaldehyde TLC stains, followed by heating. Flash chromatography employed Merck Kiesegel 60 silica gel (230–400 mesh). Et_3N-deactivated SiO_2 was prepared by loading the column with a slurry of SiO_2 in eluent with 1% Et_3N added, and flushing with one column volume of eluent before use. Solvent compositions are given in (v/v). PS 40–60 °C refers to petroleum spirits, boiling point fraction 40–60 °C.

X-Ray Crystallography

Single crystal X-ray data were collected on either a Nonius KappaCCD (Mo X-ray radiation source for **3d, 4d, 4e, 4g, 4h, 16, 17a, 17b**), Agilent Technologies SuperNova (Cu X-ray radiation source for **4f, 4k, 4l, 4o, 4t, 20**) or Agilent Technologies xCalibur (Mo X-ray radiation source for **4b, 4p, 4q**) diffractometer. Data were measured using Bruker proprietary software

(51) or CrysAlisPRO *(52)*. Structures were solved with SIR92 *(53)* or ShelXT *(54)* and refined with Crystals *(55)* or ShelXL *(56)* using OLEX2 *(57)*.

Ultra-High Pressure Reactor Setup

a)

b)

Fig. S1.

Ultra-High Pressure Reactor Setup; a) Ultra-high pressure reactor, digital and manual control panels; b) Teflon ultra-high pressure reaction vessel.

Methods

Neat [3]Dendralene (2)

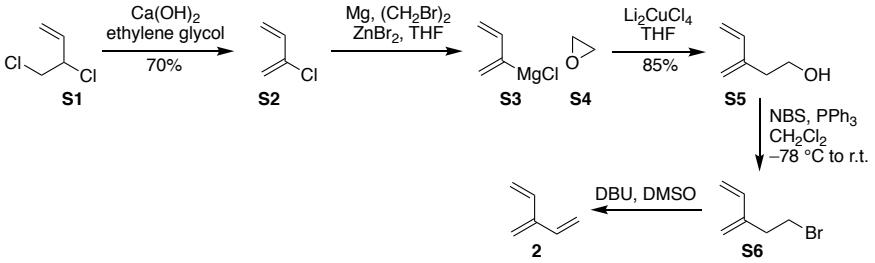

Chloroprene (S2)

Although industrially available on ton scale, chloroprene is difficult to obtain commercially on gram scale and so was prepared according to the published patent of Tassara and co-workers *(58)*.

A 500 mL 3-neck round bottom flask was equipped with a non-equalizing dropping funnel and a vigreux-column 1-piece distillation apparatus with condenser (–10 °C). The distillation apparatus was fitted with a thermometer and receiving flask and the reaction set-up placed under Ar. To the receiving flask was added BHT (1-2 crystals) and the flask cooled in a –78 °C dry ice-acetone bath. BHT (500 mg), $Ca(OH)_2$ (14.82 g, 0.200 mol, 0.50 mol. equiv.) and ethylene glycol (160 mL) were added to the reaction flask and the resulting solution heated to 105 °C. The non-equalizing dropping funnel was charged with 1,2-dichlorobutene (50.0 g, 43.0 mL, 0.400 mol, 1.0 mol. equiv.). 1,2-dichlorobutene was added dropwise to the reaction mixture until chloroprene was observed condensing in the distillation apparatus. Slow dropwise addition of the 1,2-dichlorobutene was then continued at such a rate as to maintain slow distillation of chloroprene. Once distillation was complete, the chloroprene (26.0 mL, 24.9 g, 0.281 mol, 70%) was dried with $CaCO_3$, kept under Ar and used immediately.

2-(1,3-Butadienyl)magnesium chloride (S3)

2-(1,3-butadienyl)magnesium chloride solution in THF was prepared according to the procedure described by Sherburn and co-workers *(59)*.

1,3-Butadiene S5

1,3-Butadiene **S5** was prepared in adaptation of the procedure reported by Toombs-Ruane *(60)*. A 3-neck round bottom flask equipped with an addition funnel was charged with LiCl (dried at 100 °C >24h, 1.08 g, 25.4 mmol, 0.12 mol. equiv.), anhydrous $CuCl_2$ (1.71 g, 12.7 mmol, 0.06 mol. equiv.), and THF (139 mL). The resulting solution was cooled in a 0 °C ice bath and treated with ethylene oxide solution (3.43 M solution in THF, 74.2 mL, 255 mmol, 1.2 mol.

equiv.). 2-(1,3-butadienyl)magnesium chloride **S3** solution (0.819 M solution in THF, 259 mL, 212 mmol, 1.0 mol. equiv.) was then added dropwise, and the reaction mixture allowed to slowly warm to room temperature and stirred for 13 h. Et_2O (280 mL) and H_2O (280 mL) were then added to the reaction mixture and the pH adjusted to 4 using 2M aq. HCl solution. The aqueous layer was then separated and extracted with Et_2O (2 x 200 mL). The organic layers were combined, washed with brine, dried over $MgSO_4$, filtered (celite) and concentrated under reduced pressure (50 mbar, 0°C). Distillation (27 mbar, 61-70 °C, BHT added to distilling flask) afforded 1,3-butadiene **S5** as a clear colorless oil (17.72 g, 0.181 mol, 85%). ^{1}H NMR spectroscopic data was in accordance with that reported previously *(61)(62)*.

[3]dendralene (2)

Neat [3]dendralene (**2**) was prepared from alcohol **S5** *via* bromide **S6** according to the procedure outlined by Sherburn and co-workers *(63)*.

Dienophiles

3,3-Dimethoxycyclopropene (1a)

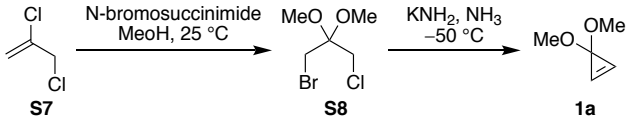

S7 **S8** **1a**

3,3-Dimethoxycyclopropene (**1a**) was prepared from 2,3-dichloro-1-propene (**S7**) according to the procedure outlined by Breslow and co-workers *(64)*.

Cyclobut-2-en-1-one (1b)

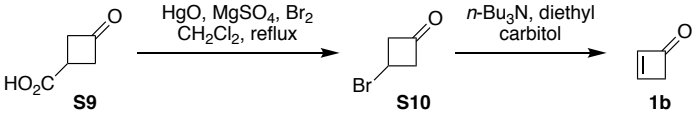

S9 **S10** **1b**

Cyclobut-2-en-1-one (**1b**) was prepared from 3-oxocyclobutane-1-carboxylic acid (**S9**) according to the procedure outlined by Danishefsky and co-workers *(65)*.

Cyclooct-2-en-1-one (1f)

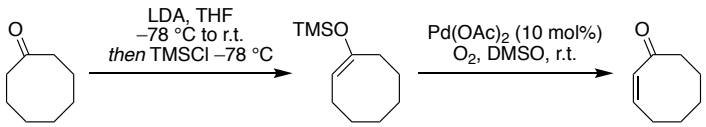

S11 **S12** **1f**

Cyclooct-2-en-1-one (**1f**) was prepared from cyclooctanone (**S11**) according to the procedure outlined by Reisinger *(66)*.

2-(trimethylsilyl)phenyl trifluoromethanesulfonate S15

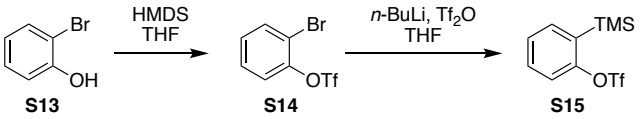

S13 **S14** **S15**

2-(trimethylsilyl)phenyl trifluoromethanesulfonate **S15** was prepared from 2-bromophenol **S13**, according to the procedure outlined by Peng and co-workers *(67)*.

Optimization Data

The following table summarizes results that led to use of optimized conditions presented in the paper.

Table S1.

Optimization of catalyst and temperature for regioselective reaction of [3]dendralene with cyclohexenone[a,b]

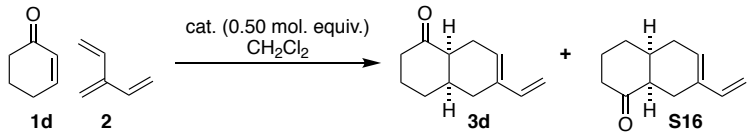

entry	catalyst	temperature (°C)	ratio (**3d**:**S16**)
1	$MeAlCl_2$	0	3:1
2	$MeAlCl_2$	–20	5:1
3	$TiCl_4$	–20	1:1
4	Me_2AlCl	–20	10:1
5	Me_2AlCl	–30	>95:5

[a] Conditions: 2 mol. equiv. [3]dendralene, 1 mol. equiv. cyclohexenone, 0.5 mol. equiv. Lewis acid catalyst; reactions performed on 0.62 mmol scale; concentration 0.62 mol L^{-1} with respect to cyclohexenone; [b] Regioselectivity determined by analysis of crude ^1H NMR spectra.

Mono-adducts

Bicyclic diene 3a

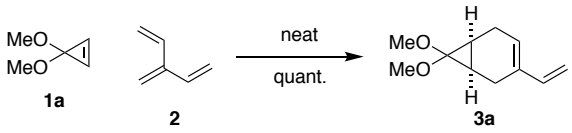

Ketal **1a** (110 mg, 1.10 mmol, 1.0 mol. equiv.) and [3]dendralene (**2**) (341 mg, 4.26 mmol, 3.88 mol. equiv.) were combined, the reaction flask sealed, and the reaction mixture stirred at 25 °C for 14.5 h. Concentration under reduced pressure and purification by flash column chromatography (Et_3N-deactivated SiO_2; 5% EtOAc in PS 40–60 °C), afforded bicyclic diene **3a** as a clear colorless oil (quant.).

R_f = 0.37 (10 % EtOAc in PS 40–60 °C);

^{1}H NMR (400 MHz, $CDCl_3$): δ 6.35 (dd, J = 10.8, 17.6 Hz, 1H), 5.63 (br s, 1H), 5.05 (d, J = 17.5 Hz, 1H), 4.88 (d, J = 10.8 Hz, 1H), 3.39 (s, 3H), 3.33 (s, 3H), 2.46 (dd, J = 6.9, 19.8 Hz), 2.39-2.25 (m, 3H), 1.50-1.43 (m, 1H), 1.39-1.30 (m, 1H) ppm;

^{13}C NMR (100 MHz, $CDCl_3$): δ 140.0 (CH), 132.2 (C_q) 126.6 (CH), 109.4 (CH_2), 92.6 (C_q), 53.6 (CH_3), 52.9 (CH_3), 20.2 (CH_2), 19.4 (CH), 18.6 (CH), 17.7 (CH_2) ppm;

IR (thin film): ν_{max} = 2936, 2895, 2830, 1654, 1607 cm^{-1};

LRMS (70 eV, EI): m/z (%): 180 (30, $[M]^{+\bullet}$), 165 (10), 133 (10), 105 (100), 91 (29), 77 (25);

HRMS (70 eV, EI): m/z calc. for $C_{11}H_{16}O_2$ $[M]^{+\bullet}$:180.1149; found 180.1150.

Bicyclic diene 3b

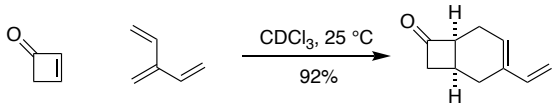

1b **2** **3b**

A solution of [3]dendralene (**2**) in $CDCl_3$ (400 µL, 3.25 M, 1.30 mmol, 2.52 mol. equiv.) was added to a solution of cyclobutenone (**1b**) in $CDCl_3$ (600 µL, 0.858 M, 0.515 mmol, 1.00 mol. equiv.) at 25 °C. The reaction flask was sealed and the reaction mixture stirred for 62 h at 25 °C, then concentrated under reduced pressure to afford the crude material as a yellow oil. Regio/diastereo-selectivity was determined to be >95:5 by analysis of crude ^{1}H NMR spectra. Purification by flash column chromatography (SiO_2; 5% EtOAc in PS 40–60 °C), afforded bicyclic diene **3b** as a clear colorless oil (70.3 mg, 0.474 mmol, 92%).

R_f = 0.34 (10 % EtOAc in PS 40–60 °C);

^{1}H NMR (400 MHz, $CDCl_3$): δ 6.24 (dd, J = 17.5, 10.7 Hz, 1H), 5.89 (s, 1H), 5.16 (d, J = 17.5 Hz, 1H), 4.97 (d, J = 10.8 Hz, 1H), 3.51-3.40 (m, 1H), 3.25-3.13 (m, 1H), 2.97-2.86 (m, 1H), 2.54-2.40 (m, 3H), 2.36-2.25 (m, 1H), 2.24-2.14 (m, 1H) ppm;

^{13}C NMR (100 MHz, $CDCl_3$): δ 213.2 (C_q), 139.3 (CH), 136.2 (C_q), 127.9 (CH), 110.8 (CH_2), 56.5 (CH), 51.6 (CH_2), 25.0 (CH_2), 23.0 (CH_2), 22.0 (CH) ppm;

IR (thin film): ν_{max} = 2924, 1772, 1738, 1636, 1601 cm^{-1};

LRMS (70 eV, EI): m/z (%): 148 (3, $[M]^{+\bullet}$), 120 (27), 106 (33), 91 (100),78 (60);

HRMS (70 eV, EI): m/z calc. for $C_{10}H_{12}O$ $[M]^{+\bullet}$: 148.0888; found 148.0890.

General procedure 1: Me_2AlCl catalyzed Diels–Alder reactions between [3]dendralene and cyclic enones

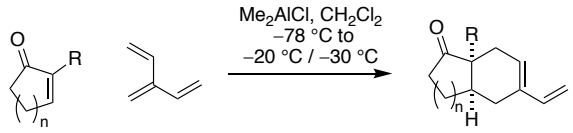

1 **2** **3**

A stirred solution of [3]dendralene (**2**) (1.25 mmol, 2.02 mol. equiv.) in CH_2Cl_2 (1.0 mL) cooled in a –78 °C dry ice-acetone bath under Ar was treated with enone **1** (1.0 mol. equiv.), followed by the dropwise addition of Me_2AlCl (1.0 M solution in hexane, 0.50 mol. equiv.). The resulting solution was transferred to a –20 °C to –30 °C bath (IPA, Huber Chiller) and was stirred at this temperature for 18-70 h. Triethylamine (0.10 mL) was then added, the reaction mixture removed from the cold bath, sat. aq. potassium sodium tartrate solution (5.0 mL) added and the resulting mixture allowed to stirr for 30 min. The mixture was then poured onto water (5.0 mL) and extracted with CH_2Cl_2 (3 x 5.0 mL). The organic layers were combined, washed with brine (5.0 mL), dried over $MgSO_4$ and concentrated under reduced pressure. Purification by flash column chromatography afforded the Diels–Alder monoadduct **3**.

Bicyclic diene 3c

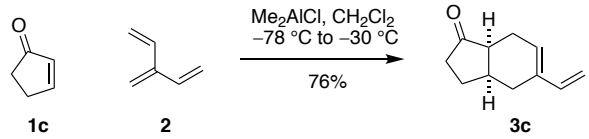

1c **2** **3c**

Bicyclic diene **3c** was prepared according to **General Procedure 1** with [3]dendralene (**2**) (342 mg, 4.27 mmol, 2.02 mol. equiv.), cyclopent-2-en-1-one (**1c**) (173 mg, 177 uL, 2.11 mmol, 1.0 mol. equiv.) and Me_2AlCl (1.0 M solution in hexane, 1.06 mL, 1.06 mmol, 0.50 mol. equiv.) at –30 °C for 70 h. Regio/diastereo-selectivity was determined to be >95:5 by analysis of crude ^1H NMR spectra. Purification by flash column chromatography (SiO_2; CH_2Cl_2) afforded bicyclic diene **3c** as a clear colorless oil (269 mg, 1.66 mmol, 76%).

$\boldsymbol{R_f}$ = 0.44 (CH_2Cl_2);

^{1}H NMR (400 MHz, $CDCl_3$): δ 6.34 (dd, J = 17.5, 10.8 Hz, 1H), 5.69 (s, 1H), 5.06 (d, J = 17.5 Hz, 1H), 4.92 (d, J = 10.8 Hz, 1H), 2.63-2.50 (m, 2H), 2.46-2.33 (m, 3H), 2.33-2.23 (m, 2H), 2.16-1.99 (m, 1H), 1.91-1.81 (m, 1H), 1.79-1.67 (m, 1H) ppm;

^{13}C NMR (100 MHz, $CDCl_3$): δ 219.3 (C_q), 139.6 (CH), 134.5 (C_q), 127.2 (CH), 110.4 (CH_2), 47.0 (CH), 34.3 (CH_2), 32.6 (CH), 26.7 (CH_2), 24.7 (CH_2), 22.3 (CH_2) ppm;

IR (thin film): ν_{max} = 2936, 2880, 2837, 1736, 1646, 1607 cm^{-1};

LRMS (70 eV, EI): m/z (%): 162 (82, $[M]^{+\bullet}$), 118 (100), 105 (90), 91 (78), 79 (50);

HRMS (70 eV, EI): m/z calc. for $C_{11}H_{14}O$ $[M]^{+\bullet}$:162.1045; found 162.1047.

Bicyclic diene 3d

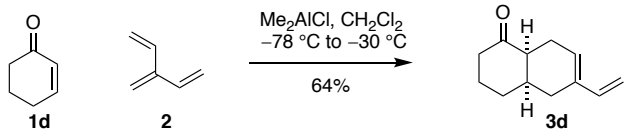

Bicyclic diene **3d** was prepared according to **General Procedure 1** with [3]dendralene (**2**) (316 mg, 3.94 mmol, 2.02 mol. equiv.), cyclohex-2-en-1-one (**1d**) (188 mg, 189 µL, 1.95 mmol, 1.0 mol. equiv.) and Me_2AlCl (1.0 M solution in hexane, 975 uL, 0.975 mmol, 0.50 mol. equiv.) at –30 °C for 46 h. Regio/diastereo-selectivity was determined to be >95:5 by analysis of crude ^1H NMR spectra. Purification by flash column chromatography (SiO_2; 5% EtOAc in PS 40–60 °C) afforded bicyclic diene **3d** as a white solid (219 mg, 1.24 mmol, 64%). Recrystallization from EtOAc gave white crystals suitable for single crystal X-ray analysis.

m.p. = 37–39 °C (EtOAc);

$\boldsymbol{R_f}$ = 0.22 (5% EtOAc in hexanes);

^{1}H NMR (400 MHz, $CDCl_3$): δ 6.33 (dd, J = 17.5, 10.8 Hz, 1H), 5.69 (s, 1H), 5.01 (d, J = 17.5 Hz, 1H), 4.89 (d, J = 10.8 Hz, 1H), 2.78-2.67 (m, 1H), 2.63 (d, J = 19.0 Hz, 1H), 2.50-2.36 (m, 2H), 2.36-2.21 (m, 1H), 2.20-1.87 (m, 6H), 1.84-1.71 (m, 1H) ppm;

^{13}C NMR (100 MHz, $CDCl_3$): δ 212.4 (C_q), 139.7 (CH), 134.1 (C_q), 126.7 (CH), 110.1 (CH_2), 48.3 (CH), 40.3 (CH_2), 36.0 (CH), 28.8 (CH_2), 25.9 (CH_2), 24.6 (CH_2), 24.1 (CH_2) ppm;

IR (KBr): ν_{max} = 2928, 1708, 1645, 1606 cm^{-1};

LRMS (70 eV, EI): m/z (%): 176 (100, $[M]^{+\bullet}$), 130 (90), 105 (90), 84 (78);

HRMS (70 eV, EI): m/z calc. for $C_{12}H_{16}O$ $[M]^{+\bullet}$: 176.1201; found 176.1201.

Bicyclic diene 3e

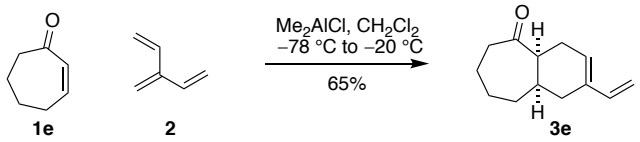

Bicyclic diene **3e** was prepared according to **General Procedure 1** with [3]dendralene (**2**) (50 mg, 0.62 mmol, 2.0 mol. equiv.), cyclohept-2-en-1-one (**1e**) (34 mg, 35 µL, 0.31 mmol, 1.0 mol. equiv.) and Me_2AlCl (1.0 M solution in hexane, 155 uL, 0.155 mmol, 0.50 mol. equiv.) at –20 °C for 20 h. Regio/diastereo-selectivity was determined to be >95:5 by analysis of crude ^1H NMR spectra. Purification by flash column chromatography (SiO_2; 5% EtOAc in PS 40–60 °C) afforded bicyclic diene **3e** as a clear colorless oil (38.3 mg, 0.201 mmol, 65%).

R_f = 0.35 (10% EtOAc in PS 40–60 °C);

^{1}H NMR (400 MHz, $CDCl_3$): δ 6.34 (dd, J = 17.5, 10.7 Hz, 1H), 5.73 (s, 1H), 5.02 (d, J = 17.5 Hz, 1H), 4.90 (d, J = 10.7 Hz, 1H), 2.76 (td, J = 6.6, 6.6, 3.3 Hz, 1H), 2.72-2.61 (m, 1H), 2.50-2.33 (m, 4H), 2.31-2.21 (m, 1H), 2.08-1.98 (m, 1H), 1.86-1.58 (m, 6H) ppm;

^{13}C NMR (100 MHz, $CDCl_3$): δ 215.0 (C_q), 139.7 (CH), 134.6 (C_q), 127.7 (CH), 110.3 (CH_2), 49.8 (CH), 43.9 (CH_2), 34.0 (CH), 33.5 (CH_2), 30.3 (CH_2), 27.5 (CH_2), 26.9 (CH_2), 24.3 (CH_2) ppm;

IR (thin film): ν_{max} = 2922, 1693, 1644, 1606 cm^{-1};

LRMS (70 eV, EI): m/z (%):190 (83, $[M]^{+\bullet}$), 133 (44), 117 (44), 105 (100), 91 (87), 79 (54);

HRMS (70 eV, EI): m/z calc. for $C_{13}H_{18}O$ $[M]^{+\bullet}$: 190.1358; found 190.1359.

Bicyclic diene 3f

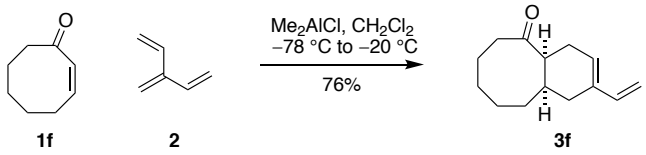

1f **2** **3f**

Bicyclic diene **3f** was prepared according to **General Procedure 1** with [3]dendralene (**2**) (326 mg, 4.07 mmol, 2.02 mol. equiv.), cyclooct-2-en-1-one (**1f**) (250 mg, 2.01 mmol, 1.0 mol. equiv.) and Me_2AlCl (1.0 M solution in hexane, 1.01 mL, 1.01 mmol, 0.50 mol. equiv.) at –20 °C for 24 h. Regio/diastereo-selectivity was determined to be >95:5 by analysis of crude ^1H NMR spectra. Purification by flash column chromatography (SiO_2; 5% EtOAc in PS 40–60 °C) afforded bicyclic diene **3f** as a clear colorless oil (310 mg, 1.52 mmol, 76%).

R_f = 0.41 (10% EtOAc in PS 40–60 °C);

^{1}H NMR (400 MHz, $CDCl_3$): δ 6.38 (dd, J = 17.5, 10.7 Hz, 1H), 5.77 (s, 1H), 5.06 (d, J = 17.5 Hz, 1H), 4.91 (d, J = 10.8 Hz, 1H), 3.06-2.94 (m, 1H), 2.91-2.79 (td, J = 3.4, 12.2, 12.2 Hz, 1H), 2.57-2.40 (m, 3H), 2.30-2.14 (m, 2H), 2.07 (d, J = 16.8 Hz, 1H), 199-1.89 (m, 1H), 1.89-1.78 (m, 1H), 1.78-1.56 (m, 3H), 1.43-1.22 (m, 2H), 0.95-0.78 (m, 1H) ppm;

^{13}C NMR (100 MHz, $CDCl_3$): δ 217.4 (C_q), 139.8 (CH), 134.0 (C_q), 127.7 (CH), 110.2 (CH_2), 49.7 (CH), 39.4 (CH_2), 32.0 (CH_2), 31.3 (CH_2), 30.3 (CH_2), 29.7 (CH), 26.3 (CH_2), 24. 3 (CH_2), 22.8 (CH_2) ppm;

IR (thin film): ν_{max} = 2924, 1695, 1643, 1605 cm^{-1};

LRMS (70 eV, EI): m/z (%): 204 (92, $[M]^{+\bullet}$), 161 (34), 133 (44), 120 (32), 117 (32), 105 (100), 91 (77), 79 (49), 77 (49);

HRMS (70 eV, EI): m/z calc. for $C_{14}H_{20}O$ $[M]^{+\bullet}$: 204.1514; found 204.1515.

Bicyclic diene 3g

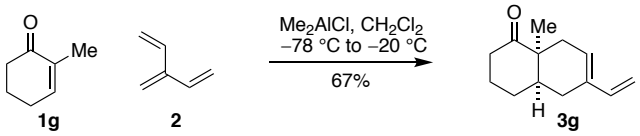

Bicyclic diene **3g** was prepared according to **General Procedure 1** with [3]dendralene (**2**) (50 mg, 0.62 mmol, 2.0 mol. equiv.), 2-methylcyclohex-2-en-1-one (**1g**) (34 mg, 36 uL, 0.31 mmol, 1.0 mol. equiv.) and Me_2AlCl (1.0 M solution in hexane, 155 uL, 0.155 mmol, 0.50 mol. equiv.) at –20 °C for 20 h. Regio/diastereo-selectivity was determined to be >95:5 by analysis of crude ^1H NMR spectra. Purification by flash column chromatography (SiO_2; 10% EtOAc in hexanes) afforded bicyclic diene **3g** as a clear colorless oil (39 mg, 0.20 mmol, 67%).

$\boldsymbol{R_f}$ = 0.31 (10% EtOAc in hexanes);

^{1}H NMR (400 MHz, $CDCl_3$): δ 6.34 (dd, J = 17.6, 11.2 Hz, 1H), 5.65 (s, 1H), 5.06 (d, J = 17.6 Hz, 1H), 4.92 (d, J = 11.2 Hz, 1H), 2.64-2.54 (m, 2H), 2.34-2.28 (m, 2H), 2.07-2.00 (m, 2H), 1.88-1.78 (m, 2H), 1.72-1.62 (m, 3H), 1.09 (s, 3H) ppm;

^{13}C NMR (100 MHz, $CDCl_3$): δ 215.3 (C_q), 139.7 (CH), 133.0 (C_q), 125.2 (CH), 110.6 (CH_2), 47.9 (C_q), 41.2 (CH), 37.3 (CH_2), 32.2 (CH_2), 27.9 (CH_2), 26.9 (CH_2), 25.1 (CH_2), 20.7 (CH_3) ppm;

IR (thin film): ν_{max} = 2931, 2865, 1703, 1676, 1646, 1607, cm_{-1};

LRMS (70 eV, EI): m/z (%): 190 (63, $[M]^{+\bullet}$); 175 (83), 147 (52), 130 (100), 91 (83);

HRMS (70 eV, EI): m/z calc. for $C_{13}H_{18}O$ $[M]^{+\bullet}$: 190.1358; found 190.1354.

Bicyclic diene 3h

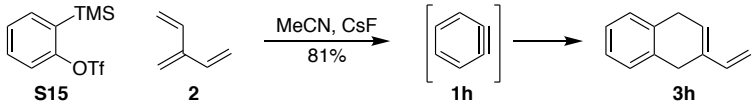

S15 **2** **1h** **3h**

CsF (69 mg, 0.45 mmol, 3.0 mol. equiv.) was dried under reduced pressure for 3 h at 190 °C, then cooled to room temperature and flushed with Ar. MeCN (0.50 mL) and [3]dendralene (**2**) (50 mg, 0.61 mmol, 4.0 mol. equiv.) were added, followed by the dropwise addition of benzyne precursor **S15** (45 mg, 37 µL, 0.15 mmol, 1.0 mol. equiv.). The reaction vessel was sealed, and the reaction stirred at 25 °C for 18 h. The reaction mixture was then diluted with CH_2Cl_2 (3.0 mL), washed with water (3 x 3.0 mL) and brine (3.0 mL), dried over $MgSO_4$ and concentrated under reduced pressure. Purification by flash column chromatography (SiO_2; pentane) afforded bicyclic diene **3h** as a colorless oil (19 mg, 0.12 mmol, 81%). ^{1}H NMR and ^{13}C NMR data were consistent with those reported previously *(68)*.

R_f = 0.55 (pentane);

^{1}H NMR (400 MHz, $CDCl_3$): δ 7.23-7.17 (m, 4H), 6.53 (dd, J = 17.2, 10.4 Hz, 1H), 5.99 (s, 1H), 5.25 (d, J = 17.2 Hz, 1H), 5.07 (d, 10.4 Hz, 1H), 3.64-3.45 (m, 4H) ppm;

^{13}C NMR (100 MHz, $CDCl_3$): δ 139.0 (CH), 134.1 (C_q), 134.0 (C_q), 133.7 (C_q), 128.8 (CH), 128.3 (CH), 126.7 (CH), 126.2 (CH), 126.1 (CH), 111.1 (CH_2), 30.8 (CH_2), 28.8 (CH_2) ppm;

IR (thin film): ν_{max} = 3086, 3046, 3022, 3006, 2868, 2817, 1609, cm^{-1};

LRMS (70 eV, EI): m/z (%): 156 (100, $[M]^{+\bullet}$), 141 (100), 128 (100), 115 (90);

HRMS (70 eV, EI): m/z calc. for $C_{12}H_{12}$ $[M]^{+\bullet}$: 156.0939; found 156.0937.

Bis-adducts

General Procedure 2: Ultra-high pressure Diels–Alder reactions

Semicyclic diene **3** (0.25 mmol, 1.0 mol. equiv.) and enone **1** (5.0 mol. equiv.) were added to a Teflon high-pressure reaction tube and dissolved in CH_2Cl_2 (1.0 mL). The reaction vessel was sealed and compressed at 19 kbar for 72-120 h using a PSIKA 20 kbar reactor. The solvent was then removed under reduced pressure. Purification by flash column chromatography afforded the tetracyclic Diels–Alder adducts **4**.

General Procedure 3: Zinc chloride catalyzed Diels–Alder reactions

Zinc chloride catalyzed Diels-Alder reactions were performed in adaptation of the procedure reported by Danishefsky and co-workers *(65)*. Zinc chloride (4.0 mol. equiv.) was dried under reduced pressure for 15 h at 140 °C, then cooled to room temperature and flushed with N_2. MeCN (652 uL) and cyclobutenone (**1b**) solution (0.305 mmol, 1.0 mol. equiv., 1.85M in $CDCl_3$) were added and the resulting mixture allowed to stir for 30 minutes at room temperature. Semicyclic diene **3** (4.0 mol. equiv.) and $CDCl_3$ (272 uL) were then added and the reaction mixture heated to 45 °C for 21 hours (flask equipped with reflux condenser). After this time, the reaction was cooled to room temperature, diluted with $CDCl_3$ (1.0mL), filtered, and concentrated under reduced pressure. Purification by flash column chromatography afforded the tetracyclic Diels–Alder adducts **4**.

Tetracycle 4a

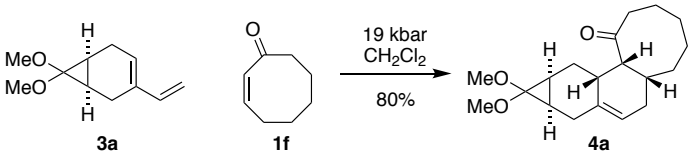

Tetracycle **4a** was prepared according to **General Procedure 2** with semicyclic diene **3a** (60 mg, 0.33 mmol, 1.0 mol. equiv.) and cyclooct-2-en-1-one (**1f**) (207 mg, 1.66 mmol, 5.0 mol. equiv.) for 72 h, with the addition of 3,5-di-tert-4-butylhydroxytoluene (7.3 mg, 0.033 mmol, 0.10 mol. equiv.) to the reaction mixture. Regio/diastereo-selectivity was determined to be >95:5 by analysis of crude ^{1}H NMR spectra. Purification by flash column chromatography (Et_3N-deactivated SiO_2; 5% EtOAc in PS 40–60 °C) afforded tetracycle **4a** as a clear colorless oil (80.9 mg, 0.266 mmol, 80%). (Note: decomposition/isomerization was observed on characterization/storage)

$\boldsymbol{R_f}$ = 0.34 (20% EtOAc in PS 40–60 °C);

^{1}H NMR (400 MHz, $CDCl_3$): δ 5.42 (br s, 1H), 3.50 (s, 3H), 3.20 (s, 3H), 2.74-2.64 (m, 1H), 2.61-2.53 (m, 1H), 2.47 (dd, J = 8.6, 15.1 Hz, 1H), 2.41-2.30 (m, 2H), 2.15-2.02 (m, 3H), 2.01-1.89 (m, 2H), 1.72-1.62 (m, 1H), 1.62-1.01 (m, 10 H) ppm;

^{13}C NMR (100 MHz, $CDCl_3$): δ 214.0 (C_q), 135.6 (C_q), 118.6 (CH), 93.9 (C_q), 53.3 (CH_3), 52.4 (CH_3), 50.5 (CH), 44.8 (CH_2), 34.9 (CH), 34.4 (CH), 33.0 (CH_2), 31.2 (CH_2), 28.6 (CH_2), 27.6 (CH_2), 26.1 (CH_2), 23.3 (CH_2), 22.9 (CH_2), 22.4 (CH), 21.6 (CH) ppm;

IR (thin film): ν_{max} = 2930, 2832, 1695 cm^{-1};

LRMS (70 eV, EI): m/z (%): 304 (15, $[M]^{+\bullet}$), 257 (12), 179 (45), 101 (100);

HRMS (70 eV, EI): m/z calc. for $C_{19}H_{28}O_3$ $[M]^{+\bullet}$: 304.2038; found 304.2034.

Tetracycle 4b

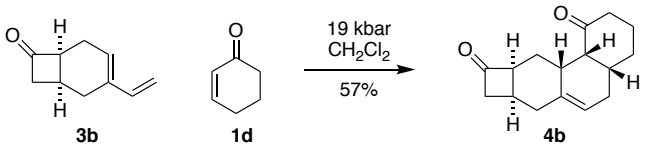

3b **1d** **4b**

Tetracycle **4b** was prepared according to **General Procedure 2** with semicyclic diene **3b** (50.0 mg, 0.337mmol, 1.0 mol. equiv.) and cyclohex-2-en-1-one (**1d**) (162 mg, 163 uL, 1.69 mmol, 5.0 mol. equiv.) for 72 h, with the addition of 3,5-di-tert-4-butylhydroxytoluene (7.3 mg, 0.034 mmol, 0.10 mol. equiv.) to the reaction mixture. No regio/diastereo-isomers were observable by analysis of crude ^{1}H NMR spectra. Purification by flash column chromatography (SiO_2; 20% EtOAc in PS 40–60 °C) afforded tetracycle **4b** as a white solid (46.9 mg, 0.192 mmol, 57%). Recrystallization from EtOAc afforded white crystals suitable for single crystal X-ray analysis.

m.p. = 102–105 °C (EtOAc);

R_f = 0.27 (20% EtOAc in PS 40–60 °C);

^{1}H NMR (400 MHz, $CDCl_3$): δ 5.31 (br s, 1H), 3.51-3.40 (m, 1H), 3.11 (ddd, J = 4.3, 7.7, 16.4 Hz, 1H), 2.88-2.58 (m, 5H), 2.37-2.19 (m, 4H), 2.17-2.02 (m, 2H), 2.01-1.86 (m, 4H), 1.71-1.59 (m, 2H) ppm;

^{13}C NMR (100 MHz, $CDCl_3$): δ 216.2 (C_q), 211.4 (C_q), 134.0 (C_q), 120.3 (CH), 59.2 (CH), 53.7 (CH), 51.3 (CH_2), 43.1 (CH_2), 39.6 (CH), 36.4 (CH), 32.0 (CH_2), 30.0 (CH_2), 27.7 (CH_2), 25.0 (CH_2), 24.2 (CH_2), 22.9 (CH) ppm;

IR (thin film): ν_{max} = 2962, 2930, 2875, 1766, 1703 cm^{-1};

LRMS (70 eV, EI): m/z (%): 244 (9, $[M]^{+\bullet}$), 207 (18), 97 (96), 44 (100);

HRMS (70 eV, EI): m/z calc. for $C_{16}H_{20}O_2$ $[M]^{+\bullet}$: 244.1463; found 244.1461.

Tetracycle 4c

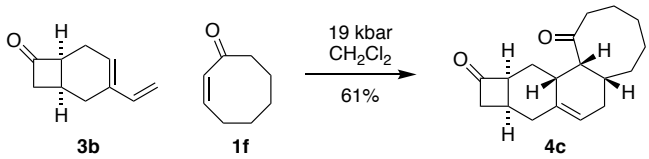

3b **1f** **4c**

Tetracycle **4c** was prepared according to **General Procedure 2** with semicyclic diene **3b** (50.0 mg, 0.337mmol, 1.0 mol. equiv.) and cyclooct-2-en-1-one (**1f**) (210 mg, 1.69 mmol, 5.0 mol. equiv.) for 72 h with the addition of 3,5-di-tert-4-butylhydroxytoluene (7.3 mg, 0.034 mmol, 0.10 mol. equiv.) to the reaction mixture. Regio/diastereo-selectivity was determined to be >90:10 by analysis of crude ^{1}H NMR spectra. Purification by flash column chromatography (SiO_2; 20% EtOAc in PS 40–60 °C) afforded tetracycle **4c** as a white foam (55.8 mg, 0.205 mmol, 61%).

R_f = 0.22 (20% EtOAc in PS 40–60 °C);

^{1}H NMR (400 MHz, $CDCl_3$): δ 5.48 (br s, 1H), 3.41-3.27 (m, 2H), 3.12 (ddd, J = 4.7, 10.2, 14.8 Hz, 1H), 2.81-2.65 (m, 3H), 2.39-2.15 (m, 5H), ppm; 2.15-2.03 (m, 1H), 2.02-1.89 (m, 2H), 1.85-1.53 (m, 5H), 1.53-1.26 (m, 4H) ppm;

^{13}C NMR (100 MHz, $CDCl_3$): δ 216.1 (C_q), 214.6 (C_q), 132.8 (C_q), 122.1 (CH), 58.5 (CH), 52.1 (CH_2), 48.6 (CH), 47.5 (CH_2), 38.4 (CH), 37.7 (CH), 32.7 (CH_2), 31.6 (CH_2), 29.5 (CH_2), 29.4 (CH_2), 25.0 (CH_2), 23.1 (CH), 22.8 (CH_2), 21.7 (CH_2) ppm;

IR (thin film): ν_{max} = 2925, 2852, 2834, 1774, 1698 cm^{-1};

LRMS (70 eV, EI): m/z (%): 272 (23, $[M]^{+\bullet}$), 230 (46), 125 (80), 91 (100);

HRMS (70 eV, EI): m/z calc. for $C_{18}H_{24}O_2$ $[M]^{+\bullet}$: 272.1776; found 272.1771.

Tetracycle 4d

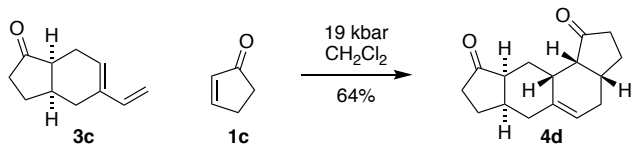

Tetracycle **4d** was prepared according to **General Procedure 2** with semicyclic diene **3c** (60 mg, 0.37 mmol, 1.0 mol. equiv.) and cyclopent-2-en-1-one (**1c**) (152 mg, 155 uL, 1.85 mmol, 5.0 mol. equiv.) for 72 h, with the addition of 3,5-di-tert-4-butylhydroxytoluene (8.2 mg, 0.037 mmol, 0.10 mol. equiv.) to the reaction mixture. Regio/diastereo-selectivity was determined to be >90:10 by analysis of crude ^{1}H NMR spectra. Purification by flash column chromatography (SiO_2; 20% EtOAc in PS 40–60 °C) afforded tetracycle **4d** as a white solid (57.9 mg, 0.237 mmol, 64%). Recrystallization from EtOAc afforded white crystals suitable for single crystal X-ray analysis.

m.p. = 117–119 °C (EtOAc);

R_f = 0.16 (15% EtOAc in hexanes);

^{1}H NMR (400 MHz, $CDCl_3$): δ 5.42 (br s, 1H), 2.50-2.07 (m, 13H), 2.04-1.90 (m, 2H), 1.87-1.75 (m, 1H), 1.75-1.60 (m, 3H) ppm;

^{13}C NMR (100 MHz, $CDCl_3$): δ 219.9 (C_q), 218.8 (C_q), 136.9 (C_q), 119.3 (CH), 50.3 (CH), 50.2 (CH), 36.91 (CH_2), 36.86 (CH), 36.4 (CH_2), 34.8 (CH_2), 34.5 (CH), 32.8 (CH), 26.8 (CH_2), 26.6 (CH_2), 25.9 (CH_2), 25.1 (CH_2) ppm;

IR (KBr): ν_{max} = 2918, 2873, 2838, 1734, 1709 cm^{-1};

LRMS (70 eV, EI): m/z (%): 244 (54, $[M]^{+\bullet}$), 162 (33), 131 (32), 118 (91), 83 (100);

HRMS (70 eV, EI): m/z calc. for $C_{16}H_{20}O_2$ $[M]^{+\bullet}$: 244.1463; found 244.1460.

Tetracycle 4e

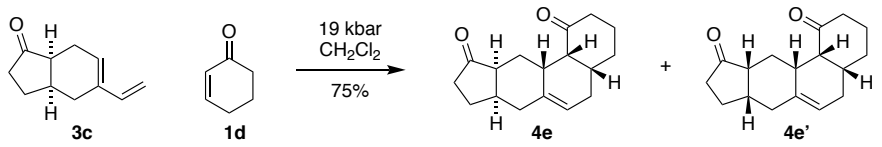

Tetracycle **4e** was prepared according to **General Procedure 2** with semicyclic diene **3c** (100 mg, 0.616 mmol, 1.0 mol. equiv.) and cyclohex-2-en-1-one (**1d**) (290 mg, 292 uL, 3.10 mmol, 5.0 mol. equiv.) for 72 h. Regio/diastereo-selectivity was determined to be >85:15 by analysis of crude ^{1}H NMR spectra. Purification by flash column chromatography (SiO_2; 5%–20% EtOAc gradient in hexanes) afforded tetracycle **4e** as a white solid (120 mg, 0.464 mmol, 75%). Recrystallization from EtOAc afforded white crystals suitable for single crystal X-ray analysis, containing a 95:5 mixture of diastereomers (**4e**:**4e**').

Major: Tetracycle 4e

m.p. = 105–107 °C (EtOAc);

R_f = 0.13 (15% EtOAc in hexanes);

^{1}H NMR (400 MHz, $CDCl_3$): δ 5.32 (br s, 1H), 2.91 (t, J = 4.7 Hz, 1H), 2.61-2.50 (m, 1H), 2.44-2.14 (m, 8H), 2.07-1.59 (m, 11H) ppm;

^{13}C NMR (100 MHz, $CDCl_3$): δ 220.8 (C_q), 212.1 (C_q), 135.6 (C_q), 119.2 (CH), 53.2 (CH), 49.6 (CH), 43.7 (CH_2), 40.0 (CH), 35.6 (CH), 35.4 (CH_2), 35.2 (CH_2), 35.0 (CH), 30.0 (CH_2), 26.7 (CH_2), 26.1 (CH_2), 25.5 (CH_2), 23.7 (CH_2) ppm;

IR (KBr): ν_{max} = 2939, 2915, 2893, 2875, 2824, 1730, 1703 cm^{-1};

LRMS (70 eV, EI): m/z (%): 258 (100, $[M]^{+\bullet}$), 240 (10), 132 (39), 91 (56), 83 (64);

HRMS (70 eV, EI): m/z calc. for $C_{17}H_{22}O_2$ $[M]^{+\bullet}$: 258.1620; found 258.1619.

Tetracycle 4f

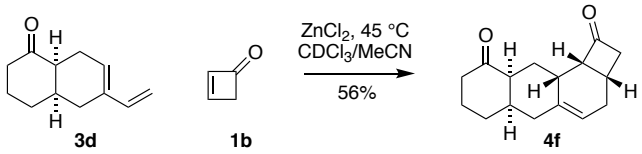

Tetracycle **4f** was prepared according to **General Procedure 3** with zinc chloride (77.3 mg, 0.567 mmol, 4.0 mol. equiv.), cyclobut-2-en-1-one (**1b**) (9.65 mg, 0.142 mmol, 1.0 mol. equiv.) and semicyclic diene **3d** (100 mg, 0.567 mmol, 4.0 mol. equiv.) for 21 h. Regio/diastereoselectivity was determined to be >85:15 by analysis of crude ^{1}H NMR spectra. Purification by flash column chromatography (SiO_2; 10% EtOAc in PS 40–60 °C) afforded tetracycle **4f** as a white solid (19.3 mg, 0.0790 mmol, 56%). Recrystallization from EtOAc afforded white crystals suitable for single crystal X-ray analysis.

m.p. = 106–108 °C (EtOAc);

R_f = 0.16 (CH_2Cl_2);

^{1}H NMR (400 MHz, $CDCl_3$): δ 5.41 (br s, 1H), 3.53-3.44 (m, 1H), 3.14 (ddd, J = 3.3, 8.9, 17.1 Hz, 1H) 2.77-2.61 (m, 2H), 2.60-2.49 (m, 1 H), 2.48-2.23 (m, 5H), 2.11-1.83 (m, 7H), 1.76 (td, J = 5.0, 13.0 Hz, 1H), 1.66 (d, J = 10.8 Hz, 1H) ppm;

^{13}C NMR (100 MHz, $CDCl_3$): δ 213.3 (C_q), 211.9 (C_q), 138.3 (C_q), 118.7 (CH), 60.6 (CH), 52.9 (CH_2), 49.7 (CH), 41.8 (CH_2), 39.4 (CH), 35.6 (CH_2), 30.9 (CH), 30.3 (CH_2), 27.8 (CH_2), 27.2 (CH_2), 22.6 (CH_2), 21.6 (CH) ppm;

IR (thin film): ν_{max} = 2919, 2851, 1768, 1706 cm^{-1};

LRMS (70 eV, EI): m/z (%): 244 (90, $[M]^{+\bullet}$), 183 (61), 141 (62), 97 (100), 91 (100);

HRMS (70 eV, EI): m/z calc. for $C_{16}H_{20}O_2$ $[M]^{+\bullet}$: 244.1436; found 244.1462.

Tetracycle 4g

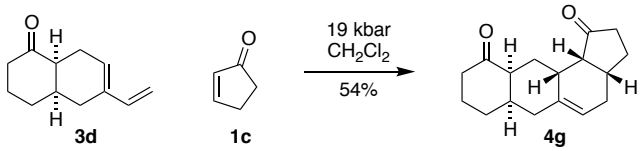

Tetracycle **4g** was prepared according to **General Procedure 2** with semicyclic diene **3d** (60 mg, 0.31 mmol, 1.0 mol. equiv.) and cyclopent-2-en-1-one (**1c**) (125 mg, 127 uL 1.55 mmol, 5.0 mol. equiv.) for 72 h. Regio/diastereo-selectivity was determined to be >95:5 by analysis of crude ^{1}H NMR spectra. Purification by flash column chromatography (SiO_2; 5%–20% EtOAc gradient in hexanes) afforded tetracycle **4g** as a white solid (43 mg, 0.17 mmol, 54%). Recrystallization from EtOAc afforded white crystals suitable for single crystal X-ray analysis.

m.p. = 127–129 °C (EtOAc);

R_f = 0.27 (15% EtOAc in hexanes);

^{1}H NMR (400 MHz, $CDCl_3$): δ 5.30 (br s, 1H), 2.78-2.68 (m, 2H), 2.48 (t, J = 6.9 Hz, 1H), 2.42-2.26 (m, 5H), 2.26-2.02 (m, 4H), 2.02-1.85 (m, 6H), 1.81-1.65 (m, 3H) ppm;

^{13}C NMR (100 MHz, $CDCl_3$): δ 218.6 (C_q), 213.2 (C_q), 137.8 (C_q), 118.5 (CH), 50.8 (CH), 50.0 (CH), 42.0 (CH_2), 40.4 (CH), 36.8 (CH_2), 35.7 (CH_2), 34.6 (CH), 32.1 (CH), 30.5 (CH_2), 27.0 (CH_2), 26.7 (CH_2), 25.9 (CH_2), 22.6 (CH_2) ppm;

IR (KBr): ν_{max} = 2920, 2876, 2848, 1732, 1697, cm^{-1};

LRMS (70 eV, EI): m/z (%): 258 (100 $[M]^{+\bullet}$), 240 (52), 176 (70), 141 (26) 117 (26);

HRMS (70 eV, EI): m/z calc. for $C_{17}H_{22}O_2$ $[M]^{+\bullet}$: 258.1620; found 258.1621.

Tetracycle 4h

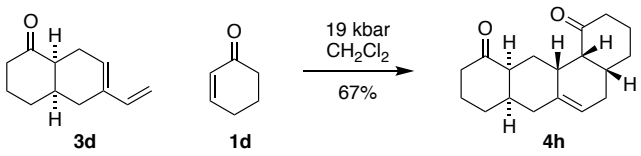

3d **1d** **4h**

Tetracycle **4h** was prepared according to **General Procedure 2** with semicyclic diene **3d** (100 mg, 0.567 mmol, 1.0 mol. equiv.) and cyclohex-2-en-1-one (**1d**) (274 mg, 275 uL, 2.85 mmol, 5.0 mol. equiv.) for 72 h. No regio/diastereo-isomers were observable by analysis of crude ^{1}H NMR spectra. Purification by flash column chromatography (SiO_2; 5%–20% EtOAc gradient in hexanes) afforded tetracycle **4h** as a white solid (95 mg, 0.38 mmol, 67%). Recrystallization from EtOAc gave white crystals suitable for single crystal X-ray analysis.

m.p. = 155–158 °C (EtOAc);

R_f = 0.19 (15% EtOAc in hexanes);

^{1}H NMR (400 MHz, $CDCl_3$): δ 5.24 (br s, 1H), 2.97 (t, J = 4.8 Hz, 1H), 2.68 (t, J = 4.0 Hz, 1H), 2.54-2.17 (m, 7H), 2.12-1.85 (m, 10H), 1.81-1.60 (m, 4H) ppm;

^{13}C NMR (100 MHz, $CDCl_3$): δ 213.8 (C_q), 212.2 (C_q), 136.8 (C_q), 118.2 (CH), 53.1 (CH), 49.9 (CH), 43.9 (CH_2), 41.9 (CH_2), 40.2 (CH), 39.4 (CH), 35.9 (CH_2), 34.2 (CH),30.4 (CH_2), 30.2 (CH_2), 26.4 (CH_2), 26.1 (CH_2), 25.7 (CH_2), 22.5 (CH_2) ppm;

IR (thin film): ν_{max} = 2918, 2907, 2850, 1704, 1700 cm^{-1};

LRMS (70 eV, EI): m/z (%): 272 (100, $[M]^{+\bullet}$), 254 (65), 236 (23), 183 (31), 91 (38);

HRMS (70 eV, EI): m/z calc. for $C_{18}H_{24}O_2$ $[M]^{+\bullet}$: 272.1776; found 272.1777.

S27

Tetracycle 4i

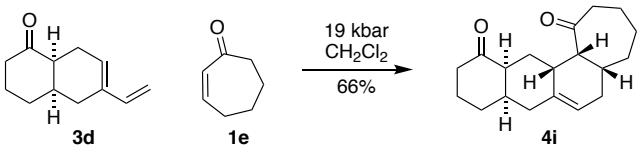

3d **1e** **4i**

Tetracycle **4i** was prepared according to **General Procedure 2** with semicyclic diene **3d** (50 mg, 0.28 mmol, 1.0 mol. equiv.) and cyclohept-2-en-1-one (**1e**) (156 mg, 158 uL, 1.42 mmol, 5.0 mol. equiv.) for 72 h. No regio/diastereo-isomers were observable by analysis of crude ^{1}H NMR spectra. Purification by flash column chromatography (SiO_2; 20% EtOAc in PS 40–60 °C) afforded tetracycle **4i** as a white solid (53.4 mg, 0.186 mmol, 66%).

m.p. = 124–126 °C (EtOAc);

R_f = 0.32 (20% EtOAc in PS 40–60 °C);

^{1}H NMR (400 MHz, $CDCl_3$): δ 5.31 (br s, 1H), 3.27 (t, J = 4.5 Hz, 1 H), 2.68-2.50 (m, 2H), 2.49-2.19 (m, 5 H), 2.09-1.56 (m, 15 H), 1.42 (td, J = 5.1, 12.8 Hz, 1H), 1.25 (t, J = 12.2 Hz, 1H) ppm;

^{13}C NMR (100 MHz, $CDCl_3$): δ 213.6 (C_q), 213.0 (C_q), 137.2 (C_q), 119.6 (CH), 52.2 (CH), 49.8 (CH), 46.4 (CH_2), 41.9 (CH_2), 39.6 (CH), 36.3 (CH_2), 36.1 (CH), 35.7 (CH_2), 35.6 (CH), 30.4 (CH_2), 28.7 (CH_2), 26.7 (CH_2), 23.6 (CH_2), 23.4 (CH_2), 22.4 (CH_2) ppm;

IR (thin film): ν_{max} = 2916, 2856, 1696 cm^{-1};

LRMS (70 eV, EI): m/z (%): 286 (100, $[M]^{+\bullet}$), 183 (21), 97 (54), 91 (50);

HRMS (70 eV, EI): m/z calc. for $C_{19}H_{26}O_2$ $[M]^{+\bullet}$: 286.1933; found 286.1936.

Tetracycle 4j

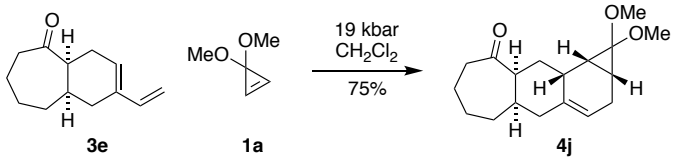

3e **1a** **4j**

Tetracycle **4j** was prepared according to **General Procedure 2** with semicyclic diene **3e** (60.0 mg, 0.315 mmol, 1.0 mol. equiv.) and ketal (**1a**) (158 mg, 1.58 mmol, 5.0 mol. equiv.) for 72 h, with the addition of 3,5-di-tert-4-butylhydroxytoluene (6.9 mg, 0.032 mmol, 0.10 mol. equiv.) to the reaction mixture. Regio/diastereo-selectivity was determined to be >85:15 by analysis of crude ^{1}H NMR spectra. Purification by flash column chromatography (Et_3N-deactivated SiO_2; 5% EtOAc in PS 40–60 °C) afforded tetracycle **4j** as a white foam (68.6 mg, 0.236 mmol, 75%).

R_f = 0.13 (10% EtOAc in PS 40–60 °C);

^{1}H NMR (400 MHz, $CDCl_3$): δ 5.21 (s, 1H), 3.40 (s, 3H), 3.30 (s, 3H), 2.91 (br s, 1H), 2.62-2.47 (m, 2H), 2.44-2.34 (m, 1H), 2.32-2.20 (m, 2H), 2.09 (d, J = 17.2 Hz, 1H), 2.01-1.76 (m, 4H), 1.75-1.61 (m, 4H), 1.57-1.45 (m, 1H), 1.39-1.23 (m, 2H), 0.99 (d, 10.7 Hz, 1H) ppm;

^{13}C NMR (100 MHz, $CDCl_3$): δ 215.6 (C_q), 137.2 (C_q), 115.5 (CH), 92.4 (C_q), 53.5 (CH_3), 53.0 (CH_3), 50.4 (CH), 44.4 (CH_2), 39.6 (CH_2), 39.3 (CH), 36.6 (CH_2), 34.1 (CH_2), 27.2 (CH), 26.0 (CH), 23.9 (CH_2), 23.7 (CH_2), 19.1 (CH_2), 18.1 (CH) ppm;

IR (thin film): ν_{max} = 2922, 2834, 1739, 1700 cm^{-1};

LRMS (70 eV, EI): m/z (%): 290 (89, $[M]^{+\bullet}$), 243 (38), 129 (61), 117 (65), 91 (100);

HRMS (70 eV, EI): m/z calc. for $C_{18}H_{26}O_3$ $[M]^{+\bullet}$:290.1877; found 290.1882.

Tetracycle 4k

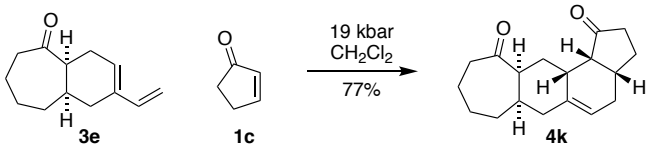

Tetracycle **4k** was prepared according to **General Procedure 2** with semicyclic diene **3e** (60.0 mg, 0.315 mmol, 1.0 mol. equiv.) and cyclopent-2-en-1-one (**1c**) (129 mg, 132 uL, 1.58 mmol, 5.0 mol. equiv.) for 72 h, with the addition of 3,5-di-tert-4-butylhydroxytoluene (6.9 mg, 0.032 mmol, 0.10 mol. equiv.) to the reaction mixture. No regio/diastereo-isomers were observable by analysis of crude ^{1}H NMR spectra. Purification by flash column chromatography (SiO_2; 10% EtOAc in PS 40–60 °C) afforded tetracycle **4k** as a white solid (66.0 mg, 0.242 mmol, 77%). Recrystallization from EtOAc afforded white crystals suitable for single crystal X-ray analysis.

m.p. = 101–104 °C (EtOAc);

R_f = 0.39 (20% EtOAc in PS 40–60 °C);

^{1}H NMR (400 MHz, $CDCl_3$): δ 5.28 (br s, 1H), 3.08-2.98 (m, 1H), 2.97-2.84 (m, 1H), 2.58 (ddd, J = 4.2,7.4, 15.1 Hz, 1H), 2.50-2.39 (m, 2H), 2.39-2.26 (m, 2H), 2.26-1.87 (m, 8H), 1.84-1.45 (m, 8H) ppm;

^{13}C NMR (100 MHz, $CDCl_3$): δ 218.8 (C_q), 215.8 (C_q), 137.9 (C_q), 118.4 (CH), 51.6 (CH), 50.4 (CH), 44.6 (CH_2), 38.0 (CH_2), 37.5 (CH), 35.7 (CH_2), 35.0 (CH_2), 34.6 (CH), 32.6 (CH), 28.5 (CH_2), 27.0 (CH_2), 26.3 (CH_2), 24.9 (CH_2), 24.4 (CH_2) ppm;

IR (thin film): ν_{max} = 2922, 1736, 1697 cm^{-1};

LRMS (70 eV, EI): m/z (%): 272 (100, $[M]^{+\bullet}$), 254 (75), 169 (57), 111 (98), 91 (82), 55 (54);

HRMS (70 eV, EI): m/z calc. for $C_{18}H_{24}O_2$ $[M]^{+\bullet}$:272.1776; found 272.1778.

Tetracycle 4l

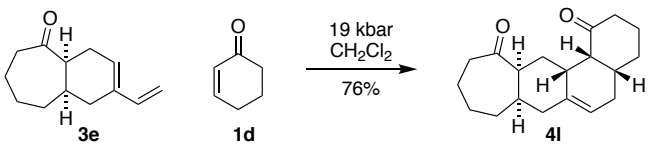

Tetracycle **4l** was prepared according to **General Procedure 2** with semicyclic diene **3e** (60.0 mg, 0.315 mmol, 1.0 mol. equiv.) and cyclohex-2-en-1-one (**1d**) (152 mg, 153 uL, 1.58 mmol, 5.0 mol. equiv.) for 72 h, with the addition of 3,5-di-tert-4-butylhydroxytoluene (6.9 mg, 0.032 mmol, 0.10 mol. equiv.) to the reaction mixture. No regio/diastereo-isomers were observable by analysis of crude ^{1}H NMR spectra. Purification by flash column chromatography (SiO_2; 20% EtOAc in petrol 40-60°) afforded tetracycle **4l** as a white solid (68.6 mg, 0.240 mmol, 76%). Recrystallization from EtOAc afforded white crystals suitable for single crystal X-ray analysis.

m.p. = 94–96 °C (EtOAc);

$\boldsymbol{R_f}$ = 0.30 (20% EtOAc in PS 40–60 °C);

^{1}H NMR (400 MHz, $CDCl_3$): δ 5.22 (br s, 1H), 3.06-2.97 (m, 1H), 2.90 (t, J = 4.8 Hz, 1H), 2.71-2.55 (m, 2H), 2.50 (dd, J = 5.4, 11.6 Hz, 1H), 2.44-2.27 (m, 2H), 2.27-2.16 (m, 2H), 2.15-2.02 (m, 2H), 2.02-1.76 (m, 8H), 1.75-1.50 (m, 6H) ppm;

^{13}C NMR (100 MHz, $CDCl_3$): δ 216.0 (C_q), 212.1 (C_q), 136.9 (C_q), 117.5 (CH), 53.3 (CH), 50.7 (CH), 44.6 (CH_2), 43.6 (CH_2), 40.0 (CH), 37.3 (CH_2), 36.9 (CH), 35.3 (CH_2), 34.7 (CH), 30.0 (CH_2), 28.5 (CH_2), 26.4 (CH_2), 25.3 (CH_2), 25.1 (CH_2), 24.3 (CH_2) ppm;

IR (thin film): ν_{max} = 2914, 1709, 1699, 1695 cm^{-1};

LRMS (70 eV, EI): m/z (%): 286 (100, $[M]^{+\bullet}$), 268 (20), 183 (18), 111 (54), 91 (57);

HRMS (70 eV, EI): m/z calc. for $C_{19}H_{26}O_2$ $[M]^{+\bullet}$: 286.1933; found 286.1935.

Tetracycle 4m

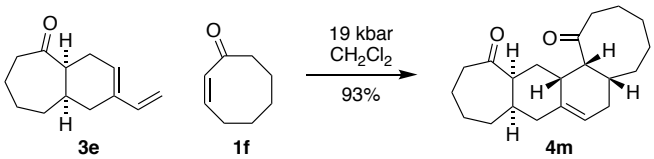

3e **1f** **4m**

Tetracycle **4m** was prepared according to **General Procedure 2** with semicyclic diene **3e** (60 mg, 0.32 mmol, 1.0 mol. equiv.) and cyclooct-2-en-1-one (**1f**) (196 mg, 1.58 mmol, 5.0 mol. equiv.) for 72 h. No regio/diastereo-isomers were observable by analysis of crude ^{1}H NMR spectra. Purification by flash column chromatography (SiO_2; 10% EtOAc in PS 40–60 °C) afforded tetracycle **4m** as a clear colorless oil (92 mg, 0.29 mmol, 93%).

R_f = 0.11 (10% EtOAc in PS 40–60 °C);

^{1}H NMR (400 MHz, $CDCl_3$): δ 5.38 (br s, 1H), 3.46 (br s, 1H), 2.85-2.79 (m, 1H), 2.78-2.69 (m, 1H), ppm; 2.57 (dt, J = 5.1, 15.7 Hz, 1H), 2.37-1.85 (m, 10H), 1.82-1.48 (m, 10 H), 1.47-1.17 (m, 5H) ppm;

^{13}C NMR (100 MHz, $CDCl_3$): δ 217.3 (C_q), 215.9 (C_q), 136.4 (C_q), 119.9 (CH), 50.7 (CH), 48.0 (CH_2), 47.9 (CH), 44.7 (CH_2), 37.9 (CH), 37.7 (CH), 37.7 (CH_2), 36.3 (CH), 35.0 (CH_2), 31.5 (CH_2), 29.9 (CH_2), 29.5 (CH_2), 28.2 (CH_2), 24.5 (CH_2), 24.0 (CH_2), 22.8 (CH_2), 21.6 (CH_2) ppm;

IR (thin film): ν_{max} = 2922, 2856, 1699, 1695 cm^{-1};

LRMS (70 eV, EI): m/z (%): 314 (100, $[M]^{+\bullet}$), 286 (57), 187 (50), 91 (75);

HRMS (70 eV, EI): m/z calc. for $C_{21}H_{30}O_2$ $[M]^{+\bullet}$: 314.2246; found 314.2244.

Tetracycle 4n

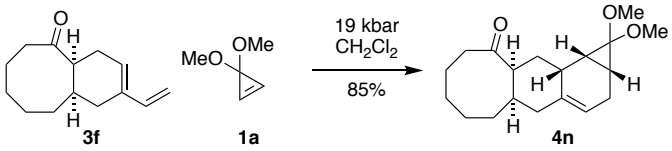

Tetracycle **4n** was prepared according to **General Procedure 2** with semicyclic diene **3f** (50 mg, 0.25 mmol,1.0 mol. equiv.) and ketal **1a** (123 mg, 1.23 mmol, 5.0 mol. equiv.) for 72 h, with the addition of 3,5-di-tert-4-butylhydroxytoluene (5.4 mg, 0.025 mmol, 0.10 mol. equiv.) to the reaction mixture. Regio/diastereo-selectivity was determined to be >85:15 by analysis of crude ^{1}H NMR spectra. Purification by flash column chromatography (Et_3N-deactivated SiO_2; 5% EtOAc in PS 40–60 °C) afforded tetracycle **4n** as a clear colorless oil (63.1 mg, 0.207 mmol, 85%).

R_f = 0.28 (10% EtOAc in PS 40–60 °C);

^{1}H NMR (400 MHz, $CDCl_3$): δ 5.20 (s, 1H), 3.45 (s, 3 H), 3.39-3.33 (m, 1H), 3.30 (s, 3H), 3.04 (d, J = 12.8 Hz, 1H), 2.60-2.49 (m, 1H), 2.32-2.07 (m, 4H), 2.04-1.92 (m, 2H), 1.89-1.53 (m, 6 H), 1.45-1.30 (m, 3H), 1.30-1.13 (m, 2H), 0.93 (d, J = 10.9 Hz, 1H) ppm;

^{13}C NMR (100 MHz, $CDCl_3$): δ 218.8 (C_q), 137.6 (C_q), 115.0 (CH), 92.4 (C_q), 53.6 (CH_3), 52.9 (CH_3), 46.3 (CH_2), 44.1 (CH), 43.5 (CH), 39.9 (CH_2), 37.1 (CH_2), 32.8 (CH_2), 29.9 (CH_2), 26.4 (CH), 25.8 (CH), 24.3 (CH_2), 24.3 (CH_2), 19.2 (CH_2), 17.8 (CH) ppm;

IR (thin film): ν_{max} = 2928, 2852, 1739, 1695 cm^{-1};

LRMS (70 eV, EI): m/z (%): 304 (85, $[M]^{+\bullet}$), 131 (68), 117 (79), 91 (100);

HRMS (70 eV, EI): m/z calc. for $C_{19}H_{28}O_3$ $[M]^{+\bullet}$: 304.2038; found 304.2044.

Tetracycle 4o

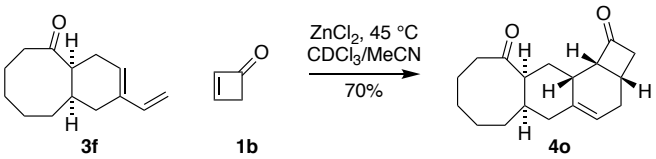

3f **1b** **4o**

Tetracycle **4o** was prepared according to **General Procedure 3** with zinc chloride (166 mg, 1.22 mmol, 4.0 mol. equiv.), semicyclic diene **3f** (250 mg, 1.22 mmol, 4.0 mol. equiv.) and cyclobut-2-en-1-one (**1b**) (20 mg, 0.31 mmol, 1.0 mol. equiv.) for 21 h. No regio/diastereo-isomers were observable by analysis of crude ^{1}H NMR spectra. Purification by flash column chromatography (SiO_2; 10% EtOAc in PS 40–60 °C) afforded tetracycle **4o** as a white solid (58.1 mg, 0.213 mmol, 70%), and recovered diene **3f** (94.9 mg, 0.464 mmol). Recrystallization of tetracycle **4o** from EtOAc afforded white crystals suitable for single crystal X-ray analysis.

m.p. = 104–106 °C (EtOAc);

R_f = 0.19 (100%; CH_2Cl_2);

^{1}H NMR (400 MHz, $CDCl_3$): δ 5.45 (br s, 1H), 3.39 (ddd, J = 3.5, 7.1, 10.3 Hz, 1H), 3.33-3.27 (m, 1H), 3.10 (ddd, J = 3.6, 9.0, 17.5 Hz, 1H), 2.97-2.86 (m, 1H), 2.79-2.68 (m, 1H), 2.58-2.45 (m, 1H), 2.44-2.41 (m, 1H), 2.40-2.29 (m, 1H), 2.26-2.08 (m, 3H), 2.08-1.90 (m, 4H), 1.89-1.75 (m, 2H), 1.74-1.60 (m, 2H), 1.49-1.37 (m, 3H), 1.36-1.23 (m, 1H) ppm;

^{13}C NMR (100 MHz, $CDCl_3$): δ 218.7 (C_q), 213.3 (C_q), 139.5 (C_q), 118.3 (CH), 61.7 (CH), 52.4 (CH_2), 45.4 (CH_2), 44.4 (CH), 39.0 (CH), 36.0 (CH_2), 32.1 (CH_2), 31.7 (CH), 29.5 (CH_2), 29.4 (CH_2), 27.6 (CH_2), 23.4 (CH_2), 22.4 (CH_2), 22.3 (CH) ppm;

IR (thin film): ν_{max} = 2931, 2912, 2883, 1761, 1681 cm^{-1};

LRMS (70 eV, EI): m/z (%): 272 (18, $[M]^{+\bullet}$), 230 (25), 145 (64),117 (51), 91 (100), 55 (46);

HRMS (70 eV, EI): m/z calc. for $C_{18}H_{24}O_2$ $[M]^{+\bullet}$: 272.1776; found 272.1779.

Tetracycle 4p

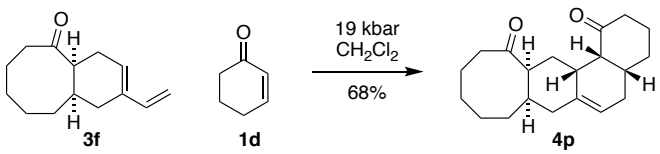

Tetracycle **4p** was prepared according to **General Procedure 2** with semicyclic diene **3f** (65 mg, 0.32 mmol,1.0 mol. equiv.) and cyclohex-2-en-1-one (**1d**) (153 mg, 154 uL, 1.59 mmol, 5.0 mol. equiv.) for 72 h. No regio/diastereo-isomers were observable by analysis of crude ^{1}H NMR spectra. Purification by flash column chromatography (SiO_2; 10% EtOAc in PS 40–60 °C) afforded tetracycle **4p** as a white solid (65 mg, 0.22 mmol, 68%). Recrystallization from EtOAc afforded white crystals suitable for single crystal X-ray analysis.

m.p. = 127–129 °C (EtOAc);

R_f = 0.18 (10% EtOAc in PS 40–60 °C);

^{1}H NMR (400 MHz, $CDCl_3$): δ 5.21 (br s, 1 H), 3.31 (br s, 1H), 2.99 (br s, 1H), 2.83 (t, J = 4.8 Hz, 1H), 2.57-2.42 (m, 2H), 2.40-2.26 (m, 1H), 2.23-2.07 (m, 4H), 2.06-1.85 (m, 8H), 1.83-1.62 (m, 5H), 1.50-1.35 (m, 3H), 1.34-1.24 (m, 1H) ppm;

^{13}C NMR (100 MHz, $CDCl_3$): δ 219.4 (C_q), 212.3 (C_q), 137.4 (C_q), 117.2 (CH), 53.2 (CH), 45.9 (CH_2), 44.0 (CH), 43.8 (CH_2), 40.3 (CH), 40.1 (CH), 36.4 (CH_2), 34.6 (CH), 32.3 (CH_2), 30.2 (CH_2), 29.8 (CH_2), 29.7 (CH_2), 26.5 (CH_2), 25.5 (CH_2), 23.2 (CH_2), 22.2 (CH_2) ppm;

IR (thin film): ν_{max} = 2906, 2859, 1708, 1693 cm^{-1};

LRMS (70 eV, EI): m/z (%): 300 (100, $[M]^{+\bullet}$), 272 (18), 183 (45), 91 (81);

HRMS (70 eV, EI): m/z calc. for $C_{20}H_{28}O_2$ $[M]^{+\bullet}$: 300.2089; found 300.2087.

S35

Tetracycle 4q

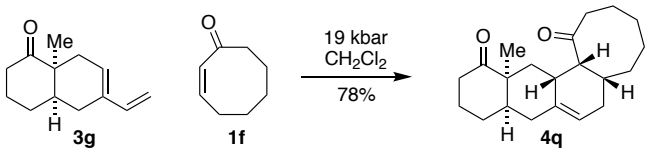

Tetracycle **4q** was prepared according to **General Procedure 2** with semicyclic diene **3g** (50 mg, 0.26 mmol, 1.0 mol. equiv.) and cyclooct-2-en-1-one (**1f**) (163 mg, 1.31 mmol, 5.0 mol. equiv.) for 120 h. No regio/diastereo-isomers were observable by analysis of crude ^{1}H NMR spectra. Purification by flash column chromatography (SiO_2; 20% EtOAc in PS 40–60 °C), followed by recrystallization from *n*-pentane afforded tetracycle **4q** as a white solid (64.1 mg, 0.204 mmol, 78%), with white crystals suitable for single crystal X-ray analysis.

m.p. = 110–112 °C (pentane);

R_f = 0.37 (20% EtOAc in PS 40–60 °C);

^{1}H NMR (400 MHz, CDCl3): δ 5.40 (d, J = 5.5 Hz, 1H), 3.52 (s, 1H), 2.64-2.45 (m 2 H), 2.38-2.08 (m, 5H), 2.05-1.84 (m, 8H), 1.82-1.59 (m, 4H), 1.51-1.29 (m, 5H), 1.71 (s, 3H), 0.86 (t, J = 12.8, 1H) ppm;

^{13}C NMR (100 MHz, CDCl3): δ 217.2 (C_q), 216.5 (C_q), 136.6 (C_q), 119.9 (CH), 49.8 (C_q), 48.1 CH_2), 47.4 (CH), 44.7 (2 x CH, coincident), 37.9 (CH_2), 36.9 (CH_2), 36.8 (CH_2), 36.5 (CH), 31.6 (CH_2), 29.6 (CH_2), 28.2 (CH_2), 27.3 (CH_3), 25.6 (CH_2), 23.0 (CH_2), 21.8 (2x CH_2, coincident) ppm;

IR (thin film): ν_{max} = 2910, 1702, 1700 cm^{-1};

LRMS (70 eV, EI): m/z (%): 314 (50, $[M]^{+\bullet}$), 204 (18), 119 (31), 111 (100), 105(26), 91 (35);

HRMS (70 eV, EI): m/z calc. for $C_{21}H_{30}O_2$ $[M]^{+\bullet}$: 314.2246; found 314.2246.

Tetracycle 4r

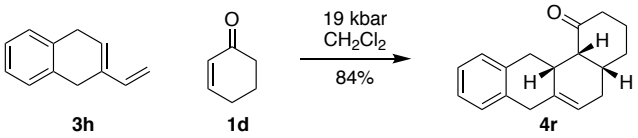

3h **1d** **4r**

Tetracycle **4r** was prepared according to **General Procedure 2** with semicyclic diene **3h** (40 mg, 0.25 mmol, 1.0 mol. equiv.) and cyclohex-2-en-1-one (**1d**) (123 mg, 127 uL, 1.25 mmol, 5.0 mol. equiv.) for 72 h. Regio/diastereo-selectivity was determined to be >95:5 by analysis of crude ^{1}H NMR spectra. Purification by flash column chromatography (SiO_2; 0%-10% gradient EtOAc in hexanes) afforded tetracycle **4r** as a white solid (54.3 mg, 0.21 mmol, 84%).

m.p. = 91–94 °C (EtOAc)

R_f = 0.37 (10% EtOAc in hexanes);

^{1}H NMR (400 MHz, $CDCl_3$): δ 7.17-7.07 (m, 4H), 5.43 (br s, 1H), 3.68 (dt, J = 3.2, 18.0, 1H), 3.46-3.30 (m, 2H), 2.95 (t, J = 4.7 Hz, 1H), 2.65-2.54 (m, 1H), 2.50 (dd, J = 14.1, 4.6 Hz, 1H), 2.45-2.35 (m, 1H), 2.34-2.23 (m, 2H), 2.11-1.92 (m, 5H), 1.76-1.64 (m, 1H) ppm;

^{13}C NMR (100 MHz, $CDCl_3$): δ 211.6 (C_q), 139.9 (C_q), 137.0 (C_q), 134.9 (C_q), 127.4 (CH), 127.1 (CH), 126.1 (CH), 125.7 (CH), 117.5 (CH), 53.2 (CH), 43.2 (CH_2), 39.6 (CH), 38.9 (CH), 36.2 (CH_2), 33.1 (CH_2), 30.0 (CH_2), 27.4 (CH_2), 24.5 (CH_2) ppm;

IR (thin film): ν_{max} =2926, 1708, cm^{-1};

LRMS (70 eV, EI): m/z (%): 252 (72, $[M]^{+\bullet}$), 234 (20), 207 (39), 179 (42), 142 (66), 97 (59), 44 (100);

HRMS (70 eV, EI): m/z calc. for $C_{18}H_{20}O$ $[M]^{+\bullet}$: 252.1514; found 252.1515.

Tetracycle 4s

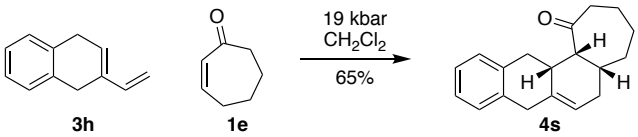

3h **1e** **4s**

Tetracycle **4s** was prepared according to **General Procedure 2** with semicyclic diene **3h** (50 mg, 0.32 mmol, 1.0 mol. equiv.) and cyclohept-2-en-1-one (**1e**) (176 mg, 178 uL, 1.60 mmol, 5.0 mol. equiv.) for 72 h. Regio/diastereo-selectivity was determined to be >90:10 by analysis of crude ^{1}H NMR spectra. Purification by flash column chromatography (SiO_2; 10% EtOAc in PS 40–60 °C) afforded tetracycle **4s** as a white solid (55 mg, 0.21 mmol, 65%).

m.p. = 97–99 °C (EtOAc);

R_f = 0.29 (10% EtOAc in PS 40–60 °C);

^{1}H NMR (400 MHz, $CDCl_3$): δ 7.17-7.04 (m, 4H), 5.51 (br s, 1H), 3.69 (d, J = 18.9 Hz, 1H), 3.49 (d, J = 18.7 Hz, 1H), 3.23 (t, J = 4.1 Hz, 1H), 2.95 (t, J = 14.2 Hz, 1H), 2.64-2.47 (m, 3H), 2.47-2.36 (m, 1H), 2.30 (dt, J = 5.0, 9.9 Hz, 1H), 2.06-1.91 (m, 2H), 1.90-1.69 (m, 5H), 1.46-1.33 (m, 1H) ppm;

^{13}C NMR (100 MHz, $CDCl_3$): δ 212.6 (C_q), 139.0 (C_q), 136.8 (C_q), 135.2 (C_q), 127.6 (CH), 127.4 (CH), 126.1 (CH), 125.6 (CH), 118.2 (CH), 52.9 (CH), 45.6 (CH_2), 40.5 (CH), 36.5 (CH), 36.2 (CH_2), 35.5 (CH_2), 33.2 (CH_2), 29.9 (CH_2), 24.4 (CH_2), 23.5 (CH_2) ppm;

IR (thin film): ν_{max} = 2913, 2888, 2857, 1683 cm^{-1};

LRMS (70 eV, EI): m/z (%): 266 (45, $[M]^{+\bullet}$), 165 (44), 142 (100), 141 (70), 124 (73), 111 (86);

HRMS (70 eV, EI): m/z calc. for $C_{19}H_{22}O$ $[M]^{+\bullet}$: 266.1671; found 266.1673.

Tetracycle 4t

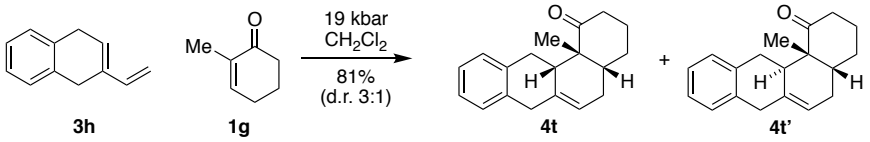

3h **1g** **4t** **4t'**

Tetracycles **4t** and **4t'** were prepared according to **General Procedure 2** with semicyclic diene **3h** (60 mg, 0.38 mmol, 1.0 mol. equiv.) and 2-methyl-2-cyclohex-en-1-one (**1g**) (211 mg, 218 uL, 1.92 mmol, 5.0 mol. equiv.) for 120 h. Regio/diastereo-selectivity was determined to be 3:1 by analysis of crude ^{1}H NMR spectra. Purification by flash column chromatography (SiO_2; 20% EtOAc in PS 40–60 °C) afforded tetracycles **4t** and **4t'** as a white solid and a 3:1 mixture of diastereomers (83.2 mg, 0.312 mmol, 81%). For characterization purposes, diastereomers **4t** and **4t'** were separated *via* normal phase preparative HPLC (Phenomenex Luna 5 μm Silica column, 150 x 10.0 mm, 2.5% EtOAc in hexanes, flow 3mL/min, λmax=264.4 nm, major diastereomer **4t** t_R=4.074 min, minor diastereomer **4t'** t_R=3.859 min). Recrystallization of the major diastereomer **4t** from 50% IPA in hexanes afforded white crystals suitable for single crystal X-ray analysis.

Major: Tetracycle 4t

m.p. = 85–87 °C (50% IPA in hexanes);

R_f = 0.54 (20% EtOAc in PS 40–60 °C);

^{1}H NMR (400 MHz, $CDCl_3$): δ 7.16-7.05 (m, 4H), 5.48 (br s, 1H), 3.62 (d, J = 17.5 Hz, 1H), 3.43 (d, J = 17.7 Hz, 1H), 3.21 (t, J = 13.4 Hz, 1H), 2.75 (dd, J = 4.7, 14.2 Hz, 1H), 2.67 (dt, J = 8.0 Hz, 15.8 Hz, 1H), 2.30-2.17 (m, 2H), 2.16-1.89 (m, 6H), 1.62-1.55 (m, 1H), 1.43 (s, 3H) ppm;

^{13}C NMR (100 MHz, $CDCl_3$): δ 215.3 (C_q), 139.0 (C_q), 137.1 (C_q), 135.2 (C_q), 127.7 (CH), 127.4 (CH), 126.2 (CH), 125.7 (CH), 117.2 (CH), 51.1 (C_q), 44.9 (CH), 42.7 (CH), 39.6 (CH_2), 37.8 (CH_2), 32.5 (CH_2), 28.4 (CH_2), 26.3 (CH_2), 23.8 (CH_3), 23.2 (CH_2) ppm;

IR (thin film): ν_{max} = 2934, 2870, 2840, 1703 cm^{-1};

LRMS (70 eV, ESI): m/z (%): 289 (100, $[M+Na]^+$), 267 $[M+H]^+$ (5), 145 (6), 102 (11);

HRMS (70 eV, EI): m/z calc. for $C_{19}H_{22}ONa$ $[M+Na]^+$: 289.1568; found 289.1563

Minor: Tetracycle 4t'

m.p. = 88–90 °C (CH_2Cl_2/pentane);

R_f = 0.54 (20% EtOAc in PS 40–60 °C);

^{1}H NMR (400 MHz, $CDCl_3$): δ 7.19-7.04 (m, 4H), 5.56 (br s, 1H), 3.52 (s, 2H), 2.80-2.70 (m,

1H), 2.59 (td, *J* = 6.7, 13.7 Hz, 1H), 2.48 (t, *J* = 13.1 Hz, 1H), 2.41-2.26 (m, 2H), 2.05-1.96 (m, 1H), 1.89 (d, *J* = 19.3 Hz, 1H), 1.83-1.77 (m, 2H), 1.68 (dd, *J* = 4.2, 12.7 Hz, 1H), 1.53-1.47 (m, 1H), 1.34-1.23 (m, 1H), 1.06 (s, 3H) ppm;

^{13}C NMR (100 MHz, $CDCl_3$): δ 215.4 (C_q), 138.7 (C_q), 136.6 (C_q), 132.3 (C_q), 127.6 (CH), 127.4 (CH), 126.5 (CH), 126.0 (CH), 118.4 (CH), 51.8 (C_q), 43.4 (CH), 38.2 (CH), 37.8 (CH_2), 36.5 (CH_2), 30.1 (CH_2), 29.2 (CH_2), 28.1 (CH_2), 26.0 (CH_2), 15.6 (CH_3) ppm;

IR (thin film): ν_{max} = 2933, 2870, 1700 cm^{-1};

LRMS (70 eV, ESI): m/z (%): 289 ($[M+Na]^+$), 267 ($[M+H]^+$);

HRMS (70 eV, ESI): m/z calc. for $C_{19}H_{23}O$ $[M+H]^+$: 267.1743; found 267.1749.

Total Synthesis: Synthesis of dienophile (±)-8

Two step sequence to (E)-4-ethoxy-3-methylbut-3-en-2-one (S20)

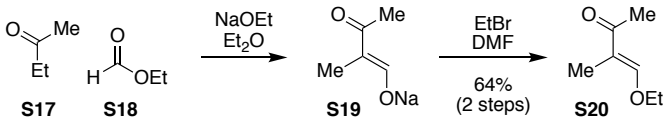

(E)-4-ethoxy-3-methylbut-3-en-2-one **S20** was prepared in adaptation of the procedures reported by Clark and co-workers *(69)*.

*Synthesis of sodium enolate **S19***

A solution of methyl ethyl ketone **S17** (78.4 mL, 63.1 g, 0.875 mol, 1.0 mol. equiv.) and ethyl formate **S18** (69.9 mL, 64.1 g, 0.875 mol, 1.0 mol. equiv.) in Et_2O (20 mL) was added slowly to a suspension of freshly prepared sodium ethoxide (59.5 g, 0.875 mol, 1.0 mol. equiv.) in Et_2O (600 mL) at 0 °C. The resulting suspension was allowed to warm to ambient room temperature and stirred for 18 h. The precipitate was then collected *via* filtration, washed with Et_2O (3 × 50 mL) and dried under reduced pressure to yield sodium enolate **S19** as a white solid (103.8 g), which was used directly without further purification.

Williamson ether synthesis

Sodium enolate **S19** (103.8 g, 0.850 mol, 1.0 mol. equiv.) was dissolved in DMF (590 mL) at ambient room temperature and treated dropwise with bromoethane (114 mL, 166 g, 1.53 mol, 1.8 mol. equiv.). The resulting solution was heated to 50 °C and stirred for 18 h, before being allowed to cool to ambient room temperature, whereupon the solution was partitioned between Et_2O (300 mL) and H_2O (300 mL). The organic layer was separated and the aqueous layer was extracted with Et_2O (2 × 250 mL). The organic layers were combined, washed with 5% aq. LiCl solution (3 × 200 mL), dried over $MgSO_4$ and concentrated under reduced pressure. Purification by vacuum distillation (70-72 °C, 7.8 mbar) afforded enone **S20** *(70)* as a pale yellow oil (70.0 g, 0.546 mol, 64 % over two steps).

R_f = 0.47 (50% EtOAc in PS 40–60 °C);

^{1}H NMR (400 MHz, $CDCl_3$): δ 7.39 (s, 1H), 4.08 (q, J = 7.4, 7.1 Hz, 2H), 2.21 (s, 3H), 1.72 (s, 3H), 1.36 (t, J = 7.08 Hz, 3H) ppm;

^{13}C NMR (100 MHz, $CDCl_3$): δ 197.5 (C_q), 159.2 (CH), 117.5 (C_q), 70.1 (CH_2), 25.2 (CH_3), 15.4 (CH_3), 8.3 (CH_3) ppm;

IR (thin film): ν_{max} = 2982, 2930, 2900, 1630 cm^{-1};

LRMS (70 eV, EI): m/z (%): 128 (23, $[M]^{+\bullet}$), 113 (21), 85 (100);

HRMS (70 eV, EI): m/z calc. for $C_7H_{12}O_2$ $[M]^{+\bullet}$: 128.0837; found 128.0832.

S41

Diene S21

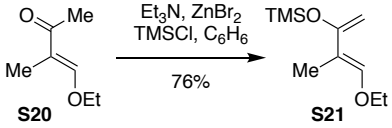

Diene **S21** was prepared in adaptation of the procedures reported by Clark and co-workers *(69)* and Danishefsky co-workers *(71)(72)*. A solution of anhydrous zinc bromide (2.70 g, 12 mmol, 3.0 mol %) in THF was concentrated under reduced pressure. The resulting residue was treated with dry Et_3N (128 mL, 0.92 mol, 2.3 mol. equiv.) and the ensuing solution stirred for 1 h. To this solution was then added sequentially ethoxy enone **S20** (50.9 g, 0.40 mol, 1.0 mol. equiv.) in dry C_6H_6 (142 mL) and TMSCl (121 mL, 0.81 mol, 2.0 mol. equiv.). The reaction was then heated to 40 °C for 14 h, before being allowed to cool to ambient room temperature, whereupon Et_2O (500 mL) was added and the slurry filtered. The filtrate was washed with H_2O (3 × 200 mL), brine (200 mL), dried over $MgSO_4$ and concentrated under reduced pressure. Purification by vacuum distillation (70 °C, 7.7 mbar) afforded diene **S21** as a clear colorless oil (60.7 g, 0.30mol, 76%).

R_f = 0.39 (50% EtOAc in PS 40–60 °C);

^{1}H NMR (400 MHz, C_6D_6): δ 6.83 (s, 1H), 4.40 (s, 1H), 4.31 (s, 1H), 3.46 (q, J = 7.1 Hz, 2 H), 1.94 (s, 3H), 0.95 (t, J = 7.06 Hz, 3H), 0.23 (s, 3H) ppm;

^{13}C NMR (100 MHz, C_6D_6): δ 157.0 (C_q), 146.5 (CH), 111.5 (C_q), 89.1 (CH_2), 68.3 (CH_2), 15.4 (CH_3), 10.7 (CH_3), 0.2 (CH_3) ppm;

IR (thin film): ν_{max} = 2979, 2961, 2880, 1655 cm^{-1};

LRMS (70 eV, EI): m/z (%):200 (39, $[M]^{+\bullet}$), 185 (77), 155 (78), 73 (100);

HRMS (70 eV, EI): m/z calc. for $C_{10}H_{20}O_2Si$ $[M]^{+\bullet}$: 200.1233; found 200.1238.

Dienophile (±)-8

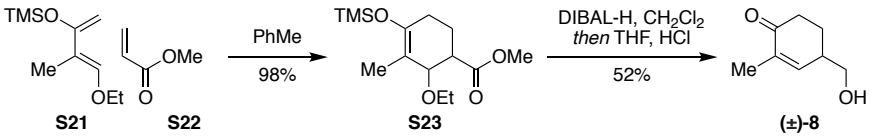

S21 **S22** **S23** **(±)-8**

Diels–Alder

Diene **S21** (45.4 g, 0.227 mol, 1.0 mol. equiv.) and methyl acrylate (**S22**) (41.5 mL, 0.454 mol, 2.0 mol. equiv.) were combined in PhMe (72 mL). The resulting stirred solution was heated to reflux for 14 h, before being allowed to cool to ambient room temperature. Concentration under reduced pressure afforded ester **S23** as a yellow oil (64.2 g, 0.22 mol, 98%) as a 2:3 ratio of diastereomers as determined by analysis of crude ^{1}H NMR spectra. Ester **S23** was used directly without further purification.

Reduction-deprotection-elimination

DIBAL-H (1.0 M solution in PhMe, 109.1 mL, 109.1 mmol, 2.5 mol. equiv.) was added dropwise to a stirred solution of ester **S23** (12.5 g, 43.5 mmol, 1.0 mol. equiv.) in CH_2Cl_2 (150 mL) at –78 °C (dry-ice acetone bath). The reaction was then warmed to ambient room temperature and stirred for 3 h. The reaction was cooled in a 0 °C ice bath and a solution of THF (200 mL) and 2M aq. HCl solution (50 mL) was added slowly. The reaction was allowed to warm to room temperature and stirred for 18 h. The reaction was then diluted with CH_2Cl_2 (300 mL) and poured onto a mixture of sat. aq. $NaHCO_3$ solution (500 mL) and sat. aq. potassium sodium tartrate solution (500 mL) and stirred for 6 h. The organic layer was separated and the aqueous layer extracted with CH_2Cl_2 (x3). The organic layers were combined, dried over $MgSO_4$ and concentrated under reduced pressure. Purification by flash column chromatography (SiO_2; 50% EtOAc in hexanes) afforded cyclohexenone (±)-**8** as a yellow oil (3.16 g, 22.5 mmol, 52%).

R_f = 0.21 (60 % EtOAc in hexanes);

^{1}H NMR (400 MHz, $CDCl_3$): δ 6.70-6.69 (m, 1H), 3.72-3.63 (m, 2H), 2.65-2.53 (m, 2H), 2.43-2.34 (m, 1H), 2.20 (br s, 1H), 2.14-2.07 (m, 1H), 1.83-1.73 (m, 4H) ppm;

^{13}C NMR (100 MHz, $CDCl_3$): δ 199.9 (C_q), 146.1 (CH), 136.7 (C_q), 65.9 (CH_2), 39.4 (CH), 37.0 (CH_2), 26.0 (CH_2), 16.3 (CH_3) ppm;

IR (thin film): ν_{max} = 3414, 2924, 1658 cm^{-1};

LRMS (70 eV, EI): m/z (%): 140.0 (46, $[M]^{+\bullet}$), 110.1 (92), 95.0 (100), 81.0 (92);

HRMS (70 eV, EI): m/z calc. for $C_8H_{12}O_2$ $[M]^{+\bullet}$: 140.0837; found 140.0835;

S43

(+) and (−) enantiomers of alcohol **8** were separable by preparative chiral HPLC (Kromasil Chiral AmyCoat Part# KRWP5-AMYCOAT-21.2X250 (21.2 x 250 mm), 100% acetonitrile, 10 mL/min, (+) enantiomer t_R = 8.14 min, (−) enantiomer t_R = 8.62 min).

Organocatalyst 12

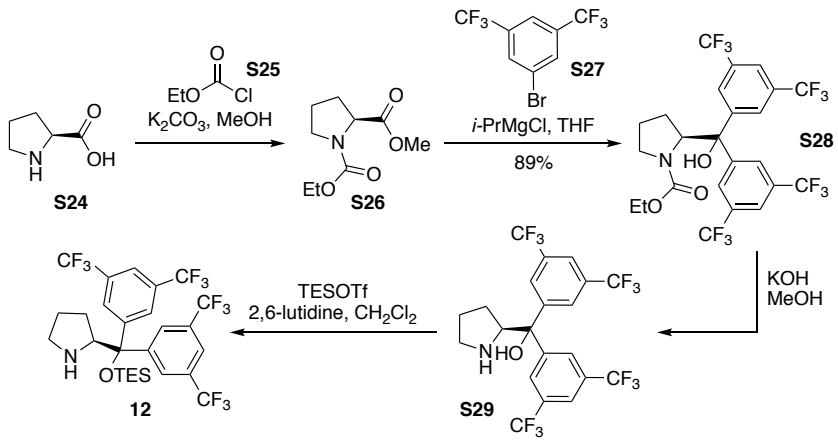

Pyrrolidine S26

Pyrrolidine **S26** was prepared from proline (**S24**) according to the procedure reported by Zhou and co-workers *(73)*.

Ester S28

Pyrrolidine **S26** was converted to ester **S28** in adaptation of procedures reported by Zhou and co-workers *(73)* and Soos and co-workers *(74)*.

A 3-neck round bottom flask fitted with a water condenser and an internal thermometer was charged with 3,5-bis(trifluoromethyl)-5-bromobenzene **S27** (1.30 mL, 2.21 g, 7.54 mmol, 3.0 mol. equiv.) and THF (6.25 mL) and the resulting solution cooled in a 0 °C ice-bath. *i*-PrMgCl (1.71M solution in THF, 4.60 mL, 7.88 mmol, 3.15 mol. equiv.) was added dropwise and the reaction stirred at 0 °C for 1 h. Pyrrolidine **S26** (500 mg, 2.48 mmol, 1.0 mol. equiv.) in THF (1.75 mL) was added dropwise and the reaction stirred for 1 h at 0 °C, before being quenched by the slow addition of sat. aq. NH_4Cl solution (9.0 mL). The organic layer was separated, and the aqueous layer extracted with CH_3Cl (3 x 9.0 mL). The organic layers were combined, dried over Na_2SO_4 and concentrated under reduced pressure to afford ester **S28** as a cream solid (1.33 g, 2.23 mmol, 89%) which was used directly without further purification.

Amine S29 and organocatalyst 12

Ester **S28** was subsequently converted to amine **S29** according to the procedure outlined by Soos and co-workers *(74)* and amine **S29** converted to organocatalyst **12** according to the procedure outlined by Zhou and co-workers *(73)*.

Total synthesis of (+)-xestoquinone

Diene 11

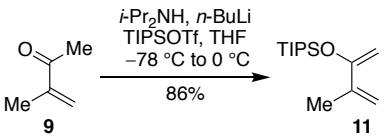

9 **11**

Diene **11** was prepared in adaptation of the procedure described by Corey and Mukherjee *(75)*. To a solution of diisopropylamine[1] (5.8 g, 8.0 mL, 57 mmol, 1.2 mol. equiv.) in THF (60 mL) at –78 °C was added dropwise *n*-BuLi (1.44 M in hexane, 36 mL, 52 mmol, 1.1 mol. equiv.) over 5 min. The resulting solution was stirred at –78 °C for 25 min. Ketone **9** (4.0 g, 4.7 mL, 48 mmol, 1.0 mol. equiv.) was then added dropwise and the reaction stirred at –78 °C for 45 min, before the dropwise addition of TIPSOTf (16.0 g, 14 mL, 52 mmol, 1.1 mol. equiv.) over 10 min. The resulting solution was stirred at –78 °C for 30 min, then was warmed to 0 °C and stirred for 15 min. The reaction was then poured onto sat. aq. $NaHCO_3$ solution (120 mL). The organic layer was separated and the aqueous layer extracted with PS 40–60 °C. The organic layers were combined, washed with brine, dried over Na_2SO_4 and concentrated under reduced pressure. Purification by flash column chromatography (SiO_2; 1% triethylamine in PS 40–60 °C) afforded diene **11** *(76)* as a colorless oil (9.88 g, 41.1 mmol, 86%). (Note: Purification by distillation (0.51 mbar, 80-82 °C) afforded diene **11** as a colorless oil (10.22 g, 42.5 mmol, 89 %), which contained minor impurities that were found to inhibit subsequent organocatalyzed Diels–Alder reaction with acrolein).

R_f = 0.68 (PS 40–60 °C);

^{1}H NMR (400 MHz, toluene-d8): δ 5.69 (d, J = 2.5 Hz, 1H), 4.94 (d, J = 1.4 Hz, 1H), 4.41 (s, 1H), 4.33 (s, 1H), 1.78 (s, 3H), 1.15-1.10 (m, 21 H) ppm;

^{13}C NMR (100 MHz, toluene-d8): δ 157.4 (C_q), 140.1 (C_q), 113.9 (CH_2), 91.6 (CH_2), 20.0 (CH_3), 18.4 (CH_3), 13.4 (CH) ppm;

IR (thin film): ν_{max} = 2945, 2894, 2868, 1590 cm^{-1};

LRMS (70 eV, EI): m/z (%): 240.1 (15, $[M]^{+\bullet}$), 197.1 (100), 155.0 (100)

HRMS (70 eV, EI): m/z calc. for $C_{14}H_{28}OSi$ $[M]^{+\bullet}$: 240.1909; found 240.1914.

[1] Distilled (b.p. 83.5 °C) over NaOH directly prior to use.

Alcohol (+)-13

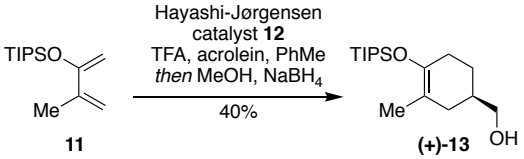

To a solution of diene **11** (1.00 g, 4.16 mmol, 1.0 mol. equiv.) in PhMe (1.44 mL) at 0 °C was added Hayashi-Jørgensen catalyst **12** (66.5 mg, 0.104 mmol, 2.5 mol %) and TFA[2] (200 uL, 1.04M solution in PhMe, 0.208 mmol, 5.0 mol%). Acrolein[3] (1.40 mL, 20.8 mmol, 5.0 mol. equiv.) was then added dropwise *via* syringe pump (46.3 uL min^{-1}, 30 min) and the reaction allowed to stir for a further 30 min at 0 °C. The reaction was then treated sequentially with MeOH (0.40 mL), and $NaBH_4$ (472 mg, 12.5 mmol, 3.0 mol. equiv.) in 5 portions (vigorous effervescence). When TLC indicated complete reaction (10 min), the reaction mixture was quenched by the slow addition of sat. aq. NH_4Cl solution (1.5 mL). The organic layer was separated and the aqueous layer extracted with EtOAc (3x 5.0 mL). The combined organic layers were washed with brine (5.0 mL), dried over Na_2SO_4 and concentrated under reduced pressure. Purification by flash column chromatography (SiO_2; 1% Et_3N and 20% EtOAc in PS 40–60 °C) afforded alcohol (+)-**13** as a yellow oil (492 mg, 1.65 mmol, 40%).

$[\alpha]_D$ = +27.39 ° (c = 1.11, MeOH);

R_f **=** 0.48 (30% EtOAc in PS 40–60 °C);

^{1}H NMR (400 MHz, C_6D_6): δ 3.34-3.26 (m, 2H), 2.19-2.03 (m, 2H), 1.94-1.89 (m, 1H), 1.79-1.56 (m, 6H), 1.32-1.22 (m, 1H), 1.14-1.12 (m, 21 H) ppm;

^{13}C NMR (100 MHz, C_6D_6): δ 143.6 (C_q), 109.3 (C_q), 67.3 (CH_2), 37.1 (CH), 33.6 (CH_2), 30.2 (CH_2), 26.7 (CH_2), 18.4 (CH_3), 16.9 (CH_3), 13.6 (CH) ppm;

IR (thin film): ν_{max} = 2866, 1687 cm^{-1};

LRMS (70 eV, EI): m/z (%): 298.1 (25, $[M]^{+\bullet}$), 255.1 (65), 131.0 (50), 103.0 (100);

HRMS (70 eV, EI): m/z calc. for $C_{17}H_{34}O_2Si$ $[M]^{+\bullet}$: 298.2328; found 298.2321.

[2] Distilled (b.p. 72.4 °C) directly prior to use.
[3] Distilled (b.p. 53 °C) directly prior to use.

Organocatalysed Diels-Alder Reaction Optimization Data

The following tables summarize attempts to optimize the organocatalyzed Diels-Alder reaction for preparation of cyclohexenone (+)-**8**.

Table S2.
Screening of prolinol-derived catalysts for reaction of diene **11** with acrolein (**10**)[a,b]

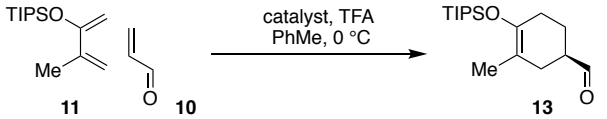

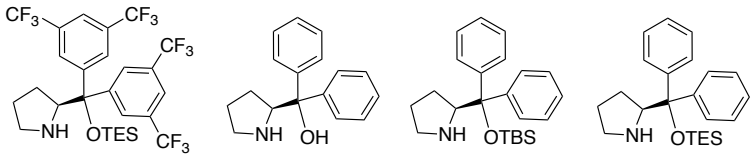

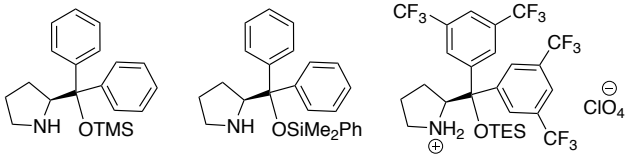

entry	catalyst	time (h)	yield (%)
1	**12**	19	35
2	**S30**	19	0
3	**S31**	24	30
4	**S32**	19	10
5	**S33**	24	3
6	**S34**	19	15
7[c]	**S35**	1	14

[a] Conditions: 1.0 mol. equiv. diene **11**, 3.0 mol. equiv. acrolein (**10**), 10 mol. % catalyst, 5 mol. % TFA; reactions performed on 50 mg scale; concentration 2.4 mol L^{-1} with respect to diene; [b] Yields determined by analysis of ^1H NMR spectra with durene as an internal standard. [c]Alternative conditions *(77)*: 1.0 mol. equiv. diene **11**, 4.0 mol. equiv. acrolein (**10**), 10 mol. % catalyst, H_2O.

Table S3.

Optimization of temperature, catalyst and co-catalyst (TFA) loading, and dienophile equivalents for organocatalyzed Diels–Alder reaction of diene **11**[a,b]

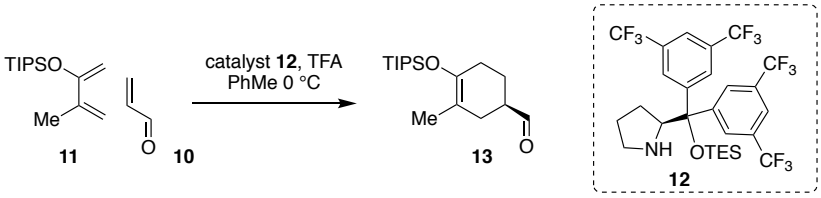

entry	diene (mol. equiv.)	dienophile (mol. equiv.)	catalyst (mol. %)	TFA (mol. %)	temperature (°C)	yield (%)
1	1.0	1.5	2.5	5	0	31
2	1.0	1.5	2.5	5	r.t.	32
3	1.0	1.5	2.5	5	–10	22
4	1.0	3.0	2.5	5	0	38
5	1.0	3.0	2.5	2.5	0	10
6	1.0	5.0	2.5	5	0	41
7	1.0	10.0	2.5	5	0	31
8	1.0	5.0	10	20	0	28
9	1.0	1.2[c]	2.5	5	0	73

[a] Reactions performed with acrolein as the dienophile unless otherwise specified; concentration 2.4 mol L^{-1} with respect to diene in PhMe; [b] Yields determined by analysis of ^{1}H NMR spectra with durene as an internal standard.[c] Dienophile ethyl 4-oxo-2-butenoate.

Reactions summarized in **Table S3** were performed with the slow addition of acrolein (**10**) last to the reaction mixture. Reactions with alternative orders of addition were lower yielding; pre-stirring of acrolein, TFA and catalyst before diene addition hindered reaction progress. In reactions using acrolein as the dienophile prolonged reaction times (> 1h) did not improve yield, with no further significant reaction progress observed through monitoring by ^{1}H NMR spectroscopy. Notably, use of the alternative dienophile, ethyl 4-oxo-2-butenoate, in place of acrolein, resulted in significantly higher yields, which are comparable to those reported in the literature previously *(78)*.

Cyclohexenone (+)-8

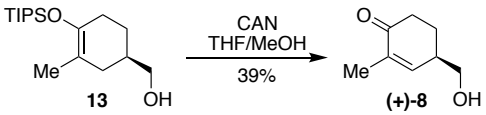

13 **(+)-8**

To a solution of silylenol ether (+)-**13** (3.47 g, 11.6 mmol, 1.0 mol. equiv.) in THF/MeOH (1.6:1, 111 mL) was added CAN (19.11 g, 34.9 mmol, 3.0 mol. equiv.) in 3 portions and the resulting solution allowed to stir for 20 min. The reaction mixture was then concentrated under reduced pressure, and diluted with H_2O (20 mL) and EtOAc (30 mL). The organic layer was separated and the aqueous layer extracted with EtOAc (3 x 30 mL). The combined organic layers were washed with sat. aq. $NaHCO_3$ solution (30 mL), brine (30 mL), dried over Na_2SO_4 and concentrated under reduced pressure. Purification by flash column chromatography (SiO_2; 50% EtOAc in PS 40–60 °C) afforded enantioenriched cyclohexenone (+)-**8** as a yellow oil (0.639 g, 4.56 mmol, 39%), e.r. 93:7, as determined by analytical chiral HPLC (AS-H (0.46 cm x 25cm), 10% IPA in hexane, 1 mL/min, major (+) enantiomer t_R = 10.6 min, minor (−) enantiomer t_R = 12.6 min). Spectroscopic data were consistent with those reported above. (Note: When conducting the Diels–Alder-reduction-oxidation sequence to generate enantioenriched cyclohexenone (+)-**8** on greater than 1.5 g scale, some deterioration in e.r. was observed.)

$[\alpha]_D$ = +89.64 ° (c = 0.975, $CHCl_3$).

Mono-adduct 16

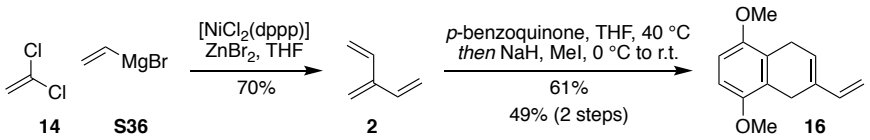

14 **S36** **2** **16**

Synthesis of [3]dendralene (**2**)

A 3-neck 1 L round-bottomed flask was charged with anhydrous $ZnBr_2$ solution (1.14 M in THF, 174 mL, 199 mmol, 2.75 mol. equiv.) and cooled to 0 °C. $Ni(dppp)Cl_2$ (0.391 g, 0.721 mmol, 1.0 mol%) was added, followed by the dropwise addition of vinylmagnesium bromide (**S36**) solution (0.86 M in THF, 230 mL, 199 mmol, 2.75 mol. equiv.). The resulting golden-brown slurry was stirred for 30 min at 0 °C and 1,1-dichloroethylene (**14**) (7.00 g, 72.2 mmol, 1.00 mol. equiv.) was then added dropwise over 15 min (ensure internal temperature stays below 10 °C). The reaction mixture was warmed to ambient room temperature and stirred for 2 h. The reaction was quenched at 0 °C with 1M aq. HCl solution (40 mL) and stirred for 10 min. Distillation of the quenched reaction mixture using a rotary evaporator (dry ice-acetone condenser, 50 mbar) afforded pure [3]dendralene (**2**) as a THF solution (0.233 M, 50.7 mmol, 70%).

One-pot Diels–Alder-methylation

To a 3-neck 500 mL round-bottomed flask was added [3]dendralene (**2**) (0.233 M in THF, 34.4 mmol, 1.00 mol. equiv.) and freshly purified *p*-benzoquinone (3.72 g, 34.4 mmol, 1.00 mol. equiv.). The resulting solution was stirred at 40 °C for 16 h and an NMR aliquot was taken to ensure the Diels–Alder reaction had reached completion. The reaction mixture was cooled to 0 °C and NaH (60% w/w dispersion in mineral oil, 6.88 g, 172 mmol, 5.00 mol. equiv.) was added in 5 portions over 10 min. MeI (14.7 g, 103 mmol, 3.00 mol. equiv.) was then added and the reaction mixture was warmed to ambient room temperature and stirred for 2 h. After this time, the reaction was cooled to 0 °C, quenched with sat. aq. NH_4Cl solution (50 mL), and diluted with Et_2O (100 mL). The aqueous phase was separated and extracted with Et_2O (100 mL). The organic layers were combined, washed with brine (100 mL), and dried over $MgSO_4$. Purification by flash column chromatography (SiO_2; 4:1 to 2:1 to 1:1 to 0:1 PS 40–60 °C in CH_2Cl_2) furnished **16** as a light yellow solid (4.54 g, 21.0 mmol, 61%). Recrystallization from Et_2O/hexanes gave yellow crystals, which were suitable for single crystal X-ray analysis.

Diene 16:

m.p. = 57–59°C (Et_2O/hexanes);

$\boldsymbol{R_f}$ = 0.66 (10% EtOAc in hexanes);

^{1}H NMR (400 MHz, $CDCl_3$): δ 6.67 (s, 2H), 6.51 (dd, J = 17.1, 10.4 Hz, 1H), 5.94 (s, 1H), 5.30 (d, 17.4 Hz, 1H), 5.05 (d, J = 10.6 Hz, 1H), 3.82 (s, 3H), 3.79 (s, 3H), 3.43-3.37 (m, 4H) ppm.

^{13}C NMR (100 MHz, $CDCl_3$): δ 151.2 (C_q), 151.0 (C_q), 139.3 (CH), 132.7 (C_q), 125.9 (CH), 124.3 (C_q), 123.9 (C_q), 111.2 (CH_2), 107.0 (CH), 106.9 (CH), 55.72 (CH_3), 55.69 (CH_3), 25.7 (CH_2), 23.4 (CH_2) ppm;

IR (KBr): ν_{max} = 3085, 2994, 2935, 2896, 2831 cm^{-1};

LRMS (70 eV, EI): m/z (%): 216.1 (100, $[M]^{+\bullet}$), 201.1 (28), 185.1 (41), 175.1 (25);

HRMS (70 eV, EI): m/z calc. for $C_{14}H_{16}O_2$ $[M]^{+\bullet}$: 216.1150; found 216.1148.

Tetracycles 17a and 17b

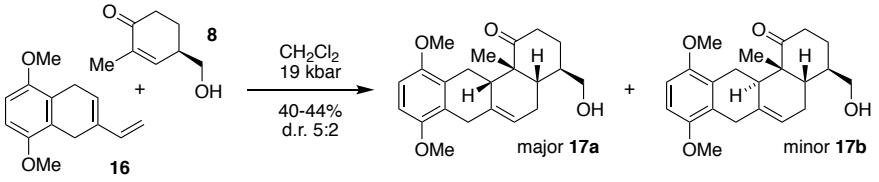

Diene **16** (2.70 g, 12.5 mmol, 1.00 mol. equiv.) and substituted cyclohexenone (±)-**8** (5.25 g, 37.5 mmol, 3.00 mol. equiv.) were added to a Teflon high-pressure reaction vessel and dissolved in CH_2Cl_2 (9.0 ml). The reaction vessel was sealed and compressed at 19 kbar for 5 days. The solvent was removed under reduced pressure to give crude target material as a mixture of isomers (5:2:1, as determined by analysis of crude ^{1}H NMR spectra). Purification by flash column chromatography (SiO_2; 50% EtOAc in PS 40–60 °C) afforded tetracycles **(±)-17a** and **(±)-17b** as a white solid (1.98 g, 5.56 mmol, 5:2 d.r., 44%). For synthetic purposes, this inconsequential mixture of diastereomers was subjected to the next step without further purification. For characterization purposes, diastereomers **(±)-17a** and **(±)-17b** were separated *via* normal-phase preparative HPLC (Phenomenex Luna 5 μm Silica column, 150 x 21.2 mm, 9:1 CH_2Cl_2/EtOAc, t_R(minor) = 23.50 min, t_R(major) = 29.05 min). Recrystallization from MeOH afforded colorless crystals suitable for single crystal X-ray analysis.

According to the same procedure, enantio-enriched dienophile **(+)-8** (1.50 g, 10.7 mmol, 3.0 mol. equiv.) and diene **16** (771 mg, 3.57 mmol, 1.0 mol. equiv.) were converted to enantioenriched tetracycles **17a** and **17b** (512 mg, 1.44 mmol, 40%). Spectroscopic data were consistent with those of the racemic compounds and this inconsequential mixture of diastereomers was subjected to the next step without further purification.

Tetracycle 17a (major)

m.p. = 155–157 °C (EtOAc/hexanes);

R_f = 0.43 (50% EtOAc in hexanes);

^{1}H NMR (400 MHz, $CDCl_3$): δ 6.61 (d, J = 8.8 Hz, 1H), 6.57 (d, J = 8.8 Hz, 1H), 5.56 (br s, 1H), 3.77 (s, 3H), 3.71 (s, 3H), 3.74-3.69 (m, 1H), 3.65-3.59 (m, 1H), 3.46-3.29 (m, 2H), 2.95 (dd, J = 15.6, 5.1 Hz, 1H), 2.69 (dt, J = 16.7, 6.7 Hz, 1H), 2.58–2.47 (m, 2H), 2.30 (br s, 2H), 2.22-2.06 (m, 2H), 2.06-1.92 (m, 1H), 1.91-1.76 (m, 2H), 1.27 (s, 3H) ppm;

^{13}C NMR (100 MHz, $CDCl_3$): δ 216.5 (C_q), 151.0 (C_q), 150.9 (C_q), 134.1 (C_q), 126.5 (C_q), 126.2 (C_q), 116.0 (CH), 107.2 (CH), 106.8 (CH), 66.2 (CH_2), 55.71 (CH_3), 55.66 (CH_3), 49.1 (C_q), 41.4 (CH), 39.5 (CH_2), 39.2 (CH), 36.3 (CH), 33.8 (CH_2), 30.2 (CH_2), 25.9 (CH_2), 25.4 (CH_3), 24.0 (CH_2) ppm;

IR (KBr): ν_{max} = 3456, 2914, 2892, 2834, 1672, 1601 cm^{-1};

LRMS (70 eV, EI): m/z (%): 356.2 (25, $[M]^{+\bullet}$), 216.1 (100), 215.1 (40), 141.1 (46);

HRMS (70 eV, EI): m/z calc. for $C_{22}H_{28}O_4$ $[M]^{+\bullet}$: 356.1988; found 356.1987.

Tetracycle 17b (minor)

m.p. = 177–179 °C (EtOAc/hexanes);

R_f = 0.43 (50% EtOAc in hexanes);

^{1}H NMR (400 MHz, $CDCl_3$): δ 6.64 (d, J = 8.9 Hz, 1H), 6.61 (d, J = 8.9 Hz, 1H), 5.61 (br s, 1H), 3.78 (s, 3H), 3.77-3.74 (m, 1H), 3.73 (s, 3H), 3.72-3.58 (m, 2H), 3.33 (d, J = 20.5 Hz, 1H), 2.83-2.64 (m, 3H), 2.38 (ddd, J = 14.7, 5.0, 2.4 Hz, 1H), 2.27-2.19 (m, 2H), 2.19-2.08 (m, 2H), 2.04-1.93 (m, 1H), 1.74-1.58 (m, 2H), 1.13 (s, 3H) ppm;

^{13}C NMR (100 MHz, $CDCl_3$): δ 214.5 (C_q), 150.7 (C_q x2, coincident), 132.9 (C_q), 127.5 (C_q), 125.7 (C_q), 118.0 (CH), 107.5 (CH), 107.4 (CH), 65.5 (CH_2), 55.9 (CH_3 x2, coincident), 50.7 (C_q), 44.9 (CH), 37.8 (CH), 37.3 (CH_2) 36.3 (CH), 29.9 (CH_2), 29.8 (CH_2), 24.0 (CH_2), 22.5 (CH_2), 16.3 (CH_3) ppm;

IR (KBr): ν_{max} = 3453, 2920, 2872, 1686, 1603 cm^{-1};

LRMS (70 eV, ESI): m/z (%): 379.5 (100, $[M + Na]^+$), 357.5 (23), 339.5 (10);

HRMS (70 eV, ESI): m/z calc. for $C_{22}H_{28}O_4$ $[M + Na]^+$: 379.1885; found 379.1885.

Two-step sequence to alcohol 19

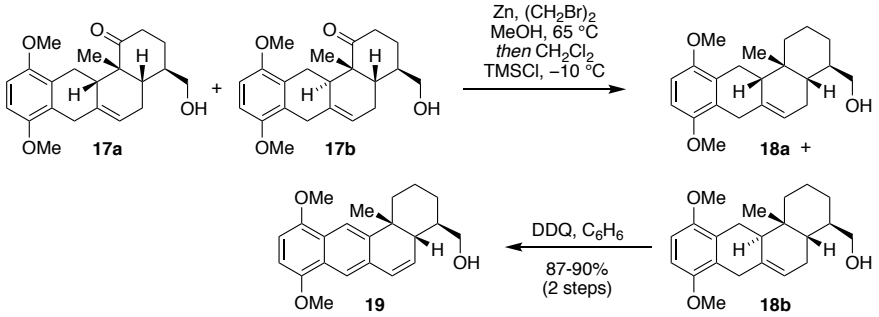

Clemmensen reduction

To a 3-neck 1L round-bottomed flask, equipped with a reflux condenser and an equalizing addition funnel was added zinc powder (15.4 g, 236 mmol, 120 mol. equiv.), one crushed glass pipette tip, and dry MeOH (80 mL). 1,2-Dibromoethane (0.840 mL, 9.70 mmol, 4.90 mol. equiv.) was added and the reaction mixture was heated to 65 ^{o}C (effervescence observed over course of heating). After 20 min, the reaction mixture was cooled to –10 ^{o}C (acetone-ice bath). A solution of tetracycles **(±)-17a** and **(±)-17b** (5:2 d.r., 0.700 g, 1.97 mmol, 1.00 mol. equiv.) in CH_2Cl_2 (35 mL) was added, after which TMSCl (29.8 mL, 236 mmol, 120 mol. equiv.) was added dropwise over 25 min. The reaction mixture was stirred for a further 90 min at –10 ^{o}C at which time an NMR aliquot was taken to ensure the reaction had reached completion. The reaction was quenched with H_2O (20 mL) and stirred for a further 30 min (or until TLC analysis confirmed no O-TMS silylated product remained). The reaction mixture was diluted with sat. aq. $NaHCO_3$ solution (200 mL) and EtOAc (200 mL). The aqueous phase was separated and extracted with EtOAc (100 mL). The organic layers were combined, washed with H_2O (2 x 100 mL), brine (100 mL), and dried over $MgSO_4$. Concentration under reduced pressure furnished a mixture of alcohols **(±)-18a** and **(±)-18b** as a white foam that was subjected crude to the next step without further purification (0.714 g crude mass). (Note: Crushed glass is added to deter aggregation of the zinc powder. It is important to quench the reaction with water prior to $NaHCO_3$ otherwise substantial amounts of the surprisingly robust silylated (O-TMS) product are formed).

DDQ oxidation

To a 100 mL round-bottomed flask containing alcohols **(±)-18a** and **(±)-18b** (0.714 g crude mass) was added dry C_6H_6 (25 mL). DDQ (0.980 g, 4.32 mmol, 2.2 mol. equiv.) was added and a reflux condenser was fitted. The reaction mixture was heated at 80 ^{o}C for 19 h and then

cooled to ambient room temperature. The reaction was diluted with EtOAc (30 ml) and stirred for 20 min. Filtration through a plug of neutral alumina (EtOAc, thorough rinsing) and concentration under reduced pressure furnished the title compound **(±)-19** as a golden foamy solid (0.600 g, 1.77 mmol, 90%). No additional purification was required. (Note: Long reaction times are required to obtain good yields. Stir vigorously with EtOAc prior to filtration for high recovery and wash neutral alumina thoroughly).

According to the same procedure, enantio-enriched tetracycles **17a** and **17b** (500 mg, 1.40 mmol, 1.0 mol. equiv.) were converted to tetracycle **(−)-19** (412 mg, 1.23 mmol, 87%), e.r. 97:3, determined by analytical chiral SFC (Waters Trefoil Cel-1, 2.5 um (3.0 x 150 mm), CO_2/MeOH 98:2, 1 mL/min, 40 °C, 270 nm, major (−) enantiomer t_R = 6.64 min, minor (+) enantiomer t_R = 6.85 min). Spectroscopic data were consistent with those of the racemic compound.

$[\alpha]_D$ = −44.69 ° (c = 0.989, $CHCl_3$);

m.p. = 144–146 °C (MeOH);

R_f **=** 0.37 (70:30 *n*-hexane/EtOAc);

^{1}H NMR (400 MHz, MeOD): δ 8.01 (s, 1H), 7.78 (s, 1H), 6.68 (d, *J* = 8.4 Hz, 1H), 6.65 (d, *J* = 8.4 Hz, 1H), 6.58 (d, *J* = 9.6 Hz, 1H), 6.19 (dd, *J* = 9.7, 6.3 Hz, 1H), 3.92 (s, 3H), 3.90 (s, 3H), 3.55-3.44 (m, 2H), 2.57 (d, *J* = 13.5 Hz, 1H), 1.94 (dd, *J* = 10.7, 6,4 Hz ,1H), 1.74-1.37 (m, 5H), 1.19-1.08 (m, 1H), 1.12 (s, 3H) ppm;

^{13}C NMR (100 MHz, MeOD): δ 150.8 (C_q), 150.6 (C_q), 141.2 (C_q), 133.2 (CH), 133.0(C_q), 128.0 (CH), 127.2 (C_q), 126.2(C_q), 120.7 (CH), 118.1 (CH), 104.3 (CH), 104.1 (CH), 66.0 (CH_2), 56.1 (CH_3), 56.0 (CH_3), 46.4 (CH), 44.5 (CH), 39.8 (C_q), 36.3 (CH_2), 31.8 (CH_3), 31.0 (CH_2), 23.0 (CH_2) ppm;

IR (thin film): ν_{max} = 3444, 2960, 2923, 2854, 1737, 1596 cm^{-1};

LRMS (70 eV, ESI): m/z (%): 361.2 (100, $[M + Na]^+$), 339.1 (82), 321.2 (30), 227.0 (32);

HRMS (70 eV, ESI): m/z calc. for $C_{22}H_{26}O_3$ $[M + Na]^+$: 361.1780; found 361.1781;

Lactol 20

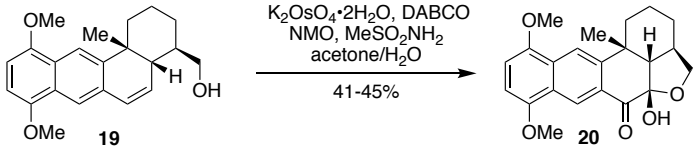

To a round-bottomed flask containing alcohol **(±)-19** (250 mg, 0.739 mmol, 1.0 mol. equiv.) was added NMO (693 mg, 5.91 mmol, 8.0 mol. equiv.), DABCO (11.9 mg, 0.106 mmol, 14.4 mol%), $MeSO_2NH_2$ (146 mg, 1.54 mmol, 2.08 mol. equiv.) and acetone/water (3:1, 14.2 mL). $K_2OsO_4.2H_2O$ (54.5 mg, 0.148 mmol, 20 mol%) was then added and the round-bottomed flask was stoppered, placed in an oil bath pre-set at 25 °C, and the reaction stirred for 15 h. The reaction was quenched with Na_2SO_3 (188 mg) and diluted with EtOAc (11 mL) and sat. aq. NH_4Cl solution (11 mL). The aqueous phase was separated and extracted with EtOAc (60 mL). The organic layers were combined, washed with H_2O (50 mL), brine (50 mL), dried over $MgSO_4$ and concentrated under reduced pressure. Purification by flash column chromatography (SiO_2; CH_2Cl_2 to 1% to 2% MeOH in CH_2Cl_2) furnished lactol **(±)-20** as a golden orange solid (123 mg, 0.334 mmol, 45%). Recrystallization from CH_2Cl_2/hexanes afforded orange crystals suitable for single crystal X-ray analysis.

According to the same procedure, enantio-enriched tetracycle **(−)-19** (250 mg, 0.739 mmol, 1.0 mol. equiv.) was converted to lactol **(+)-20** (111 mg, 0.301 mmol, 41%), e.r. 96:4, determined by analytical chiral SFC (Waters Trefoil Cel-1, 2.5 um (3.0 x 150 mm), CO_2/MeOH 98:2, 1 mL/min, 40 °C, 270 nm, minor (−) enantiomer t_R = 5.56 min, major (+) enantiomer t_R = 5.86 min). Spectroscopic data were consistent with those of the racemic compound.

$[\alpha]_D$ = +23.57 ° (c = 0.980, $CHCl_3$);

m.p. = 220 °C (decomposition);

***R_f* =** 0.45 (2:1 PS 40–60 °C in EtOAc)

^{1}H NMR ($CDCl_3$, 400 MHz): δ 8.97 (s, 1H), 8.10 (s, 1H), 6.83 (d, *J* = 8.4 Hz, 1H), 6.70 (d, *J* = 8.4 Hz, 1H), 3.98 (s, 3H), 3.96 (s, 3H), 3.79 (br. t, *J* = 6.8 Hz, 1H), 3.70 (dd, *J* = 10.8, 7.5 Hz, 1H), 2.71 (d, *J* = 12.0 Hz, 1H) 2.13 (d, *J* = 12.1 Hz, 1H), 1.87-1.68 (m, 3H), 1.63-1.46 (m, 2H), 1.33 (s, 3H), 1.31-1.26 (m, 1H) ppm;

^{13}C NMR ($CDCl_3$, 150 MHz): δ 195.6 (C_q), 151.1 (C_q), 149.0 (C_q), 144.0 (C_q), 129.1 (C_q), 128.0 (C_q), 126.6 (CH), 124.8 (C_q), 118.2 (CH), 107.0 (CH), 103.7 (CH), 99.9 (C_q), 71.4 (CH_2), 57.9 (CH), 56.0 (CH_3), 55.9 (CH_3), 44.4 (CH), 38.2 (C_q), 36.0 (CH_2), 33.9 (CH_3), 27.0 (CH_2), 22.5 (CH_2) ppm;

IR (thin film): ν_{max} = 3448, 2932, 1686, 1624, 1189 cm^{-1};

LRMS (70 eV, ESI): m/z (%): 391.2 (70, $[M + Na]^+$), 369.3 (50, [M+H]);

HRMS (ESI) m/z calc. for $C_{22}H_{24}O_5$ $[M + Na]^+$: 391.1521; found 391.1515.

Furan 21

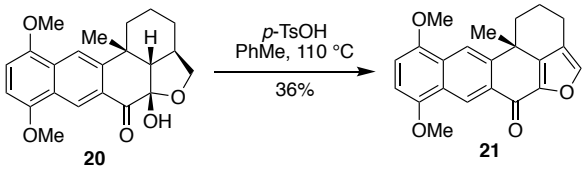

Lactol **(±)-20** (30 mg, 0.081 mmol, 1.0 mol. equiv.) was dissolved in d8-toluene (3.00 mL) in a round-bottomed flask fitted with a water condenser and drying tube (packed $CaCl_2$) under air. The resulting stirred solution was treated with *p*-toluenesulfonic acid monohydrate (15.4 mg, 0.0810 mmol, 1.0 mol. equiv.) and heated in a 110 °C oil bath for 46 h, before being allowed to cool to room temperature. The reaction was quenched by the addition of sat. aq. $NaHCO_3$ solution (3.0 mL). The aqueous layer was separated and extracted with EtOAc (3x 3.0 mL). The combined organic layers were washed with brine (3.0 mL), dried over $MgSO_4$ and concentrated under reduced pressure. Purification by flash column chromatography (SiO_2; CH_2Cl_2 to 5% MeOH in CH_2Cl_2) afforded furan **(±)-21** as an orange paste (10.2 mg, 0.0293 mmol, 36%). Spectroscopic data were consistent with those reported previously *(27)*.

According to the above procedure, enantio-enriched lactol **(+)-20** (50.0 mg, 0.136 mmol, 1.0 mol. equiv.) was converted to furan **(+)-21** (17.1 mg, 0.0491 mmol, 36%), e.r. 96:4 determined by analytical chiral SFC (Waters Trefoil AMY1, 2.5 um (3.0 x 150 mm), CO_2/MeOH 80:20, 2 mL/min, 40 °C, 305 nm, minor (−) enantiomer t_R = 4.85, major (+) enantiomer t_R = 5.73). (Note: a reaction heating time of 24 h was found to be sufficient). Spectroscopic data were consistent with those of the racemic compound and those reported previously *(27)*.

$[\alpha]_D$ = +88.33 ° (c = 0.600, $CHCl_3$); (lit. $[\alpha]_D$ = +93.70° (c = 0.650, $CHCl_3$) *(27)*).

Xestoquinone (5)

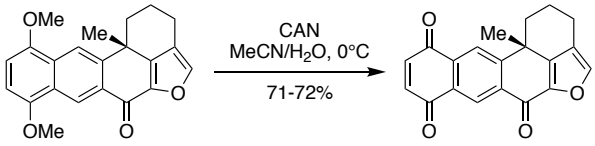

Xestoquinone (**5**) was prepared in adaptation of the procedure reported by Harada and co-workers (*27*). To a 25 mL round-bottomed flask containing furan **(±)-21** (11.2 mg, 0.0321 mmol, 1.0 mol. equiv.) was added CH_3CN (2 mL) and H_2O (1 mL). The resulting solution was cooled to 0 ^oC and CAN (53.0 mg, 0.0967 mmol, 3.0 mol. equiv.) was added. The reaction mixture was stirred for 10 min then quenched with sat. aq. $NaHCO_3$ solution (2 mL) and diluted with CH_2Cl_2 (2 mL). The aqueous phase was separated and extracted with CH_2Cl_2 (5 mL). The organic layers were combined, washed with H_2O (5 mL), brine (5 mL), and dried over $MgSO_4$. Concentration under reduced pressure furnished (±)-xestoquinone (**5**) as an orange-brown paste (7.3 mg, 0.0229 mmol, 71%). Spectroscopic data were consistent with those reported previously *(27)*.

According to the above procedure, enantio-enriched furan **(+)-21** (10.0 mg, 0.0287 mmol, 1.0 mol. equiv.) was converted to (+)-xestoquinone (**5**) (6.6 mg, 0.021 mmol, 72%), e.r. 98:2 determined by analytical chiral SFC (Waters Trefoil CEL2, 2.5 um (3.0 x 150 mm), CO_2/MeOH 65:35, 2 mL/min, 40 °C, 305 nm, major (+) enantiomer t_R = 5.03, minor (−) enantiomer t_R = 6.70). Spectroscopic data were consistent with those of the racemic compound and those reported previously *(27)*.

Alternative two step route to furan 21:

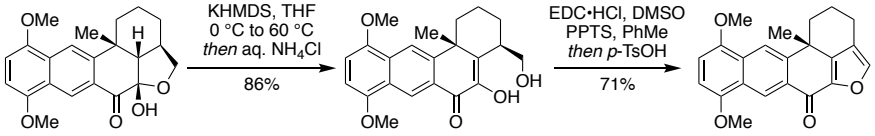

Tautomerization

To a 3-neck 25 mL round-bottomed flask was added lactol **(±)-20** (14.0 mg, 0.0380 mmol, 1.0 mol. equiv.) and dry THF (1.0 mL). The resulting solution was cooled to 0 °C and KHMDS (0.5 M in PhMe, 0.114 mL, 0.0570 mmol, 1.5 mol. equiv.) was added dropwise. The reaction mixture was warmed to 60 °C and stirred for 90 min, after which time TLC analysis indicated the complete consumption of starting material. The vessel was removed from the oil bath and the reaction was quenched with sat. aq. NH_4Cl solution (5 mL) and diluted with EtOAc (5 mL). The aqueous phase was separated and extracted with EtOAc (10 mL). The organic layers were combined, washed with sat. aq. NH_4Cl solution (10 mL), brine (10 mL), and dried over $MgSO_4$. Concentration under reduced pressure furnished diosphenol **(±)-S37** as a golden brown solid (12.1 mg, 0.0330 mmol, 86%). No additional purification was required. (Note: The reaction outcome was found to be highly dependent on temperature)

Diosphenol (±)-S37

m.p. = 120 °C (decomposition);

R_f = 0.22 (2:1 PS 40–60 °C in EtOAc);

^{1}H NMR ($CDCl_3$, 800 MHz): δ 9.14 (s, 1H), 8.35 (s, 1H), 6.92 (s, 1H), 6.79 (d, J = 8.3 Hz, 1H), 6.68 (d, J = 8.3 Hz, 1H), 3.98 (s, 3H), 3.98 (s, 3H), 3.97-3.90 (m, 2H), 3.65 (q, J = 7.7 Hz, 1H), 2.68 (d, J = 11.2 Hz, 1H), 2.03-1.97 (m, 2H), 1.81-1.75 (m, 1H), 1.70 (td, J = 12.9, 3.9 Hz, 1H), 1.65-1.59 (m, 1H), 1.55 (s, 3H) ppm;

^{13}C NMR ($CDCl_3$, 200 MHz): δ 180.0 (C_q), 150.8 (C_q), 148.9 (C_q), 148.6 (C_q), 144.5 (C_q), 135.9 (C_q), 128.6 (C_q), 126.1 (C_q), 124.8 (C_q), 123.1 (CH), 118.4 (CH), 106.0 (CH), 103.1 (CH), 65.5 (CH_2), 55.9 (CH_3), 55.8 (CH_3), 39.7 (C_q), 38.6 (CH_2), 38.3 (CH), 32.3 (CH_3), 26.1 (CH_2), 18.6 (CH_2) ppm;

IR (thin film): ν_{max} = 3391, 2933, 2863, 1620, 1268 cm^{-1};

LRMS (70 eV, ESI): m/z (%): 391.2 (20, $[M+Na]^+$), 369.2 (50, $[M+H]$);

HRMS (ESI) m/z calc. for $C_{22}H_{24}O_5$ $[M+Na]^+$: 391.1521; found 391.1523.

Oxidation-cyclization-dehydration

To a 3-neck 25 mL round-bottomed flask was added diosphenol **(±)-S37** (60.0 mg, 0.162 mmol, 1.0 mol. equiv.), PhMe (5.4 mL) and dry DMSO (1.8 mL). Freshly recrystallized anhydrous EDC•HCl (156 mg, 0.810 mmol, 5.0 mol. equiv.) and PPTS (73.0 mg, 0.290 mmol, 1.8 mol. equiv.) were added and the resulting solution was stirred at ambient room temperature for 3 h (check conversion by ^{1}H NMR aliquot). Anhydrous *p*-TsOH (28 mg, 0.16 mmol, 1.0 mol. equiv.) was added and the reaction mixture was warmed to 35 ^{o}C and stirred for 16 h. At this time an additional portion of *p*-TsOH (10.0 mg, 0.058 mmol, 0.40 mol. equiv.) was added and the reaction mixture was warmed to 45 ^{o}C and stirred for 90 min. The reaction was quenched with sat. aq. NH_4Cl solution (5.0 mL) and diluted with EtOAc (5.0 mL). The aqueous phase was separated and extracted with EtOAc (10 mL). The organic layers were combined, washed with H_2O (2 x 10 mL), brine (10 mL), dried over $MgSO_4$ and concentrated under reduced pressure. Purification by flash column chromatography (SiO_2; CH_2Cl_2 to 5:1 to 4:1 CH_2Cl_2 in EtOAc) furnished furan **(±)-21** as a red-orange paste (40.3 mg, 0.116 mmol, 71%) and a small amount of unreacted starting material **(±)-S37** (15.0 mg, 0.0407 mmol, 25%). Spectroscopic data were consistent with those reported above and previously *(27)*.

Alternative preparation of mono-adduct 16:

3,6-Dimethoxy-2-trimethylsilyl-benzene-1-trifluoromethanesulfonate (benzyne precursor) S42

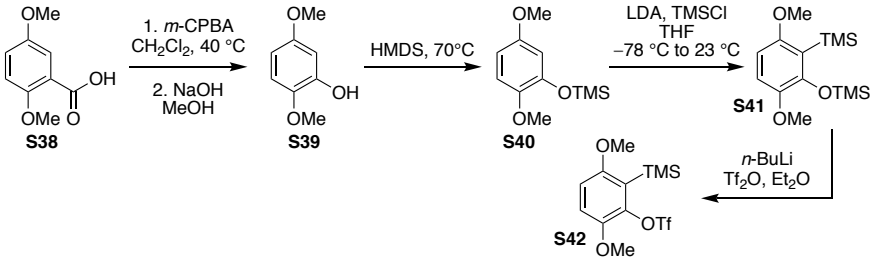

3,6-Dimethoxy-2-trimethylsilyl-benzene-1-trifluoromethanesulfonate **S42** was prepared according to the procedure outlined by Sherburn and co-workers *(79)*.

Mono-adduct 16

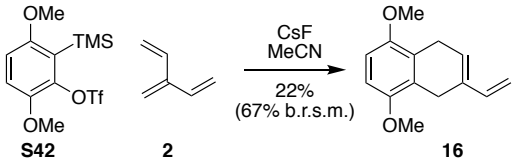

A solution of 3,6-dimethoxy-2-(trimethylsilyl)phenyl trifluoromethanesulfonate **S42** (1.49 g, 4.16 mmol, 1.0 mol. equiv.) in dry MeCN (2.0 mL) was added dropwise to a mixture of freshly prepared [3]dendralene (**2**) (1.00 g, 12.5 mmol, 3.0 mol. equiv.), CsF (1.26 g, 8.32 mmol, 2.0 mol. equiv.) and 3,5-di-tert-4-butylhydroxytoluene (1 crystal) in dry MeCN (8.0 mL). The resulting mixture was stirred at ambient room temperature for 20 h, whereupon it was diluted with CH_2Cl_2 (20 mL), washed with H_2O (x3), brine (x1), dried over $MgSO_4$ and concentrated under reduced pressure. Purification by flash column chromatography (SiO_2; 0% to 10% EtOAc in hexanes) furnished bicyclic diene **16** as a pale yellow solid (199 mg, 0.920 mmol, 22% yield, 67% b.r.s.m). Spectroscopic data were consistent with those reported above.

X-Ray Crystallography

Bicyclic diene 3d

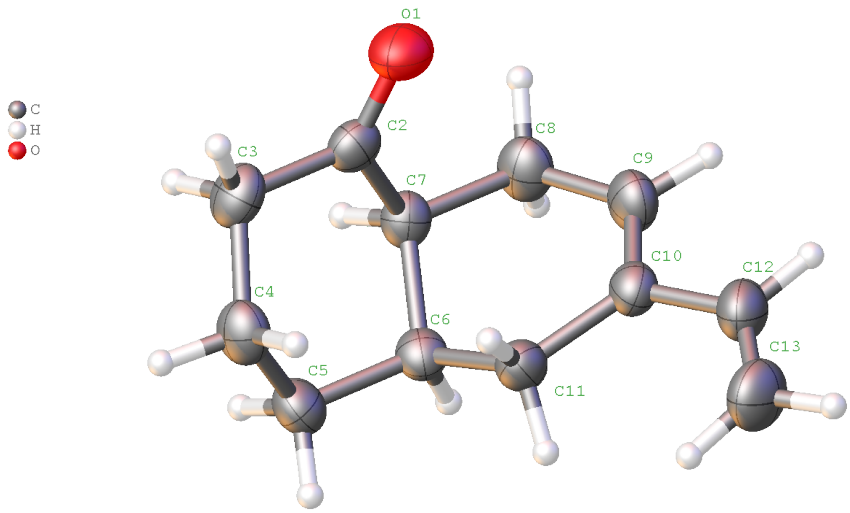

Fig. S2.
Molecular structure of **3d** (dataset ID: she1124). Atomic displacement parameters shown at 50% probability level.

Crystal Data. $C_{12}H_{16}O$, M_r = 176.26, monoclinic, $C2/c$ (No. 15), a = 22.5516(6) Å, b = 5.3223(1) Å, c = 16.8301(4) Å, β = 96.7003(13)°, $\alpha = \gamma$ = 90°, V = 2006.26(8) Å^3, T = 200.00 K, Z = 8, Z' = 1, $\mu(MoK_\alpha)$ = 0.07, 21686 reflections measured, 2275 unique (R_{int} = 0.028) which were used in all calculations. The final wR_2 was 0.106 (all data) and R_1 was 0.040 (I > 2(I)).

Tetracycle 4b

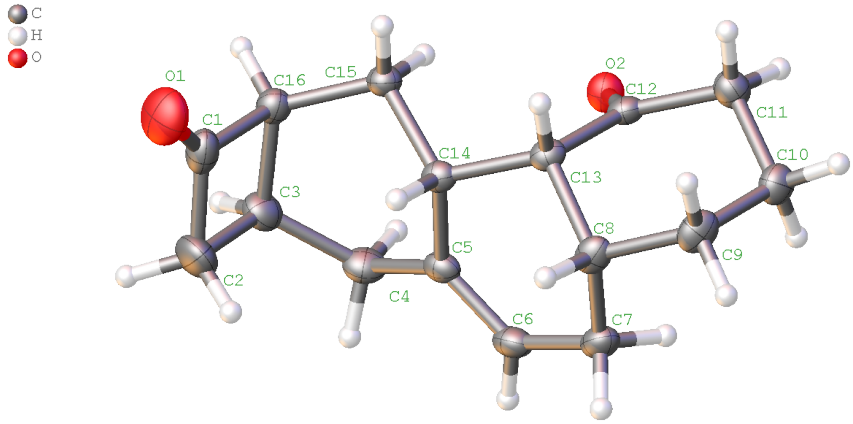

Fig. S3.
Molecular structure of **4b** (dataset ID: NSSF168-c2_f19-27scaled). Atomic displacement parameters shown at 50% probability level.

Crystal Data. $C_{16}H_{20}O_2$, M_r = 244.32, monoclinic, $P2_1/c$ (No. 14), a = 12.6498(7) Å, b = 7.8189(5) Å, c = 12.8557(8) Å, β = 93.163(5)°, $\alpha = \gamma$ = 90°, V = 1269.59(13) Å^3, T = 150.00(10) K, Z = 4, Z' = 1, μ(MoK$_\alpha$) = 0.082, 7306 reflections measured, 3069 unique (R_{int} = 0.0222) which were used in all calculations. The final wR_2 was 0.1156 (all data) and R_1 was 0.0451 (I > 2(I)).

Tetracycle 4d

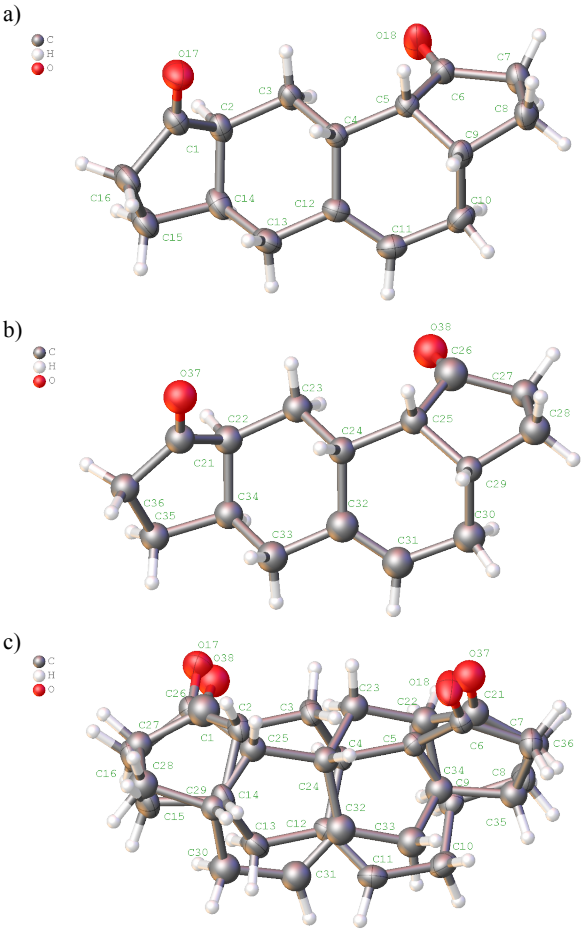

Fig. S4.

Molecular structure of **4d** (dataset ID: she1139). Atomic displacement parameters shown at 50% probability level. The molecule is disordered over two site occupancies; (a) shows the main occupancy (92%), (b) shows the minor occupancy (8%) and (c) overlay of both occupancies.

Crystal Data. $C_{16}H_{20}O_2$, M_r = 244.33, triclinic, *P-1* (No. 2), a = 6.9877(2) Å, b = 9.6419(3) Å, c = 9.7193(3) Å, α = 78.5491(18)˚, β = 80.908(2)˚, γ = 86.575(2)˚, V = 633.47(3) Å^3, T = 200.00 K, Z = 2, Z' = 1, μ(MoK$_\alpha$) = 0.08, 17142 reflections measured, 3700 unique (R_{int} = 0.029) which were used in all calculations. The final wR_2 was 0.121 (all data) and R_1 was 0.048 (I > 2(I)).

Tetracycle 4e

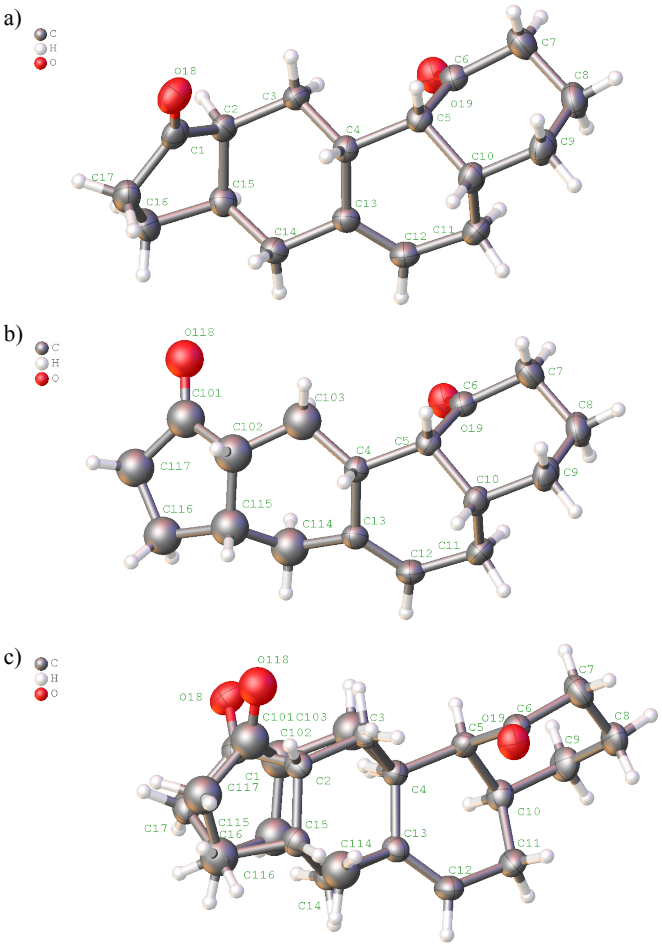

Fig. S5.

Molecular structure of **4e** (dataset ID: she1137). Atomic displacement parameters shown at 50% probability level. The structure features a mixture of diastereomers; (a) shows the main occupancy (95% of **4e**), (b) shows the minor occupancy (5% of the diastereomer) and (c) overlay of both occupancies.

Crystal Data. $C_{17}H_{22}O_2$, M_r = 258.36, monoclinic, $P2_1/n$ (No. 14), a = 5.4050(1) Å, b = 11.4876(3) Å, c = 22.1384(5) Å, β = 92.5486(13)°, $\alpha = \gamma$ = 90°, V = 1373.22(5) Å^3, T = 200.00 K, Z = 4, Z' = 1, μ(MoK$_\alpha$) = 0.08, 23050 reflections measured, 3134 unique (R_{int} = 0.046)-which were used in all calculations. The final wR_2 was 0.114 (all data) and R_1 was 0.046 (I > 2(I)).

Tetracycle 4f

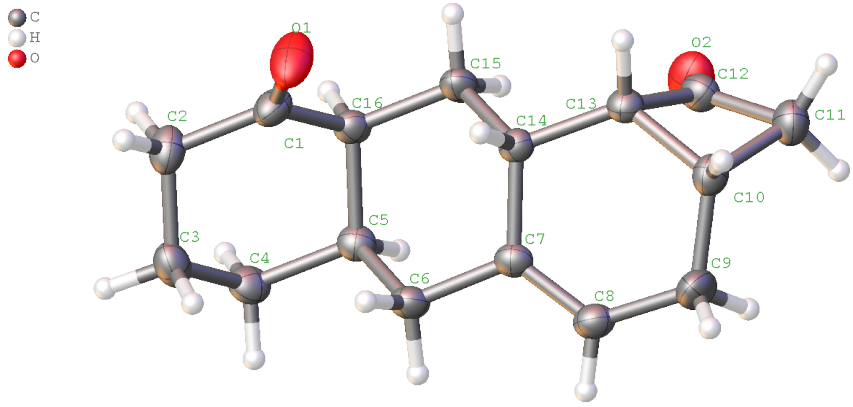

Fig. S6.
Molecular structure of **4f** (dataset ID: NSSG38_f20-45scaled). Atomic displacement parameters shown at 50% probability level.

Crystal Data. $C_{16}H_{20}O_2$, M_r = 244.32, monoclinic, $P2_1/n$ (No. 14), a = 11.2167(3) Å, b = 10.5908(2) Å, c = 11.4952(2) Å, β = 112.059(2)°, $\alpha = \gamma$ = 90°, V = 1265.60(5) Å^3, T = 150.00(10) K, Z = 4, Z' = 1, μ(CuK$_\alpha$) = 0.651, 6729 reflections measured, 2546 unique (R_{int} = 0.0172) which were used in all calculations. The final wR_2 was 0.1046 (all data) and R_1 was 0.0392 (I > 2(I)).

Tetracycle 4g

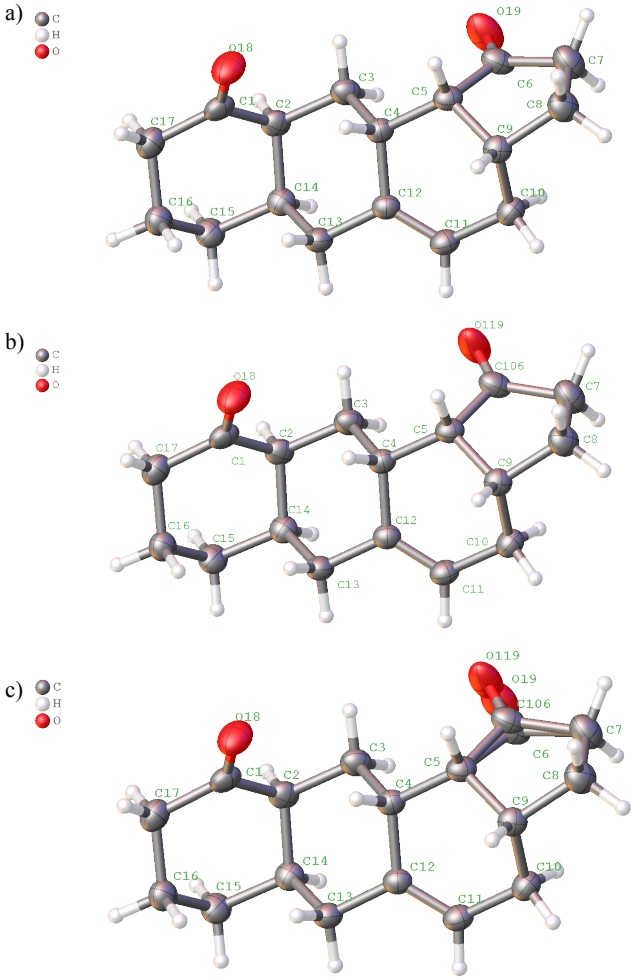

Fig. S7.

Molecular structure of **4g** (dataset ID: she1130). Atomic displacement parameters shown at 50% probability level. The molecule is disordered over two site occupancies; (a) shows the main occupancy (68%), (b) shows the minor occupancy (32%) and (c) overlay of both occupancies.

Crystal Data. $C_{17}H_{22}O_2$, M_r = 258.36, orthorhombic, *Pbca* (No. 61), a = 10.9052(2) Å, b = 9.1538(1) Å, c = 27.0213(4) Å, $\alpha = \beta = \gamma = 90^{\circ}$, V = 2697.37(7) Å^3, T = 200.00 K, Z = 8, Z' = 1, μ(MoK$_\alpha$) = 0.08, 30580 reflections measured, 3078 unique (R_{int} = 0.037) which were used in all calculations. The final wR_2 was 0.089 (all data) and R_1 was 0.037 (I > 2(I)).

S69

Tetracycle 4h

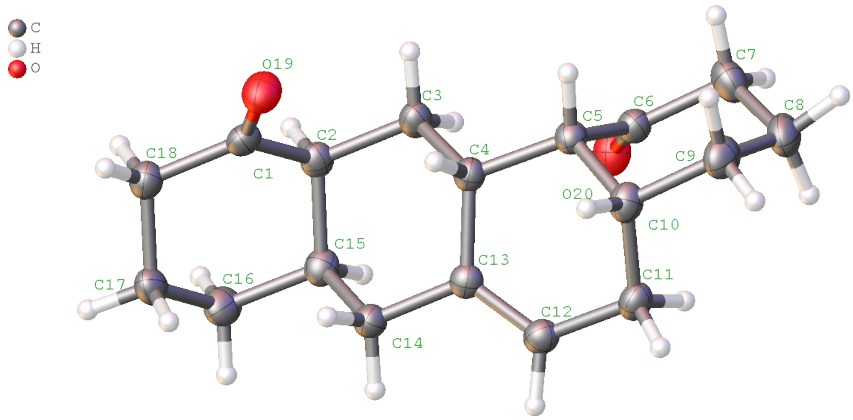

Fig. S8.
Molecular structure of **4h** (dataset ID: she1128). Atomic displacement parameters shown at 50% probability level.

Crystal Data. $C_{18}H_{24}O_2$, M_r = 272.39, monoclinic, $P2_1/a$ (No. 14), a = 9.1638(2) Å, b = 10.3911(2) Å, c = 15.1030(3) Å, β = 93.4520(13)˚, $\alpha = \gamma$ = 90˚, V = 1435.53 (5) Å^3, T = 200.00 K, Z = 4, Z' = 1, μ(MoK$_\alpha$) = 0.08, 32027 reflections measured, 3268 unique (R_{int} = 0.038) which were used in all calculations. The final wR_2 was 0.094 (all data) and R_1 was 0.037 (I > 2(I)).

Tetracycle 4k

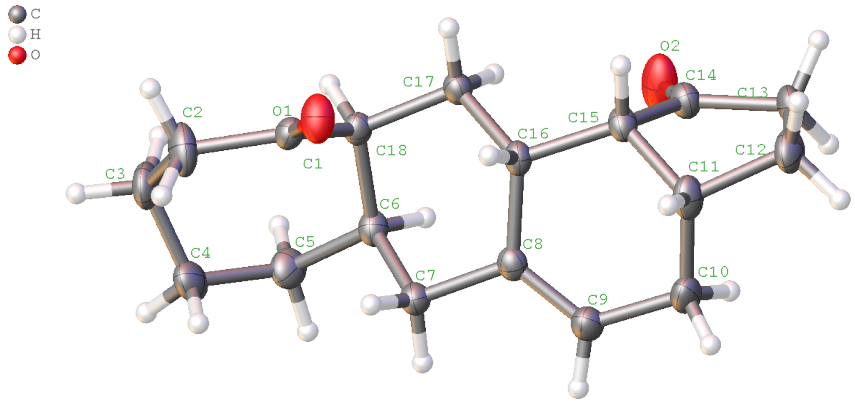

Fig. S9.
Molecular structure of **4k** (dataset ID: NSSG3_f30-45scaled). Atomic displacement parameters shown at 50% probability level.

Crystal Data. $C_{18}H_{24}O_2$, M_r = 272.37, monoclinic, $P2_1/c$ (No. 14), a = 11.2646(3) Å, b = 12.8502(2) Å, c = 11.0432(3) Å, β = 115.731(3)˚, $\alpha = \gamma$ = 90˚, V = 1440.02(7) Å^3, T = 150.00(10) K, Z = 4, Z' = 1, $\mu(CuK_\alpha)$ = 0.623, 14549 reflections measured, 2898 unique (R_{int} = 0.0244) which were used in all calculations. The final wR_2 was 0.1074 (all data) and R_1 was 0.0416 (I > 2(I)).

Tetracycle 4l

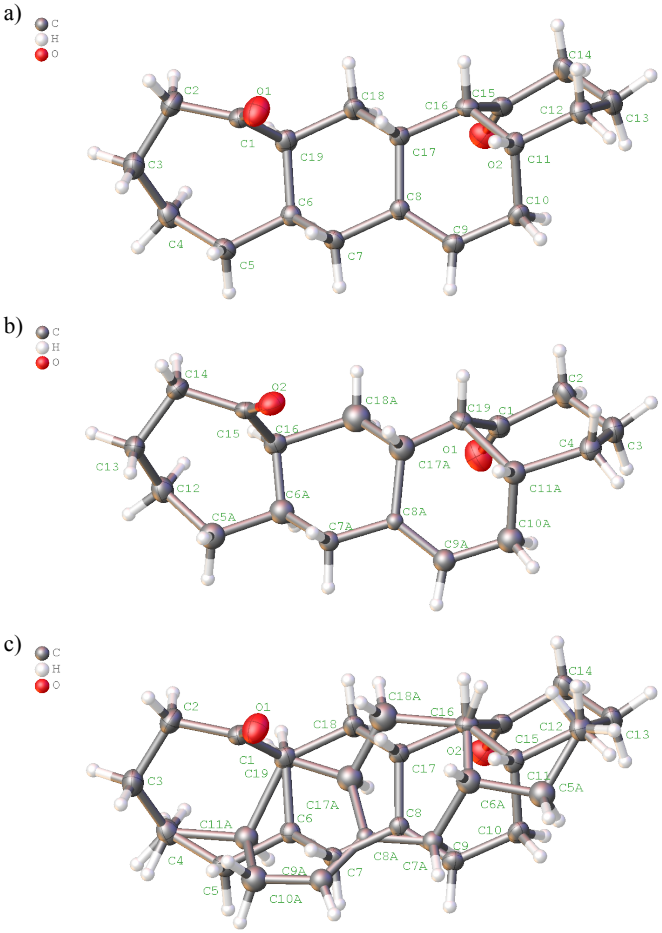

Fig. S10.

Molecular structure of **4l** (dataset ID: NSSG4_f10-13ascaled). Atomic displacement parameters shown at 50% probability level. The molecule is disordered over two site occupancies; (a) shows the main occupancy (90%), (b) shows the minor occupancy (10%) and (c) overlay of both occupancies.

Crystal Data. $C_{19}H_{26}O_2$, M_r = 286.40, triclinic, *P*-1 (No. 2), a = 7.0685(3) Å, b = 10.0469(7) Å, c = 12.3347(5) Å, α = 112.709(5)˚, β = 106.387(4)˚, γ = 90.373(5)˚, *V* = 768.61(8) Å^3, *T* = 150.00(10) K, *Z* = 2, *Z*′ = 1, μ(CuK$_\alpha$) = 0.607, 6722 reflections measured, 3084 unique (R_{int} = 0.0196) which were used in all calculations. The final wR_2 was 0.1192 (all data) and R_1 was 0.0466 (I > 2(I)).

Tetracycle 4o

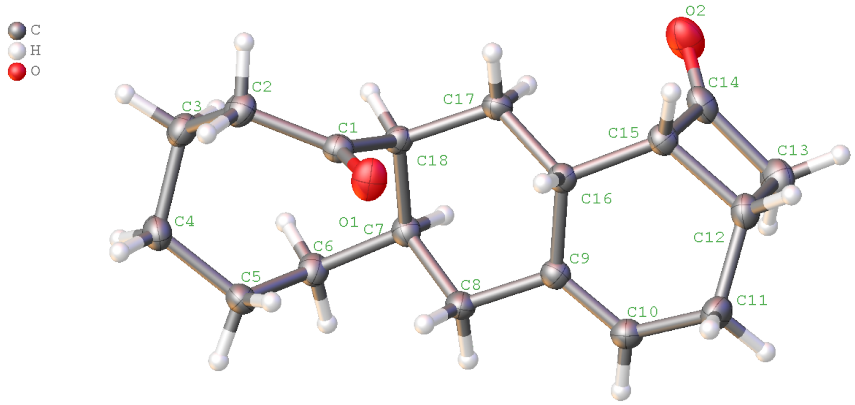

Fig. S11.
Molecular structure of **4o** (dataset ID: NSSG39_f28-40scaled). Atomic displacement parameters shown at 50% probability level.

Crystal Data. $C_{18}H_{24}O_2$, M_r = 272.37, monoclinic, $P2_1/n$ (No. 14), a = 11.8603(2) Å, b = 5.56720(10) Å, c = 21.9033(4) Å, β = 99.032(2)˚, $\alpha = \gamma$ = 90˚, V = 1428.31(4) Å^3, T = 150.00(10) K, Z = 4, Z' = 1, μ(CuK$_\alpha$) = 0.628, 8051 reflections measured, 2869 unique (R_{int} = 0.0202) which were used in all calculations. The final wR_2 was 0.1015 (all data) and R_1 was 0.0373 (I > 2(I)).

Tetracycle 4p

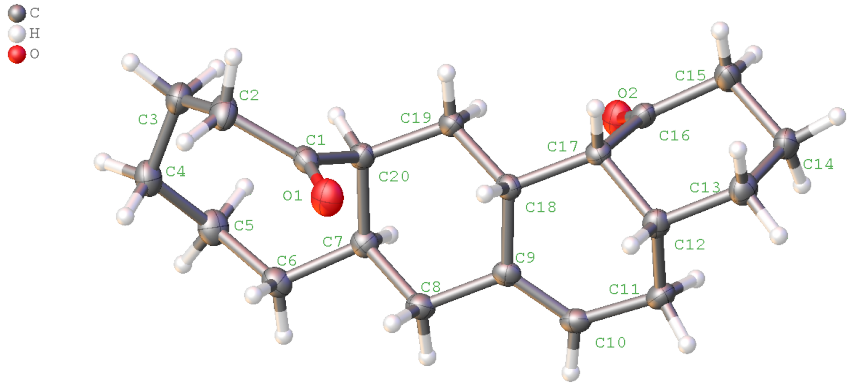

Fig. S12.
Molecular structure of **4p** (dataset ID: NSSF117_c2_f11-21scaled). Atomic displacement parameters shown at 50% probability level.

Crystal Data. $C_{20}H_{28}O_2$, M_r = 300.42, triclinic, *P*-1 (No. 2), a = 6.8680(2) Å, b = 10.2026(4) Å, c = 12.6848(4) Å, α = 110.059(3)˚, β = 100.954(2)˚, γ = 95.904(2)˚, V = 805.99(5) Å^3, T = 150.02(10) K, Z = 2, Z' = 1, μ(MoK$_\alpha$) = 0.078, 61115 reflections measured, 4333 unique (R_{int} = 0.0303) which were used in all calculations. The final wR_2 was 0.1110 (all data) and R_1 was 0.0413 (I > 2(I)).

Tetracycle 4q

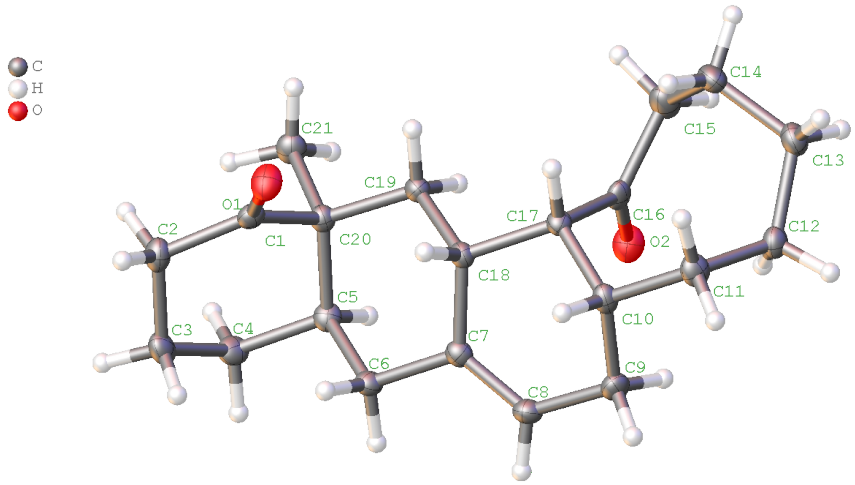

Fig. S13.
Molecular structure of **4q** (dataset ID: NSSG15_f23-38scaled). Atomic displacement parameters shown at 50% probability level.

Crystal Data. $C_{21}H_{30}O_2$, M_r = 314.45, monoclinic, $P2_1/c$ (No. 14), a = 11.6493(8) Å, b = 10.3574(7) Å, c = 14.6161(10) Å, β = 103.393(7)°, $\alpha = \gamma$ = 90°, V = 1715.6(2) Å^3, T = 150.00(10) K, Z = 4, Z' = 1, μ(MoK$_\alpha$) = 0.076, 9638 reflections measured, 4139 unique (R_{int} = 0.0296) which were used in all calculations. The final wR_2 was 0.1145 (all data) and R_1 was 0.0513 (I > 2(I)).

Tetracycle 4t

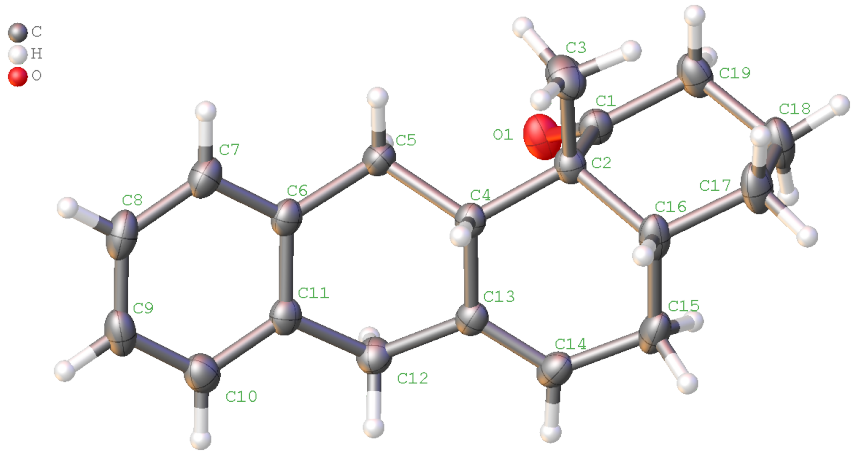

Fig. S14.
Molecular structure of **4t** (dataset ID: NSSF162scaled). Atomic displacement parameters shown at 50% probability level.

Crystal Data. $C_{19}H_{22}O$, M_r = 266.36, triclinic, *P*-1 (No. 2), a = 8.6679(5) Å, b = 8.6791(5) Å, c = 10.5367(6) Å, α = 80.791(5)˚, β = 67.622(6)˚, γ = 87.330(5)˚, V = 723.44(8) Å^3, T = 150.00(10) K, Z = 2, Z' = 1, μ(CuK$_\alpha$) = 0.560, 7487 reflections measured, 2909 unique (R_{int} = 0.0160) which were used in all calculations. The final wR_2 was 0.1021 (all data) and R_1 was 0.0376 (I > 2(I)).

Mono-adduct 16

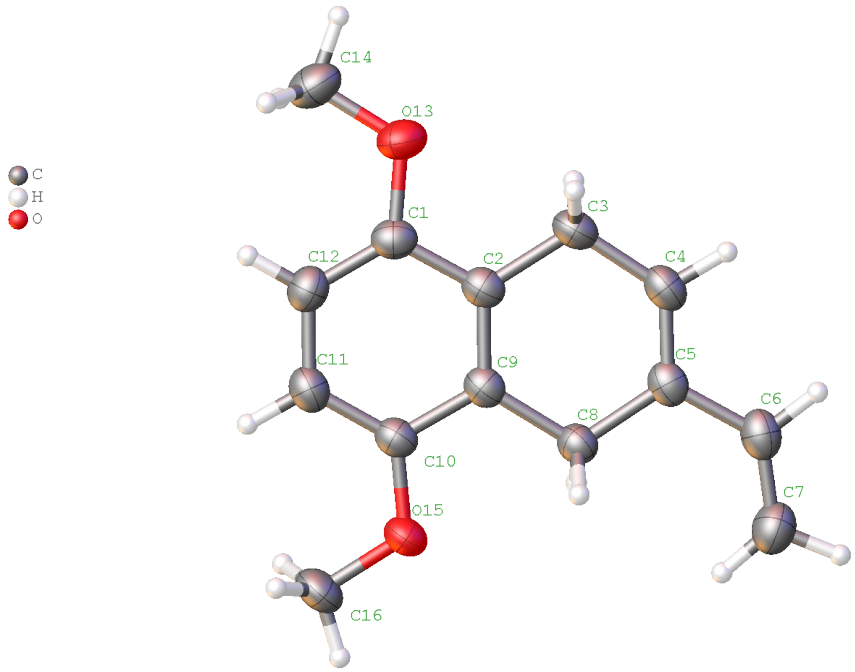

Fig. S15.
Molecular structure of **16** (dataset ID: she1207). Atomic displacement parameters shown at 50% probability level.

Crystal Data. $C_{14}H_{16}O_2$, M_r = 216.28, monoclinic, $P2_1/n$ (No. 14), a = 15.5545(4) Å, b = 4.1242(1) Å, c = 17.8711(5) Å, β = 90.8518(14)˚, $\alpha = \gamma$ = 90˚, V = 1146.30 (5) Å^3, T = 200.00 K, Z = 4, Z' = ,1 μ(MoK$_\alpha$) = 0.08, 23327 reflections measured, 2640 unique (R_{int} = 0.046) which were used in all calculations. The final wR_2 was 0.110 (all data) and R_1 was 0.043 (I > 2(I)).

S77

Tetracycle 17a

a)

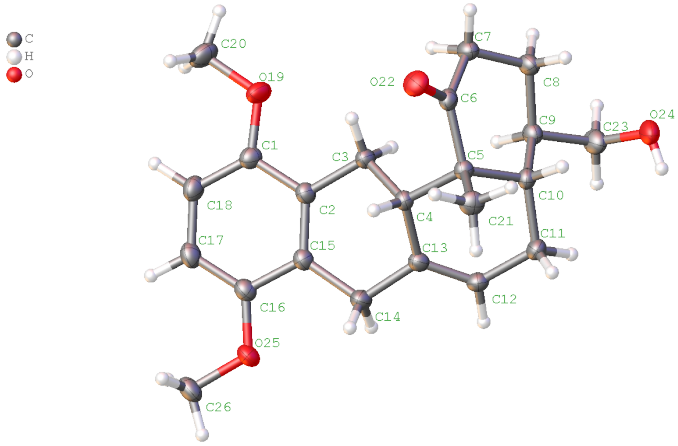

b)

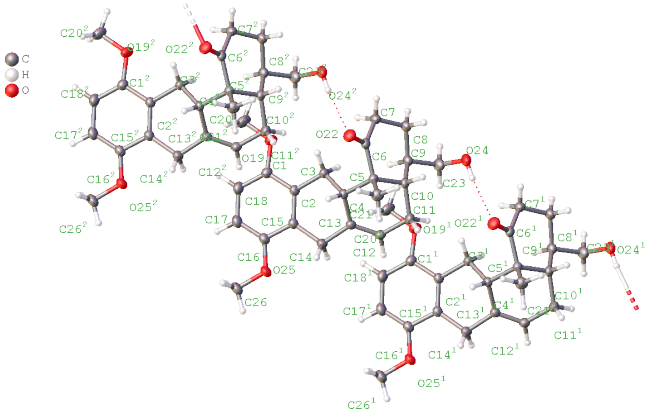

Fig. S16.

Molecular structure of **17a** (dataset ID: she1314). Atomic displacement parameters shown at 50% probability level. (a) shows the asymmetric unit and (b) a portion of the extended H-bonded structure ([1] denotes symmetry operator 1+*x*,*y*,*z*, [2] denotes symmetry operator -1+*x*,*y*,*z*).

Crystal Data. $C_{22}H_{28}O_4$, M_r = 356.46, monoclinic, $P2_1/c$ (No. 14), a = 7.55730(1) Å, b = 19.1020(3) Å, c = 13.2888(2) Å, β = 103.7200(8)°, $\alpha = \gamma$ = 90°, V = 1863.63 (5) Å^3, T = 200.00 K, Z = 4, Z' = 1, μ(MoK$_\alpha$) = 0.09, 46356 reflections measured, 5460 unique (R_{int} = 0.032) which were used in all calculations. The final wR_2 was 0.102 (all data) and R_1 was 0.039 (I > 2(I)).

Tetracycle 17b

a)

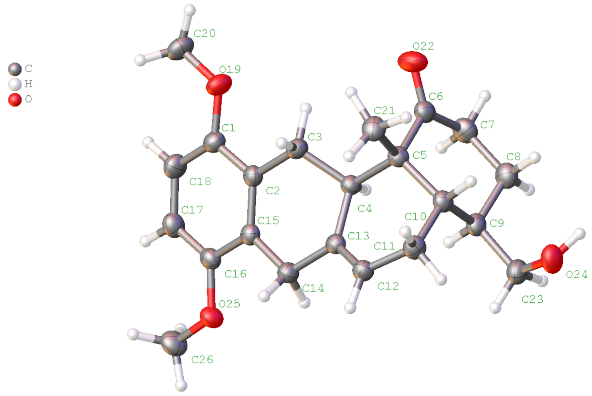

b)

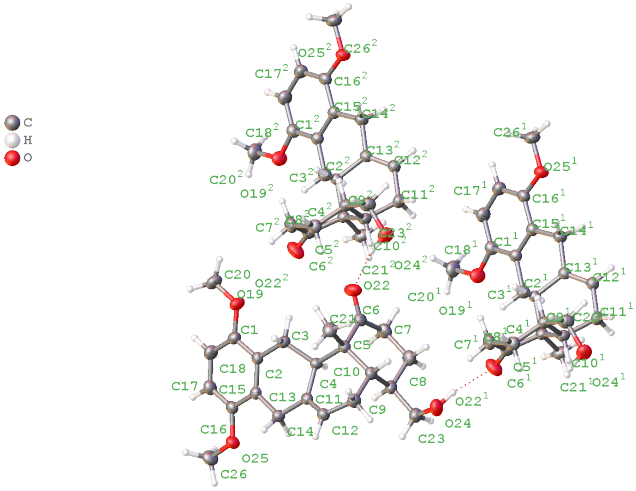

Fig. S17.

Molecular structure of **17b** (dataset ID: she1315). Atomic displacement parameters shown at 50% probability level. (a) shows the asymmetric unit and (b) a portion of the extended H-bonded structure ([1] denotes symmetry operator 1/2-x,-1/2+y,3/2-z, [2] denotes symmetry operator 1/2-x,1/2+y,3/2-z).

Crystal Data. $C_{22}H_{28}O_4$, M_r = 356.46, monoclinic, *C2/c* (No. 15), a = 21.8445(8) Å, b = 11.5206(5) Å, c = 14.4658(3) Å, β = 92.862(2)˚, $\alpha = \gamma$ = 90˚, V = 3635.9 (2) Å^3, T = 200.00 K, Z = 8, Z' = 1, μ(MoK$_\alpha$) = 0.09, 22581 reflections measured, 3214 unique (R_{int} = 0.058) which were used in all calculations. The final wR_2 was 0.101 (all data) and R_1 was 0.041 (I > 2(I)).

Lactol 20

a)

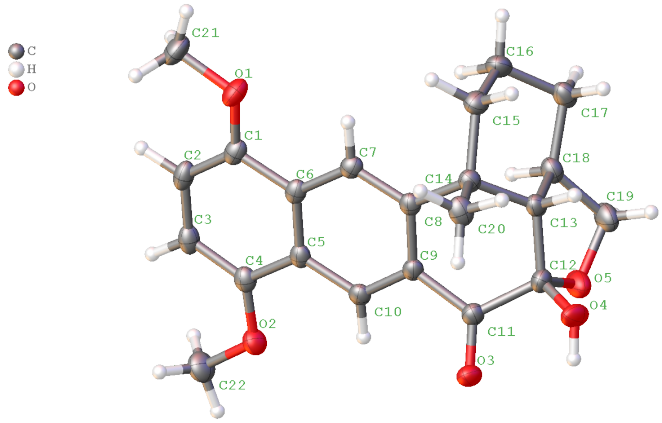

b)

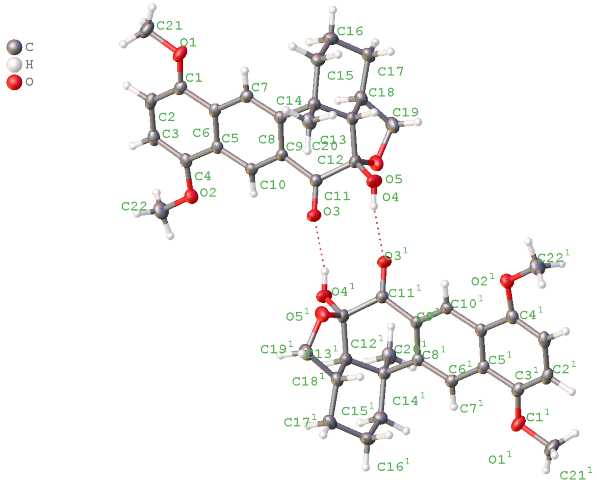

Fig. S18.

Molecular structure of **20** (dataset ID: she1526SN). Atomic displacement parameters shown at 50% probability level. (a) shows the asymmetric unit and (b) the dimeric H-bonded structure (^{1} denotes symmetry operator 1-*x*,-*y*,-*z*).

Crystal Data. $C_{22}H_{24}O_5$, M_r = 368.43, monoclinic, $P2_1/n$ (No. 14), a = 11.6171(1) Å, b = 10.0998(1) Å, c = 16.1499(1) Å, β = 103.5384(8)°, $\alpha = \gamma$ = 90°, V = 1842.22 (3) Å^3, T = 110.00 K, Z = 4, Z' = 1, μ(CuK$_\alpha$) = 0.76, 28014 reflections measured, 3634 unique (R_{int} = 0.015) which were used in all calculations. The final wR_2 was 0.095 (all data) and R_1 was 0.036 (I > 2(I)).

Compound	Dataset ID	CCDC Deposition Number
3d	she1124	2008993
4b	nssf168-c2_f19-27	2008994
4d	she1139	2008995
4e	she1137	2008996
4f	nssg38_f20-45scaled	2008997
4g	she1130	2008998
4h	she1128	2008999
4k	nssg3_f30-45scaled	2009000
4l	nssg4-f10_13ascaled	2009001
4o	nssg39-f28-40scaled	2009002
4p	nssf117_c2_f11-21scaled	2009003
4q	nssg15-f23-38scaled	2009004
4t	nssf162scaled	2009005
16	she1207	2009006
17a	she1314	2009007
17b	she1315	2009008
20	she1526SN	2009009

Table S4.

CCDC deposition numbers for supplementary crystallographic data. This data can be obtained free of charge from The Cambridge Crystallographic Data Centre *via* www.ccdc.cam.ac.uk/data_request/cif.

Analytical Chiral HPLC Traces
Cyclohexenone 8 (Organocatalyzed DA product)

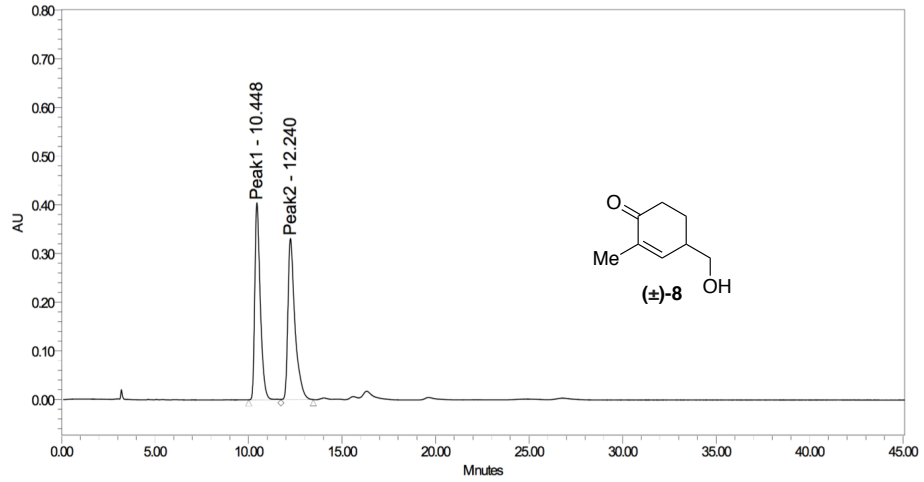

	Peak Name	RT	Area	% Area	Height
1	Peak1	10.448	8239147	48.63	404873
2	Peak2	12.240	8703907	51.37	331294

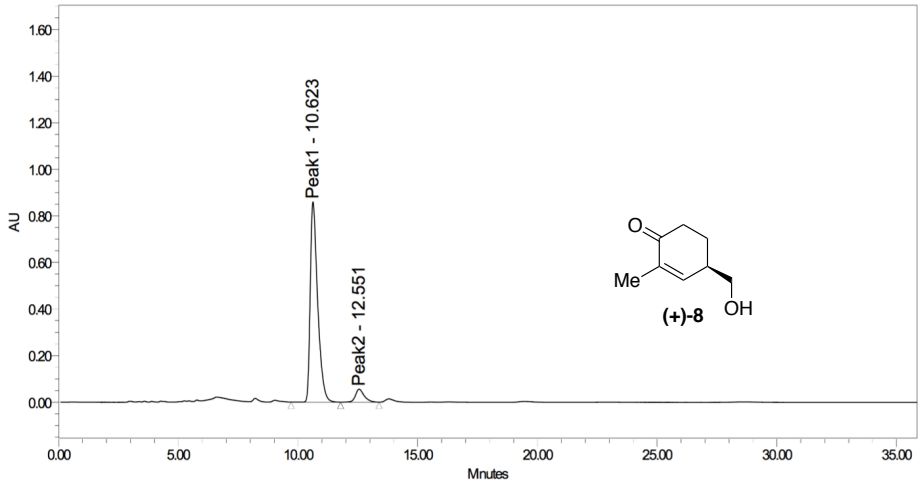

	Peak Name	RT	Area	% Area	Height
1	Peak1	10.623	18485294	92.86	860140
2	Peak2	12.551	1421452	7.14	56190

Cyclohexenone 8 (Starting material for HP)

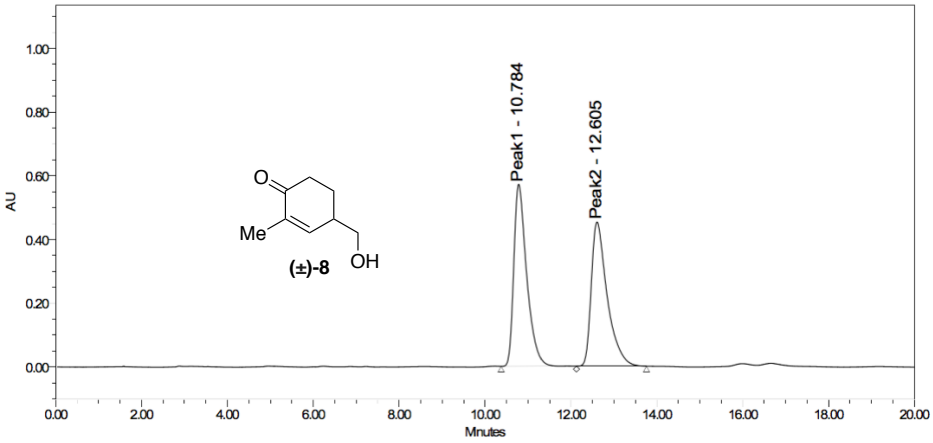

	Peak Name	RT	Area	% Area	Height
1	Peak1	10.784	11940616	50.62	571496
2	Peak2	12.605	11648498	49.38	452928

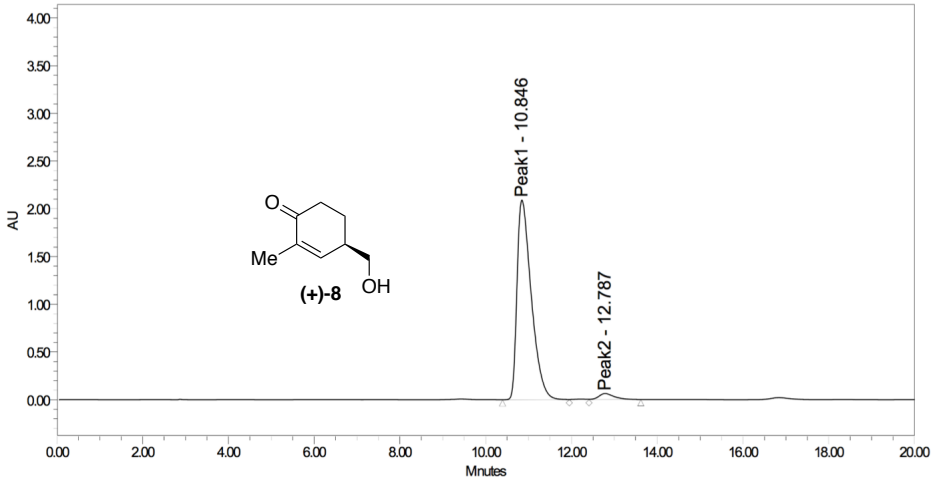

	Peak Name	RT	Area	% Area	Height
1	Peak1	10.846	48316156	96.81	2091586
2	Peak2	12.787	1592752	3.19	63453

S83

Chiral SFC Traces
Tetracycle 19

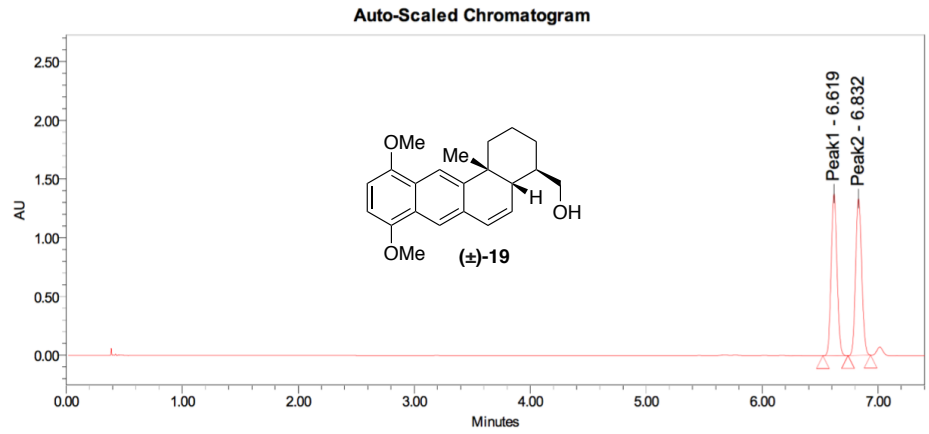

Peak Results

Peak1	6.619	4921583	50.10
Peak2	6.832	4901322	49.90

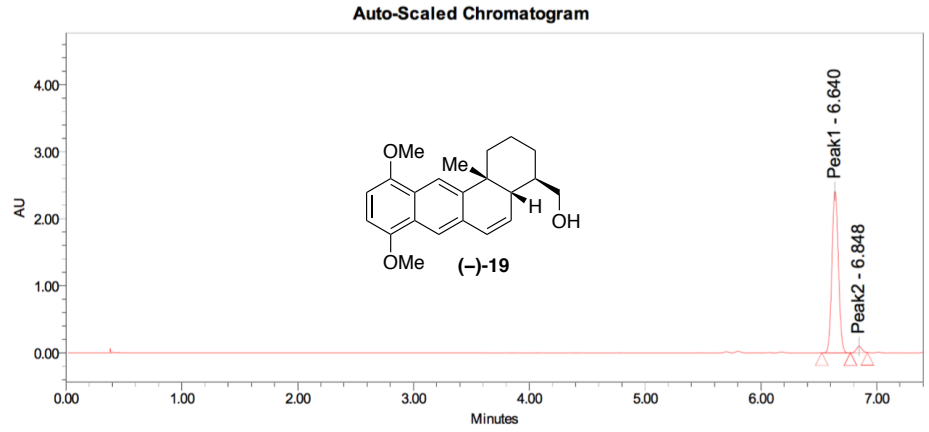

Peak Results

Peak1	6.640	9368519	96.71
Peak2	6.848	319185	3.29

Lactol 20

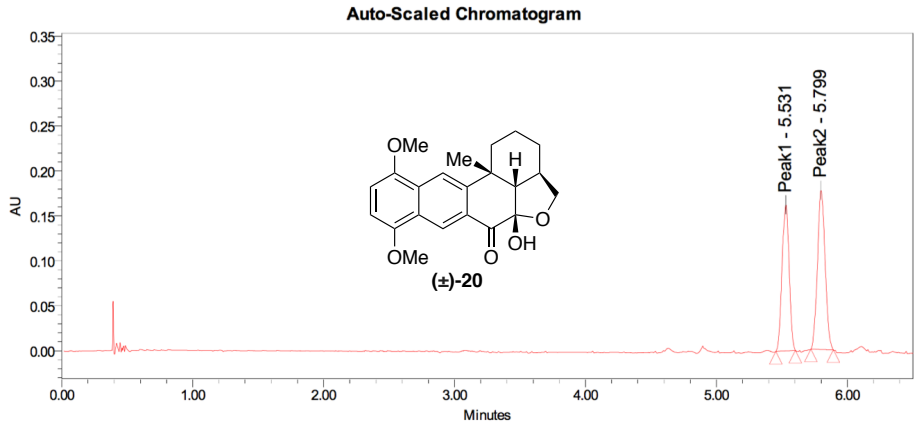

Peak Results

Peak1	5.531	612002	45.95
Peak2	5.799	719838	54.05

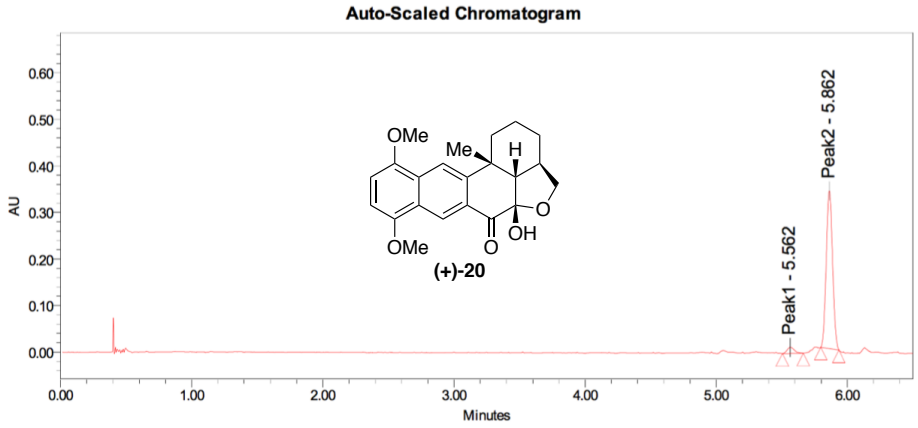

Peak Results

Peak1	5.562	50879	4.28
Peak2	5.862	1138628	95.72

S85

Furan 21

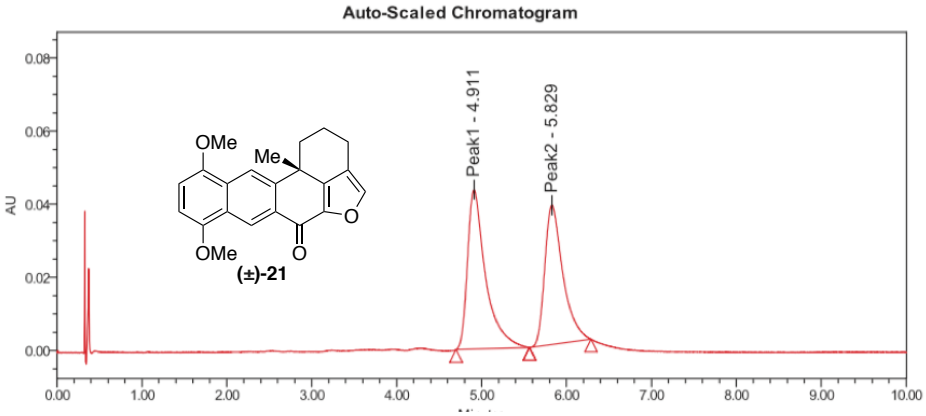

Peak Results

	Name	RT	Area	% Area
1	Peak1	4.911	649285	53.09
2	Peak2	5.829	573703	46.91

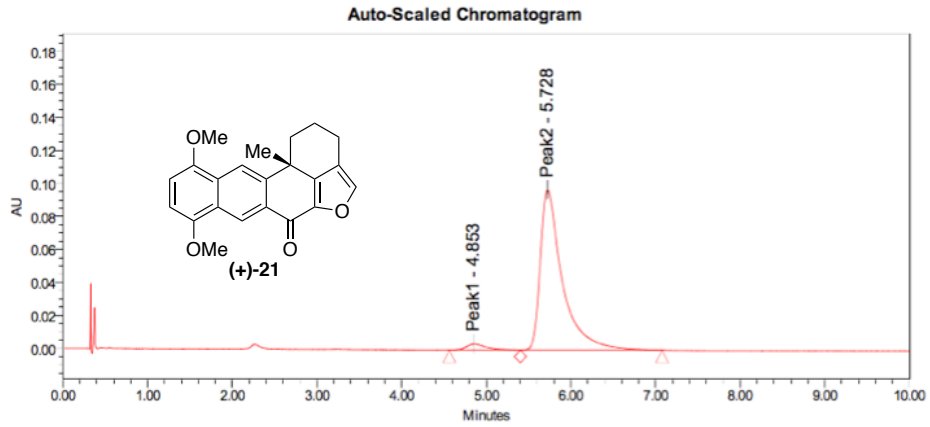

Peak Results

Peak1	4.853	64167	3.51
Peak2	5.728	1762360	96.49

Xestoquinone (5)

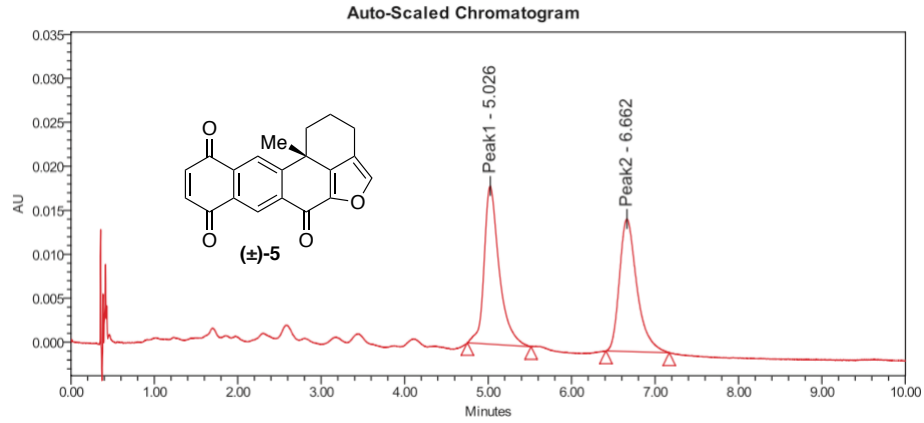

Peak Results

	Name	RT	Area	% Area
1	Peak1	5.026	226176	50.75
2	Peak2	6.662	219534	49.25

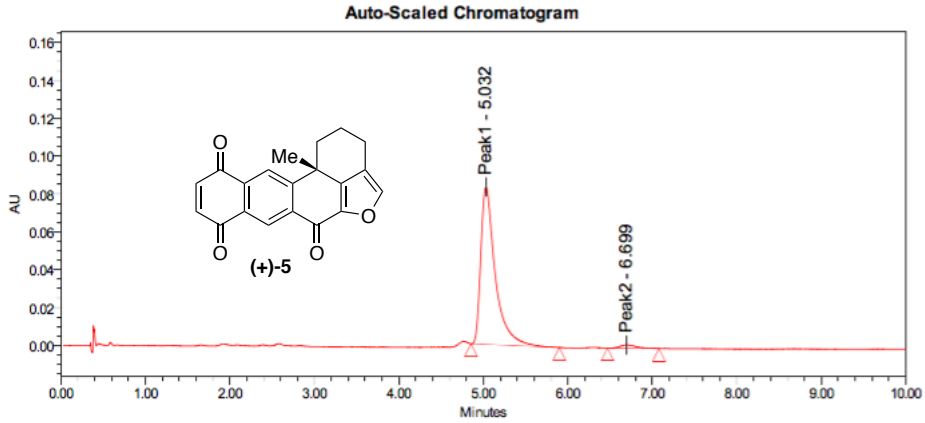

Peak Results

Peak1	5.032	990221	97.63
Peak2	6.699	24008	2.37

S87

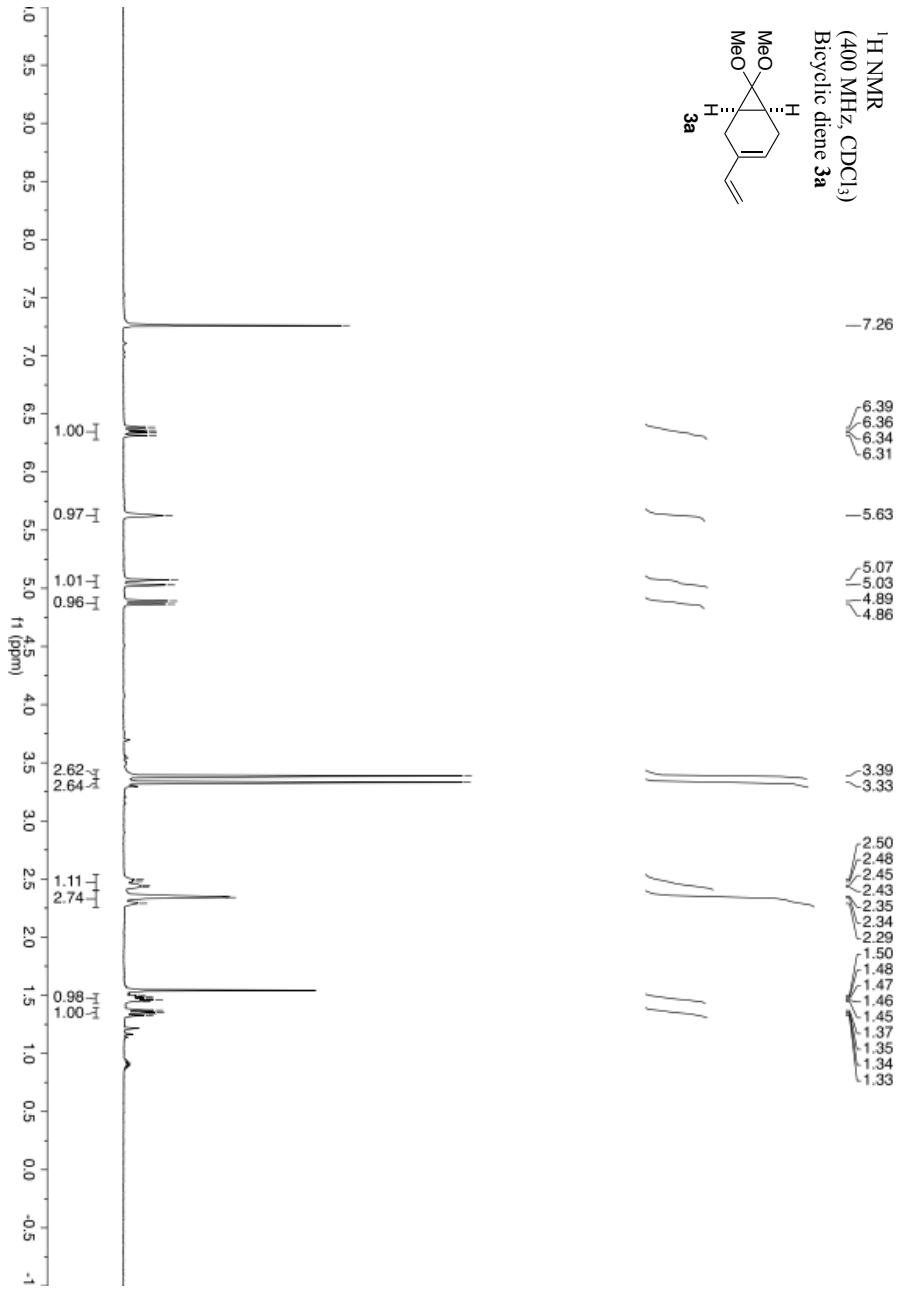
^{1}H NMR
(400 MHz, $CDCl_3$)
Bicyclic diene **3a**
MeO
MeO
H
H
3a
7.26
6.39
6.36
6.34
6.31
5.63
5.07
5.03
4.89
4.86
3.39
3.33
2.50
2.48
2.45
2.43
2.35
2.34
2.29
1.50
1.48
1.47
1.46
1.45
1.37
1.35
1.34
1.33
1.00
0.97
1.01
0.96
2.62
2.64
1.11
2.74
0.98
1.00
f1 (ppm)

S88

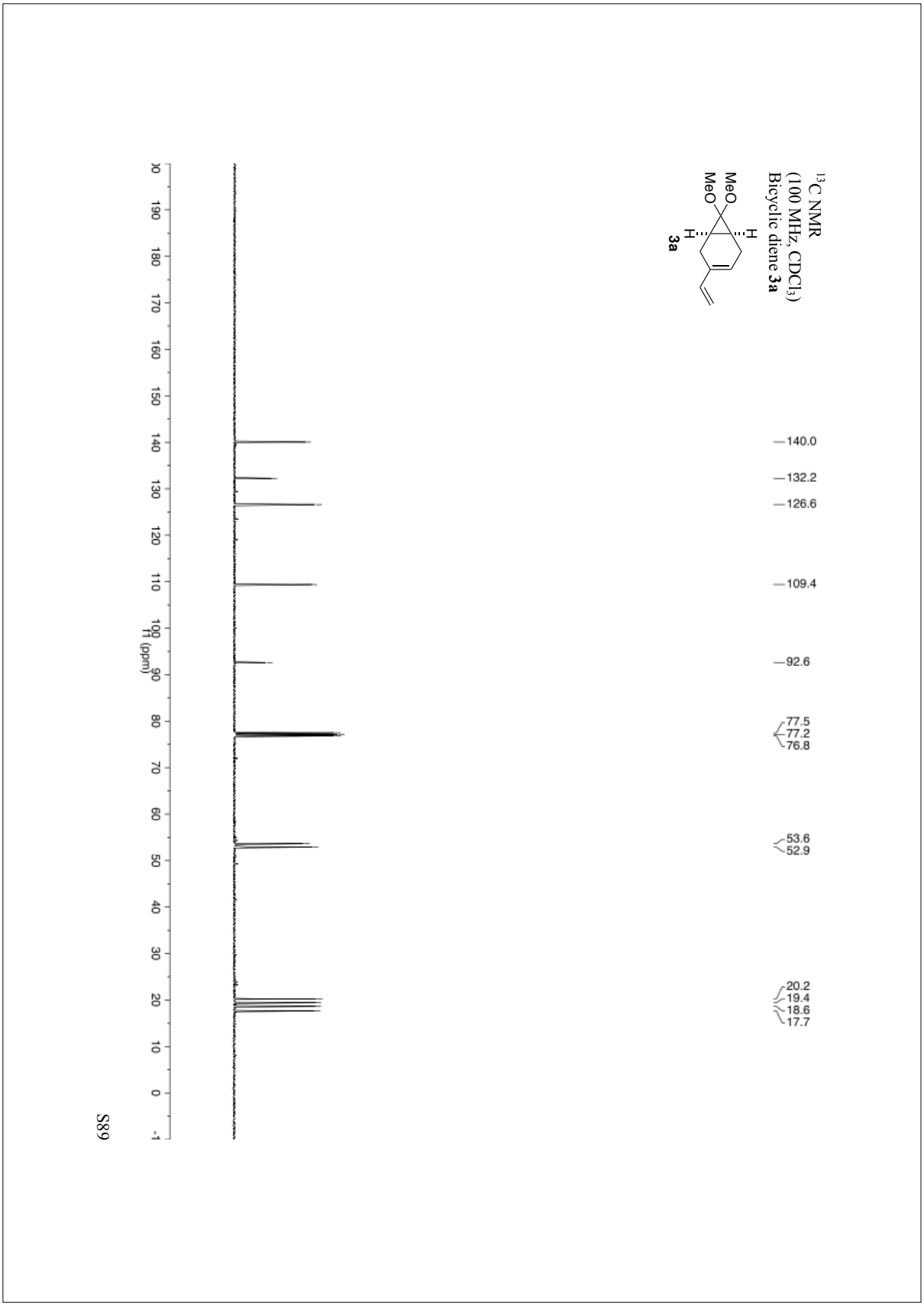
^{13}C NMR
(100 MHz, $CDCl_3$)
Bicyclic diene **3a**
MeO
MeO
H
H
3a
140.0
132.2
126.6
109.4
92.6
77.5
77.2
76.8
53.6
52.9
20.2
19.4
18.6
17.7
f1 (ppm)

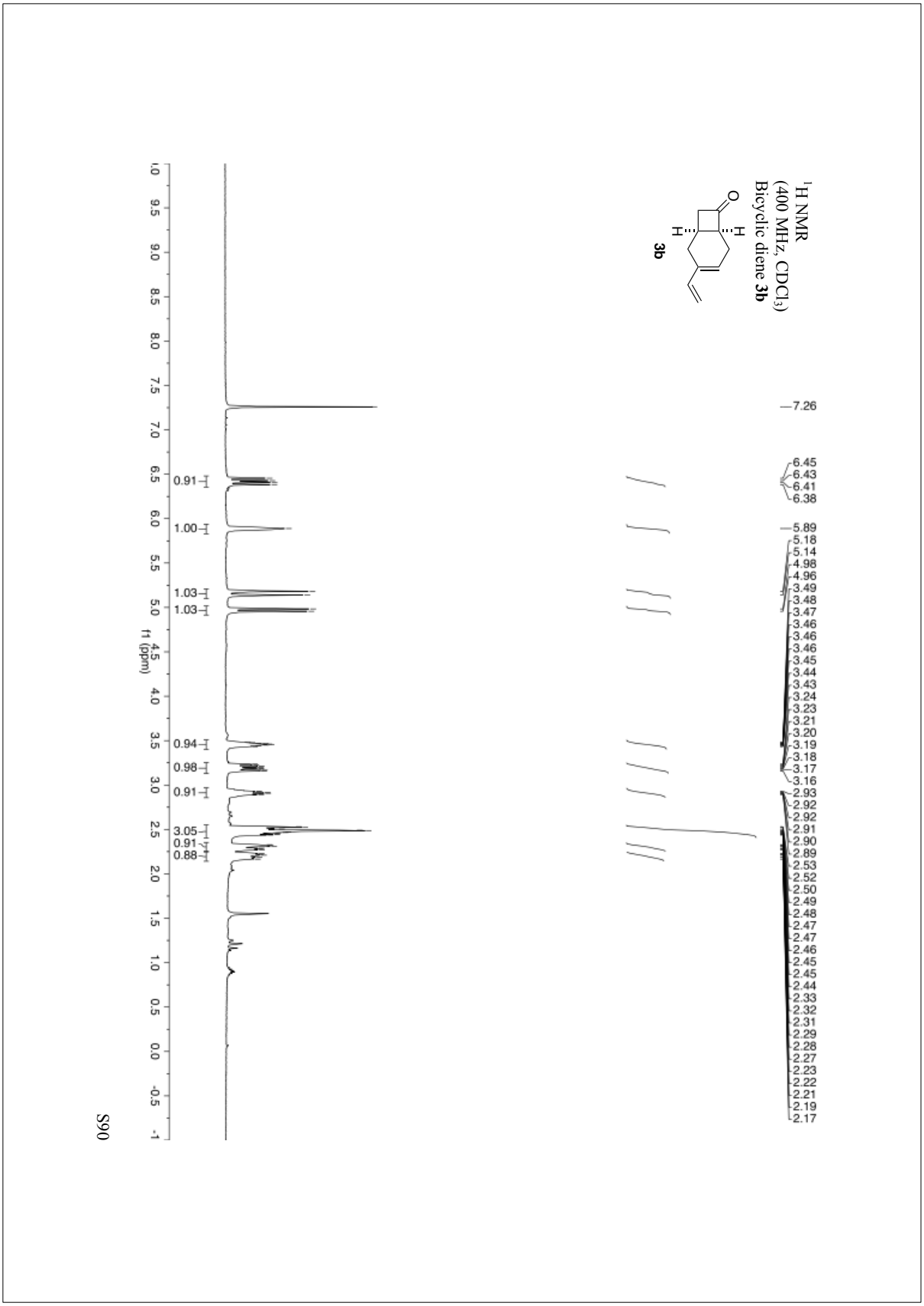
^{1}H NMR
(400 MHz, $CDCl_3$)
Bicyclic diene **3b**
3b
7.26
6.45
6.43
6.41
6.38
5.89
5.18
5.14
4.98
4.96
3.49
3.48
3.47
3.46
3.46
3.46
3.45
3.44
3.43
3.24
3.23
3.21
3.20
3.19
3.18
3.17
3.16
2.93
2.92
2.92
2.91
2.90
2.89
2.53
2.52
2.50
2.49
2.48
2.47
2.47
2.46
2.45
2.45
2.44
2.33
2.32
2.31
2.29
2.28
2.27
2.23
2.22
2.21
2.19
2.17
0.91
1.00
1.03
1.03
0.94
0.98
0.91
3.05
0.91
0.88
f1 (ppm)
S90

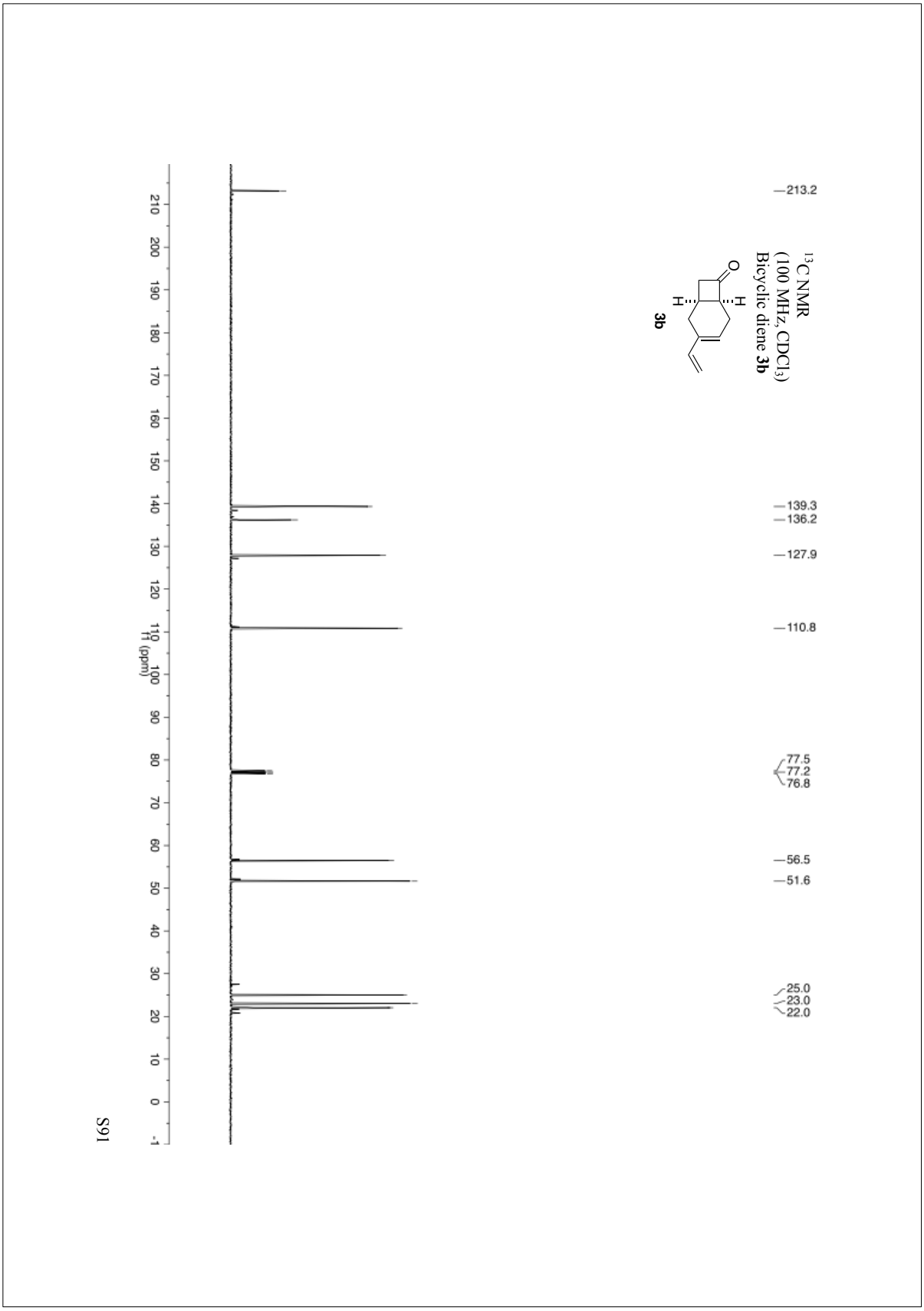
^{13}C NMR
(100 MHz, $CDCl_3$)
Bicyclic diene **3b**
3b
213.2
139.3
136.2
127.9
110.8
77.5
77.2
76.8
56.5
51.6
25.0
23.0
22.0
f1 (ppm)
S91

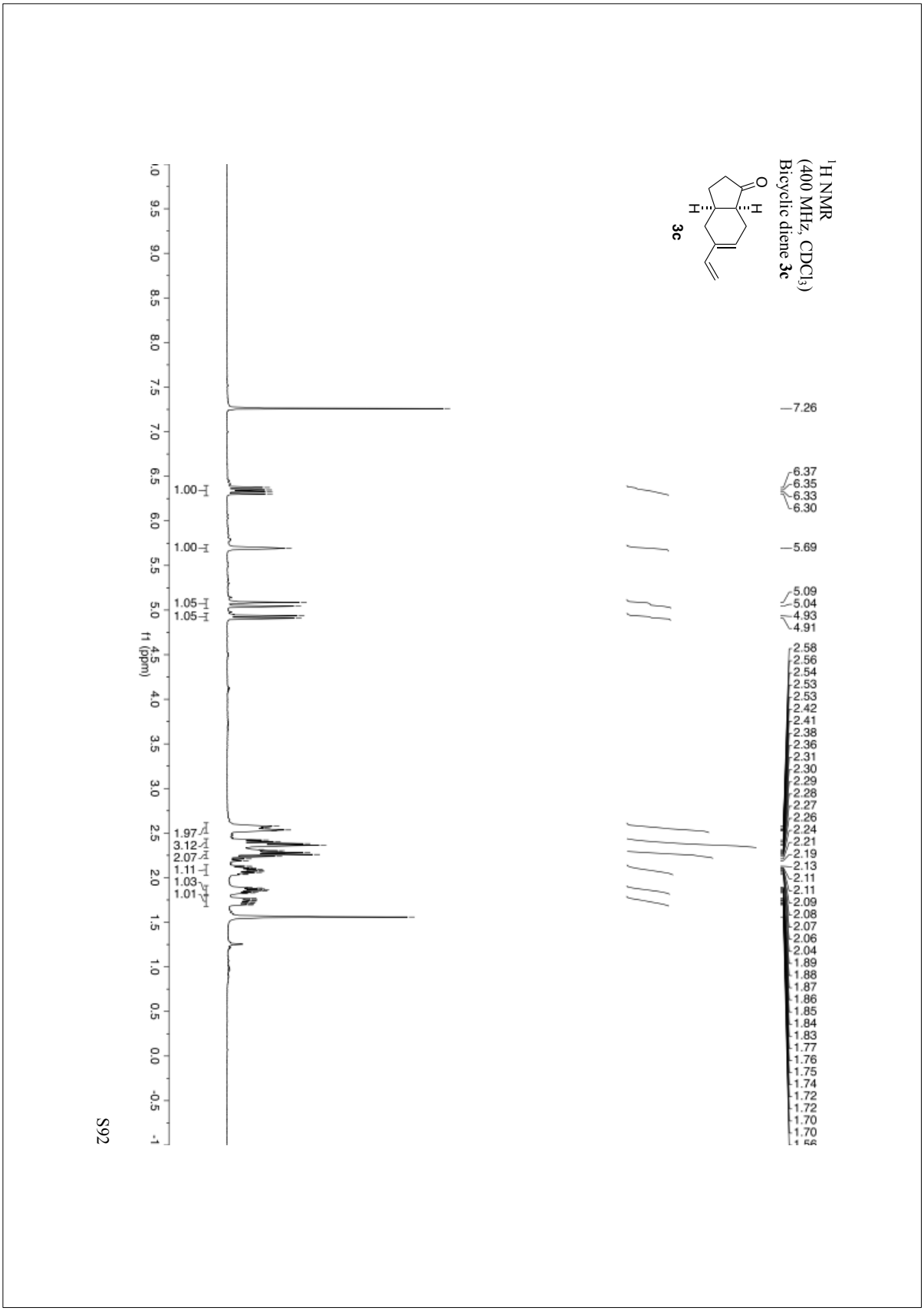
^{1}H NMR
(400 MHz, $CDCl_3$)
Bicyclic diene **3c**
3c
7.26
6.37
6.35
6.33
6.30
5.69
5.09
5.04
4.93
4.91
2.58
2.56
2.54
2.53
2.53
2.42
2.41
2.38
2.36
2.31
2.30
2.29
2.28
2.27
2.26
2.24
2.21
2.19
2.13
2.11
2.11
2.09
2.08
2.07
2.06
2.04
1.89
1.88
1.87
1.86
1.85
1.84
1.83
1.77
1.76
1.75
1.74
1.72
1.72
1.70
1.70
1.00
1.00
1.05
1.05
1.97
3.12
2.07
1.11
1.03
1.01
f1 (ppm)

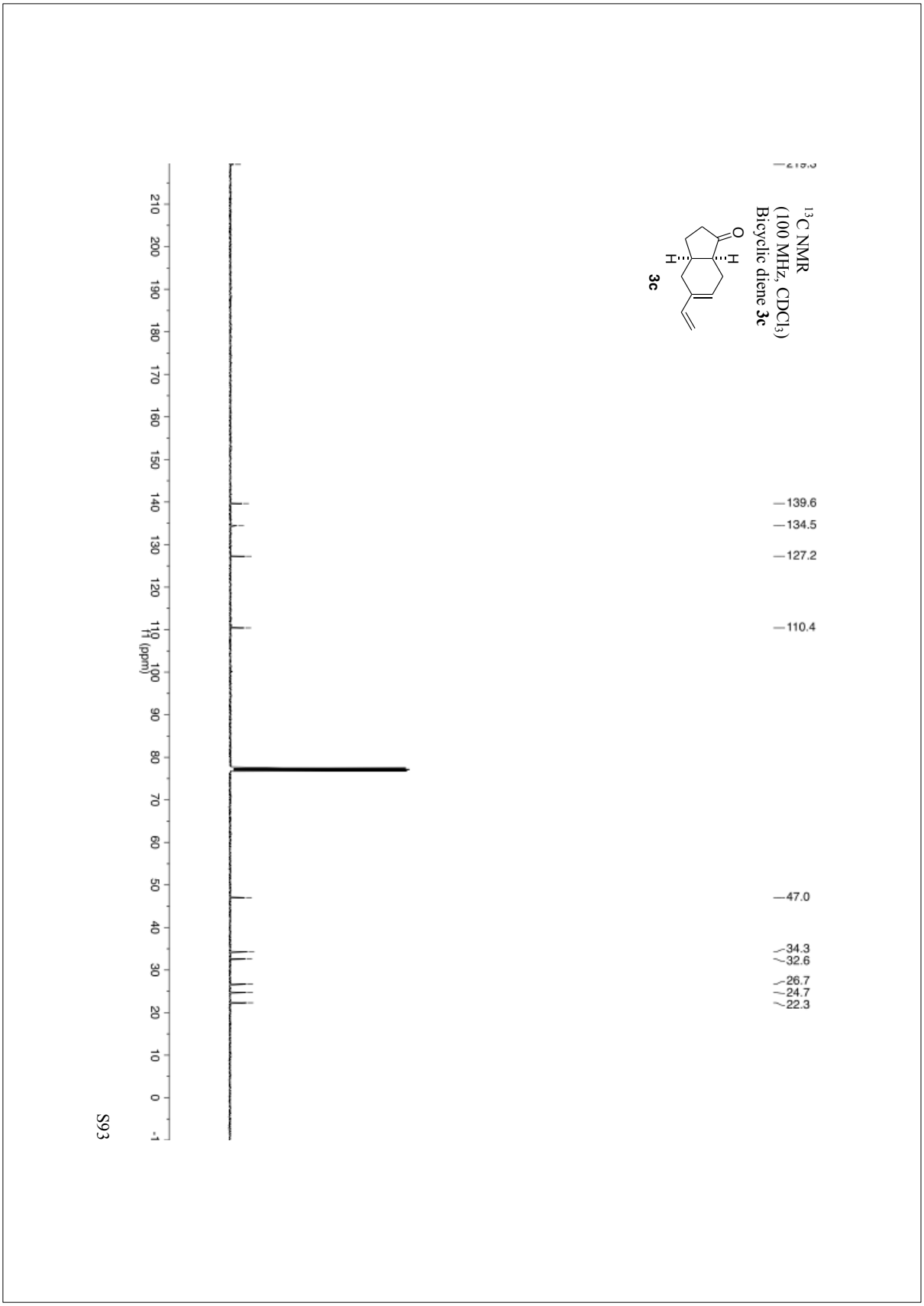
^{13}C NMR
(100 MHz, CDCl$_3$)
Bicyclic diene **3c**
3c
139.6
134.5
127.2
110.4
47.0
34.3
32.6
26.7
24.7
22.3
f1 (ppm)
S93

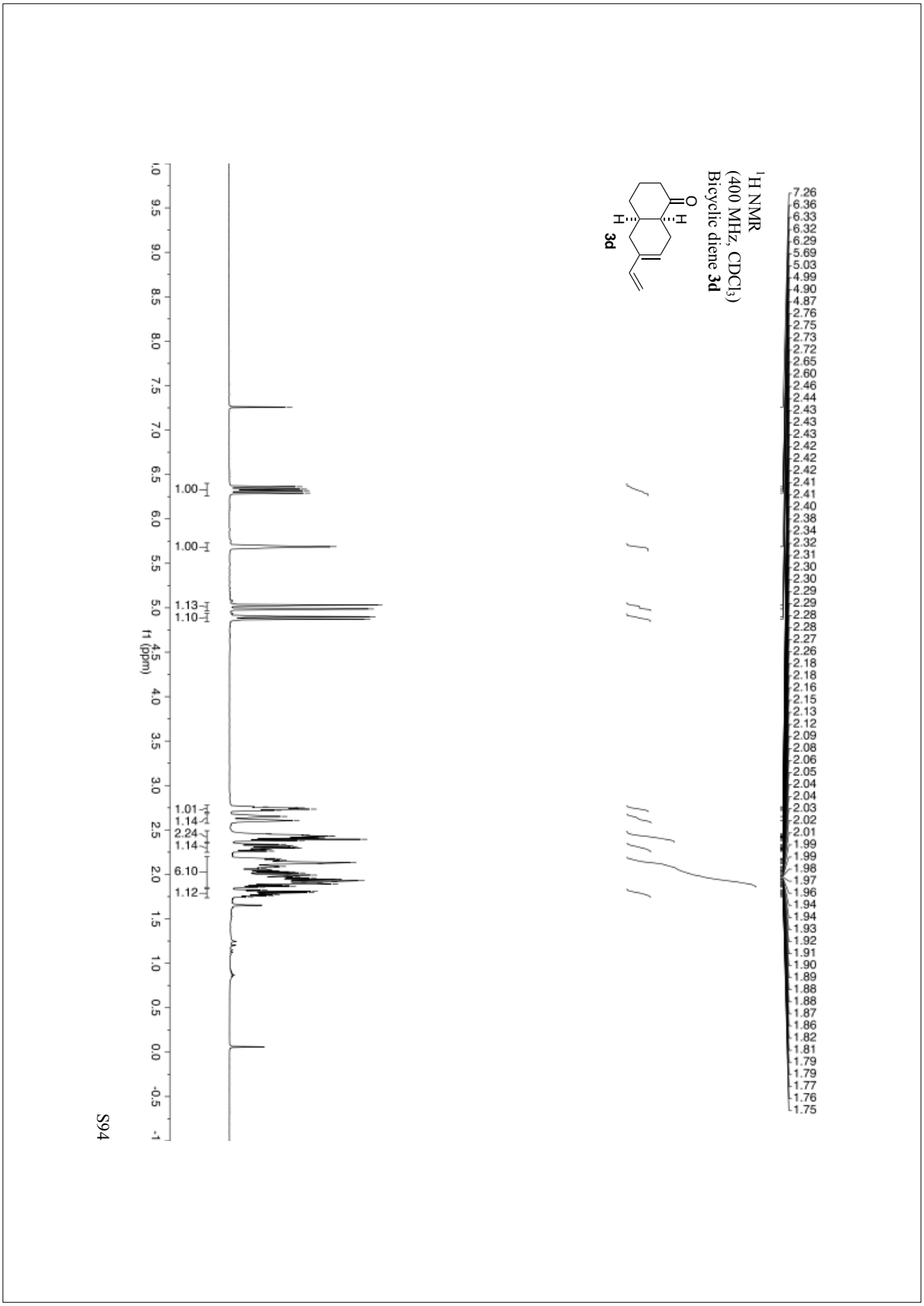
^{1}H NMR
(400 MHz, $CDCl_3$)
Bicyclic diene **3d**
3d
7.26
6.36
6.33
6.32
6.29
5.69
5.03
4.99
4.90
4.87
2.76
2.75
2.73
2.72
2.65
2.60
2.46
2.44
2.43
2.43
2.43
2.42
2.42
2.42
2.41
2.41
2.40
2.38
2.34
2.32
2.31
2.30
2.30
2.29
2.29
2.28
2.28
2.27
2.26
2.18
2.18
2.16
2.15
2.13
2.12
2.09
2.08
2.06
2.05
2.04
2.04
2.03
2.02
2.01
1.99
1.99
1.98
1.97
1.96
1.94
1.94
1.93
1.92
1.91
1.90
1.89
1.88
1.88
1.87
1.86
1.82
1.81
1.79
1.79
1.77
1.76
1.75
1.00
1.00
1.13
1.10
1.01
1.14
2.24
1.14
6.10
1.12
f1 (ppm)

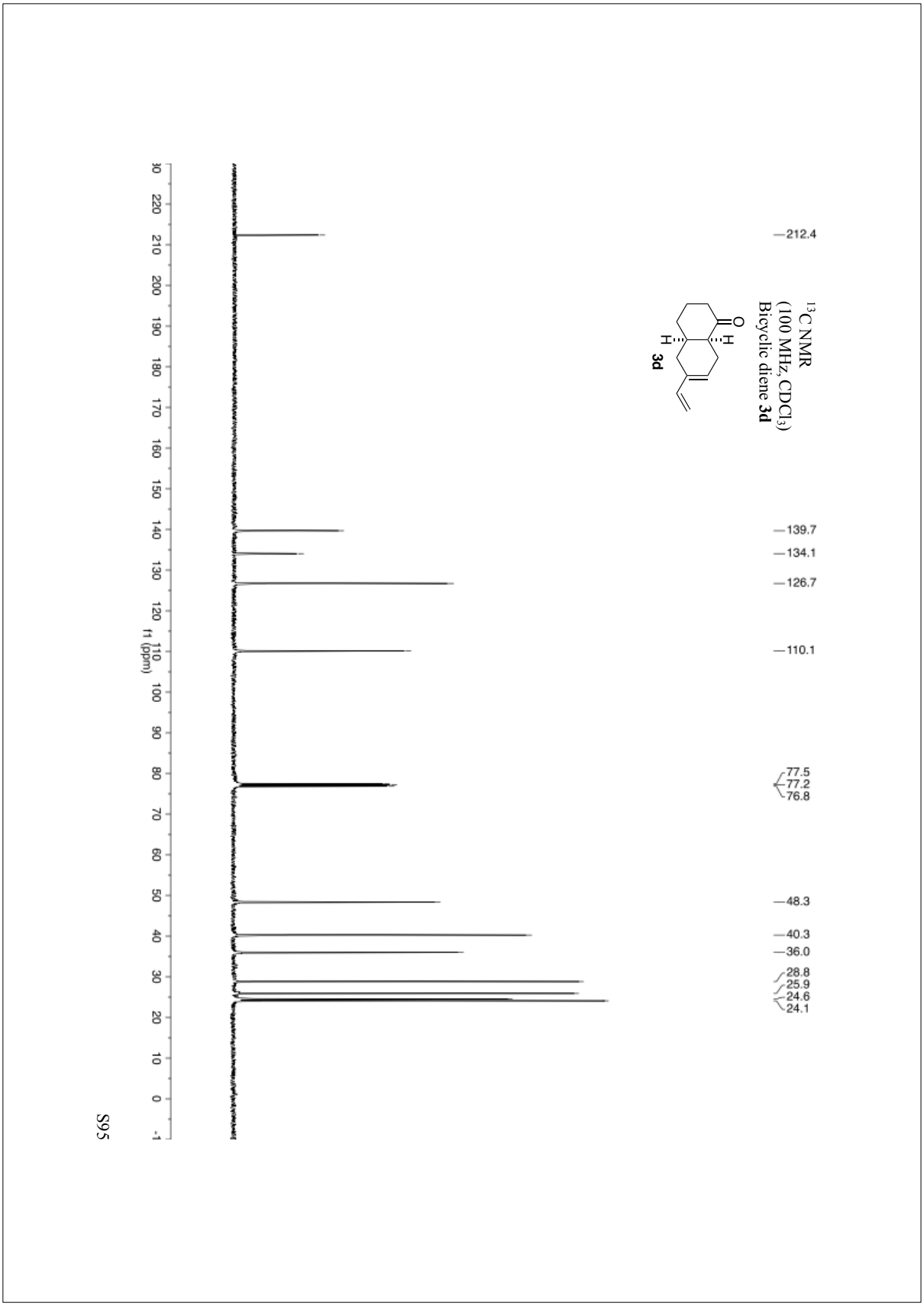
^{13}C NMR
(100 MHz, $CDCl_3$)
Bicyclic diene **3d**
3d
212.4
139.7
134.1
126.7
110.1
77.5
77.2
76.8
48.3
40.3
36.0
28.8
25.9
24.6
24.1
f1 (ppm)
S95

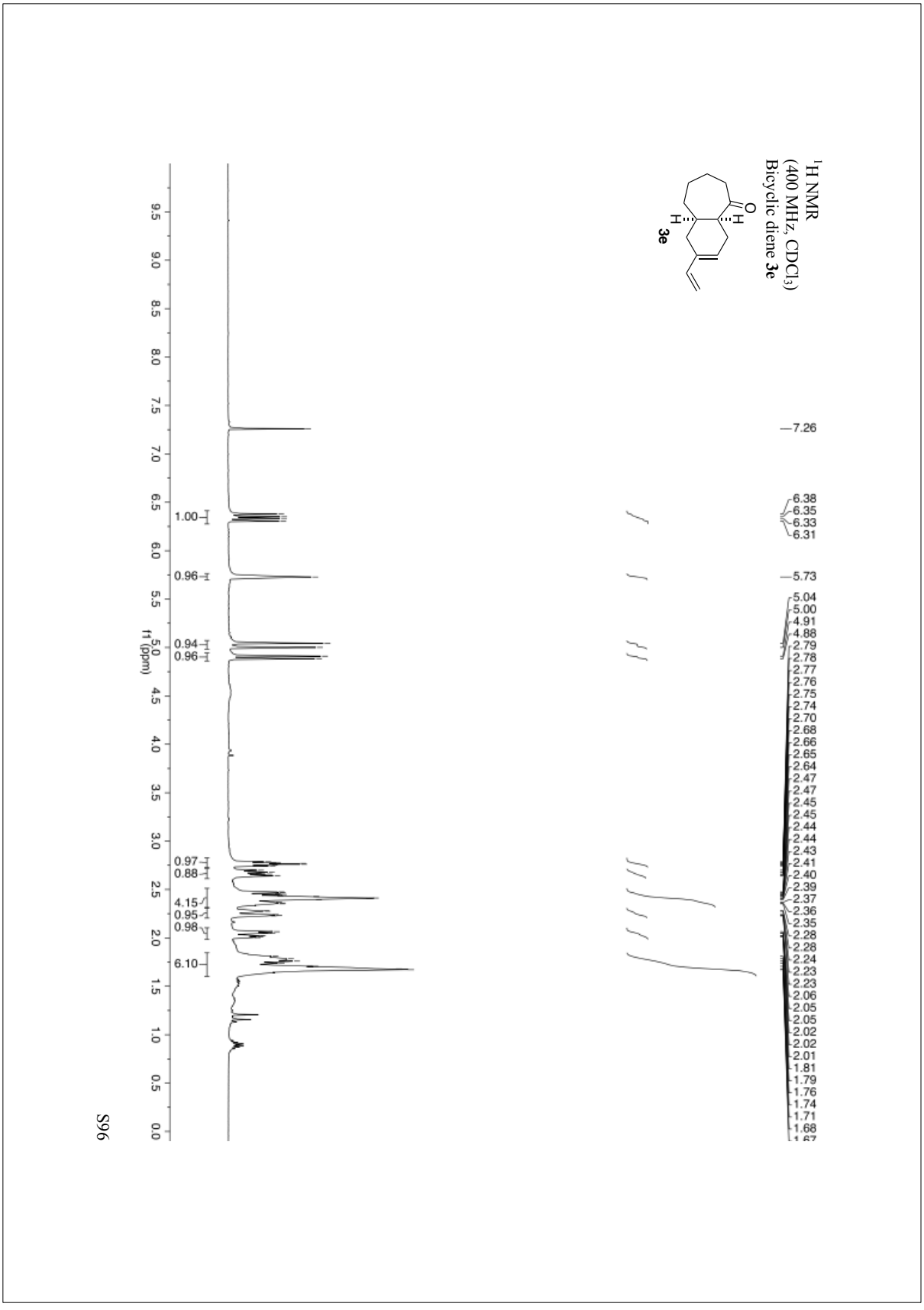
^{1}H NMR
(400 MHz, CDCl$_3$)
Bicyclic diene **3e**
3e
7.26
6.38
6.35
6.33
6.31
5.73
5.04
5.00
4.91
4.88
2.79
2.78
2.77
2.76
2.75
2.74
2.70
2.68
2.66
2.65
2.64
2.47
2.47
2.45
2.45
2.44
2.44
2.43
2.41
2.40
2.39
2.37
2.36
2.35
2.28
2.28
2.24
2.23
2.23
2.06
2.05
2.05
2.02
2.02
2.01
1.81
1.79
1.76
1.74
1.71
1.68
1.00
0.96
0.94
0.96
0.97
0.88
4.15
0.95
0.98
6.10
f1 (ppm)

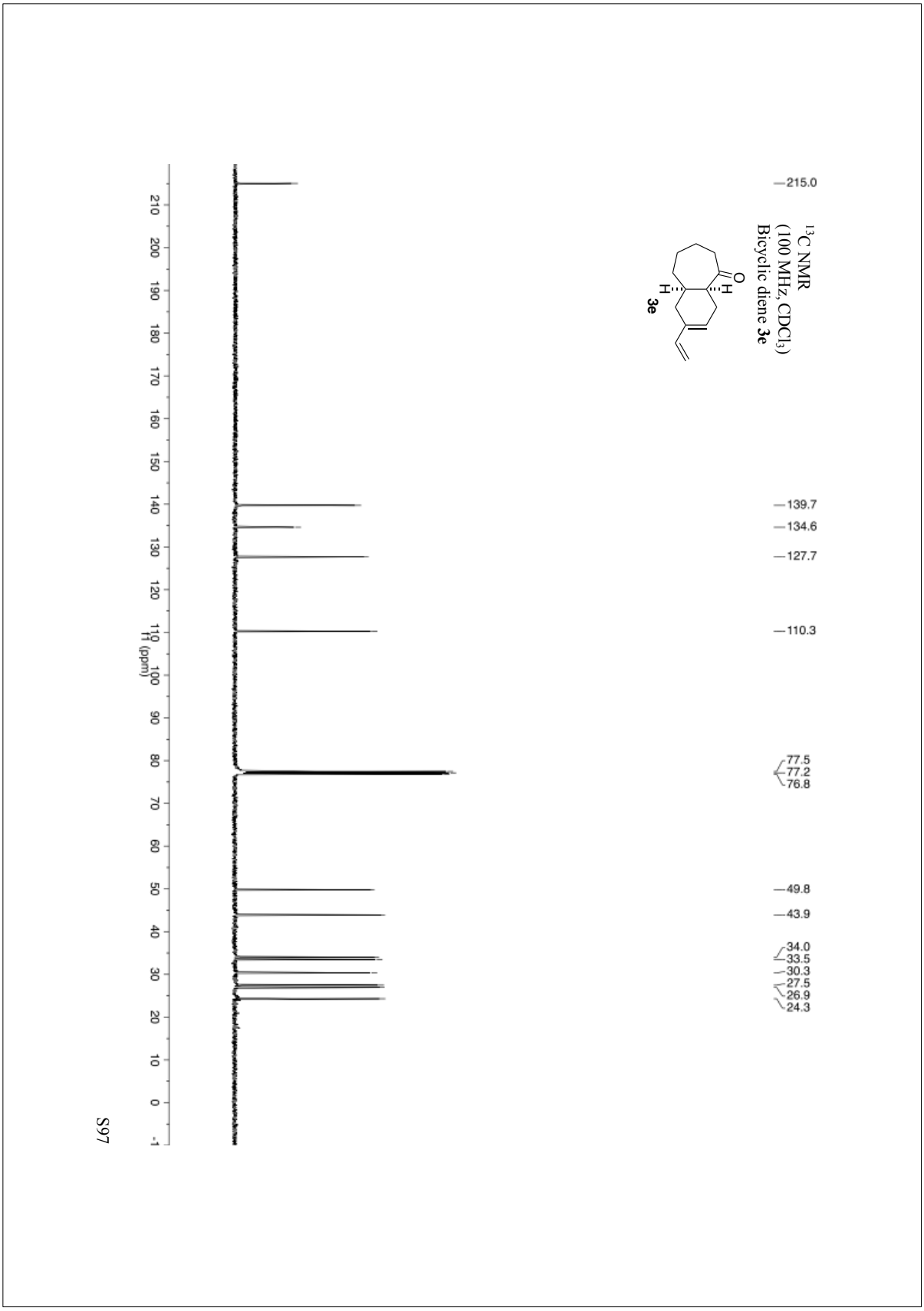
^{13}C NMR
(100 MHz, CDCl$_3$)
Bicyclic diene **3e**
3e
215.0
139.7
134.6
127.7
110.3
77.5
77.2
76.8
49.8
43.9
34.0
33.5
30.3
27.5
26.9
24.3
f1 (ppm)
S97

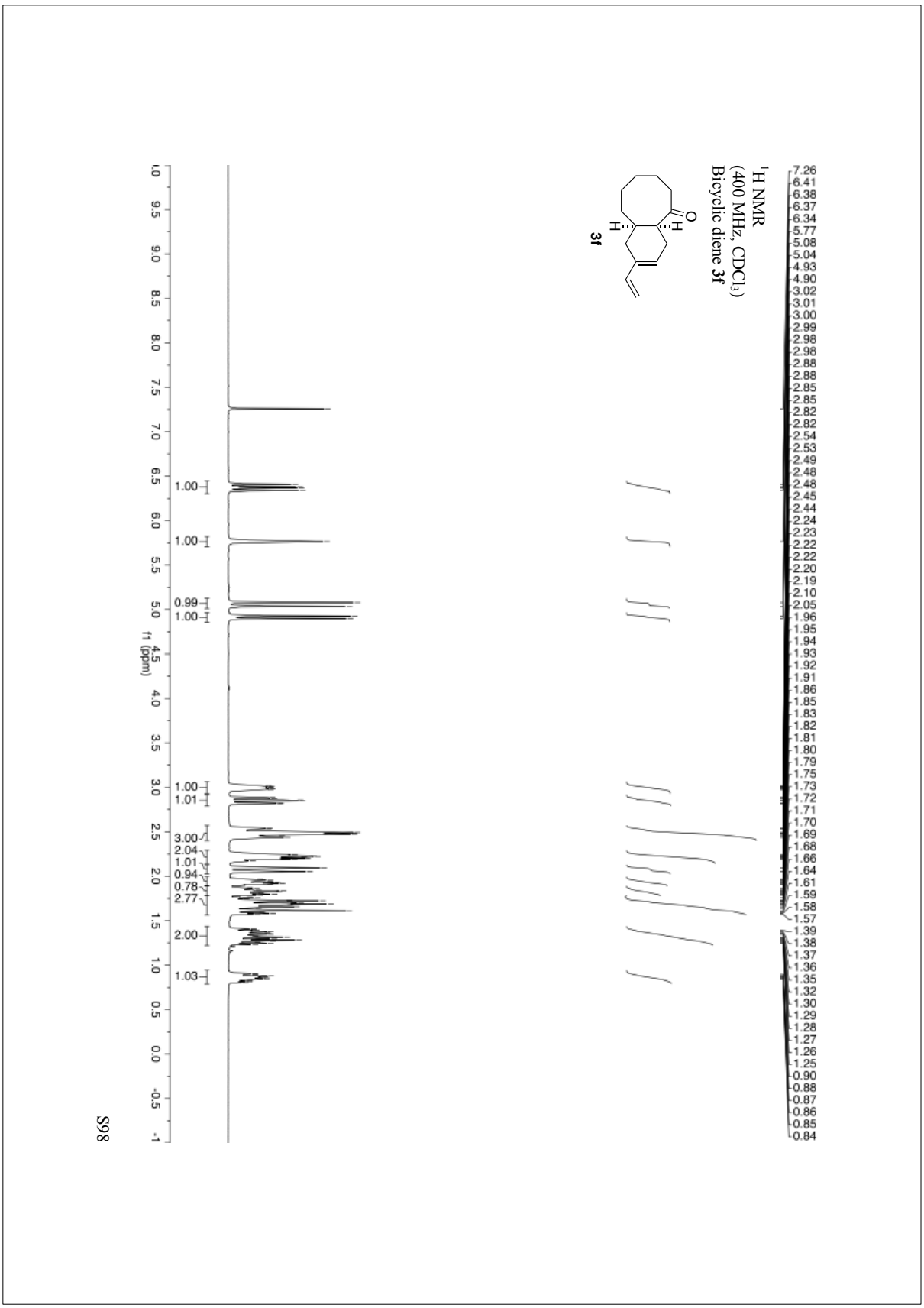
^{1}H NMR
(400 MHz, $CDCl_3$)
Bicyclic diene **3f**
3f
f1 (ppm)
1.00
1.00
0.99
1.00
1.00
1.01
3.00
2.04
1.01
0.94
0.78
2.77
2.00
1.03

S98

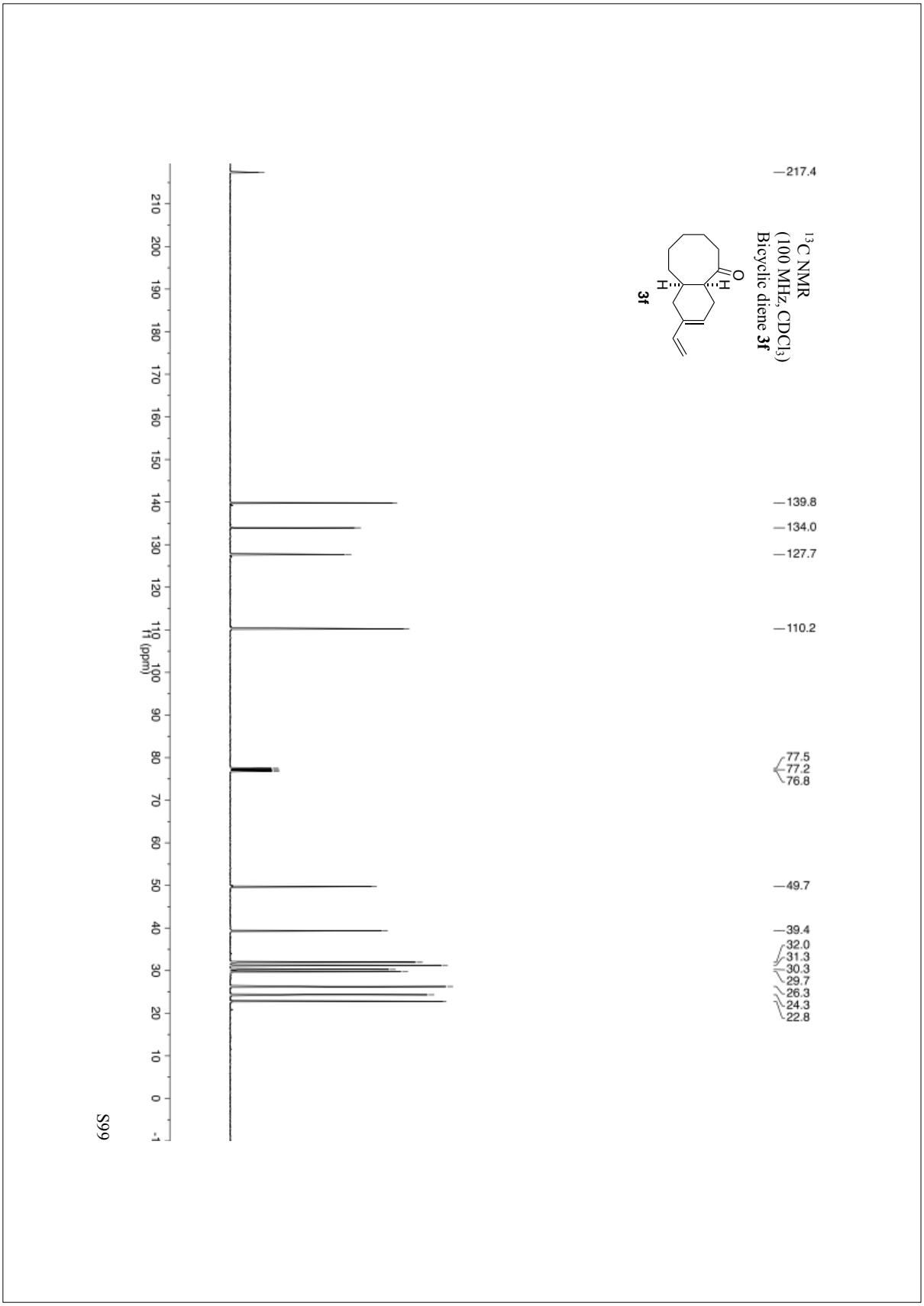
^{13}C NMR
(100 MHz, $CDCl_3$)
Bicyclic diene **3f**
3f
—217.4
—139.8
—134.0
—127.7
—110.2
77.5
77.2
76.8
—49.7
—39.4
32.0
31.3
30.3
29.7
26.3
24.3
22.8
f1 (ppm)
S99

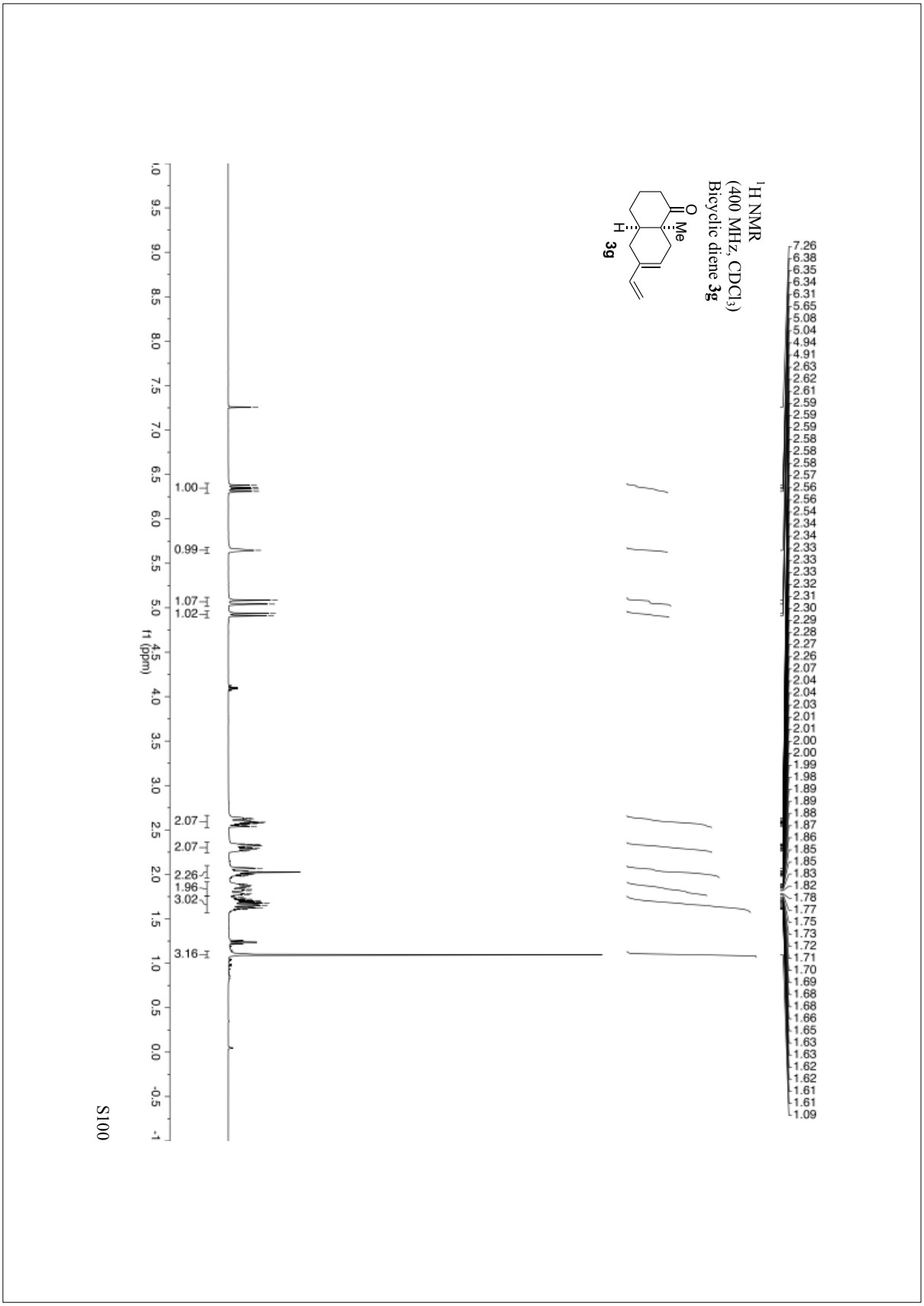
^{1}H NMR
(400 MHz, $CDCl_3$)
Bicyclic diene **3g**
O
Me
H
3g
7.26
6.38
6.35
6.34
6.31
5.65
5.08
5.04
4.94
4.91
2.63
2.62
2.61
2.59
2.59
2.59
2.59
2.58
2.58
2.58
2.57
2.56
2.56
2.54
2.34
2.34
2.33
2.33
2.33
2.32
2.31
2.30
2.29
2.28
2.27
2.26
2.07
2.04
2.04
2.03
2.01
2.01
2.00
2.00
1.99
1.98
1.89
1.89
1.89
1.88
1.87
1.86
1.85
1.85
1.83
1.82
1.78
1.77
1.75
1.73
1.72
1.71
1.70
1.69
1.68
1.68
1.66
1.65
1.63
1.63
1.62
1.62
1.61
1.61
1.09
1.00
0.99
1.07
1.02
2.07
2.07
2.26
1.96
3.02
3.16
f1 (ppm)
10.0
9.5
9.0
8.5
8.0
7.5
7.0
6.5
6.0
5.5
5.0
4.5
4.0
3.5
3.0
2.5
2.0
1.5
1.0
0.5
0.0
-0.5
-1.0

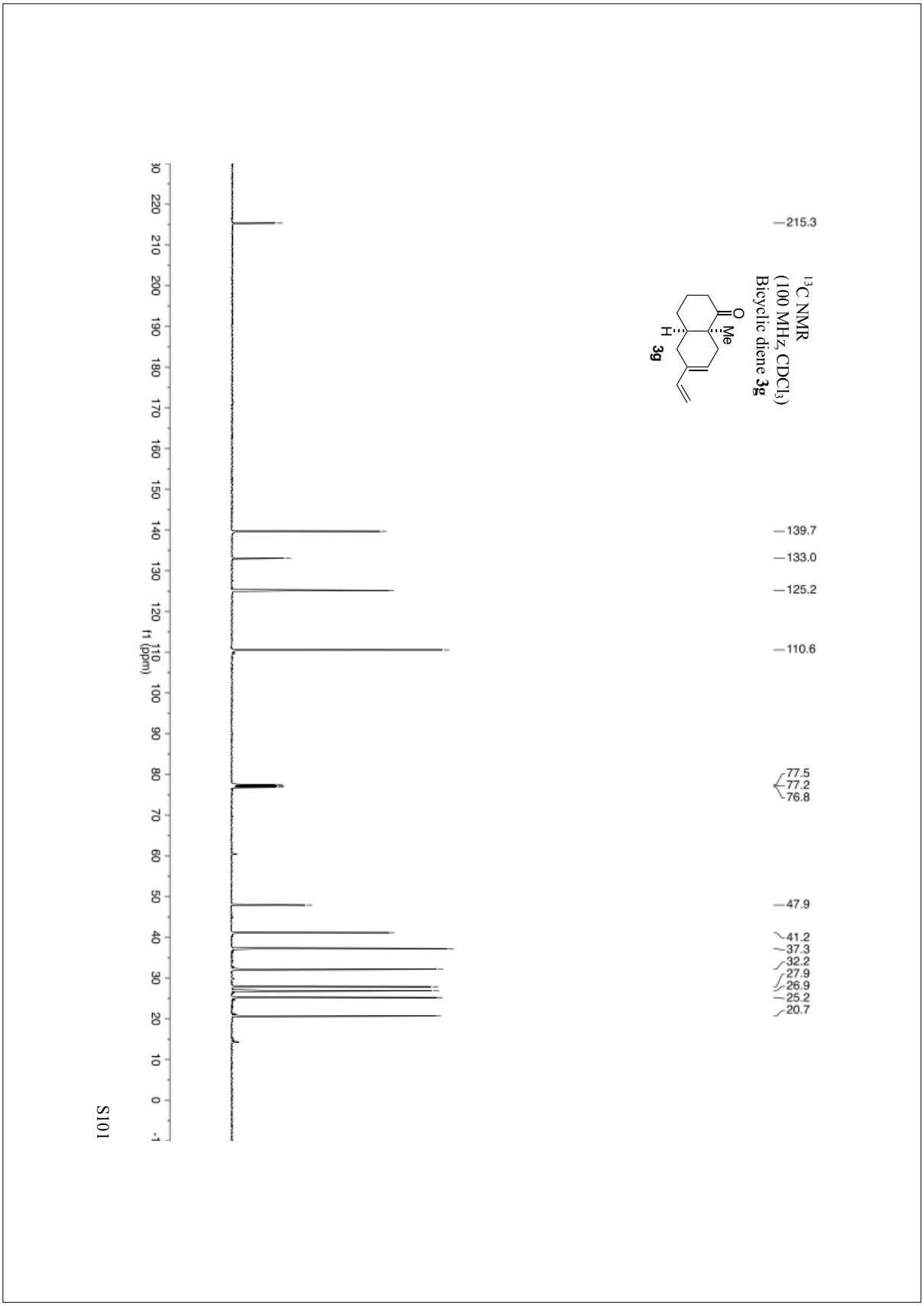
^{13}C NMR
(100 MHz, $CDCl_3$)
Bicyclic diene **3g**
O
Me
H
3g
215.3
139.7
133.0
125.2
110.6
77.5
77.2
76.8
47.9
41.2
37.3
32.2
27.9
26.9
25.2
20.7
f1 (ppm)
S101

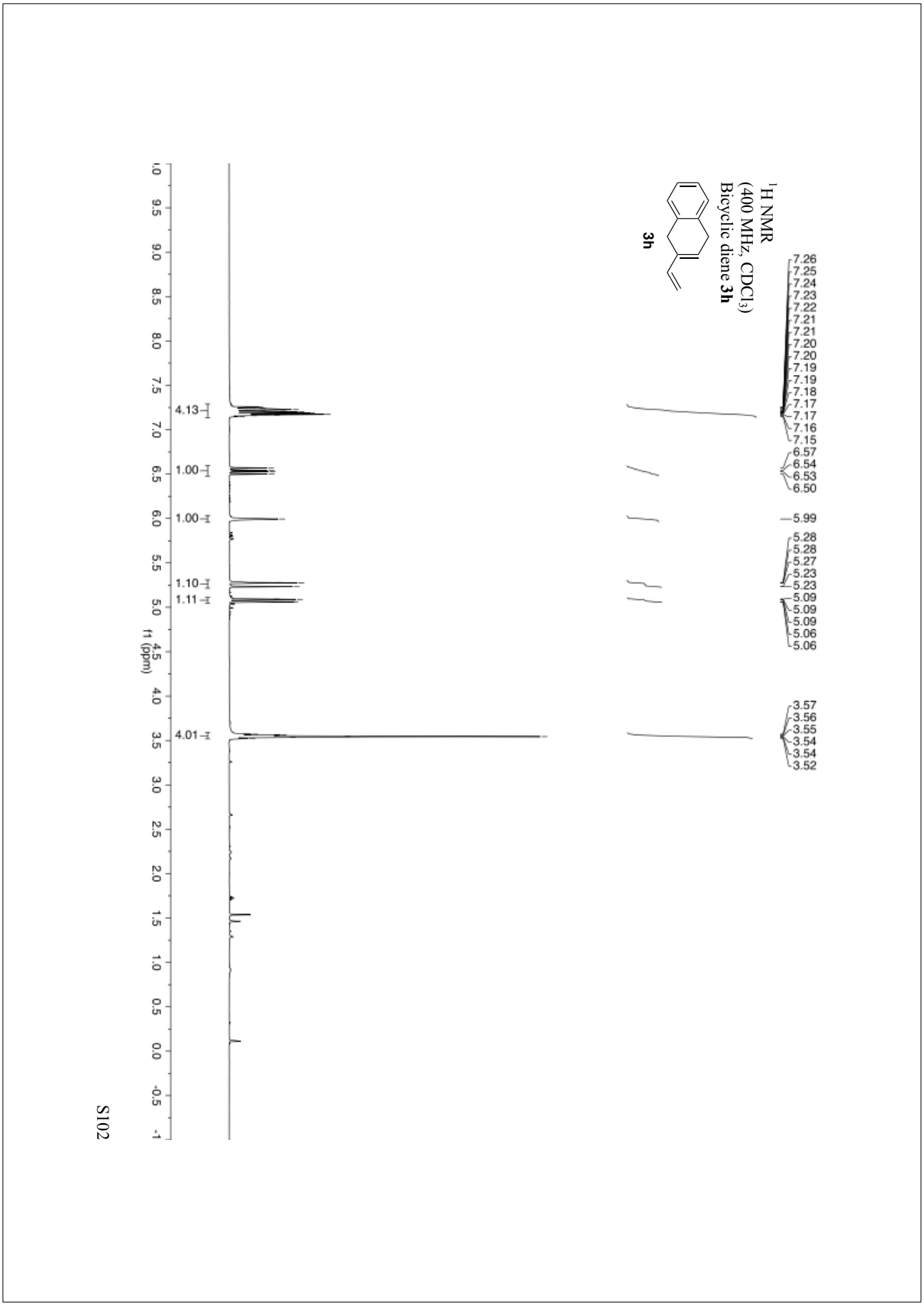
^{1}H NMR
(400 MHz, $CDCl_3$)
Bicyclic diene **3h**
3h
7.26
7.25
7.24
7.23
7.22
7.21
7.21
7.20
7.20
7.19
7.19
7.18
7.17
7.17
7.16
7.15
6.57
6.54
6.53
6.50
5.99
5.28
5.28
5.27
5.23
5.23
5.09
5.09
5.09
5.06
5.06
3.57
3.56
3.55
3.54
3.54
3.52
4.13
1.00
1.00
1.10
1.11
4.01
f1 (ppm)
S102

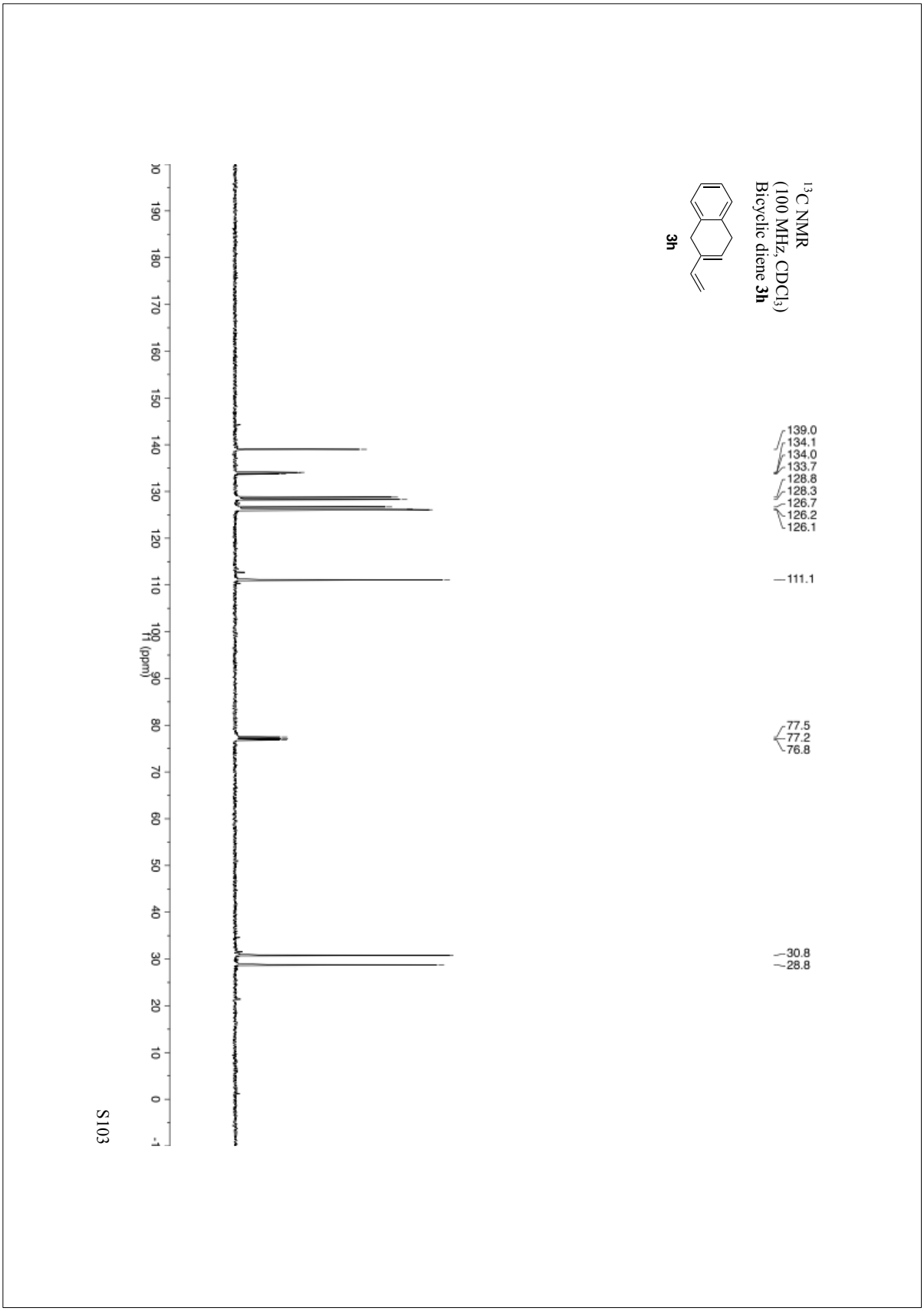
^{13}C NMR
(100 MHz, $CDCl_3$)
Bicyclic diene **3h**
3h
139.0
134.1
134.0
133.7
128.8
128.3
126.7
126.2
126.1
111.1
77.5
77.2
76.8
30.8
28.8
f1 (ppm)
S103

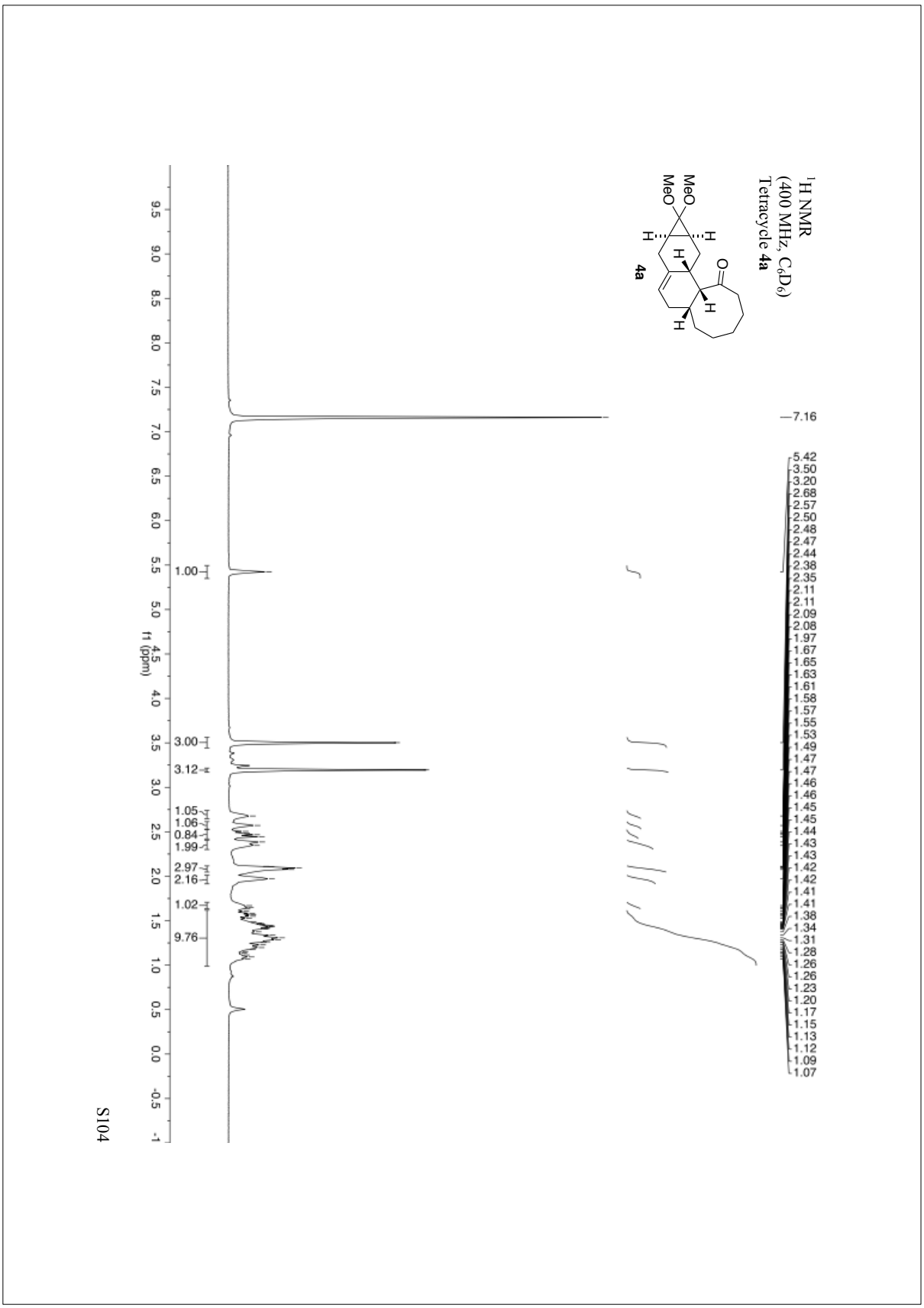
^{1}H NMR
(400 MHz, C_6D_6)
Tetracycle **4a**
MeO
MeO
H
H
H
H
H
O
4a
7.16
5.42
3.50
3.20
2.68
2.57
2.50
2.48
2.47
2.44
2.38
2.35
2.11
2.11
2.09
2.08
1.97
1.67
1.65
1.63
1.61
1.58
1.57
1.55
1.53
1.49
1.47
1.47
1.46
1.46
1.45
1.45
1.44
1.43
1.43
1.42
1.42
1.41
1.41
1.38
1.34
1.31
1.28
1.26
1.26
1.23
1.20
1.17
1.15
1.13
1.12
1.09
1.07
1.00
3.00
3.12
1.05
1.06
0.84
1.99
2.97
2.16
1.02
9.76
f1 (ppm)
9.5
9.0
8.5
8.0
7.5
7.0
6.5
6.0
5.5
5.0
4.5
4.0
3.5
3.0
2.5
2.0
1.5
1.0
0.5
0.0
-0.5
-1

S104

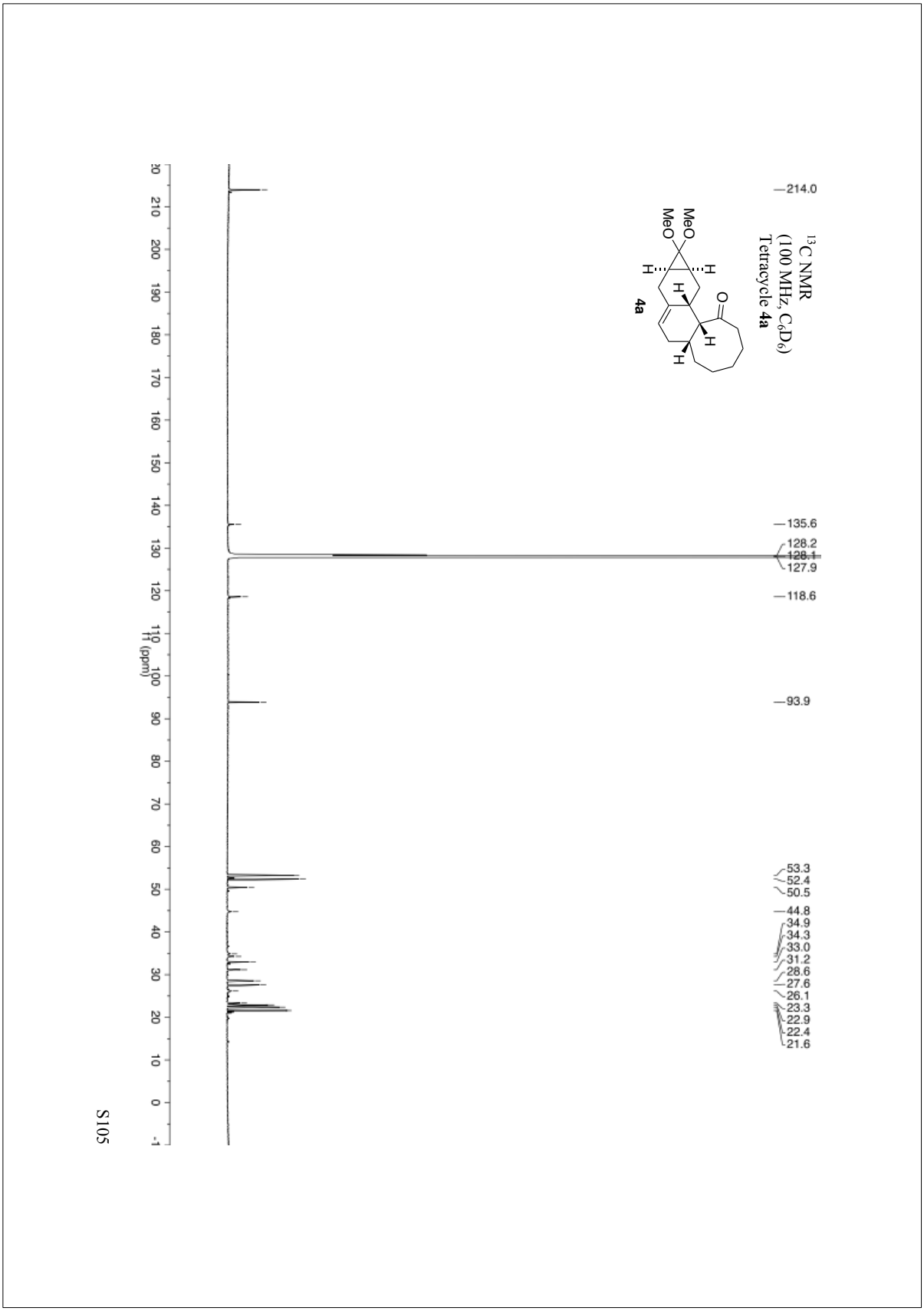
^{13}C NMR
(100 MHz, C_6D_6)
Tetracycle **4a**
MeO
MeO
H
H
H
H
O
H
H
4a
214.0
135.6
128.2
128.1
127.9
118.6
93.9
53.3
52.4
50.5
44.8
34.9
34.3
33.0
31.2
28.6
27.6
26.1
23.3
22.9
22.4
21.6
f1 (ppm)
S105

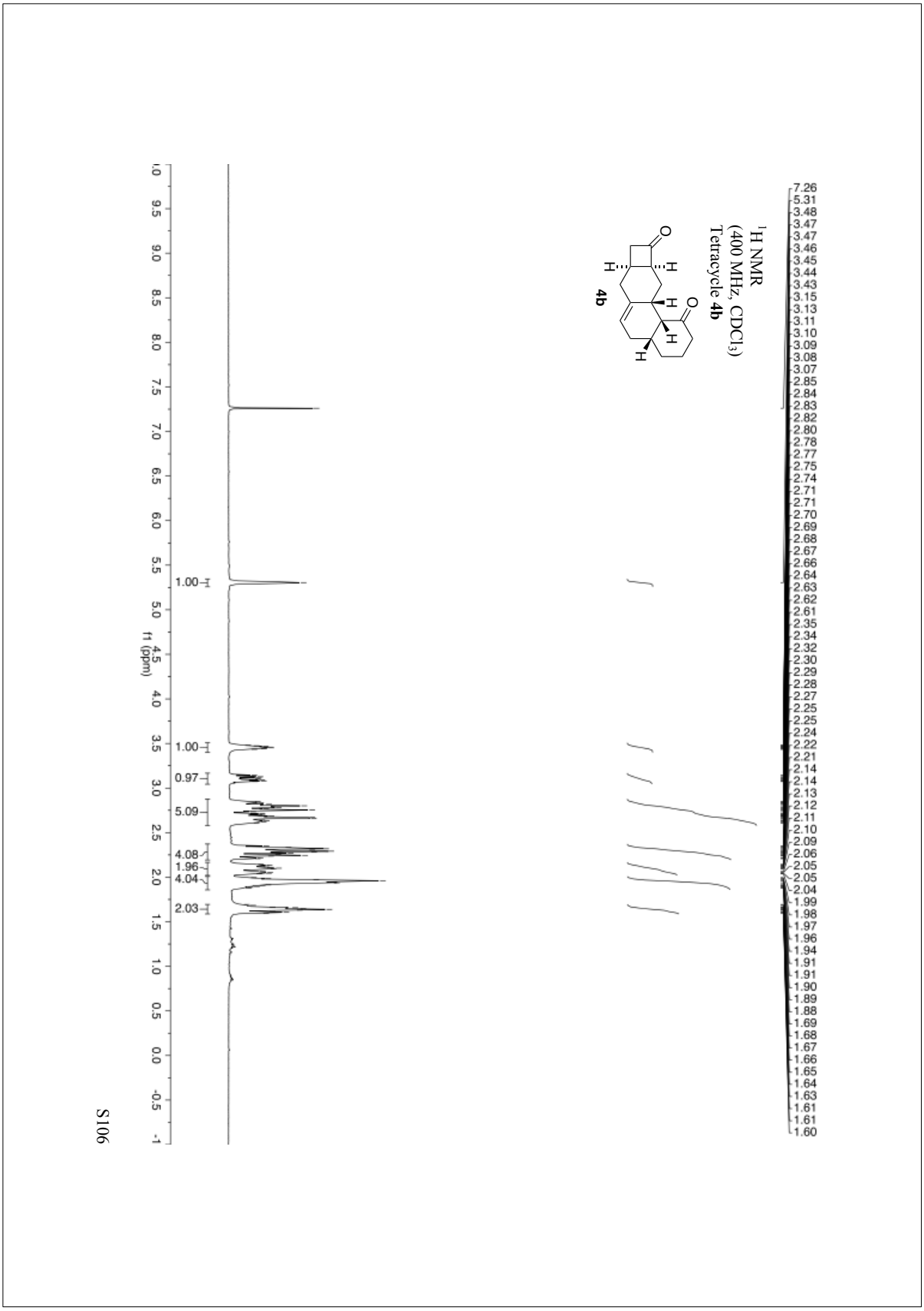
^{1}H NMR
(400 MHz, $CDCl_3$)
Tetracycle **4b**
4b
7.26
5.31
3.48
3.47
3.47
3.46
3.45
3.44
3.43
3.15
3.13
3.11
3.10
3.09
3.08
3.07
2.85
2.84
2.83
2.82
2.80
2.78
2.77
2.75
2.74
2.71
2.71
2.70
2.69
2.68
2.67
2.66
2.64
2.63
2.62
2.61
2.35
2.34
2.32
2.30
2.29
2.28
2.27
2.25
2.25
2.24
2.22
2.21
2.14
2.14
2.13
2.12
2.11
2.10
2.09
2.06
2.05
2.05
2.04
1.99
1.98
1.97
1.96
1.94
1.91
1.91
1.90
1.89
1.88
1.69
1.68
1.67
1.66
1.65
1.64
1.63
1.61
1.61
1.60
1.00
1.00
0.97
5.09
4.08
1.96
4.04
2.03
f1 (ppm)
S106

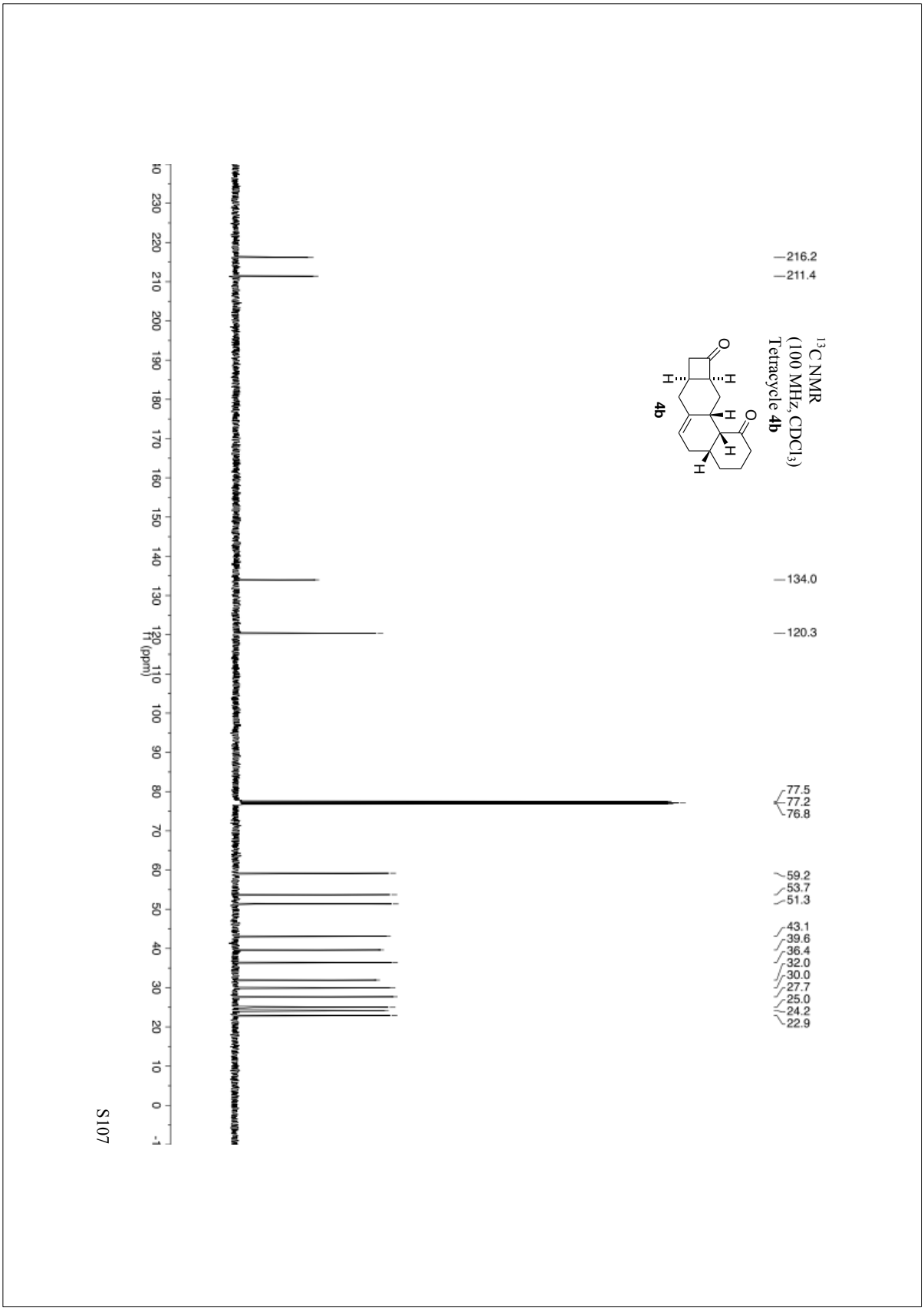
^{13}C NMR
(100 MHz, CDCl$_3$)
Tetracycle **4b**
4b
216.2
211.4
134.0
120.3
77.5
77.2
76.8
59.2
53.7
51.3
43.1
39.6
36.4
32.0
30.0
27.7
25.0
24.2
22.9
f1 (ppm)
S107

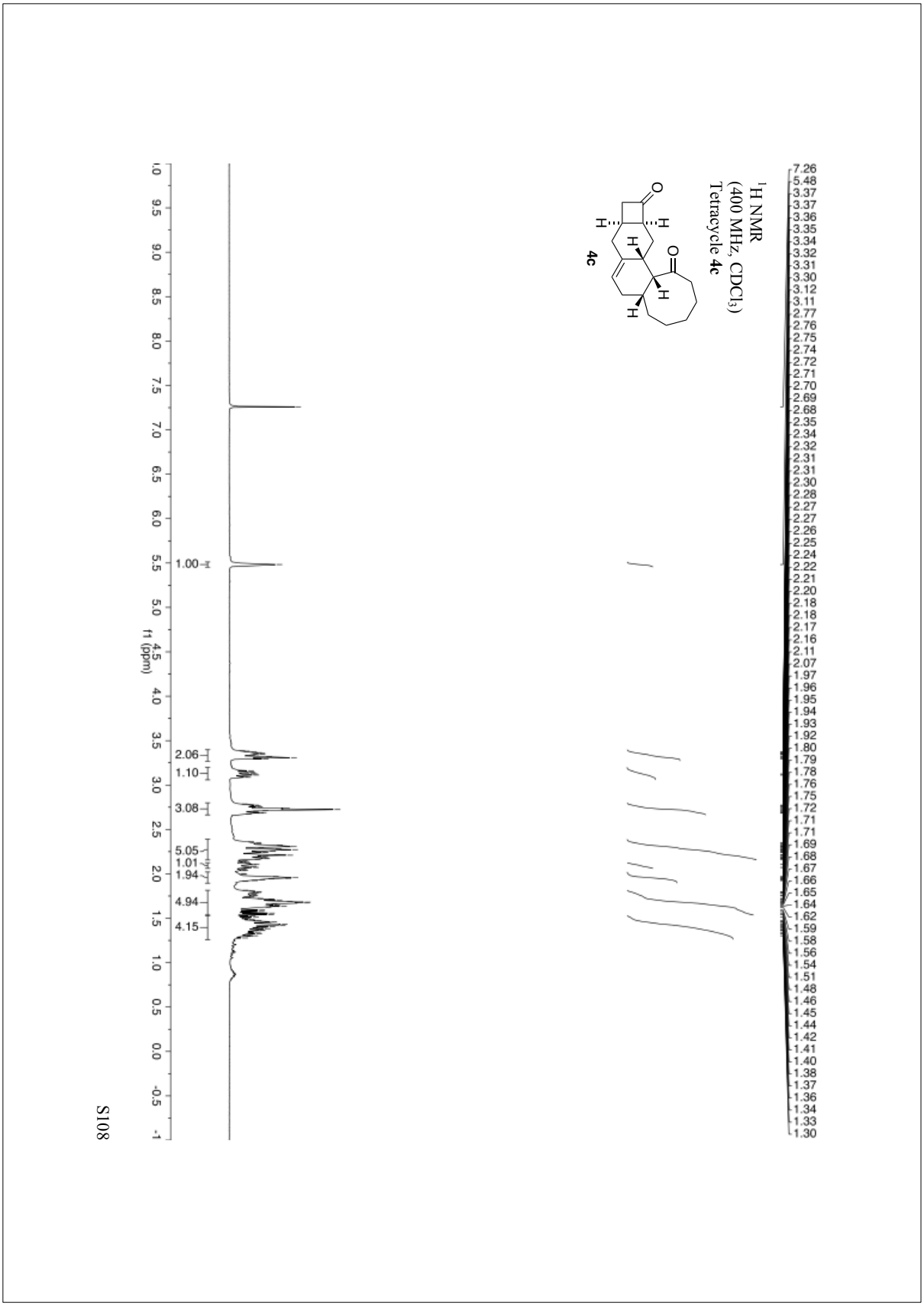
^{1}H NMR
(400 MHz, $CDCl_3$)
Tetracycle **4c**
4c
f1 (ppm)
1.00
2.06
1.10
3.08
5.05
1.01
1.94
4.94
4.15
S108

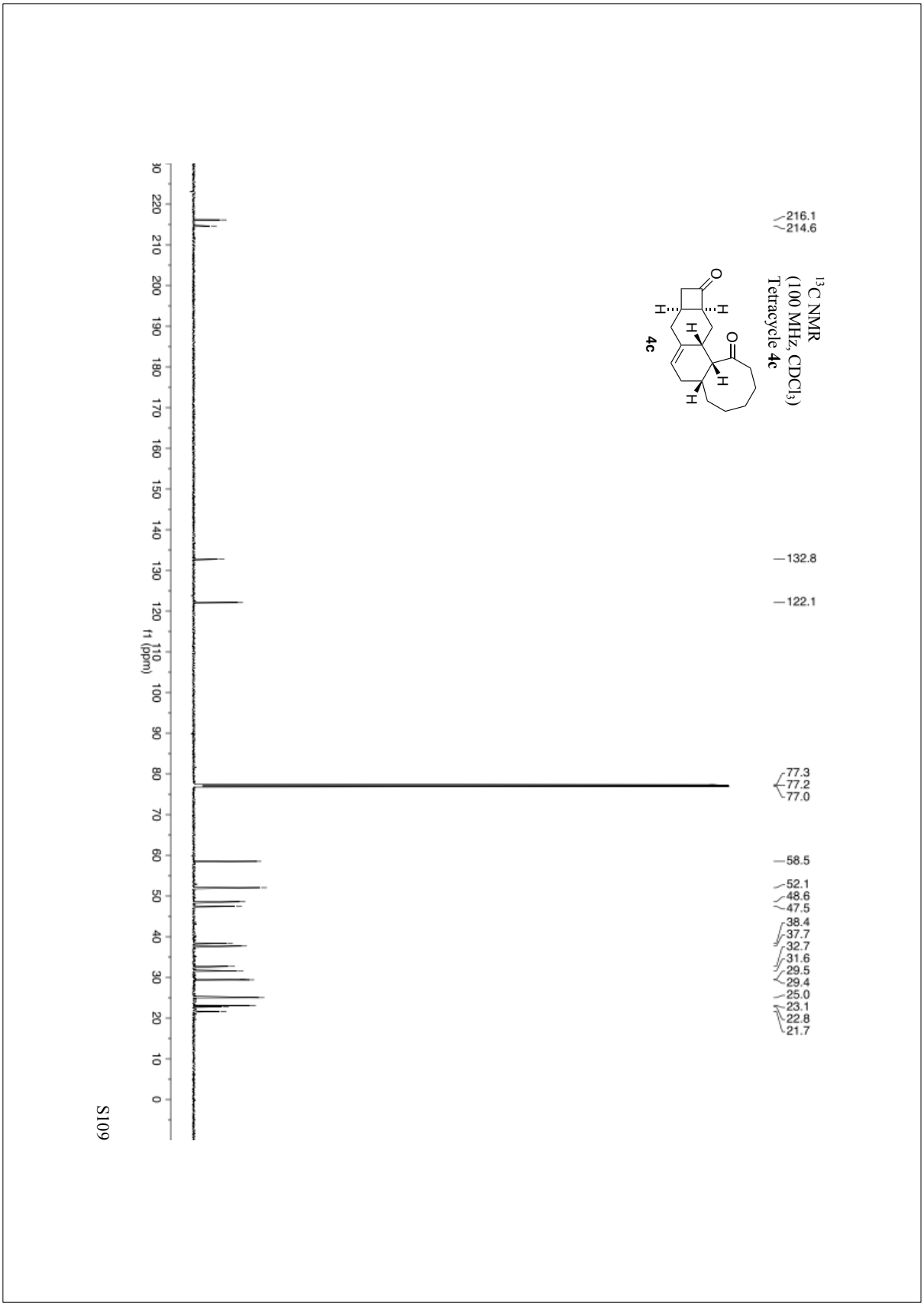
^{13}C NMR
(100 MHz, CDCl$_3$)
Tetracycle **4c**
4c
216.1
214.6
132.8
122.1
77.3
77.2
77.0
58.5
52.1
48.6
47.5
38.4
37.7
32.7
31.6
29.5
29.4
25.0
23.1
22.8
21.7
f1 (ppm)
S109

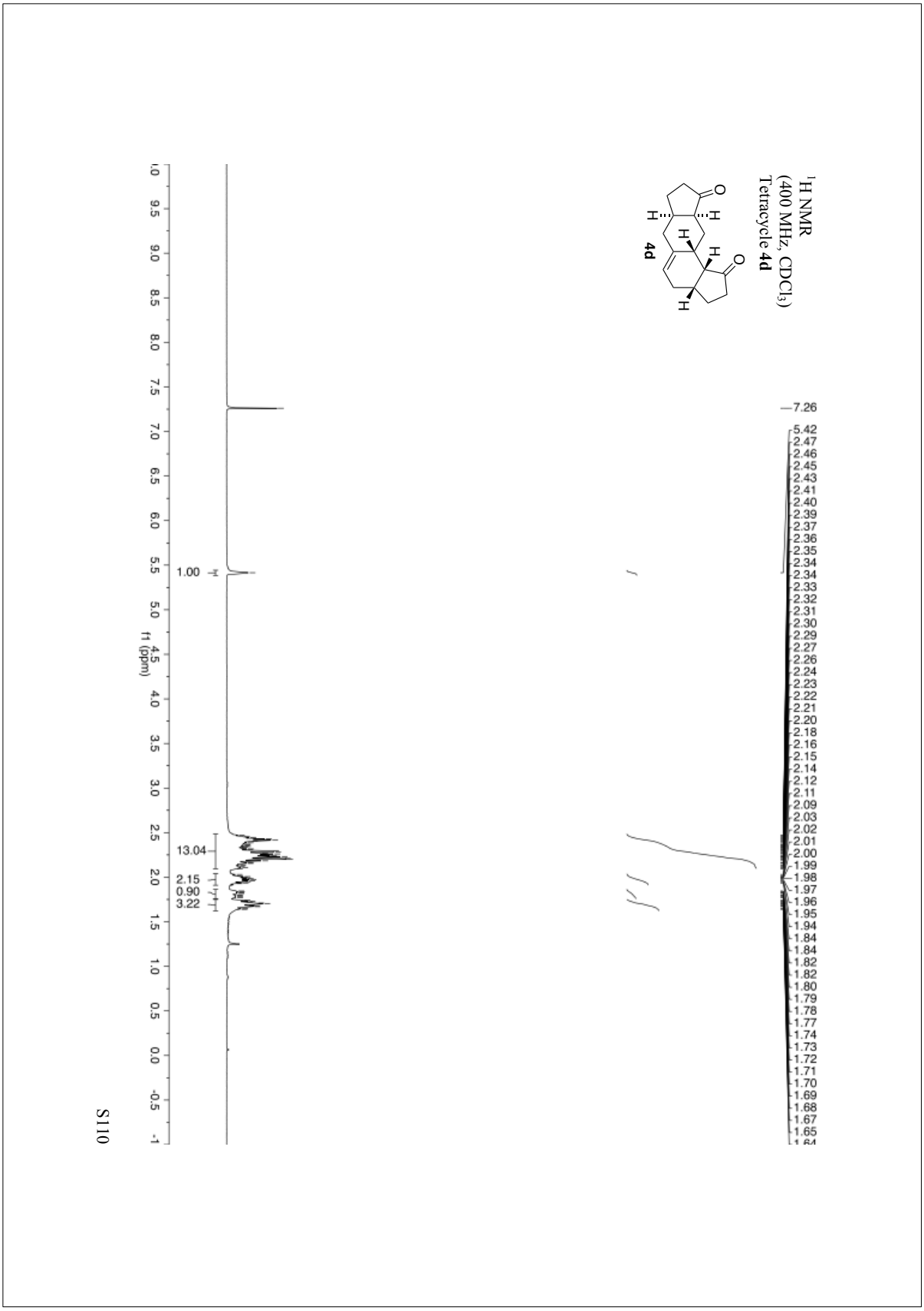
^{1}H NMR
(400 MHz, $CDCl_3$)
Tetracycle **4d**
4d
7.26
5.42
2.47
2.46
2.45
2.43
2.41
2.40
2.39
2.37
2.36
2.35
2.34
2.34
2.33
2.32
2.31
2.30
2.29
2.27
2.26
2.24
2.23
2.22
2.21
2.20
2.18
2.16
2.15
2.14
2.12
2.11
2.09
2.03
2.02
2.01
2.00
1.99
1.98
1.97
1.96
1.95
1.94
1.84
1.84
1.82
1.82
1.80
1.79
1.78
1.77
1.74
1.73
1.72
1.71
1.70
1.69
1.68
1.67
1.65
1.00
13.04
2.15
0.90
3.22
f1 (ppm)

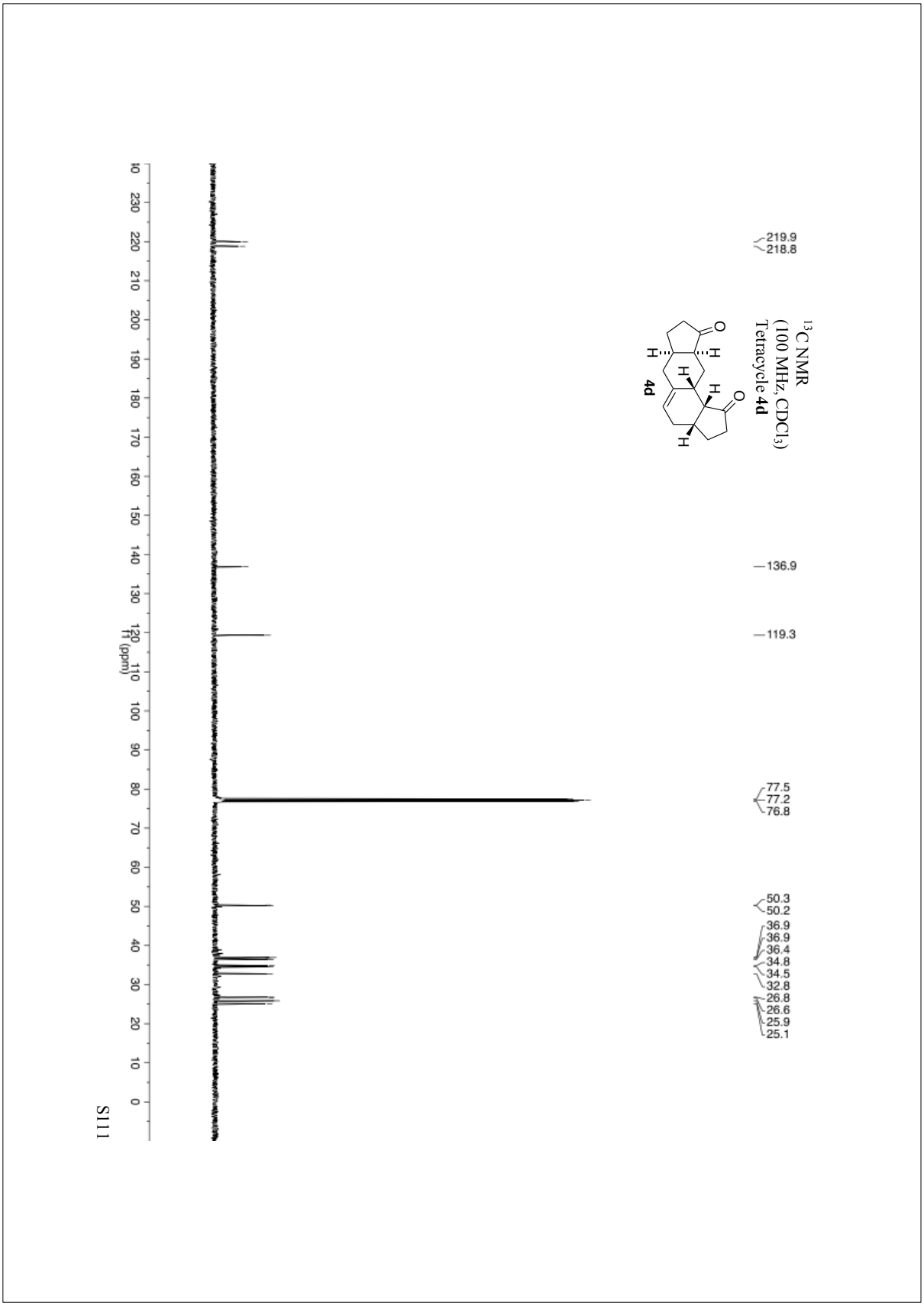
^{13}C NMR
(100 MHz, CDCl$_3$)
Tetracycle **4d**
4d
219.9
218.8
136.9
119.3
77.5
77.2
76.8
50.3
50.2
36.9
36.9
36.4
34.8
34.5
32.8
26.8
26.6
25.9
25.1
f1 (ppm)
S111

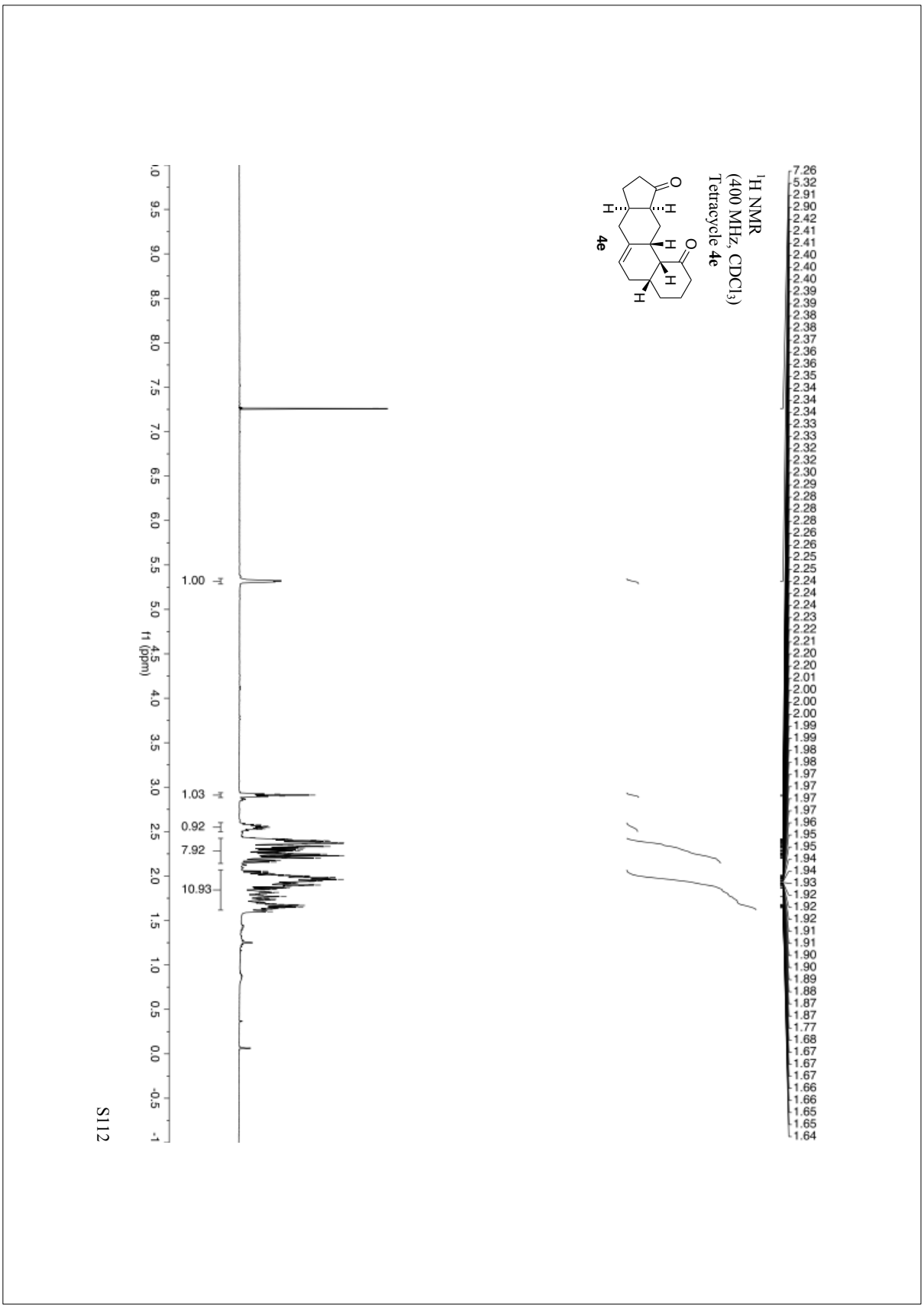
^{1}H NMR
(400 MHz, $CDCl_3$)
Tetracycle **4e**
4e
f1 (ppm)
1.00
1.03
0.92
7.92
10.93
S112

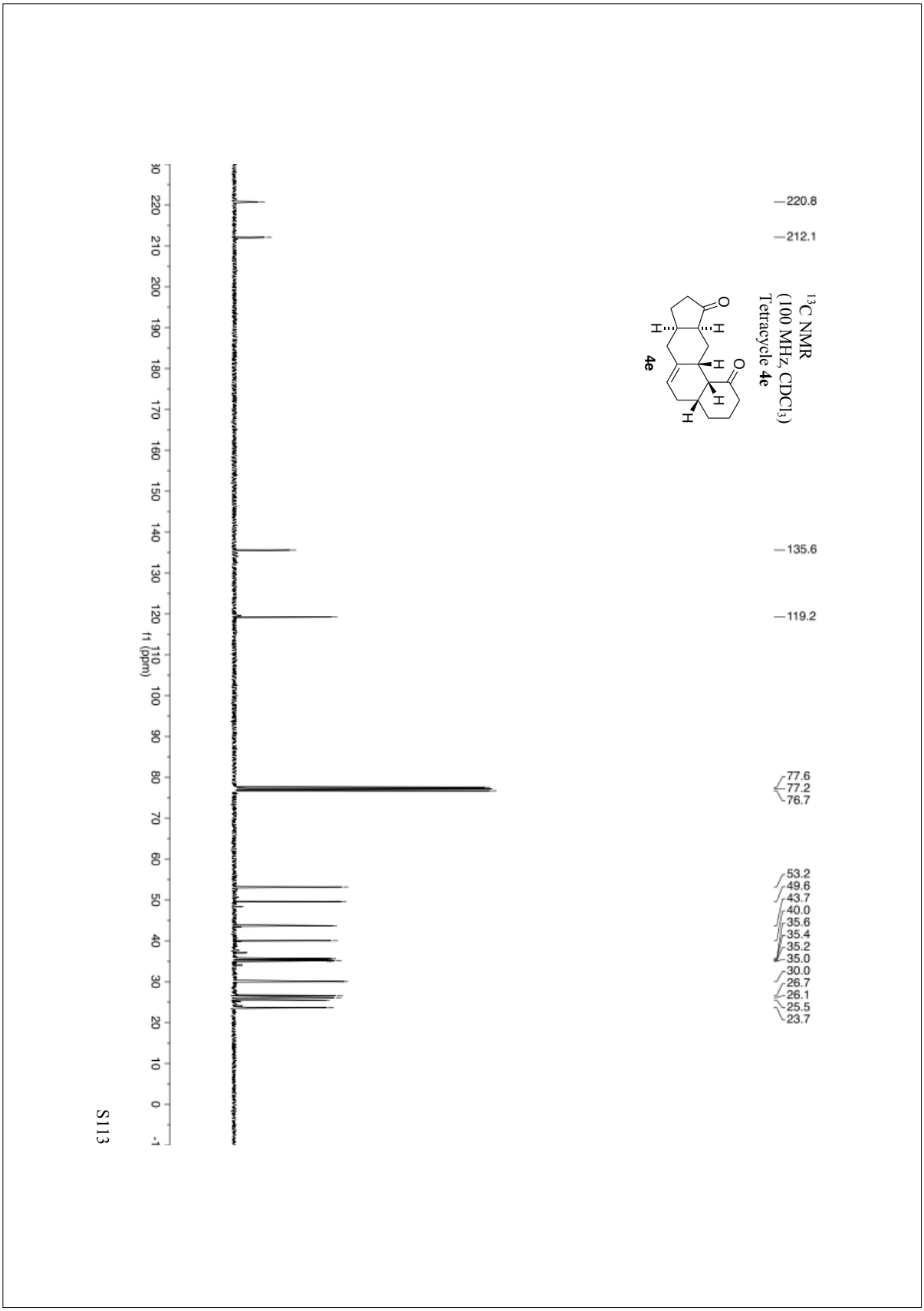
^{13}C NMR
(100 MHz, $CDCl_3$)
Tetracycle **4e**
4e
220.8
212.1
135.6
119.2
77.6
77.2
76.7
53.2
49.6
43.7
40.0
35.6
35.4
35.2
35.0
30.0
26.7
26.1
25.5
23.7
f1 (ppm)
S113

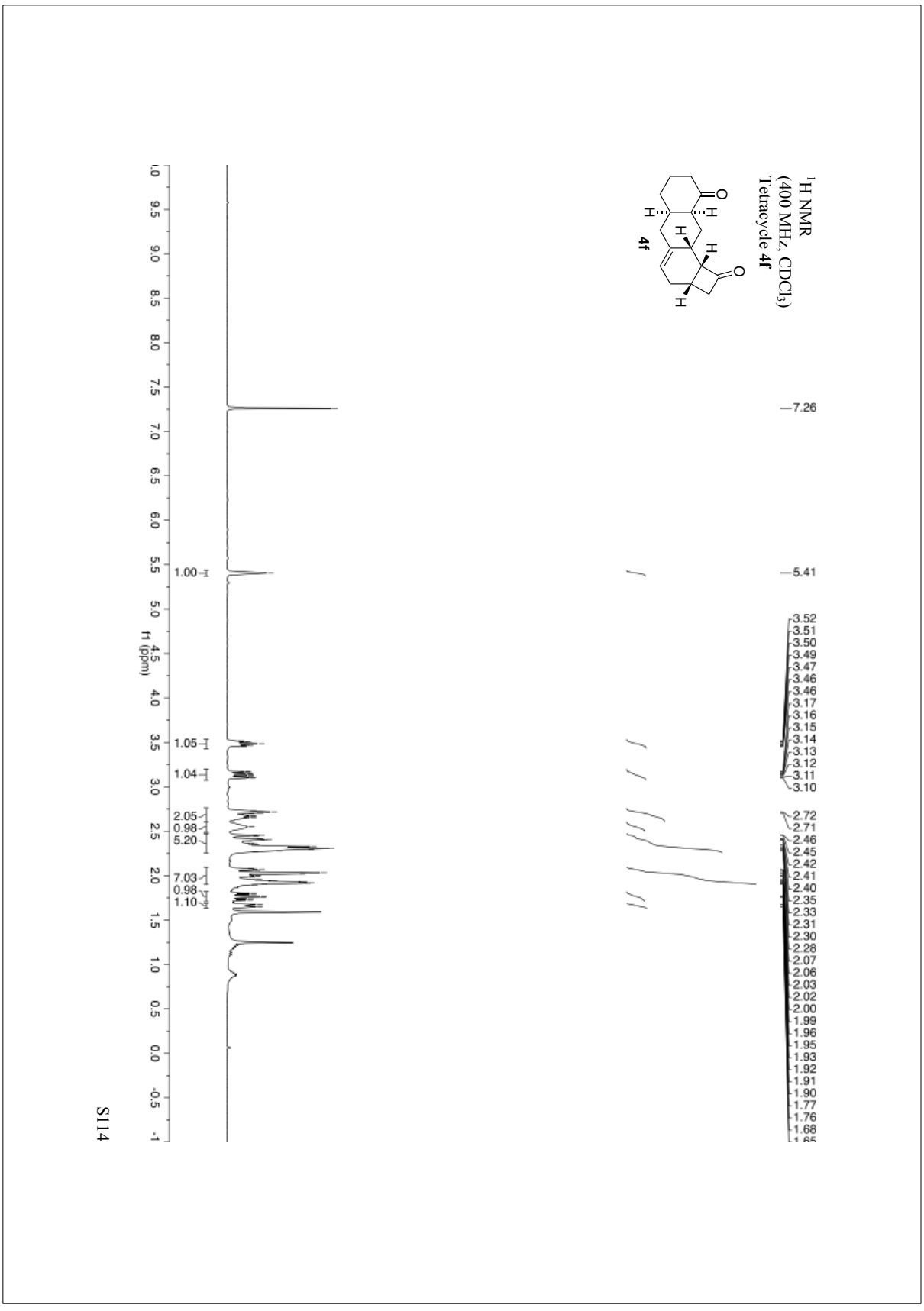
^{1}H NMR
(400 MHz, $CDCl_3$)
Tetracycle **4f**
4f
7.26
5.41
3.52
3.51
3.50
3.49
3.47
3.46
3.46
3.17
3.16
3.15
3.14
3.13
3.12
3.11
3.10
2.72
2.71
2.46
2.45
2.42
2.41
2.40
2.35
2.33
2.31
2.30
2.28
2.07
2.06
2.03
2.02
2.00
1.99
1.96
1.95
1.93
1.92
1.91
1.90
1.77
1.76
1.68
1.00
1.05
1.04
2.05
0.98
5.20
7.03
0.98
1.10
f1 (ppm)
S114

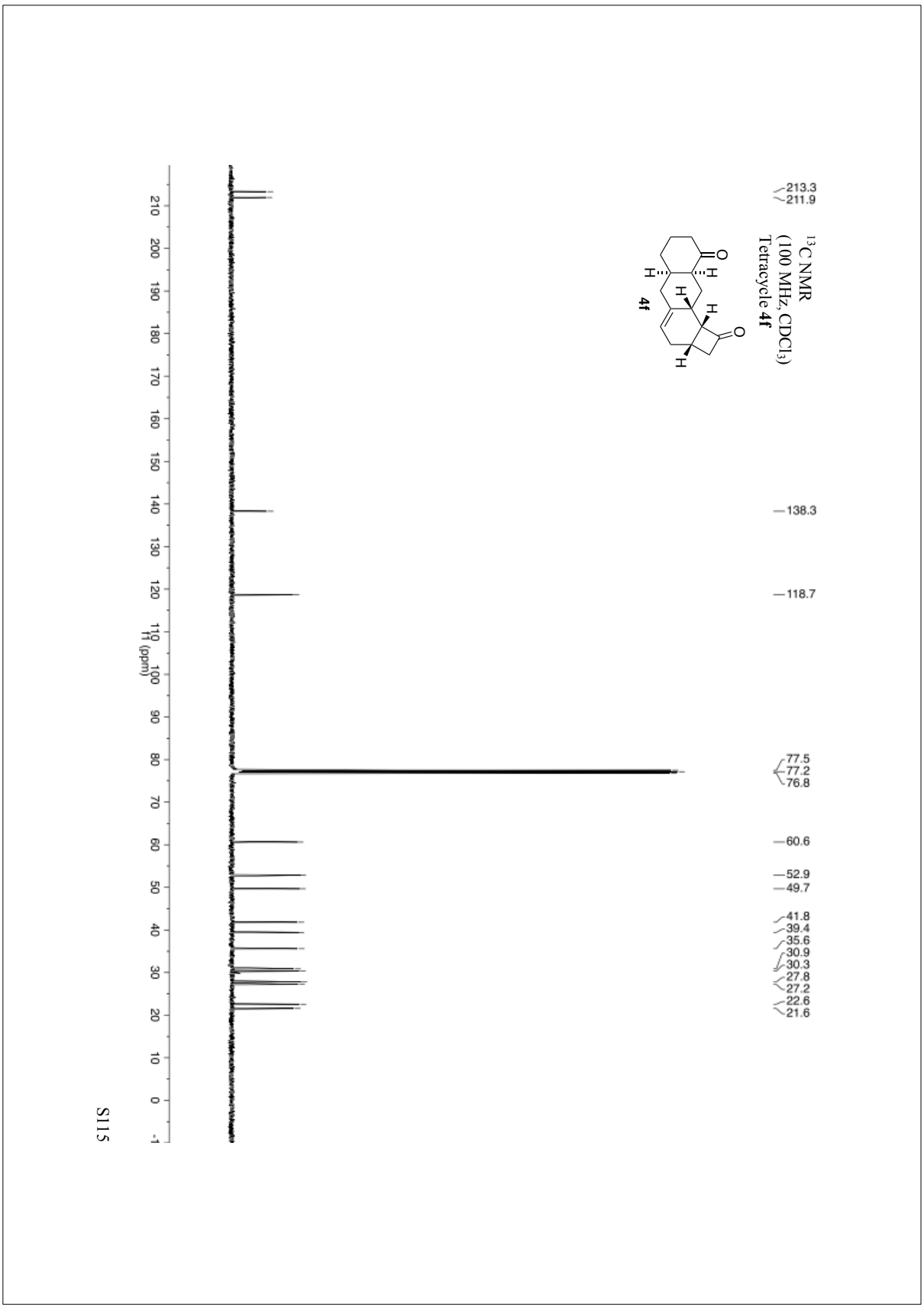
^{13}C NMR
(100 MHz, CDCl$_3$)
Tetracycle **4f**
4f
213.3
211.9
138.3
118.7
77.5
77.2
76.8
60.6
52.9
49.7
41.8
39.4
35.6
30.9
30.3
27.8
27.2
22.6
21.6
f1 (ppm)
S115

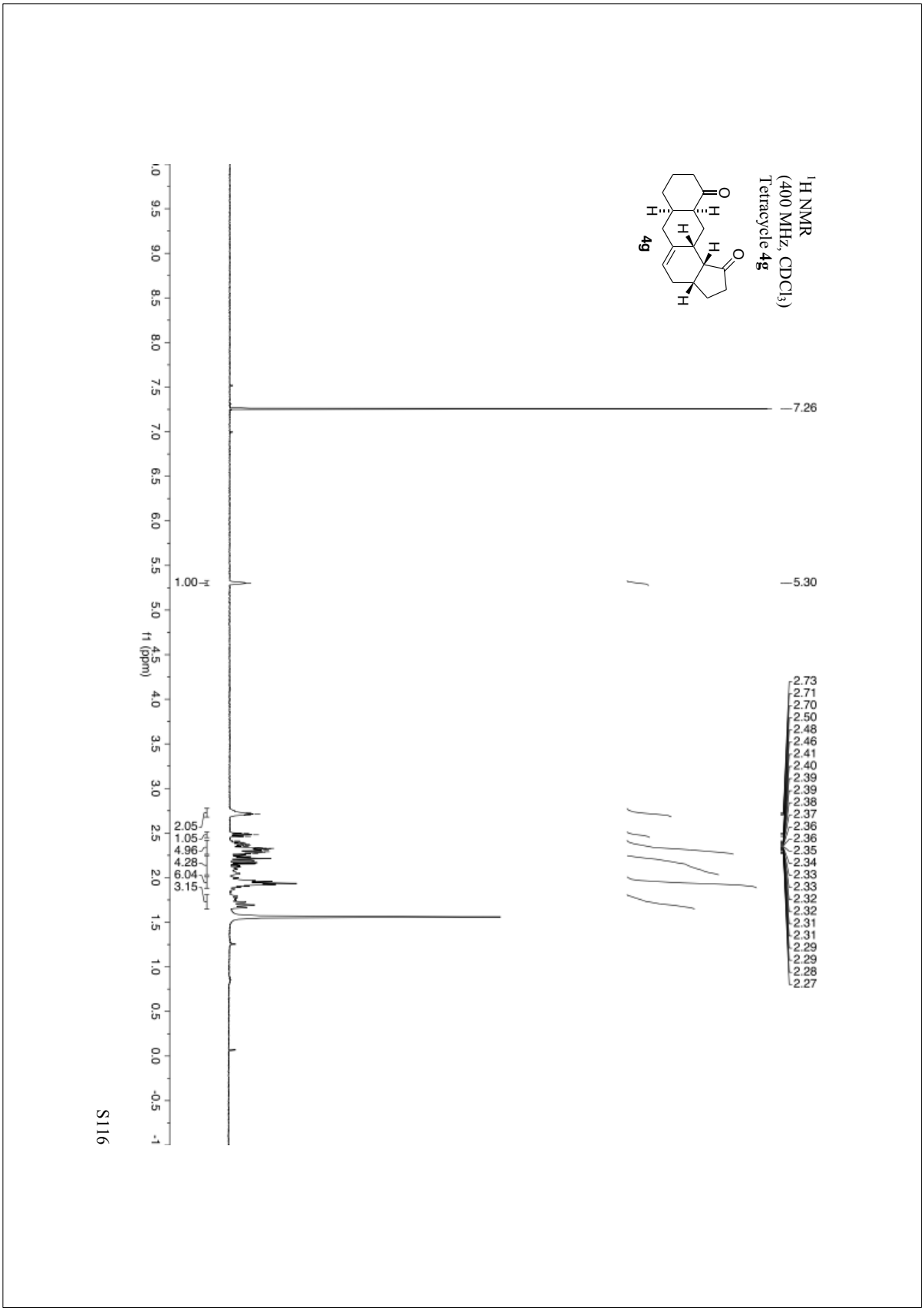
^{1}H NMR
(400 MHz, $CDCl_3$)
Tetracycle **4g**
4g
7.26
5.30
2.73
2.71
2.70
2.50
2.48
2.46
2.41
2.40
2.39
2.39
2.38
2.37
2.36
2.36
2.35
2.34
2.33
2.33
2.32
2.32
2.31
2.31
2.29
2.29
2.28
2.27
1.00
2.05
1.05
4.96
4.28
6.04
3.15
f1 (ppm)

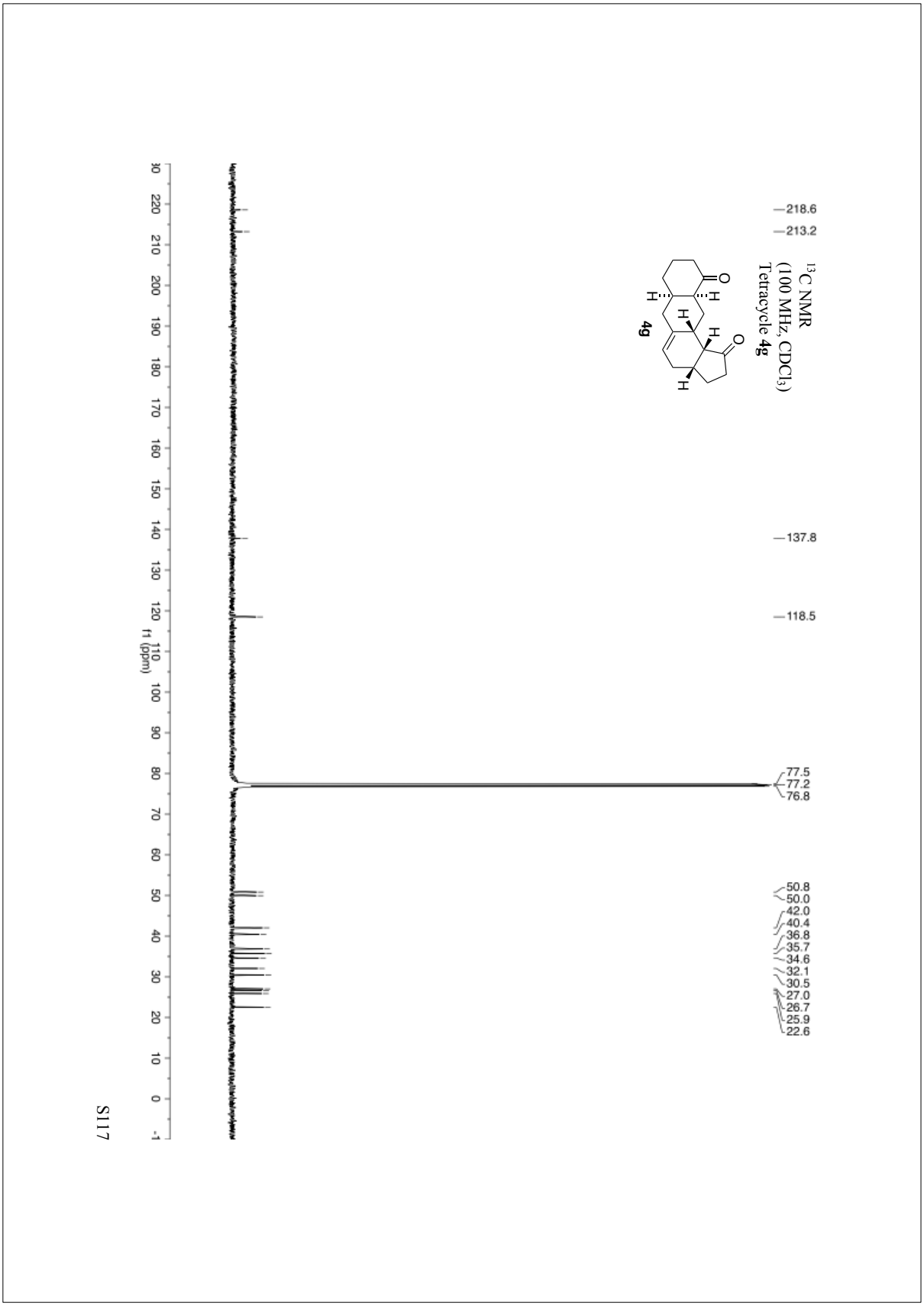
^{13}C NMR
(100 MHz, CDCl$_3$)
Tetracycle **4g**
4g
218.6
213.2
137.8
118.5
77.5
77.2
76.8
50.8
50.0
42.0
40.4
36.8
35.7
34.6
32.1
30.5
27.0
26.7
25.9
22.6
f1 (ppm)
S117

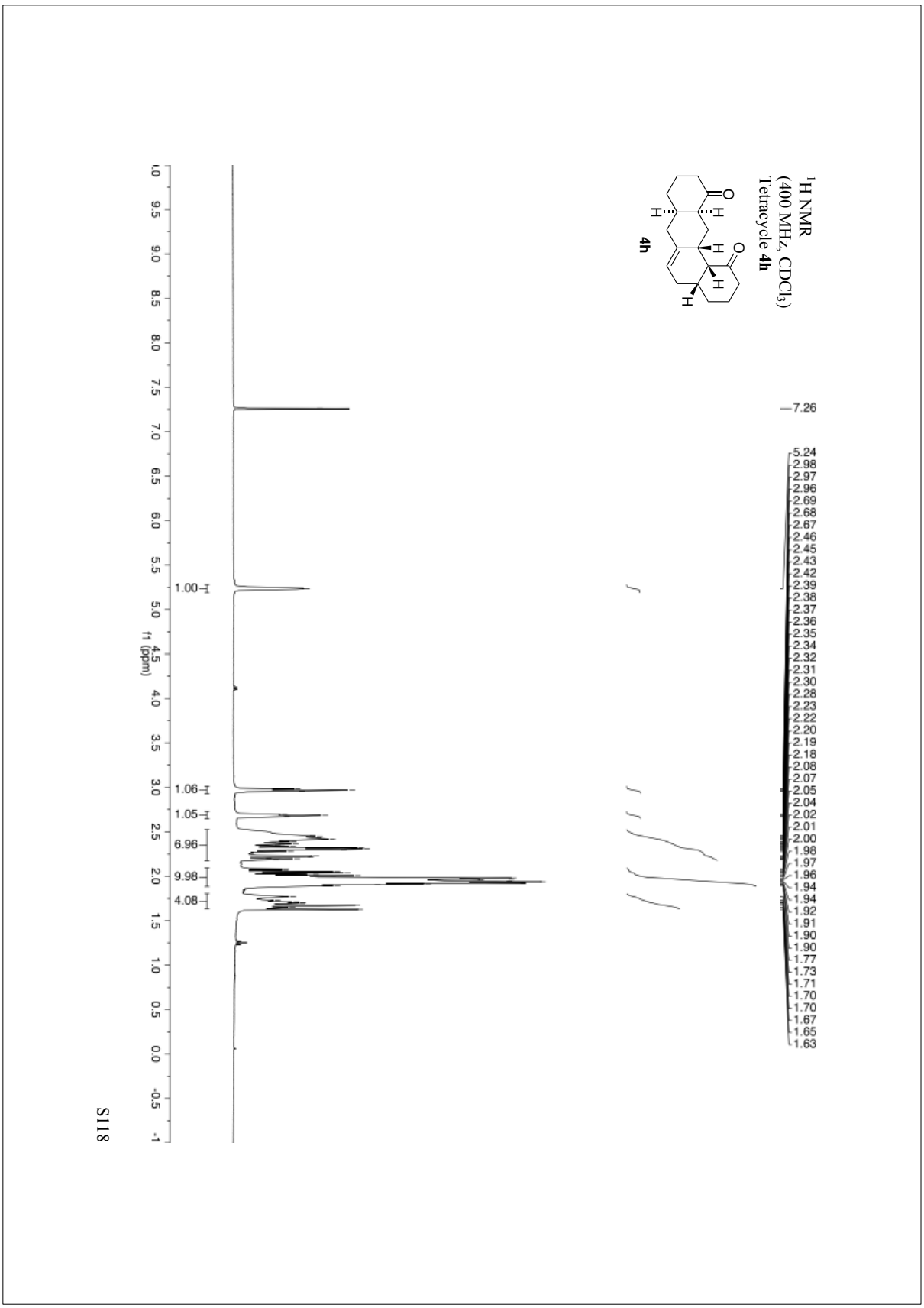
^{1}H NMR
(400 MHz, CDCl$_3$)
Tetracycle **4h**
4h
7.26
5.24
2.98
2.97
2.96
2.69
2.68
2.67
2.46
2.45
2.43
2.42
2.39
2.38
2.37
2.36
2.35
2.34
2.32
2.31
2.30
2.28
2.23
2.22
2.20
2.19
2.18
2.08
2.07
2.05
2.04
2.02
2.01
2.00
1.98
1.97
1.96
1.94
1.94
1.92
1.91
1.90
1.90
1.77
1.73
1.71
1.70
1.70
1.67
1.65
1.63
1.00
1.06
1.05
6.96
9.98
4.08
f1 (ppm)
S118

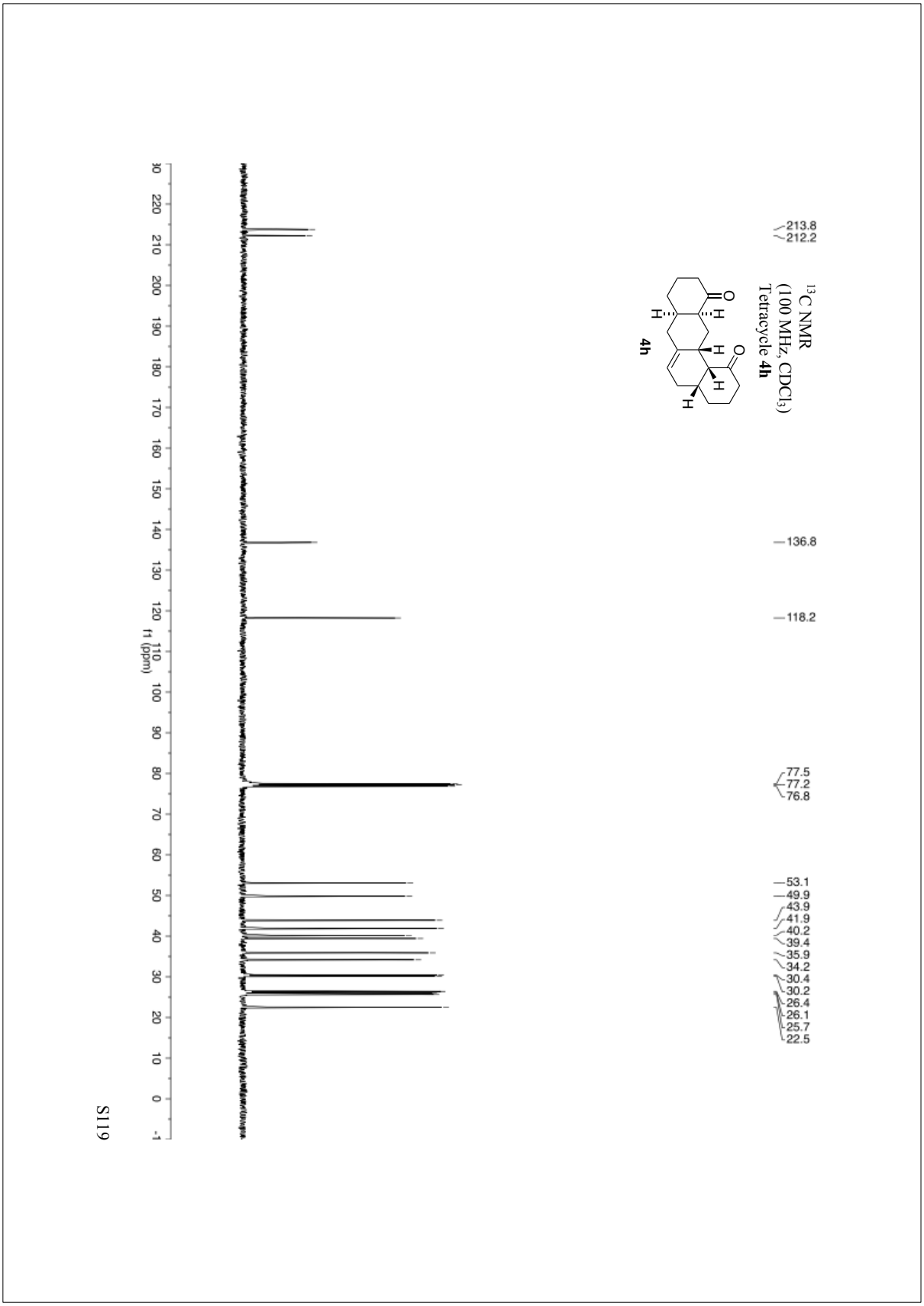
^{13}C NMR
(100 MHz, CDCl$_3$)
Tetracycle **4h**
4h
213.8
212.2
136.8
118.2
77.5
77.2
76.8
53.1
49.9
43.9
41.9
40.2
39.4
35.9
34.2
30.4
30.2
26.4
26.1
25.7
22.5
f1 (ppm)
S119

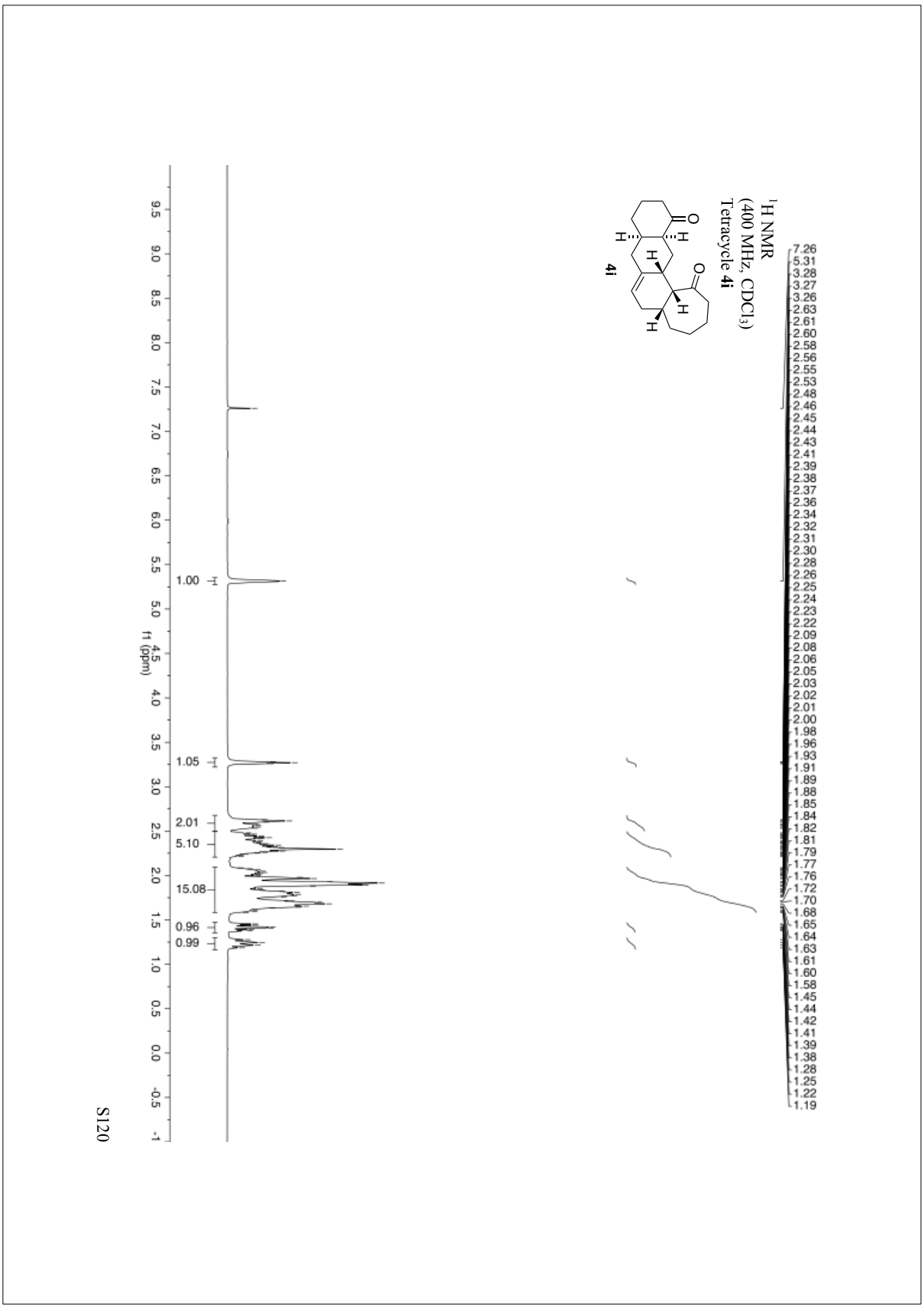
^{1}H NMR
(400 MHz, $CDCl_3$)
Tetracycle **4i**
4i
7.26
5.31
3.28
3.27
3.26
2.63
2.61
2.60
2.58
2.56
2.55
2.53
2.48
2.46
2.45
2.44
2.43
2.41
2.39
2.38
2.37
2.36
2.34
2.32
2.31
2.30
2.28
2.26
2.25
2.24
2.23
2.22
2.09
2.08
2.06
2.05
2.03
2.02
2.01
2.00
1.98
1.96
1.93
1.91
1.89
1.88
1.85
1.84
1.82
1.81
1.79
1.77
1.76
1.72
1.70
1.68
1.65
1.64
1.63
1.61
1.60
1.58
1.45
1.44
1.42
1.41
1.39
1.38
1.28
1.25
1.22
1.19
1.00
1.05
2.01
5.10
15.08
0.96
0.99
f1 (ppm)

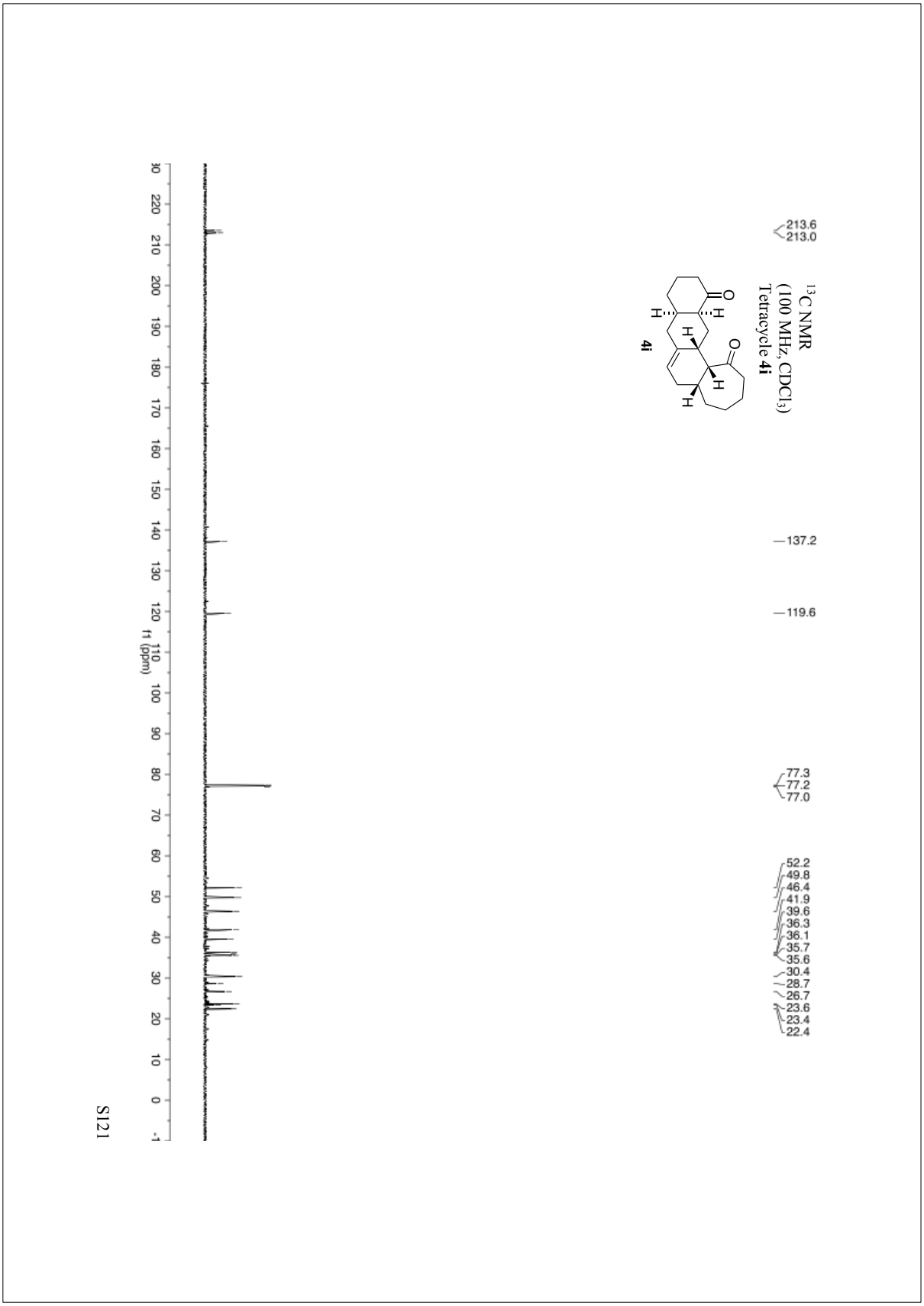
^{13}C NMR
(100 MHz, CDCl$_3$)
Tetracycle **4i**
4i
213.6
213.0
137.2
119.6
77.3
77.2
77.0
52.2
49.8
46.4
41.9
39.6
36.3
36.1
35.7
35.6
30.4
28.7
26.7
23.6
23.4
22.4
f1 (ppm)
S121

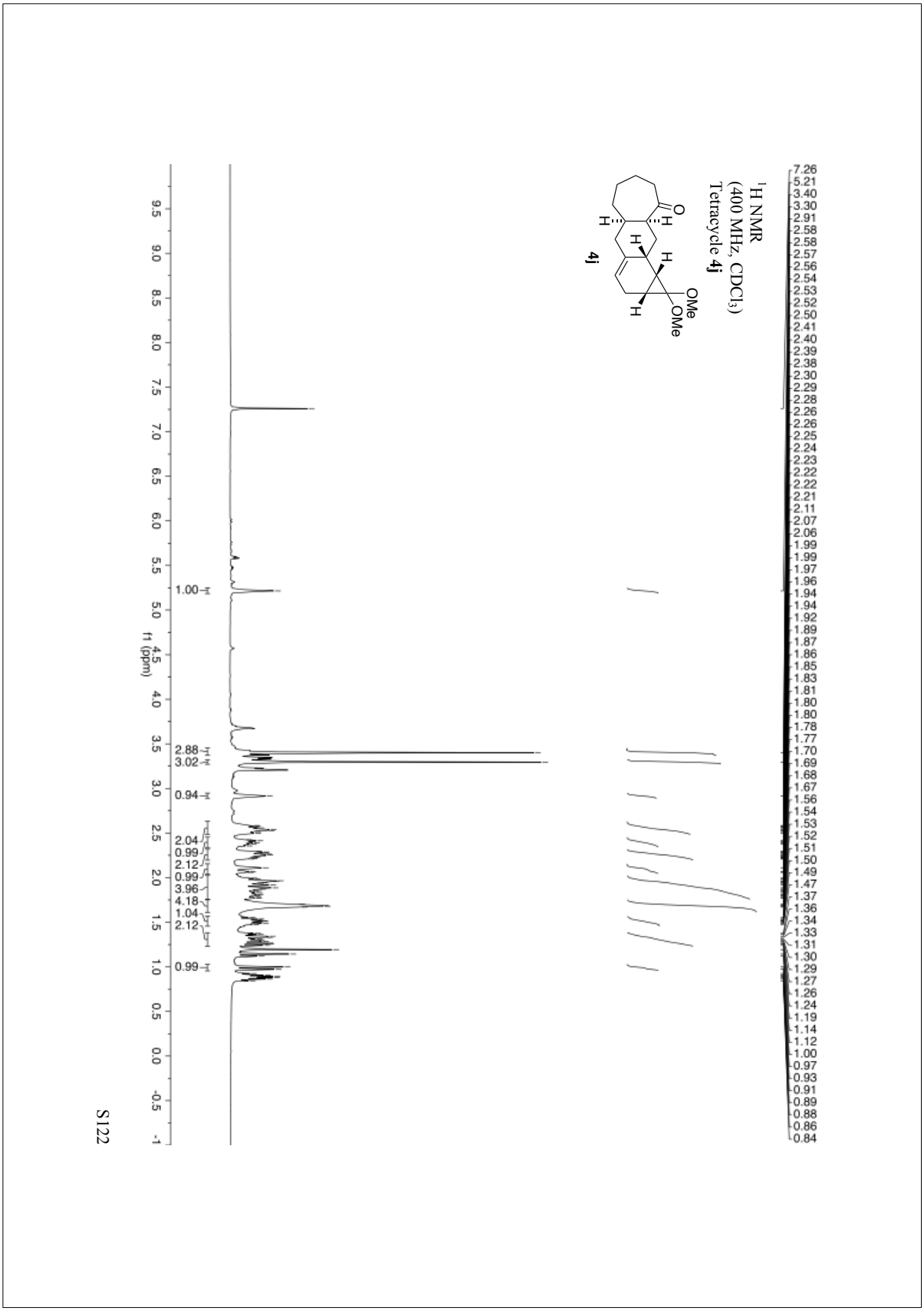
^{1}H NMR
(400 MHz, CDCl$_3$)
Tetracycle **4j**
4j
OMe
OMe
f1 (ppm)
1.00
2.88
3.02
0.94
2.04
0.99
2.12
0.99
3.96
4.18
1.04
2.12
0.99

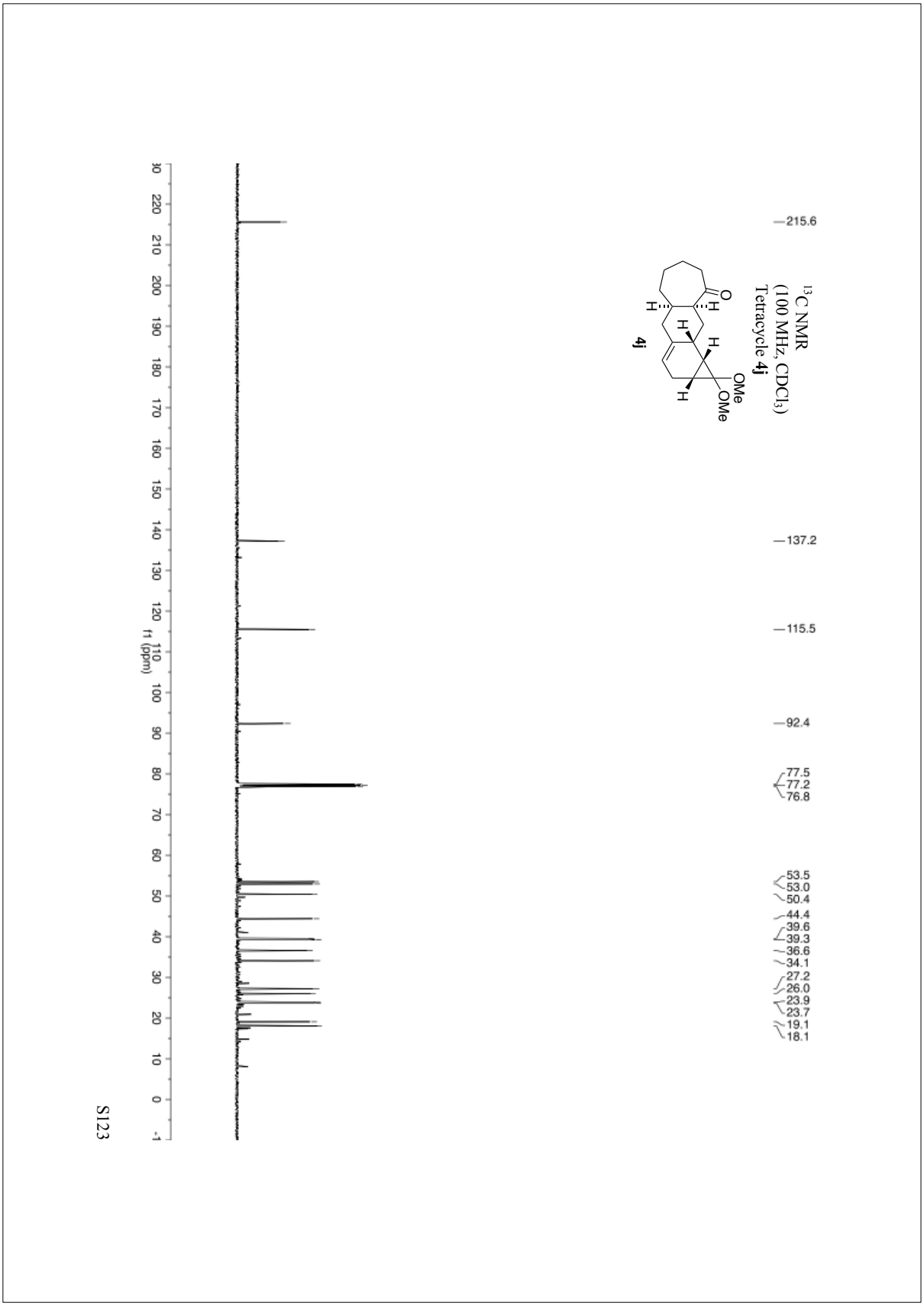
^{13}C NMR
(100 MHz, CDCl$_3$)
Tetracycle **4j**
4j
OMe
OMe
—215.6
—137.2
—115.5
—92.4
77.5
77.2
76.8
53.5
53.0
50.4
44.4
39.6
39.3
36.6
34.1
27.2
26.0
23.9
23.7
19.1
18.1
f1 (ppm)
S123

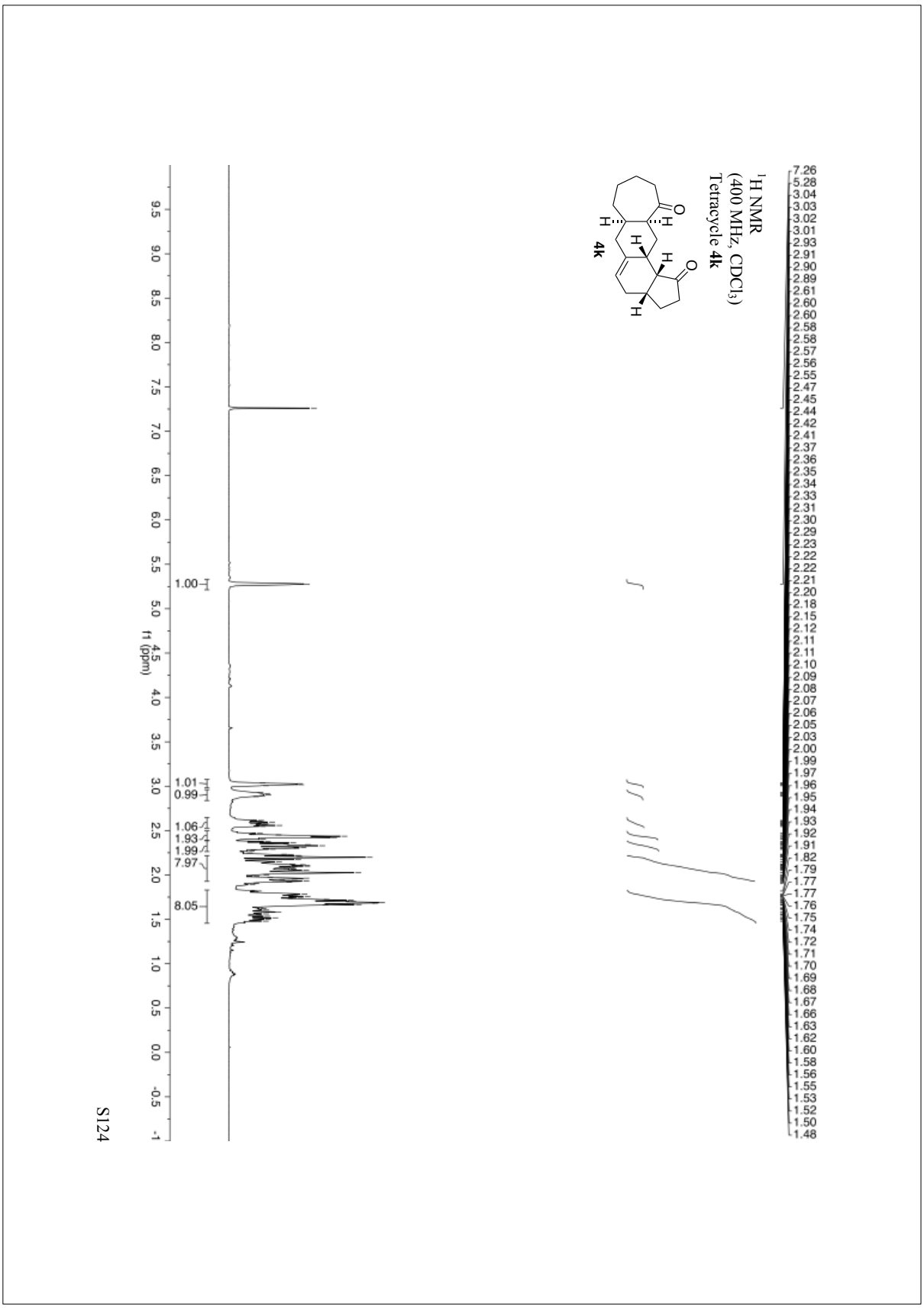
^{1}H NMR
(400 MHz, $CDCl_3$)
Tetracycle **4k**
4k
f1 (ppm)
1.00
1.01
0.99
1.06
1.93
1.99
7.97
8.05

S124

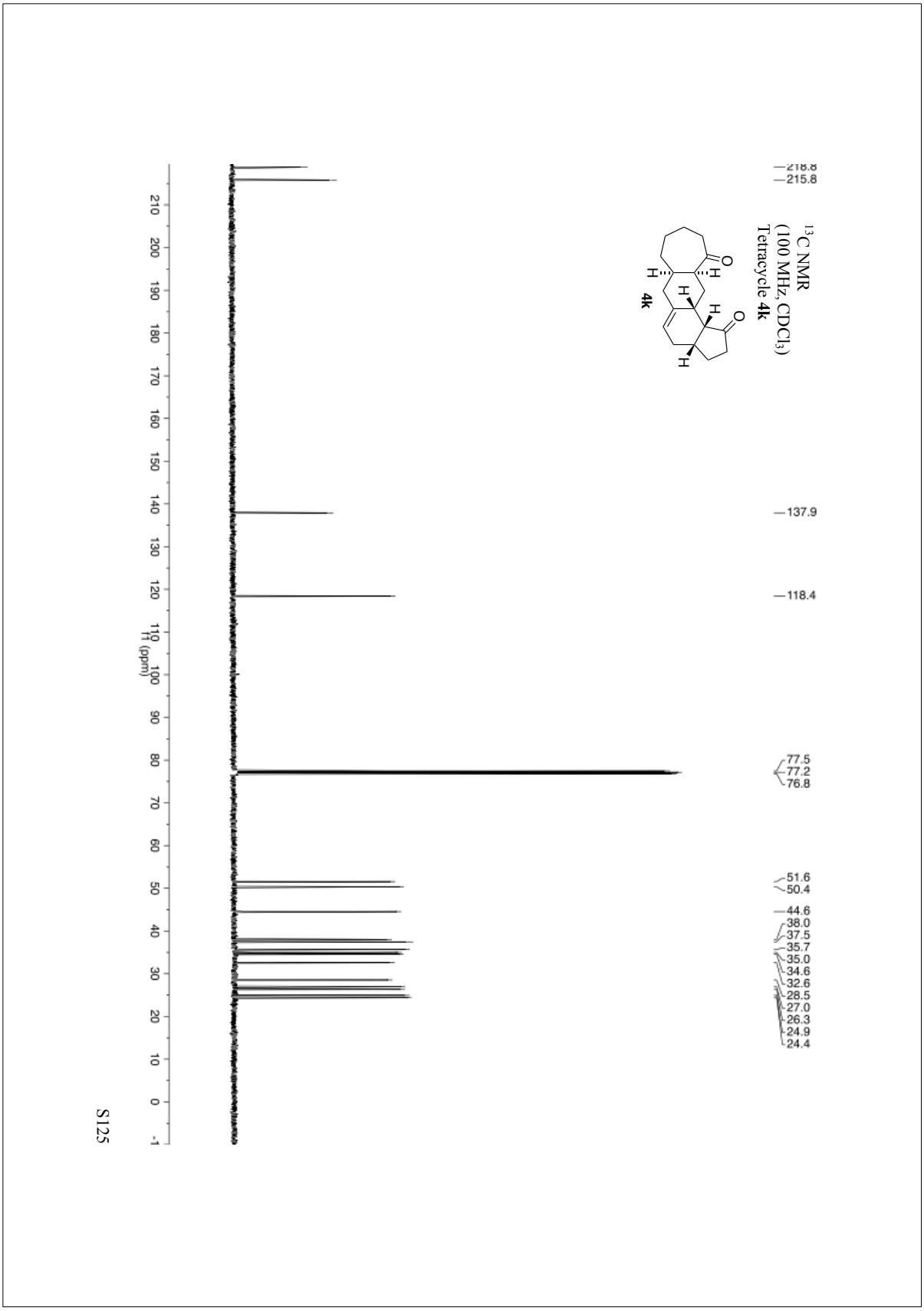
218.8
215.8
137.9
118.4
77.5
77.2
76.8
51.6
50.4
44.6
38.0
37.5
35.7
35.0
34.6
32.6
28.5
27.0
26.3
24.9
24.4
f1 (ppm)
210 200 190 180 170 160 150 140 130 120 110 100 90 80 70 60 50 40 30 20 10 0 -1
^{13}C NMR
(100 MHz, CDCl$_3$)
Tetracycle **4k**
4k
S125

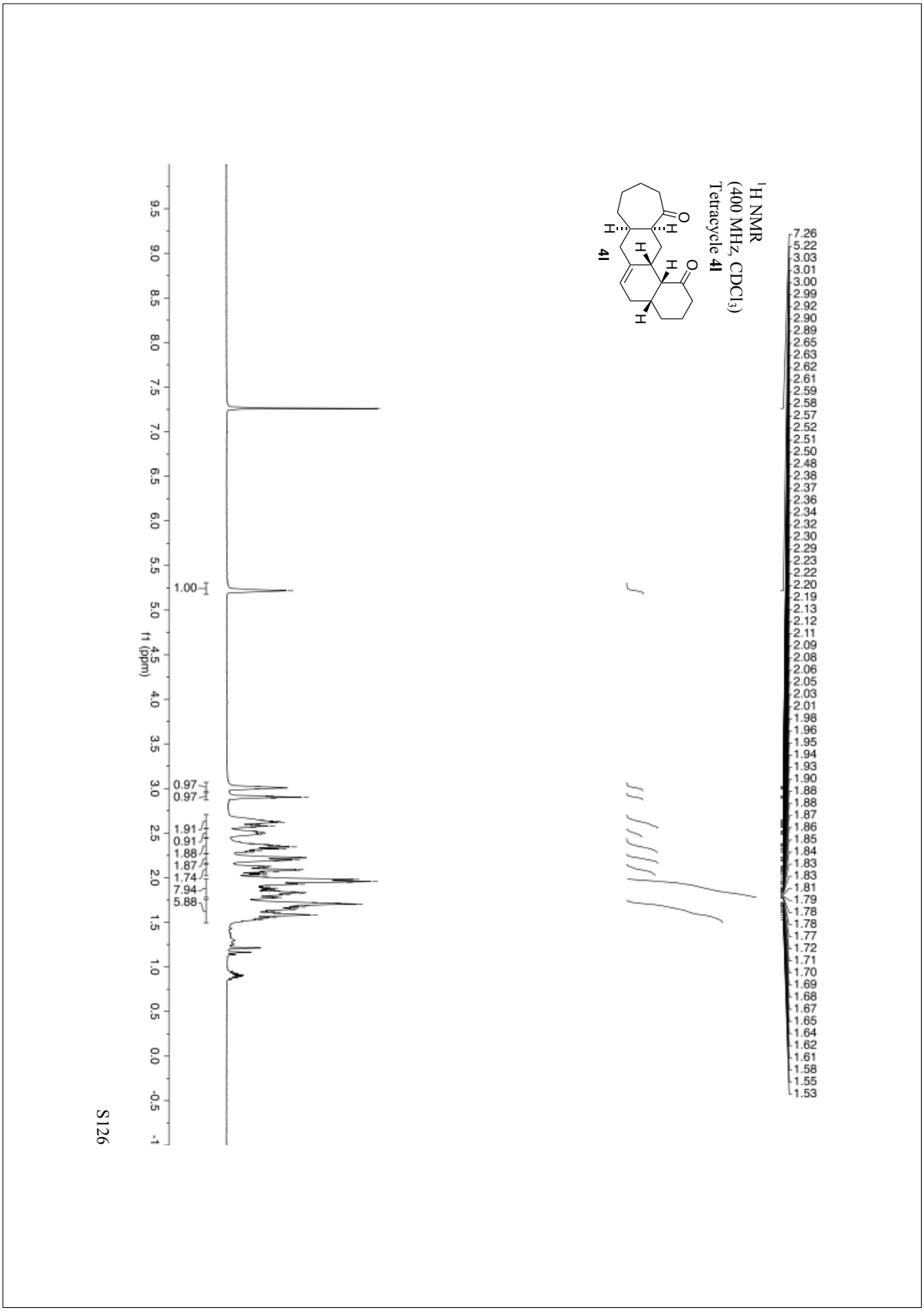
^{1}H NMR
(400 MHz, $CDCl_3$)
Tetracycle **4l**
4l
7.26
5.22
3.03
3.01
3.00
2.99
2.92
2.90
2.89
2.65
2.63
2.62
2.61
2.59
2.58
2.57
2.52
2.51
2.50
2.48
2.38
2.37
2.36
2.34
2.32
2.30
2.29
2.23
2.22
2.20
2.19
2.13
2.12
2.11
2.09
2.08
2.06
2.05
2.03
2.01
1.98
1.96
1.95
1.94
1.93
1.90
1.88
1.88
1.87
1.86
1.85
1.84
1.83
1.83
1.81
1.79
1.78
1.78
1.77
1.72
1.71
1.70
1.69
1.68
1.67
1.65
1.64
1.62
1.61
1.58
1.55
1.53
1.00
0.97
0.97
1.91
0.91
1.88
1.87
1.74
7.94
5.88
f1 (ppm)
9.5 9.0 8.5 8.0 7.5 7.0 6.5 6.0 5.5 5.0 4.5 4.0 3.5 3.0 2.5 2.0 1.5 1.0 0.5 0.0 -0.5 -1

S126

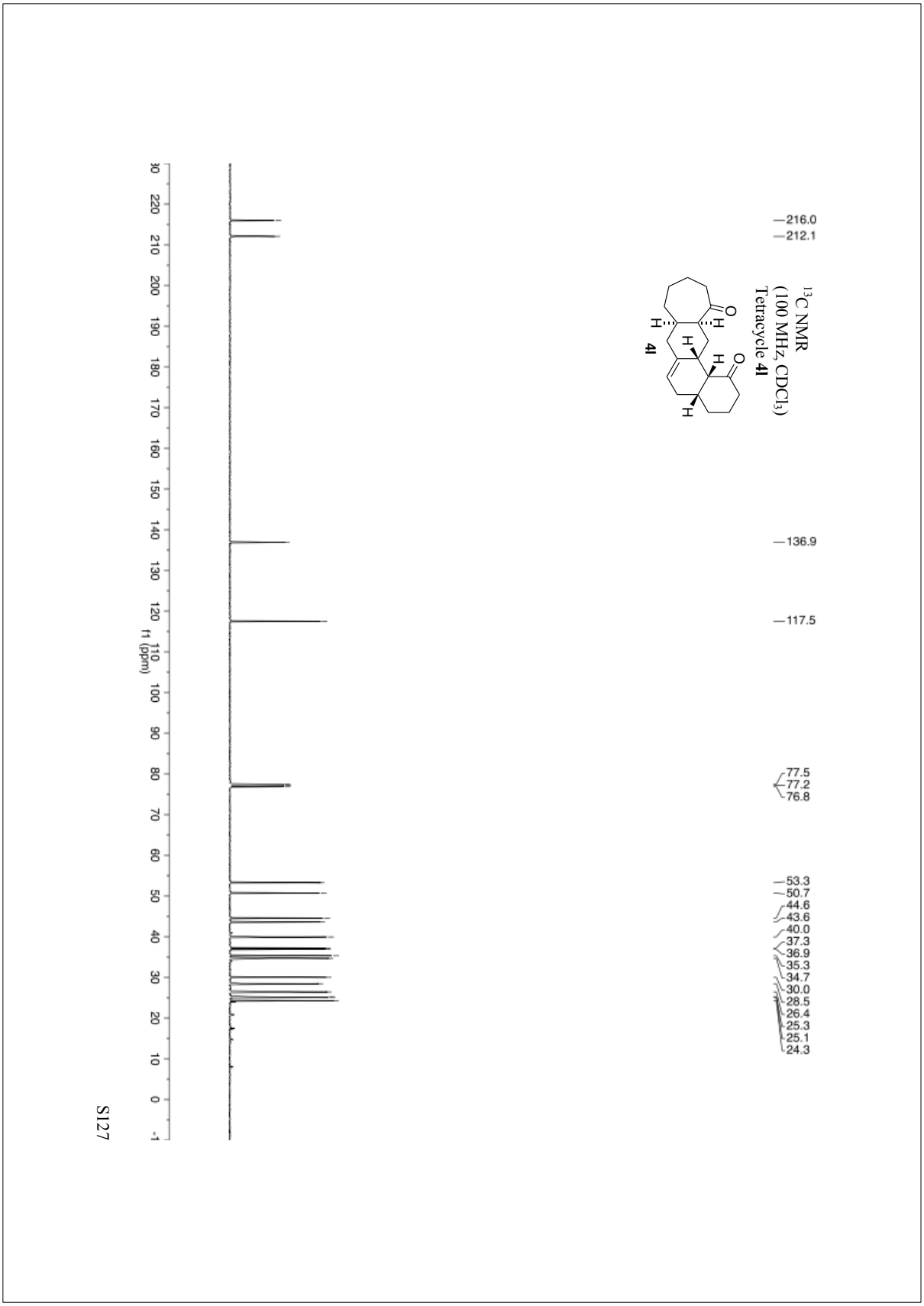
^{13}C NMR
(100 MHz, CDCl$_3$)
Tetracycle **4l**
4l
216.0
212.1
136.9
117.5
77.5
77.2
76.8
53.3
50.7
44.6
43.6
40.0
37.3
36.9
35.3
34.7
30.0
28.5
26.4
25.3
25.1
24.3
f1 (ppm)
S127

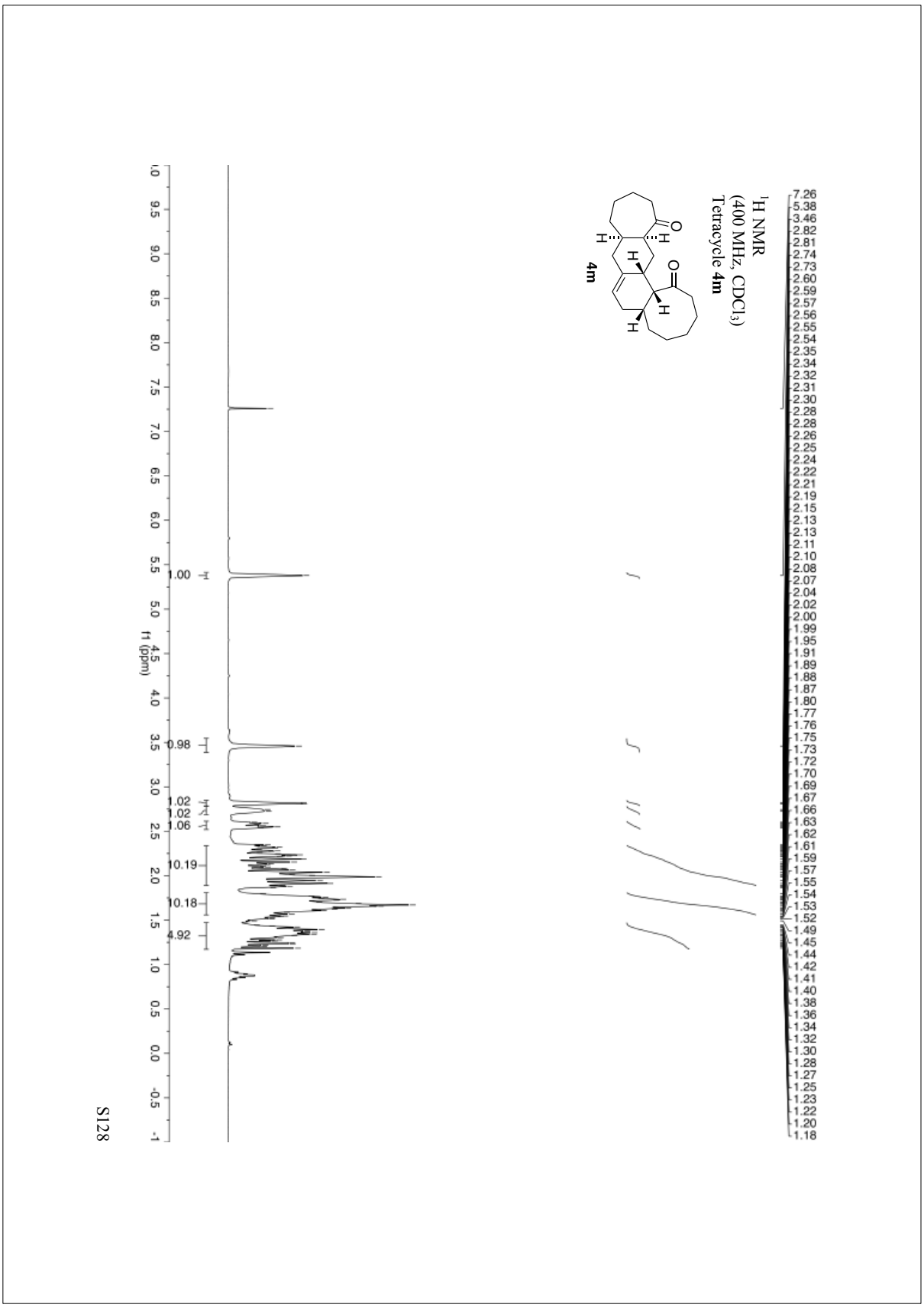
^{1}H NMR
(400 MHz, $CDCl_3$)
Tetracycle **4m**
4m
f1 (ppm)
1.00
0.98
1.02
1.02
1.06
10.19
10.18
4.92

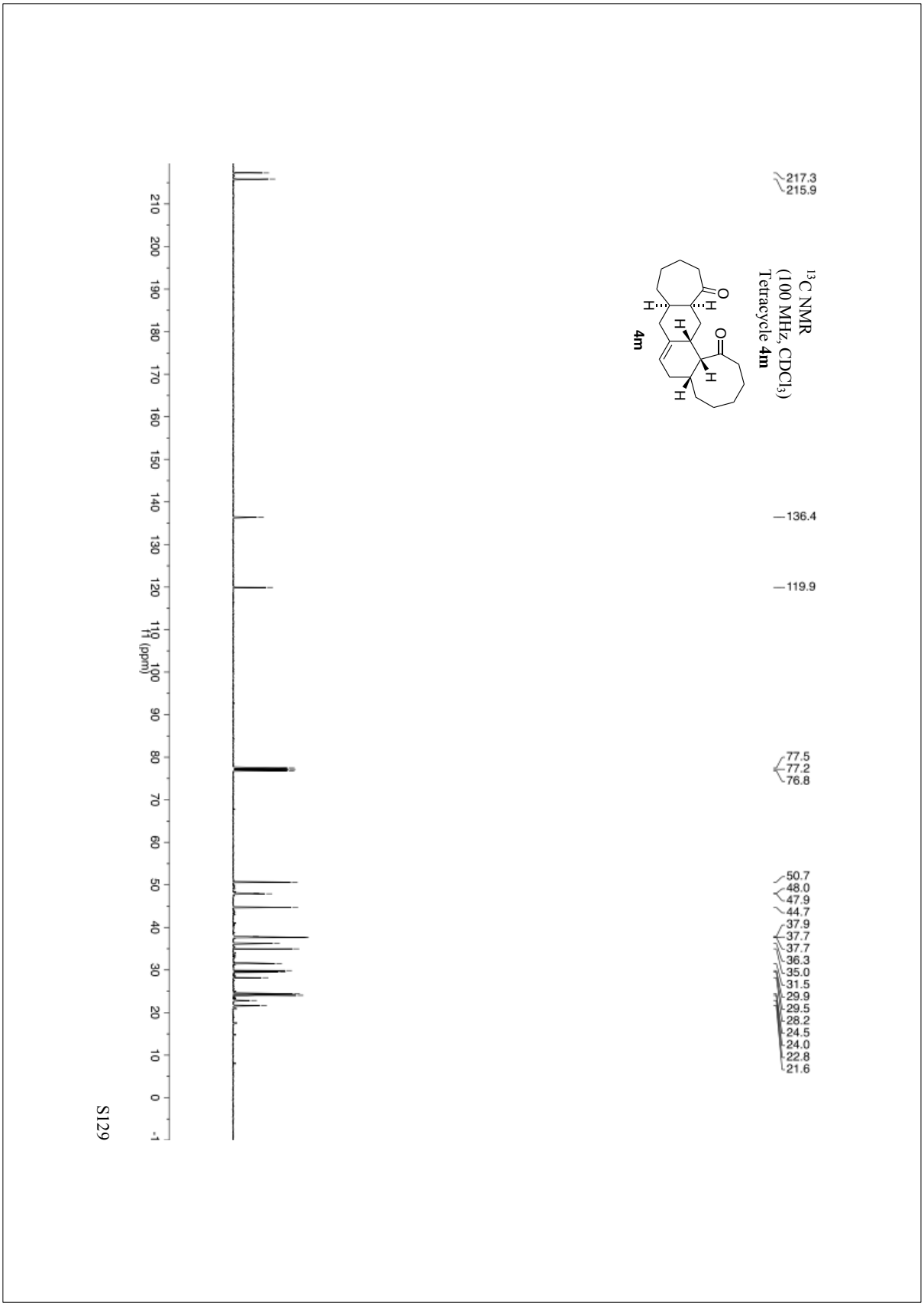
^{13}C NMR
(100 MHz, CDCl$_3$)
Tetracycle **4m**
4m
217.3
215.9
136.4
119.9
77.5
77.2
76.8
50.7
48.0
47.9
44.7
37.9
37.7
37.7
36.3
35.0
31.5
29.9
29.5
28.2
24.5
24.0
22.8
21.6
f1 (ppm)
S129

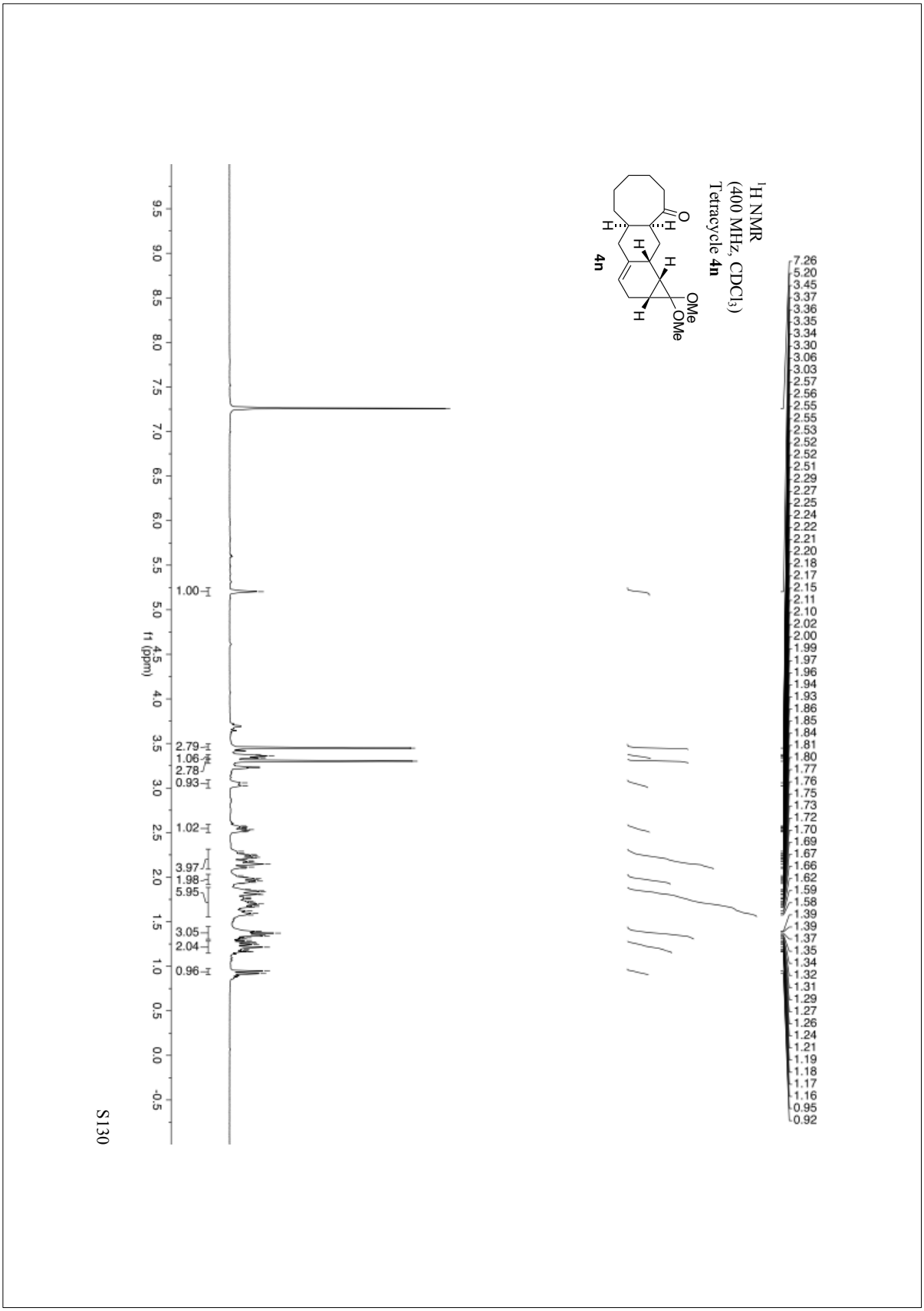
^{1}H NMR
(400 MHz, $CDCl_3$)
Tetracycle **4n**
4n
OMe
OMe
7.26
5.20
3.45
3.37
3.36
3.35
3.34
3.30
3.06
3.03
2.57
2.56
2.55
2.55
2.53
2.52
2.52
2.51
2.29
2.27
2.25
2.24
2.22
2.21
2.20
2.18
2.17
2.15
2.11
2.10
2.02
2.00
1.99
1.97
1.96
1.94
1.93
1.86
1.85
1.84
1.81
1.80
1.77
1.76
1.75
1.73
1.72
1.70
1.69
1.67
1.66
1.62
1.59
1.58
1.39
1.39
1.37
1.35
1.34
1.32
1.31
1.29
1.27
1.26
1.24
1.21
1.19
1.18
1.17
1.16
0.95
0.92
1.00
2.79
1.06
2.78
0.93
1.02
3.97
1.98
5.95
3.05
2.04
0.96
f1 (ppm)

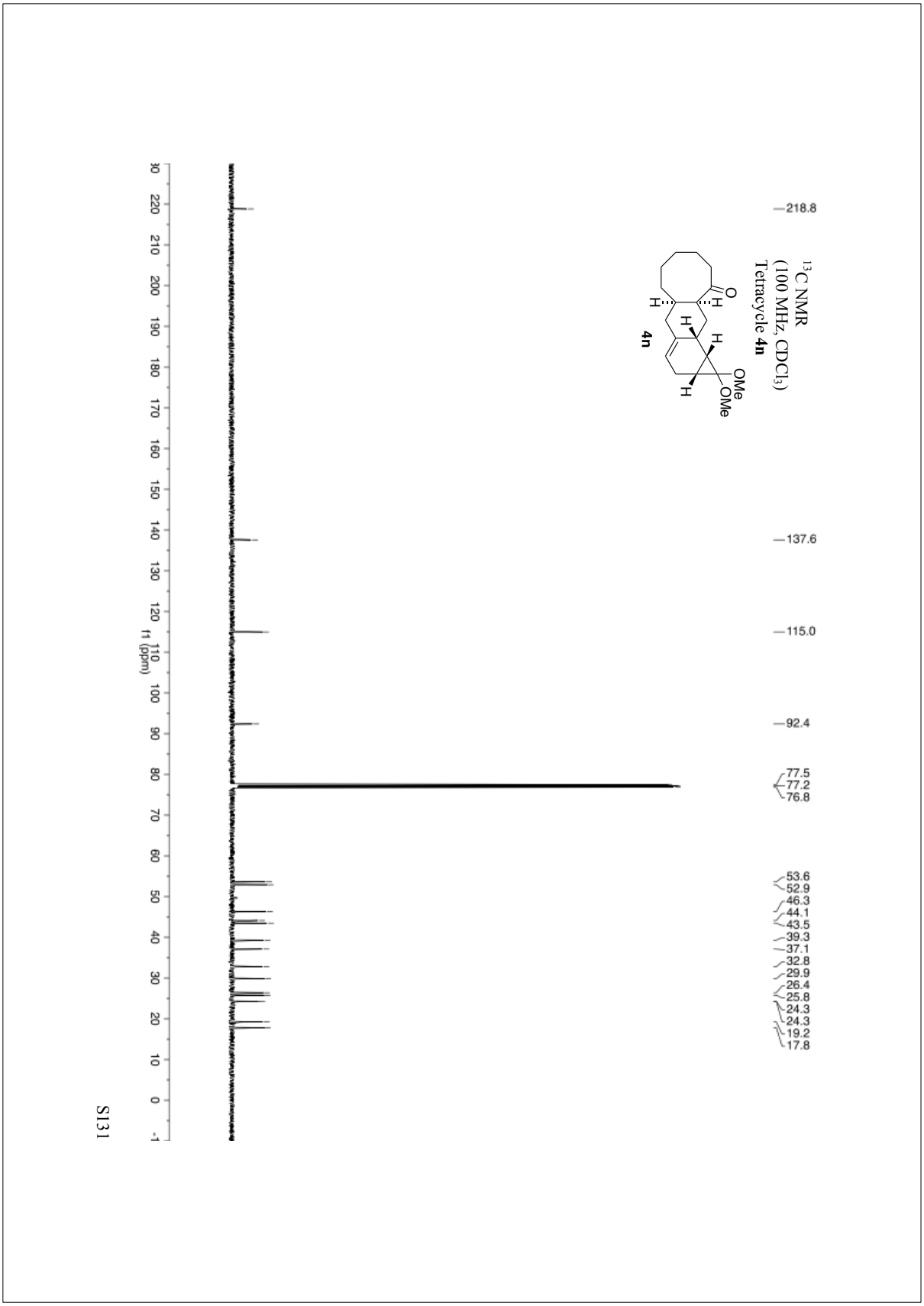
^{13}C NMR
(100 MHz, $CDCl_3$)
Tetracycle **4n**
4n
OMe
OMe
218.8
137.6
115.0
92.4
77.5
77.2
76.8
53.6
52.9
46.3
44.1
43.5
39.3
37.1
32.8
29.9
26.4
25.8
24.3
24.3
19.2
17.8
f1 (ppm)
S131

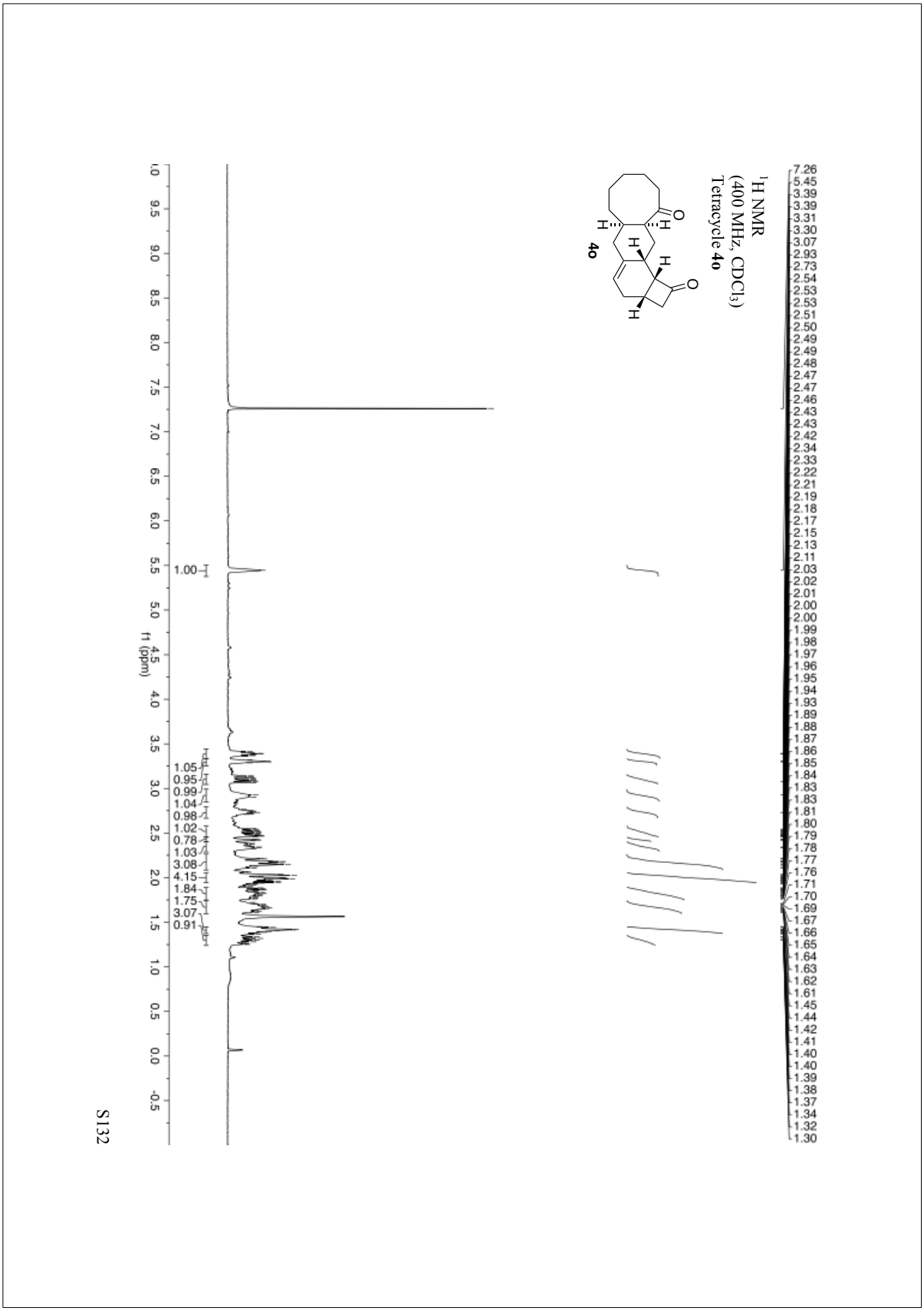
^{1}H NMR
(400 MHz, $CDCl_3$)
Tetracycle **4o**
4o
f1 (ppm)
1.00
1.05
0.95
0.99
1.04
0.98
1.02
0.78
1.03
3.08
4.15
1.84
1.75
3.07
0.91

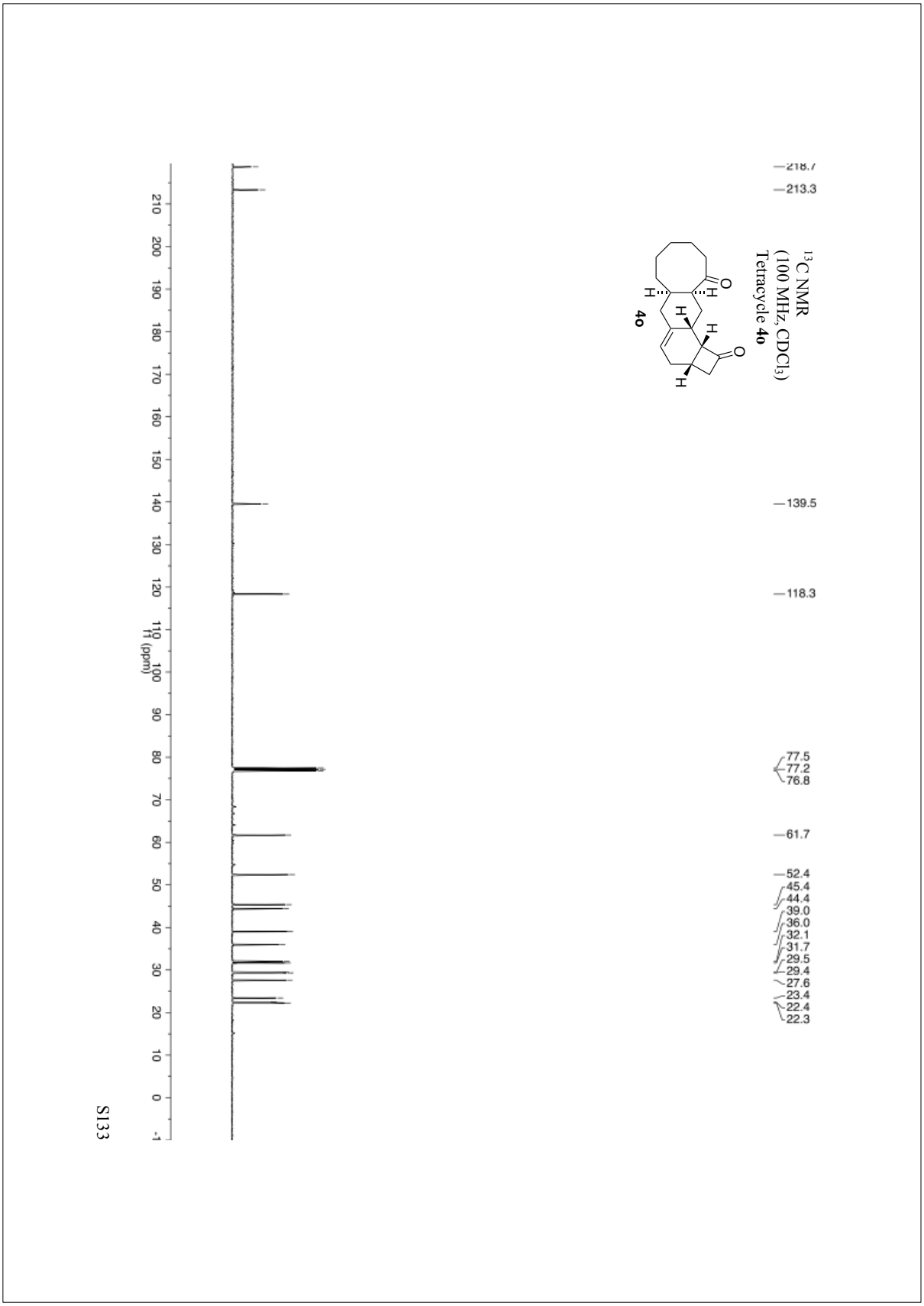
218.7
213.3
139.5
118.3
77.5
77.2
76.8
61.7
52.4
45.4
44.4
39.0
36.0
32.1
31.7
29.5
29.4
27.6
23.4
22.4
22.3
^{13}C NMR
(100 MHz, CDCl$_3$)
Tetracycle **4o**
4o
f1 (ppm)
S133

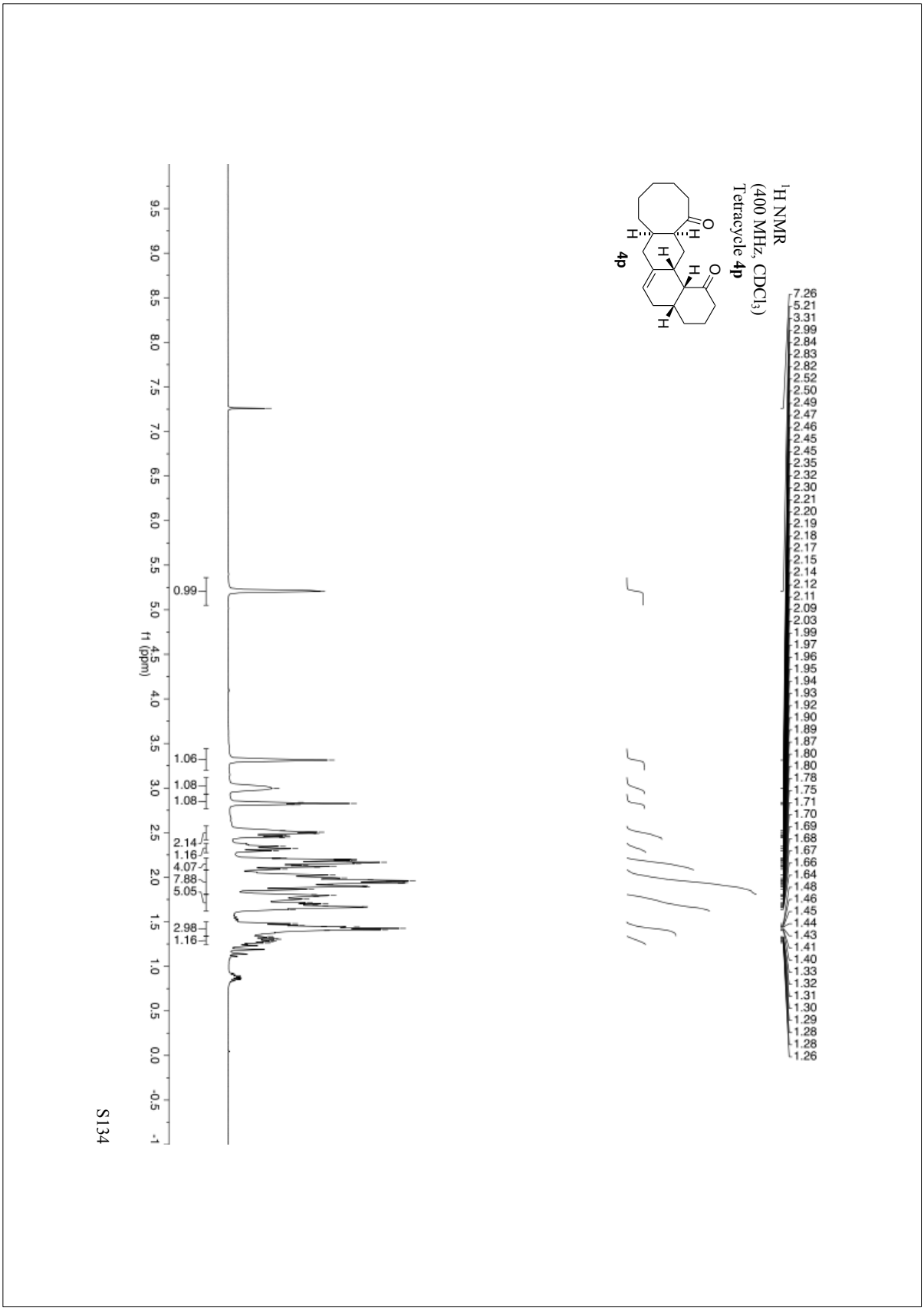
^{1}H NMR
(400 MHz, $CDCl_3$)
Tetracycle **4p**
4p
7.26
5.21
3.31
2.99
2.84
2.83
2.82
2.52
2.50
2.49
2.47
2.46
2.45
2.45
2.35
2.32
2.30
2.21
2.20
2.19
2.18
2.17
2.15
2.14
2.12
2.11
2.09
2.03
1.99
1.97
1.96
1.95
1.94
1.93
1.92
1.90
1.89
1.87
1.80
1.80
1.78
1.75
1.71
1.70
1.69
1.68
1.67
1.66
1.64
1.48
1.46
1.45
1.44
1.43
1.41
1.40
1.33
1.32
1.31
1.30
1.29
1.28
1.28
1.26
0.99
1.06
1.08
1.08
2.14
1.16
4.07
7.88
5.05
2.98
1.16
f1 (ppm)
9.5 9.0 8.5 8.0 7.5 7.0 6.5 6.0 5.5 5.0 4.5 4.0 3.5 3.0 2.5 2.0 1.5 1.0 0.5 0.0 -0.5 -1

S134

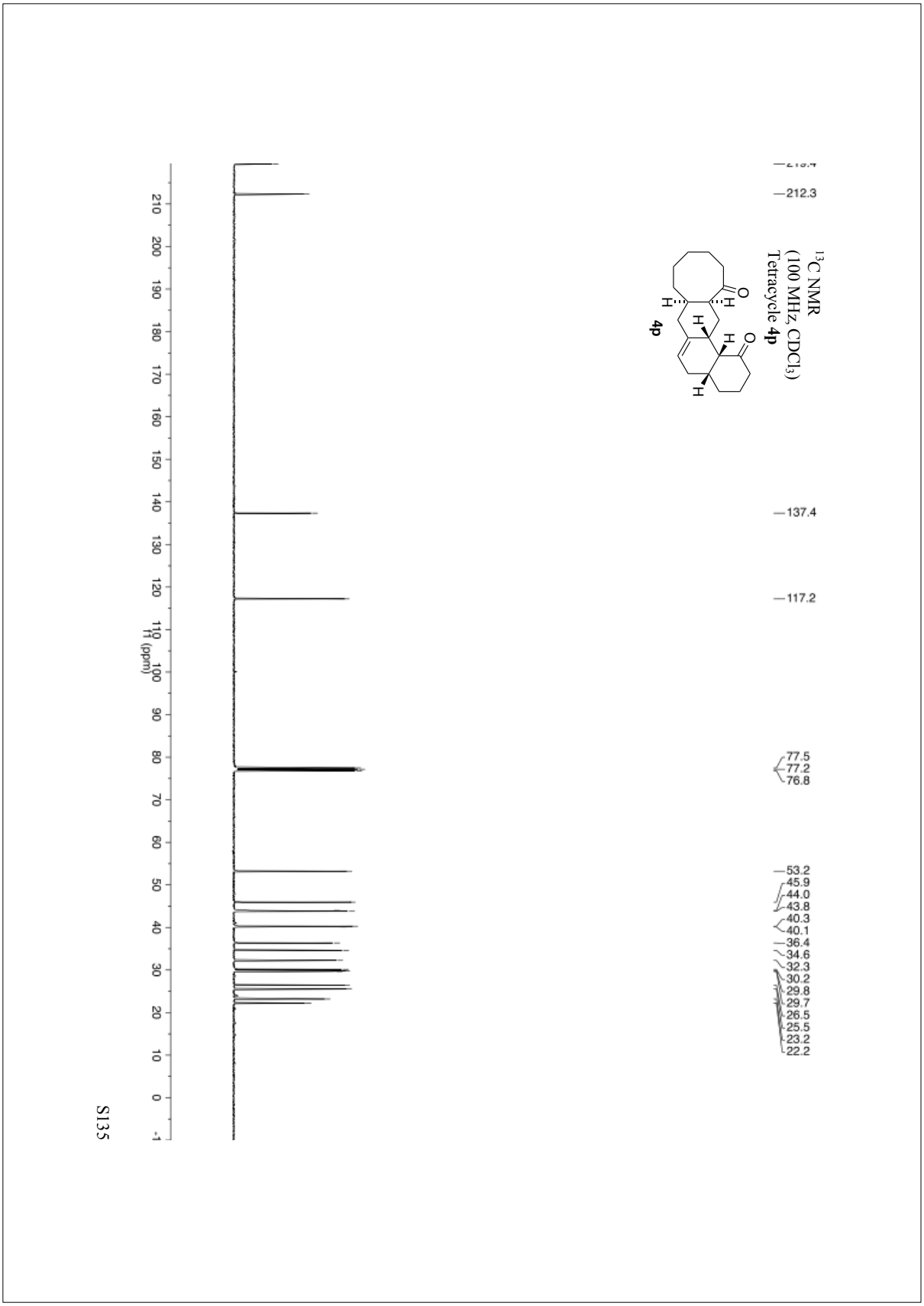
^{13}C NMR
(100 MHz, CDCl$_3$)
Tetracycle **4p**
4p
—212.3
—137.4
—117.2
77.5
77.2
76.8
—53.2
45.9
44.0
43.8
40.3
40.1
36.4
34.6
32.3
30.2
29.8
29.7
26.5
25.5
23.2
22.2
f1 (ppm)
S135

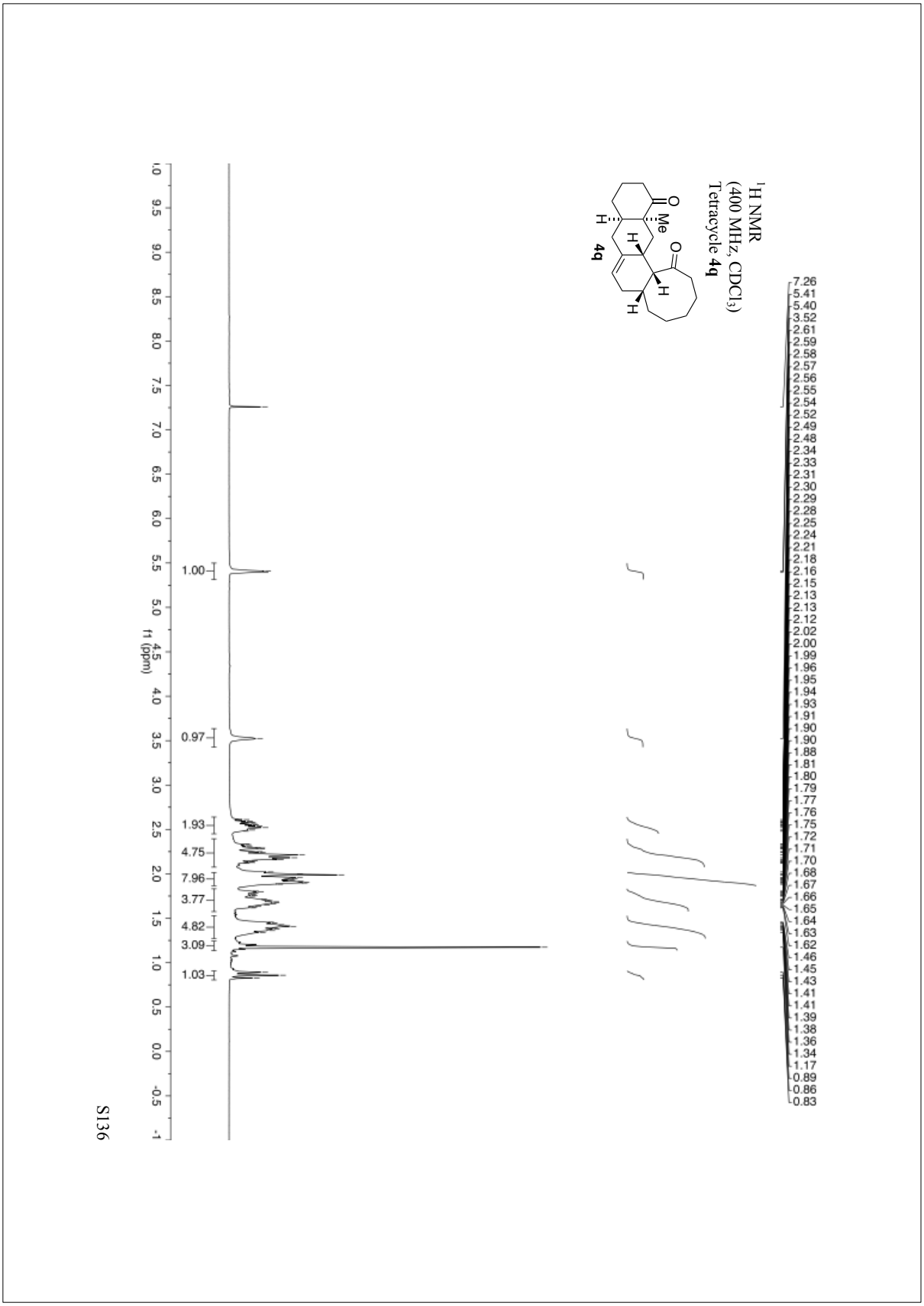
^{1}H NMR
(400 MHz, $CDCl_3$)
Tetracycle **4q**
4q
f1 (ppm)
1.00
0.97
1.93
4.75
7.96
3.77
4.82
3.09
1.03
7.26
5.41
5.40
3.52
2.61
2.59
2.58
2.57
2.56
2.55
2.54
2.52
2.49
2.48
2.34
2.33
2.31
2.30
2.29
2.28
2.25
2.24
2.21
2.18
2.16
2.15
2.13
2.13
2.12
2.02
2.00
1.99
1.96
1.95
1.94
1.93
1.91
1.90
1.90
1.88
1.81
1.80
1.79
1.77
1.76
1.75
1.72
1.71
1.70
1.68
1.67
1.66
1.65
1.64
1.63
1.62
1.46
1.45
1.43
1.41
1.41
1.39
1.38
1.36
1.34
1.17
0.89
0.86
0.83

S136

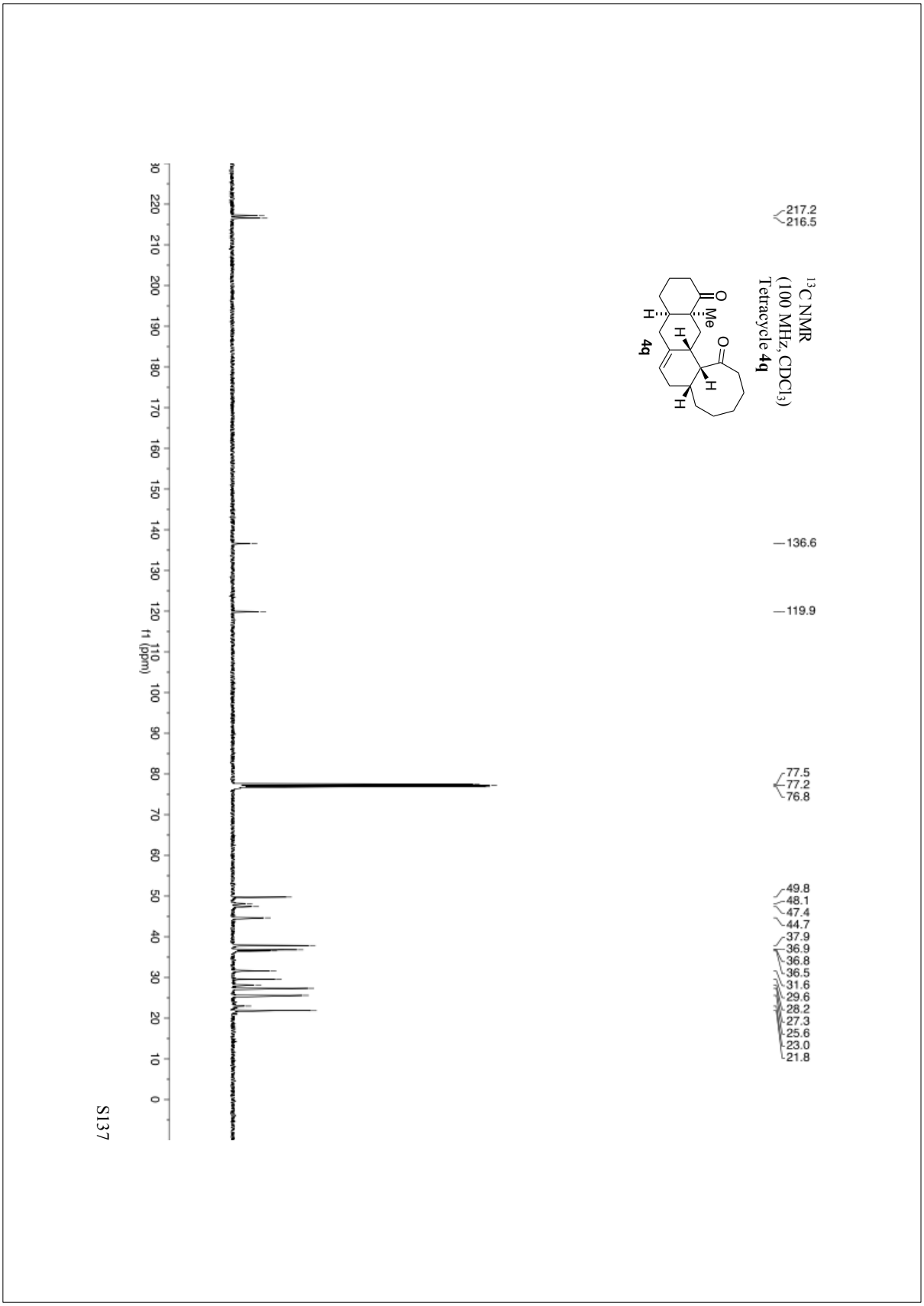
^{13}C NMR
(100 MHz, CDCl$_3$)
Tetracycle **4q**
4q
O
Me
H
H
O
H
H
217.2
216.5
136.6
119.9
77.5
77.2
76.8
49.8
48.1
47.4
44.7
37.9
36.9
36.8
36.5
31.6
29.6
28.2
27.3
25.6
23.0
21.8
f1 (ppm)
S137

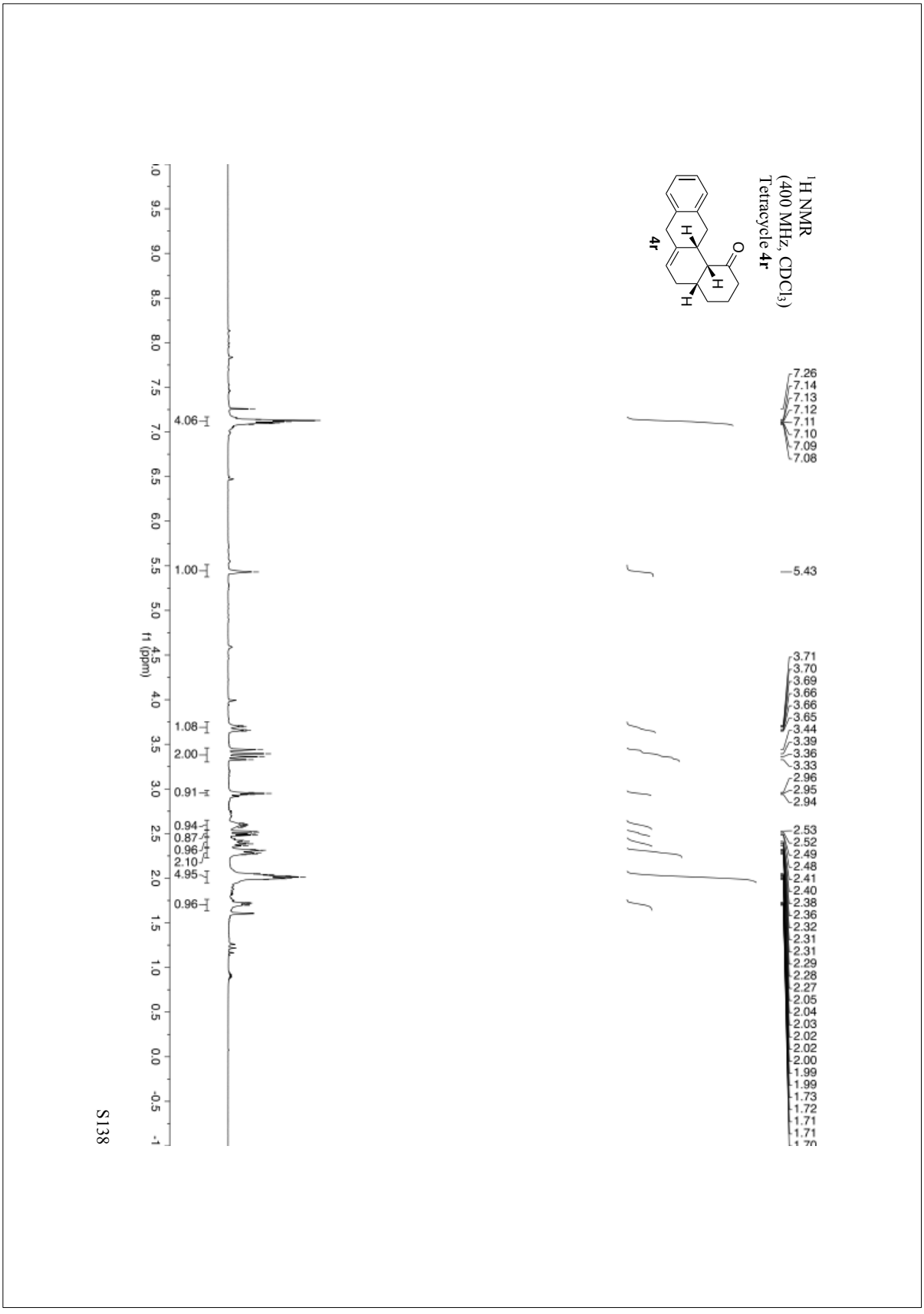
^{1}H NMR
(400 MHz, $CDCl_3$)
Tetracycle **4r**
4r
7.26
7.14
7.13
7.12
7.11
7.10
7.09
7.08
5.43
3.71
3.70
3.69
3.66
3.66
3.65
3.44
3.39
3.36
3.33
2.96
2.95
2.94
2.53
2.52
2.49
2.48
2.41
2.40
2.38
2.36
2.32
2.31
2.31
2.29
2.28
2.27
2.05
2.04
2.03
2.02
2.02
2.00
1.99
1.99
1.73
1.72
1.71
1.71
4.06
1.00
1.08
2.00
0.91
0.94
0.87
0.96
2.10
4.95
0.96
f1 (ppm)

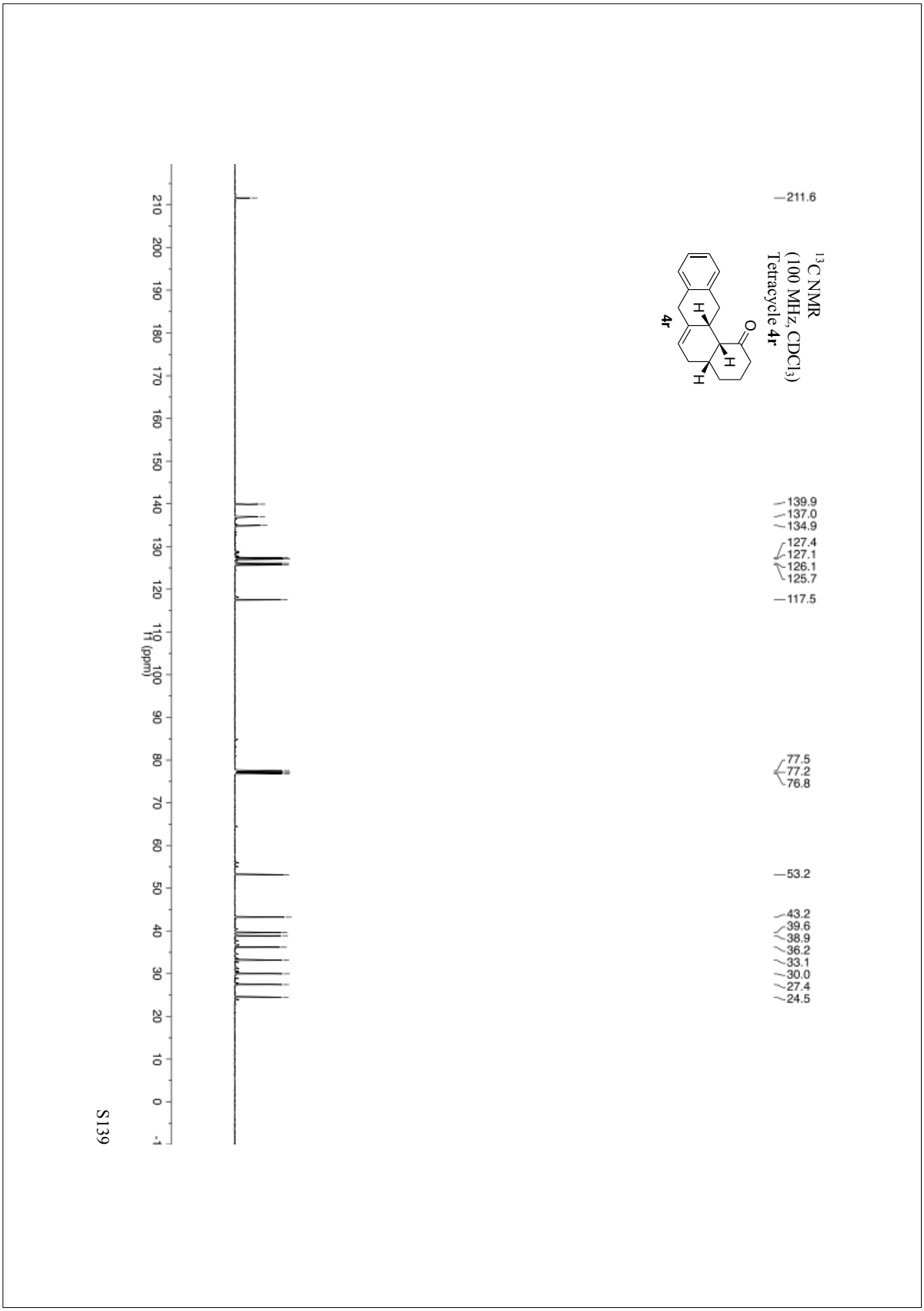
^{13}C NMR
(100 MHz, $CDCl_3$)
Tetracycle **4r**
4r
211.6
139.9
137.0
134.9
127.4
127.1
126.1
125.7
117.5
77.5
77.2
76.8
53.2
43.2
39.6
38.9
36.2
33.1
30.0
27.4
24.5
f1 (ppm)

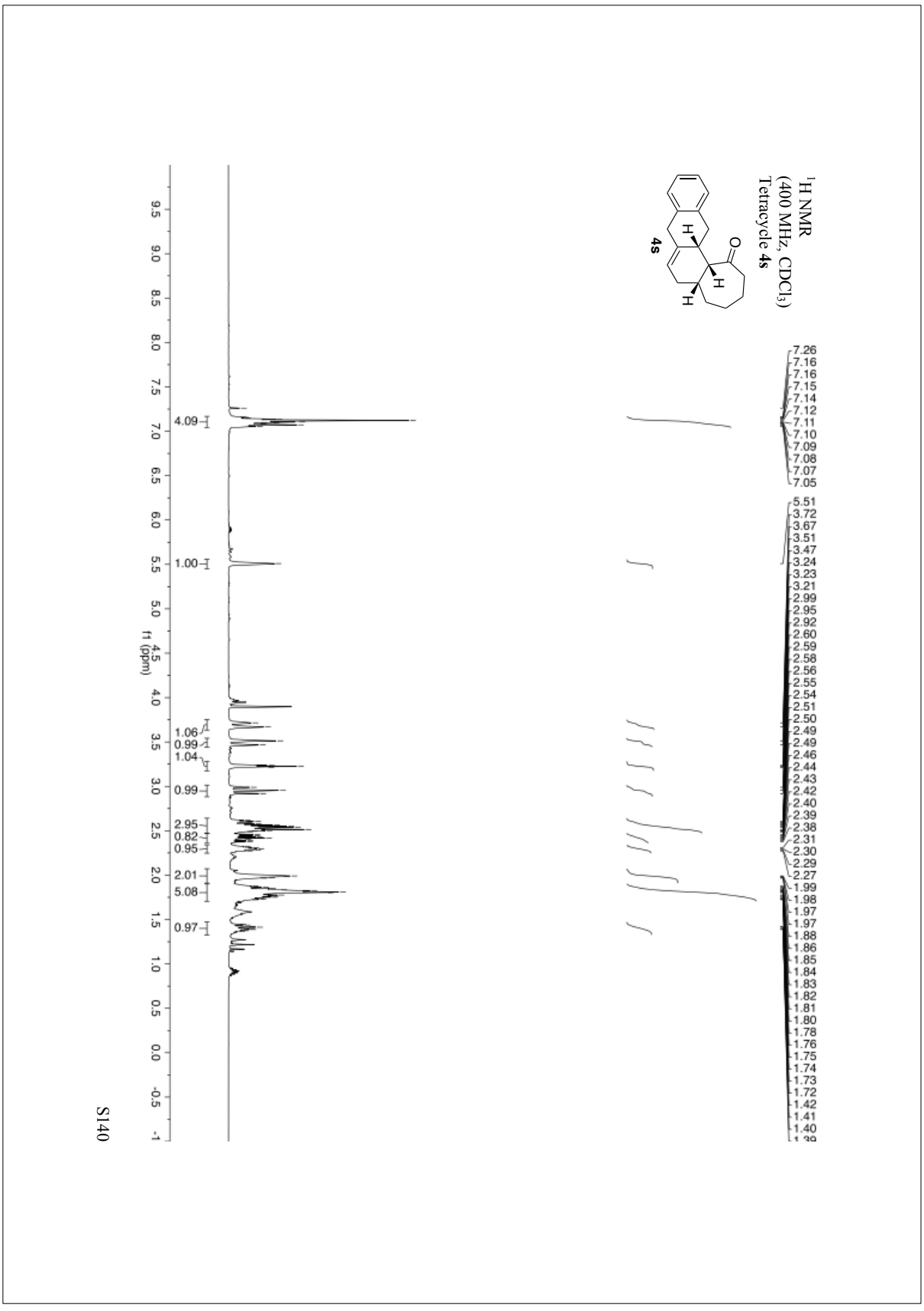
^{1}H NMR
(400 MHz, $CDCl_3$)
Tetracycle **4s**
4s
7.26
7.16
7.16
7.15
7.14
7.12
7.11
7.10
7.09
7.08
7.07
7.05
5.51
3.72
3.67
3.51
3.47
3.24
3.23
3.21
2.99
2.95
2.92
2.60
2.59
2.58
2.56
2.55
2.54
2.51
2.50
2.49
2.49
2.46
2.44
2.43
2.42
2.40
2.39
2.38
2.31
2.30
2.29
2.27
1.99
1.98
1.97
1.97
1.88
1.86
1.85
1.84
1.83
1.82
1.81
1.80
1.78
1.76
1.75
1.74
1.73
1.72
1.42
1.41
1.40
4.09
1.00
1.06
0.99
1.04
0.99
2.95
0.82
0.95
2.01
5.08
0.97
f1 (ppm)

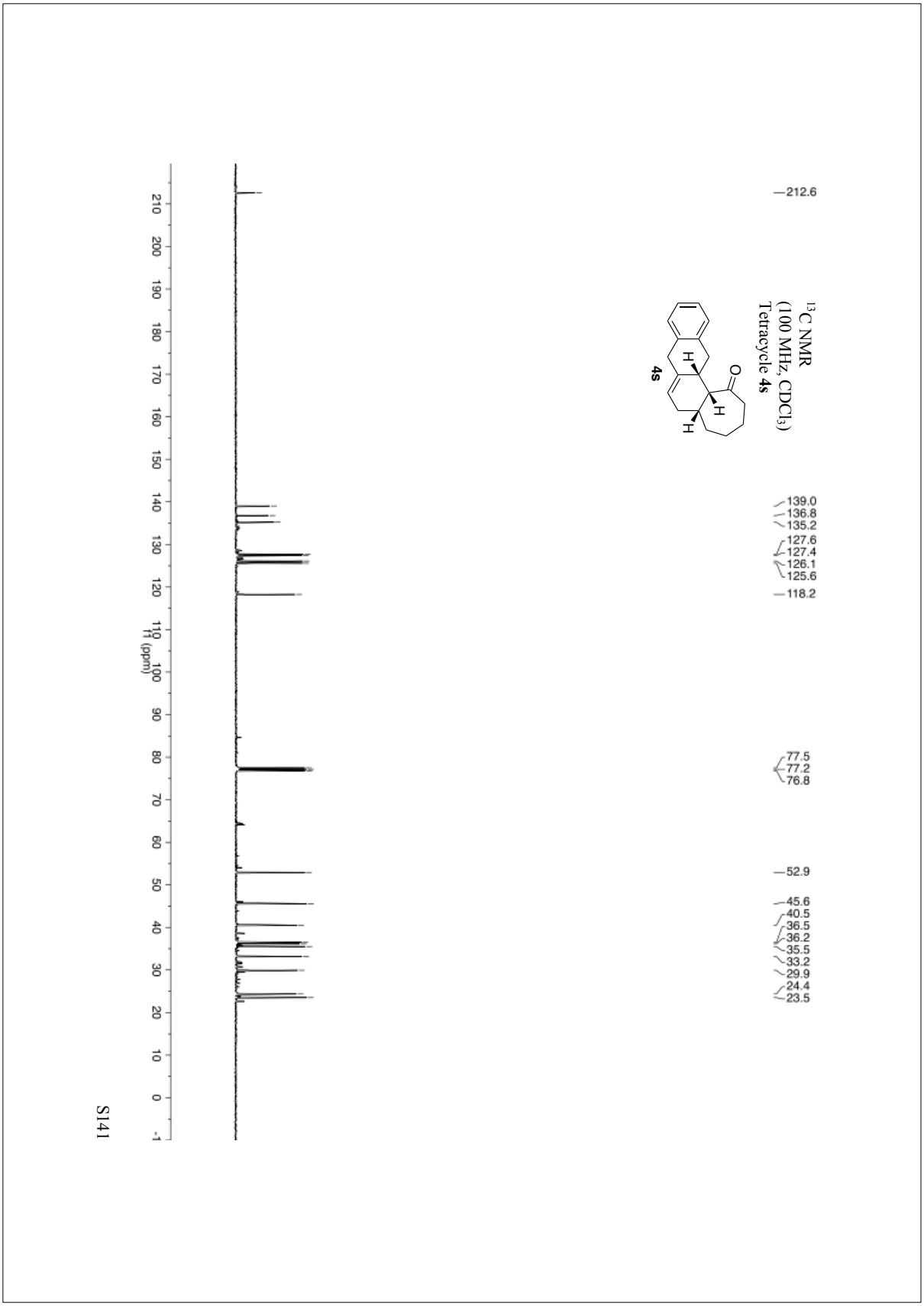
^{13}C NMR
(100 MHz, CDCl$_3$)
Tetracycle **4s**
4s
O
H
H
H
212.6
139.0
136.8
135.2
127.6
127.4
126.1
125.6
118.2
77.5
77.2
76.8
52.9
45.6
40.5
36.5
36.2
35.5
33.2
29.9
24.4
23.5
f1 (ppm)
S141

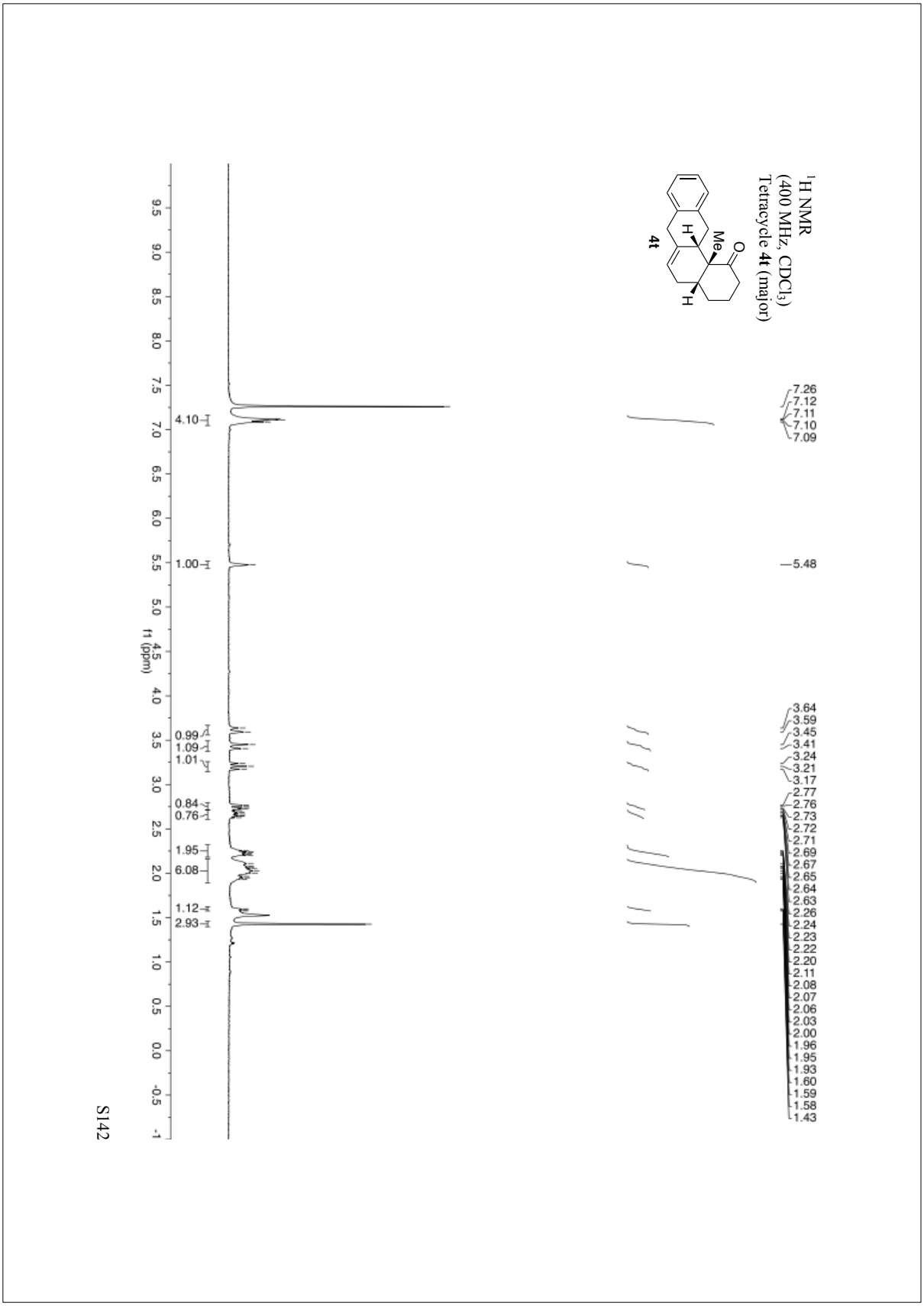
^{1}H NMR
(400 MHz, $CDCl_3$)
Tetracycle **4t** (major)
4t
Me
O
H
H
7.26
7.12
7.11
7.10
7.09
5.48
3.64
3.59
3.45
3.41
3.24
3.21
3.17
2.77
2.76
2.73
2.72
2.71
2.69
2.67
2.65
2.64
2.63
2.26
2.24
2.23
2.22
2.20
2.11
2.08
2.07
2.06
2.03
2.00
1.96
1.95
1.93
1.60
1.59
1.58
1.43
4.10
1.00
0.99
1.09
1.01
0.84
0.76
1.95
6.08
1.12
2.93
f1 (ppm)

S142

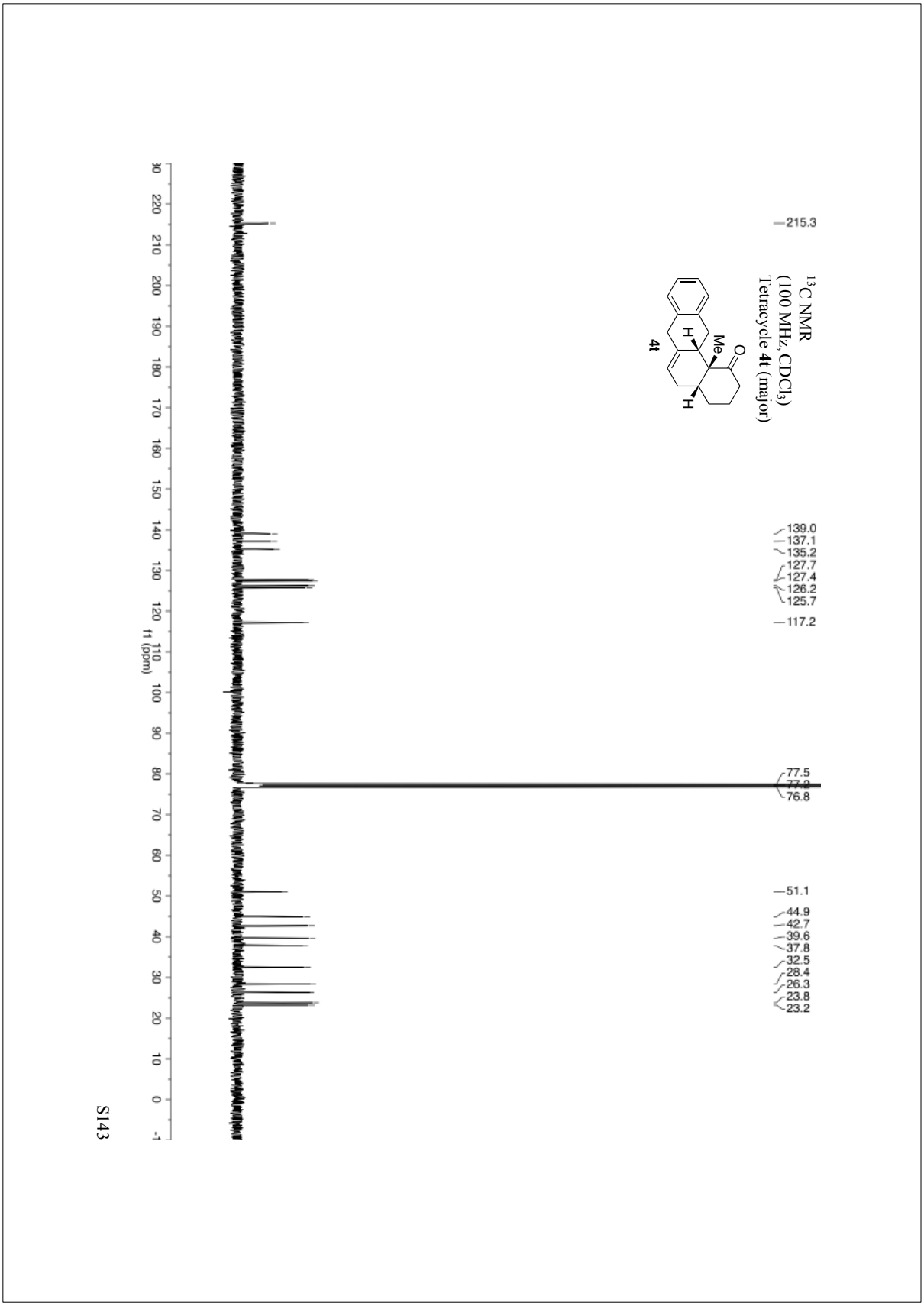
^{13}C NMR
(100 MHz, $CDCl_3$)
Tetracycle **4t** (major)
4t
Me
O
H
H
215.3
139.0
137.1
135.2
127.7
127.4
126.2
125.7
117.2
77.5
77.2
76.8
51.1
44.9
42.7
39.6
37.8
32.5
28.4
26.3
23.8
23.2
f1 (ppm)
S143

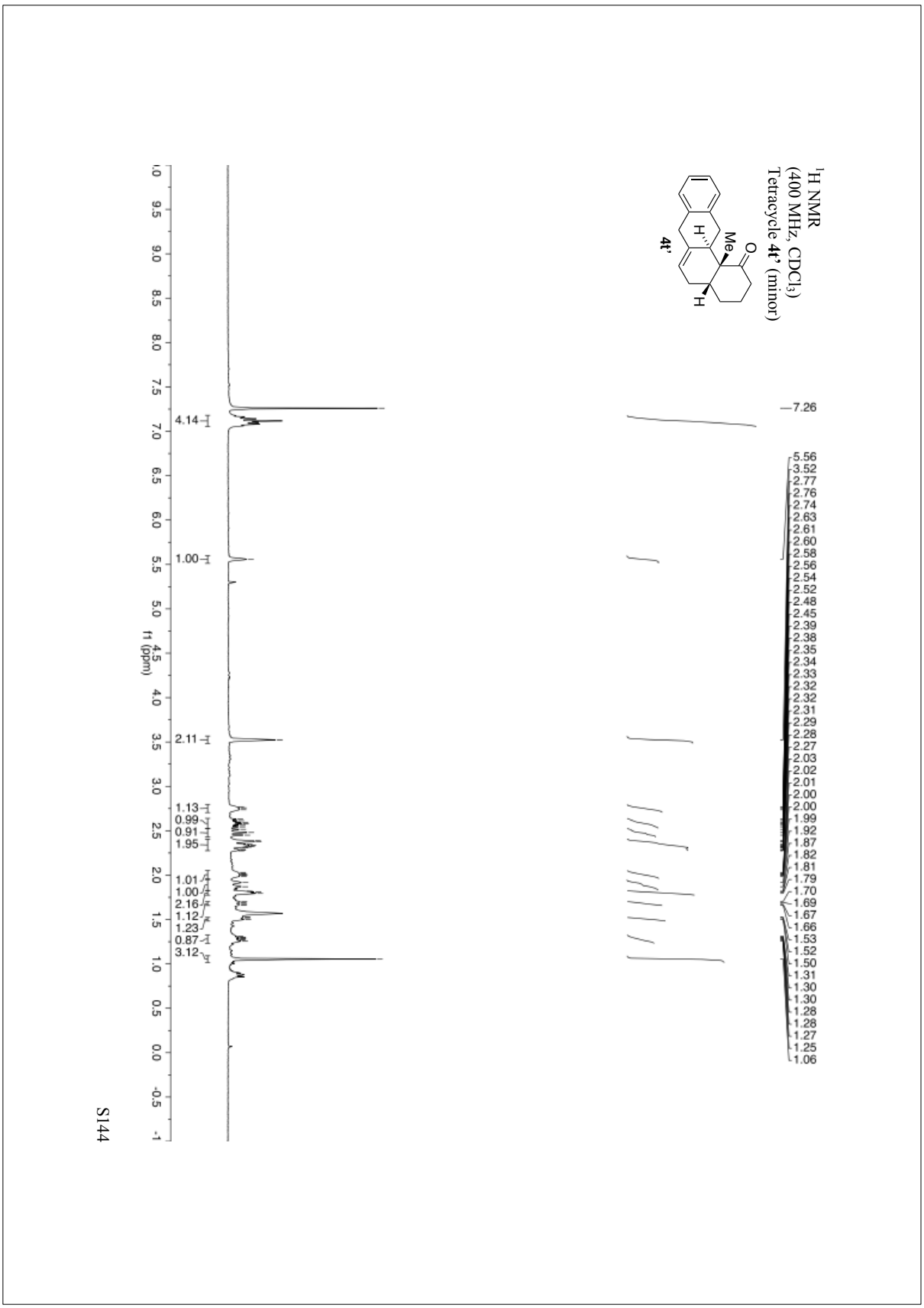
^{1}H NMR
(400 MHz, $CDCl_3$)
Tetracycle **4t'** (minor)
4t'
Me
O
H
H
7.26
5.56
3.52
2.77
2.76
2.74
2.63
2.61
2.60
2.58
2.56
2.54
2.52
2.48
2.45
2.39
2.38
2.35
2.34
2.33
2.32
2.32
2.31
2.29
2.28
2.27
2.03
2.02
2.01
2.00
2.00
1.99
1.92
1.87
1.82
1.81
1.79
1.70
1.69
1.67
1.66
1.53
1.52
1.50
1.31
1.30
1.30
1.28
1.28
1.27
1.25
1.06
4.14
1.00
2.11
1.13
0.99
0.91
1.95
1.01
1.00
2.16
1.12
1.23
0.87
3.12
f1 (ppm)

S144

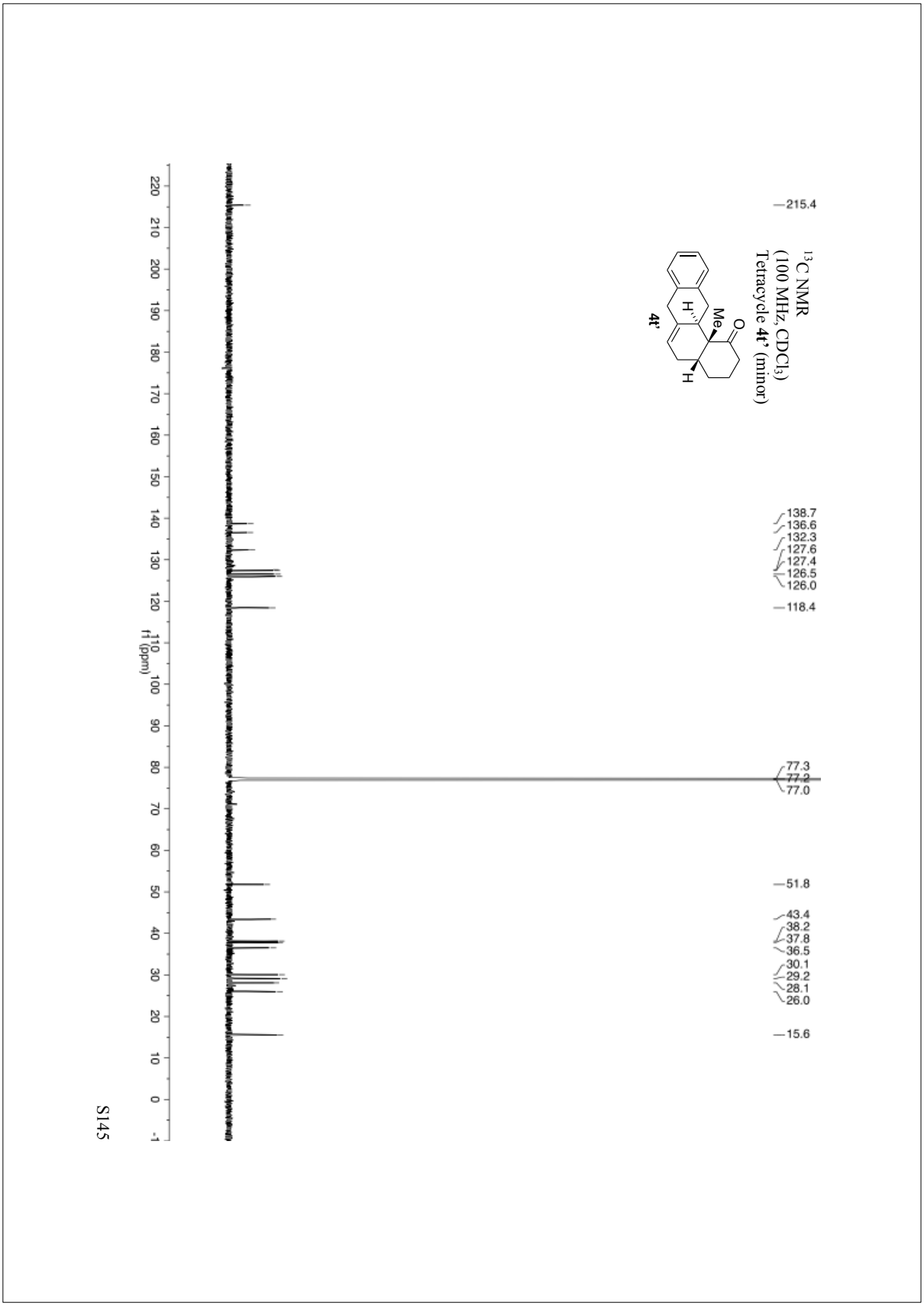
^{13}C NMR
(100 MHz, $CDCl_3$)
Tetracycle **4t'** (minor)
4t'
Me
O
H
H
215.4
138.7
136.6
132.3
127.6
127.4
126.5
126.0
118.4
77.3
77.2
77.0
51.8
43.4
38.2
37.8
36.5
30.1
29.2
28.1
26.0
15.6
f1 (ppm)
S145

HSCQ ($CDCl_3$)
Tetracycle **4t'** (minor)

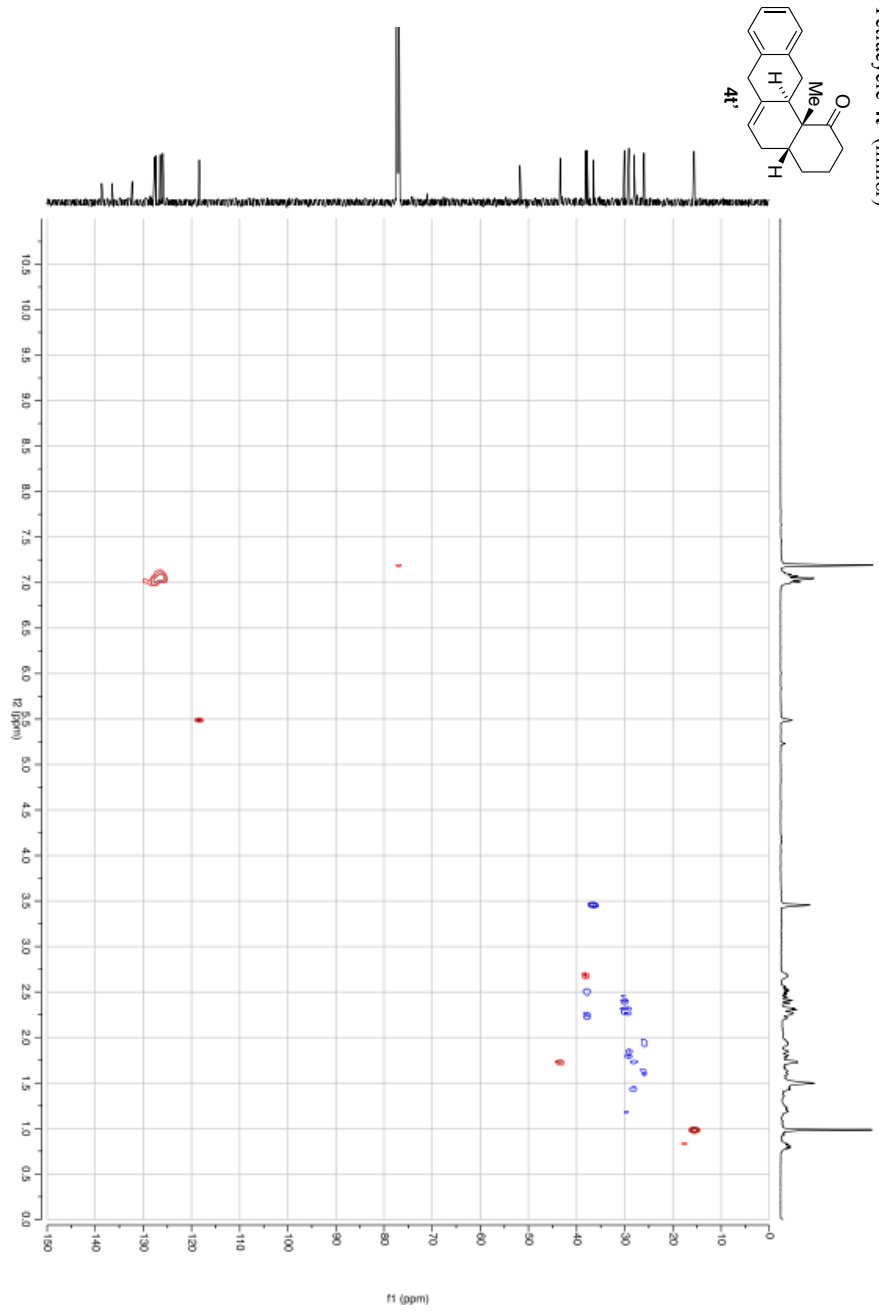

HMBC ($CDCl_3$)
Tetracycle **4t'** (minor)

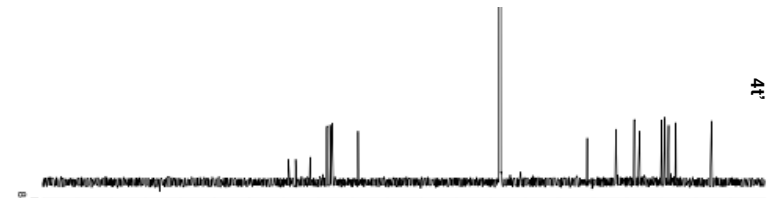

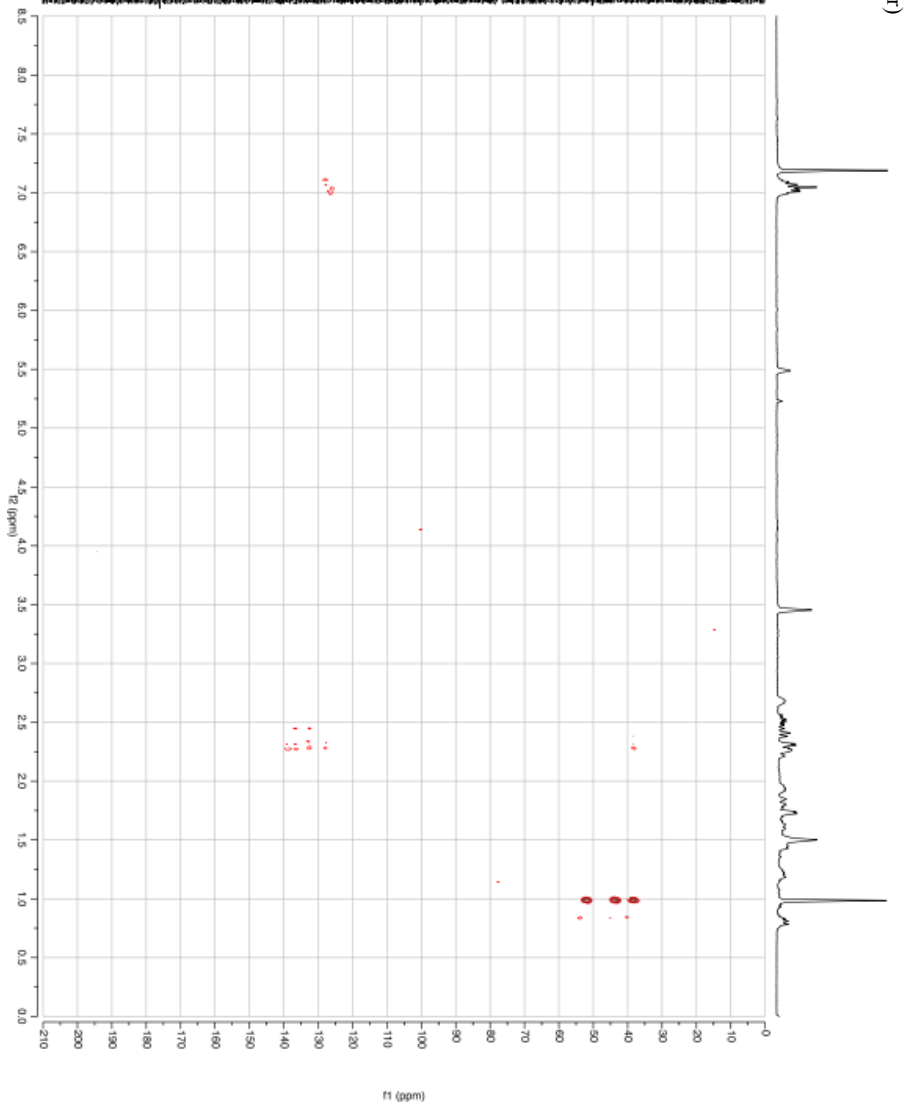

S147

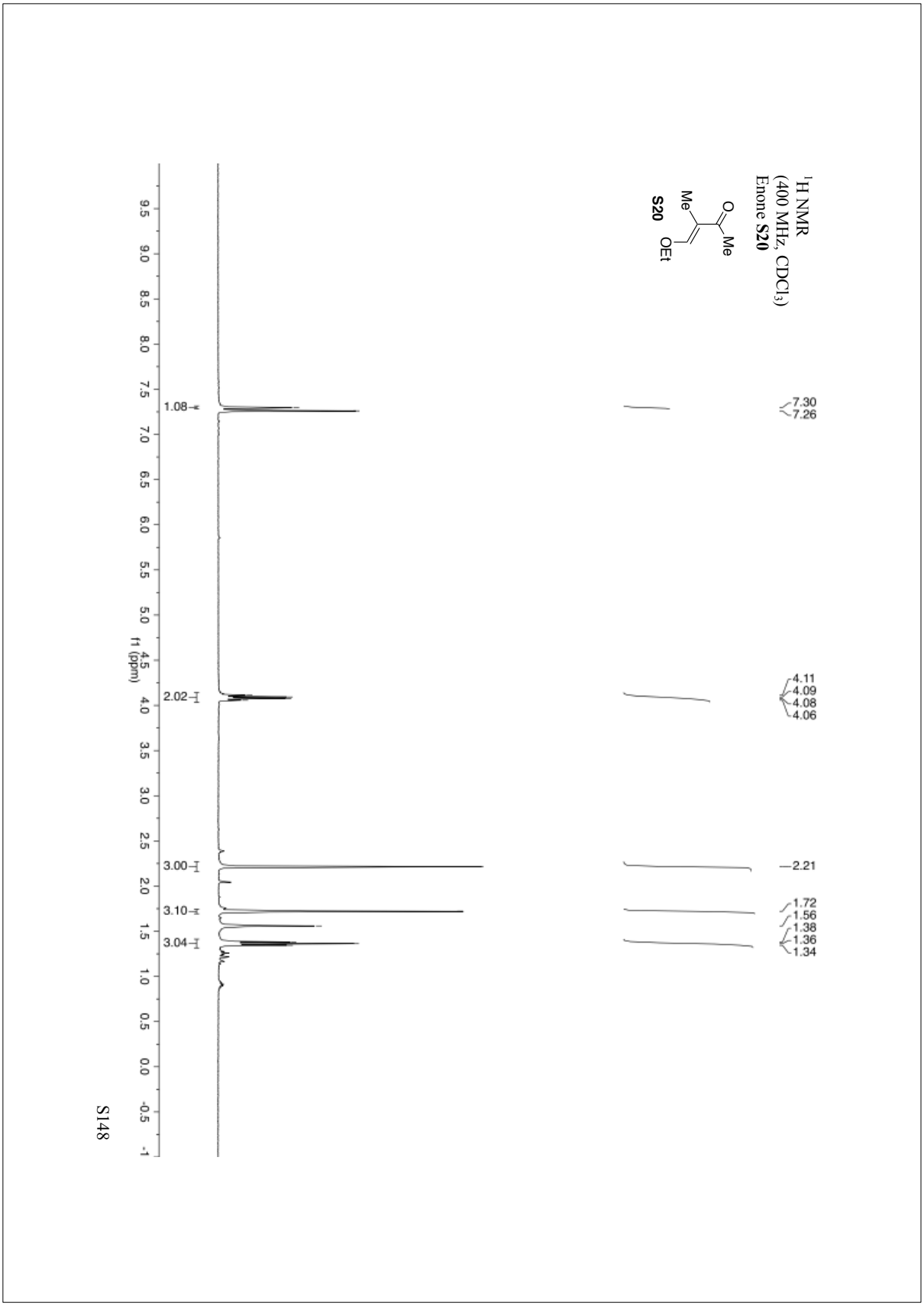
^{1}H NMR
(400 MHz, CDCl$_3$)
Enone **S20**
S20
Me
Me
OEt
7.30
7.26
4.11
4.09
4.08
4.06
2.21
1.72
1.56
1.38
1.36
1.34
1.08
2.02
3.00
3.10
3.04
f1 (ppm)

S148

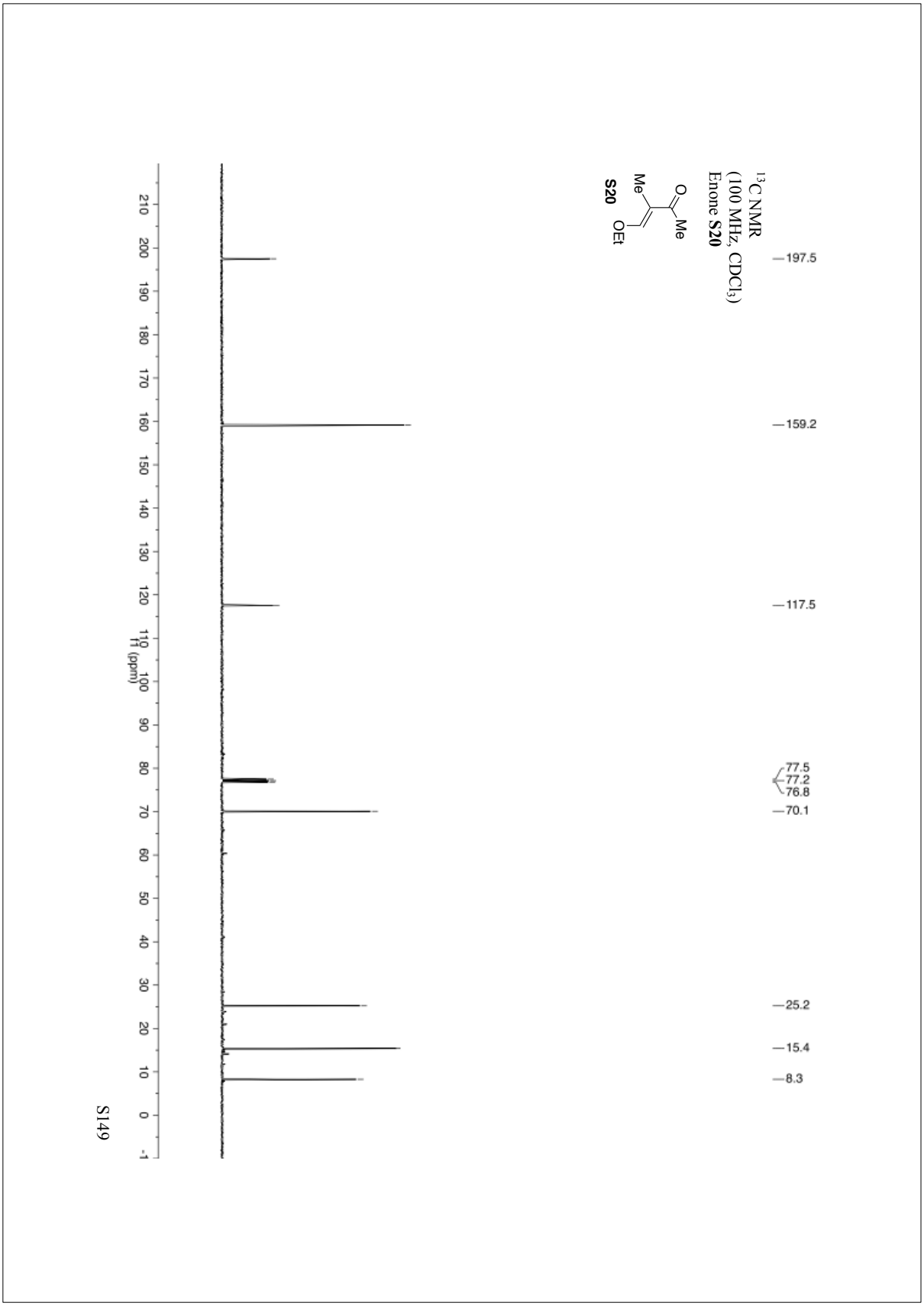
^{13}C NMR
(100 MHz, $CDCl_3$)
Enone **S20**
Me
O
Me
OEt
S20
197.5
159.2
117.5
77.5
77.2
76.8
70.1
25.2
15.4
8.3
f1 (ppm)
210 200 190 180 170 160 150 140 130 120 110 100 90 80 70 60 50 40 30 20 10 0 -1

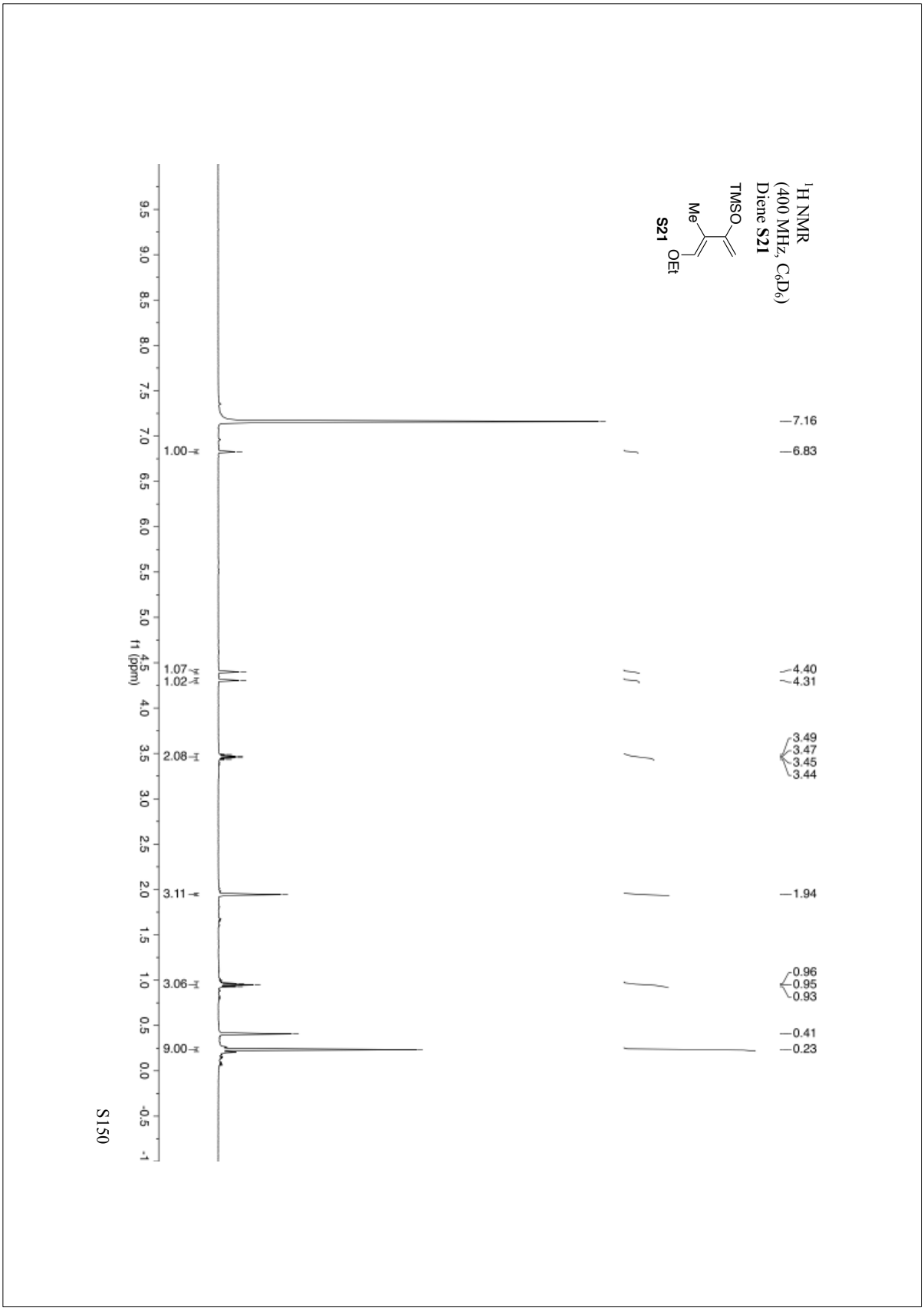
^{1}H NMR
(400 MHz, C_6D_6)
Diene **S21**
TMSO
Me
OEt
S21
7.16
6.83
4.40
4.31
3.49
3.47
3.45
3.44
1.94
0.96
0.95
0.93
0.41
0.23
1.00
1.07
1.02
2.08
3.11
3.06
9.00
f1 (ppm)

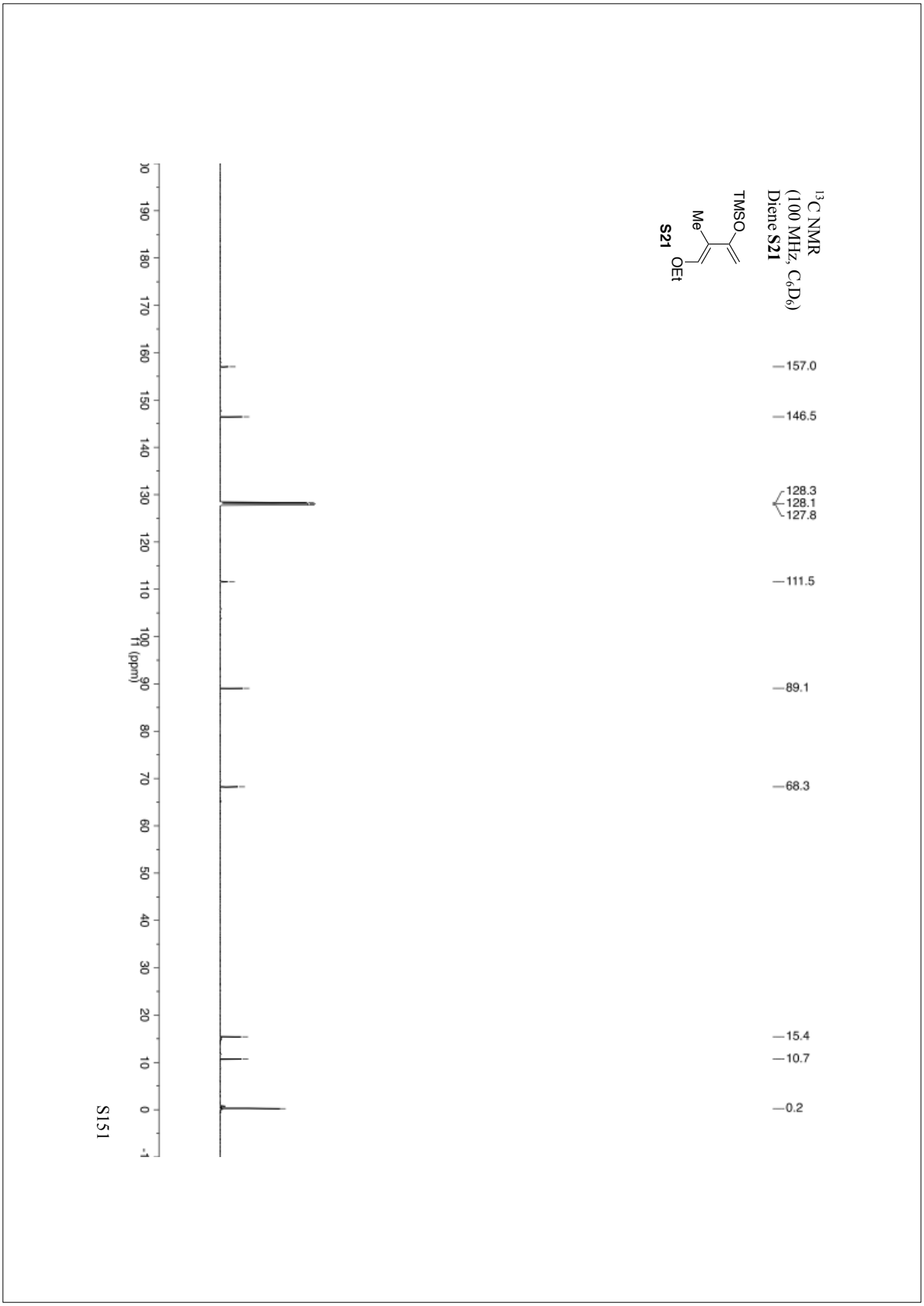
^{13}C NMR
(100 MHz, C_6D_6)
Diene **S21**
TMSO
Me
OEt
S21
157.0
146.5
128.3
128.1
127.8
111.5
89.1
68.3
15.4
10.7
0.2
f1 (ppm)
S151

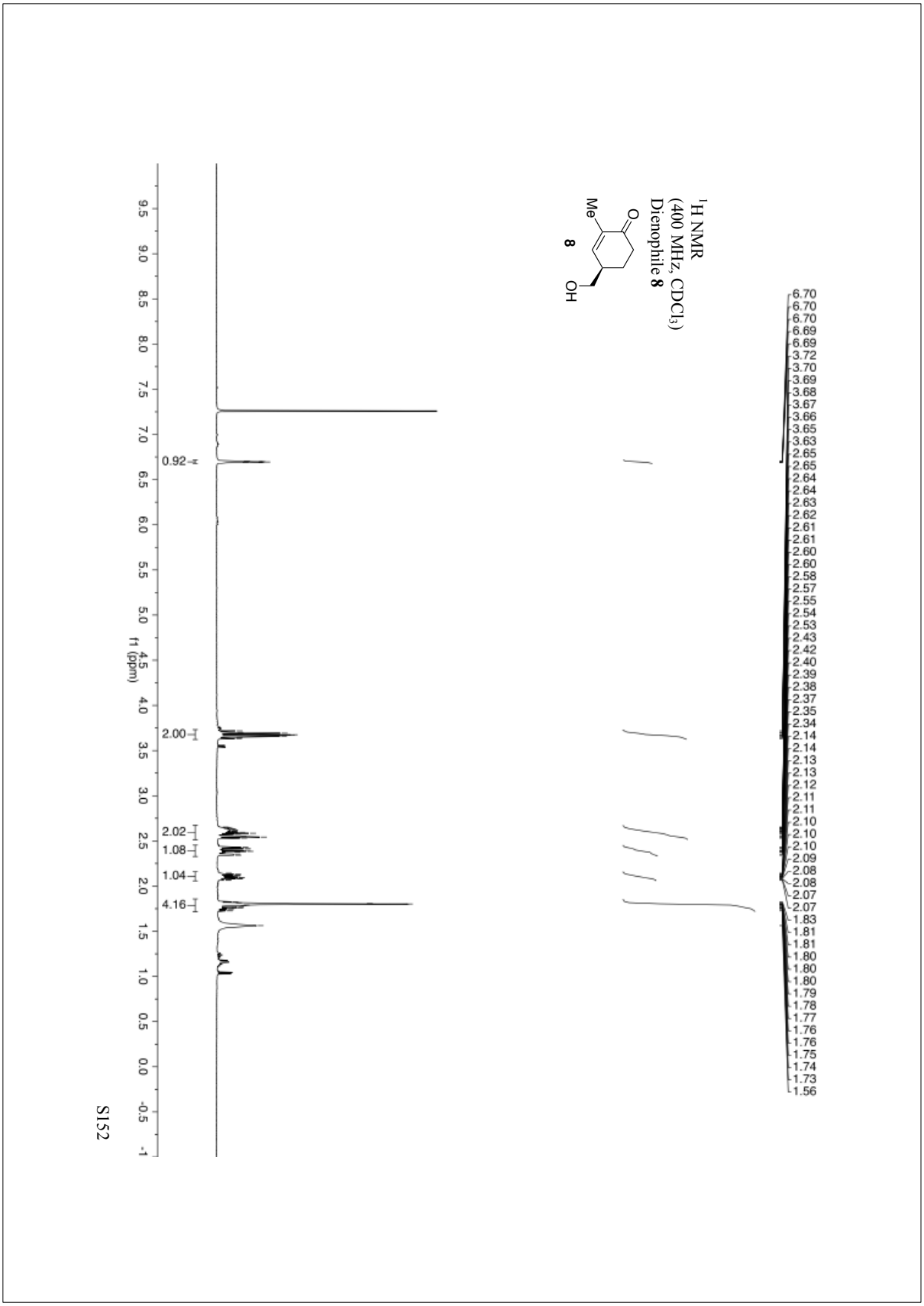
^{1}H NMR
(400 MHz, $CDCl_3$)
Dienophile **8**
Me
O
OH
8
6.70
6.70
6.70
6.69
6.69
3.72
3.70
3.69
3.68
3.67
3.66
3.65
3.63
2.65
2.65
2.64
2.64
2.63
2.62
2.61
2.61
2.60
2.60
2.58
2.57
2.55
2.54
2.53
2.43
2.42
2.40
2.39
2.38
2.37
2.35
2.34
2.14
2.14
2.13
2.13
2.12
2.11
2.11
2.10
2.10
2.10
2.09
2.08
2.08
2.07
2.07
1.83
1.81
1.81
1.80
1.80
1.80
1.79
1.78
1.77
1.76
1.76
1.75
1.74
1.73
1.56
0.92
2.00
2.02
1.08
1.04
4.16
f1 (ppm)
9.5 9.0 8.5 8.0 7.5 7.0 6.5 6.0 5.5 5.0 4.5 4.0 3.5 3.0 2.5 2.0 1.5 1.0 0.5 0.0 -0.5 -1
S152

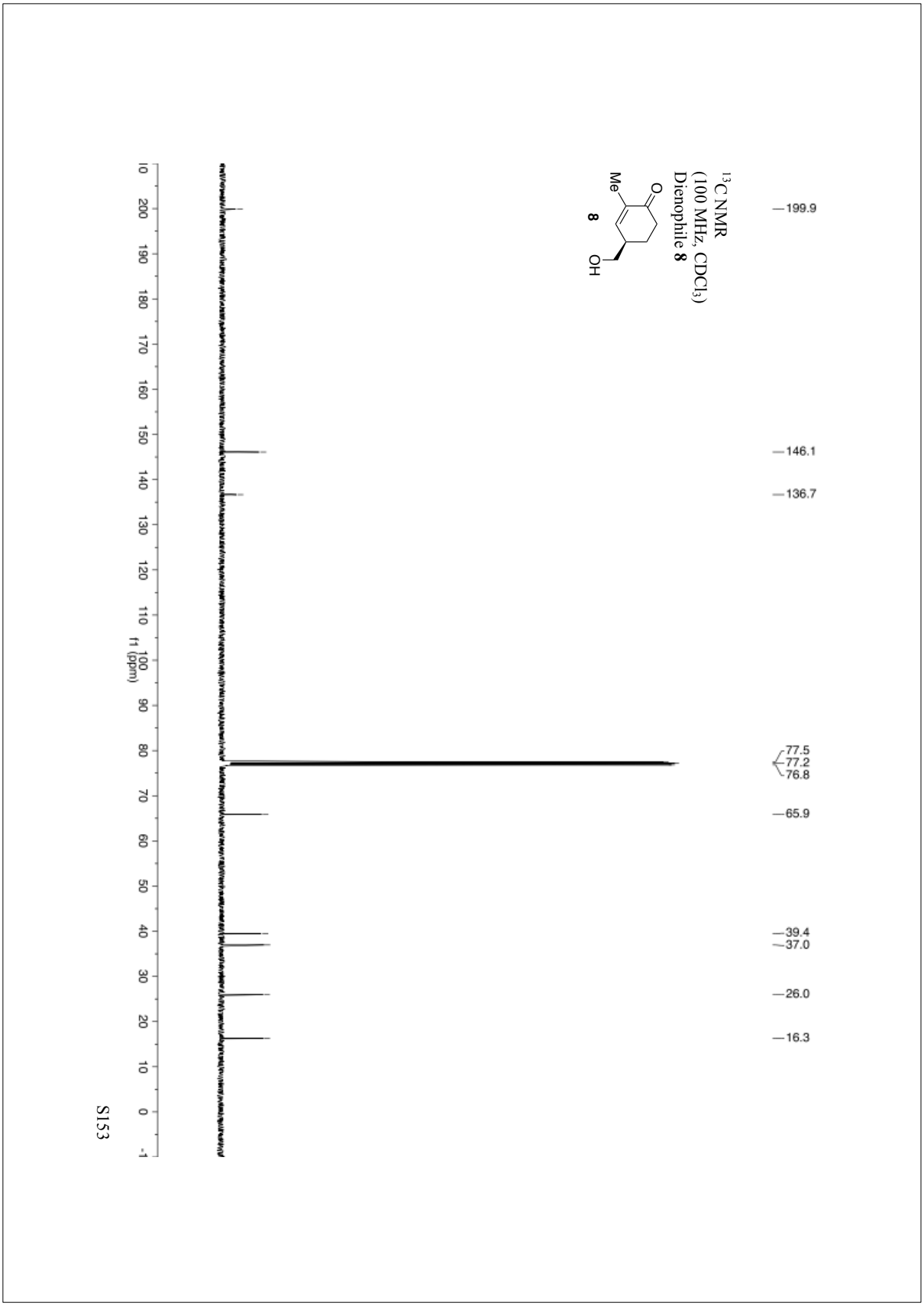
^{13}C NMR
(100 MHz, $CDCl_3$)
Dienophile **8**
Me
O
OH
8
199.9
146.1
136.7
77.5
77.2
76.8
65.9
39.4
37.0
26.0
16.3
f1 (ppm)
S153

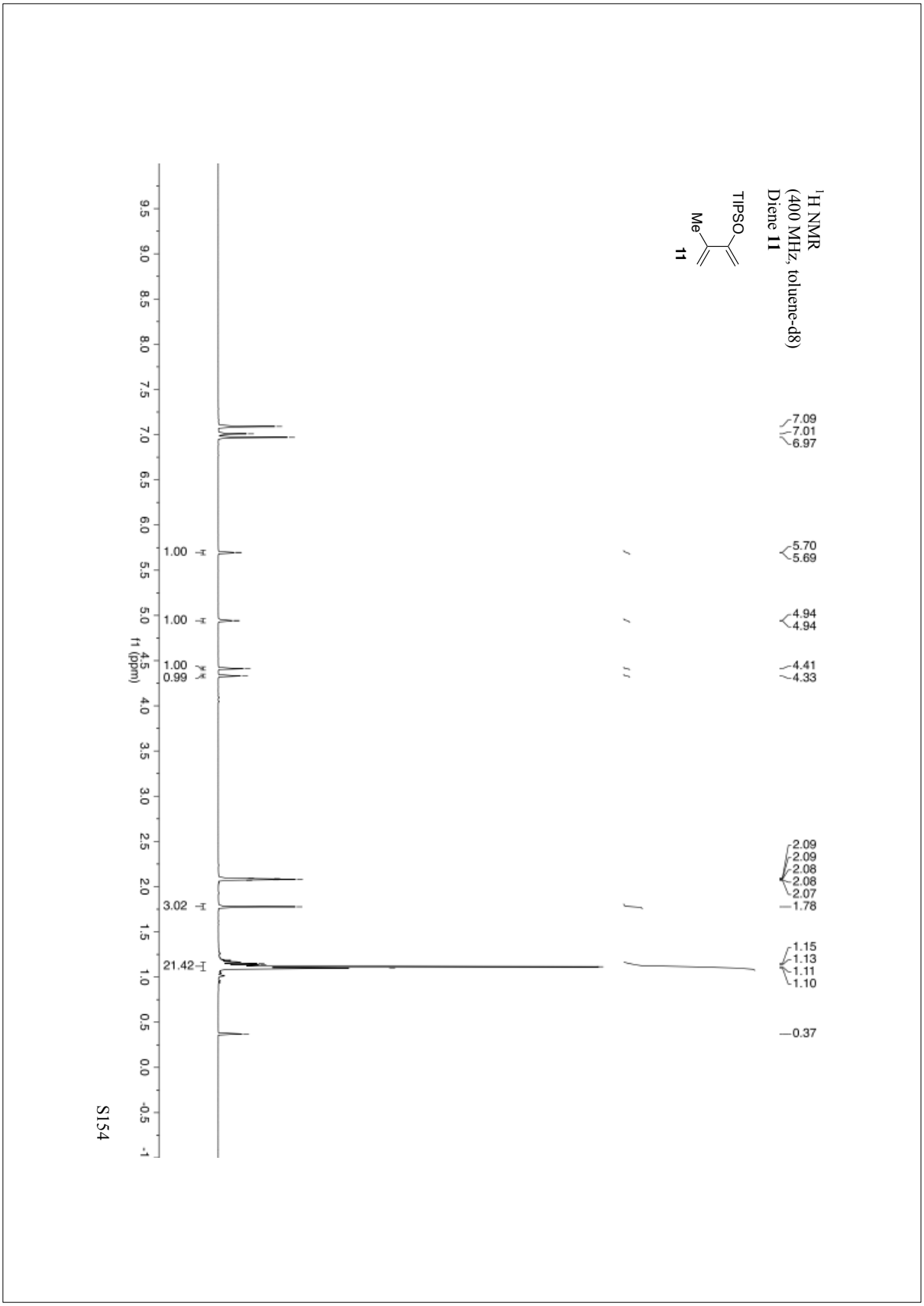
^{1}H NMR
(400 MHz, toluene-d8)
Diene **11**
TIPSO
Me
11
7.09
7.01
6.97
5.70
5.69
4.94
4.94
4.41
4.33
2.09
2.09
2.08
2.08
2.07
1.78
1.15
1.13
1.11
1.10
0.37
1.00
1.00
1.00
0.99
3.02
21.42
f1 (ppm)
S154

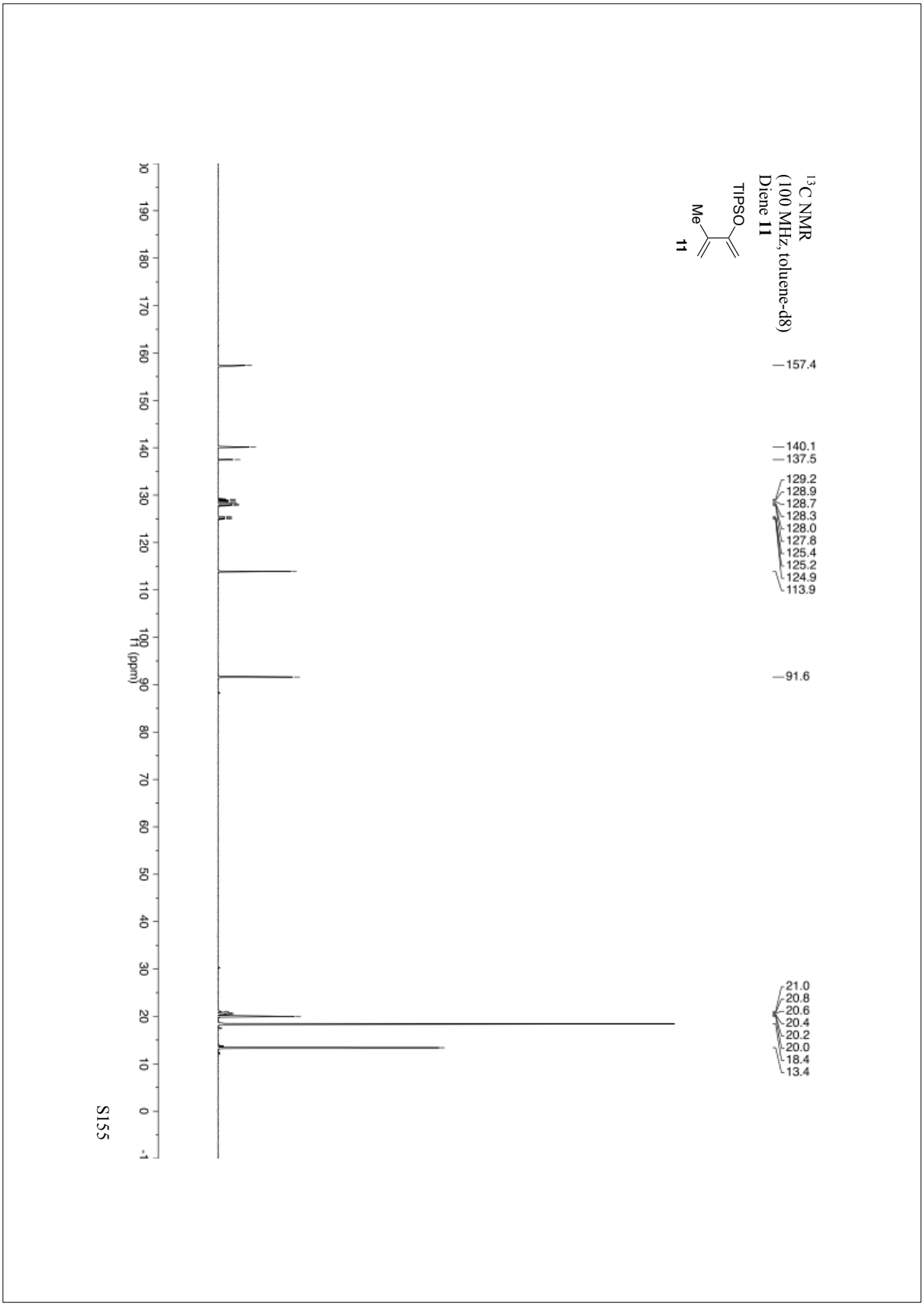
^{13}C NMR
(100 MHz, toluene-d8)
Diene **11**
TIPSO
Me
11
157.4
140.1
137.5
129.2
128.9
128.7
128.3
128.0
127.8
125.4
125.2
124.9
113.9
91.6
21.0
20.8
20.6
20.4
20.2
20.0
18.4
13.4
f1 (ppm)
S155

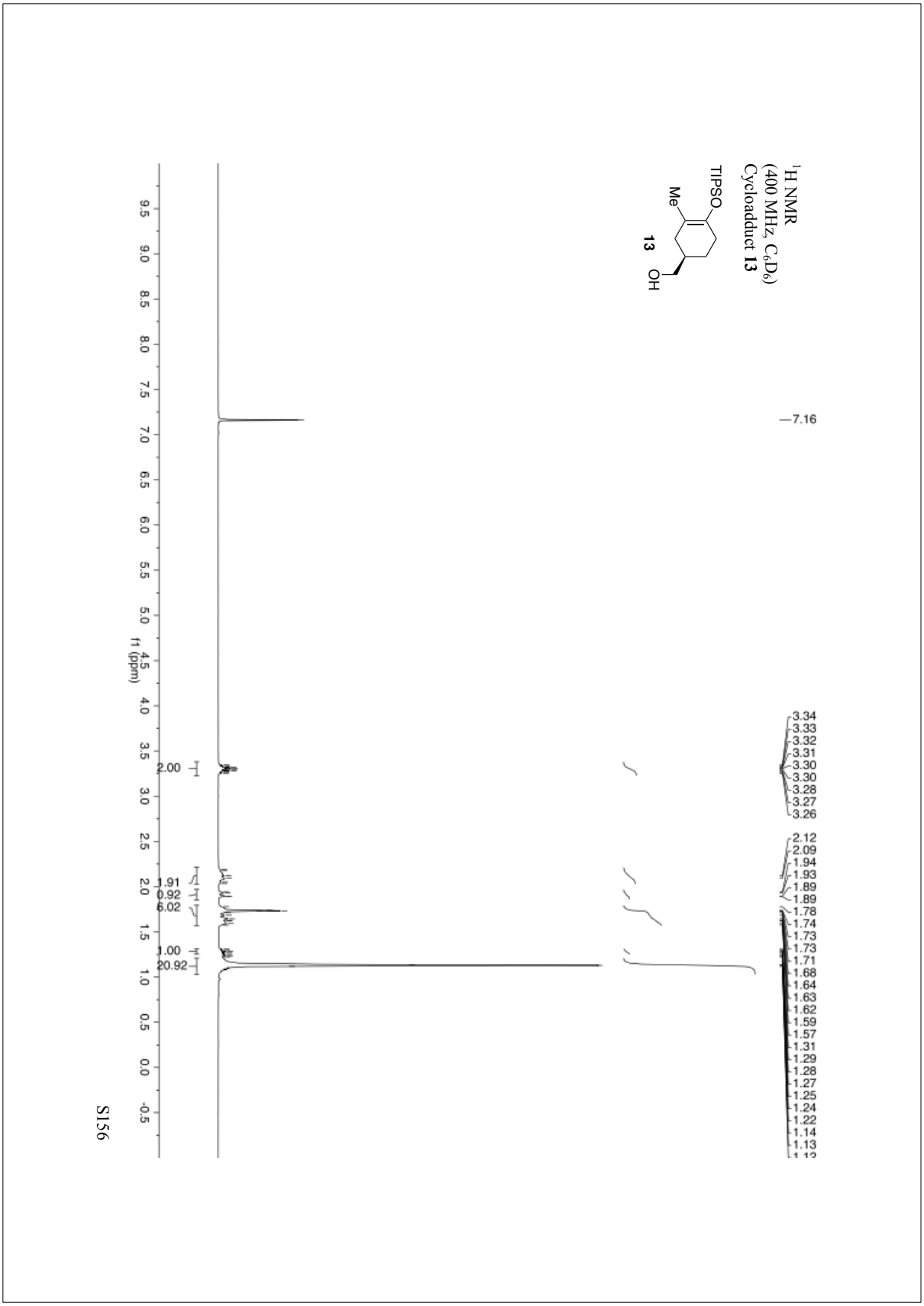
^{1}H NMR
(400 MHz, C_6D_6)
Cycloadduct **13**
TIPSO
Me
13
OH
7.16
3.34
3.33
3.32
3.31
3.30
3.30
3.28
3.27
3.26
2.12
2.09
1.94
1.93
1.89
1.89
1.78
1.74
1.73
1.73
1.71
1.68
1.64
1.63
1.62
1.59
1.57
1.31
1.29
1.28
1.27
1.25
1.24
1.22
1.14
1.13
2.00
1.91
0.92
6.02
1.00
20.92
f1 (ppm)

S156

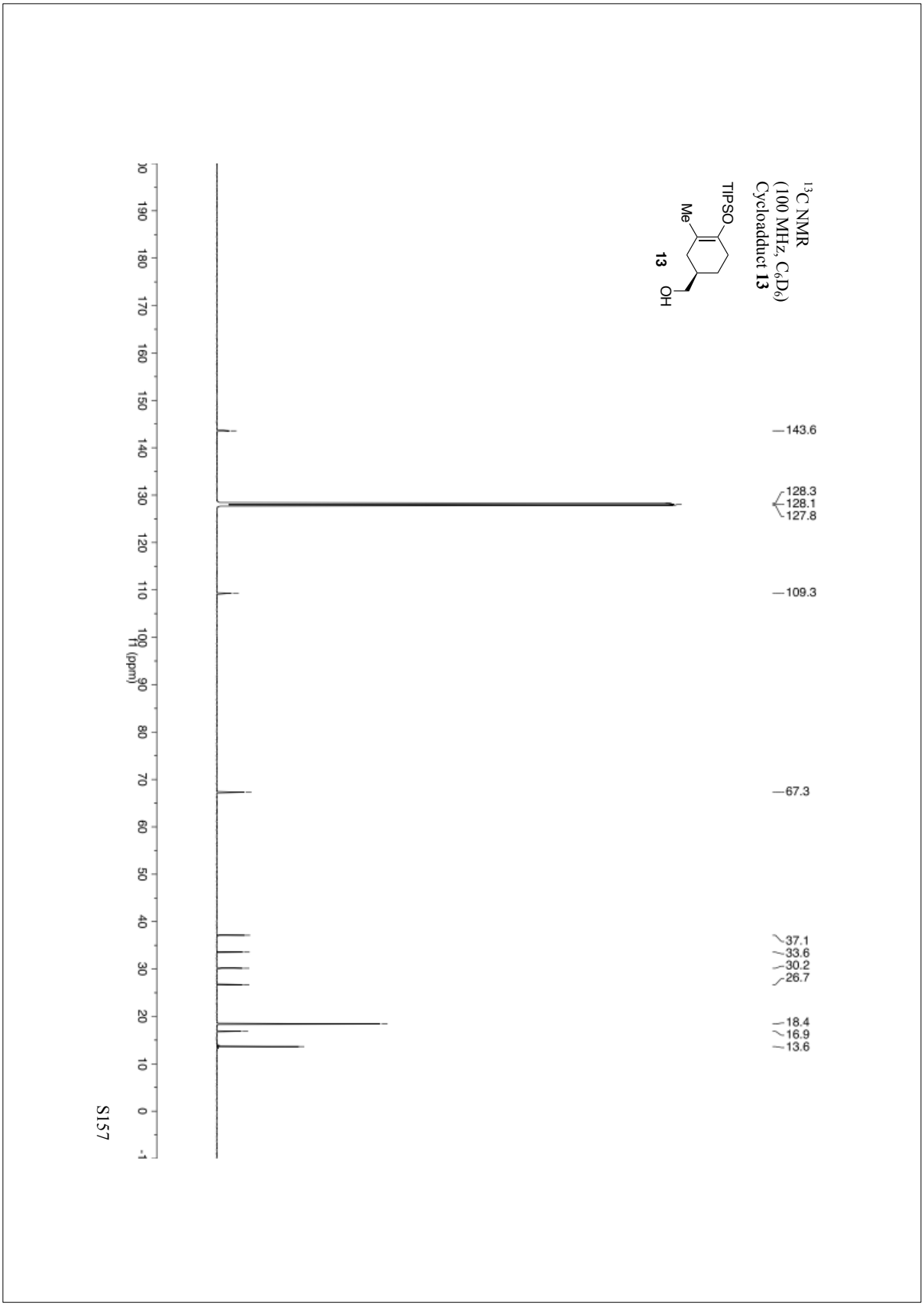
^{13}C NMR
(100 MHz, C_6D_6)
Cycloadduct **13**
TIPSO
Me
13
OH
143.6
128.3
128.1
127.8
109.3
67.3
37.1
33.6
30.2
26.7
18.4
16.9
13.6
f1 (ppm)
S157

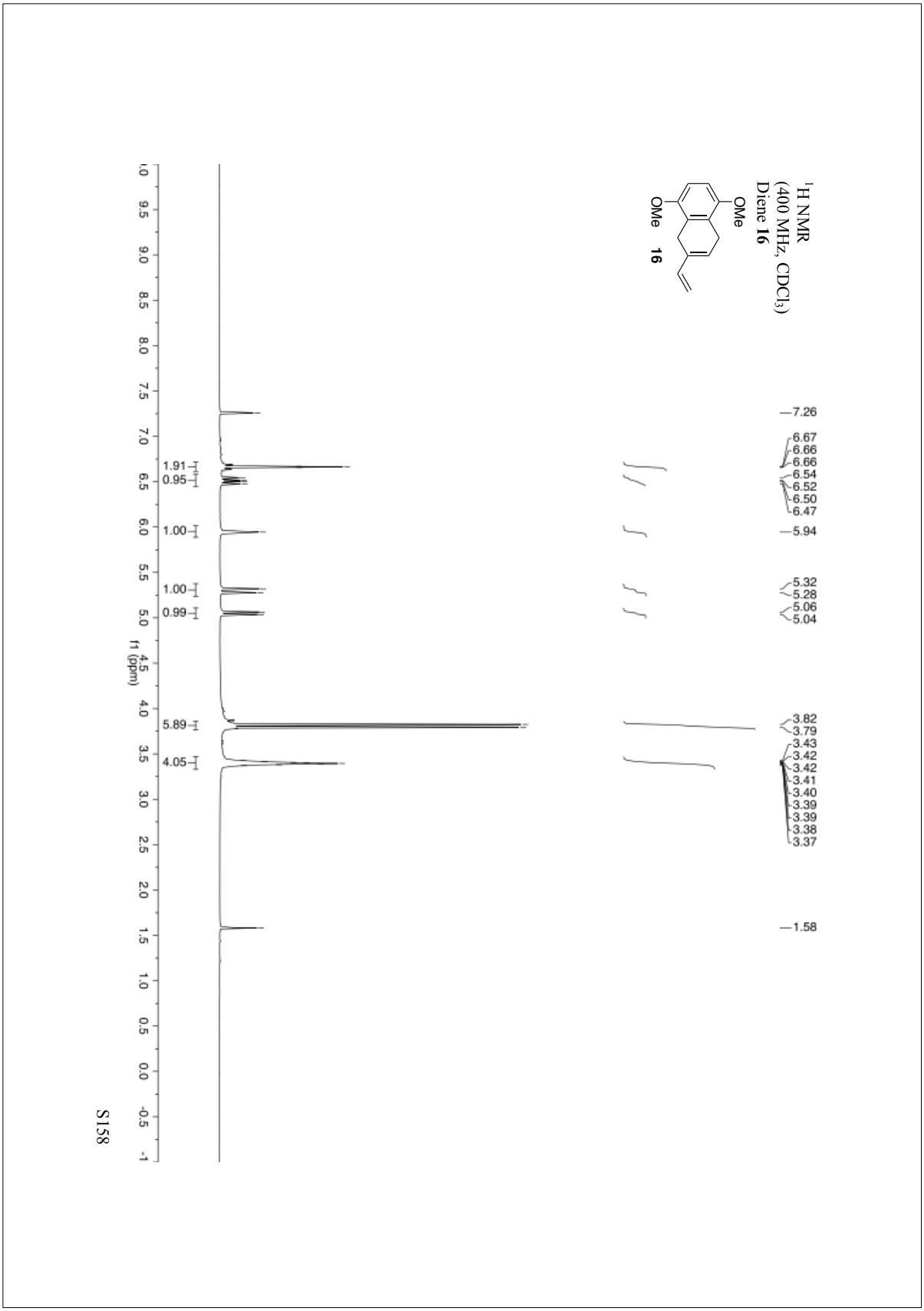
^{1}H NMR
(400 MHz, $CDCl_3$)
Diene **16**
OMe
OMe
16
7.26
6.67
6.66
6.66
6.54
6.52
6.50
6.47
5.94
5.32
5.28
5.06
5.04
3.82
3.79
3.43
3.42
3.42
3.41
3.40
3.39
3.39
3.38
3.37
1.58
1.91
0.95
1.00
1.00
0.99
5.89
4.05
f1 (ppm)
S158

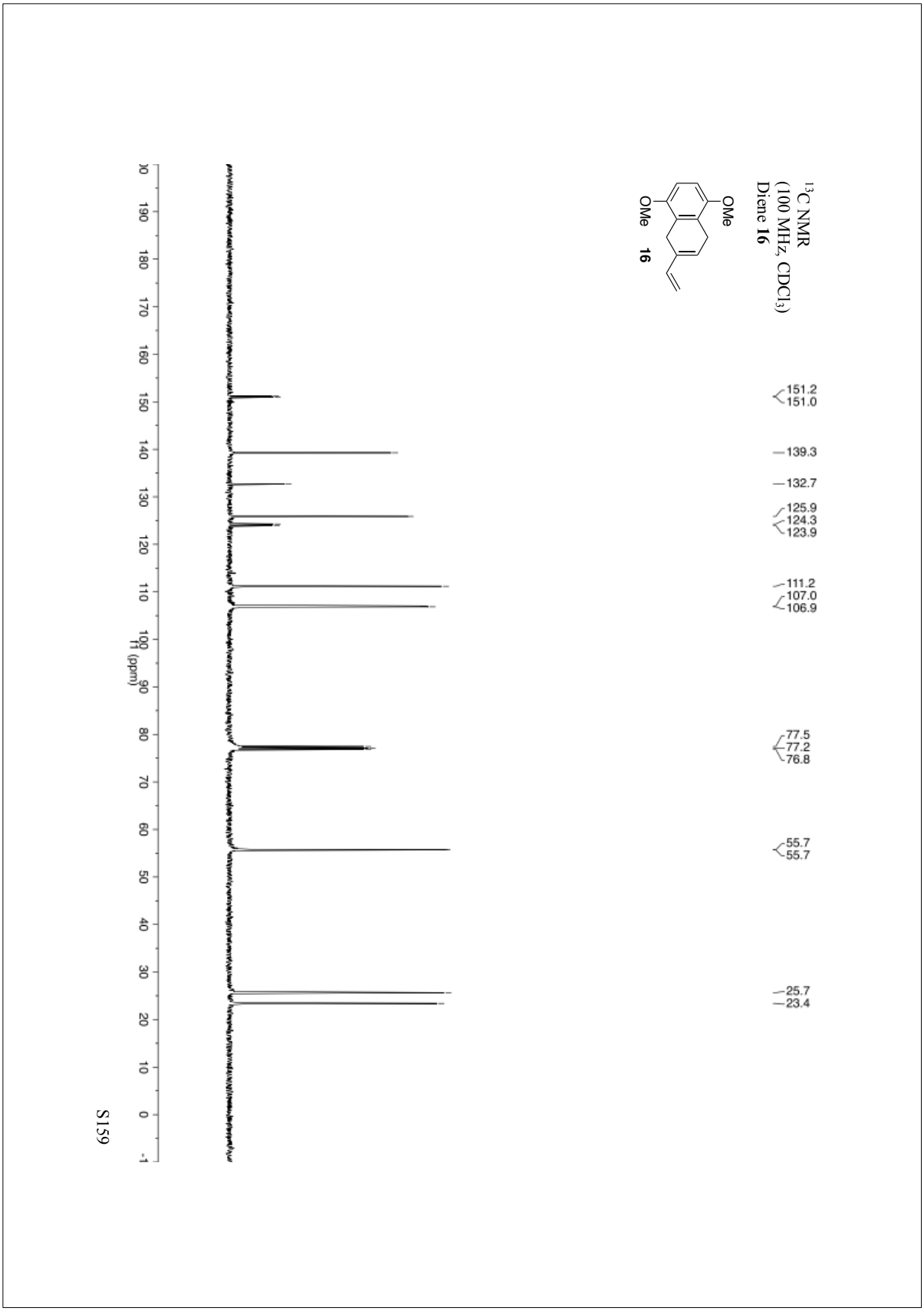
^{13}C NMR
(100 MHz, CDCl$_3$)
Diene **16**
OMe
OMe
16
151.2
151.0
139.3
132.7
125.9
124.3
123.9
111.2
107.0
106.9
77.5
77.2
76.8
55.7
55.7
25.7
23.4
f1 (ppm)
S159

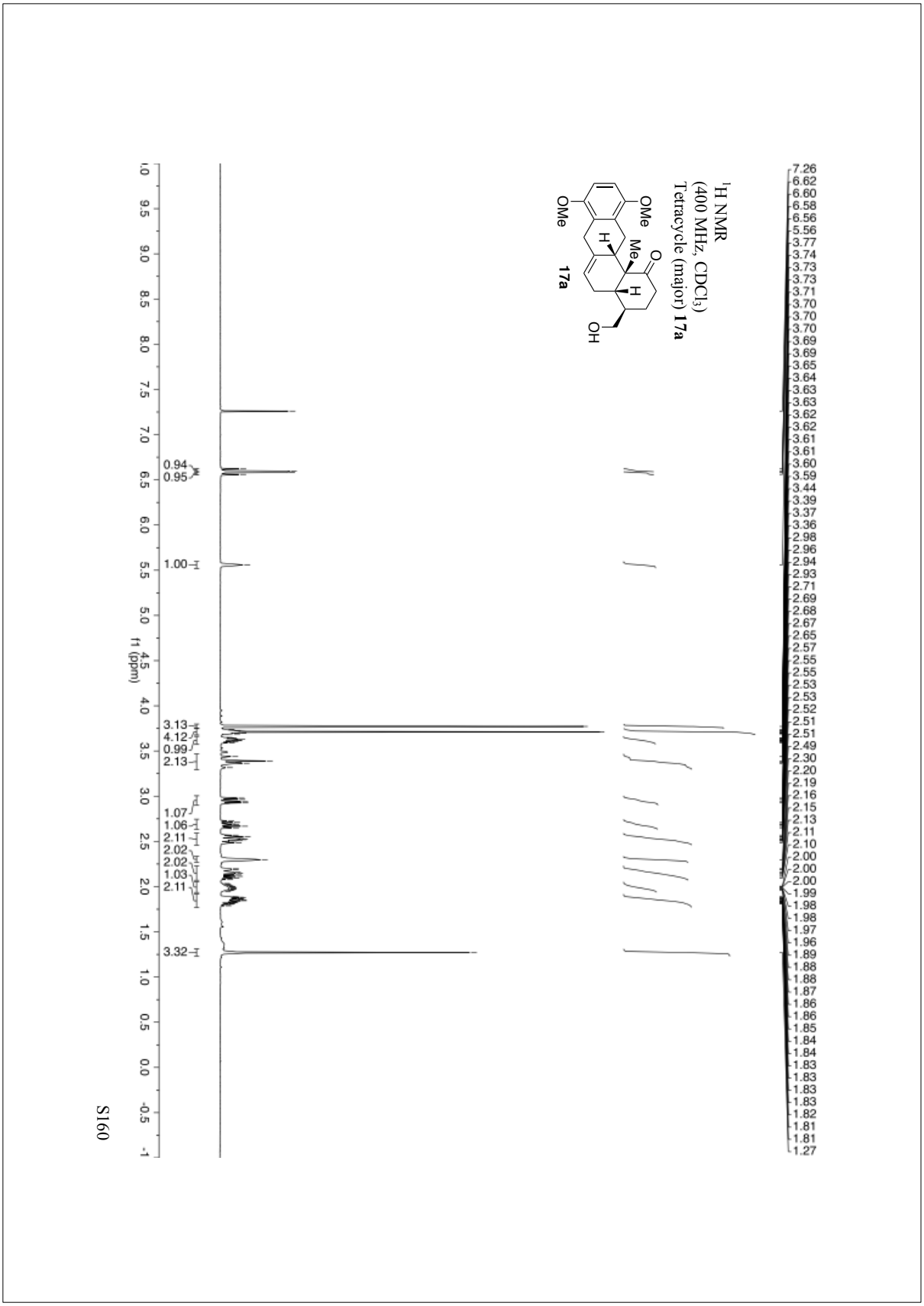
^{1}H NMR
(400 MHz, $CDCl_3$)
Tetracycle (major) **17a**
OMe
OMe
Me
O
H
H
OH
17a
f1 (ppm)
0.94
0.95
1.00
3.13
4.12
0.99
2.13
1.07
1.06
2.11
2.02
2.02
1.03
2.11
3.32

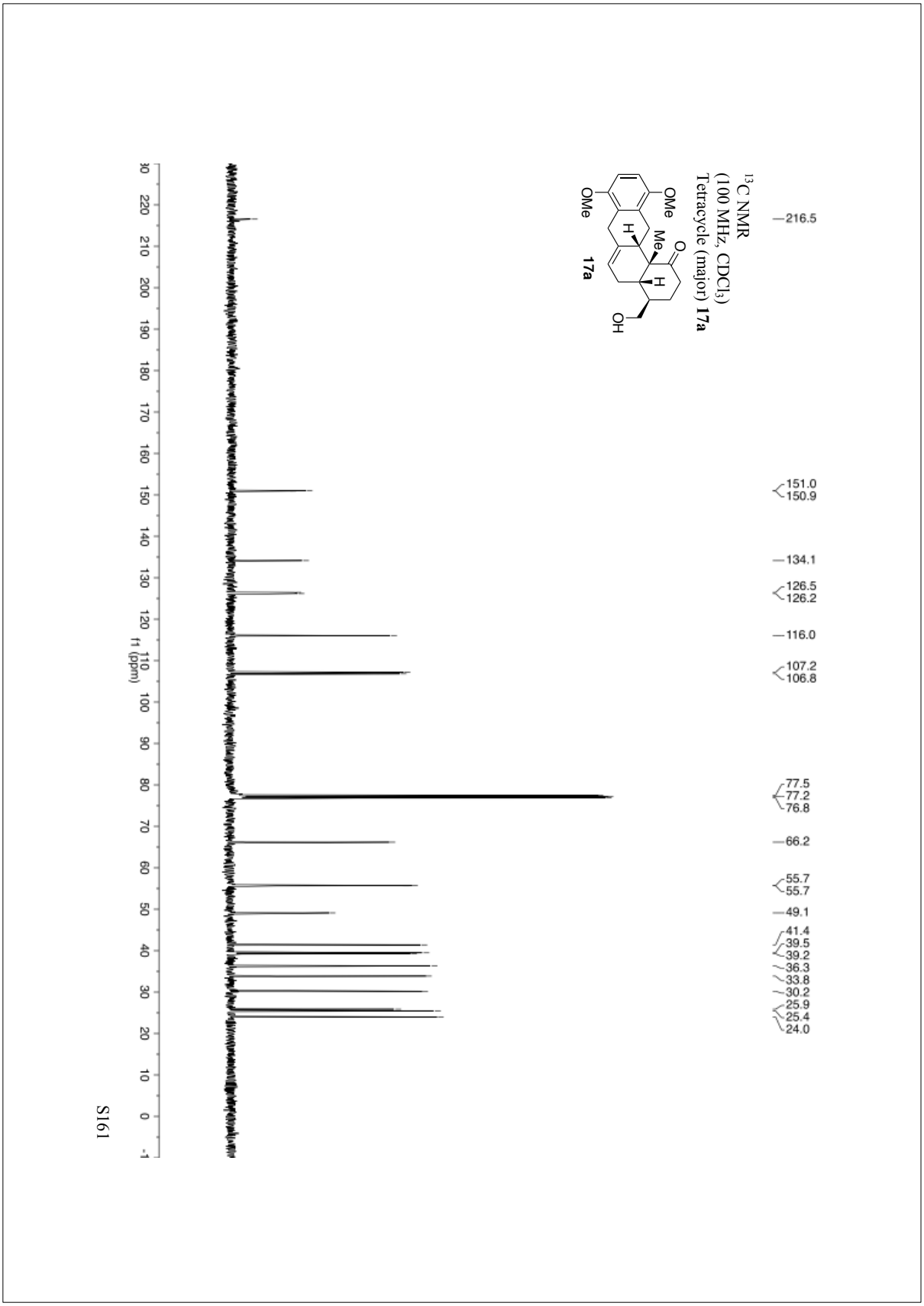
^{13}C NMR
(100 MHz, $CDCl_3$)
Tetracycle (major) **17a**
OMe
OMe
Me
H
H
O
OH
17a
216.5
151.0
150.9
134.1
126.5
126.2
116.0
107.2
106.8
77.5
77.2
76.8
66.2
55.7
55.7
49.1
41.4
39.5
39.2
36.3
33.8
30.2
25.9
25.4
24.0
f1 (ppm)
S161

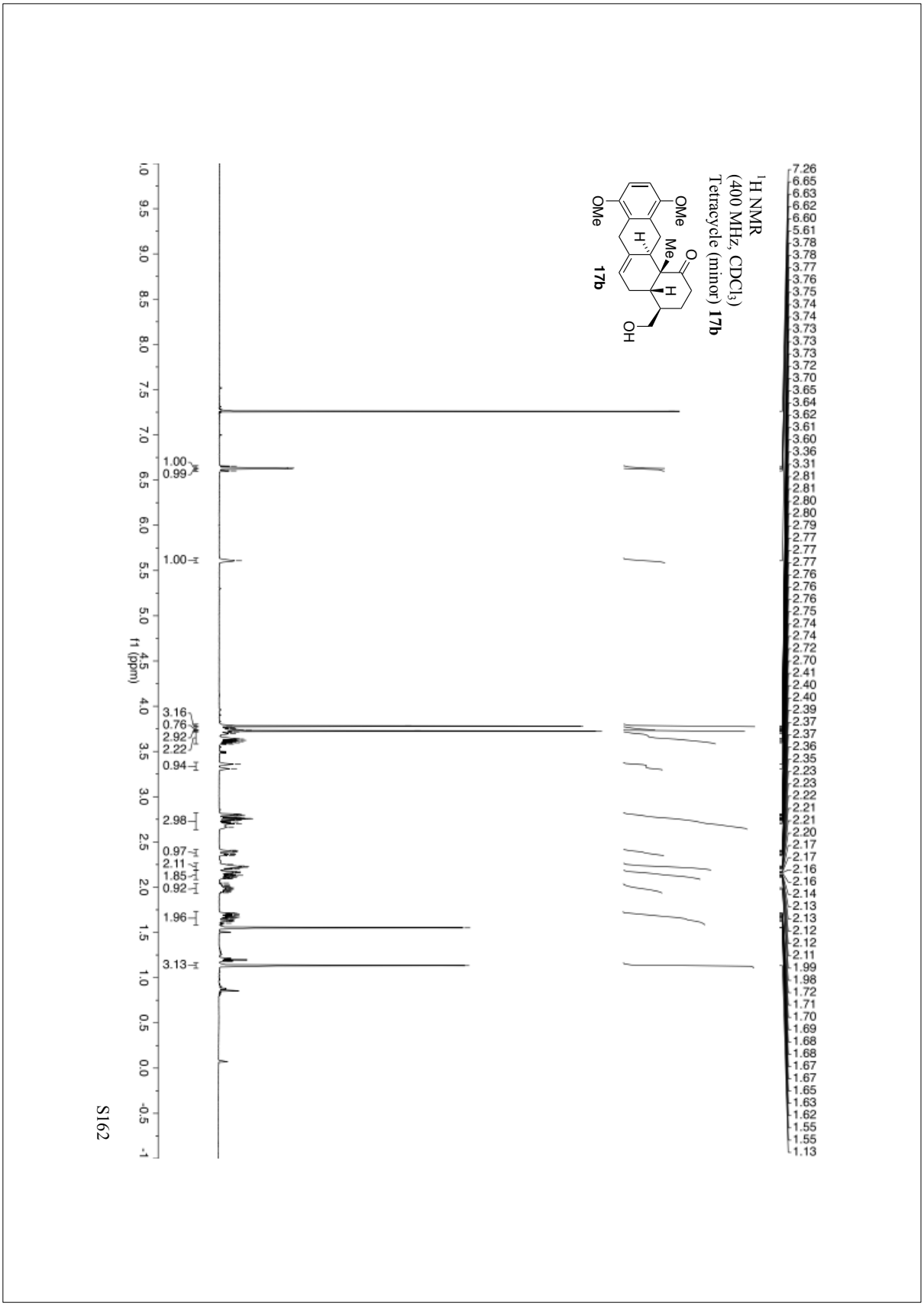
^{1}H NMR
(400 MHz, $CDCl_3$)
Tetracycle (minor) **17b**
OMe
OMe
Me
O
H
H
OH
17b
f1 (ppm)
1.00
0.99
1.00
3.16
0.76
2.92
2.22
0.94
2.98
0.97
2.11
1.85
0.92
1.96
3.13

S162

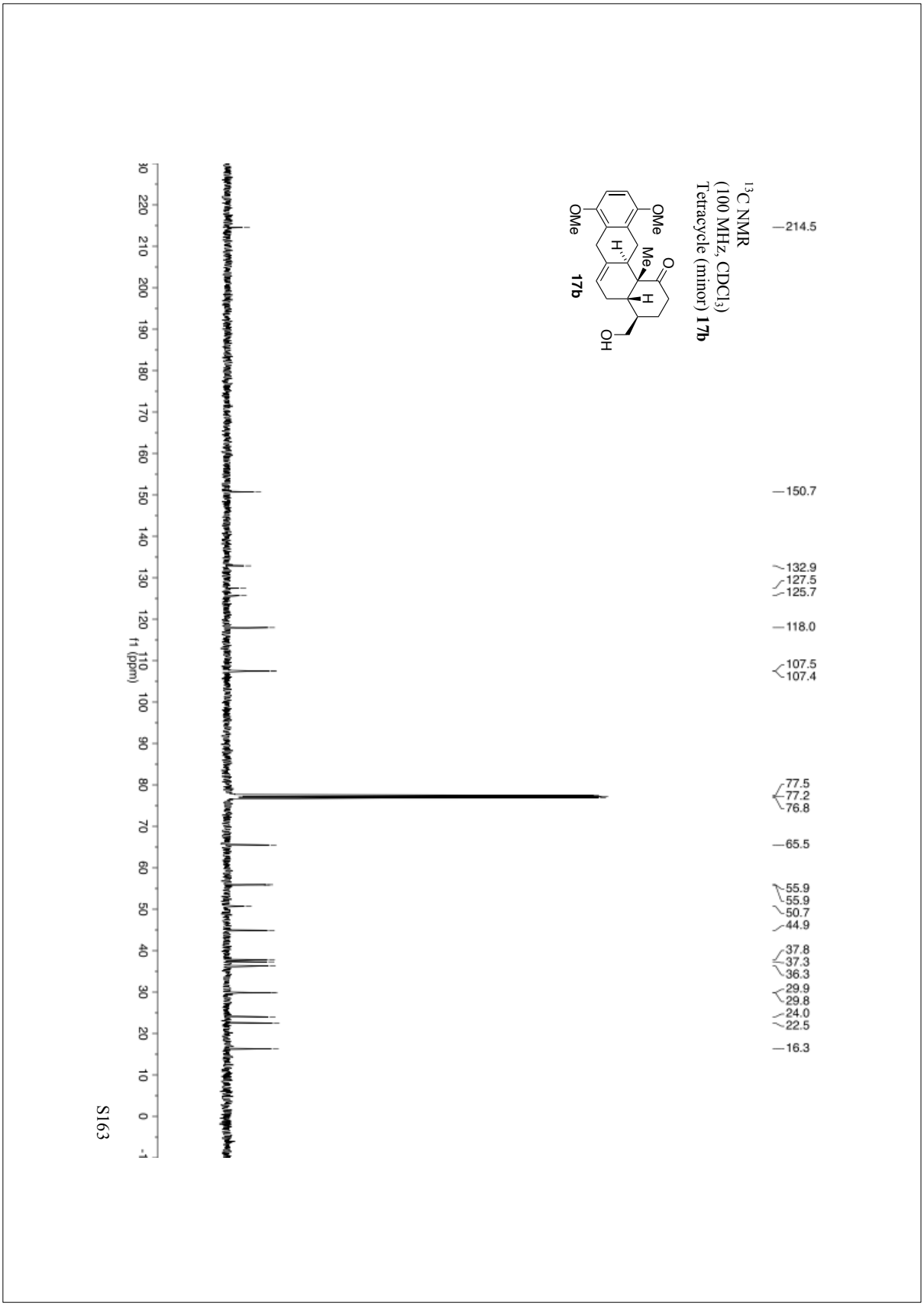
^{13}C NMR
(100 MHz, $CDCl_3$)
Tetracycle (minor) **17b**
OMe
OMe
Me
H
H
O
OH
17b
214.5
150.7
132.9
127.5
125.7
118.0
107.5
107.4
77.5
77.2
76.8
65.5
55.9
55.9
50.7
44.9
37.8
37.3
36.3
29.9
29.8
24.0
22.5
16.3
f1 (ppm)
S163

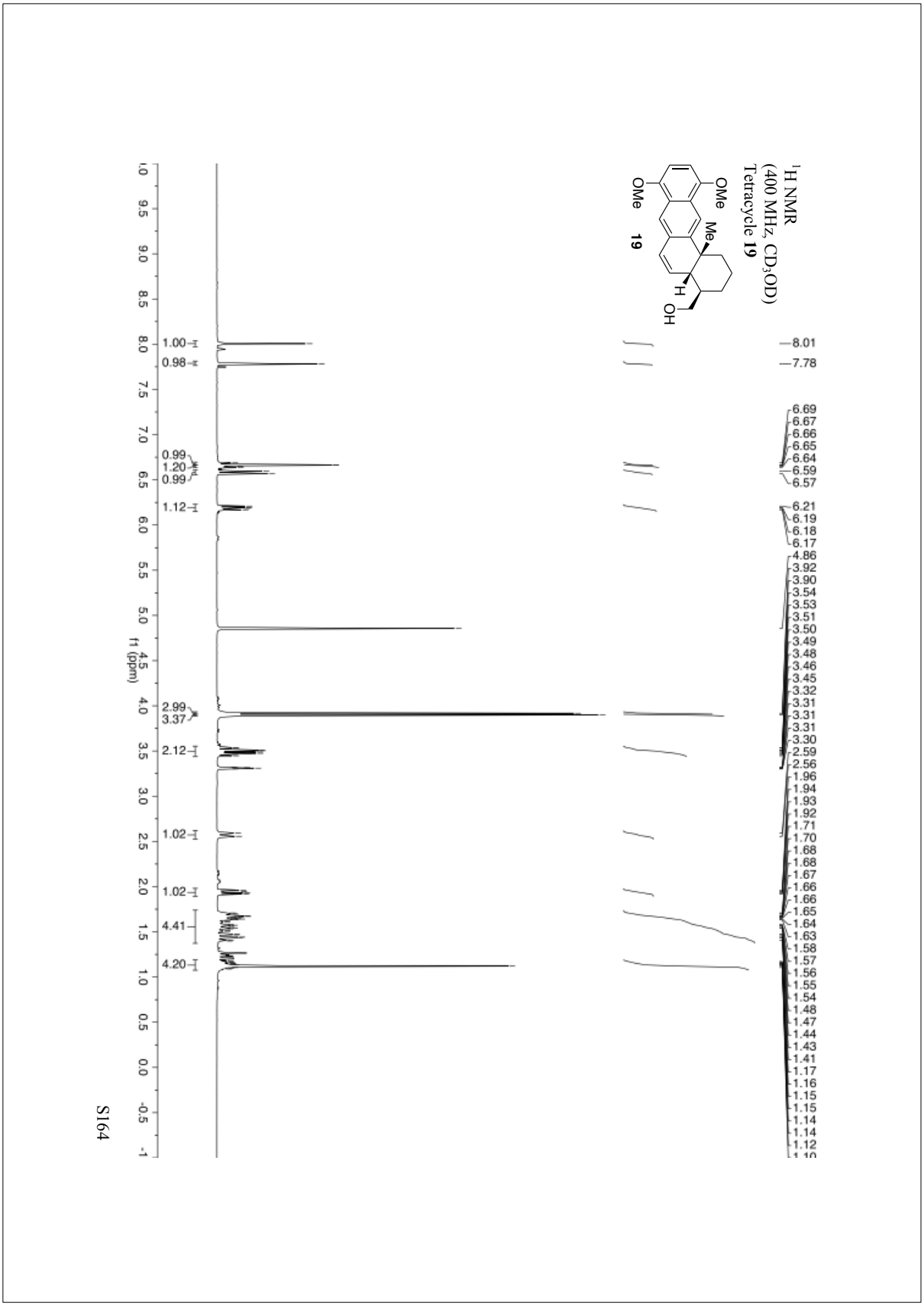
^{1}H NMR
(400 MHz, CD_3OD)
Tetracycle **19**
OMe
Me
H
OH
OMe
19
f1 (ppm)
1.00
0.98
0.99
1.20
0.99
1.12
2.99
3.37
2.12
1.02
1.02
4.41
4.20
8.01
7.78
6.69
6.67
6.66
6.65
6.64
6.59
6.57
6.21
6.19
6.18
6.17
4.86
3.92
3.90
3.54
3.53
3.51
3.50
3.49
3.48
3.46
3.45
3.32
3.31
3.31
3.31
3.30
2.59
2.56
1.96
1.94
1.93
1.92
1.71
1.70
1.68
1.68
1.67
1.66
1.66
1.65
1.64
1.63
1.58
1.57
1.56
1.55
1.54
1.48
1.47
1.44
1.43
1.41
1.17
1.16
1.15
1.15
1.14
1.14
1.12

S164

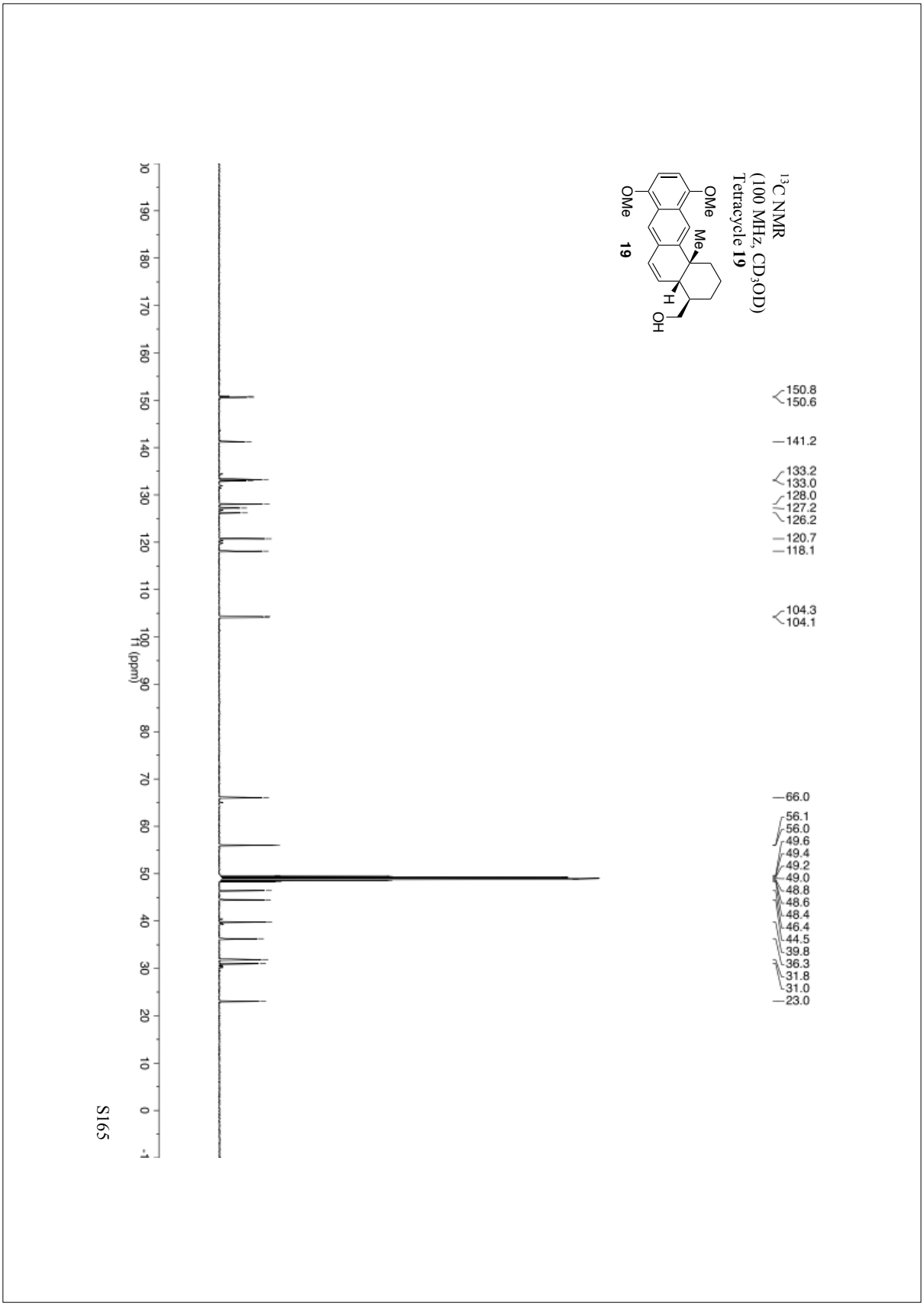
^{13}C NMR
(100 MHz, CD_3OD)
Tetracycle **19**
OMe
Me
OMe **19**
H
OH
150.8
150.6
141.2
133.2
133.0
128.0
127.2
126.2
120.7
118.1
104.3
104.1
66.0
56.1
56.0
49.6
49.4
49.2
49.0
48.8
48.6
48.4
46.4
44.5
39.8
36.3
31.8
31.0
23.0
f1 (ppm)
S165

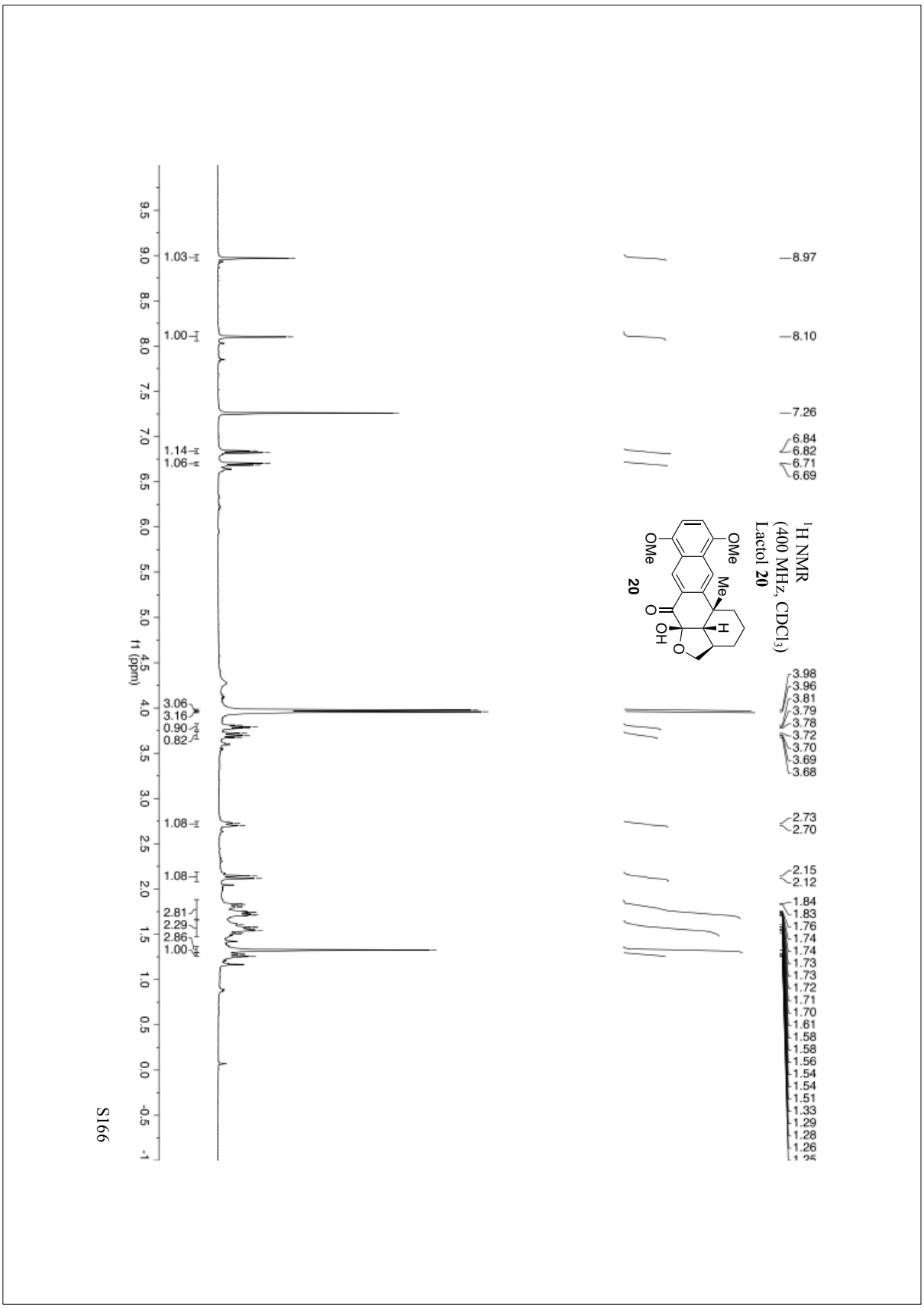
^{1}H NMR
(400 MHz, CDCl$_3$)
Lactol **20**
20
OMe
OMe
Me
H
O
OH
O
8.97
8.10
7.26
6.84
6.82
6.71
6.69
3.98
3.96
3.81
3.79
3.78
3.72
3.70
3.69
3.68
2.73
2.70
2.15
2.12
1.84
1.83
1.76
1.74
1.74
1.73
1.73
1.72
1.71
1.70
1.61
1.58
1.58
1.56
1.54
1.54
1.51
1.33
1.29
1.28
1.26
1.03
1.00
1.14
1.06
3.06
3.16
0.90
0.82
1.08
1.08
2.81
2.29
2.86
1.00
f1 (ppm)

S166

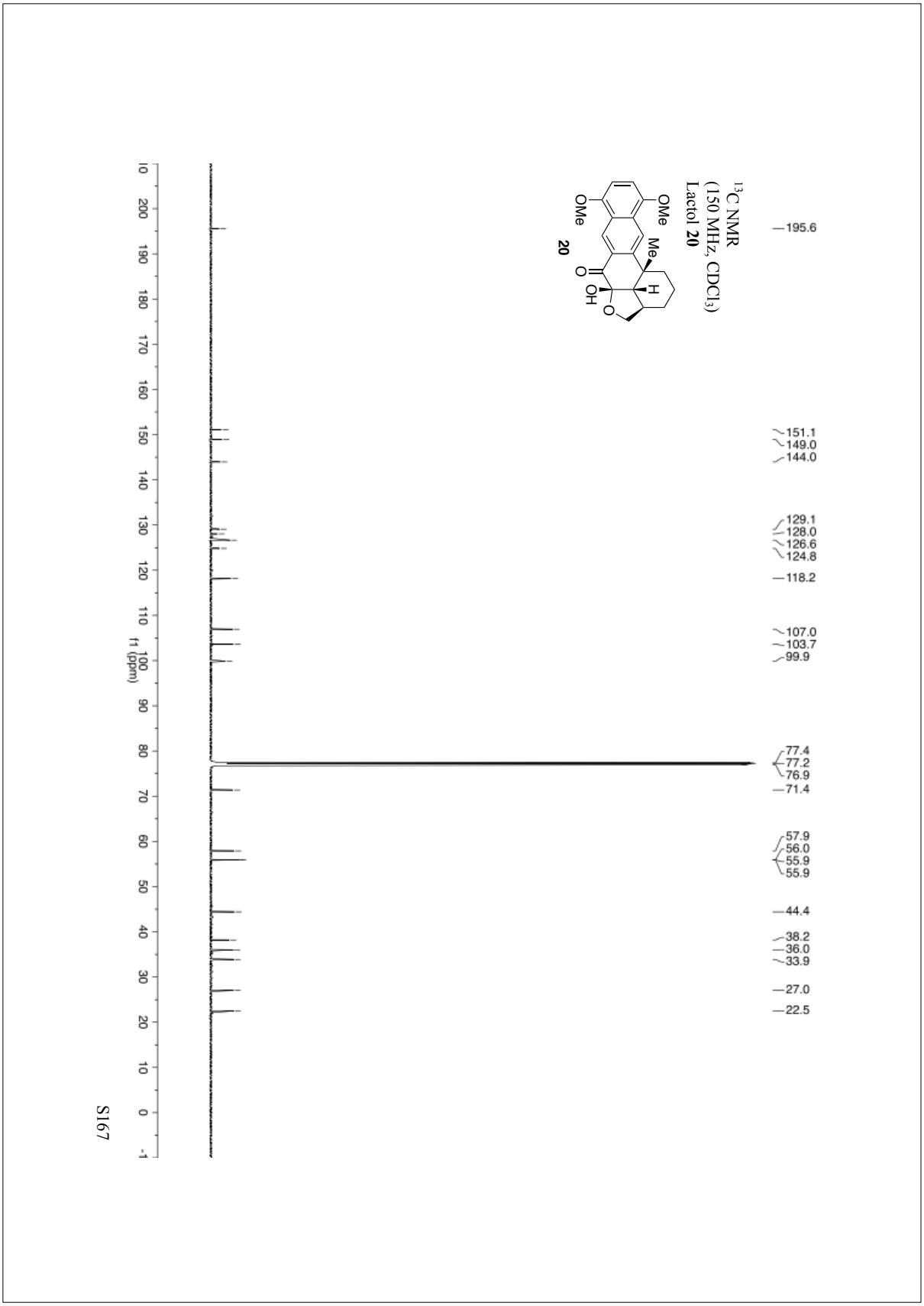
^{13}C NMR
(150 MHz, CDCl$_3$)
Lactol **20**
OMe
OMe
Me
H
O
OH
O
20
195.6
151.1
149.0
144.0
129.1
128.0
126.6
124.8
118.2
107.0
103.7
99.9
77.4
77.2
76.9
71.4
57.9
56.0
55.9
55.9
44.4
38.2
36.0
33.9
27.0
22.5
f1 (ppm)
S167

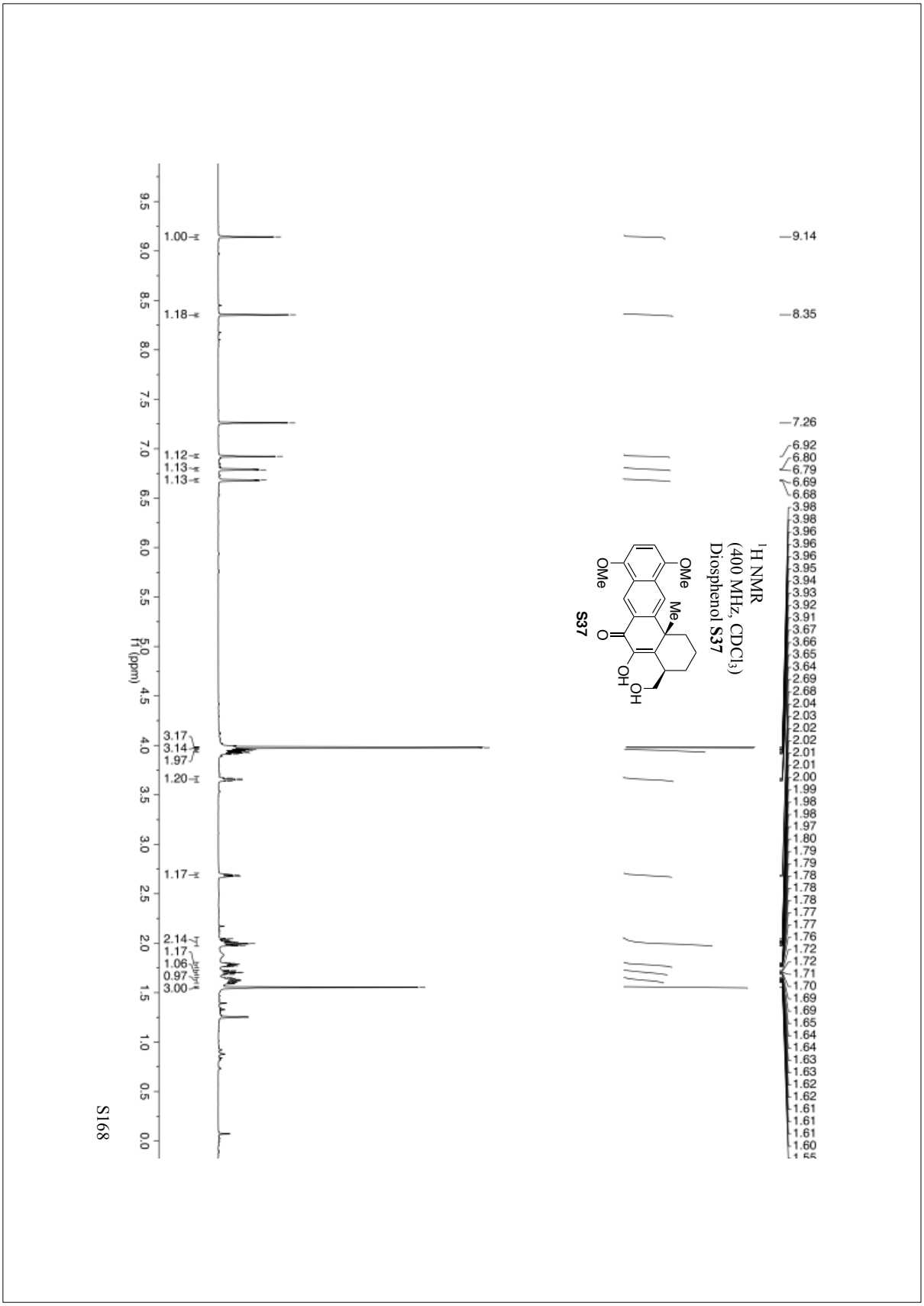
^{1}H NMR
(400 MHz, $CDCl_3$)
Diosphenol **S37**
S37
OMe
OMe
Me
O
OH
OH
9.14
8.35
7.26
6.92
6.80
6.79
6.69
6.68
3.98
3.96
3.95
3.94
3.93
3.92
3.91
3.67
3.66
3.65
3.64
2.69
2.68
2.04
2.03
2.02
2.01
2.00
1.99
1.98
1.97
1.80
1.79
1.78
1.77
1.76
1.72
1.71
1.70
1.69
1.65
1.64
1.63
1.62
1.61
1.60
1.00
1.18
1.12
1.13
1.13
3.17
3.14
1.97
1.20
1.17
2.14
1.17
1.06
0.97
3.00
f1 (ppm)
S168

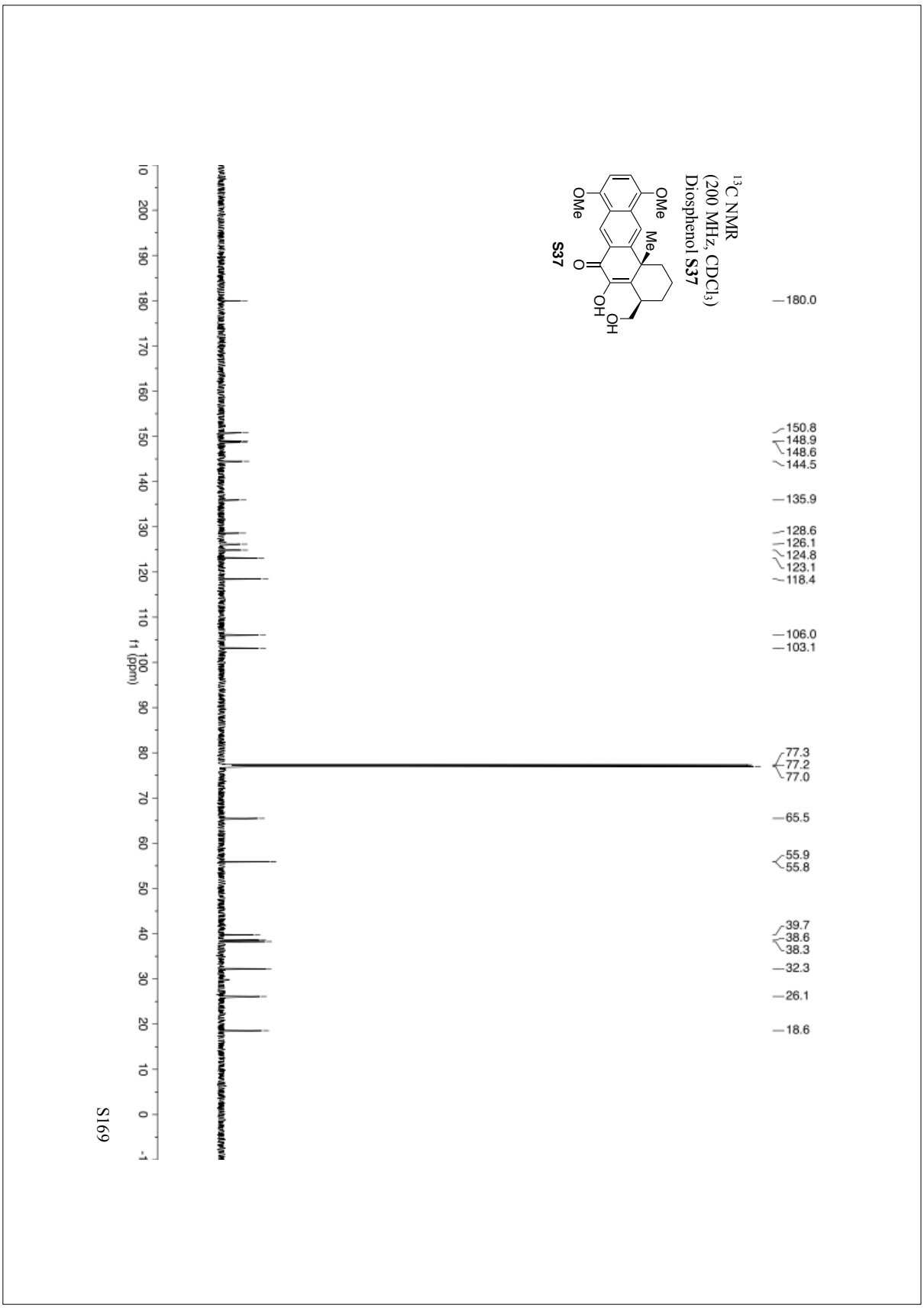
^{13}C NMR
(200 MHz, $CDCl_3$)
Diosphenol **S37**
S37
OMe
OMe
Me
O
OH
OH
180.0
150.8
148.9
148.6
144.5
135.9
128.6
126.1
124.8
123.1
118.4
106.0
103.1
77.3
77.2
77.0
65.5
55.9
55.8
39.7
38.6
38.3
32.3
26.1
18.6
f1 (ppm)
S169

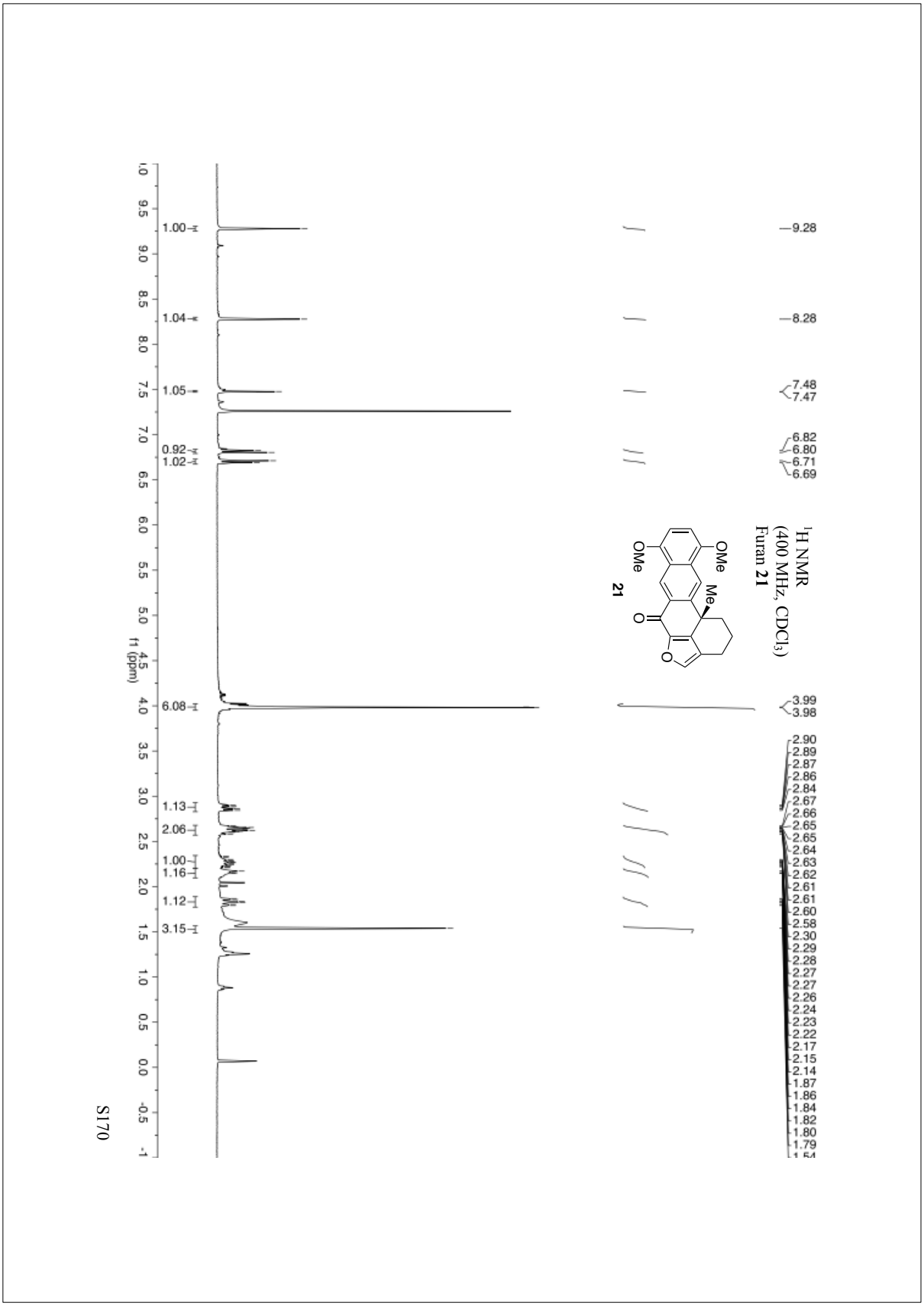
^{1}H NMR
(400 MHz, $CDCl_3$)
Furan **21**
OMe
OMe
Me
O
O
21
9.28
8.28
7.48
7.47
6.82
6.80
6.71
6.69
3.99
3.98
2.90
2.89
2.87
2.86
2.84
2.67
2.66
2.65
2.65
2.64
2.63
2.62
2.61
2.61
2.60
2.58
2.30
2.29
2.28
2.27
2.27
2.26
2.24
2.23
2.22
2.17
2.15
2.14
1.87
1.86
1.84
1.82
1.80
1.79
1.00
1.04
1.05
0.92
1.02
6.08
1.13
2.06
1.00
1.16
1.12
3.15
f1 (ppm)
S170

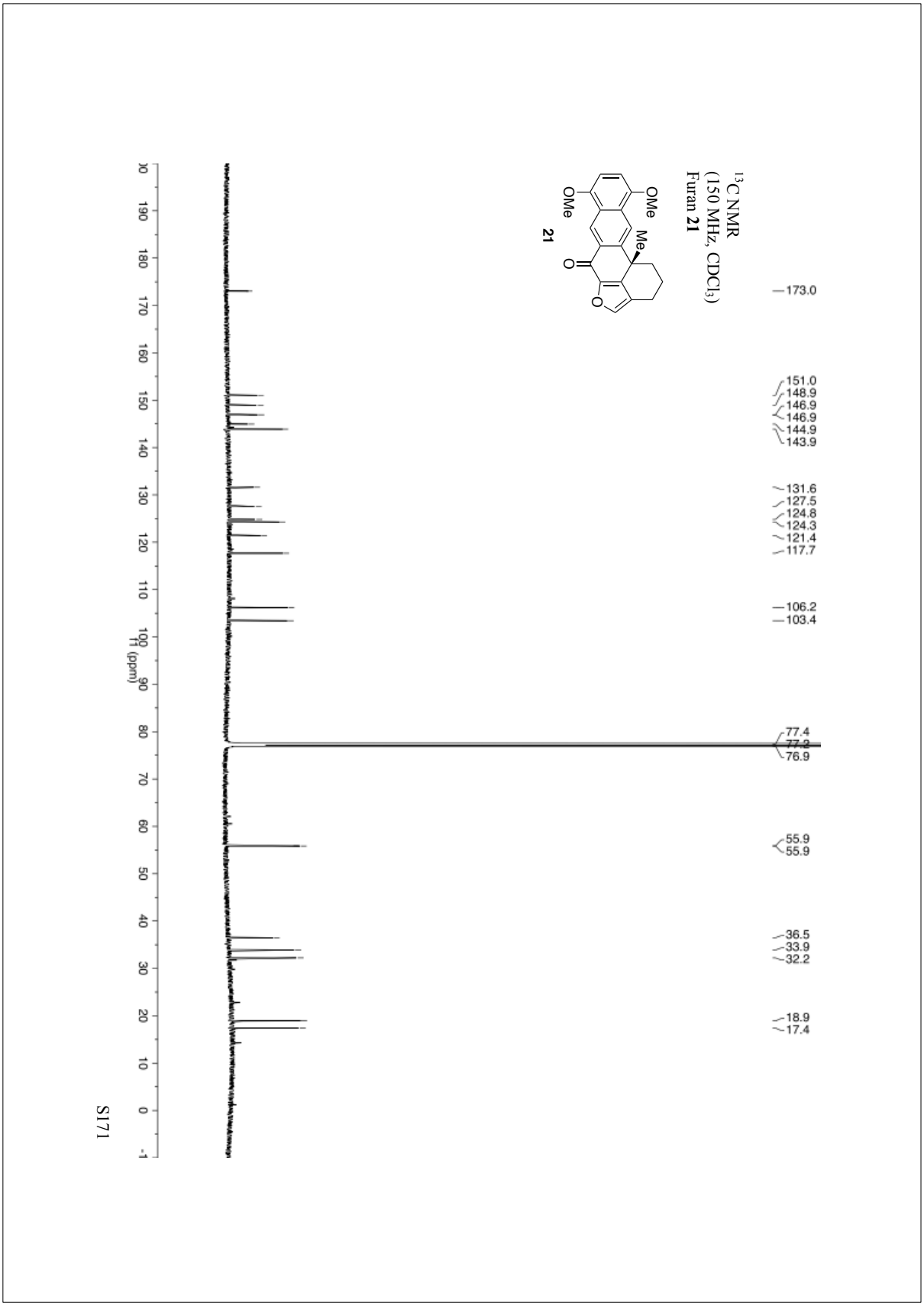
^{13}C NMR
(150 MHz, $CDCl_3$)
Furan **21**
OMe
OMe
Me
O
O
21
173.0
151.0
148.9
146.9
146.9
144.9
143.9
131.6
127.5
124.8
124.3
121.4
117.7
106.2
103.4
77.4
77.2
76.9
55.9
55.9
36.5
33.9
32.2
18.9
17.4
f1 (ppm)
S171

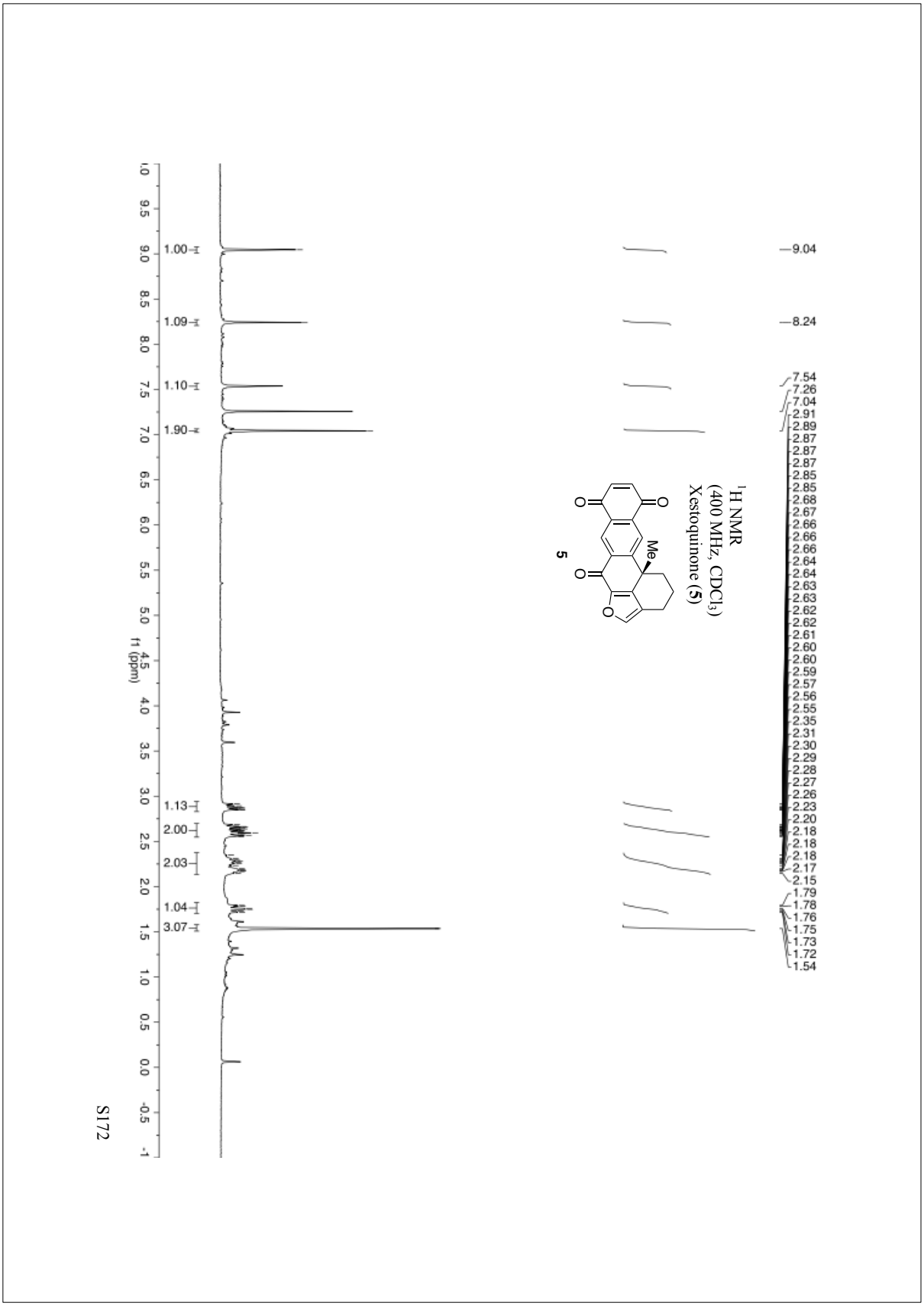
^{1}H NMR
(400 MHz, CDCl$_3$)
Xestoquinone (**5**)
Me
5
9.04
8.24
7.54
7.26
7.04
2.91
2.89
2.87
2.87
2.87
2.85
2.85
2.68
2.67
2.66
2.66
2.66
2.64
2.64
2.63
2.63
2.62
2.62
2.61
2.60
2.60
2.59
2.57
2.56
2.55
2.35
2.31
2.30
2.29
2.28
2.27
2.26
2.23
2.20
2.18
2.18
2.18
2.17
2.15
1.79
1.78
1.76
1.75
1.73
1.72
1.54
1.00
1.09
1.10
1.90
1.13
2.00
2.03
1.04
3.07
f1 (ppm)

S172

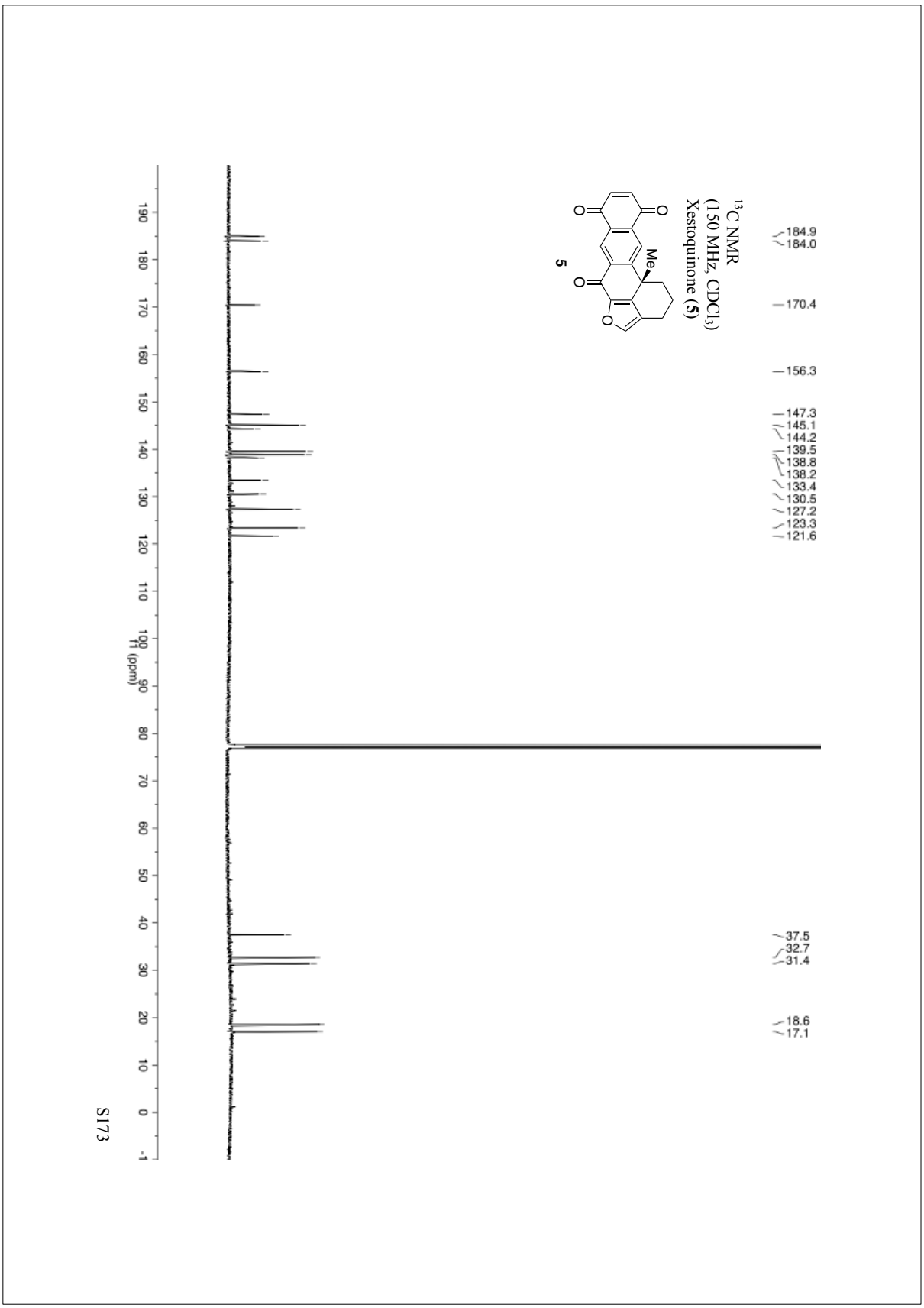
^{13}C NMR
(150 MHz, $CDCl_3$)
Xestoquinone (**5**)
5
Me
184.9
184.0
170.4
156.3
147.3
145.1
144.2
139.5
138.8
138.2
133.4
130.5
127.2
123.3
121.6
37.5
32.7
31.4
18.6
17.1
f1 (ppm)
S173

References and Notes:

(1) I. Abe, Enzymatic Synthesis Of Cyclic Triterpenes. *Nat. Prod. Rep*. **24**, 1311-1331 (2007).
(2) W. D. Nes, Biosynthesis Of Cholesterol And Other Sterols. *Chem. Rev*. **111**, 6423-6451 (2011).
(3) K. C. Nicolaou, S. A. Snyder, T. Montagnon, G. Vassilikogiannakis, The Diels–Alder Reaction In Total Synthesis. *Angew. Chem. Int. Ed*. **41**, 1668-1698 (2002).
(4) L. Gao, C. Su, X. Du, R. Wang, S. Chen, Y. Zhou, C. Liu, X. Liu, R. Tian, L. Zhang, K. Xie, S. Chen, Q. Guo, L. Guo, Y. Hano, M. Shimazaki, A. Minami, H. Oikawa, N. Huang, K. N. Houk, L. Huang, J. Dai, X. Lei, FAD-Dependent Enzyme-Catalysed Intermolecular [4+2] Cycloaddition In Natural Product Biosynthesis. *Nat. Chem*. **12**, 620-628 (2020)
(5) H. Hopf, M. S. Sherburn, Dendralenes Branch Out: Cross-Conjugated Oligoenes Allow The Rapid Generation Of Molecular Complexity. *Angew. Chem. Int. Ed*. **51**, 2298-2338 (2012).
(6) W. G. Dauben, A. P. Kozikowski, Organic reactions at high pressure. Cycloadditions of enamines and dienamines. *J. Am. Chem. Soc.* **96**, 3664-3666 (1974).
(7) I. Fleming, Frontier Orbitals And Organic Chemical Reactions. London: Wiley (1978).
(8) The only previously reported carbocyclic dienophiles in diene-transmissive Diels-Alder reaction sequences are *para*-benzoquinone and benzyne.
(9) H. Lachance, S. Wetzel, K. Kumar, H. Waldmann, Charting, Navigating, And Populating Natural Product Chemical Space For Drug Discovery. *J. Med. Chem*., **55**, 5989-6001 (2012).
(10) C. J. O'Connor, H. S. G. Beckmann, D. R. Spring, Diversity-Oriented Synthesis: Producing Chemical Tools For Dissecting Biology. *Chem. Soc. Rev*., **41**, 4444-4456 (2012).
(11) D. M. Roll, P. J. Scheuer, G. K. Matsumoto, J. Clardy, Halenaquinone, A Pentacyclic Polyketide From A Marine Sponge. *J. Am. Chem. Soc*. **105**, 6177-6178 (1983).
(12) H. Nakamura, J. Kobayashi, M. Kobayashi, Y. Ohizumi, Y. Hirata, Xestoquinone. A Novel Cardiotonic Marine Natural Product Isolated From The Okinawan Sea Sponge Xestospongia Sapra. *Chem. Lett*. 713-716 (1985).
(13) F. J. Schmitz, S. J. Bloor, Xesto- And Halenaquinone Derivatives From A Sponge, Adocia Sp., From Truk Lagoon. *J. Org. Chem*. **53**, 3922-3925 (1988).
(14) J. Kobayashi, T. Hirase, H. Shigemori, M. Ishibashi, New Pentacyclic Compounds From The Okinawan Marine Sponge Xestospongia Sapra. *J. Nat. Prod*. **55**, 994-998 (1992).
(15) G. P. Concepcion, T. A. Foderaro, G. S. Eldredge, E. Lobkovsky, J. Clardy, L. R. Barrows, C. M. Ireland, Topoisomerase II-Mediated DNA Cleavage By Adocia- And Xestoquinones From The Philippine Sponge Xestospongia Sp. *J. Med. Chem*. **38**, 4503-4507 (1995).
(16) T. Kubota, Y. Kon, J. Kobayashi, Xestosaprol C, A New Pentacyclic Hydroquinone Sulfate From A Marine Sponge Xestospongia Sapra. *Heterocycles* **76**, 1571-1575 (2008).
(17) N. Millan-Anguinaga, I. E. Soria-Mercado, P. Williams, Xestosaprol D And E From The Indonesian Marine Sponge Xestospongia sp. *Tet. Lett*. **51**, 751-753 (2010).
(18) J. Dai, A. Sorribas, W. Y. Yoshida, M. Kelly, P. G. Williams, Xestosaprols From The Indonesian Marine Sponge Xestospongia sp. *J. Nat. Prod*. **73**, 1188-1191 (2010).
(19) Y.-J. Lee, C.-K. Kim, S.-K. Park, J. S. Kang, J.-S. Lee, H. J. Shin, H.-S. Lee, Halenaquinone Derivatives From Tropical Marine Sponge Xestospongia sp. *Heterocycles* **85**, 895-901 (2012).
(20) R. M. Centko, A. Steino, F. I. Rosell, B. O. Patrick, N. de Voogd, A. G. Mauk, R. J. Andersen, Indoleamine 2,3-Dioxygenase Inhibitors Isolated From The Sponge Xestospongia Vansoesti: Structure Elucidation, Analogue Synthesis, And Biological Activity. *Org. Lett.* **16**, 6480-6483 (2014).
(20) H. Nakamura, J. Kobayashi, M. Kobayashi, Y. Ohizumi, Y. Hirata, Xestoquinone. A Novel Cardiotonic Marine Natural Product Isolated From The Okinawan Sea Sponge Xestospongia Sapra. *Chem. Lett*. 713-716 (1985).
(21) M. Nakamura, T. Kakauda, J. Qi, M. Hirata, T. Shintani, Y. Yoshioka, T. Okamoto, Y. Oba, H. Nakamura, M. Ojika, Novel Relationship Between The Antifungal Activity And Cytotoxicity Of

Marine-Derived Metabolite Xestoquinone And Its Family. *Biosci. Biotechnol. Biochem*. **69**, 1749–1752 (2005).
(22) D. Laurent, V. Jullian, A. Parenty, M. Knibiehler, D. Dorin, S. Schmitt, O. Lozach, N. Lebouvier, M. Frostin, F. Alby, S. Maurel, C. Doerig, L. Meijer, M. Sauvain. Antimalarial Potential Of Xestoquinone, A Protein Kinase Inhibitor Isolated From A Vanuatu Marine Sponge Xestospongia sp. *Bioorg. Med. Chem*. **14**, 4477–4482 (2006).
(23) M. Ito, Y. Hirata, H. Nakamura, Y. Ohizumi, Xestoquinone, Isolated From Sea Sponge, Causes Ca^{2+} Release Through Sulfhydryl Modification From Skeletal Muscle Scaroplasmic Reticulum. *J. Pharmacol. Exp. Ther*. **291**, 976-981 (1999).
(24) M. Kobayashi, H. Nakamura, J. Kobayashi, Y. Ohizumi, Mechanism Of Inotropic Action Of Xestoquinone, A Novel Cardiotonic Agent Isolated From A Sea Sponge. *J. Pharmacol. Exp. Ther*. **257**, 82-89 (1991).
(25) M. Nakamura, T. Kakauda, J. Qi, M. Hirata, T. Shintani, Y. Yoshioka, T. Okamoto, Y. Oba, H. Nakamura, M. Ojika, Novel Relationship Between The Antifungal Activity And Cytotoxicity Of Marine-Derived Metabolite Xestoquinone And Its Family. *Biosci. Biotechnol. Biochem*. **69**, 1749–1752 (2005).
(26) G. M. Schwarzwalder, C. D. Vandwerwal, Strategies For The Synthesis Of The Halenaquinol And Xestoquinol Families Of Natural Products. *Eur. J. Org. Chem*. 1567–1577 (2017).
(27) N. Harada, T. Sugioka, H. Uda, T. Kuriki, Total Synthesis And Absolute Stereochemistry Of (+)-Xestoquinone And Xestoquinol. *J. Org. Chem*. **55**, 3158-3163 (1990).
(28) K. Kanematsu, S. Soejima, G. Wang, Formal Total Synthesis Of Xestoquinone Via Furan Ring Transfer Reaction Strategy. *Tetrahedron. Lett*. **32**, 4761-4764 (1991).
(29) R. Carlini, K. Higgs, C. Older, S. Randhawa, Intramolecular Diels-Alder And Cope Reactions Of *Ortho*-Quinonoid Monoketals And Their Adducts: Efficient Syntheses Of (±)-Xestoquinone And Heterocycles Related To Viridin. *J. Org. Chem*. **62**, 2330-2331 (1997).
(30) H. S. Sutherland, K. C. Higgs, N. J. Taylor, R. Rodrigo, Isobenzofurans And *Ortho*-Benzoquinone Monoketals In Syntheses Of Xestoquinone And Its 9- And 10-Methoxy Derivatives. *Tetrahedron* **57**, 309-317 (2001).
(31) S. P. Maddaford, N. G. Andersen, W. A. Cristofoli, B. A. Keay, Total Synthesis Of (+)-Xestoquinone Using An Asymmetric Palladium-Catalysed Polyene Cyclization. *J. Am. Chem. Soc*. **118**, 10766-10773 (1996).
(32) F. Miyazaki, K. Uotsu, M. Shibasaki, Silver Salt Effects On An Asymmetric Heck Reaction. Catalytic Asymmetric Total Synthesis Of (+)-Xestoquinone. *Tetrahedron* **54**, 13073-13078 (1998).
(33) N. Harada, T Sugioka, Y. Ando, H. Uda, T. Kuriki, Total Synthesis Of (+)-Halenaquinol And (+)-Halenaquinone. Experimental Proof Of Their Absolute Stereostructures Theoretically Determined. *J. Am. Chem. Soc.* **110**, 8483-8487 (1988).
(34) H. S. Sutherland, F. E. S. Souza, R. G. A. Rodrigo, A Short Synthesis Of (±)-Halenaquinone. *J. Org. Chem.* **66**, 3639-3641 (2001).
(35) A. Kojima, T. Takemoto, M. Sodeoka, M. Shibasaki, Catalytic Asymmetric Synthesis Of Halenaquinone And Halenaquinol. *J. Org. Chem*. **61**, 4876-4877 (1996).
(36) A. Kojima, T. Takemoto, M. Sodeoka, M. Shibasaki, Catalytic Asymmetric Synthesis Of Halenaquinone And Halenaquinol. *Synthesis* 581-589 (1998).
(37) M. A. Kienzler, S. Suseno, D. Trauner, Vinyl Quinones As Diels-Alder Dienes: Concise Synthesis Of (-)-Halenaquinone. *J. Am. Chem. Soc*. **130**, 8604-8605 (2008).
(38) S. Goswami, K. Harada, M. F. El-Mansy, R. Lingampally, R. G. Carter, Enantioselective Synthesis Of (-)-Halenaquinone. *Angew. Chem. Int. Ed*. **57**, 9117-9121 (2018).

(39) Several syntheses of [3]dendralene have been previously reported (see reference 3) but all involve high temperature eliminations and/or lengthy preparations. The method reported here is much more convenient and scalable.
(40) This diene could also be generated in one step from [3]dendralene *via* Diels-Alder reaction with a substituted benzyne, generated *in situ* from 3,6-dimethoxy-2-(trimethylsilyl)phenyl trifluoro-methanesulfonate by cesium fluoride. This synthetic route was, however, lower yielding and required a 5 step synthesis of the benzyne precursor (See Supporting Information).
(41) This straightforward removal of the now superfluous carbonyl activating group also confirms the versatility of the cyclic enone dienophiles employed in the methodological section of this project.
(42) C. K. Jana, R. Scopelliti, K. Gademann, Connecting C19 Norditerpenoids To C20 Diterpenes: Total Syntheses Of 6-Hydroxy-5,6-Dehydrosugiol, 6-Hydroxysugiol, And Taiwaniaquinone H, And Formal Synthesis Of Dichroanone. *Synthesis* **2010**, 2223-2232.
(43) The requisite furan functionality could also be installed via a two-step sequence involving: 1) ring opening of the lactol with KHMDS and 2) oxidation of the primary alcohol to the aldehyde by EDC•HCl, followed by cyclisation and dehydration under acidic conditions. See Supporting Information for details.
(44) B. M. Trost, The Atom Economy: A Search For Synthetic Efficiency. *Science*, **254**, 1471-1477 (1991).
(45) N. A. Miller, A. C. Willis, M. S. Sherburn, Formal Total Synthesis Of Triptolide. *Chem. Commun.* 1226- 1228 (2008).
(46) S. V. Pronin, R. A. Shenvi, Synthesis Of A Potent Antimalarial Amphilectene. *J. Am. Chem. Soc*. **134**, 19604-19606 (2012).
(47) C. G. Newton, S. L. Drew, A. L. Lawrence, A. C. Willis, M. N. Paddon-Row, M. S. Sherburn, Pseudopterosin Synthesis From A Chiral Cross-Conjugated Hydrocarbon Through A Series Of Cycloadditions. *Nat. Chem*. **7**, 82–86 (2015).
(48) H.-H. Lu, S. V. Pronin, Y. Antonova-Koch, S. Meister, E. A. Winzeler, R. A. Shenvi, Synthesis Of (+)-7,20-Diisocyanoadociane And Liver-Stage Antiplasmodial Activity Of The Isocyanoterpene Class. *J. Am. Chem. Soc*. **138**, 7268-7271 (2016).
(49) A. B. Pangborn, M. A. Giardello, R. H. Grubbs, R. K. Rosen, F. J. Timmers, Safe And Convenient Procedure For Solvent Purification. *Organometallics* **15**, 1518 (1996).
(50) W. L. F. Armarego, C. L. L. Chai, Purification Of Laboratory Chemicals. (Butterworth-Heineman, Oxford, ed. Seventh Edition, 2013).
(51) Nonius (1997-2001). COLLECT. Nonius BV, Delft, The Netherlands.
(52) CrysAlisPro Software System, Rigaku Oxford Diffraction (2018).
(53) A. Altomare, G. Cascarano, C. Giacovazzo, A. Guagliardi, M. C. Burla, G. Polidori, M. Camalli, SIR92 - A Program For Automatic Solution Of Crystal Structures By Direct Methods. *J. Appl. Cryst*. **27**, 435 (1994).
(54) G. M. Sheldrick, SHELXT-Integrated Space-Group And Crystal-Structure Determination. *Acta Cryst.* **A71**, 3-8 (2015).
(55) P. W. Betteridge, J. R. Carruthers, R. I. Cooper, K. Prout, D. J. Watkin, CRYSTALS Version 12: Software For Guided Crystal Structure Analysis. *J. Appl. Cryst*. **36**, 1487 (2003).
(56) G. M. Sheldrick, Crystal Structure Refinement With SHELXL. *Acta Cryst*. **C71**, 3-8 (2015).
(57) O. V. Dolomanov, L. J. Bourhis, R. J. Gildea, J. A. K. Howard, H. Puschmann, Olex2: A Complete Structure Solution, Refinement And Analysis Program. *J. Appl. Cryst*., **42**, 339-341 (2009).
(58) J.-P. Tassara, M. Baudoin, in Eur. Pat. Appl. EP646561. (1995).
(59) K. M. Cergol, C. G. Newton, A. L. Lawrence, A. C. Willis, M. N. Paddon-Row, M. S. Sherburn, 1,1-Divinylallene. *Angew. Chem. Int. Ed*. **50**, 10425-10428 (2011).
(60) H. Toombs-Ruane, Australian National University, Australia (2013).

(61) S. Fielder, D. D. Rowan, M. S. Sherburn, First Synthesis Of The Dendralene Family Of Fundamental Hydrocarbons. *Angew. Chem. Int. Ed*. **39**, 4331 (2000).
(62) W. S. Trahanovsky, K. A. Koeplinger, Synthesis And Dimerization Of Two Cross-Conjugated Trienes: 3-Methylene-1,4-Pentadiene And 1,2,3-Trimethylenecyclohexane. *J. Org. Chem.* **57**, 4711-4716 (1992).
(63) T. A. Bradford, A. D. Payne, A. C. Willis, M. N. Paddon-Row, M. S. Sherburn, Practical Synthesis And Reactivity Of [3]Dendralene. *J. Org. Chem*. **75**, 491 (2010).
(64) R. Breslow, J. Pecoraro, T. Sugimoto, Cyclopropenone. *Org. Synth*. **57**, 41 (1977).
(65) X. Li, S. J. Danishefsky, Cyclobutenone As A Highly Reactive Dienophile: Expanding Upon Diels−Alder Paradigms. *J. Am. Chem. Soc*. **132**, 11004-11005 (2010).
(66) C. Reisinger, University of Köln, Köln (2010).
(67) F. Peng, M. Dai, A. R. Angeles, S. J. Danishefsky, Permuting Diels–Alder And Robinson Annulation Stereopatterns. *Chemical Science* **3**, 3076-3080 (2012).
(68) J. Barluenga, E. Campos-Gomez, A. Minatti, D. Rodriguez, J. M. Gonzalez, Iodoarylation Reactions of Allenes: Inter- and Intramolecular Processes. *Eur. J. Chem* **15**, 8946-8950 (2009).
(69) J. Lin, M. M. Nikaido, G. Clark, Convergence With Mutual Kinetic Resolution. 1. Studies Defining Methodology For The Taxol C/D Ring Fragment And Synthesis Of The A Ring Fragment. *J. Org. Chem.* **52**, 3745-3752 (1987).
(70) S. Sugasawa, S. I. Yamada, M. J. Narachi, Synthesis Of 2-(p-Aminobenzenesulfonamido)-4,5-dimethylpyrimidine. *J. Pharm. Soc. Jpn*. **71**, 1345-1349 (1951).
(71) S. Danishefsky et al., Derivatives Of 1-Methoxy-3-trimethylsilyloxy-1,3-butadiene for Diels-Alder Reactions. *J. Am. Chem. Soc.* **101**, 7001-7008 (1979).
(72) S. Danishefsky, T. Kitahara, Useful Diene for the Diels-Alder Reaction. *J. Am. Chem. Soc.* **96**, 7807-7808 (1974).
(73) Q. Lin et al., Enantioselective Synthesis of Janus Kinase Inhibitor INCB018424 Via An Organocatalytic Aza-Michael Reaction. *Org. Lett.* **11**, 1999-2002 (2009).
(74) Z. Dalicsek, F. Pollreisz, T. Soos, Efficient Separation Of A Trifluoromethyl Substituted Organocatalyst: Just Add Water. *Chem. Commun*., 4587-4589 (2009).
(75) S. Mukherjee, E. J. Corey, Highly Enantioselective Diels-Alder Reactions Of Maleimides Catalyzed By Activated Chiral Oxazaborolidines. *Org. Lett*. **12**, 632-635 (2010).
(76) H.-J. Liu, D.-X. Wang, J. B. Kim, E. N. C. Browne, Y. Wang, Activated Cyclooctenones Are Effective Dienophiles. *Can. J. Chem*. **75**, 899-912 (1997).
(77) Y. Hayashi, S. Samanta, H. Gotoh, H. Ishikawa, Asymmetric Diels–Alder Reactions Of α,β-Unsaturated Aldehydes Catalyzed By A Diarylprolinol Silyl Ether Salt In The Presence Of Water. *Angew. Chem. Int. Ed*. **47**, 6634-6637 (2008).
(78) L. You et al., Asymmetric Total Synthesis Of Propindilactone G. *J. Am. Chem. Soc*. **137**, 10120-10123 (2015).
(79) J. George, J. S. Ward, M. S. Sherburn, Diene-Transmissive Diels–Alder Sequences With Benzynes. *Org. Lett*. **21**, 7529-7533 (2019).

6.2 Experimental for Chapter 4

6.2.1 General Methods

NMR Spectroscopy

^{1}H NMR spectra were recorded at 800 or 400 MHz using a Bruker AVANCE 400, Varian 400-MR or Bruker AVANCE 800 spectrometer, as indicated. Residual protio-solvent peaks were used as an internal reference for ^{1}H NMR spectra ($CDCl_3$ δ 7.26 ppm, toluene-d_8 7.09, C_6D_6 7.16, CD_3OD δ 3.31 ppm). Coupling constants (*J*) are quoted to the nearest 0.1 Hz. The assignment of proton signals was assisted by COSY, HSQC and HMBC experiments. ^{13}C NMR spectra were recorded at 100, 150 or 200 MHz using a Bruker AVANCE 400, Varian 400-MR or Bruker AVANCE 800 spectrometer. Solvent peaks were used as an internal reference for ^{13}C NMR spectra ($CDCl_3$ δ 77.16 ppm, toluene-d_8 137.48, C_6D_6 128.06, CD_3OD δ 49.00 ppm). Assignment of carbon signals was assisted by HSQC and HMBC experiments. Assignment of stereochemistry was assisted by nOe experiments. The following abbreviations (or combinations thereof) are used to denote ^{1}H NMR multiplicities: s = singlet, d = doublet, dd= doublet of doublets, t = triplet, m = multiplet, br = broad.

Infrared Spectroscopy

IR spectra were recorded on a Perkin–Elmer UATR Two spectrometer as a thin film or solid, or on a Perkin–Elmer 1600 FTIR spectrometer as a thin film (NaCl plate) or solid (KBr disc).

Mass Spectrometry

Low-resolution EI mass spectra were recorded on a Finnigan Polaris Q ion trap mass spectrometer or Agilent HP 6869 series mass spectrometer using electron impact (EI+) ionisation mode at 40 or 70 eV. High-resolution EI mass spectra were recorded on a VG Autospec mass spectrometer operating at 70 eV. Low resolution ESI mass spectra were recorded on a ZMD Micromass spectrometer with Waters Alliance 2690 HPLC. High resolution ESI mass spectra were recorded on a Waters LCT Premier time of flight (TOF) mass spectrometer.

Melting Points

Melting points were measured on a Stanford Research Systems Optimelt Automated Melting Point System and are uncorrected.

Optical Rotations

Optical rotations were measured on a Perkin–Elmer 341 polarimeter using a sodium lamp (589 nm) as the light source over a path length of 10 cm. $[\alpha]_D$ values are reported in units of 10^{-1}degcm^{2}g^{-1} at concentration (c) in g/100 mL.

Ultra-High Pressure Reactor

Ultra-high pressure reactions were conducted in Telfon reaction vessels with a Psika 20 kbar ultra-high pressure reactor.

Experimental Procedures, Reagents, Chromatography and Glassware

Reactions were conducted under a positive pressure of dry nitrogen in oven or heat gun-dried glassware and at room temperature, unless specified otherwise. Anhydrous solvents were either obtained from commercial sources or dried according to the procedure outlined by Grubbs and co-workers.[125] Commercially available chemicals were used as purchased, or where specified, purified by standard techniques.[126] Analytical thin-layer chromatography was conducted with aluminum-backed silica gel 60 F254 (0.2 mm) plates supplied by Merck, and visualised using UV fluorescence (λ_{max} = 254 nm), or developed using $KMnO_4$ or *p*-anisaldehyde TLC stains, followed by heating. Preparative thin-layer chromatography was conducted with glass-backed silica gel (1.0 mm, with fluorescent indicator) plates supplied by Merck. Flash chromatography employed Merck Kiesegel 60 silica gel (230–400 mesh). Et_3N-deactivated SiO_2 was prepared by loading the column with a slurry of SiO_2 in eluent with 1% Et_3N added, and flushing with one column volume of eluent before use. Solvent compositions are given in (v/v). PS 40–60 °C refers to petroleum spirits, boiling point fraction 40–60 °C.

X-ray Crystallography

Single crystal X-ray data was collected on a SuperNova (Dual Source) diffractometer using a SuperNova (Cu or Mo) X-ray radiation source. Crystallographic Structures were solved using CrysAlis PRO.[127]

Conformational Analysis

Calculations were carried out on isolated molecules in the gas phase using the Spartan'18 Parallel Suite package using the conformer distribution function.[i] ωB97X-V/6-31G* geometries within 15 kJ/mol of the minimum energy conformation were located employing a Monte Carlo search method.

[i] Grateful acknowledgement is given to Professor Mick Sherburn for his assistance with calculations.

6.2.2 Dienes

[3]Dendralene (25)

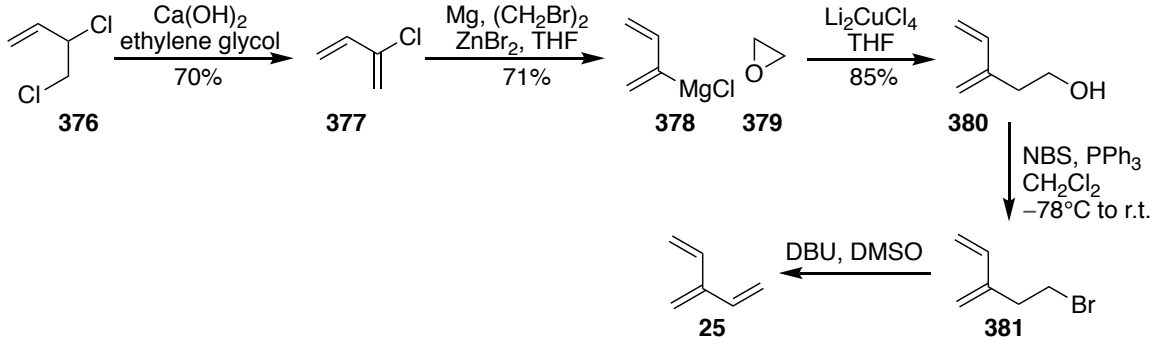

Neat [3]dendralene was prepared according to the procedure described in Chapter 2, and outlined by Sherburn and co-workers.[13]

Substituted dendralene 384

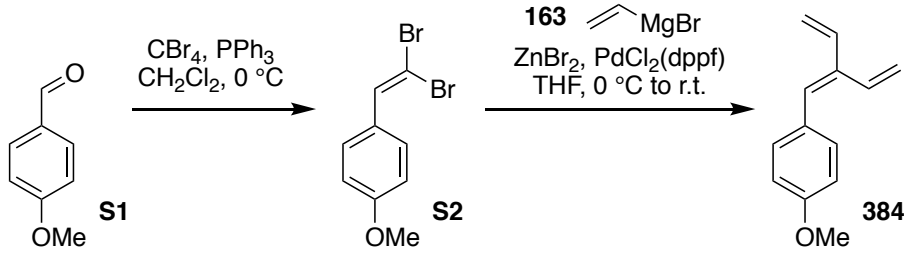

Aryl substituted dendralene **384** was prepared according to the procedure described by Sherburn and co-workers.[85]

Substituted dendralene 385

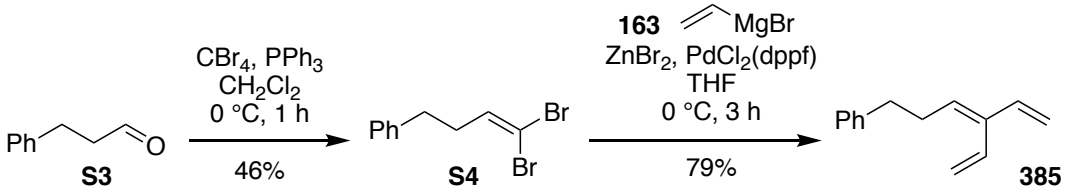

Substituted dendralene **385** was prepared according to the procedure described by Sherburn and co-workers.[85]

Achiral diene S5

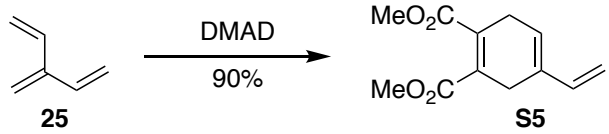

DMAD (284 mg, 245 μL, 2.00 mmol, 1.0 mol. equiv.) and [3]dendralene (240 mg, 3.00 mmol, 1.50 mol. equiv.) were combined, the reaction flask was sealed, and the reaction mixture was stirred at 25 °C for 23 h. Purification by flash column chromatography (SiO_2; 10% EtOAc in PS 40–60 °C), afforded bicyclic diene **S5** as a clear colourless oil (398 mg, 1.79 mmol, 90%).

R_f = 0.21 (10 % EtOAc in PS 40–60 °C);

^{1}H NMR (400 MHz, $CDCl_3$): δ 6.40 (dd, J = 10.8, 17.5 Hz, 1H), 5.75 (br s, 1H), 5.13 (d, J = 17.5 Hz, 1H), 506 (d, J = 10.8 Hz, 1H), 3.81 (s, 3H), 3.79 (s, 3H), 3.18-3.07 (m, 4H) ppm;

^{13}C NMR (100 MHz, $CDCl_3$): δ 168.4 (C_q), 168.0 (C_q), 137.6 (CH), 132.7 (C_q), 131.6 (C_q), 131.4 (C_q), 123.5 (CH), 112.2 (CH_2), 52.2 (CH_3), 52.1 (CH_3), 28.5 (CH_2), 26.6 (CH_2) ppm;

IR (thin film): ν_{max} = 3005, 2952, 2884, 1720, 1676, 1645, 1610 cm^{-1};

LRMS (70 eV, ESI): m/z (%): 245 (100, $[M+Na]^{+\bullet}$);

HRMS (70 eV, ESI): m/z calc. for $C_{12}H_{14}O_4Na$ $[M+Na]^{+\bullet}$: 245.07843; found 245.07829.

Achiral diene 374

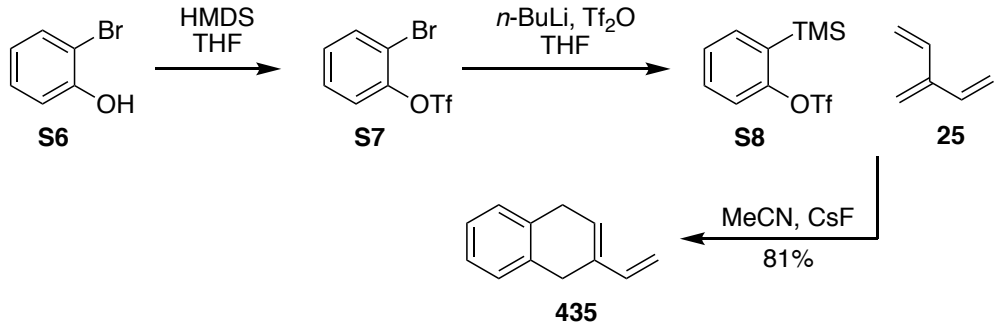

2-(Trimethylsilyl)phenyl trifluoromethanesulfonate **S8** was prepared from 2-bromophenol **S6**, according to the procedure outlined by Peng and co-workers.[128]

CsF (69 mg, 0.45 mmol, 3.0 mol. equiv.) was dried under reduced pressure for 3 h at 190 °C, then cooled to room temperature and flushed with Ar. MeCN (0.50 mL) and [3]dendralene (**25**) (50 mg, 0.61 mmol, 4.0 mol. equiv.) were added, followed by the dropwise addition of benzyne precursor **S8** (45 mg, 37 μL, 0.15 mmol, 1.0 mol. equiv.). The reaction vessel was sealed, and the reaction was stirred at 25 °C for 18 h. The reaction mixture was then diluted with CH_2Cl_2 (3.0 mL), washed with water (3 x 3.0 mL) and brine (3.0 mL), dried over $MgSO_4$ and concentrated under reduced pressure. Purification by flash column chromatography (SiO_2; pentane) afforded bicyclic diene **435** as a colorless oil (19 mg, 0.12 mmol, 81%). ^{1}H NMR and ^{13}C NMR data were consistent with those reported previously.[129]

R_f = 0.55 (pentane);

^{1}H NMR (400 MHz, $CDCl_3$): δ 7.23-7.17 (m, 4H), 6.53 (dd, J = 17.2, 10.4 Hz, 1H), 5.99 (s, 1H), 5.25 (d, J = 17.2 Hz, 1H), 5.07 (d, 10.4 Hz, 1H), 3.64-3.45 (m, 4H) ppm;

^{13}C NMR (100 MHz, $CDCl_3$): δ 139.0 (CH), 134.1 (C_q), 134.0 (C_q), 133.7 (C_q), 128.8 (CH), 128.3 (CH), 126.7 (CH), 126.2 (CH), 126.1 (CH), 111.1 (CH_2), 30.8 (CH_2), 28.8 (CH_2) ppm;

IR (thin film): ν_{max} = 3086, 3046, 3022, 3006, 2868, 2817, 1609, cm^{-1};

LRMS (70 eV, EI): m/z (%): 156 (100, $[M]^{+\bullet}$), 141 (100), 128 (100), 115 (90);

HRMS (70 eV, EI): m/z calc. for $C_{12}H_{12}$ $[M]^{+\bullet}$: 156.0939; found 156.0937.

6.2.3 Monoadducts

Monoadduct 399a

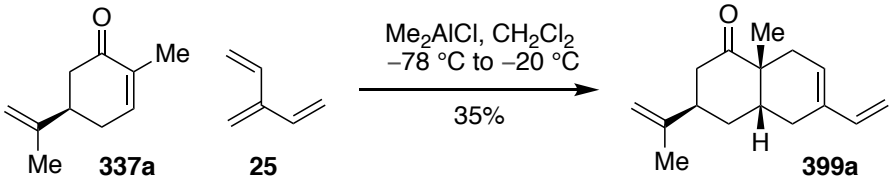

A stirred solution of [3]dendralene (**25**) (50 mg, 0.62 mmol, 2.0 mol. equiv.) in CH_2Cl_2 (0.50 mL) cooled in a –78 °C dry ice-acetone bath under Ar was treated with (*R*)-(–)-carvone (**337a**) (46 mg, 48 μL, 0.31 mmol, 1.0 mol. equiv.), followed by the dropwise addition of Me_2AlCl (1.0 M solution in hexane, 155 μL, 0.155 mmol, 0.50 mol. equiv.). The flask was transferred to a –20 °C bath (IPA, Huber Chiller) and the temperature was allowed to equilibrate. The reaction vessel was sealed and the reaction was stirred at –20 °C for 42 h. The reaction mixture was then placed under Ar, transferred to a –78 °C dry ice-acetone bath and treated dropwise with Me_2AlCl (1.0 M solution in hexane, 155 μL, 0.155 mmol, 0.50 mol. equiv.). The resulting solution was then transferred back to a –20 °C bath (IPA, Huber Chiller). The vessel was sealed and was stirred at –20 °C for a further 17 h. Triethylamine (50 μL) was then added, the reaction mixture was removed from the cold bath, sat. aq. potassium sodium tartrate solution (2.5 mL) was added and the resulting mixture was allowed to stir for 30 minutes. The mixture was then poured onto water (5.0 mL) and extracted with CH_2Cl_2 (3 x 5.0 mL). The organic layers were combined, washed with brine (5.0 mL), dried over $MgSO_4$ and concentrated under reduced pressure. Regio/diastereo-selectivity was determined to be >95:5 by analysis of crude ^{1}H NMR spectra. Purification by flash column chromatography (SiO_2; 5 % EtOAc in PS 40–60 °C) afforded bicyclic diene **399a** as a clear colourless oil (24.7 mg, 0.107 mmol, 35%).

$[\alpha]_D$ = +29.7 ° (c = 1.48, $CHCl_3$);

R_f = 0.55 (20 % EtOAc in PS 40–60 °C);

^{1}H NMR (400 MHz, $CDCl_3$): δ 6.34 (dd, *J* = 17.5, 10.7 Hz, 1H), 5.67 (s, 1H), 5.04 (d, *J* = 17.5 Hz, 1H), 4.92 (d, *J* = 10.8 Hz, 1H), 4.84 (s, 1H), 4.73 (s, 1H), 2.81-2.65 (m, 2H), 2.64-2.50 (m, 2H), 2.26 (dd, *J* = 5.8, 17.3 Hz, 1H), 2.15–2.05 (m, 1H), 2.04–1.91 (m, 2H), 1.86–1.78 (m, 2H), 1.76 (s, 3H), 1.21 (s, 3H) ppm;

^{13}C NMR (100 MHz, $CDCl_3$): δ 214.5 (Cq), 147.4 (Cq), 139.6 (CH,), 133.5 (Cq), 126.3 (CH), 111.2 (CH_2), 110.4 (CH_2), 47.5 (Cq), 41.4 (CH_2), 41.1 (CH), 37.4 (CH), 32.8 (CH_2), 30.3 (CH_2), 26.7 (CH_2), 23.4 (CH_3), 21.5 (CH_3) ppm;

IR (thin film): ν_{max} = 2969, 2931, 2998, 1703, 1645 1607 cm^{-1};

LRMS (70 eV, EI): m/z (%):231.1 ($[M+1]^{+\bullet}$, 23), 230.1 ($[M]^{+\bullet}$, 100);

HRMS (70 eV, EI): m/z calc. for $C_{16}H_{22}O$ $[M]^{+\bullet}$: 230.1671; found 230.1667.

Monoadduct 399b

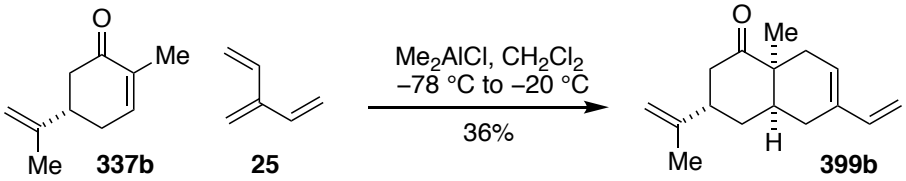

According to the above procedure, (*S*)-(+)-carvone (**337b**) (46 mg, 48 µL, 0.31mmol, 1.0 mol. equiv.) was converted to bicycle **399b** (25.6 mg, 0.111 mmol, 36 %). Regio/diastereo-selectivity of the reaction and spectroscopic data were consistent with those reported above.

$[\alpha]_D$ = –30.0 ° (c = 1.01, $CHCl_3$)

Monoadduct 408

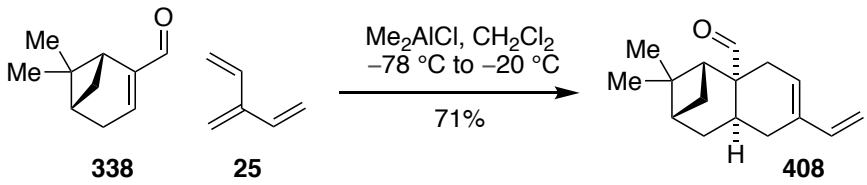

338 **25** **408**

A stirred solution of [3]dendralene (**25**) (50 mg, 0.62 mmol, 2.0 mol. equiv.) in CH_2Cl_2 (0.50 mL) cooled in a –78 °C dry ice-acetone bath under Ar was treated with (*R*)-(–)-myrtenal (**338**) (46 mg, 47 µL, 0.31 mmol, 1.0 mol. equiv.), followed by the dropwise addition of Me_2AlCl (1.0 M solution in hexane, 155 µL, 0.155 mmol, 0.50 mol. equiv.). The flask was transferred to a –20 °C bath (IPA, Huber Chiller) and the temperature was allowed to equilibrate. The reaction vessel was sealed and the reaction was stirred at –20 °C for 17 h. Triethylamine (50 µL) was then added, the reaction mixture was removed from the cold bath, sat. aq. potassium sodium tartrate solution (2.5 mL) was added and the resulting mixture was allowed to stir for 30 minutes. The mixture was then poured onto water (5.0 mL) and was extracted with CH_2Cl_2 (3 x 5.0 mL). The organic layers were combined, washed with brine (5.0 mL), dried over $MgSO_4$ and concentrated under reduced pressure. Regio/diastereo-selectivity was determined to be >95:5 by analysis of crude ^{1}H NMR spectra. Purification by flash column chromatography (5 % EtOAc in PS 40–60 °C) afforded bicyclic diene **408** as a clear colourless oil (50.8 mg, 0.221 mmol, 71%).

$[\alpha]_D$ = –153 ° (c = 0.910, $CHCl_3$);

R_f = 0.51 (10 % EtOAc in PS 40–60 °C);

^{1}H NMR (400 MHz, $CDCl_3$): δ 9.40 (s, 1H), 6.34 (dd, *J* = 10.7, 17.4 Hz, 1H), 5.71 (s, 1H), 5.23 (d, *J* = 17.4 Hz, 1H), 4.98 (d, *J* = 10.7 Hz, 1H), 2.73 (dd, *J* = 6.2, 14.3 Hz, 1H)), 2.64-2.53 (s, 1H), 2.38-2.25 (m, 2H), 2.23-2.13 (m, 2H), 2.08 (dd, *J* = 6.9, 15.7 Hz, 1H) 1.97-1.89 (m, 1H), 1.78-1.68 (m, 1H), 1.59-1.52 (m, 1H), 1.33 (d, *J* = 10.4 Hz, 1H), 1.23 (s, 3H), 0.68 (s, 3H) ppm;

^{13}C NMR (100 MHz, $CDCl_3$): δ 206.9 (CH), 141.4 (C_q), 137.4 (CH), 125.7 (CH), 111.2 (CH_2), 56.1 (C_q), 49.2 (CH), 40.1 (CH), 39.8 (C_q), 34.2 (CH_2), 33.9 (CH_2), 30.9 (CH_2), 27.2 (CH_2), 26.9 (CH), 26.8 (CH_3), 23.4 (CH_3) ppm;

IR (thin film): ν_{max} = 2933, 2910, 1722, 1634, 1600 cm^{-1};

LRMS (70 eV, EI): m/z (%): 230 (22, $[M]^{+\bullet}$), 112 (22), 131 (61), 119 (90), 105 (81), 91 (100);

HRMS (70 eV, EI): m/z calc. for $C_{16}H_{22}O$ $[M]^{+\bullet}$: 230.1671; found 230.1671.

Monoadducts 416a and 416b

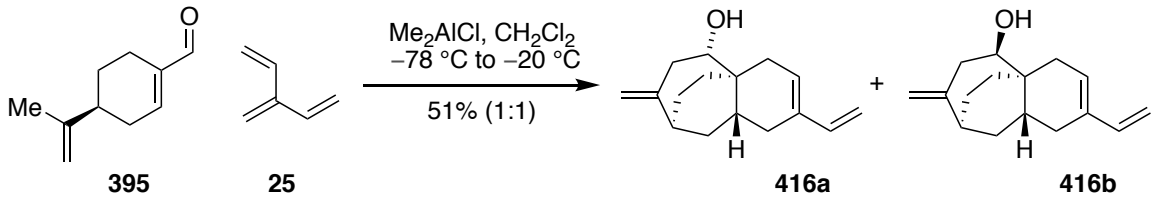

395 **25** **416a** **416b**

A stirred solution of [3]dendralene (**25**) (50 mg, 0.62 mmol, 2.0 mol. equiv.) in CH_2Cl_2 (0.50 mL) cooled in a –78 °C dry ice-acetone bath under Ar was treated with (*S*)-(–)-perillaldehyde (**395**) (46 mg, 48 μL, 0.31 mmol, 1.0 mol. equiv.), followed by the dropwise addition of Me_2AlCl (1.0 M solution in hexane, 155 μL, 0.155 mmol, 0.50 mol. equiv.). The flask was transferred to a –20 °C bath (IPA, Huber Chiller) and the temperature was allowed to equilibrate. The reaction vessel was sealed and the reaction was stirred at –20 °C for 17 h. Triethylamine (50 μL) was then added, the reaction mixture was removed from the cold bath, sat. aq. potassium sodium tartrate solution (2.5 mL) was added and the resulting mixture was allowed to stir for 30 minutes. The mixture was then poured onto water (5.0 mL) and was extracted with CH_2Cl_2 (3 x 5.0 mL). The organic layers were combined, washed with brine (5.0 mL), dried over $MgSO_4$ and concentrated under reduced pressure. Purification by flash column chromatography (5% EtOAc in PS 40–60 °C) afforded tricyclic diene **416a** (18.8 mg, 0.0816 mmol, 26%) and tricyclic diene **416b** (17.5 mg, 0.0760 mmol, 25%) as clear colourless oils.

Tricyclic diene 416a

$[\alpha]_D$ = + 23.20 ° (c = 1.03, $CHCl_3$);

R_f = 0.14 (10 % EtOAc in PS 40–60 °C);

^{1}H NMR (400 MHz, $CDCl_3$): δ 6.34 (dd, *J* = 10.8, 17.5 Hz, 1H), 5.64 (br s, 1H), 5.08 (d, *J* = 17.5 Hz, 1H), 4.92 (d, *J* = 10.7 Hz, 1H), 2.24 (br s, 1H), 3.59 (t, *J* = 5.3 Hz, 1H), 2.81 (ddt, *J* = 1.4 Hz, 5.7 Hz, 14.9 Hz, 1H), 2.55 (dt, *J* = 3.6, 6.9 Hz, 1H), 2.37-2.30 (m, 2H), 2.18-2.06 (m, 2H), 2.02 (dddd, *J* = 1.4, 2.4, 9.7, 14.4 Hz, 1H), 1.99-1.92 (m, 1H), 1.87-1.76 (m, 2H), 1.67 (dddd, *J* = 2.0, 7.6, 10.8, 14.7 Hz, 1H) 1.57-1.51 (m, 1H), 1.47-1.39 (m, 2H) ppm;

^{13}C NMR (100 MHz, $CDCl_3$): δ 151.8 (C_q), 139.3 (CH), 135.8 (C_q), 127.6 (CH), 110.1 (CH_2), 109.8 (CH_2), 78.7 (CH), 42.1 (CH_2), 38.8 (CH_2), 38.6 (C_q), 36.5 (CH), 34.2 (CH_2), 32.9 (CH_2), 31.7 (CH), 26.3 (CH_2), 19.9 (CH_2) ppm;

IR (thin film): ν_{max} = 3264, 2918, 2896, 1637 cm^{-1};

LRMS (70 eV, EI): m/z (%):230 (4, $[M]^{+\bullet}$), 212 (69, $[M-H_2O]^{+\bullet}$), 155 (100);

HRMS (70 eV, EI): m/z calc. for $C_{16}H_{22}O$ $[M]^{+\bullet}$: 230.1671; found 230.1668.

Tricyclic diene 416b

[α]$_D$ = +38.50 ° (c = 1.07 $CHCl_3$);

R_f = 0.20 (10 % EtOAc in PS 40–60 °C);

^{1}H NMR (400 MHz, $CDCl_3$): δ 6.33 (dd, *J* = 10.7, 17.5 Hz, 1H), 5.61 (br s, 1H), 5.08 (d, *J* = 17.5 Hz, 1H), 4.91 (d, *J* = 10.7 Hz, 1H), 4.73 (t, *J* = 2.2 Hz, 1H), 4.66 (t, *J* = 2.3 Hz, 1H), 3.57 (t, *J* = 4.1 Hz, 1H), 2.83 (ddt, *J* = 2.2, 4.5, 15.2, 1H), 2.56-2.48 (m, 2H), 2.38-2.31 (m, 2H), 2.15-2.10 (m, 1H), 1.96-1.88 (m, 2H), 1.82 (dddd, *J* = 4.3, 6.7, 11.2, 14.2, 1H), 1.75-1.67 (m, 2H), 1.66-1.59 (m, 2H), 1.32-1.24 (m, 1H) ppm;

^{13}C NMR (100 MHz, $CDCl_3$): δ 154.1 (C_q), 139.3 (CH), 135.9 (C_q), 128.3 (CH), 110.1 (CH_2), 109.8 (CH_2), 78.5 (CH), 41.1 (CH_2), 39.3 (CH_2), 38.3 (C_q), 37.5 (CH_2), 37.1 (CH), 32.6 (CH_2), 27.8 (CH), 24.5 (CH_2), 22.7 (CH_2) ppm;

IR (thin film): ν_{max} = 3392, 2917, 1650, 1607 cm^{-1};

LRMS (70 eV, EI): m/z (%): 230 (4, $[M]^{+\bullet}$), 212 (82, $[M-H_2O]^{+\bullet}$), 169 (96), 155 (94), 117 (100);

HRMS (70 eV, EI): m/z calc. for $C_{16}H_{22}O$ $[M]^{+\bullet}$: 230.1671; found 230.1668.

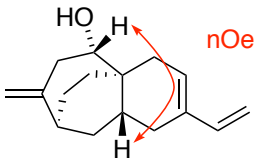

416a

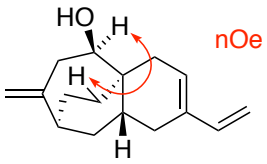

416b

Monoadduct 428

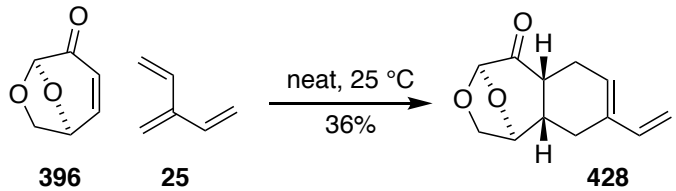

396 **25** **428**

(–)-Levoglucosenone (**396**) (29.3 mg, 0.232 mmol, 1.0 mol. equiv.) and [3]dendralene (**25**) (60 mg, 0.75 mmol, 3.2 mol. equiv.) were combined, the reaction flask was sealed, and the reaction mixture was stirred at 25 °C for 20 h. Regio/diastereo-selectivity was determined to be >95:5 by analysis of crude ^{1}H NMR spectra. Purification by flash column chromatography (Et_3N-deactivated SiO_2; 30% EtOAc in PS 40–60 °C), afforded bicyclic diene **428** as a white solid (17.0 mg, 0.0824 mmol, 36%). Recrystallisation from MeCN gave white crystals suitable for single crystal X-ray analysis.

$[\alpha]_D$ = –4.81 ° (c = 1.08 MeCN);

m.p. = 106-108 °C (C_6H_6);

R_f: 0.37 (30 % EtOAc in PS 40–60 °C);

^{1}H NMR (400 MHz, C_6D_6): δ 6.29 (dd, *J* = 10.8, 17.5 Hz, 1H), 5.48 (br s, 1H), 5.19 (s, 1H), 4.99 (dd, *J* = 17.4 Hz, 1H), 4.89 (d, *J* = 10.8 Hz, 1H), 3.64 (d, *J* = 5.0 Hz, 1H), 3.44 (dd, *J* = 5.2, 7.3 Hz), 3.36 (d, *J* = 7.4 Hz, 1H), 2.86 (d, *J* = 20.2 Hz, 1H), 2.57 (t, *J* = 7.5 Hz, 1H), 2.41-2.27 (m, 1H), 1.88 (dd, *J* = 6.1, 17.1 Hz, 1H), 1.73-1.62 (m, 1H), 1.58-1.50 (m, 1H) ppm;

^{13}C NMR (100 MHz, C_6D_6): δ 200.9 (C_q), 139.7 (CH), 134.1 (C_q), 126.7 (CH), 110.3 (CH_2), 102.2 (CH), 77.2 (CH), 67.1 (CH_2), 40.5 (CH), 38.0 (CH), 23.4 (CH_2), 21.4 (CH_2) ppm;

IR (thin film): ν_{max} = 2967, 2908, 1737, 1733, 1656, 1607 cm^{-1};

LRMS (70 eV, EI): m/z (%): 206 (23, $[M]^{+\bullet}$), 132 (22), 106 (33), 117 (100);

HRMS (70 eV, EI): m/z calc. for $C_{12}H_{14}O_3$ $[M]^{+\bullet}$: 206.0943; found 206.0941.

Monoadduct 455

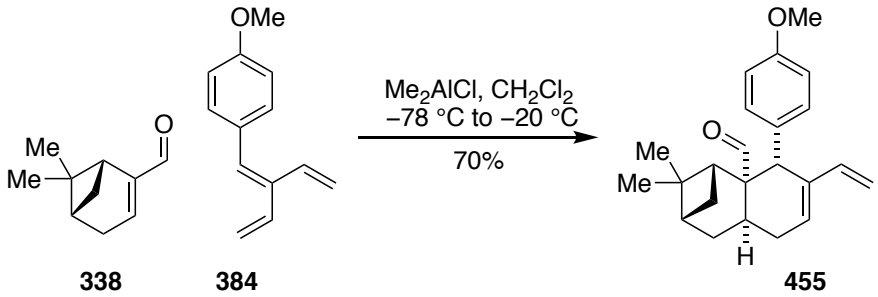

338 **384** **455**

A stirred solution of substituted [3]dendralene **384** (116 mg, 0.624 mmol, 2.02 mol. equiv.) in CH_2Cl_2 (0.50 mL) cooled in a –78 °C dry ice-acetone bath under Ar was treated with (*R*)-(–)-myrtenal (**338**) (46 mg, 47 µL, 0.31 mmol, 1.0 mol. equiv.), followed by the dropwise addition of Me_2AlCl (1.0 M solution in hexane, 155 µL, 0.155 mmol, 0.50 mol. equiv.). The flask was transferred to a –20 °C bath (IPA, Huber Chiller) and the temperature was allowed to equilibrate. The reaction vessel was sealed and the reaction was stirred at –20 °C for 21.5 h. Triethylamine (50 µL) was then added, the reaction mixture was removed from the cold bath, sat. aq. potassium sodium tartrate solution (2.5 mL) was added and the resulting mixture was allowed to stir for 30 minutes. The mixture was then poured onto water (5.0 mL) and was extracted with CH_2Cl_2 (3 x 5.0 mL). The organic layers were combined, washed with brine (5.0 mL), dried over $MgSO_4$ and concentrated under reduced pressure. Regio/diastereoselectivity was determined to be >90:10 by analysis of crude ^{1}H NMR spectra. Purification by flash column chromatography (5% EtOAc in PS 40–60 °C) afforded bicyclic diene **455** (72.8 mg, 0.216 mmol, 70%) as a clear colourless oil.

$[\alpha]_D$ = –216 ° (c = 1.16, $CHCl_3$);

R_f **=** 0.18 (5 % EtOAc in PS 40–60 °C);

^{1}H NMR (400 MHz, $CDCl_3$): δ 9.09 (s, 1H), 6.95 (d, *J* = 8.13 Hz, 2H), 6.74 (d, *J* = 8.5 Hz, 2H), 6.33-6.17 (m, 2H), 4.97 (d, *J* = 17.5 Hz, 1H), 4.84 (d, *J* = 10.9 Hz, 1H), 3.74 (s, 3H), 3.60 (s, 1H), 3.03-2.93 (m, 1H), 2.65-2.53 (m, 2H), 2.31-2.11 (m, 3H), 1.88-1.79 (m, 1H), 1.53-1.45 (m, 1H), 1.25 (s, 3H), 1.08 (d, *J* = 10.1 Hz, 1H), 0.76 (s, 3H) ppm;

^{13}C NMR (100 MHz, $CDCl_3$): δ 204.8 (CH), 158.5 (C_q), 141.6 (C_q), 137.3 (CH), 130.5 (CH), 130.2 (C_q), 128.8 (CH), 114.2 (CH), 111.8 (CH_2), 56.3 (C_q), 55.2 (CH_3), 51.7 (CH), 48.1 (CH), 40.5 (C_q), 40.1 (CH), 36.0 (CH_2), 30.1 (CH_2), 27.8 (CH_3), 27.5 (CH_2), 27.3 (CH), 22.6 (CH_3) ppm;

IR (thin film): ν_{max} = 2915, 1719, 1679, 1647, 1607 cm^{-1};

LRMS (70 eV, EI): m/z (%): 336 (10, $[M]^{+\bullet}$), 307 (29), 186 (72), 121 (100);

HRMS (70 eV, EI): m/z calc. for $C_{23}H_{28}O_2$ $[M]^{+\bullet}$: 336.2089; found 336.2084.

Monoadduct 466

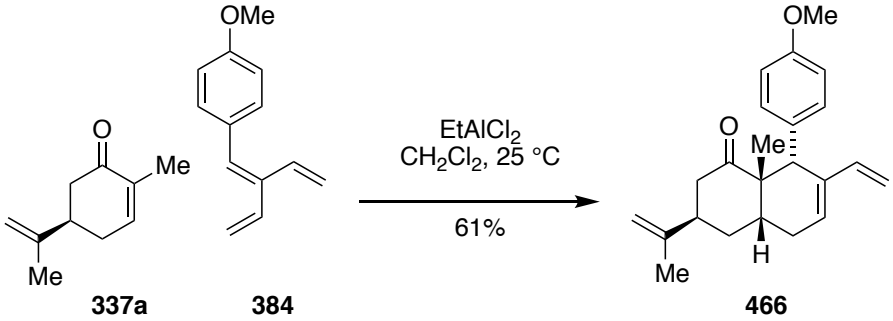

337a **384** **466**

(*R*)-(–)-carvone (**337a**) (40.3 mg, 42 μL, 0.27 mmol, 1.0 mol. equiv.) in CH_2Cl_2 (0.50 mL) with powdered 4Å mol sieves (~20 mg) was treated with $EtAlCl_2$ (1.0 M solution in hexane, 268 μL, 0.268 mmol, 1.0 mol. equiv.) at 25 °C. The resulting solution was stirred for 30 min, before the addition of substituted [3]dendralene (**25**) (50.0 mg, 0.268 mmol, 1.0 mol. equiv.) in CH_2Cl_2 (0.50 mL). The resulting solution was stirred at 25 °C for 2 h 40 min, before the addition of ice-cold sat. aq. $NaHCO_3$ solution (1.0 mL) and sat. aq. potassium sodium tartrate solution (2.0 mL). The organic layer was separated and the aqueous layer was extracted with CH_2Cl_2 (3 x 5.0 mL). The combined organic layers were dried (K_2CO_3), filtered and concentrated under reduced pressure. Regio/diastereo-selectivity was determined to be >90:10 by analysis of crude ^{1}H NMR spectra. A yield of 61% was determined by analysis of ^{1}H NMR spectra using 1,4-dinitrobenzene as an internal standard. A pure sample of monoadduct **466** was obtained as a clear colourless oil for characterisation purposes by preparative thin layer chromatography (SiO_2; CH_2Cl_2).

[α]$_D$ = –217 ° (c = 0.870, $CHCl_3$);

R$_f$ = 0.54 (CH_2Cl_2);

^{1}H NMR (400 MHz, $CDCl_3$): δ 7.09 (d, *J* = 6.9 Hz, 2H), 6.76 (d, *J* = 6.8 Hz, 2H), 6.25 (dd, *J* = 10.9, 17.6 Hz, 1H), 6.03 (br s, 1H), 4.84-4.63 (m, 3H), 4.43 (s, 1H), 3.76 (s, 3H), 3.55 (s, 1H), 2.66 (d, *J* = 19.4 Hz, 1H), 2.30 (dd, *J* = 5.6, 16.1 Hz, 1H), 2.17 (dd, *J* = 4.5, 20.2 Hz, 1H), 2.10-1.95 (m, 2H), 1.88-1.80 (m, 1H), 1.59 (s, 3H), 1.51-1.44 (m, 1H), 1.40-1.28 (m, 1H), 1.25 (s, 3H) ppm;

^{13}C NMR (100 MHz, $CDCl_3$): δ 216.5 (C_q), 158.4 (C_q), 147.9 (C_q), 138.7 (CH), 135.1 (C_q), 132.5 (C_q), 131.5 (CH), 128.5 (CH), 113.6 (CH), 112.7 (CH_2), 111.2 (CH_2), 55.3 (CH_3), 52.1 (C_q), 47.8 (CH), 44.3 (CH_2), 38.6 (CH), 33.5CH), 32.3 (CH_2), 29.6 (CH_2), 26.0 (CH_3), 21.6 (CH_3) ppm;

IR (thin film): ν_{max} = 2961, 2932, 2835, 1695, 1645, 1609 cm^{-1};

LRMS (70 eV, EI): m/z (%): 336 (5, $[M]^{+\bullet}$), 186 (100, $[M - C_{10}H_{14}O]^{+\bullet}$);

HRMS (70 eV, EI): m/z calc. for $C_{23}H_{28}O_2$ $[M]^{+\bullet}$: 336.2089; found 336.2086.

Monoadduct 399b

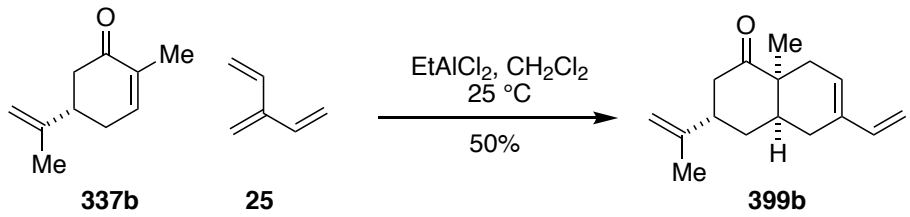

337b **25** **399b**

According to the above procedure, (*S*)-(+)-carvone (**337b**) (637 mg, 665 μL, 4.24 mmol, 1.0 mol equiv) and [3]dendralene (**25**) (340 mg, 4.24 mmol, 1.0 mol equiv) were converted to monoadduct **399b**. Regio/diastereo-selectivity was determined to be >95:5 by analysis of crude ^{1}H NMR spectra. Purification by flash column chromatography (SiO_2; 5% EtOAc in PS 40–60 °C) afforded monoadduct **399b** as a clear colourless oil (489 mg, 2.12 mmol, 50%). Spectroscopic data were consistent with those reported above.

Monoadduct 399a[ii]

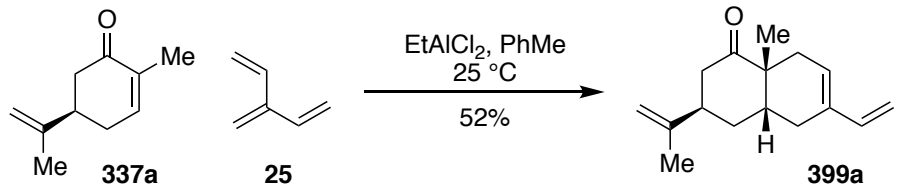

337a **25** **399a**

(*R*)-(–)-Carvone (**337a**) (375 mg, 391 μL, 2.50 mmol, 2.0 mol. equiv.) in PhMe (0.50 mL) was treated with $EtAlCl_2$ (1.0 M solution in hexane, 1.38 mL, 1.38 mmol, 1.1 mol. equiv.) at 25 °C. The resulting solution was stirred for 20 min, before the addition of [3]dendralene (**25**) (100 mg, 1.25 mmol, 1.0 mol. equiv.) in PhMe (0.50 mL). The resulting solution was stirred at 25 °C for 1 h 15 min, before the addition of ice-cold sat. aq. $NaHCO_3$ solution (1.0 mL). The organic layer was separated and the aqueous layer was extracted with Et_2O (3 x 10 mL). The combined organic layers were dried ($MgSO_4$), filtered and concentrated under reduced pressure. Regio/diastereo-selectivity was determined to be >95:5 by analysis of crude ^{1}H NMR spectra. Purification by flash column chromatography (SiO_2; 2.5% EtOAc in PS 40–60 °C) afforded monoadduct **399a** as a clear colourless oil (151 mg, 0.656 mmol, 52%). Spectral data were consistent with those reported above.

[ii] Reaction performed by undergraduate student Chloe Larcombe under direct instruction and guidance of the author.

Monoadduct 469

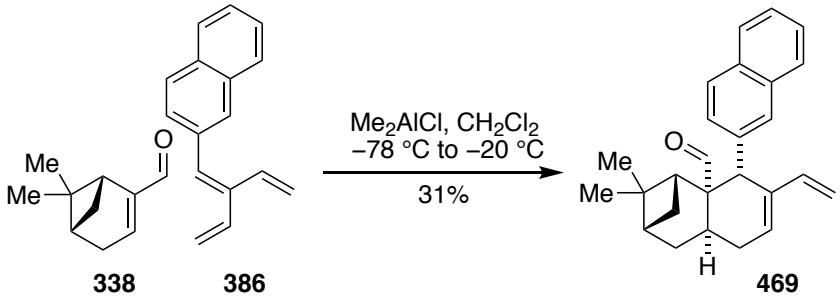

338 **386** **469**

A stirred solution of substituted [3]dendralene **386** (130 mg, 0.630 mmol, 2.02 mol. equiv.) in CH_2Cl_2 (0.50 mL) cooled in a –78 °C dry ice-acetone bath under Ar was treated with (*R*)-(–)-myrtenal (**338**) (47 mg, 48 μL, 0.31 mmol, 1.0 mol. equiv.), followed by the dropwise addition of Me_2AlCl (1.0 M solution in hexane, 156 μL, 0.156 mmol, 0.50 mol. equiv.). The flask was transferred to a –20 °C bath (IPA, Huber Chiller) and the temperature was allowed to equilibrate. The reaction vessel was sealed and the reaction was stirred at –20 °C for 29 h. Triethylamine (50 μL) was then added, the reaction mixture was removed from the cold bath, sat. aq. potassium sodium tartrate solution (2.5 mL) was added and the resulting mixture was allowed to stir for 30 minutes. The mixture was then poured onto water (5.0 mL) and was extracted zwith CH_2Cl_2 (3 x 5.0 mL). The organic layers were combined, washed with brine (5.0 mL), dried over $MgSO_4$ and concentrated under reduced pressure. Regio/diastereo-selectivity was determined to be >80:20 by analysis of crude ^{1}H NMR spectra. Purification by flash column chromatography (SiO_2; 5 % EtOAc in PS 40–60 °C) afforded monoadduct **469** (34.0 mg, 0.0954 mmol, 31%) as a clear colourless oil.

$[\alpha]_D$ = –111 ° (c = 0.996, $CHCl_3$);

R_f = 0.41 (10 % EtOAc in PS 40–60 °C);

^{1}H NMR (400 MHz, $CDCl_3$): δ 9.08 (s, 1H), 7.86-7.69 (m, 3H), 7.54 (s, 1H), 7.52-7.39 (m, 2H), 7.17 (dd, *J* = 1.83, 8.49 Hz, 1H), 6.35-6.28 (m, 2H), 5.03 (d, *J* = 17.5 Hz, 1H), 4.83 (d, *J* = 10.9 Hz, 1H), 3.85 (s, 1H), 3.08-2.98 (m, 1H), 2.77-2.66 (m, 2H), 2.40-2.20 (m, 3H), 1.93-1.84 (m, 1H), 1.58-1.53 (m, 1H), 1.28 (s, 3H), 1.19-1.15 (m, 1H), 0.78 (s, 3H) ppm;

^{13}C NMR (100 MHz, $CDCl_3$): δ 204.6 (CH), 141.2 (C_q), 137.3 (CH), 136.0 (C_q), 133.6 (C_q), 132.6 (C_q), 129.2 (CH), 128.6 (CH), 128.4 (CH), 127.9 (CH), 127.72 (CH), 127.67 (CH), 126.2 (CH), 125.9 (CH), 112.0 (CH_2), 56.6 (C_q), 51.9 (CH), 49.2 (CH), 40.6 (C_q), 40.2 (CH), 36.0 (CH_2), 30.3 (CH_2), 27.9 (CH_3), 27.6 (CH_2), 27.3 (CH), 22.6 (CH_3) ppm;

IR (thin film): ν_{max} = 2917, 2870, 1717 cm^{-1};

LRMS (70 eV, EI): m/z (%): 356 (100, $[M]^{+\bullet}$), 338 (87), 330 (71);

HRMS (70 eV, EI): m/z calc. for $C_{26}H_{28}O$ $[M]^{+\bullet}$: 356.2140; found 356.2142.

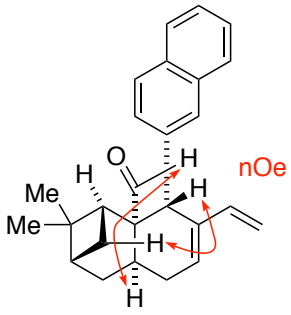

469

Monoadduct 429

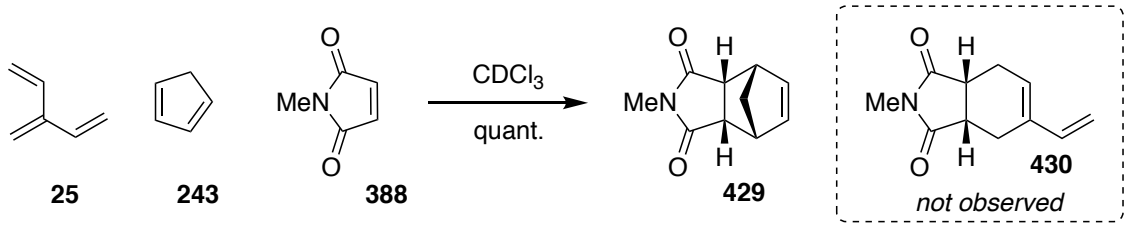

A stirred solution of dicyclopentadiene in a round bottomed flask fitted with a vigreux distillation apparatus, condenser (chilled-water) and trap (dry-ice acetone bath) was heated at 180 °C (oil bath) until distillation of cyclopentadiene (**243**) ceased. Cyclopentadiene (**243**) was used directly.

A solution of [3]dendralene (**25**) (20 mg, 0.25 mmol, 1.2 mol. equiv.) in $CDCl_3$ (2.50 mL) was treated with cyclopentadiene (**243**) (17 mg, 0.25 mmol, 1.2 mol. equiv.; freshly cracked) in $CDCl_3$ (2.50 mL), followed by NMM (**388**) (23 mg, 0.21 mmol, 1.0 mol. equiv.). The resulting solution was allowed to stir at ambient room temperature for 18.5 h. A quantitative yield of monoadduct **429** was determined by analysis of ^{1}H NMR spectra using durene as an internal standard. Spectroscopic data for monoadduct **429** were consistent with those reported previously.[130] Monoadduct **430** was not observed by analysis of ^{1}H NMR spectra.[110]

Monoadduct 478 and Bisadduct 479[iii]

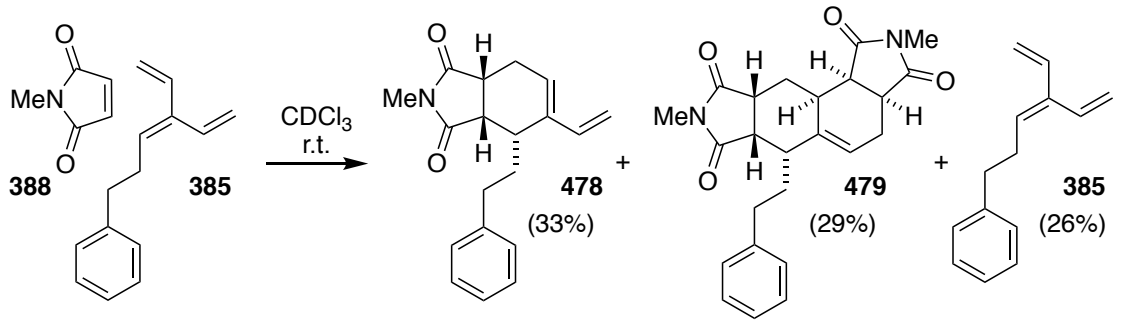

To a solution of substituted [3]dendralene **385** (108 mg, 0.586 mmol, 1.0 mol. equiv.) in $CDCl_3$ (1.0 mL) at 25 °C was added NMM (**388**) (62.0 mg, 0.558 mmol, 0.95 mol. equiv.). The resulting solution was stirred at 25 °C for 25 h, before concentration under reduced pressure. Regio/diastereo-selectivity was determined to be >95:5 by analysis of crude ^{1}H NMR spectra. Purification by flash column chromatography (SiO_2; 20% to 50% EtOAc in PS 40–60 °C) afforded monoadduct **478** as a clear colourless oil (53.3 mg, 0.180 mmol, 32%), bisadduct **479** as a clear colourless oil (64.0 mg, 0.157 mmol, 28%) and recovered dendralene **385** (25.5 mg, 0.138 mmol, 24%).

Monoadduct 478

R_f = 0.59 (50% EtOAc in PS 40–60 °C;

^{1}H NMR (400 MHz, $CDCl_3$): δ 7.42 (t, J = 6.9 Hz, 2H), 7.37-7.31 (m, 1H), 7.25 (d, J = 7.5 Hz, 2H), 6.60 (dd, J = 10.9, 17.5 Hz, 1H), 6.23-6.11 (m, 1H), 5.42 (d, 17.5 Hz, 1H), 5.23 (d, J = 10.7 Hz, 1H), 5.29-5.16 (m, 1H), 3.56-3.42 (m, 2H), 3.16 (s, 3H), 2.98-2.83 (m, 1H), 2.77-2.58 (m, 3H), 1.93-1.77 (m, 1H), 1.67-1.54 (m 1H) ppm;

^{13}C NMR (100 MHz, $CDCl_3$): δ 180.2 (C_q), 178.7 (C_q), 142.6 (C_q), 141.8 (C_q), 137.8 (CH), 128.5 (CH), 128.4 (CH), 127.0 (CH), 126.1 (CH), 112.7 (CH_2), 44.7 (CH), 39.0 (CH), 34.6 (CH_2), 33.9 (CH), 31.0 (CH_2), 24.8 (CH_3), 22.7 (CH_2) ppm;

IR (neat): ν_{max} = 3027, 2932, 2857, 1774, 1698 cm^{-1};

LRMS (70 eV, EI): m/z (%): 296 ($[M+1]^{+\bullet}$, 28), 295 ($[M]^{+\bullet}$, 92), 191 (100), 77 (100);

HRMS (70 eV, EI): calc. for $C_{19}H_{21}NO_2$ $[M]^{+\bullet}$: 295.1572; found 295.1572.

Bisadduct 479

R_f = 0.37 (70% EtOAc in PS 40–60 °C);

^{1}H NMR (400 MHz, $CDCl_3$): δ 7.29 (t, J = 7.34 Hz, 2 H), 7.19 (t, J = 8.35 Hz, 3 H), 5.67-5.60 (m, 1H), 3.28-3.21 (m, 1H), 3.18 (dd, J = 5.6, 9.6 Hz, 1H), 3.11-3.01 (m, 2H), 2.91 (s, 3H),

[iii] Reaction performed by undergraduate student Chloe Larcombe under direct instruction and guidance of the author. Purification and characterisation performed by the author.

2.90 (s, 3H), 2.88-2.81 (m, 1H), 2.81-2.71 (m, 2H), 2.58 (ddd, J = 5.3, 10.1, 13.3 Hz, 1H), 2.53-2.45 (br m, 1H), 2.36 (ddd, *J* = 2.3, 4.9, 14.2 Hz, 1H), 2.20-1.91 (m, 4H) ppm;

^{13}C NMR (100 MHz, $CDCl_3$): δ 180.0 (C_q), 179.5 (C_q), 177.9 (C_q), 177.7 (C_q), 142.0 (C_q), 140.5 (C_q), 128.6 (CH), 128.5 (CH), 126.2 (CH), 120.5 (CH), 43.3 (CH), 41.6 (CH), 40.2 (CH), 39.9 (CH), 37.4 (CH), 34.1 (CH), 33.6 (CH_2), 29.8 (CH_2), 25.0 (CH_2), 24.8 (CH_3, 2 x C; coincident), 23.1 (CH_2) ppm;

IR (neat): ν_{max} = 3448, 2926, 2854, 1771, 1690 cm^{-1};

LRMS (70 eV, EI): m/z (%): 407.1 ($[M+1]^{+\bullet}$, 21), 406.1 ($[M]^{+\bullet}$, 70), 91 (100);

HRMS (70 eV, EI): calc. for $C_{24}H_{26}N_2O_4$ $[M]^{+\bullet}$: 406.1893; found 406.1889.

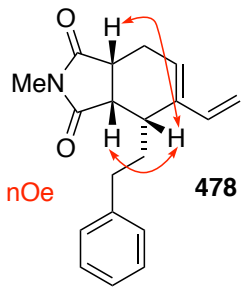

478

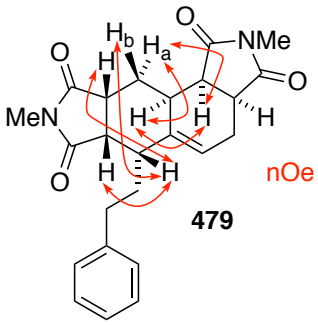

479

6.2.4 Bisadducts

Bisadduct 477

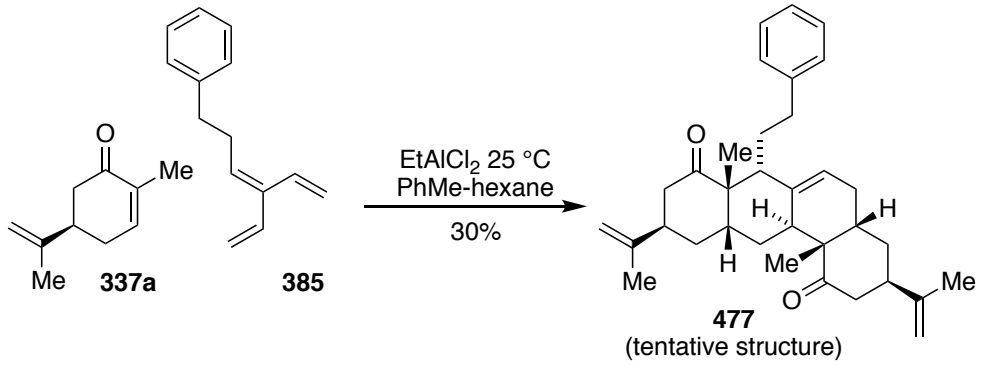

(*R*)-(–)-carvone (**337a**) (170 μL, 163 mg, 1.09 mmol, 2.0 mol equiv) in PhMe (0.50 mL) was treated with $EtAlCl_2$ (1.0 M solution in hexane, 597 μL, 0.597 mmol, 1.1 mol equiv) at 25 °C. The resulting solution was stirred for 20 min, before the addition of substituted [3]dendralene **385** (100 mg, 0.543 mmol, 1.0 mol equiv) in PhMe (0.50 mL). The resulting solution was stirred at 25 °C for 21 h, before the addition of ice-cold sat. aq. $NaHCO_3$ solution (2.0 mL), Et_2O (5.0 mL) and sat. aq. potassium sodium tartrate solution (2.0 mL). The organic layer was separated and the aqueous layer was extracted with Et_2O (2 x 5.0 mL). The combined organic layers were dried (K_2CO_3), filtered and concentrated under reduced pressure. Regio/diastereoselectivity was determined to be >80:20 by analysis of crude ^{1}H NMR spectra. A yield of 30% was determined by analysis of ^{1}H NMR spectra using 1,4-dinitrobenzene as an internal standard. A pure sample of bisadduct **477** was obtained as a white foam for characterisation purposes by flash column chromatography (SiO_2; 10% EtOAc in PS 40–60 °C).

$[\alpha]_D$ = +60.5 ° (c = 0.370, $CHCl_3$);

R_f = 0.26 (10 % EtOAc in PS 40–60 °C);

^{1}H NMR (400 MHz, $CDCl_3$): δ 7.30-7.27 (m, 4H), 7.19-7.15 (m, 1H), 5.39 (s, 1H), 4.83 (s, 1H), 4.78 (s, 1H), 4.76 (s, 1H), 4.59 (s, 1H), 2.87-2.79 (m, 2H), 2.76 (t, *J* = 11.8, 11.8 Hz, 1H), 2.71-264 (m, 2H), 2.61-2.56 (m, 1H), 2.56-2.50 (m, 1H), 2.34 (dd, *J* = 5.4, 15.8 Hz, 1H), 2.31-2.24 (m, 1H), 2.22-2.09 (m, 4H), 2.06-1.92 (m, 4H), 1.84-1.77 (m, 1H), 1.78 (s, 3H), 1.70 (s, 3H), 1.67-1.61 (m, 2H), 1.60-1.54 (m, 1H), 1.45-1.39 (m, 1H), 1.22 (s, 3H), 1.12 (s, 3H) ppm;

^{13}C NMR (100 MHz, $CDCl_3$): δ 218.2 (C_q), 213.7 (C_q), 148.0 (C_q), 147.5 (C_q), 142.9 (2 x C_q; coincident), 128.8 (CH), 128.4 (CH), 125.7 (CH), 121.3 (CH), 111.0 (2 x CH_2; coincident), 54.3 (CH), 51.8 (C_q), 49.9 (C_q), 44.6 (CH_2), 41.4 (CH_2), 41.0 (CH), 38.5 (CH), 37.0 (CH), 36.5 (CH), 35.6 (CH_2), 34.1 (CH_2), 32.0 (CH_2), 30.9 (CH), 29.9 (CH_2), 29.4 (CH_2), 27.9 (CH_2), 26.4

(CH_3), 21.3 (CH_3), 21.1 (2 x CH_3; coincident) ppm;

IR (thin film): ν_{max} = 2932, 2873, 1704, 1695 cm^{-1};

LRMS (70 eV, EI): m/z (%): 484 (80, $[M+1]^{+\bullet}$), 341 (37, $[M]^{+\bullet}$), 466 (41), 243 (59), 109 (72), 105 (77), 91 (100);

HRMS (70 eV, EI): m/z calc. for $C_{34}H_{44}O_2$ $[M]^{+\bullet}$: 484.3341; found 484.3343.

Bisadduct 497[iv]

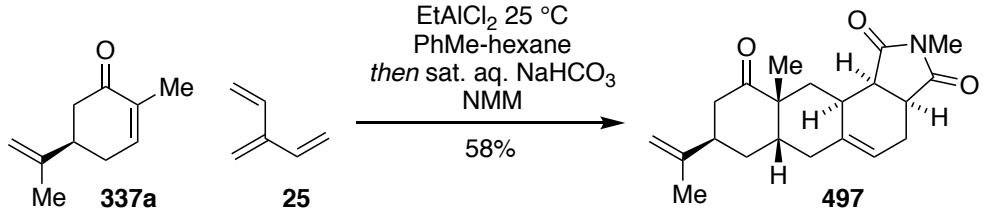

(*R*)-(–)-carvone (**337a**) (391 μL, 375 mg, 2.50 mmol, 2.0 mol. equiv.) in PhMe (0.50 mL) was treated with $EtAlCl_2$ (1.0 M solution in hexane, 1.38 mL, 1.38 mmol, 1.1 mol. equiv.) at 25 °C. The resulting solution was stirred for 20 min, before the addition of [3]dendralene (**25**) (100 mg, 1.25 mmol, 1.0 mol. equiv.) in PhMe (0.50 mL). The resulting solution was stirred at 25 °C for 1 h 15 min, before the addition of ice-cold sat. aq. $NaHCO_3$ solution (1.0 mL) and NMM (**388**) (694 mg, 6.25 mmol, 5.0 mol. equiv.). The resulting solution was stirred for 45 h. The organic layer was then separated and the aqueous layer was extracted with Et_2O (3 x 10 mL). The combined organic layers were dried ($MgSO_4$), filtered and concentrated under reduced pressure. Regio/diastereo-selectivity was determined to be >90:10 by analysis of crude ^1H NMR spectra Purification by flash column chromatography (SiO_2; 10% EtOAc in PS 40–60 °C) afforded bisadduct **497** as a white solid (248 mg, 0.726 mmol, 58%). Recrystallisation from EtOAc gave white crystals suitable for single crystal X-ray analysis.

$[\alpha]_D$ = +4.27 ° (c = 1.01, $CHCl_3$);

m.p. = 117-119 °C (EtOAc)

R_f = 0.48 (50 % EtOAc in PS 40–60 °C);

^{1}H NMR (400 MHz, $CDCl_3$): δ 5.40 (br s, 1H), 4.72 (s, 1H), 4.68 (s, 1H), 3.11 (t, *J* = 8.2 Hz, 1H), 2.95 (td, *J* = 2.9, 8.4 Hz, 1H), 2.89 (s, 3H), 2.61-2.43 (m, 4H), 2.42-2.33 (m, 1H), 2.29-2.10 (m, 3H), 2.10-1.90 (m, 3H), 1.69 (s, 3H), 1.55 (d, *J* = 13.8 Hz, 1H), 1.29-1.13 (m, 4H) ppm;

^{13}C NMR (100 MHz, $CDCl_3$): δ 214.5 (C_q), 180.0 (C_q), 178.3 (C_q), 147.4 (C_q), 139.2 (C_q), 117.2 (CH), 109.9 (CH_2), 49.1 (C_q), 44.3 (CH), 43.0 (CH_2), 41.9 (CH), 40.3 (CH), 38.6 (CH), 37.4 (CH_2), 36.6 (CH_2), 32.3 (CH_2), 32.2 (CH), 27.5 (CH_3), 24.5 (CH_3), 22.5 (CH_2), 20.6 (CH_3) ppm;

IR (thin film): ν_{max} = 2965, 2934, 2858, 1775, 1692 cm^{-1};

LRMS (70 eV, EI): m/z (%): 342 (12, $[M+1]^{+\bullet}$), 341 (37, $[M]^{+\bullet}$), 191 (66), 151 (57), 109

[iv] Reaction and purification performed by undergraduate student Chloe Larcombe under direct instruction and guidance of the author. Characterisation performed by Chloe Larcombe and the author, under direct instruction and guidance of the author. Recrystallisation for single crystal X-ray analysis performed by the author.

(100);

HRMS (70 eV, EI): m/z calc. for $C_{21}H_{27}NO_3$ $[M]^{+\bullet}$: 341.1991; found 341.1993.

Bisadduct 498[v]

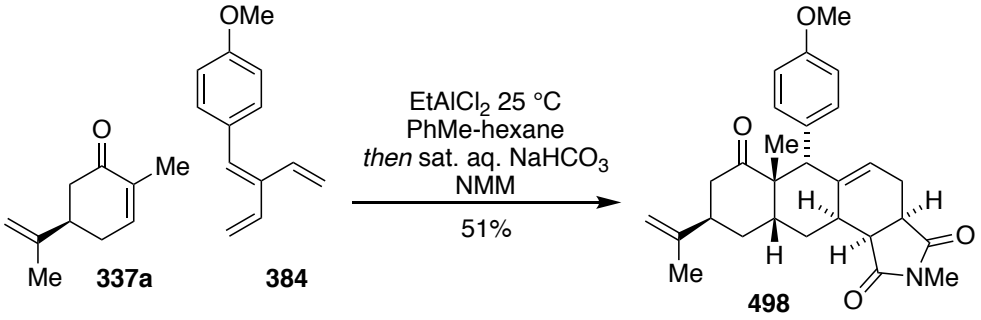

(*R*)-(–)-carvone (**337a**) (168 μL, 1.07 mmol, 2.0 mol. equiv.) in PhMe (0.50 mL) was treated with $EtAlCl_2$ (1.0 M solution in hexane, 591 μL, 0.591 mmol, 1.1 mol. equiv.) at 25 °C. The resulting solution was stirred for 20 min, before the addition of substituted [3]dendralene **384** (100 mg, 0.537 mmol, 1.0 mol. equiv.) in PhMe (0.50 mL). The resulting solution was stirred at 25 °C for 2 h, before the addition of ice-cold sat. aq. $NaHCO_3$ solution (1.0 mL) and NMM (318 mg, 2.68 mmol, 5.0 mol. equiv.). The resulting solution was stirred for 19 h. The organic layer was then separated and the aqueous layer was extracted with Et_2O (3 x 20 mL). The combined organic layers were dried ($MgSO_4$), filtered and concentrated under reduced pressure. Regio/diastereo-selectivity was determined to be >90:10 by analysis of crude ^1H NMR spectra Purification by flash column chromatography (SiO_2; 10% to 50% EtOAc in PS 40–60 °C) afforded bisadduct **498** as a pale yellow solid (122 mg, 0.272 mmol, 51%). Recrystallisation from CH_2Cl_2 gave white crystals suitable for single crystal X-ray analysis.

$[\alpha]_D$ = +121.81 ° (c = 0.981, $CHCl_3$);

m.p. = 151-153 °C (EtOAc)

R_f = 0.46 (50 % EtOAc in PS 40–60 °C);

^{1}H NMR (400 MHz, $CDCl_3$): δ 7.27 (d, *J* = 8.8 Hz, 2H), 6.80 (d, *J* = 8.8 Hz, 2H), 5.12 (br s, 1H), 4.80 (s, 1H), 4.76 (s, 1H), 3.78 (s, 3H), 3.09-2.97 (m, 3H), 2.88 (s, 3H), 2.84-2.64 (m, 2H), 2.62-2.43 (m 4H), 229-2.10 (m, 3H), 1.89 (dt, *J* = 7.7, 15.3 1H), 1.82-1.69 (m, 4H), 1.08 (s, 3H) ppm;

^{13}C NMR (100 MHz, $CDCl_3$): δ ^{13}C NMR (101 MHz, $CDCl_3$) δ 214.6 (C_q), 180.0 (C_q), 179.0 (C_q), 158.3 (C_q), 147.3 (C_q), 143.8 (C_q), 133.0 (CH), 131.0 (C_q), 119.2 (CH), 113.4 (CH), 110.1 (CH_2), 57.2 (CH), 55.2 (CH_3), 52.7 (C_q), 45.1 (CH), 44.5 (CH_2), 44.1 (CH), 42.2 (CH), 40.1 (CH), 34.0 (CH), 33.6 (CH_2), 28.4 (CH_2), 25.0 (CH_2), 24.8 (CH_3), 24.6 (CH_3), 20.7 (CH_3) ppm;

IR (thin film): ν_{max} = 2971, 2937, 2826, 1763, 1690 cm^{-1};

[v] Reaction performed by undergraduate student Chloe Larcombe under direct instruction and guidance of the author. Purification and characterisation performed by the author.

LRMS (70 eV, EI): m/z (%): 448 (37, $[M+1]^{+\bullet}$), 447 (86, $[M]^{+\bullet}$), 297 (92), 284 (58), 121 (100);

HRMS (70 eV, EI): m/z calc. for $C_{28}H_{33}NO_4$ $[M]^{+\bullet}$: 447.2410; found 148.0890.

Bisadduct 499

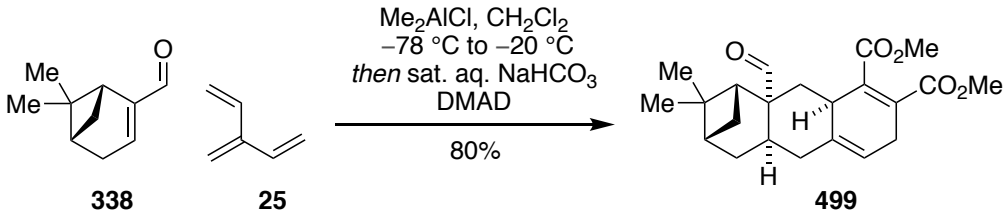

338 **25** **499**

A stirred solution of [3]dendralene (**25**) (50 mg, 0.62 mmol, 2.0 mol. equiv.) in CH_2Cl_2 (0.50 mL) cooled in a –78 °C dry ice-acetone bath under Ar was treated with (*R*)-(–)-myrtenal (**338**) (46 mg, 47 μL, 0.31 mmol, 1.0 mol. equiv.), followed by the dropwise addition of Me_2AlCl (1.0 M solution in hexane, 155 μL, 0.155 mmol, 0.50 mol. equiv.). The flask was transferred to a –20 °C bath (IPA, Huber Chiller) and the temperature was allowed to equilibrate. The reaction vessel was sealed and the reaction was stirred at –20 °C for 17 h. Sat. aq. $NaHCO_3$ solution (300 μL) was then added, and the reaction solution was allowed to warm to ambient room temperature, before the addition of DMAD (380 μL, 439 mg, 3.09 mmol, 10 mol. equiv.). The resulting reaction mixture was allowed to stir for 52 h, before the addition of sat. aq. $NaHCO_3$ solution (1.0 mL). The mixture was then poured onto water (5.0 mL) and was extracted with CH_2Cl_2 (3 x 5.0 mL). The combined organic layers were dried ($MgSO_4$) and concentrated under reduced pressure. Regio/diastereo-selectivity was determined to be >85:15 by analysis of crude ^{1}H NMR spectra. Purification by flash column chromatography (SiO_2; 10% EtOAc in PS 40–60 °C) afforded bisadduct **499** as a clear colourless oil (91.8 mg, 0.246 mmol, 80%).

$[\alpha]_D$ = –43.27 ° (c = 1.03, $CHCl_3$);

R_f = 0.44 (30 % EtOAc in PS 40–60 °C);

^{1}H NMR (400 MHz, $CDCl_3$): δ 9.41 (s, 1H), 5.48 (s, 1H), 3.77 (s, 3H), 3.74 (s, 3H), 3.11 (dt, *J* = 5.2, 5.2, 22.0 Hz, 1H), 3.02-2.91 (m, 1H), 2.91-2.69 (m, 2H), 2.49 (dd, *J* = 7.4, 15.1 Hz, 1H), 2.34-2.24 (m, 1H), 2.20-2.03 (m, 3H), 1.97-1.87 (m, 1H), 1.71-1.63 (m, 2H), 1.45 (ddd, *J* = 2.6, 6.2, 13.6 Hz, 1H), 1.29-1.17 (m, 1H), 1.23 (s, 3H), 0.79 (s, 3H), ppm;

^{13}C NMR (100 MHz, $CDCl_3$): δ 205.7 (CH), 168.6 (C_q), 167.3 (C_q), 139.4 (C_q), 135.1 (C_q), 131.0 (C_q), 116.1 (CH), 54.3 (C_q), 52.32 (CH_3), 52.36 (CH_3), 48.7 (CH), 41.4 (CH), 39.7 (CH_2), 39.1 (C_q), c), 32.7 (CH_2), 28.9 (CH_2), 27.85 (CH_3), 27.80 (CH_2), 26.0 (CH), 22.9 (CH_3) ppm;

IR (thin film): ν_{max} = 2990, 2950, 2907, 1717, 1646 cm^{-1};

LRMS (70 eV, ESI): m/z (%): 395 (100, $[M+Na]^{+\bullet}$);

HRMS (70 eV, ESI): m/z calc. for $C_{22}H_{28}O_5$ $[M+Na]^{+\bullet}$:395.1834; found 395.1829; m/z calc. for $C_{22}H_{28}O_5$ $[M+H]^{+\bullet}$:373.2015; found 373.2017

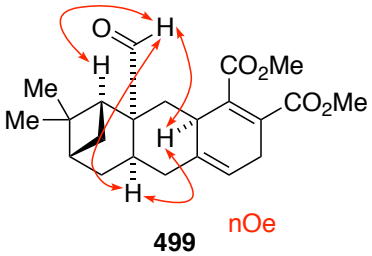

499

Bisadduct 500

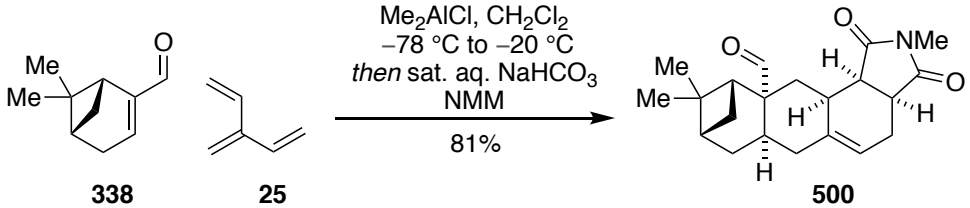

338 **25** **500**

A stirred solution of [3]dendralene (**25**) (50 mg, 0.62 mmol, 2.0 mol. equiv.) in CH_2Cl_2 (0.50 mL) cooled in a –78 °C dry ice-acetone bath under Ar was treated with (*R*)-(–)-myrtenal (**338**) (46 mg, 47 μL, 0.31 mmol, 1.0 mol. equiv.), followed by the dropwise addition of Me_2AlCl (1.0 M solution in hexane, 155 μL, 0.155 mmol, 0.50 mol. equiv.). The flask was transferred to a –20 °C bath (IPA, Huber Chiller) and the temperature was allowed to equilibrate. The reaction vessel was sealed and the reaction was stirred at –20 °C for 17 h. Sat. aq. $NaHCO_3$ solution (300 μL) was then added, and the reaction solution was allowed to warm to ambient room temperature, before the addition of NMM (**388**) (172 mg, 1.55 mmol, 5.0 mol. equiv.). The resulting reaction mixture was allowed to stir for 22 h, before the addition of sat. aq. $NaHCO_3$ solution (1.0 mL). The mixture was then poured onto water (5.0 mL) and was extracted with CH_2Cl_2 (3 x 5.0 mL). The combined organic layers were dried ($MgSO_4$) and concentrated under reduced pressure. Regio/diastereo-selectivity was determined to be >90:10 by analysis of crude ^{1}H NMR spectra. Purification by flash column chromatography (SiO_2; 20% EtOAc in PS 40–60 °C) afforded bisadduct **500** as a white foam (85.8 mg, 0.251 mmol, 81%).

$[\alpha]_D$ = 37.65 ° (c = 1.07, $CHCl_3$);

R_f = 0.46 (50 % EtOAc in PS 40–60 °C);

^{1}H NMR (400 MHz, $CDCl_3$): δ 9.45 (s, 1H), 5.55 (br s, 1H), 3.03 (t, *J* = 7.9 Hz, 1H), 2.95-2.86 (m, 1H), 2.92 (s, 3H), 2.73-2.59 (m, 2H), 2.59-2.49 (m, 1H), 2.40-2.13 (m, 4H), 2.13-1.87 (m, 4H), 1.55 (dd, *J* = 4.6, 14.6 Hz, 1H), 1.39 (d, *J* = 13.7 Hz, 1H), 1.34 (d, 10.6 Hz, 1H), 1.23 (s, 3H), 0.66 (s, 3H) ppm;

^{13}C NMR (100 MHz, $CDCl_3$): δ 207.2 (CH), 179.8 (C_q), 178.0 (C_q), 141.5 (C_q), 118.0 (CH), 54.7 (C_q), 48.9 (CH), 43.0 (CH), 41.2 (CH_2), 40.8 (CH), 40.4 (CH), 39.1 (C_q), 33.5 (CH_2), 32.0 (CH), 28.1 (CH_2), 26.8 (CH_3), 26.7 (CH_2), 26.4 (CH), 24.7 (CH_3), 24.4 (CH_2), 22.7 (CH_3) ppm;

IR (thin film): ν_{max} = 2920, 2868, 1772, 1717, 1689 cm^{-1};

LRMS (70 eV, EI): m/z (%): 341 (15, $[M]^{+\bullet}$), 280 (28), 193 (38), 112 (100);

HRMS (70 eV, EI): m/z calc. for $C_{21}H_{27}NO_3$ $[M]^{+\bullet}$: 341.1991; found 341.1190.

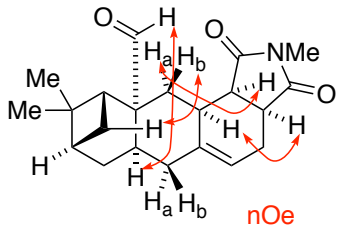

500

Bisadduct 502

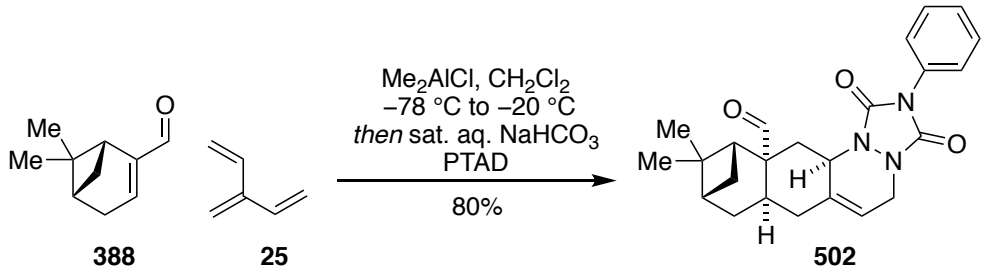

388 **25** **502**

A stirred solution of [3]dendralene (**25**) (50 mg, 0.62 mmol, 2.0 mol. equiv.) in CH_2Cl_2 (0.50 mL) cooled in a –78 °C dry ice-acetone bath under Ar was treated with (*R*)-(–)-myrtenal (**388**) (46 mg, 47 μL, 0.31 mmol, 1.0 mol. equiv.), followed by the dropwise addition of Me_2AlCl (1.0 M solution in hexane, 155 μL, 0.155 mmol, 0.50 mol. equiv.). The flask was transferred to a –20 °C bath (IPA, Huber Chiller) and the temperature was allowed to equilibrate. The reaction vessel was sealed and the reaction was stirred at –20 °C for 17 h. Sat. aq. $NaHCO_3$ solution (300 μL) was then added, and the reaction solution was allowed to warm to ambient room temperature, before the addition of PTAD (162 mg, 0.927 mmol, 3.0 mol. equiv.). The resulting reaction mixture was allowed to stir for 22 h, before the addition of sat. aq. $NaHCO_3$ solution (1.0 mL). The mixture was then poured onto water (5.0 mL) and was extracted with CH_2Cl_2 (3 x 5.0 mL). The combined organic layers were dried ($MgSO_4$) and concentrated under reduced pressure. Regio/diastereo-selectivity was determined to be >85:15 by analysis of crude ^{1}H NMR spectra. Purification by flash column chromatography (SiO_2; 30% EtOAc in PS 40–60 °C) afforded bisadduct **502** as a white solid (100 mg, 0.247 mmol, 80%).

$[\alpha]_D$ = –117.20 ° (c = 1.20, $CHCl_3$);

m.p. = 153-155 (decomposition) ($CHCl_3$)

R_f = 0.32 (30 % EtOAc in PS 40–60 °C);

^{1}H NMR (400 MHz, $CDCl_3$): δ 9.54 (s, 1H), 7.56-7.41 (m, 4H), 7.39-7.32 (m, 1H), 5.64 (s, 1H), 4.26-4.01 (m, 3H), 3.20-3.05 (m, 1H), 2.69-2.51 (m, 2H), 2.41-2.31 (m, 1H), 2.25 (dd, *J* = 5.0, 15.0 Hz, 1H), 2.29-2.21 (m, 2H), 1.97 (br s, 1H), 1.83 (t, *J* = 13.1 Hz, 1H), 1.54-1.46 (m, 1H), 1.26 (s, 3H), 1.22 (d, *J* = 10.5 Hz, 1H), 0.85 (s, 3H) ppm;

^{13}C NMR (100 MHz, $CDCl_3$): δ 204.7 (CH), 152.2 (C_q), 152.1 (C_q), 134.1(C_q), 131.2 (C_q), 129.2 (CH), 128.1 (CH), 125.4 (CH), 113.0, (CH) 53.9 (C_q), 52.5 (CH), 48.3 (CH), 43.0 (CH_2), 41.5 (CH), 38.9 (C_q), 38.3 (CH_2), 34.2 (CH_2), 31.1 (CH_2), 29.8 (CH_2), 28.2 (CH_3), 26.0 (CH), 22.7 (CH_3) ppm;

IR (thin film): ν_{max} = 2909, 2871, 1772, 1709 cm^{-1};

LRMS (70 eV, EI): m/z (%): 405 (55, $[M]^{+\bullet}$), 387 (49), 257 (52), 256 (100);

HRMS (70 eV, EI): m/z calc. for $C_{24}H_{27}N_3O_3$ $[M]^{+\bullet}$:405.2052; found 405.2054.

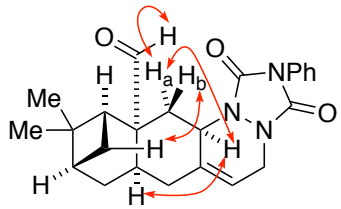

nOe **502**

Bisadduct 504

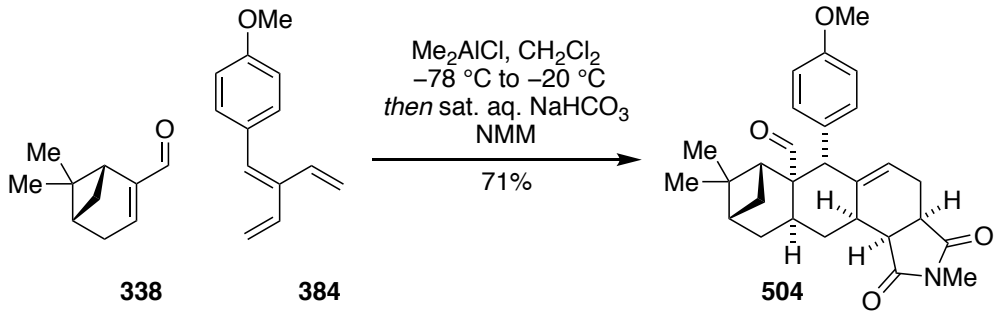

338 **384** **504**

A stirred solution of substituted [3]dendralene **384** (2.50 g, 13.4 mmol, 2.02 mol. equiv.) in CH_2Cl_2 (10.7 mL) cooled in a –78 °C dry ice-acetone bath under Ar was treated with (*R*)-(–)-myrtenal (**338**) (0.998 g, 1.01 mL, 6.64 mmol, 1.0 mol. equiv.), followed by the dropwise addition of Me_2AlCl (1.0 M solution in hexane, 3.32 mL, 3.32 mmol, 0.50 mol. equiv.). The flask was transferred to a –20 °C bath (IPA, Huber Chiller) and the temperature was allowed to equilibrate. The reaction vessel was sealed and the reaction was stirred at –20 °C for 22 h. Sat. aq. $NaHCO_3$ solution (2.0 mL) was then added, and the reaction solution was allowed to warm to ambient room temperature, before the addition of NMM (**388**) (3.69 g, 33.2 mmol, 5.0 mol. equiv.). The resulting reaction mixture was allowed to stir for 49 h, before the addition of sat. aq. $NaHCO_3$ solution (5.0 mL). The mixture was then poured onto H_2O (10.0 mL) and was extracted with CH_2Cl_2 (3 x 10.0 mL). The combined organic layers were dried ($MgSO_4$) and concentrated under reduced pressure. Regio/diastereo-selectivity was determined to be >90:10 by analysis of crude ^{1}H NMR spectra. Purification by flash column chromatography (SiO_2; 30% EtOAc in PS 40–60 °C) afforded bisadduct **504** as a white foam (2.11 g, 4.71 mmol, 71%).

$[\alpha]_D$ = –3.16° (c = 1.11, $CHCl_3$);

R_f = 0.26 (30 % EtOAc in PS 40–60 °C);

^{1}H NMR (400 MHz, $CDCl_3$): δ 9.53 (s, 1H), 6.92-6.72 (m, 4H), 5.27 (br s, 1H), 3.78 (s, 3H), 3.69 (s, 1H), 3.13-3.02 (m, 2H), 2.81 (s, 3H), 2.65-2.53 (m 2H), 2.50-2.37 (m, 2H), 2.31-2.15 (m, 3H), 2.04 (d, *J* = 12.1 Hz, 1H), 1.97-1.88 (m, 2H), 1.65 (d, *J* = 13.5 Hz, 1H), 1.43 (d, *J* = 10.32 Hz, 1H), 1.12 (s, 3H), 0.60 (s, 3H) ppm;

^{13}C NMR (100 MHz, $CDCl_3$): δ 210.6 (CH), 180.0 (C_q), 178.5 (C_q), 158.7 (C_q), 142.0 (C_q), 133.1(CH), 130.2 (CH), 127.3 (C_q), 121.1 (CH), 113.8 (CH), 113.4 (CH), 56.5 (C_q), 55.3 (CH_3), 50.2 (CH), 46.1 (CH), 43.8(CH), 40.2 (CH), 39.7 (CH), 38.4 (C_q), 36.4 (CH), 35.0 (CH_2), 34.9 (CH_2), 30.3 (CH), 27.0 (CH_3), 26.3 (CH_2), 24.9 (CH_2), 24.8(CH_3), 22.4 (CH_3) ppm;

IR (thin film): ν_{max} = 2919, 2870, 1772, 1692, 1610 cm^{-1};

LRMS (70 eV, EI): m/z (%): 447 (7, $[M]^{+\bullet}$), 299 (22), 121 (100);

HRMS (70 eV, EI): m/z calc. for $C_{28}H_{33}NO_4$ $[M]^{+\bullet}$:447.2410; found 447.2414.

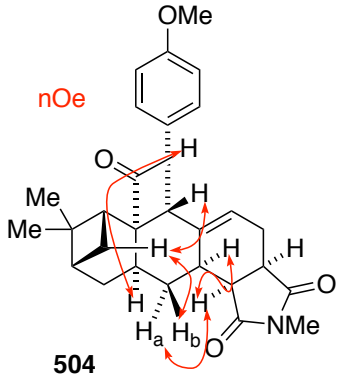

504

Bisadduct 507

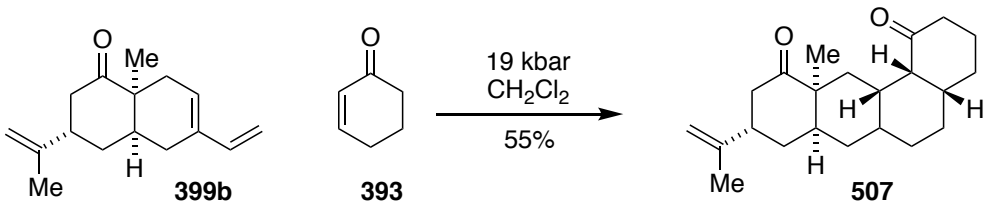

Semicyclic diene **399b** (80 mg, 0.35 mmol, 1.0 mol. equiv.) and 2-cyclohexen-1-one (**393**) (168 μL, 167 mg, 1.74 mmol, 5.0 mol. equiv.) were added to a Teflon high-pressure reaction tube with CH_2Cl_2 (1.37 mL). The reaction vessel was sealed and was compressed at 19 kbar for 72 h using a PSIKA 20 kbar reactor. The solvent was then removed under reduced pressure. Regio/diastereo-selectivity was determined to be >90:10 by analysis of crude ^{1}H NMR spectra Purification by preparative thin layer chromatography (SiO_2; CH_2Cl_2) afforded tetracycle **507** as a pale yellow oil (62.1 mg, 0.190 mmol, 55%).

$[\alpha]_D$ = –94.7° (c = 1.01, $CHCl_3$);

R_f = 0.18 (10 % EtOAc in PS 40–60 °C);

^{1}H NMR (400 MHz, $CDCl_3$): δ 5.22 (br s, 1H), 4.74 (s, 1H), 4.72 (s, 1H), 2.95 (t, *J* = 4.8 Hz, 1H), 2.66 (tt, *J* = 4.3, 12.7 Hz, 1H), 2.52 (t, *J* = 13.8 Hz, 1H), 2.45-2.31 (m, 3H), 2.27-2.10 (m, 3H), 2.08-2.00 (m, 3H), 1.99-1.82 (m, 6H), 1.79-1.67 (m, 1H), 1.71 (s, 3H), 1.66-1.59 (m, 1H), 1.54 (dd, *J* = 2.2, 13.8 Hz, 1H), 1.21 (s, 3H) ppm;

^{13}C NMR (100 MHz, $CDCl_3$): δ 215.8 (C_q), 212.2 (C_q), 147.7 (C_q), 136.8 (C_q), 117.6 (CH), 109.7 (CH_2), 52.8 (CH), 49.0 (C_q), 43.9 (CH_2), 43.6 (CH), 42.6 (CH_2), 40.5 (CH), 40.1 (CH), 37.0 (CH_2), 35.3 (CH_2), 35.2 (CH), 30.9 (CH_2), 30.1 (CH_2), 27.4 (CH_3), 26.3 (CH_2), 25.7 (CH_2), 20.5 (CH_3) ppm;

IR (thin film): ν_{max} = 2959, 2912, 1704, 1645 cm^{-1};

LRMS (70 eV, EI): m/z (%): 326 (100, $[M]^{+\bullet}$), 176 (21), 151 (41);

HRMS (70 eV, EI): m/z calc. for $C_{22}H_{30}O_2$ $[M]^{+\bullet}$:326.2246; found 326.2249.

Bisadduct 508

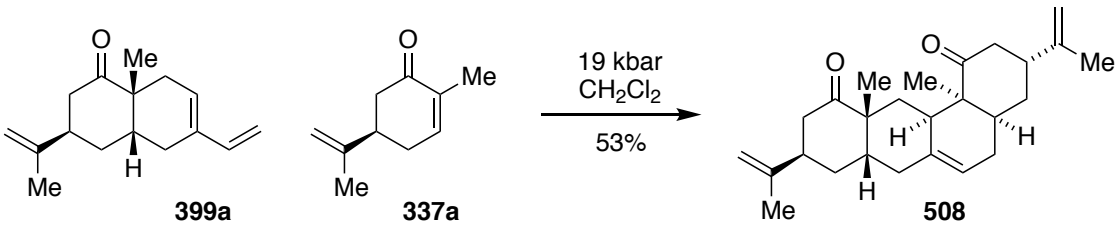

399a **337a** **508**

Semicyclic diene **399a** (23 mg, 0.099 mmol, 1.0 mol. equiv.) and (*R*)-(–)-carvone (**337a**) (78 μL, 75 mg, 0.50 mmol, 5.0 mol. equiv.) were added to a Teflon high-pressure reaction tube with CH_2Cl_2 (800 μL). The reaction vessel was sealed and was compressed at 19 kbar for 120 h using a PSIKA 20 kbar reactor. The solvent was then removed under reduced pressure. Regio/diastereo-selectivity was determined to be >95:5 by analysis of crude ^{1}H NMR spectra Purification by flash column chromatography (SiO_2; 4 % EtOAc in PS 40–60 °C) afforded tetracycle **508** as a clear colourless oil (20.3 mg, 0.0533 mmol, 53%).

$[\alpha]_D$ = +86.24 ° (c = 1.17, $CHCl_3$);

R_f = 0.23 (5 % EtOAc in PS 40–60 °C);

^{1}H NMR (400 MHz, $CDCl_3$): δ 5.27 (s, 1H), 4.82-4.72 (m, 4H), 2.80-2.63 (m, 3H), 2.55 (t, *J* = 13.8 Hz, 1H), 2.30-2.22 (m, 1H), 2.22-2.08 (m, 5H), 2.08-1.99 (m, 4H), 1.99-1.88 (m, 2H), 1.85-1.77 (m, 1H), 1.75 (s, 6H), 1.58 (d, *J* = 12.2 Hz, 2H), 1.50 (s, 3H), 1.25 (s, 3H) ppm;

^{13}C NMR (100 MHz, $CDCl_3$): δ 215.4 (C_q), 214.1 (C_q), 147.8 (C_q), 147.7 (C_q), 137.0 (C_q), 116.9(CH), 110.0 (CH_2), 109.8 (CH_2), 50.7 (C_q), 49.4 (C_q), 43.9 (CH_2), 43.8 (CH), 43.1 (CH), 42.8 (CH_2), 42.5 (CH), 42.3 (CH), 40.6 (CH), 38.0 (CH_2), 34.2 (CH_2), 31.0 (CH_2), 30.4 (CH_2), 27.6 (CH_3), 27.5 (CH_2), 23.9 (CH_3), 20.7 (CH_3), 20.6 (CH_3) ppm;

IR (thin film): ν_{max} = 2966, 2932, 1707, 1644 cm^{-1};

LRMS (70 eV, EI): m/z (%): 308 (47, $[M]^{+\bullet}$), 151 (61), 109 (100);

HRMS (70 eV, EI): m/z calc. for $C_{26}H_{36}O_2$ $[M]^{+\bullet}$:380.2715; found 380.2714.

Bisadduct 511[vi]

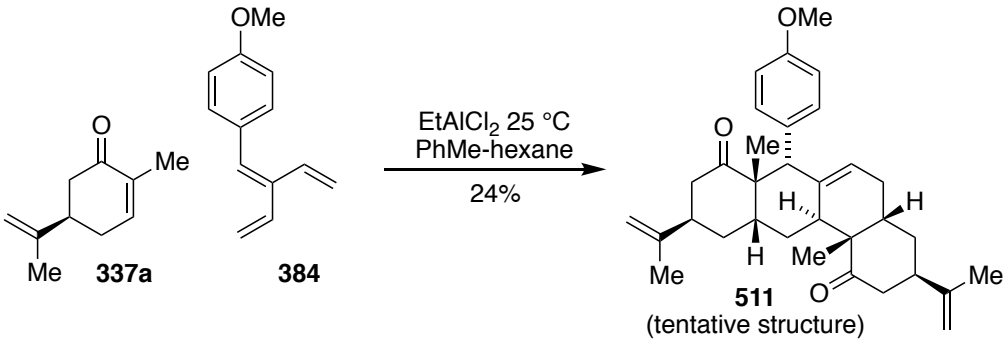

(*R*)-(–)-carvone (**337a**) (337 µL, 2.15 mmol, 4.0 mol. equiv.) in PhMe (0.50 mL) was treated with $EtAlCl_2$ (1.0 M solution in hexane, 1.18 mL, 1.18 mmol, 2.2 mol. equiv.) at 25 °C. The resulting solution was stirred for 20 min, before the addition of substituted [3]dendralene **384** (104 mg, 0.558 mmol, 1.0 mol. equiv.) in PhMe (0.50 mL). The resulting solution was stirred at 25 °C for 26 h, before the addition of ice-cold sat. aq. $NaHCO_3$ solution (1.0 mL). The organic layer was separated and the aqueous layer was extracted with Et_2O (3 x 10 mL). The combined organic layers were dried ($MgSO_4$), filtered and concentrated under reduced pressure. Regio/diastereo-selectivity was determined to be >95:5 by analysis of crude ^{1}H NMR spectra. Purification by flash column chromatography (SiO_2; 10% EtOAc in PS 40–60 °C; 60% dichloromethane in PS 40–60 °C) afforded bisadduct **511** as a white foam (62.9 mg, 0.129 mmol, 24%);

$[\alpha]_D$ = –10.49 ° (c = 0.963, $CHCl_3$);

R_f = 0.48 (20 % EtOAc in PS 40–60 °C);

^{1}H NMR (400 MHz, $CDCl_3$): δ 7.42 (d, *J* = 8.3 Hz, 2H), 6.83 (d, *J* = 8.6 Hz, 2H), 5.14 (br s, 1H), 4.86 (s, 1H), 4.77 (s, 1H), 4.67 (s, 1H), 4.64 (s, 1H), 3.80 (s, 3H), 3.16 (br s, 1H), 2.82-2.55 (m, 4H), 2.49-2.32 (m, 2H), 2.27-2.15 (m, 2H), 2.13-1.90 (m, 3H), 1.89-1.75 (m, 4H), 1.72 (s, 3H), 1.69 (s, 3H), 1.66-1.57 (m, 1H), 1.19-1.10 (m, 1H), 1.03 (s, 3H), 0.96 (s, 3H) ppm;

^{13}C NMR (100 MHz, $CDCl_3$): δ 215.2 (C_q), 214.6 (C_q), 158.2 (C_q), 147.3 (C_q), 147.3 (C_q), 136.4 (C_q), 133.2 (C_q), 133.0 (CH), 120.3 (CH), 113.4 (CH), 112.5 (CH_2), 110.6 (CH_2), 57.6 (CH), 55.3 (CH_3), 51.6 (C_q), 51.4 (C_q), 44.8 (CH_2), 42.5 (CH), 41.5 (CH), 41.3 (CH_2), 41.1 (CH), 36.8 (CH), 36.0 (CH), 34.5 (CH_2), 29.9 (CH_2), 28.6 (CH_2), 27.9 (CH_2), 25.1 (CH_3), 22.5 (CH_3), 20.9 (CH_3), 15.6 (CH_3), ppm;

[vi] Reaction performed by undergraduate student Chloe Larcombe under direct instruction and guidance of the author. Purification and characterisation performed by the author.

IR (thin film): ν_{max} = 2933, 2888, 2875, 1698 cm^{-1};

LRMS (70 eV, EI): m/z (%): 487 (29, $[M+1]^{+\bullet}$), 486 (79, $[M]^{+\bullet}$), 150 (58), 121 (90), 109 (70), 84 (100);

HRMS (70 eV, EI): m/z calc. for $C_{33}H_{42}O_3$ $[M]^{+\bullet}$: 486.3134; found 486.3133.

Bisadduct 524

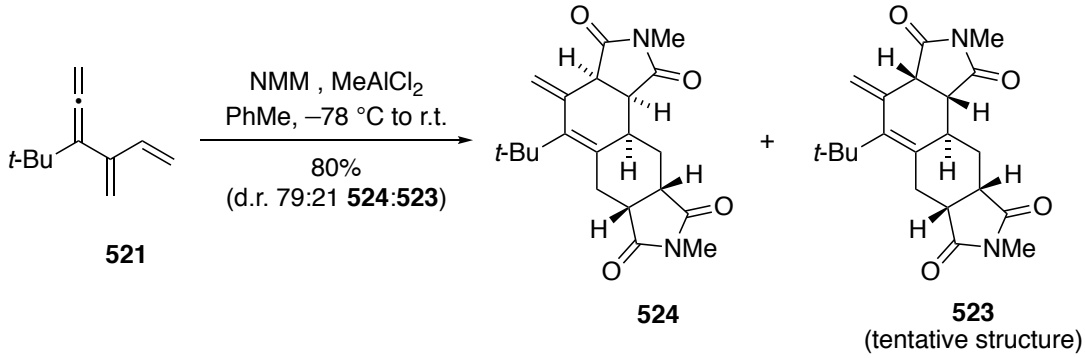

To a stirred solution of NMM (**388**) (84 mg, 0.75 mmol, 2.2 mol. equiv.) in PhMe (0.72 mL) at –78 °C was added dropwise $MeAlCl_2$ (1M in hexane, 0.47 mL, 0.47 mmol, 1.4 mol. equiv.). The resulting solution was stirred at –78 °C for 30 min, then allenic dendralene **521** (50 mg, 0.34 mmol, 1.0 mol. equiv.) in PhMe (0.36 mL) was added dropwise. The reaction was stirred at –78 °C for 30 min, then allowed to warm to r.t. over 20 min. The reaction mixture was then cooled to –78 °C, quenched with sat. aq. NH_4Cl solution (1 mL) and allowed to warm to r.t.. The mixture was diluted with H_2O (20 mL) and was extracted with Et_2O (3 x 20 mL). The combined organic layers were dried ($MgSO_4$) and concentrated under reduced pressure. Purification by flash column chromatography (SiO_2; 40% EtOAc in petrol 40–60°) afforded the bisadduct as a white solid (0.100g, 0.270 mmol, 80%) as a 79:21 mixture of diastereomers **524** and **523**. Recrystallisation from CH_2Cl_2/petrol 40–60° afforded colourless needles of major isomer **524** suitable for single crystal X-ray analysis.

m.p. = 243-245 °C (CH_2Cl_2/petrol 40–60°);

R_f = 0.56 (80% EtOAc in PS 40–60°);

^{1}H NMR ($CDCl_3$, 400 MHz): δ 5.15 (s, 1H), 4.83 (s, 1H), 3.50 (d, J = 8.2 Hz, 1H), 3.31 (dd, *J* = 15.0, 2.0 Hz, 1H), 3.23 – 3.10 (m, 2H), 2.96 (dd, *J* = 8.3, 4.5 Hz, 1H), 2.92 (s, 3H), 2.90 (s, 3H), 2.87 – 2.76 (m, 1H), 2.39 – 2.24 (m, 2H), 1.93 – 1.84 (m, 1H), 1.10 (s, 9H).ppm;

^{13}C NMR ($CDCl_3$, 101 MHz): δ 180.1 (CO), 179.3 (CO), 178.0 (CO), 176.4 (CO), 144.4 (C_q), 139.4 (C_q), 131.7 (C_q), 115.7 (CH_2), 52.1 (CH), 43.8 (CH), 39.3 (CH), 38.8 (CH), 35.5 (CH), 33.9 (C_q), 31.8 (3 x CH_3), 26.6 (CH_2), 25.0 (CH_3), 24.9 (CH_3), 23.9 (CH_2) ppm;

IR (neat): ν_{max} = 2949, 1774, 1690 cm^{-1};

LRMS (70 eV, EI): m/z (%): 370 (100, $[M]^{+\bullet}$), 355 (53), 270 (58), 143 (40);

HRMS (70 eV, EI): m/z calc. for $C_{21}H_{26}N_2O_4$ $[M]^{+\bullet}$: 370.1893; found 370.1886.

Bisadduct 523

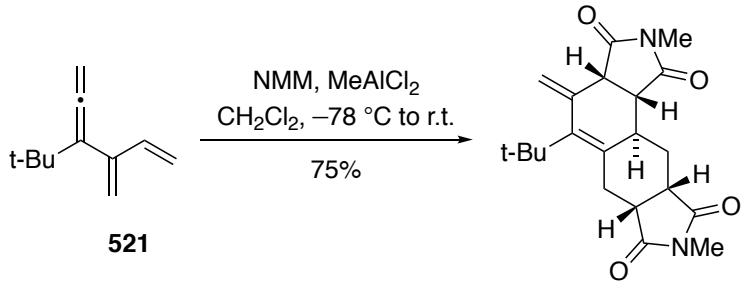

521 **523**
(tentative structure)

To a stirred solution of NMM (**388**) (117 mg, 1.06 mmol, 3.13 mol. equiv.) in CH_2Cl_2 (1.1 mL) at –78 °C was added dropwise $MeAlCl_2$ (1M in hexane, 3.16 mL, 3.16 mmol, 9.38 mol. equiv.). The resulting solution was stirred at –78 °C for 30 min, then allenic dendralene **521** (50 mg, 0.34 mmol, 1.0 mol. equiv.) in CH_2Cl_2 (0.53 mL) was added dropwise. The reaction was stirred at –78 °C for 2 h, then allowed to warm to r.t. over 20 min. The reaction mixture was then cooled to –78 °C, quenched with sat. aq. NH_4Cl solution (1 mL) and allowed to warm to r.t.. The mixture was diluted with water (20 mL) and was extracted with CH_2Cl_2 (3 x 20 mL). The combined organic layers were dried ($MgSO_4$) and concentrated under reduced pressure. Regio/diastereo-selectivity was determined to be >95:5 by analysis of crude ^{1}H NMR spectra Purification by flash column chromatography (SiO_2; 40% EtOAc in petrol 40–60°) afforded bisadduct **523** as a white solid (0.0939 g, 0.253 mmol, 75%).

m.p. = 80.8–86.6 °C (EtOAc);

R_f = (80% EtOAc in PS 40–60°) = 0.56;

^{1}H NMR ($CDCl_3$, 400 MHz): δ 5.25 (s, 1H), 4.94 (s, 1H), 3.58 (d, J = 8.2 Hz, 1H), 3.25 (dd, J = 14.6, 5.7 Hz, 1H), 3.03 (dd, J = 8.3, 4.7 Hz, 1H), 2.99 (s, 3H), 2.87 (s, 3H), 2.82 – 2.72 (m, 2H), 2.52 – 2.38 (m, 1H), 2.32 – 2.23 (m, 1H), 2.17 – 2.08 (m, 1H), 2.08 – 1.95 (m, 1H), 1.13 (s, 9H) ppm;

^{13}C NMR ($CDCl_3$, 101 MHz): δ 178.9 (CO x 2; coincident), 177.5 (CO), 176.4 (CO), 143.2 (C_q), 139.5 (C_q), 133.0 (C_q), 116.0 (CH_2), 52.3 (CH), 43.8 (CH), 39.5 (CH), 39.1 (CH), 38.4 (CH), 33.6 (C_q), 31.6 (CH_3), 26.6 (CH_2), 25.0 (CH_2), 24.9 (CH_3), 24.8 (CH_3) ppm;

IR (neat): ν_{max} = 2951, 1773, 1690 cm^{-1};

LRMS (70 eV, EI): m/z (%): 370 (100, $[M]^{+\bullet}$), 355 (35), 270 (71), 143 (56);

HRMS (70 eV, EI): m/z calc. for $C_{21}H_{26}N_2O_4$ $[M]^{+\bullet}$: 370.1893; found 370.1891.

6.2.5 X-Ray Crystallography

Monoadduct 428

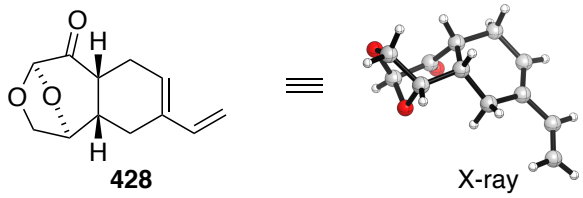

Crystal Data. $C_{12}H_{14}O_3$, M_r = 206.23, orthorhombic, $P2_12_12_1$ (No. 19), a = 5.22920(10) Å, b = 12.3287(3) Å, c = 15.9196(3) Å, $\alpha = \beta = \gamma = 90^\circ$, V = 1026.32(4) Å^3, T = 150.00(10) K, Z = 4, Z' = 1, $\mu(CuK_\alpha)$ = 0.779, 2936 reflections measured, 1899 unique (R_{int} = 0.0230) which were used in all calculations. The final wR_2 was 0.0815 (all data) and R_1 was 0.0325 (I > 2(I)).

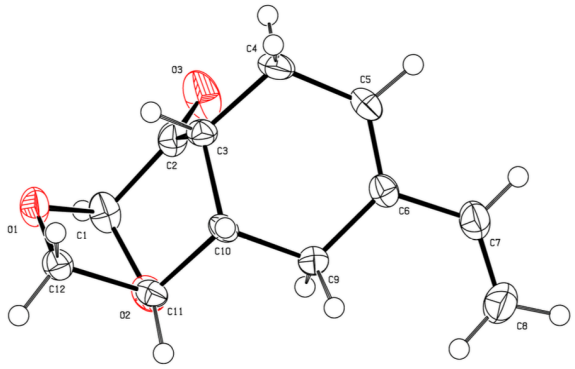

Figure 6.1 Anisotropic displacement ellipsoid plot of monoadduct **428**. Ellipsoids exhibit 50% probability levels. Hydrogen atoms are drawn as circles with small radii.

Bisadduct 497

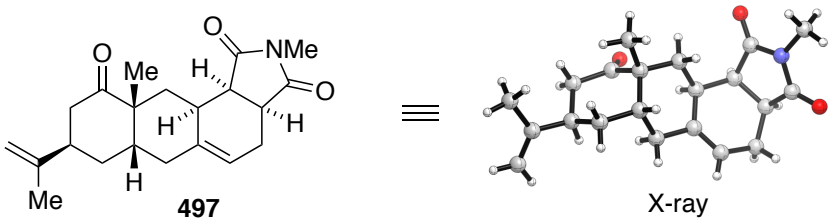

Crystal Data. $C_{21}H_{27}NO_3$, M_r = 341.43, monoclinic, $P2_1$ (No. 4), a = 9.3918(5) Å, b = 10.0409(5) Å, c = 19.2029(8) Å, β = 98.070(5)°, $\alpha = \gamma$ = 90°, V = 1792.94(15) Å^3, T = 150.01(10) K, Z = 4, Z' = 2, μ(MoK_α) = 0.084, 20439 reflections measured, 10023 unique (R_{int} = 0.0343) which were used in all calculations. The final wR_2 was 0.1207 (all data) and R_1 was 0.0568 (I > 2(I)).

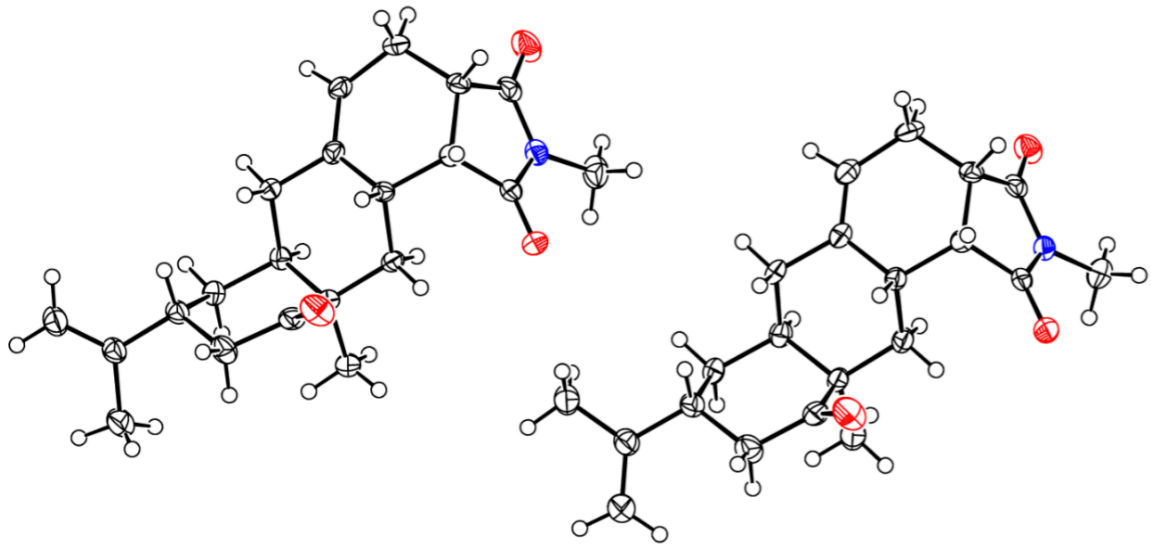

Figure 6.2 Anisotropic displacement ellipsoid plot of bisadduct **497**. Ellipsoids exhibit 50% probability levels. Hydrogen atoms are drawn as circles with small radii.

Bisadduct 498

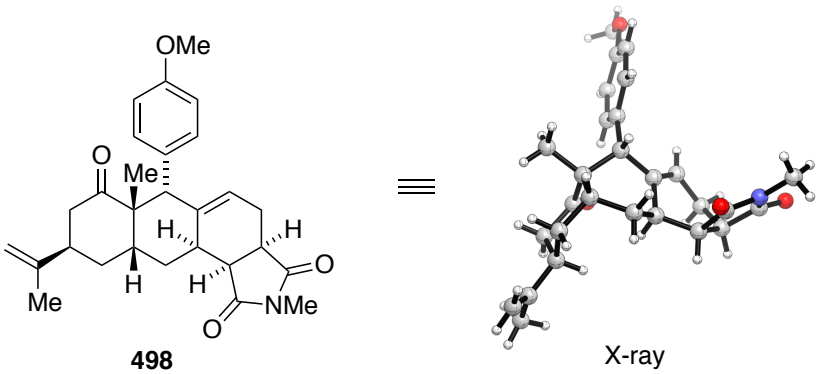

Crystal Data. $C_{28}H_{33}NO_4$, M_r = 447.55, orthorhombic, $P2_12_12_1$ (No. 19), a = 6.44720(10) Å, b = 12.7774(2) Å, c = 28.1843(4) Å, $\alpha = \beta = \gamma = 90^{\circ}$, V = 2321.78(6) Å^3, T = 150.01(10) K, Z = 4, Z' = 1, $\mu(CuK_\alpha)$ = 0.677, 13340 reflections measured, 4677 unique (R_{int} = 0.0311) which were used in all calculations. The final wR_2 was 0.0843 (all data) and R_1 was 0.0337 (I > 2(I)).

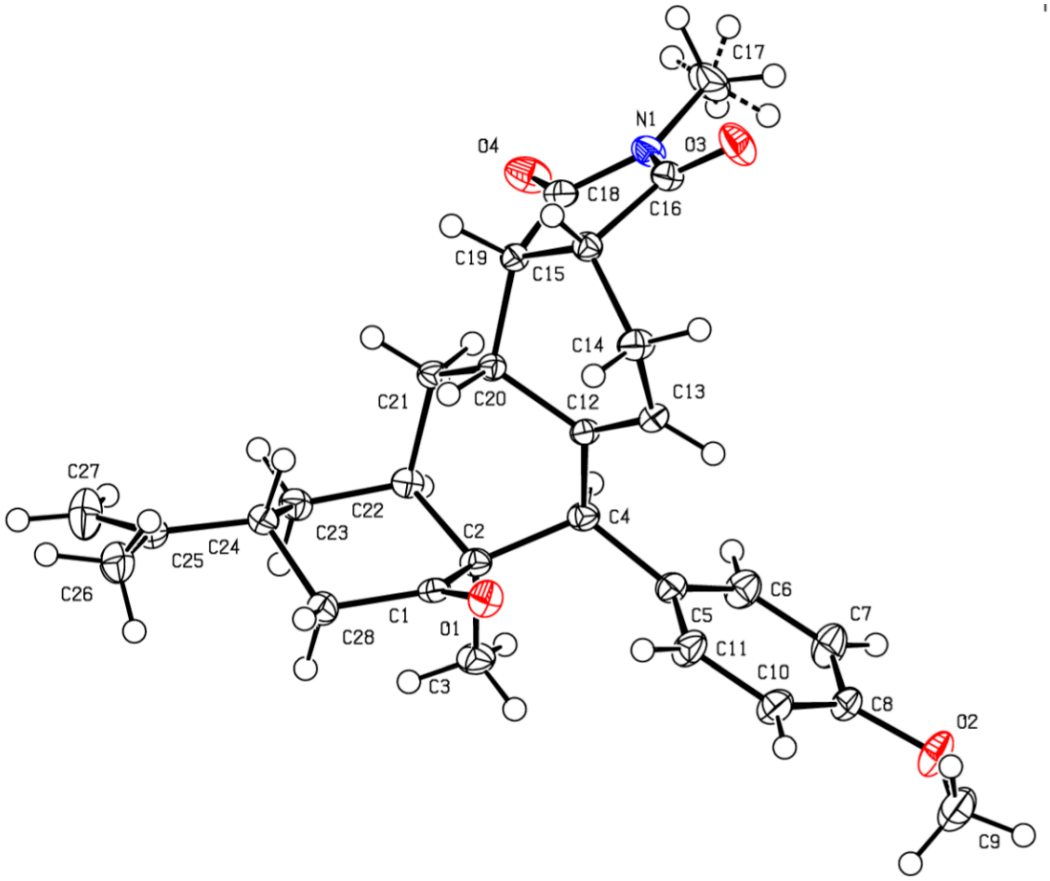

Figure 6.3 Anisotropic displacement ellipsoid plot of bisadduct **498**. Ellipsoids exhibit 50% probability levels. Hydrogen atoms are drawn as circles with small radii.

Bisadduct 524

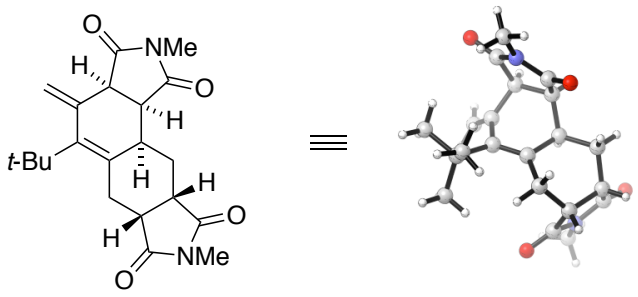

524 X-ray

Crystal Data. $C_{21}H_{26}N_2O_4$, M_r = 370.44, monoclinic, $P2_1/c$ (No. 14), a = 13.95213(8) Å, b = 16.45917(10) Å, c = 8.29699(4) Å, β = 92.2977(5)˚, $\alpha = \gamma$ = 90˚, V = 1903.79(2) Å^3, T = 150.00(10) K, Z = 4, Z' = 1, μ(CuK$_\alpha$) = 0.73, 37224 reflections measured, 3618 unique (R_{int} = 0.040) which were used in all calculations. The final wR_2 was 0.091 (all data) and R_1 was 0.035 (I > 2(I)).

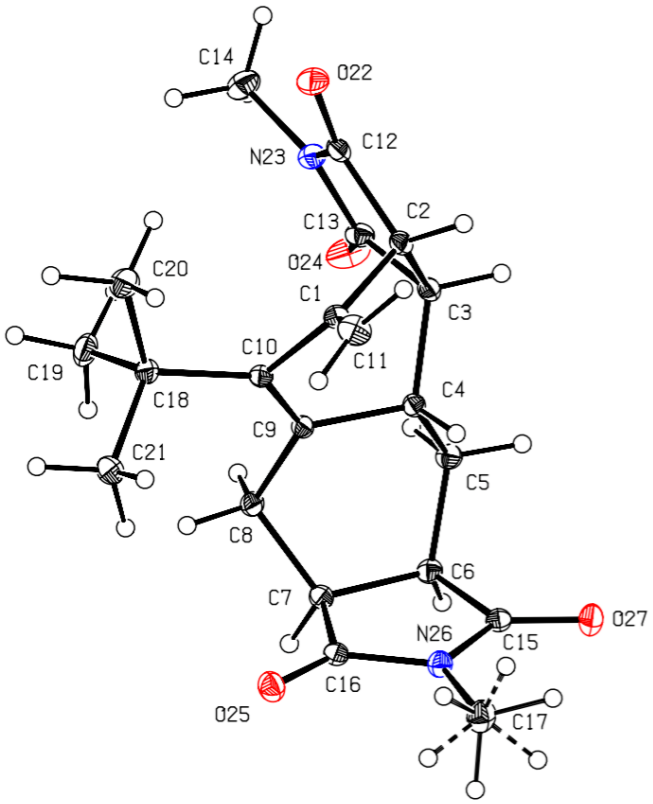

Figure 6.4 Anisotropic displacement ellipsoid plot of bisadduct **524**. Ellipsoids exhibit 30% probability levels. Hydrogen atoms are drawn as circles with small radii.

6.2.6 Conformational Analysis

The in-plane *s-trans* diene (C=C-C=C dihedral 180° +/- 2°) is the most commonly encountered conformation of the 1,3-butadiene group. The *s-cis* diene (i.e. the in-plane conformation) is not a local energy minimum structure but the skew *cisoid* diene (C=C-C=C dihedral ca 35-46°) is located in each case as a local energy minimum structure within 15 kJ/mol of the *s-trans* conformer. The *s-trans*/skew *cisoid* energy difference in the parent 1-vinylcyclohexene was calculated to be 11.16 kJ/mol, and exhibits a C=C-C=C dihedral of 38.7°.

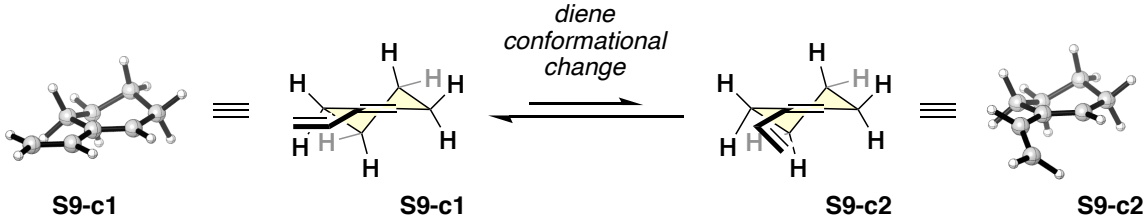

Figure 6.5 Calculated lowest energy *s-trans* (**S9-c1**) and *cisoid* (**S9-c2**) conformations of 1-vinylcyclohexene

6.2.7 ^{1}H NMR and ^{13}C NMR Spectra

^{1}H NMR and ^{13}C NMR spectra are provided on following pages.

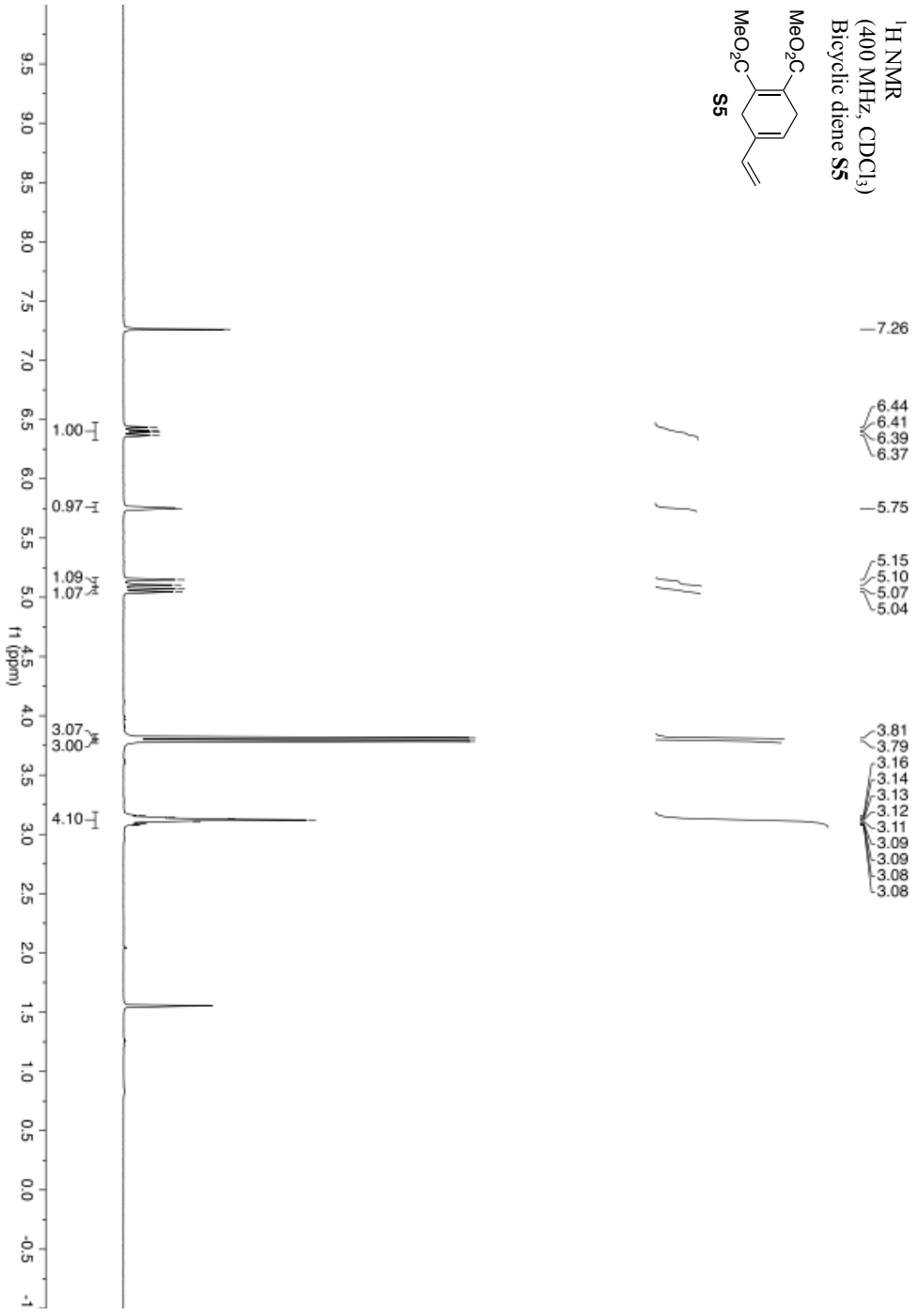
^{1}H NMR
(400 MHz, $CDCl_3$)
Bicyclic diene **S5**
MeO_2C
MeO_2C
S5
7.26
6.44
6.41
6.39
6.37
5.75
5.15
5.10
5.07
5.04
3.81
3.79
3.16
3.14
3.13
3.12
3.11
3.09
3.09
3.08
3.08
1.00
0.97
1.09
1.07
3.07
3.00
4.10
f1 (ppm)

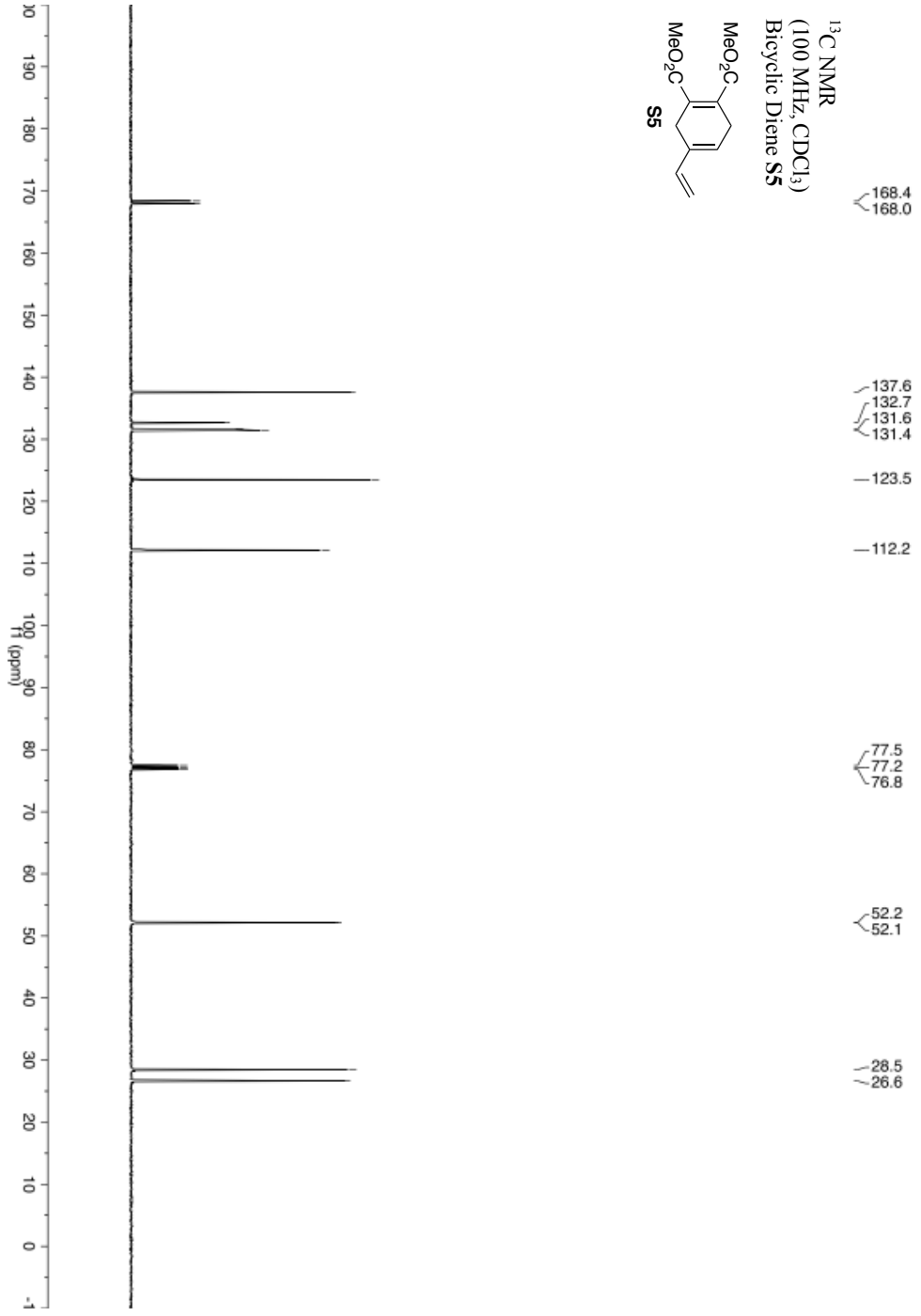
^{13}C NMR
(100 MHz, $CDCl_3$)
Bicyclic Diene **S5**
MeO_2C
MeO_2C
S5
168.4
168.0
137.6
132.7
131.6
131.4
123.5
112.2
77.5
77.2
76.8
52.2
52.1
28.5
26.6
f1 (ppm)

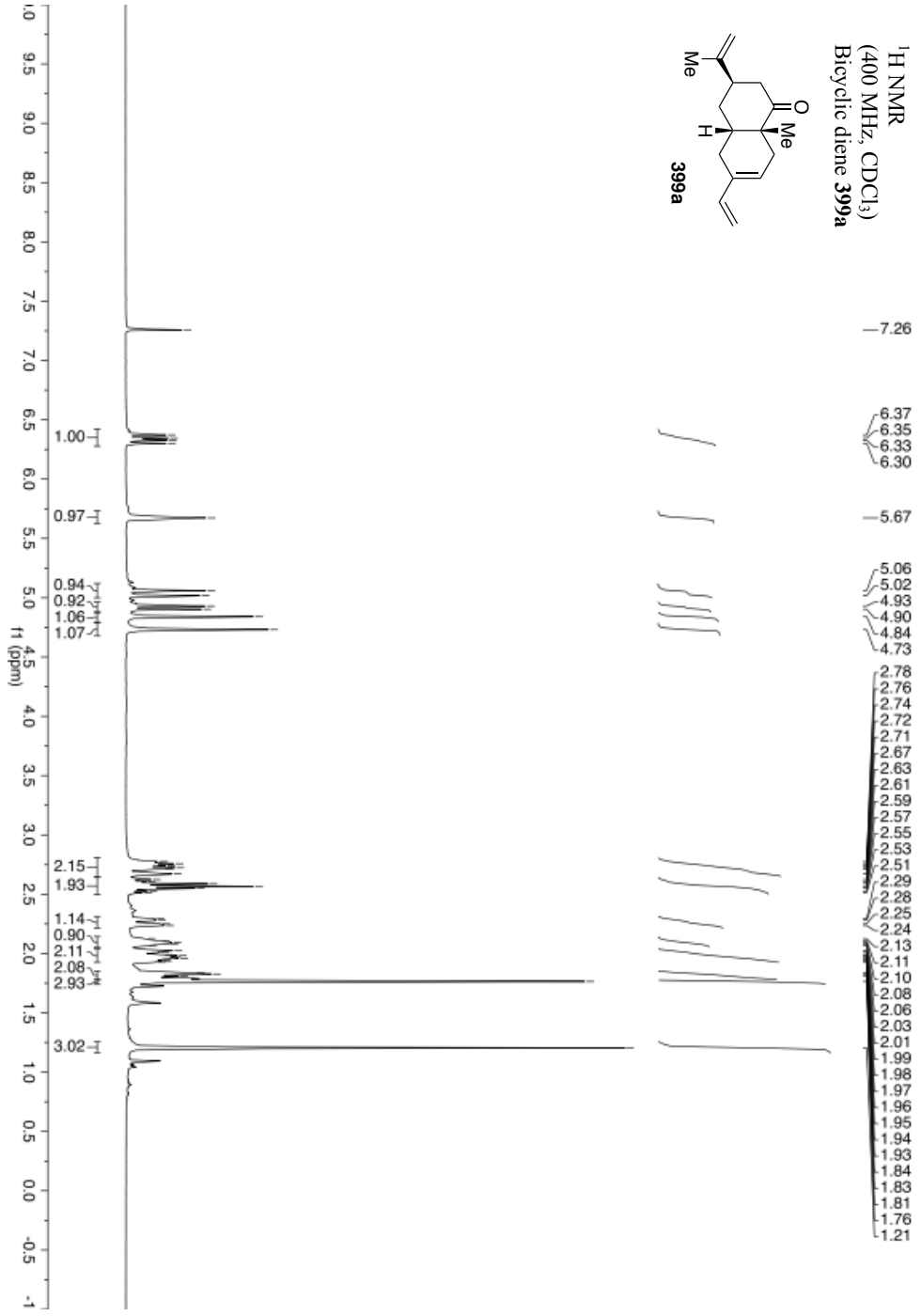
^{1}H NMR
(400 MHz, $CDCl_3$)
Bicyclic diene **399a**
Me
O
Me
H
399a
7.26
6.37
6.35
6.33
6.30
5.67
5.06
5.02
4.93
4.90
4.84
4.73
2.78
2.76
2.74
2.72
2.71
2.67
2.63
2.61
2.59
2.57
2.55
2.53
2.51
2.29
2.28
2.25
2.24
2.13
2.11
2.10
2.08
2.06
2.03
2.01
1.99
1.98
1.97
1.96
1.95
1.94
1.93
1.84
1.83
1.81
1.76
1.21
1.00
0.97
0.94
0.92
1.06
1.07
2.15
1.93
1.14
0.90
2.11
2.08
2.93
3.02
f1 (ppm)

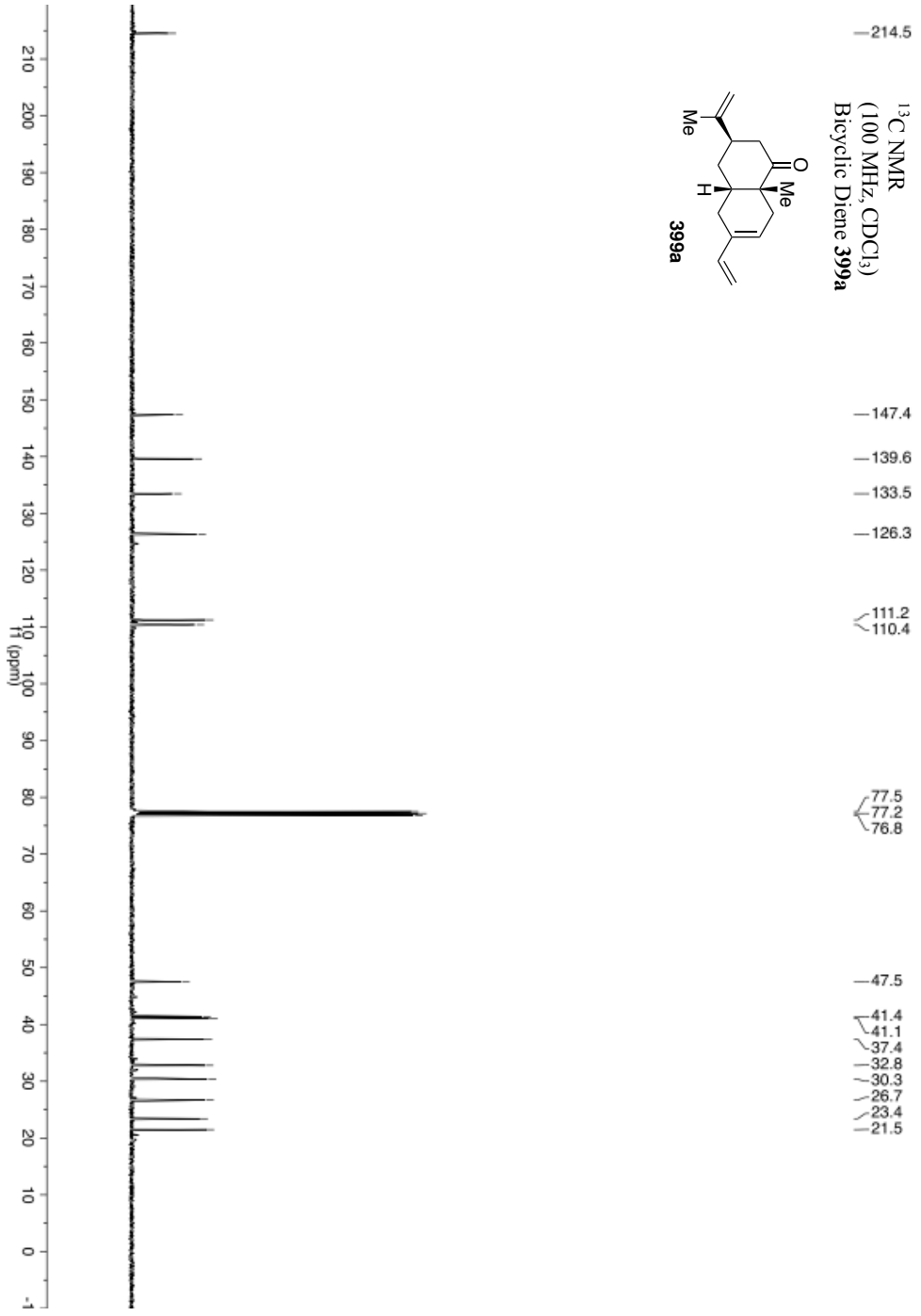
^{13}C NMR
(100 MHz, CDCl$_3$)
Bicyclic Diene **399a**
399a
Me
O
Me
H
214.5
147.4
139.6
133.5
126.3
111.2
110.4
77.5
77.2
76.8
47.5
41.4
41.1
37.4
32.8
30.3
26.7
23.4
21.5
f1 (ppm)

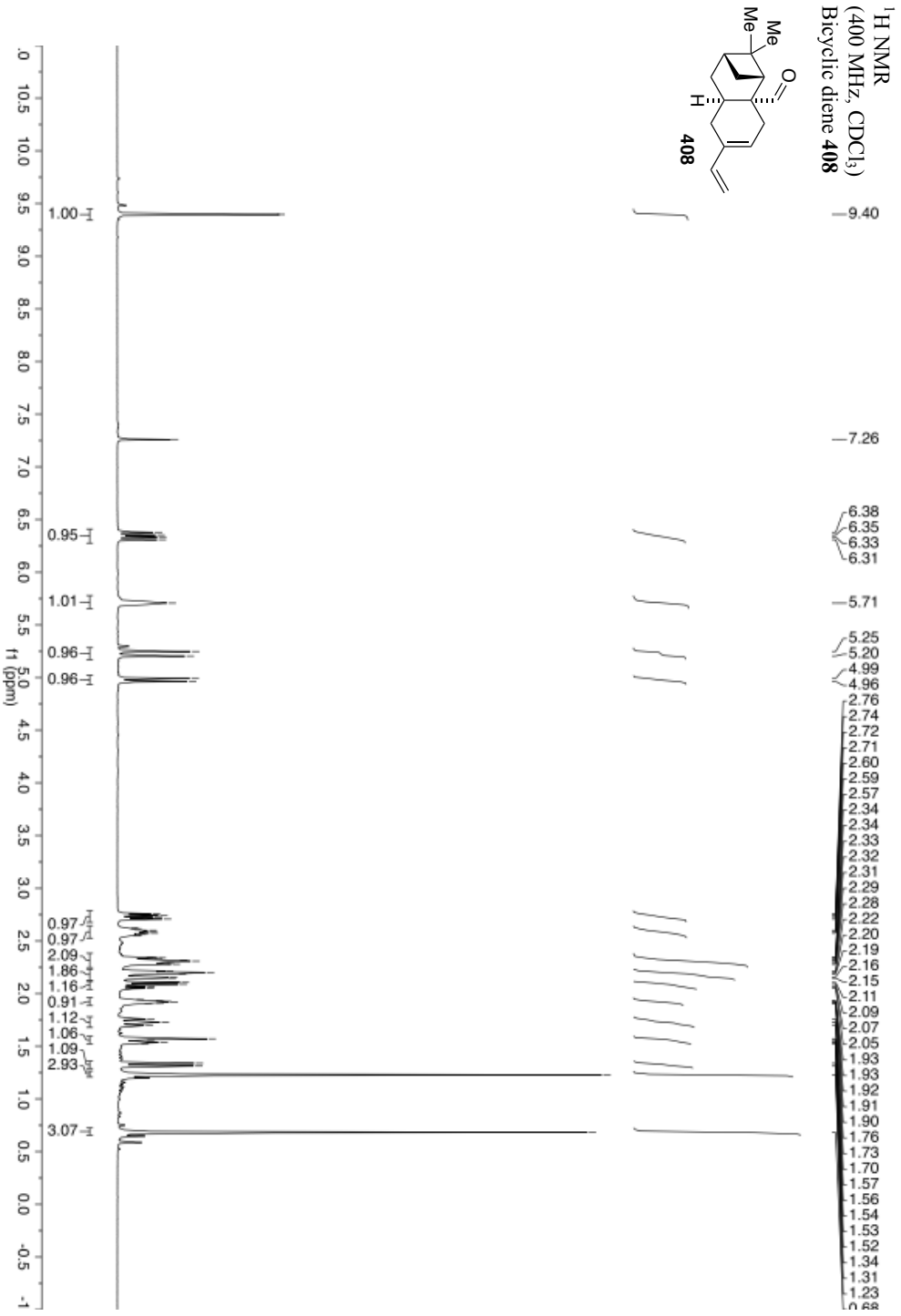
^{1}H NMR
(400 MHz, $CDCl_3$)
Bicyclic diene **408**
Me
Me
O
H
408
f1 (ppm)
1.00
0.95
1.01
0.96
0.96
0.97
0.97
2.09
1.86
1.16
0.91
1.12
1.06
1.09
2.93
3.07
9.40
7.26
6.38
6.35
6.33
6.31
5.71
5.25
5.20
4.99
4.96

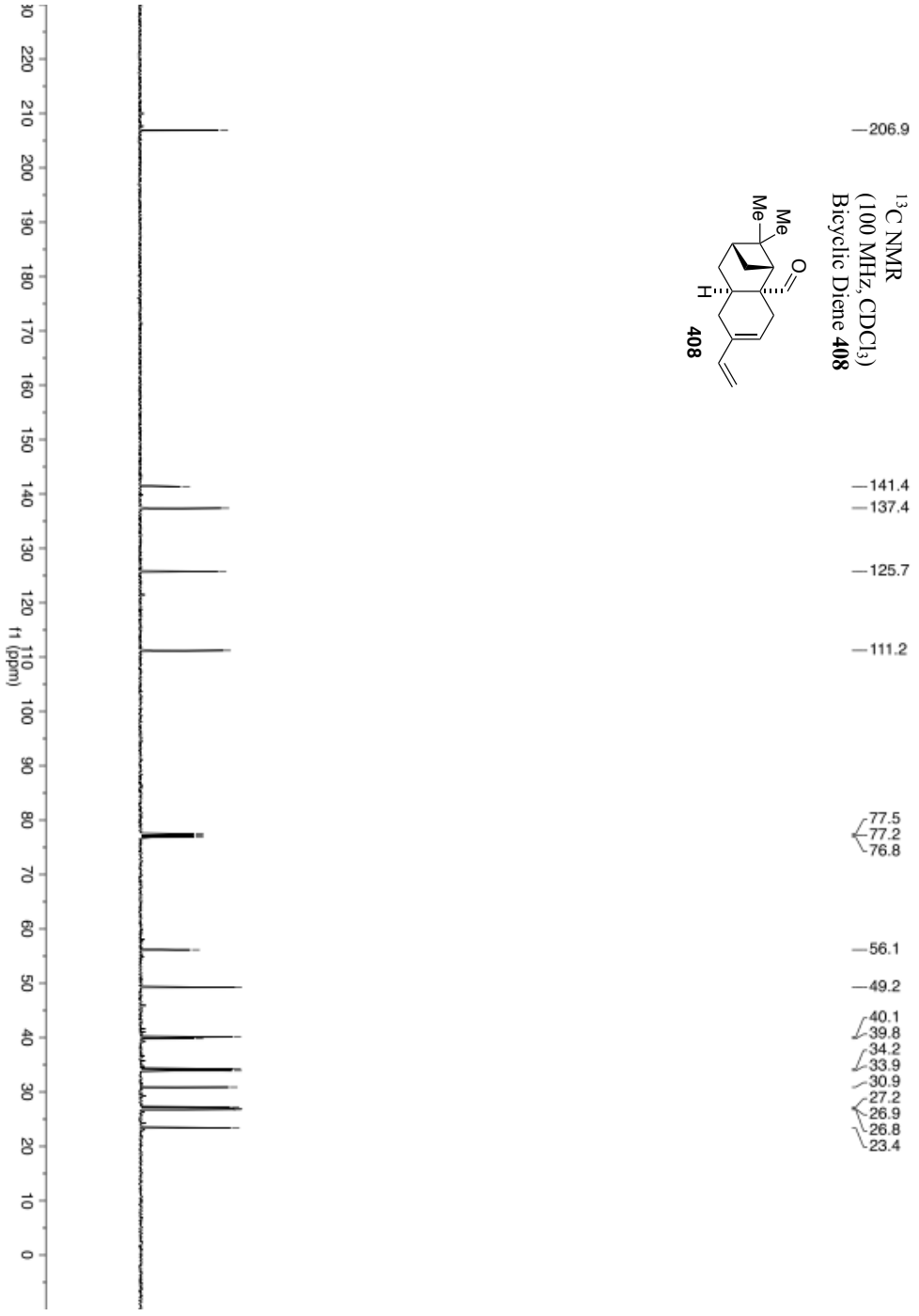
^{13}C NMR
(100 MHz, CDCl$_3$)
Bicyclic Diene **408**
Me
Me
O
H
408
206.9
141.4
137.4
125.7
111.2
77.5
77.2
76.8
56.1
49.2
40.1
39.8
34.2
33.9
30.9
27.2
26.9
26.8
23.4
f1 (ppm)

^{1}H NMR
(400 MHz, $CDCl_3$)
Tricyclic diene **416a**

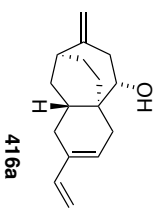

416a

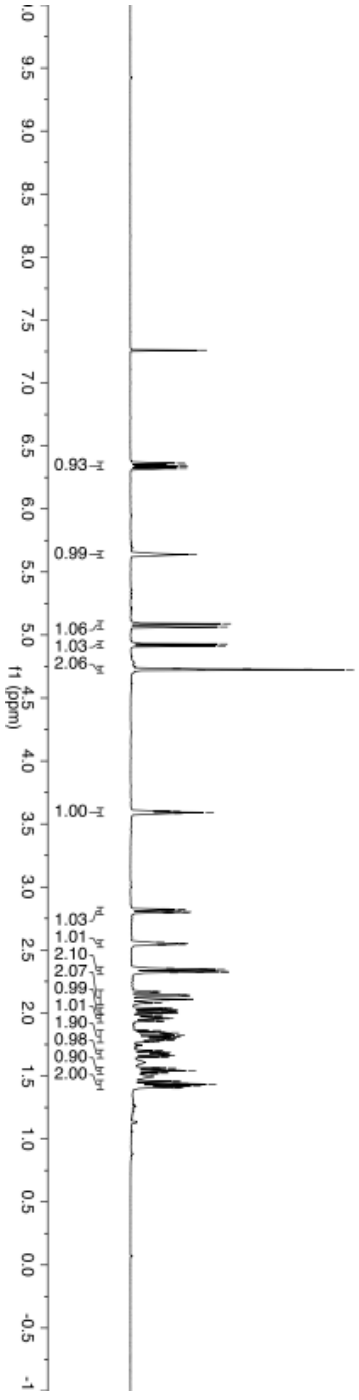

^{13}C NMR
(100 MHz, $CDCl_3$)
Tricyclic Diene **416a**

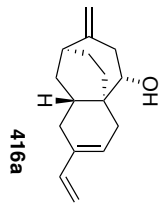

416a

151.8
139.3
135.8
127.6
110.1
109.8
78.7
77.5
77.2
76.8
42.1
38.8
38.6
36.5
34.2
32.9
31.7
26.3
19.9

f1 (ppm)

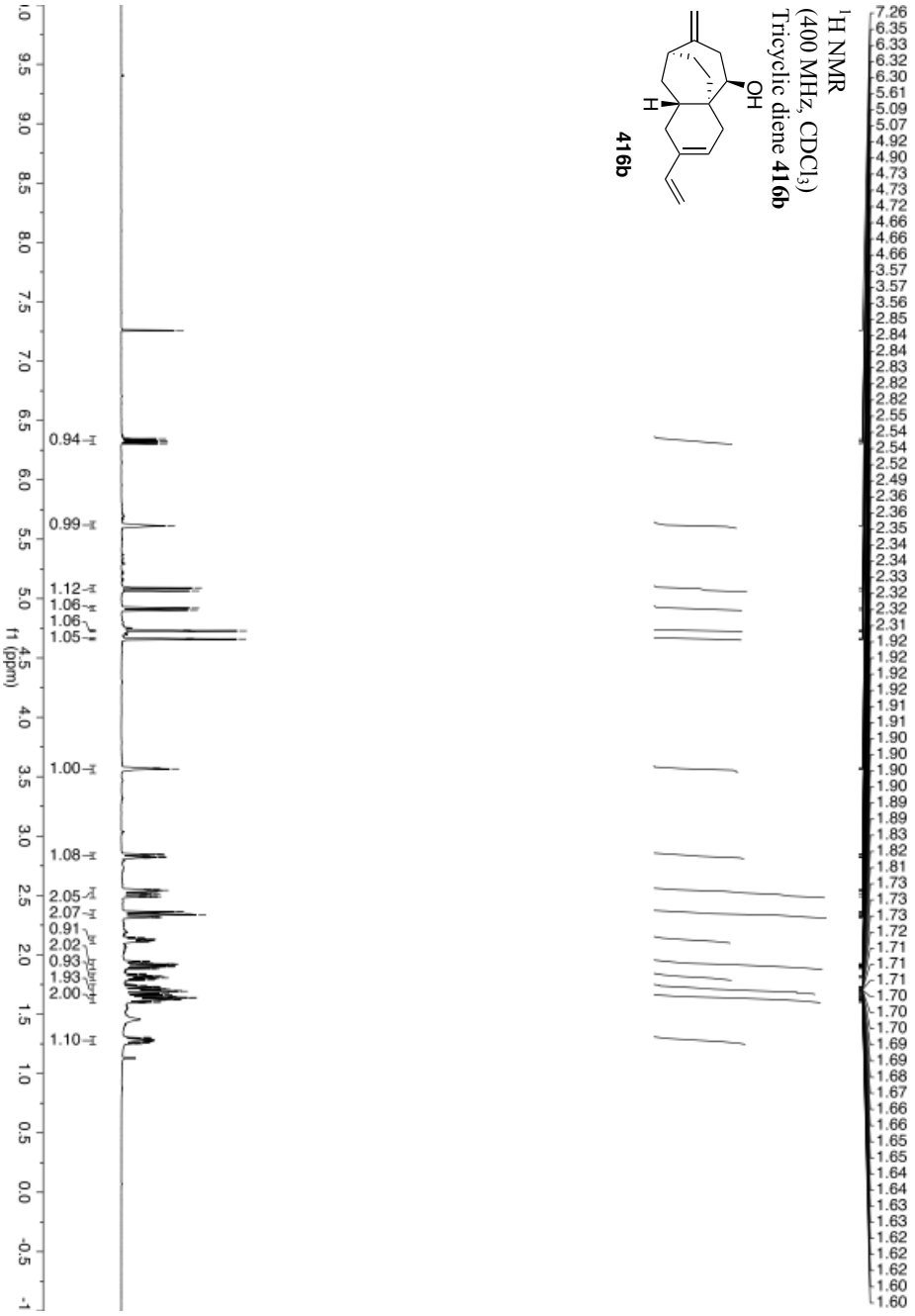
^{1}H NMR
(400 MHz, $CDCl_3$)
Tricyclic diene **416b**
OH
H
416b
f1 (ppm)
0.94
0.99
1.12
1.06
1.06
1.05
1.00
1.08
2.05
2.07
0.91
2.02
0.93
1.93
2.00
1.10

^{13}C NMR
(100 MHz, $CDCl_3$)
Tricyclic Diene **416b**

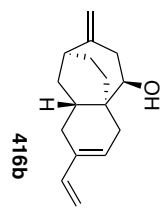

416b

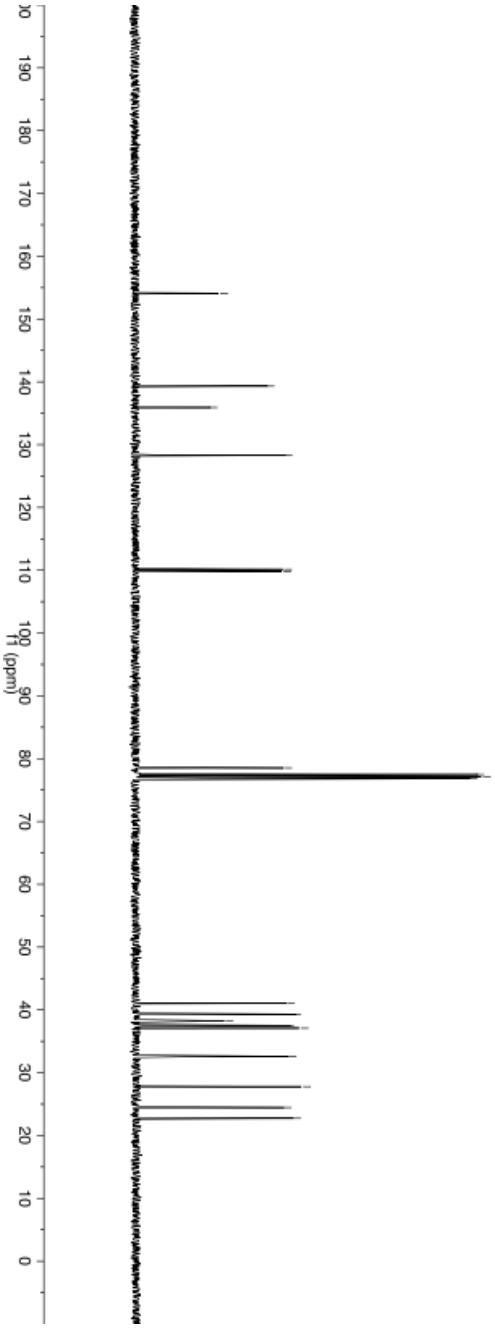

154.1
139.3
135.9
128.3
110.1
109.8
78.5
77.5
77.2
76.8
41.1
39.3
38.3
37.5
37.1
32.6
27.8
24.5
22.7

^{1}H NMR
(400 MHz, C_6D_6)
Bicyclic diene **428**

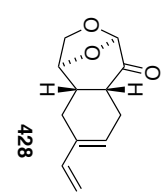

428

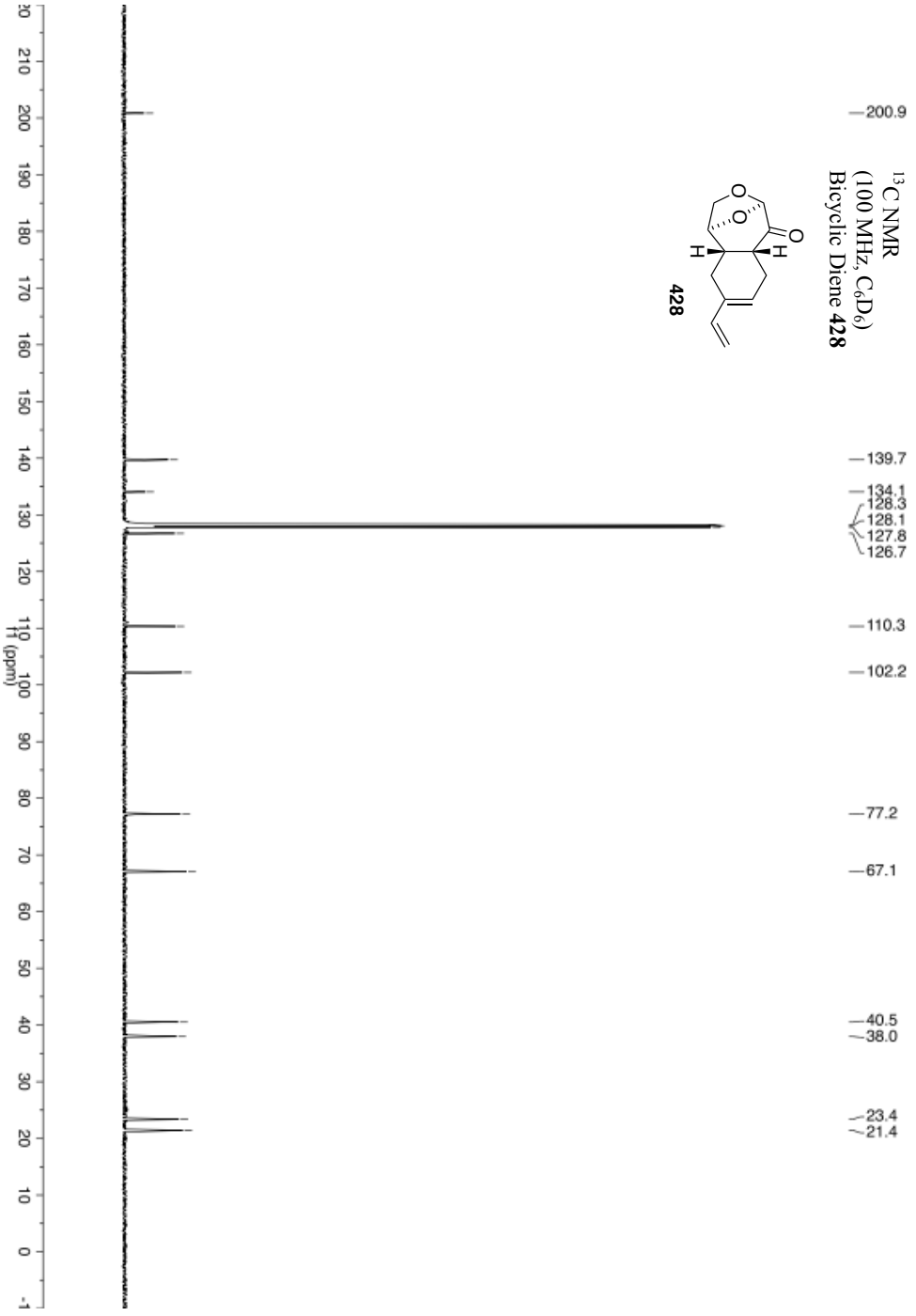
^{13}C NMR
(100 MHz, C_6D_6)
Bicyclic Diene **428**
428
200.9
139.7
134.1
128.3
128.1
127.8
126.7
110.3
102.2
77.2
67.1
40.5
38.0
23.4
21.4
f1 (ppm)

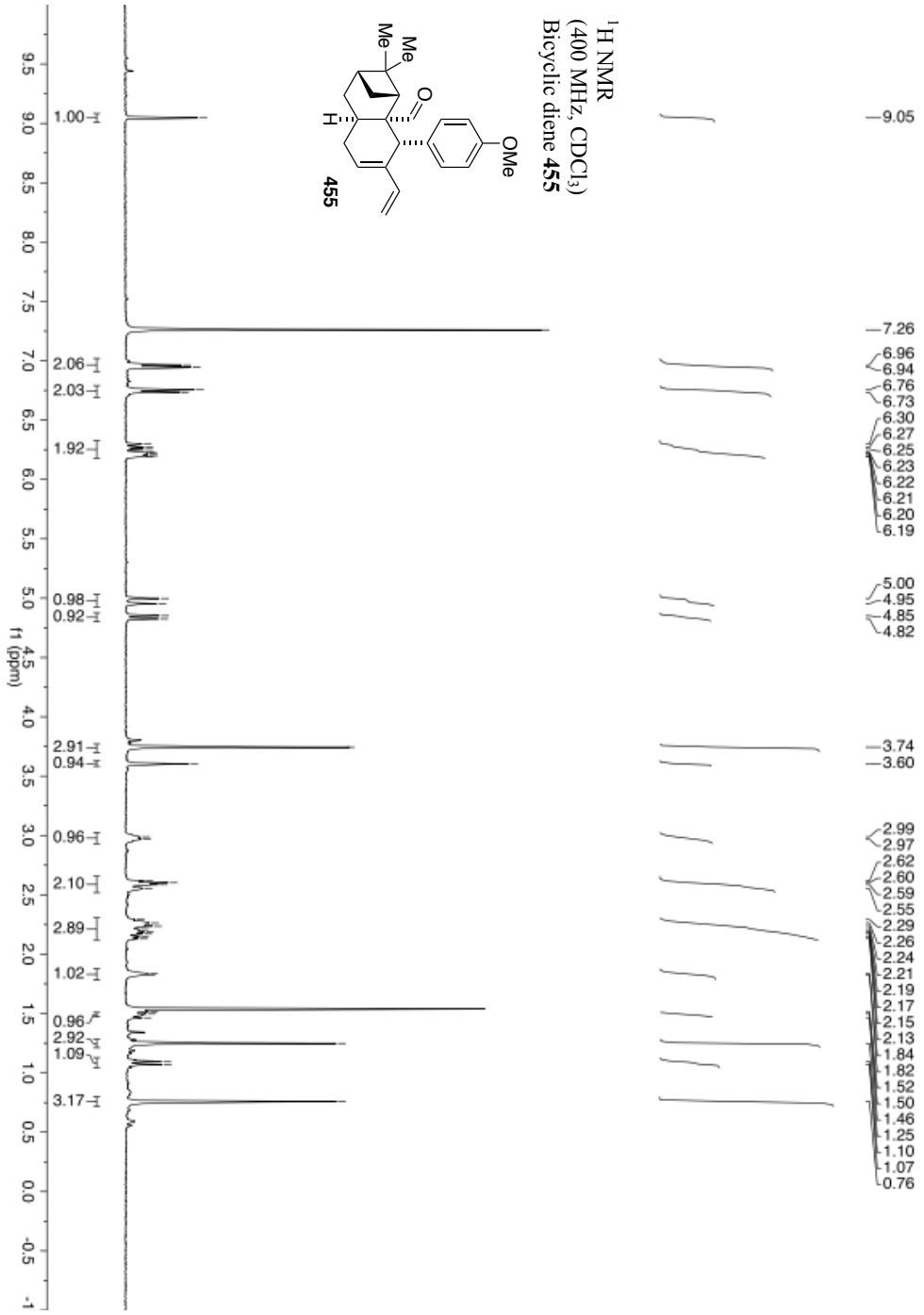
^{1}H NMR
(400 MHz, $CDCl_3$)
Bicyclic diene **455**
Me
Me
O
H
OMe
455
f1 (ppm)
1.00
2.06
2.03
1.92
0.98
0.92
2.91
0.94
0.96
2.10
2.89
1.02
0.96
2.92
1.09
3.17
9.05
7.26
6.96
6.94
6.76
6.73
6.30
6.27
6.25
6.23
6.22
6.21
6.20
6.19
5.00
4.95
4.85
4.82
3.74
3.60
2.99
2.97
2.62
2.60
2.59
2.55
2.29
2.26
2.24
2.21
2.19
2.17
2.15
2.13
1.84
1.82
1.52
1.50
1.46
1.25
1.10
1.07
0.76

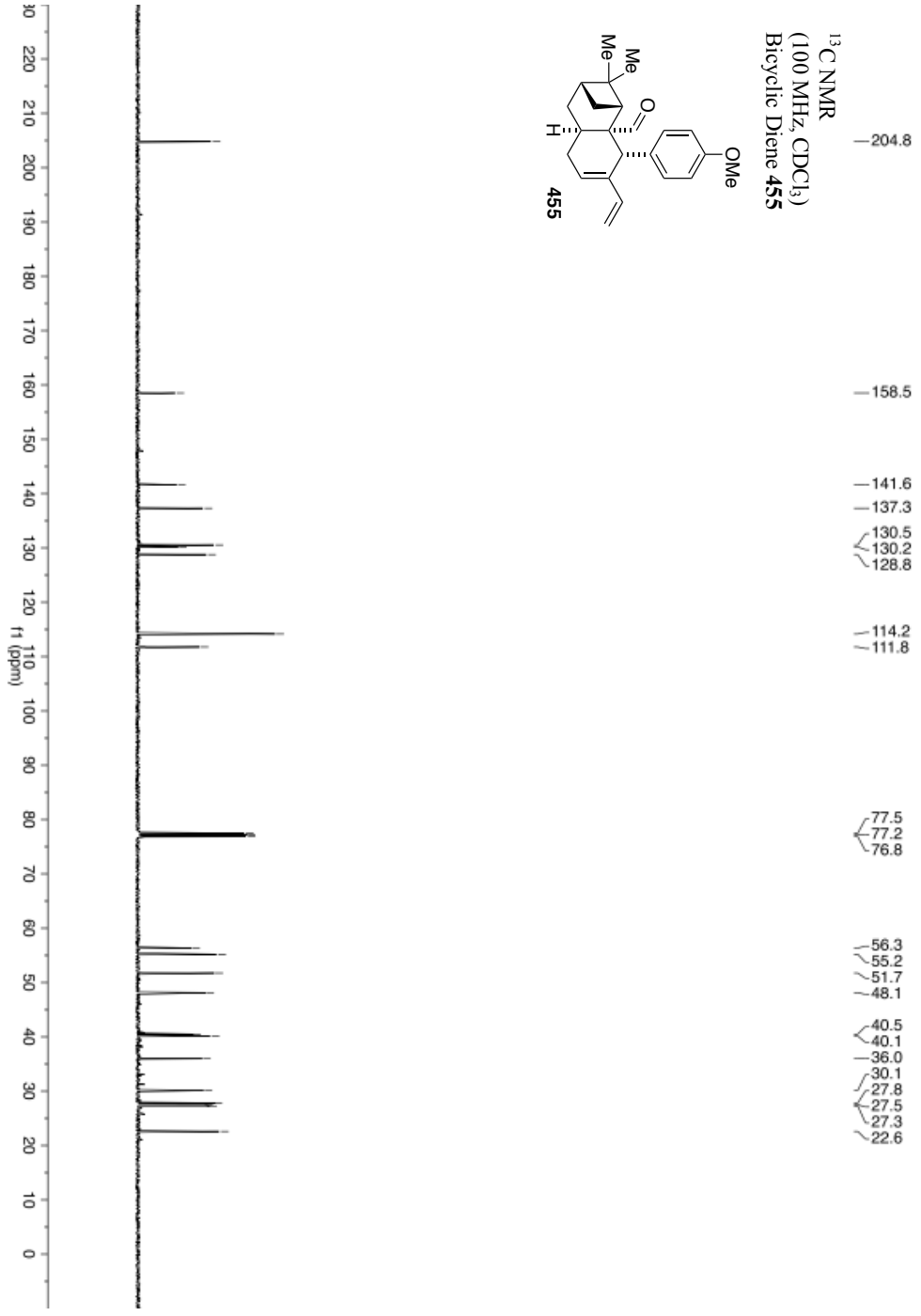
^{13}C NMR
(100 MHz, $CDCl_3$)
Bicyclic Diene **455**
Me
Me
O
H
OMe
455
204.8
158.5
141.6
137.3
130.5
130.2
128.8
114.2
111.8
77.5
77.2
76.8
56.3
55.2
51.7
48.1
40.5
40.1
36.0
30.1
27.8
27.5
27.3
22.6
f1 (ppm)

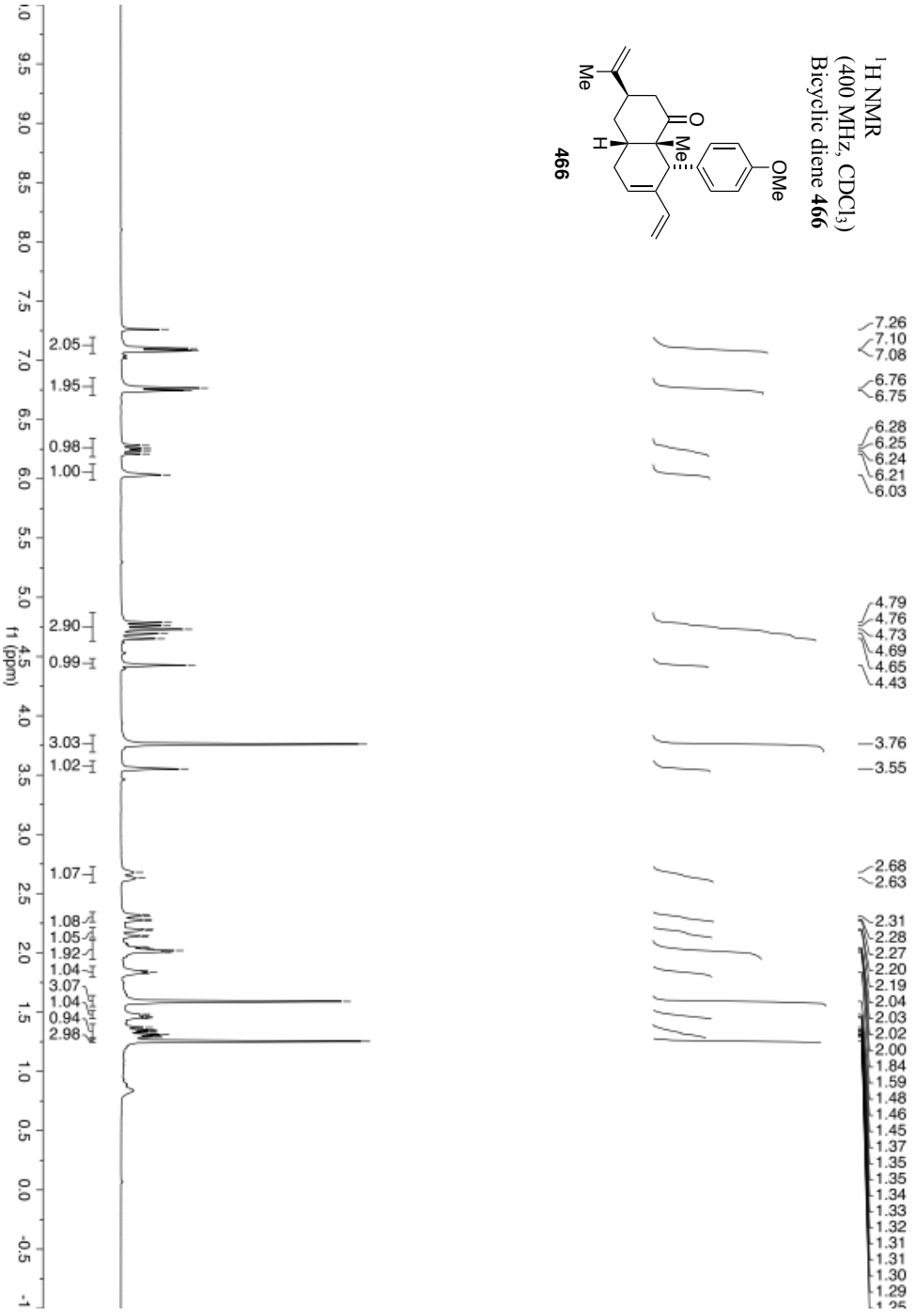
^{1}H NMR
(400 MHz, $CDCl_3$)
Bicyclic diene **466**
466
Me
O
Me
H
OMe
7.26
7.10
7.08
6.76
6.75
6.28
6.25
6.24
6.21
6.03
4.79
4.76
4.73
4.69
4.65
4.43
3.76
3.55
2.68
2.63
2.31
2.28
2.27
2.20
2.19
2.04
2.03
2.02
2.00
1.84
1.59
1.48
1.46
1.45
1.37
1.35
1.35
1.34
1.33
1.32
1.31
1.31
1.30
1.29
2.05
1.95
0.98
1.00
2.90
0.99
3.03
1.02
1.07
1.08
1.05
1.92
1.04
3.07
1.04
0.94
2.98
f1 (ppm)

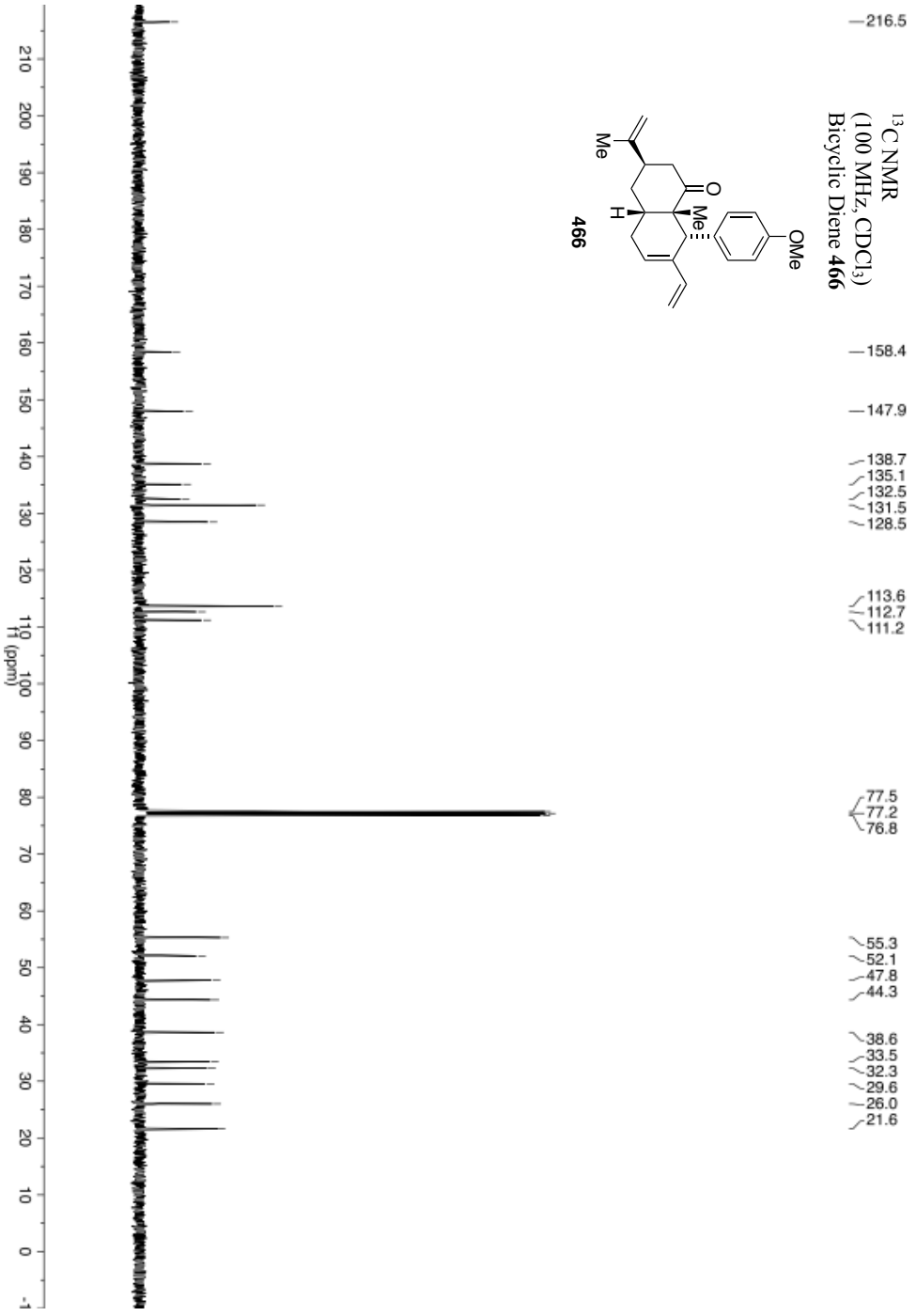
^{13}C NMR
(100 MHz, CDCl$_3$)
Bicyclic Diene **466**
466
Me
H
O
Me
OMe
216.5
158.4
147.9
138.7
135.1
132.5
131.5
128.5
113.6
112.7
111.2
77.5
77.2
76.8
55.3
52.1
47.8
44.3
38.6
33.5
32.3
29.6
26.0
21.6
f1 (ppm)

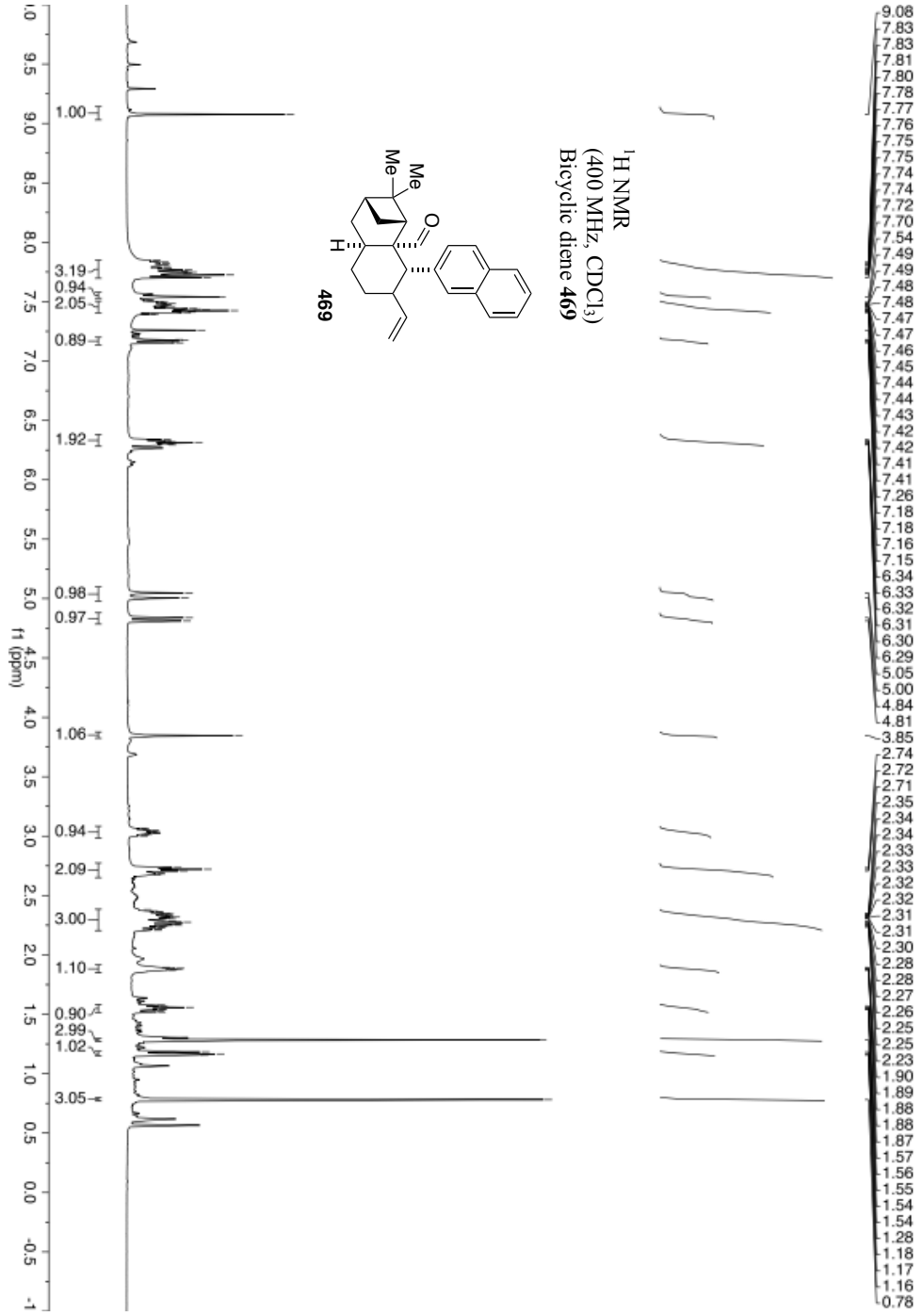
^{1}H NMR
(400 MHz, $CDCl_3$)
Bicyclic diene **469**
469
Me
Me
O
H
f1 (ppm)
1.00
3.19
0.94
2.05
0.89
1.92
0.98
0.97
1.06
0.94
2.09
3.00
1.10
0.90
2.99
1.02
3.05

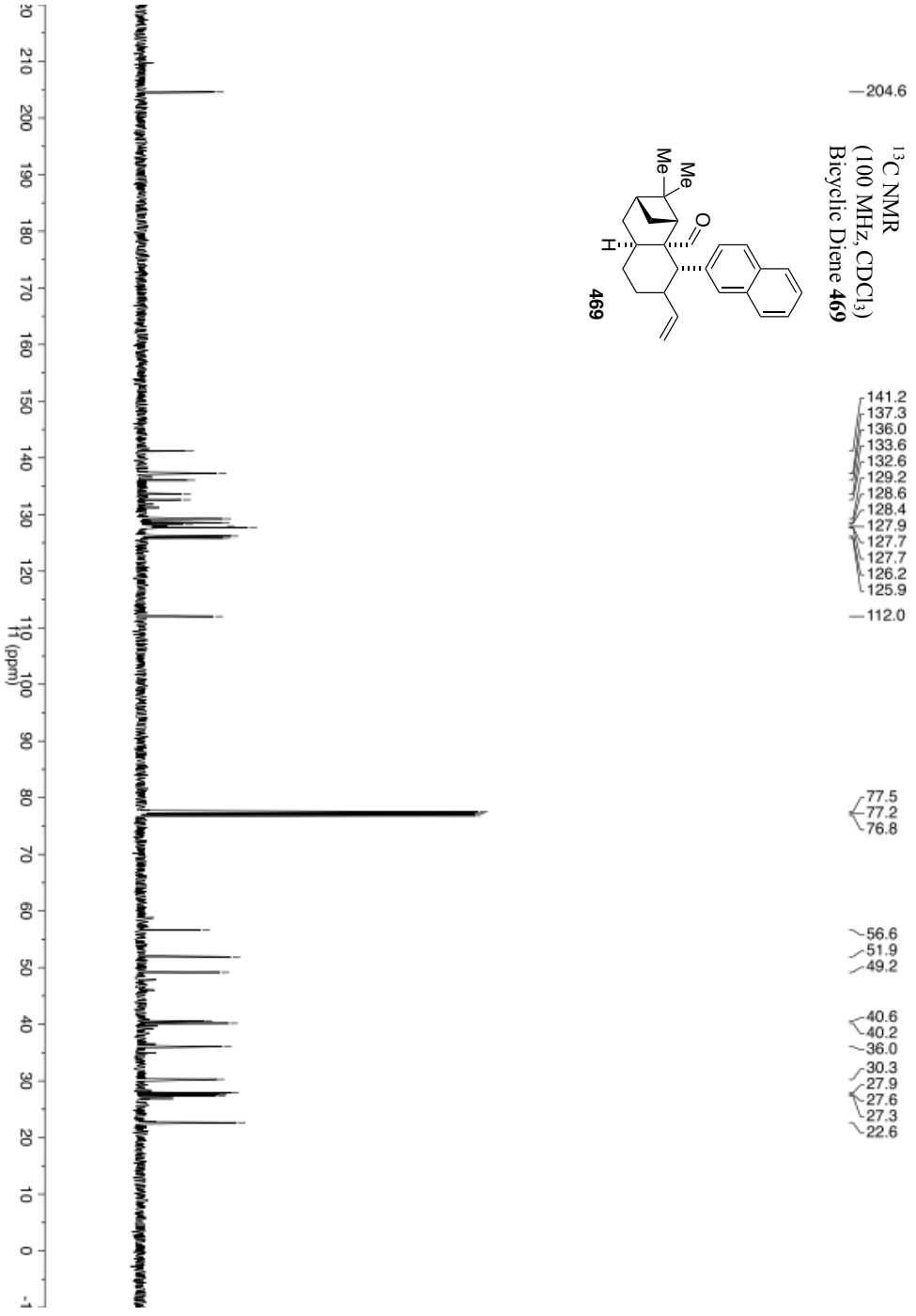
^{13}C NMR
(100 MHz, $CDCl_3$)
Bicyclic Diene **469**
Me
Me
O
H
469
204.6
141.2
137.3
136.0
133.6
132.6
129.2
128.6
128.4
127.9
127.7
127.7
126.2
125.9
112.0
77.5
77.2
76.8
56.6
51.9
49.2
40.6
40.2
36.0
30.3
27.9
27.6
27.3
22.6
f1 (ppm)

^{1}H NMR
(400 MHz, $CDCl_3$)
Bicyclic diene **478**

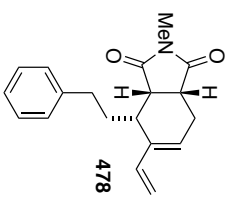

478

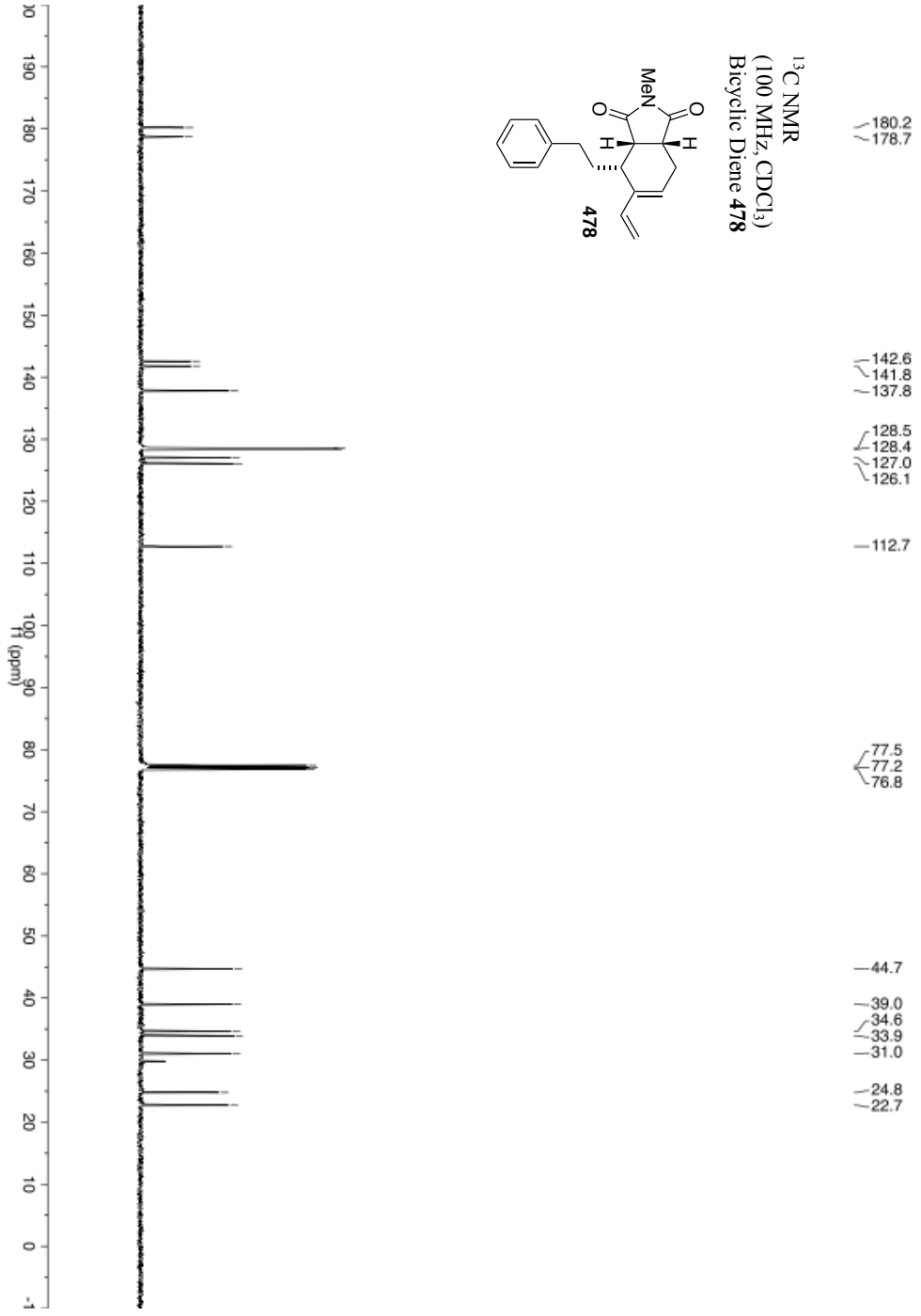
^{13}C NMR
(100 MHz, $CDCl_3$)
Bicyclic Diene **478**
478
MeN
O
O
H
H
180.2
178.7
142.6
141.8
137.8
128.5
128.4
127.0
126.1
112.7
77.5
77.2
76.8
44.7
39.0
34.6
33.9
31.0
24.8
22.7
f1 (ppm)

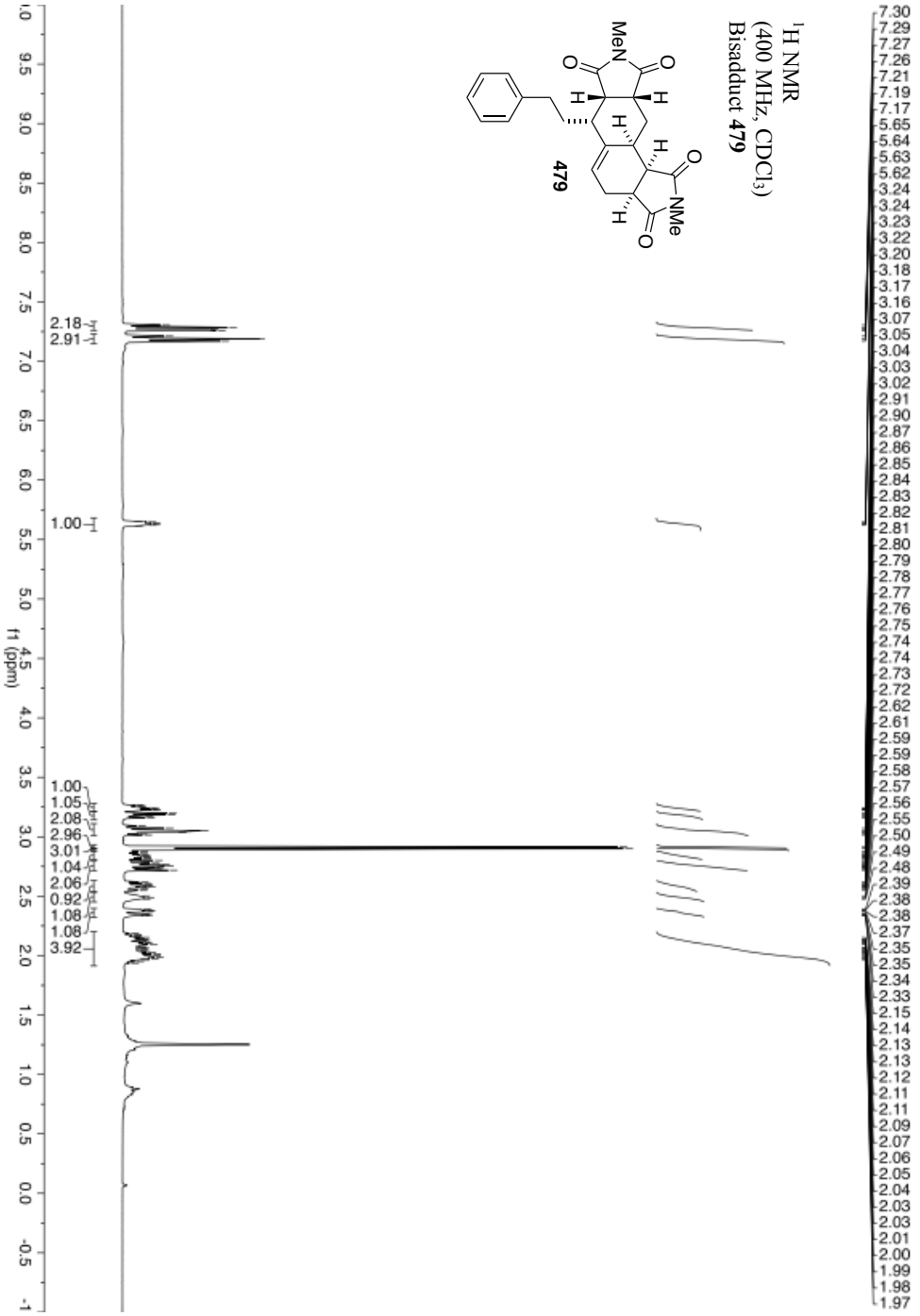
^{1}H NMR
(400 MHz, $CDCl_3$)
Bisadduct **479**
479
MeN
NMe
f1 (ppm)

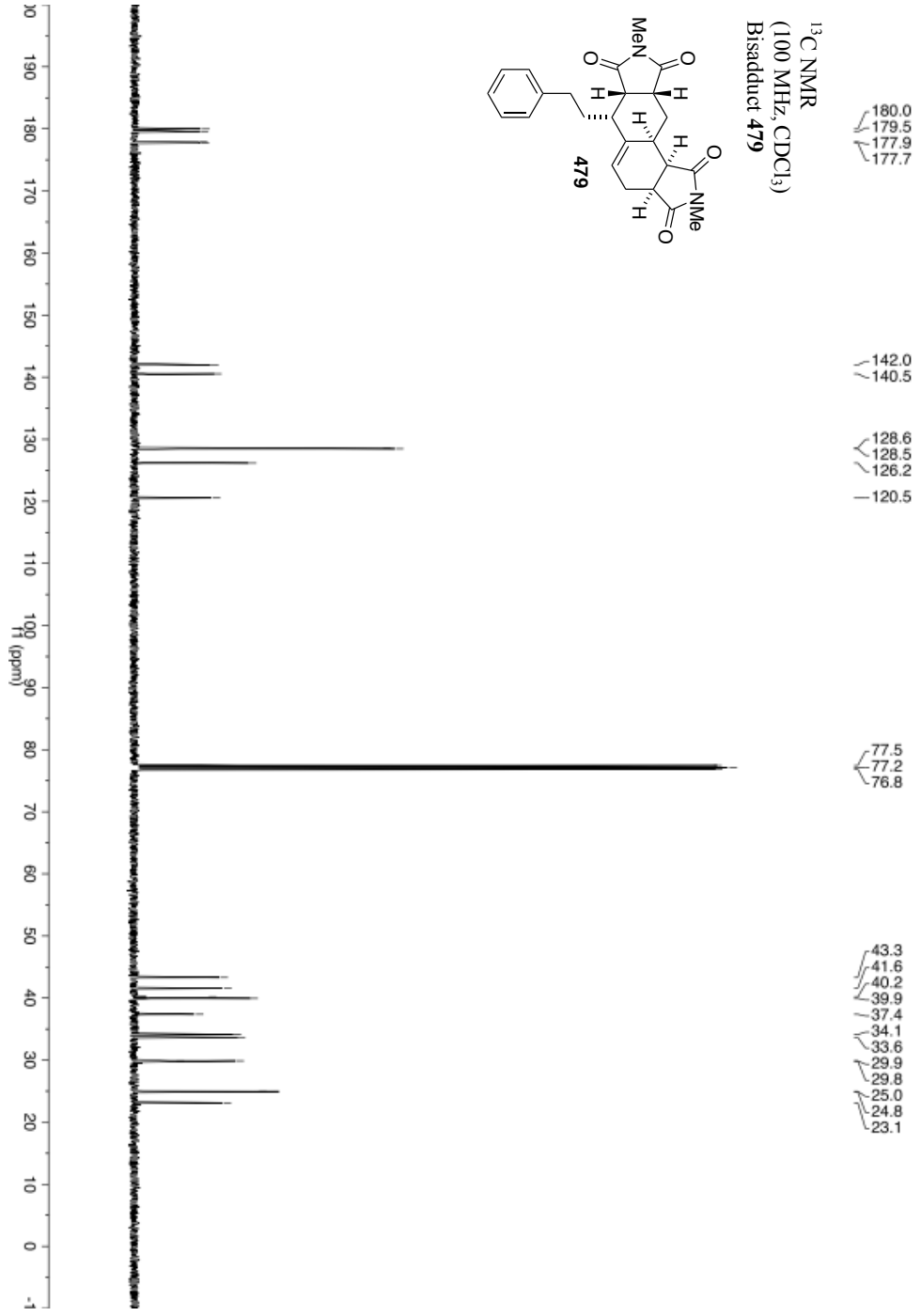
^{13}C NMR
(100 MHz, $CDCl_3$)
Bisadduct **479**
479
MeN
NMe
180.0
179.5
177.9
177.7
142.0
140.5
128.6
128.5
126.2
120.5
77.5
77.2
76.8
43.3
41.6
40.2
39.9
37.4
34.1
33.6
29.9
29.8
25.0
24.8
23.1
f1 (ppm)

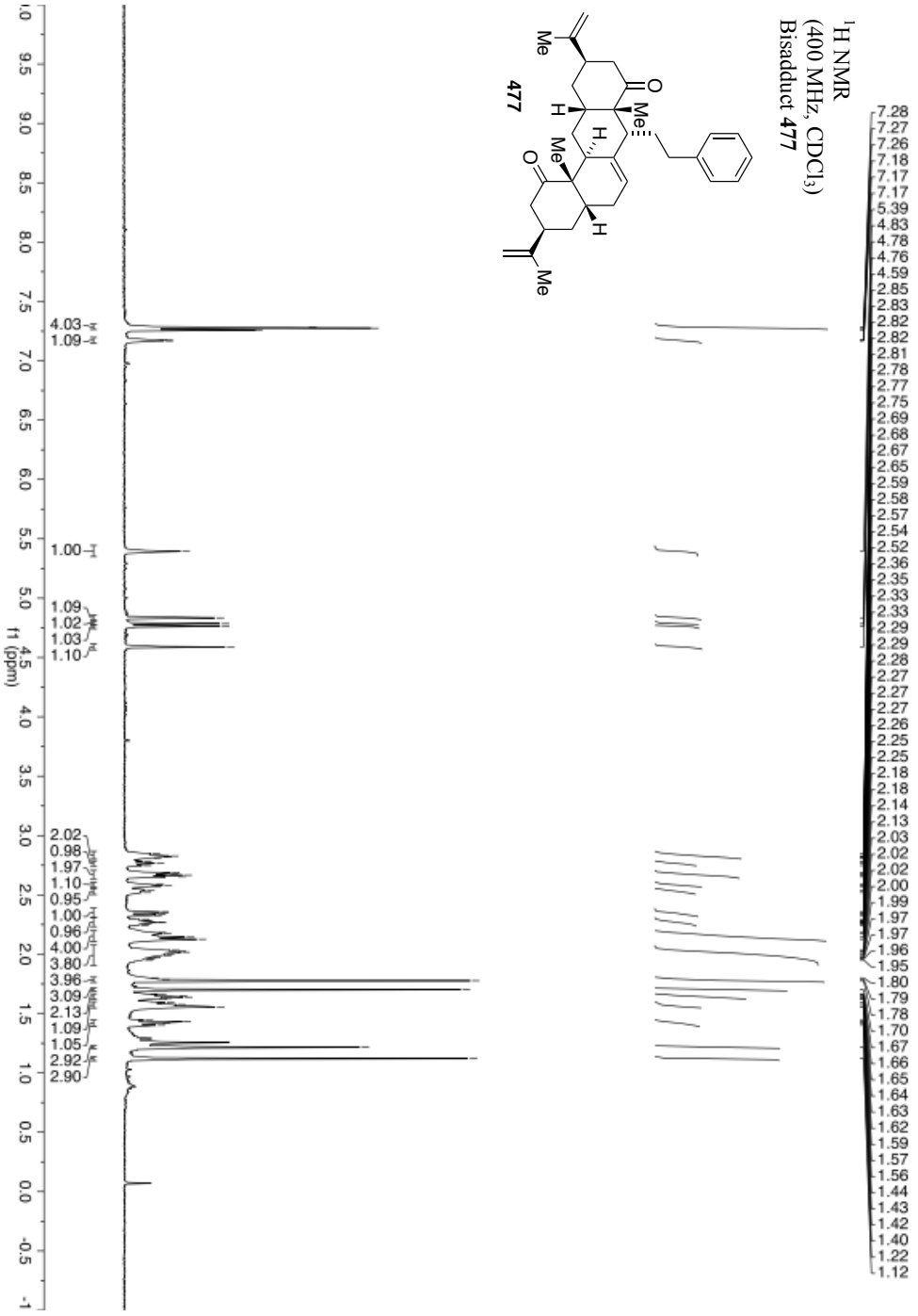
^{1}H NMR
(400 MHz, $CDCl_3$)
Bisadduct **477**
477
Me
O
Me
H
H
Me
O
H
Me
f1 (ppm)
4.03
1.09
1.00
1.09
1.02
1.03
1.10
2.02
0.98
1.97
1.10
0.95
1.00
0.96
4.00
3.80
3.96
3.09
2.13
1.09
1.05
2.92
2.90
7.28
7.27
7.26
7.18
7.17
7.17
5.39
4.83
4.78
4.76
4.59
2.85
2.83
2.82
2.82
2.81
2.78
2.77
2.75
2.69
2.68
2.67
2.65
2.59
2.58
2.57
2.54
2.52
2.36
2.35
2.33
2.33
2.29
2.29
2.28
2.27
2.27
2.27
2.26
2.25
2.25
2.18
2.18
2.14
2.13
2.03
2.02
2.02
2.00
1.99
1.97
1.97
1.96
1.95
1.80
1.79
1.78
1.70
1.67
1.66
1.65
1.64
1.63
1.62
1.59
1.57
1.56
1.44
1.43
1.42
1.40
1.22
1.12

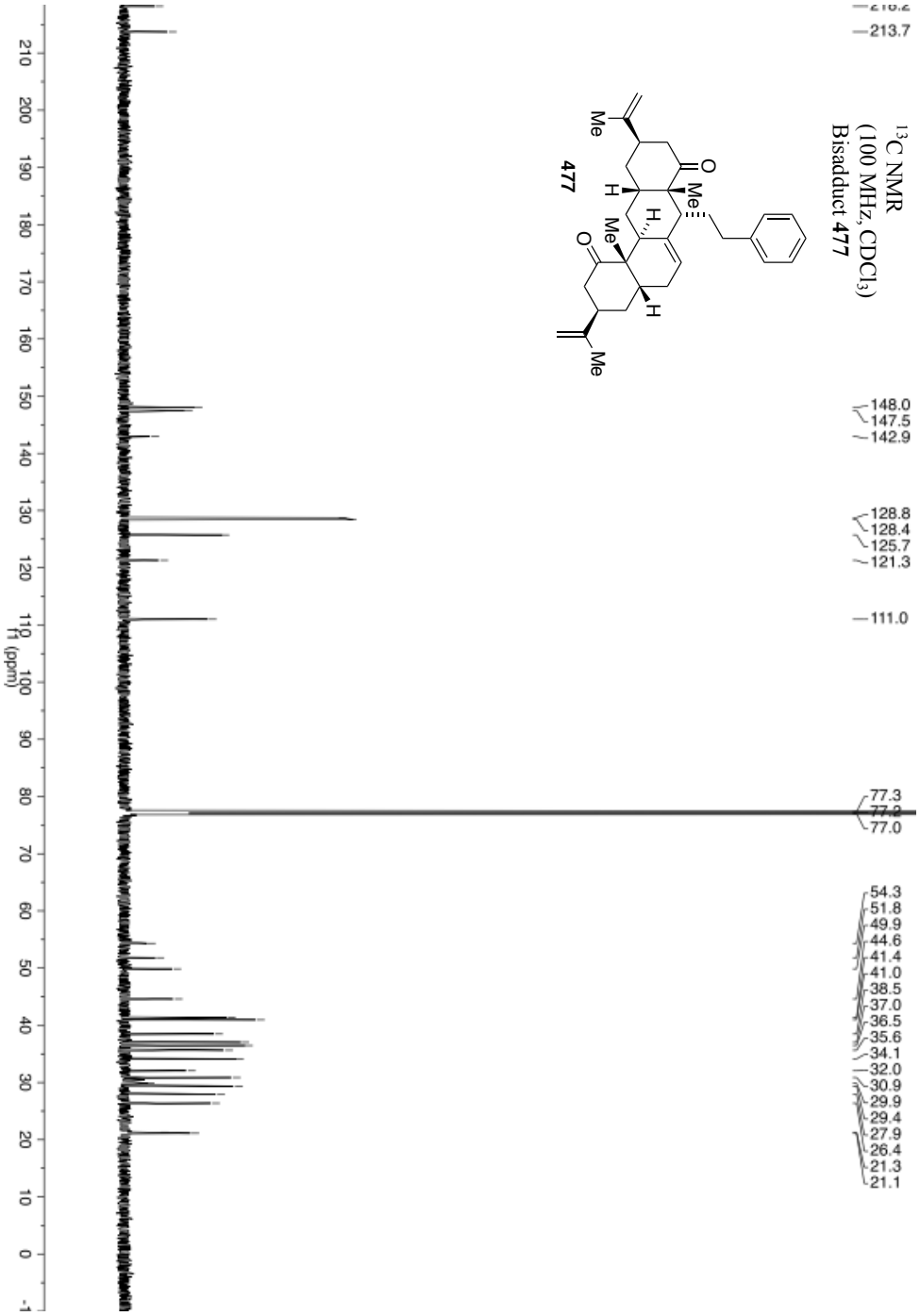
^{13}C NMR
(100 MHz, CDCl$_3$)
Bisadduct **477**
477
Me
H
Me
O
Me
H
O
H
Me
213.7
148.0
147.5
142.9
128.8
128.4
125.7
121.3
111.0
77.3
77.0
54.3
51.8
49.9
44.6
41.4
41.0
38.5
37.0
36.5
35.6
34.1
32.0
30.9
29.9
29.4
27.9
26.4
21.3
21.1
f1 (ppm)

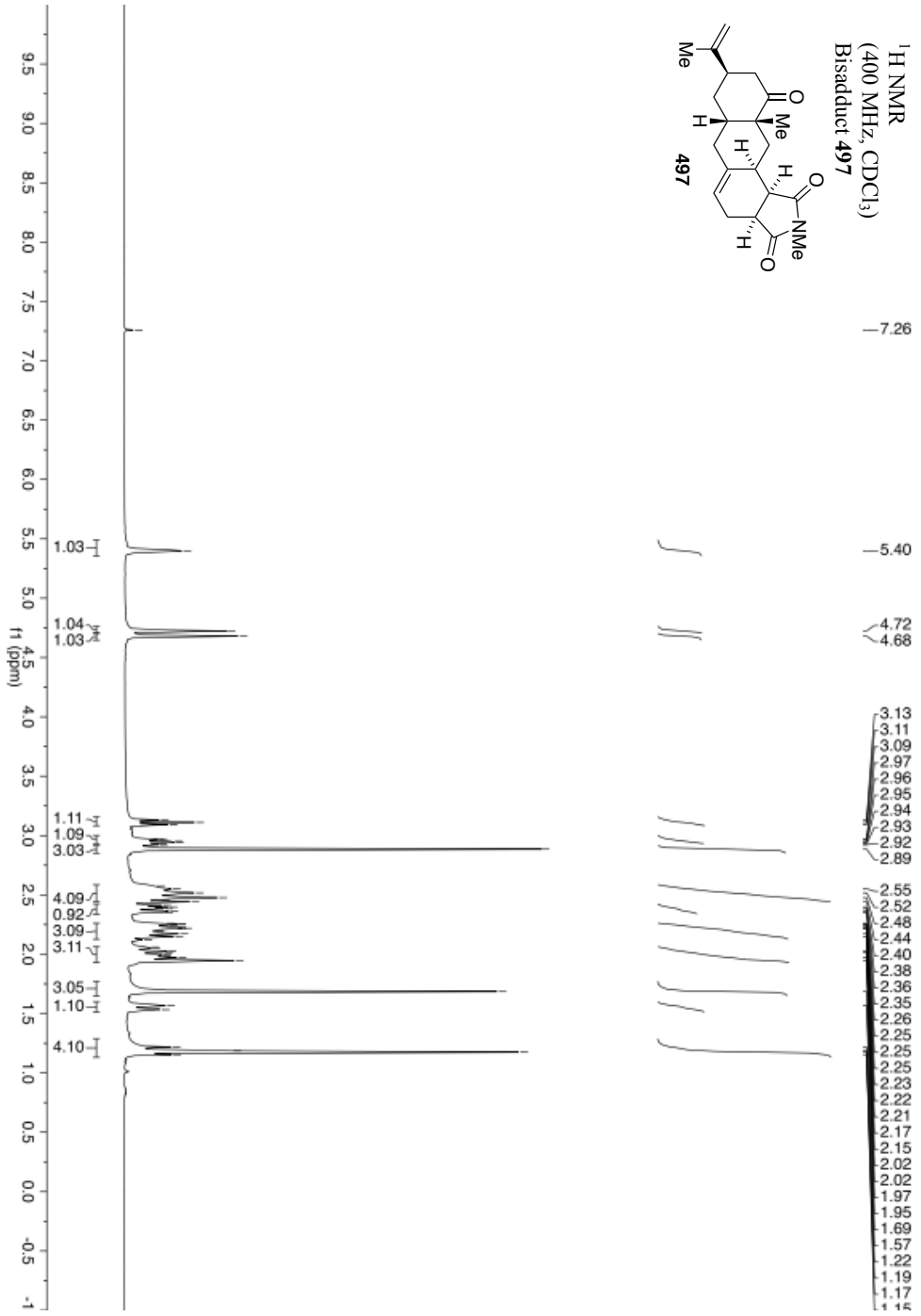
^{1}H NMR
(400 MHz, $CDCl_3$)
Bisadduct **497**
497
Me
O
Me
H
H
H
O
NMe
O
H
7.26
5.40
4.72
4.68
3.13
3.11
3.09
2.97
2.96
2.95
2.94
2.93
2.92
2.89
2.55
2.52
2.48
2.44
2.40
2.38
2.36
2.35
2.26
2.25
2.25
2.23
2.22
2.21
2.17
2.15
2.02
2.02
1.97
1.95
1.69
1.57
1.22
1.19
1.17
1.03
1.04
1.03
1.11
1.09
3.03
4.09
0.92
3.09
3.11
3.05
1.10
4.10
f1 (ppm)

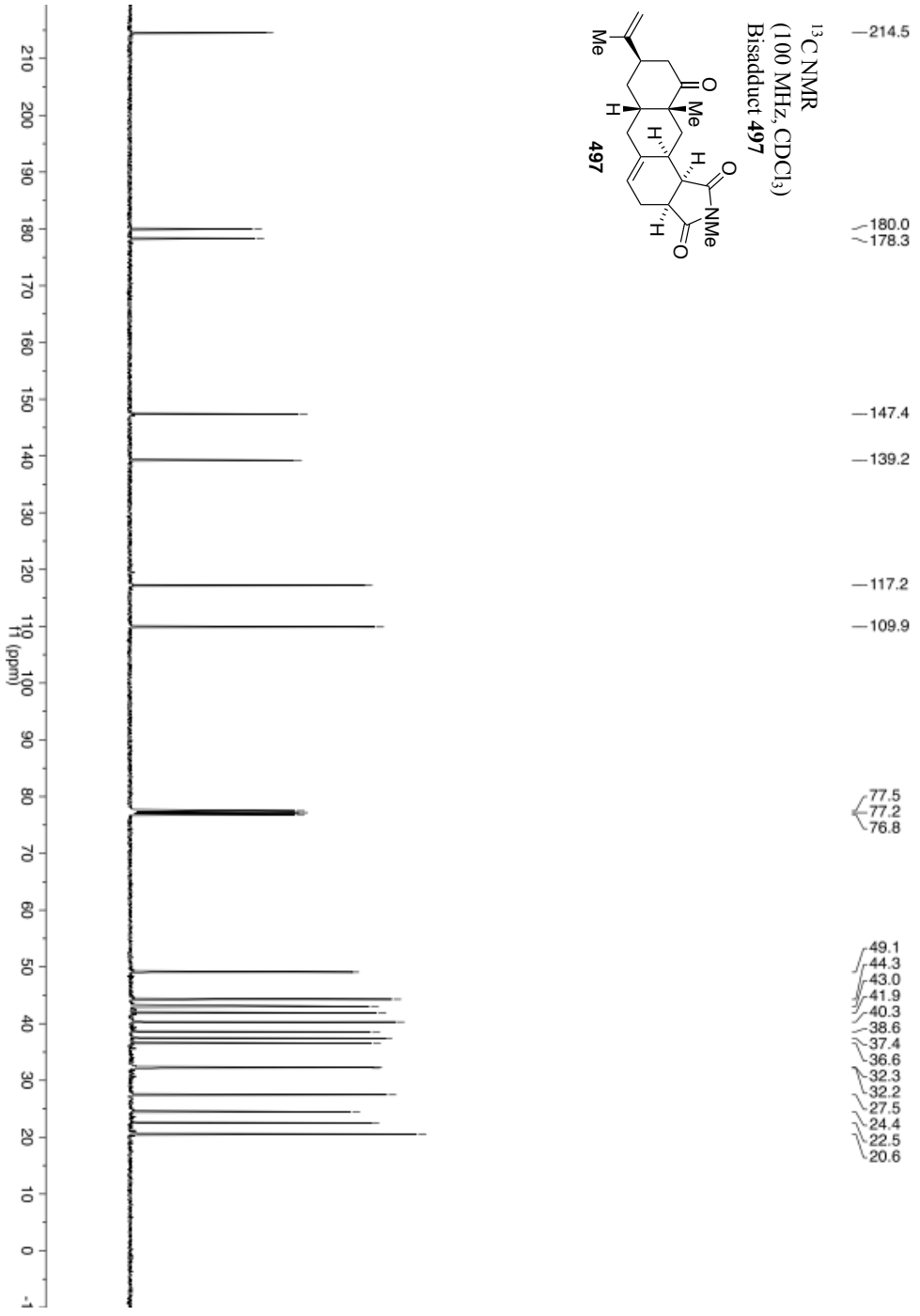
^{13}C NMR
(100 MHz, $CDCl_3$)
Bisadduct **497**
497
Me
O
Me
H
H
H
O
NMe
O
214.5
180.0
178.3
147.4
139.2
117.2
109.9
77.5
77.2
76.8
49.1
44.3
43.0
41.9
40.3
38.6
37.4
36.6
32.3
32.2
27.5
24.4
22.5
20.6
f1 (ppm)

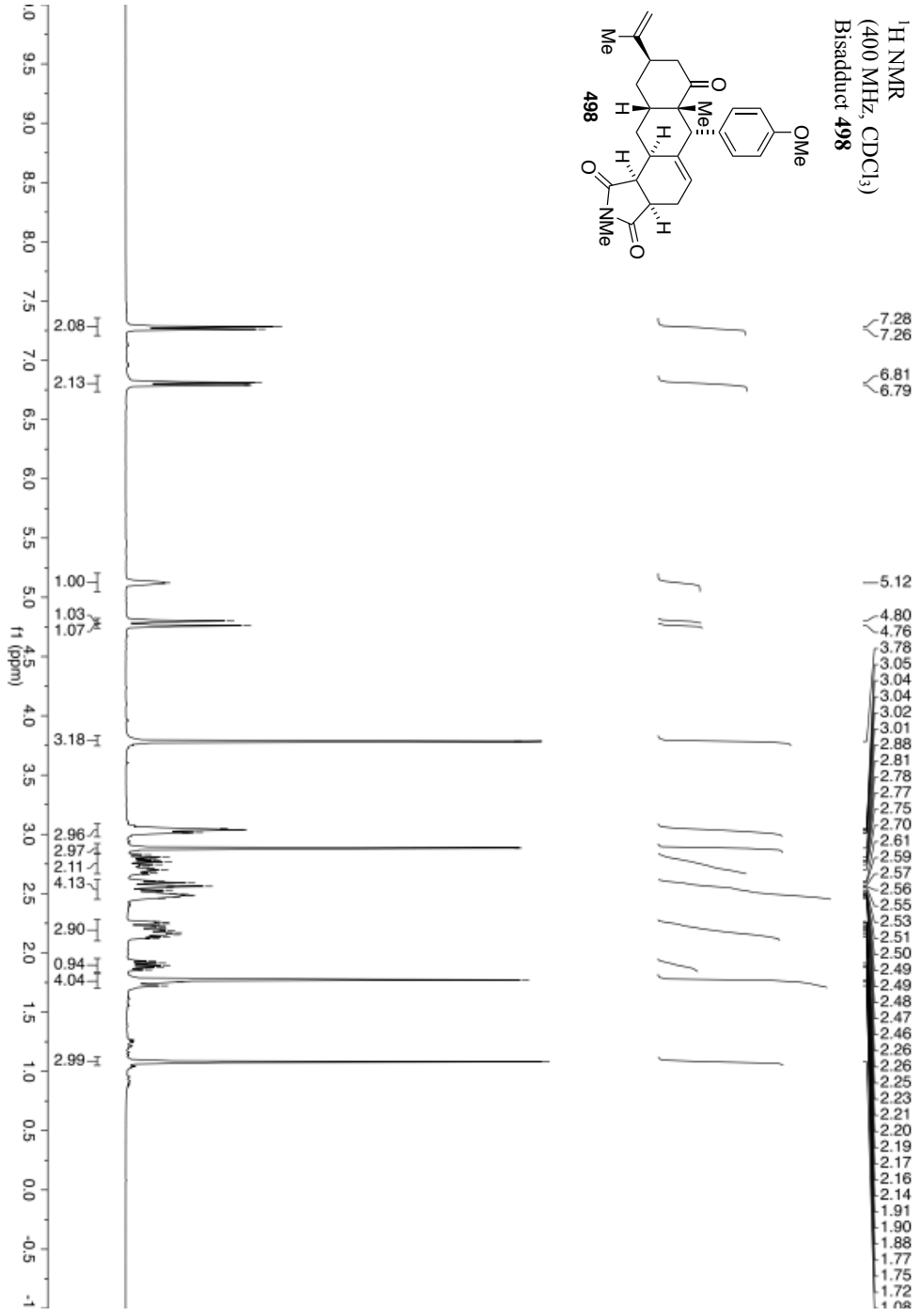
^{1}H NMR
(400 MHz, $CDCl_3$)
Bisadduct **498**
498
Me
O
Me
H
H
H
OMe
O
NMe
O
H
7.28
7.26
6.81
6.79
5.12
4.80
4.76
3.78
3.05
3.04
3.04
3.02
3.01
2.88
2.81
2.78
2.77
2.75
2.70
2.61
2.59
2.57
2.56
2.55
2.53
2.51
2.50
2.49
2.49
2.48
2.47
2.46
2.26
2.26
2.25
2.23
2.21
2.20
2.19
2.17
2.16
2.14
1.91
1.90
1.88
1.77
1.75
1.72
2.08
2.13
1.00
1.03
1.07
3.18
2.96
2.97
2.11
4.13
2.90
0.94
4.04
2.99
f1 (ppm)

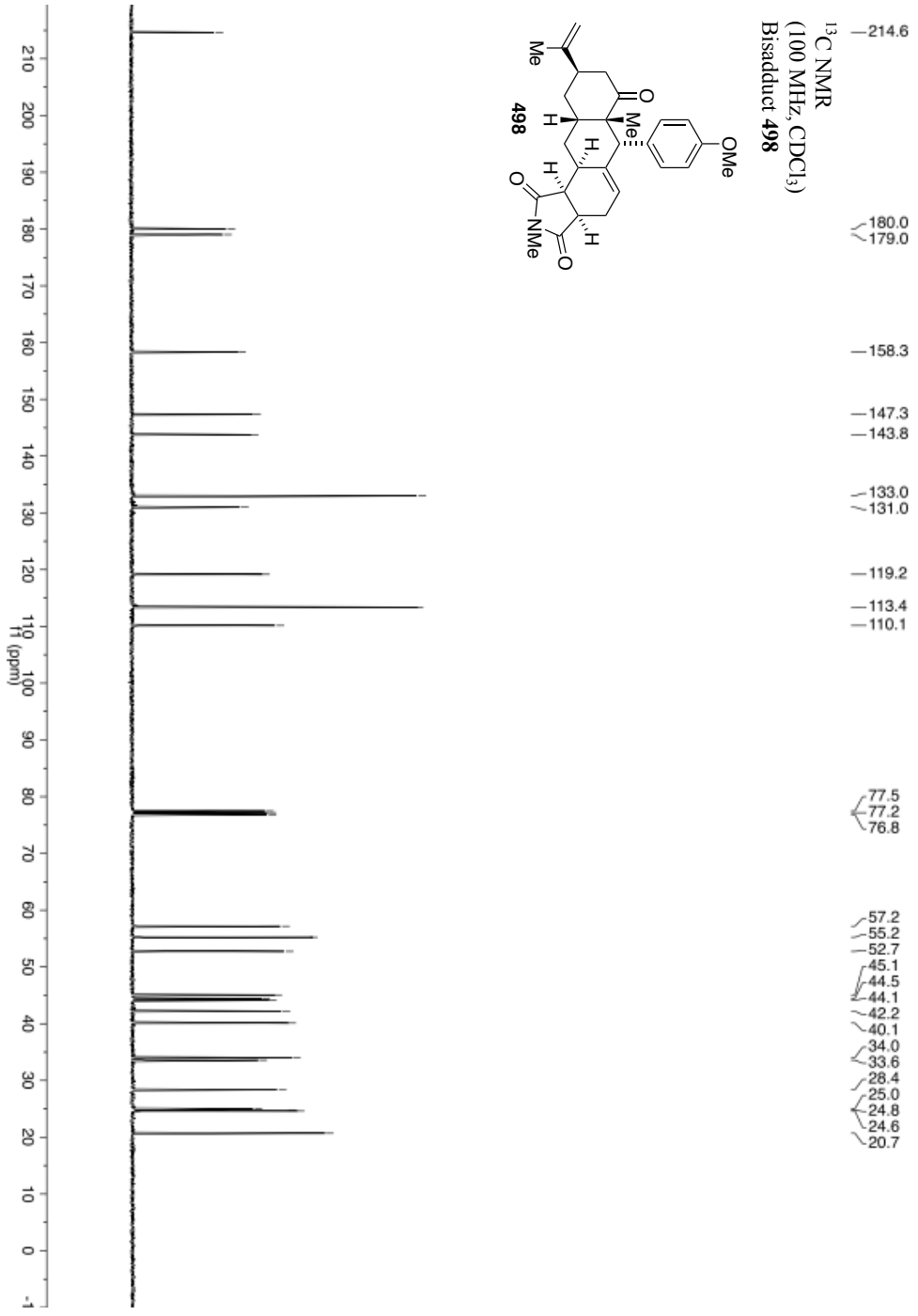
^{13}C NMR
(100 MHz, CDCl$_3$)
Bisadduct **498**
498
Me
H
O
Me
H
H
OMe
O
NMe
O
H
214.6
180.0
179.0
158.3
147.3
143.8
133.0
131.0
119.2
113.4
110.1
77.5
77.2
76.8
57.2
55.2
52.7
45.1
44.5
44.1
42.2
40.1
34.0
33.6
28.4
25.0
24.8
24.6
20.7
f1 (ppm)

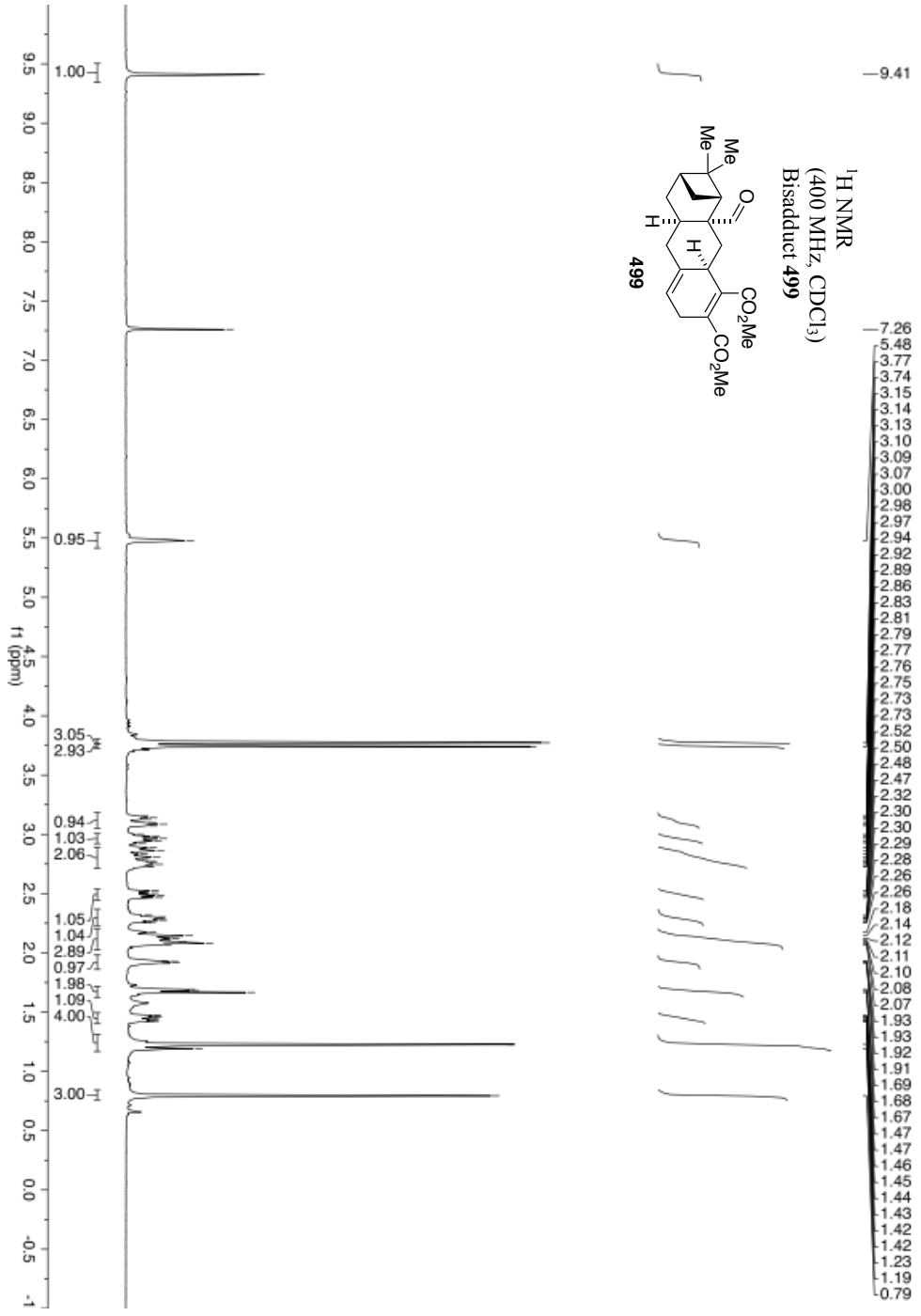
^{1}H NMR
(400 MHz, $CDCl_3$)
Bisadduct **499**
499
Me
Me
Me
O
H
H
CO_2Me
CO_2Me
f1 (ppm)
1.00
0.95
3.05
2.93
0.94
1.03
2.06
1.05
1.04
2.89
0.97
1.98
1.09
4.00
3.00
9.41
7.26
5.48
3.77
3.74
3.15
3.14
3.13
3.10
3.09
3.07
3.00
2.98
2.97
2.94
2.92
2.89
2.86
2.83
2.81
2.79
2.77
2.76
2.75
2.73
2.73
2.52
2.50
2.48
2.47
2.32
2.30
2.30
2.29
2.28
2.26
2.26
2.18
2.14
2.12
2.11
2.10
2.08
2.07
1.93
1.93
1.92
1.91
1.69
1.68
1.67
1.47
1.47
1.46
1.45
1.44
1.43
1.42
1.42
1.23
1.19
0.79

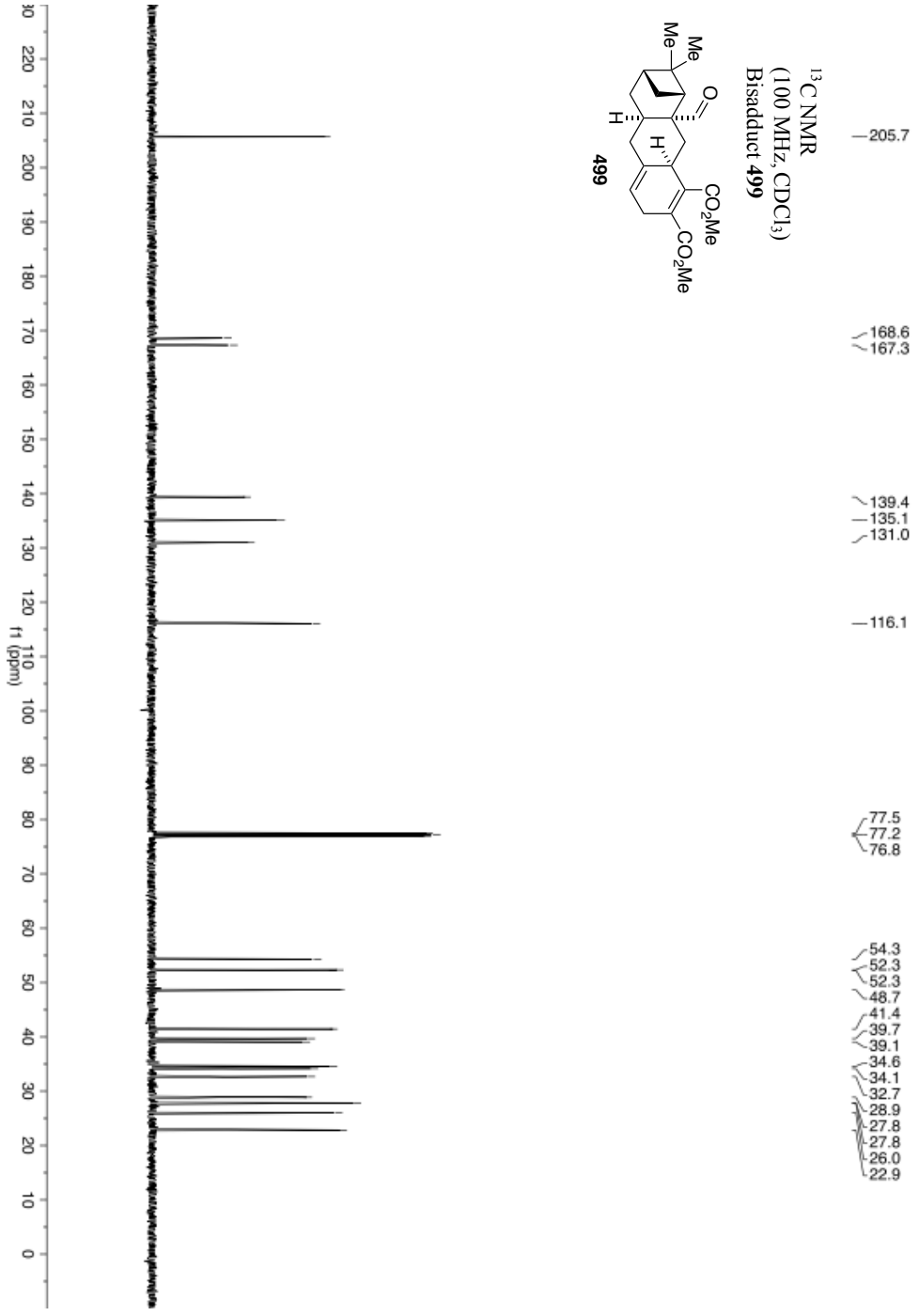
^{13}C NMR
(100 MHz, $CDCl_3$)
Bisadduct **499**
499
Me
Me
O
H
H
CO_2Me
CO_2Me
205.7
168.6
167.3
139.4
135.1
131.0
116.1
77.5
77.2
76.8
54.3
52.3
52.3
48.7
41.4
39.7
39.1
34.6
34.1
32.7
28.9
27.8
27.8
26.0
22.9
f1 (ppm)

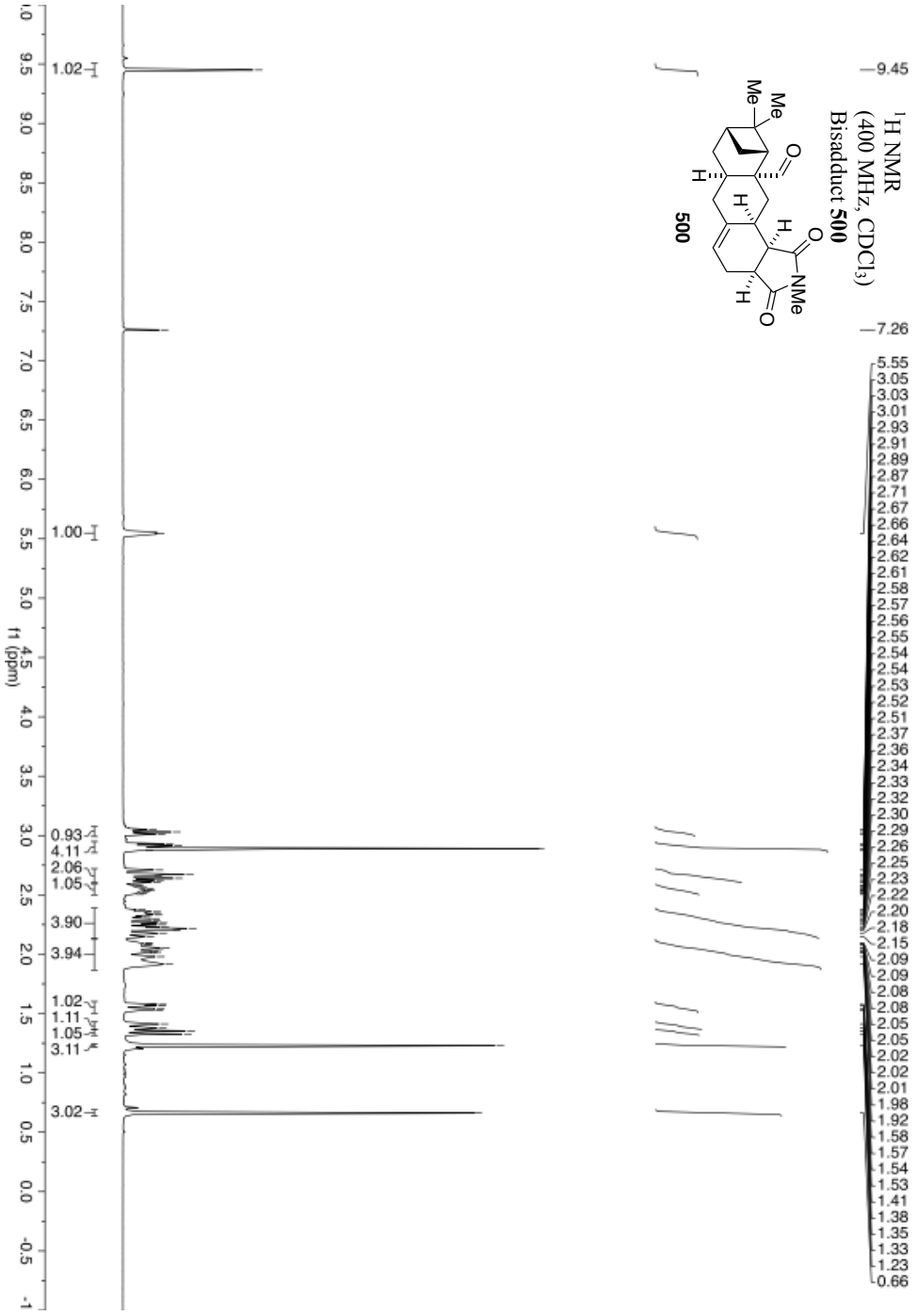
^{1}H NMR
(400 MHz, $CDCl_3$)
Bisadduct **500**
500
Me
Me
O
H
H
H
O
NMe
O
9.45
7.26
5.55
3.05
3.03
3.01
2.93
2.91
2.89
2.87
2.71
2.67
2.66
2.64
2.62
2.61
2.58
2.57
2.56
2.55
2.54
2.54
2.53
2.52
2.51
2.37
2.36
2.34
2.33
2.32
2.30
2.29
2.26
2.25
2.23
2.22
2.20
2.18
2.15
2.09
2.09
2.08
2.08
2.05
2.05
2.02
2.02
2.01
1.98
1.92
1.58
1.57
1.54
1.53
1.41
1.38
1.35
1.33
1.23
0.66
1.02
1.00
0.93
4.11
2.06
1.05
3.90
3.94
1.02
1.11
1.05
3.11
3.02
f1 (ppm)

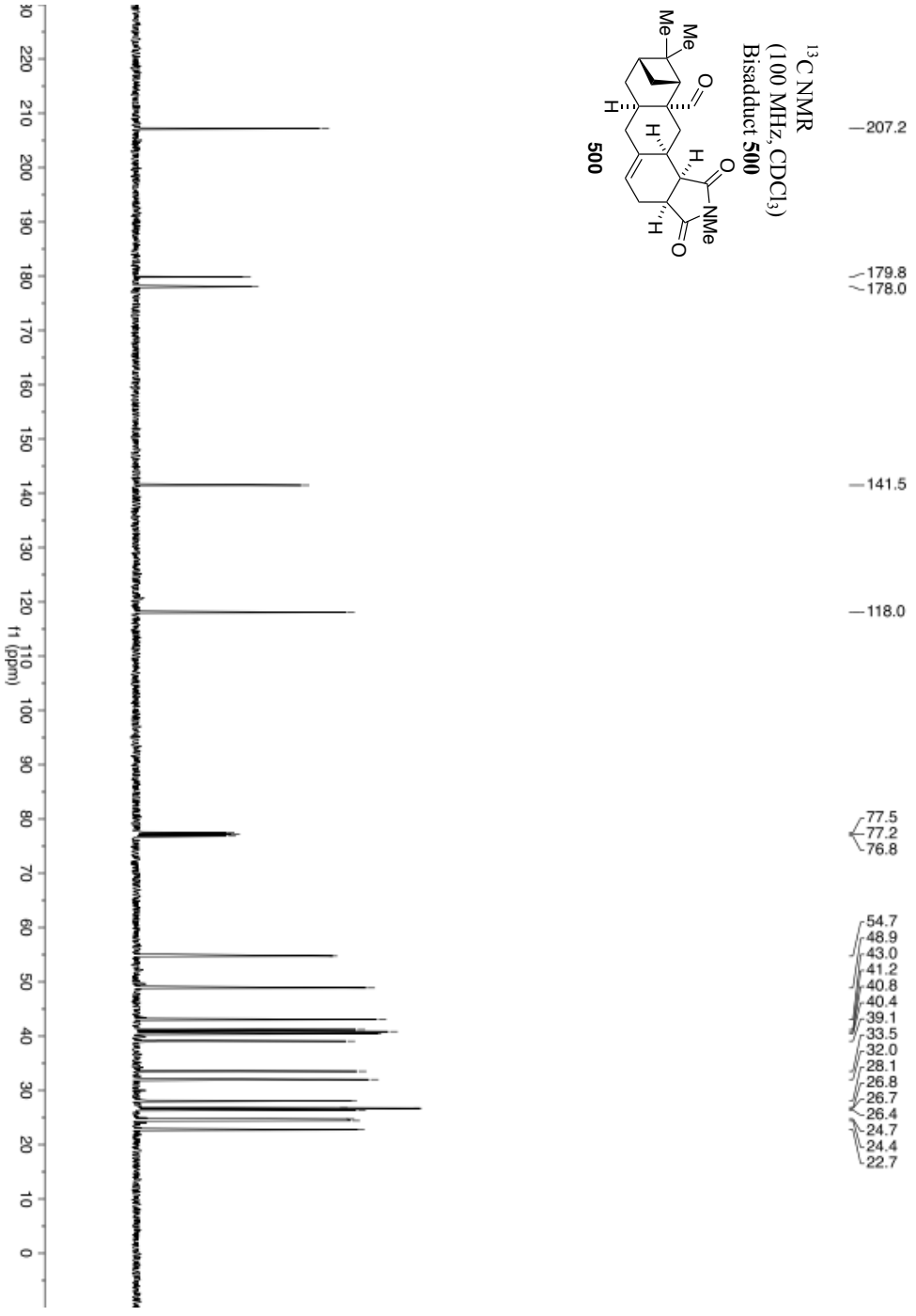
^{13}C NMR
(100 MHz, $CDCl_3$)
Bisadduct **500**
500
Me
Me
O
H
H
H
O
NMe
H
O
—207.2
—179.8
—178.0
—141.5
—118.0
77.5
77.2
76.8
54.7
48.9
43.0
41.2
40.8
40.4
39.1
33.5
32.0
28.1
26.8
26.7
26.4
24.7
24.4
22.7
f1 (ppm)

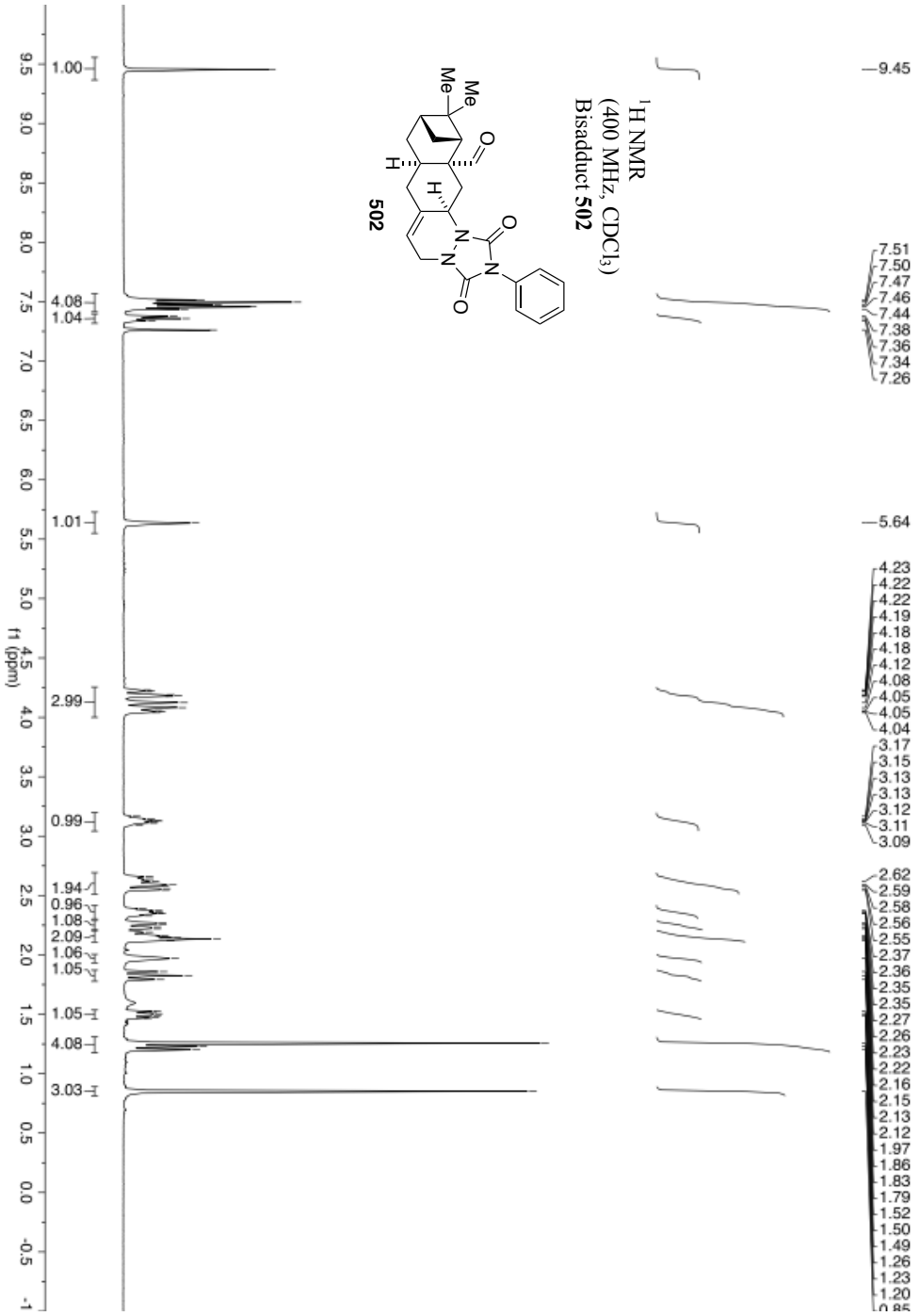
^{1}H NMR
(400 MHz, $CDCl_3$)
Bisadduct **502**
502
Me
Me
O
H
H
N
N
N
O
O
f1 (ppm)
1.00
4.08
1.04
1.01
2.99
0.99
1.94
0.96
1.08
2.09
1.06
1.05
1.05
4.08
3.03
9.45
7.51
7.50
7.47
7.46
7.44
7.38
7.36
7.34
7.26
5.64
4.23
4.22
4.22
4.19
4.18
4.18
4.12
4.08
4.05
4.05
4.04
3.17
3.15
3.13
3.13
3.12
3.11
3.09
2.62
2.59
2.58
2.56
2.55
2.37
2.36
2.35
2.35
2.27
2.26
2.23
2.22
2.16
2.15
2.13
2.12
1.97
1.86
1.83
1.79
1.52
1.50
1.49
1.26
1.23
1.20

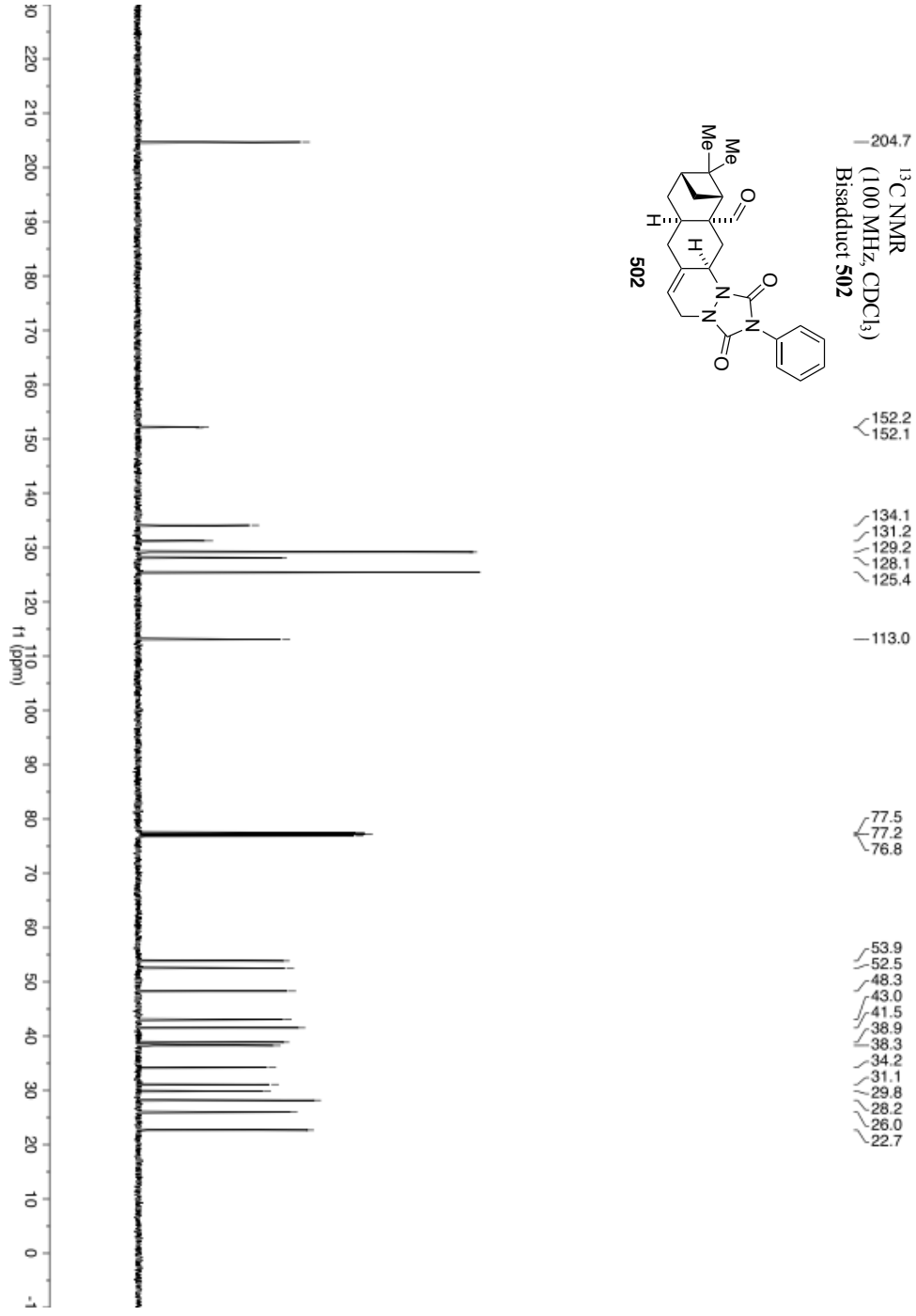
^{13}C NMR
(100 MHz, CDCl$_3$)
Bisadduct **502**
502
204.7
152.2
152.1
134.1
131.2
129.2
128.1
125.4
113.0
77.5
77.2
76.8
53.9
52.5
48.3
43.0
41.5
38.9
38.3
34.2
31.1
29.8
28.2
26.0
22.7
f1 (ppm)

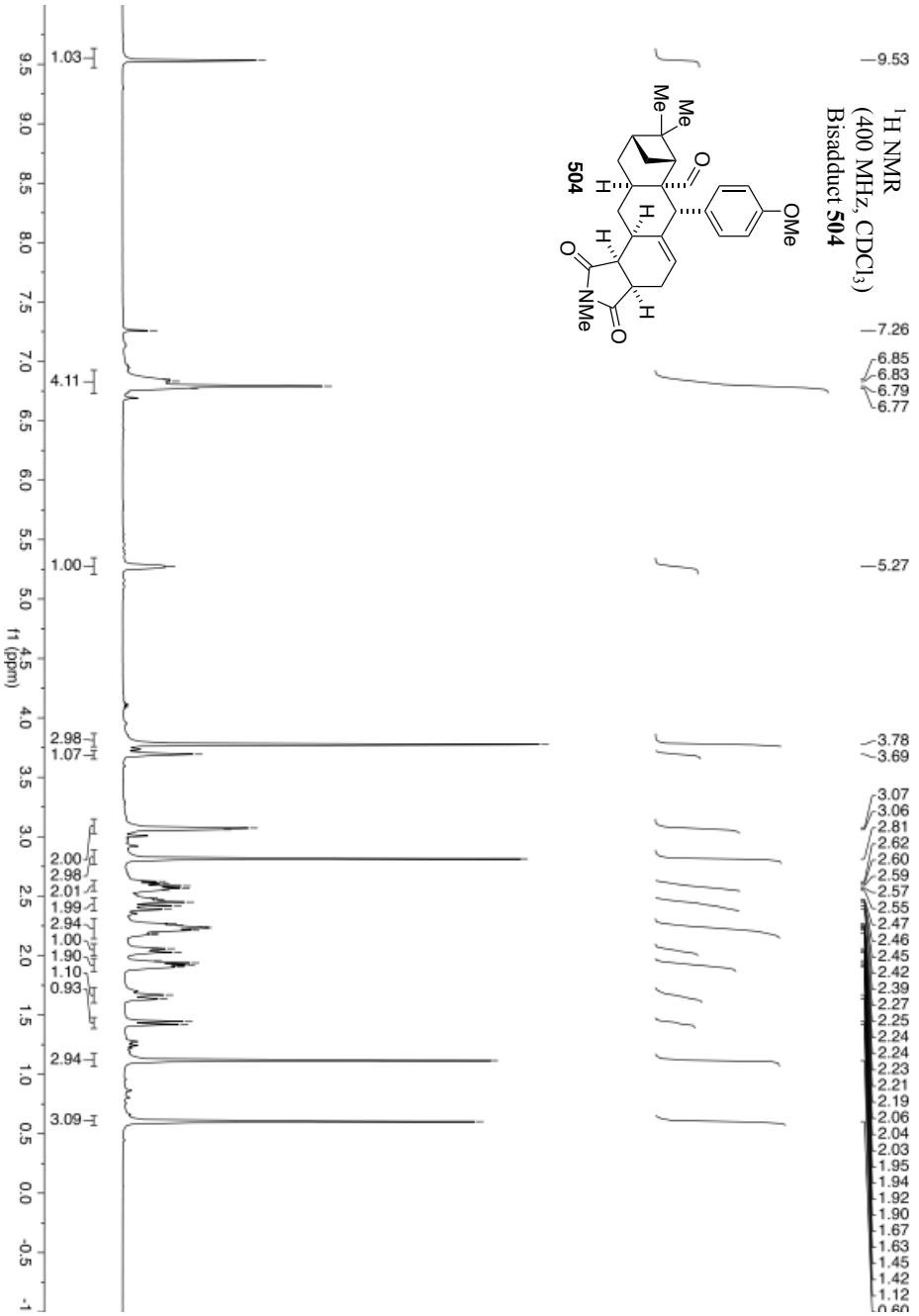
^{1}H NMR
(400 MHz, $CDCl_3$)
Bisadduct **504**
504
Me
Me
Me
O
H
H
H
O
NMe
O
H
OMe
f1 (ppm)
1.03
4.11
1.00
2.98
1.07
2.00
2.98
2.01
1.99
2.94
1.00
1.90
1.10
0.93
2.94
3.09
9.53
7.26
6.85
6.83
6.79
6.77
5.27
3.78
3.69
3.07
3.06
2.81
2.62
2.60
2.59
2.57
2.55
2.47
2.46
2.45
2.42
2.39
2.27
2.25
2.24
2.24
2.23
2.21
2.19
2.06
2.04
2.03
1.95
1.94
1.92
1.90
1.67
1.63
1.45
1.42
1.12

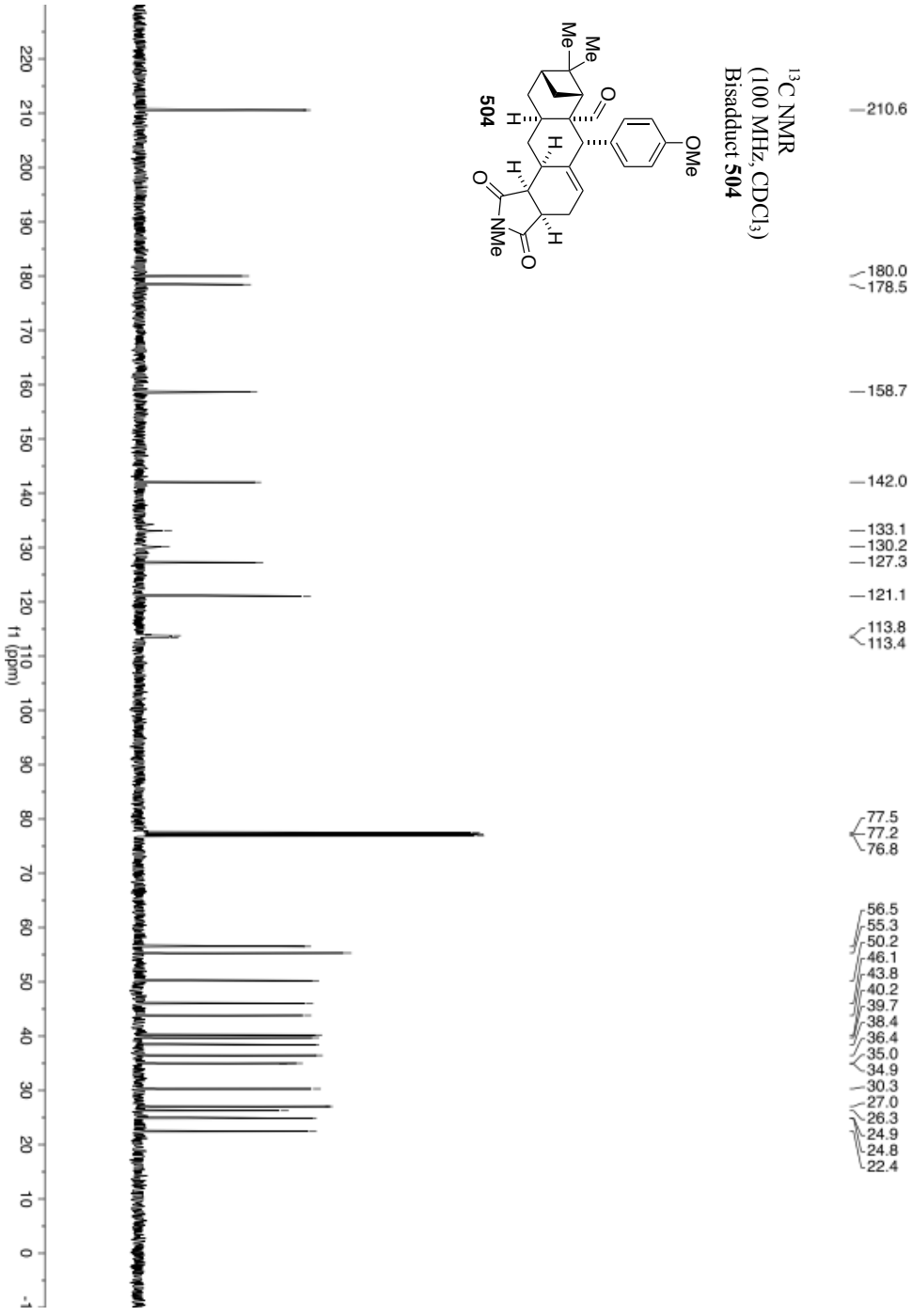
^{13}C NMR
(100 MHz, CDCl$_3$)
Bisadduct **504**
504
Me
Me
O
H
H
H
OMe
O
NMe
O
H
210.6
180.0
178.5
158.7
142.0
133.1
130.2
127.3
121.1
113.8
113.4
77.5
77.2
76.8
56.5
55.3
50.2
46.1
43.8
40.2
39.7
38.4
36.4
35.0
34.9
30.3
27.0
26.3
24.9
24.8
22.4
f1 (ppm)

^{1}H NMR
(400 MHz, $CDCl_3$)
Bisadduct **507**

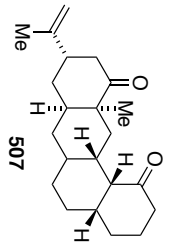

507

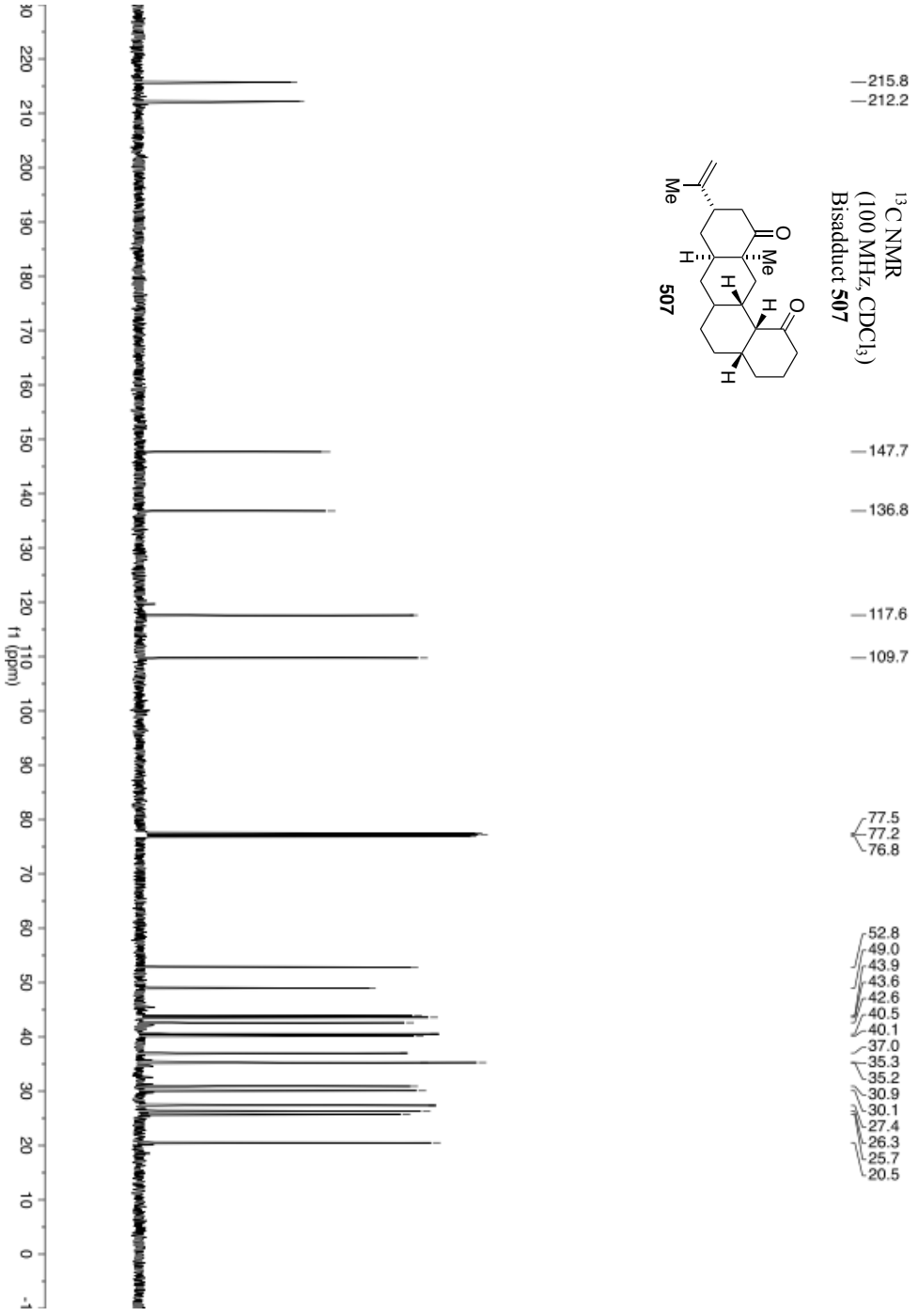
^{13}C NMR
(100 MHz, CDCl$_3$)
Bisadduct **507**
507
Me
O
Me
H
H
H
O
H
215.8
212.2
147.7
136.8
117.6
109.7
77.5
77.2
76.8
52.8
49.0
43.9
43.6
42.6
40.5
40.1
37.0
35.3
35.2
30.9
30.1
27.4
26.3
25.7
20.5
f1 (ppm)

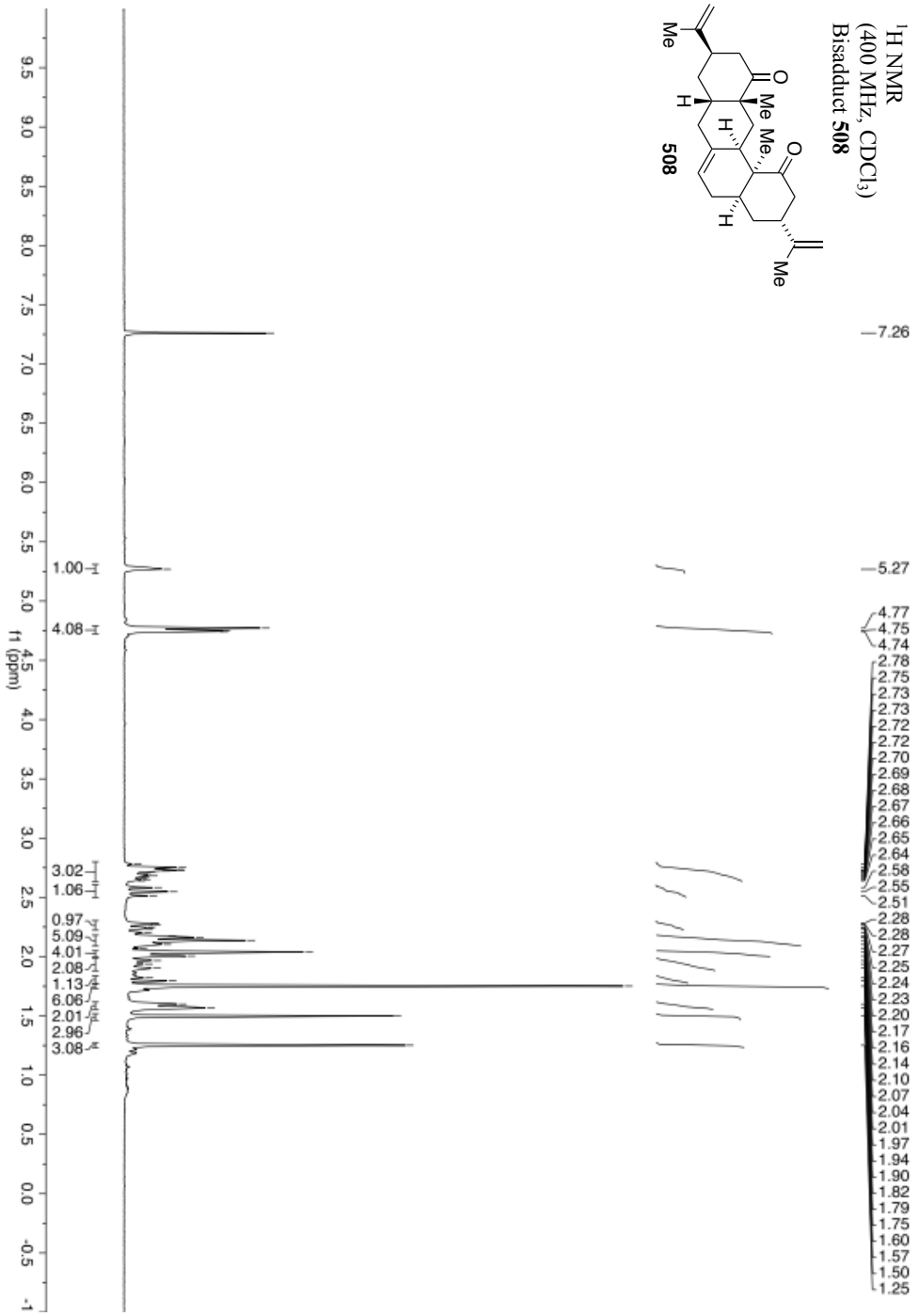
^{1}H NMR
(400 MHz, $CDCl_3$)
Bisadduct **508**
508
Me
H
O
Me
Me
H
O
H
Me
7.26
5.27
4.77
4.75
4.74
2.78
2.75
2.73
2.73
2.72
2.72
2.70
2.69
2.68
2.67
2.66
2.65
2.64
2.58
2.55
2.51
2.28
2.28
2.27
2.25
2.24
2.23
2.20
2.17
2.16
2.14
2.10
2.07
2.04
2.01
1.97
1.94
1.90
1.82
1.79
1.75
1.60
1.57
1.50
1.25
1.00
4.08
3.02
1.06
0.97
5.09
4.01
2.08
1.13
6.06
2.01
2.96
3.08
f1 (ppm)

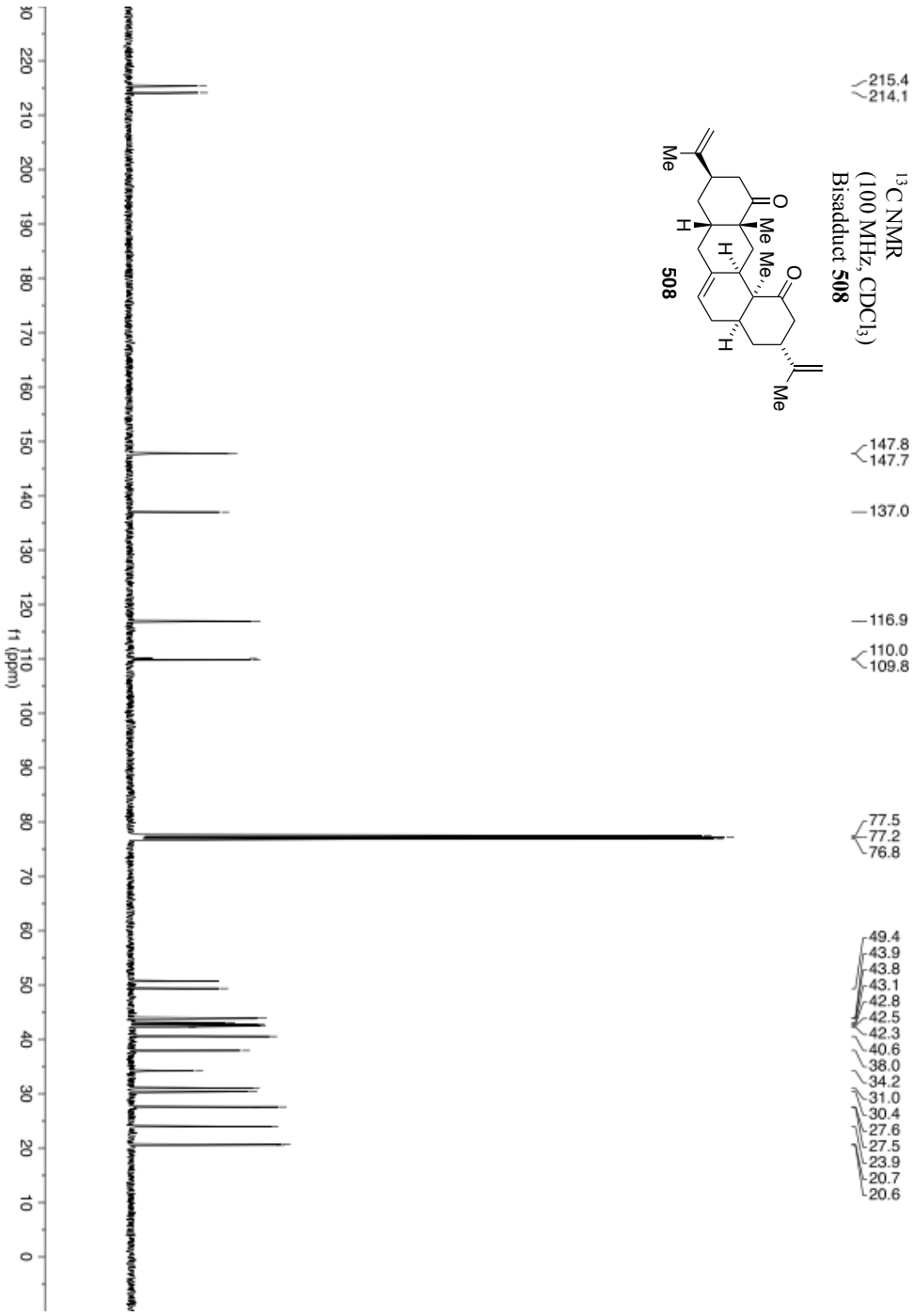
^{13}C NMR
(100 MHz, CDCl$_3$)
Bisadduct **508**
508
215.4
214.1
147.8
147.7
137.0
116.9
110.0
109.8
77.5
77.2
76.8
49.4
43.9
43.8
43.1
42.8
42.5
42.3
40.6
38.0
34.2
31.0
30.4
27.6
27.5
23.9
20.7
20.6
f1 (ppm)

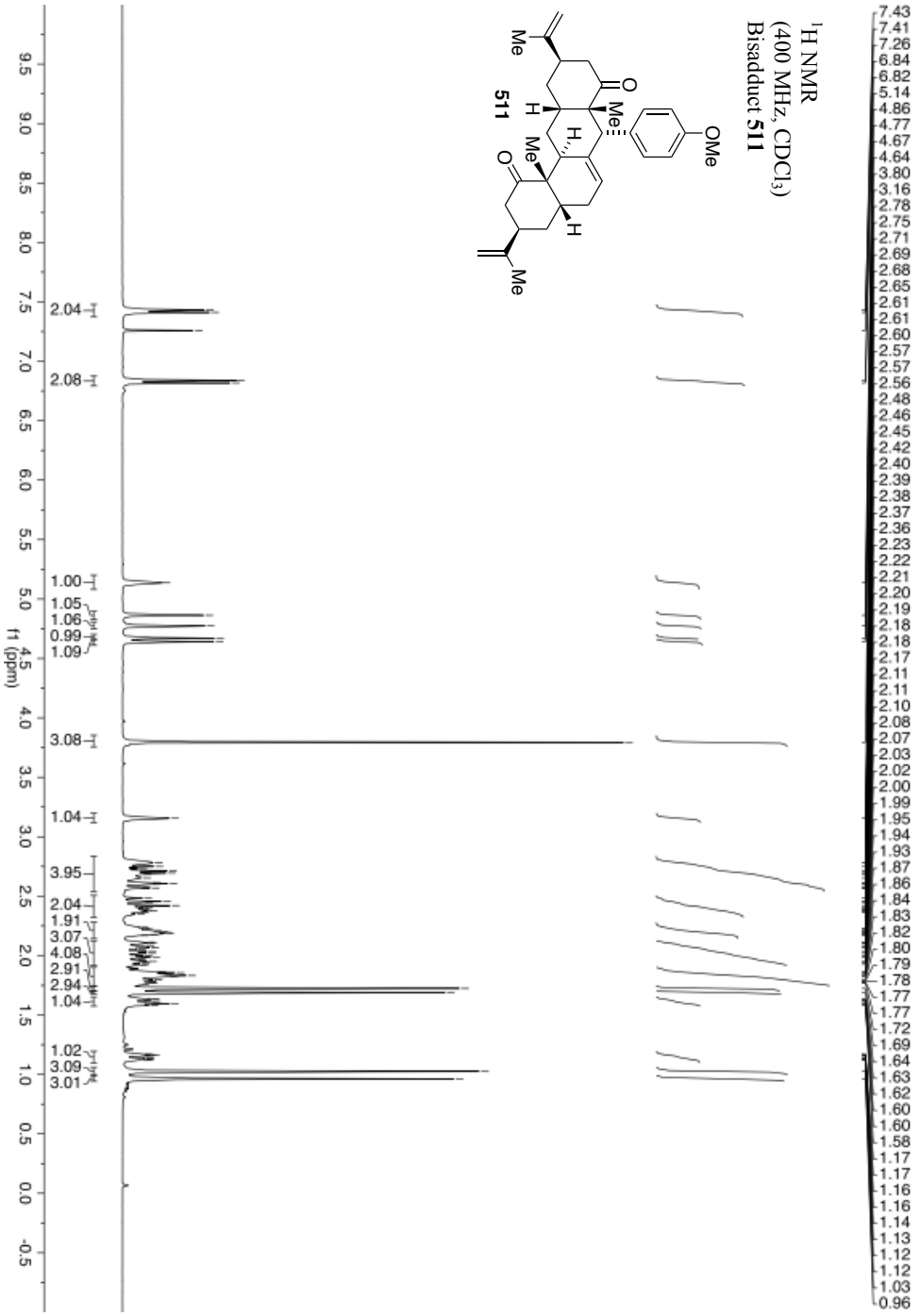
^{1}H NMR
(400 MHz, $CDCl_3$)
Bisadduct **511**
511
OMe
Me
O
H
f1 (ppm)

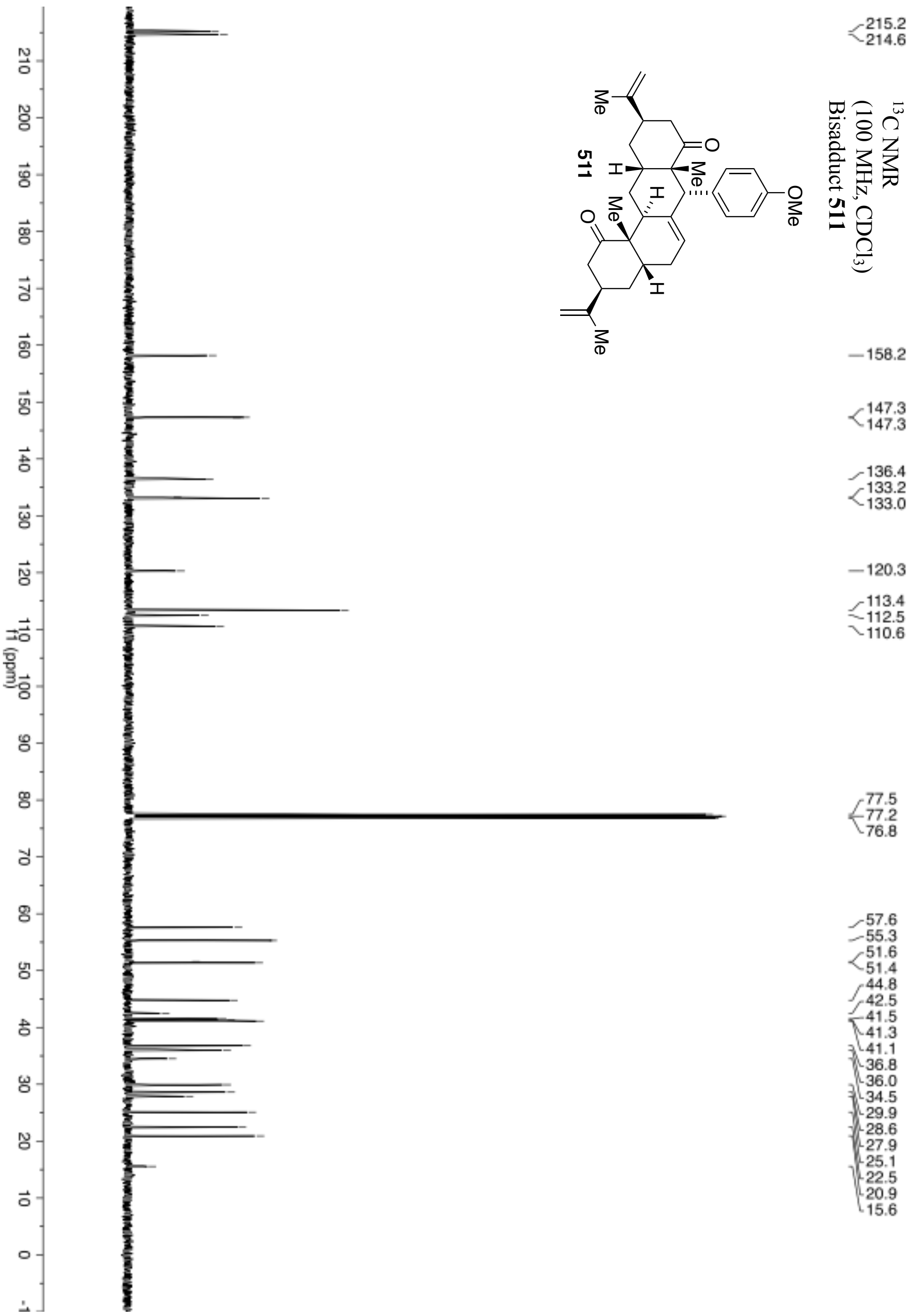
13C NMR
(100 MHz, CDCl3)
Bisadduct 511
OMe
Me
H
O
Me
511
215.2
214.6
158.2
147.3
147.3
136.4
133.2
133.0
120.3
113.4
112.5
110.6
77.5
77.2
76.8
57.6
55.3
51.6
51.4
44.8
42.5
41.5
41.3
41.1
36.8
36.0
34.5
29.9
28.6
27.9
25.1
22.5
20.9
15.6
f1 (ppm)

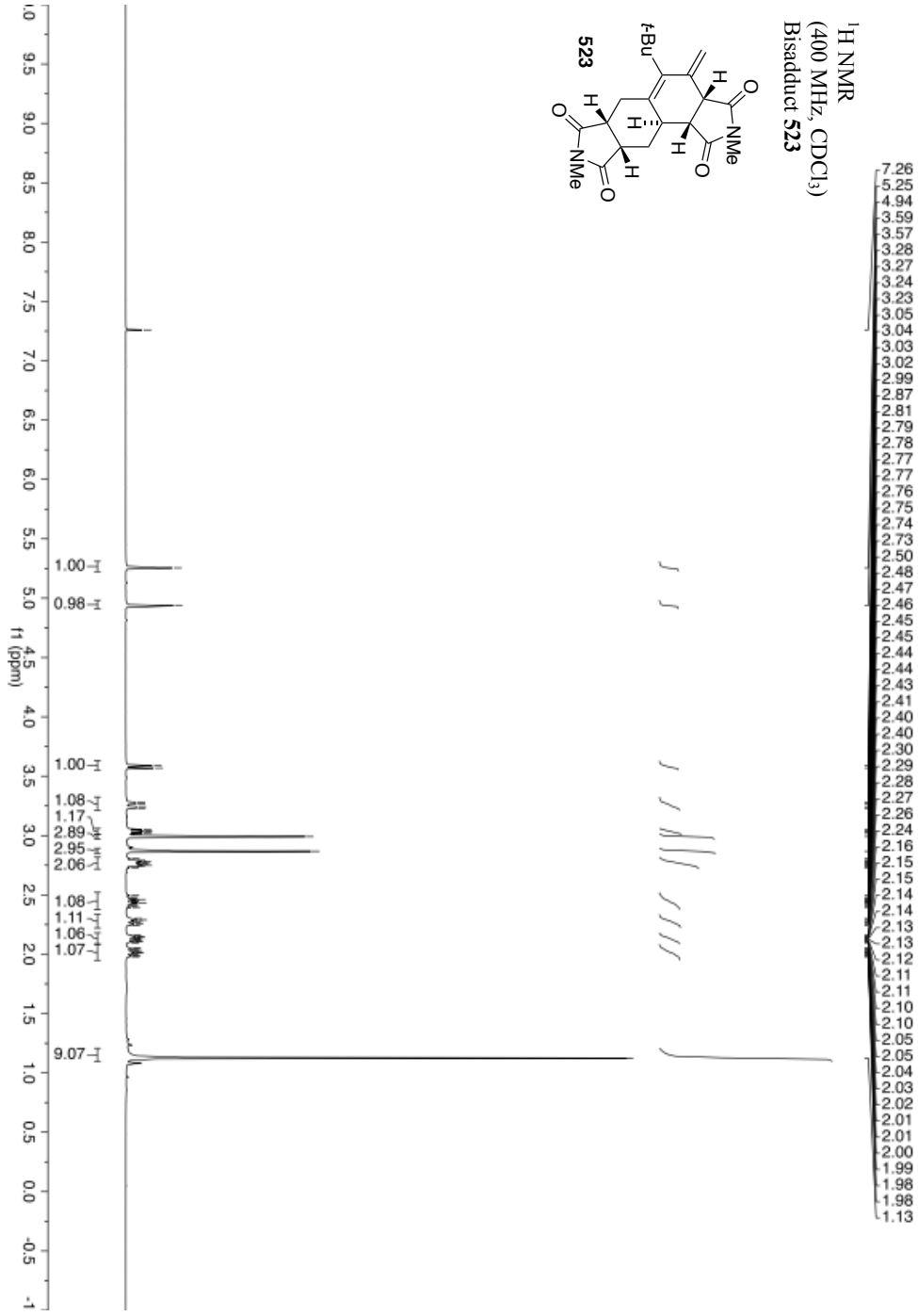
^{1}H NMR
(400 MHz, $CDCl_3$)
Bisadduct **523**
523
tBu
NMe
NMe
f1 (ppm)
1.00
0.98
1.00
1.08
1.17
2.89
2.95
2.06
1.08
1.11
1.06
1.07
9.07

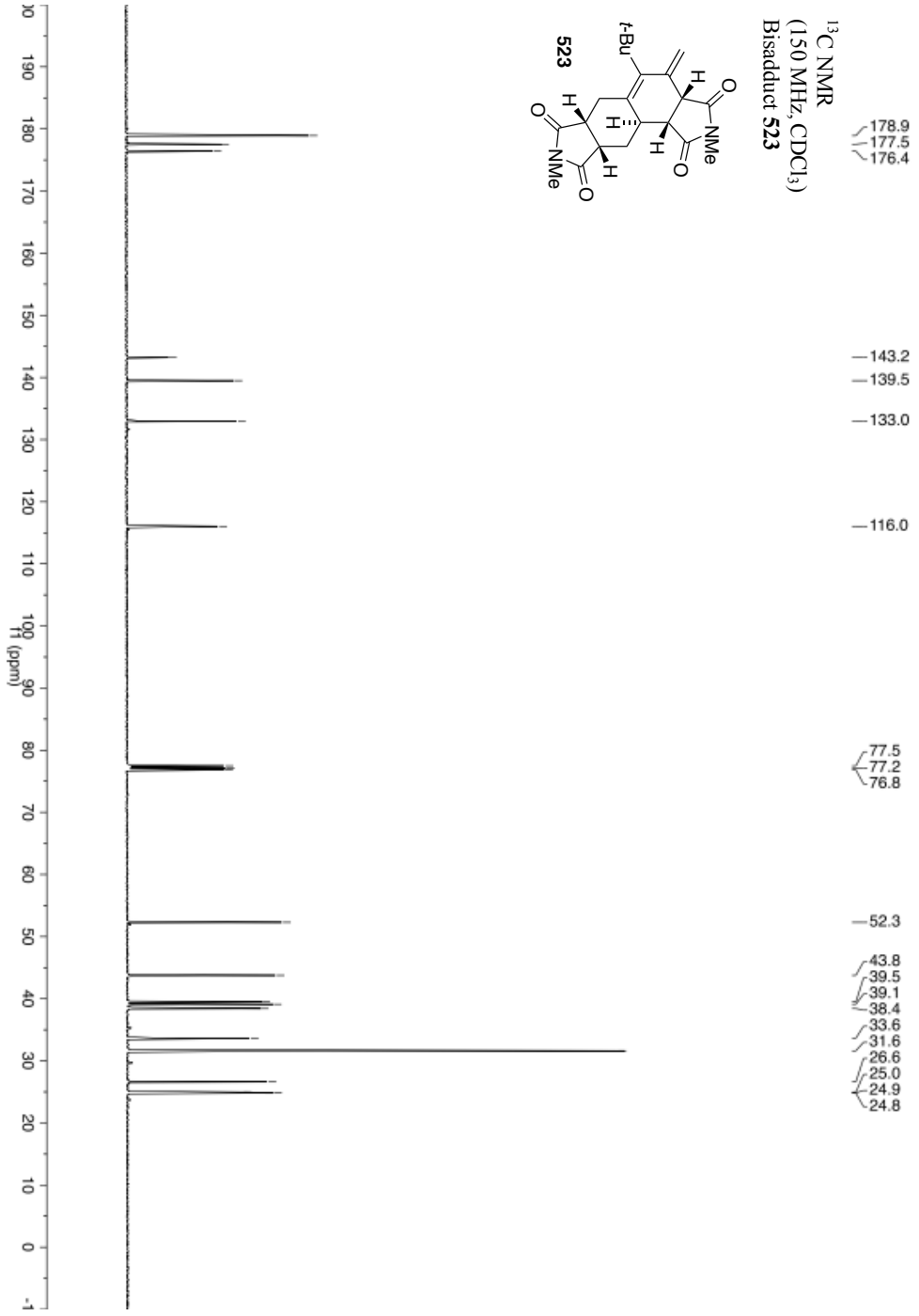
^{13}C NMR
(150 MHz, $CDCl_3$)
Bisadduct **523**
523
t-Bu
NMe
NMe
178.9
177.5
176.4
143.2
139.5
133.0
116.0
77.5
77.2
76.8
52.3
43.8
39.5
39.1
38.4
33.6
31.6
26.6
25.0
24.9
24.8
f1 (ppm)

^{1}H NMR
(400 MHz, $CDCl_3$)
Tetracycle **524**

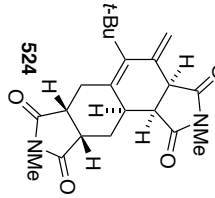

524

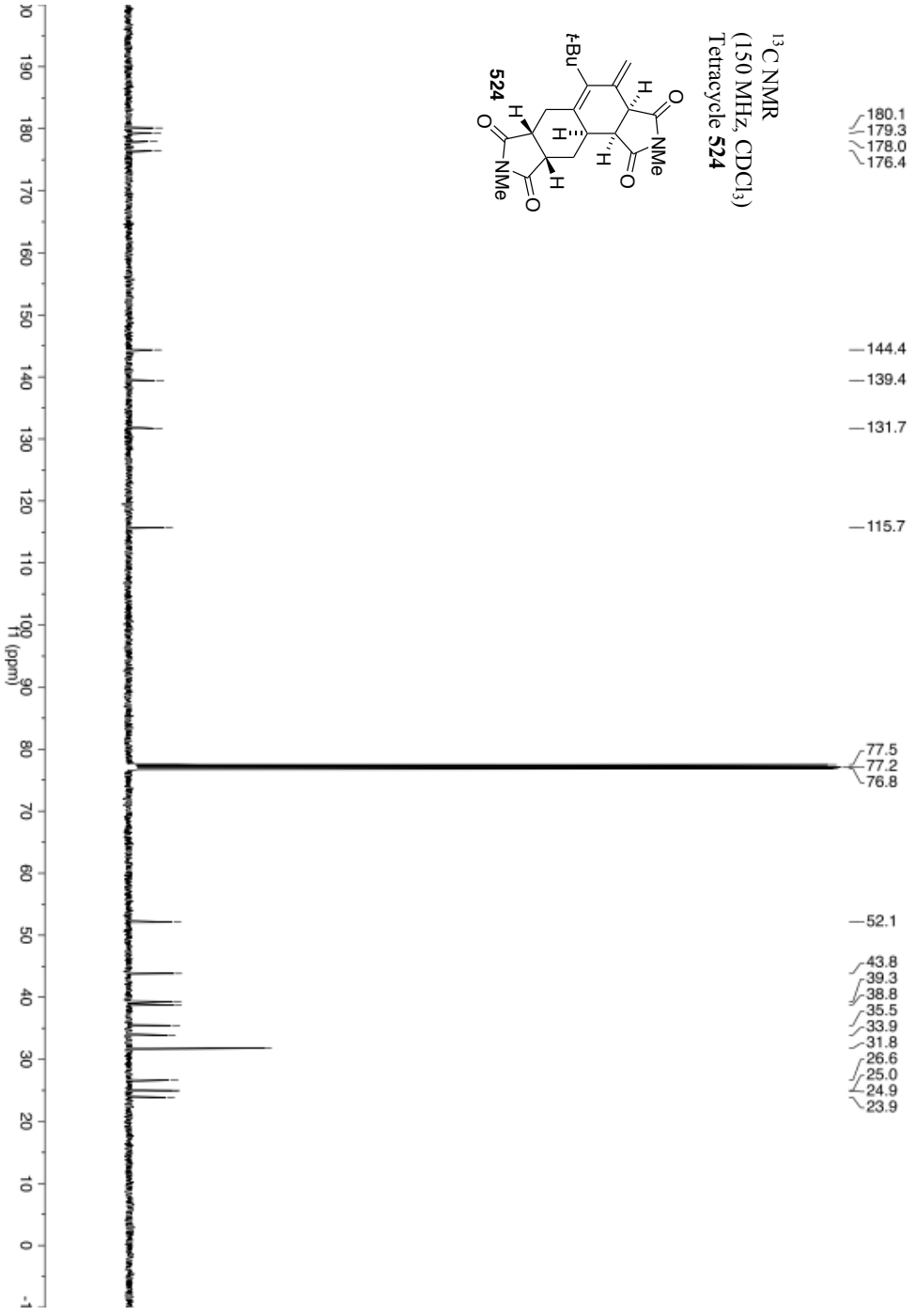
^{13}C NMR
(150 MHz, $CDCl_3$)
Tetracycle **524**
524
t-Bu
NMe
NMe
180.1
179.3
178.0
176.4
144.4
139.4
131.7
115.7
77.5
77.2
76.8
52.1
43.8
39.3
38.8
35.5
33.9
31.8
26.6
25.0
24.9
23.9
f1 (ppm)

7

References

This chapter provides references for Chapters 1 through 6.

7.1 References for Chapters 1, 3, 4 and 6

The following section provides references for Chapters 1, 3, 4 and 6.

[1] P. S. Baran, Natural Product Total Synthesis: As Exciting as Ever and Here to Stay. *J. Am. Chem. Soc.* **140**, 4751-4755 (2018).
[2] (a) P. A. Wender, B. L. Miller, *Organic Synthesis: Theory and Applications*. (JAI Press, Greenwich, 1993), vol. 2. (b) P. A. Wender, B. L. Miller, Synthesis at the Molecular Frontier. *Nature* **460**, 197-201 (2009).
[3] N. J. Green, M. S. Sherburn, Multi-Bond Forming Processes in Efficient Synthesis. *Aust. J. Chem*. **66**, 267-283 (2013).
[4] L. F. Tietze, G. Brasche, K. M. Gericke, *Domino Reactions in Organic Synthesis*. (Wiley-VCH, Weinheim, 1st ed., 2006).
[5] W. S. Johnson, M. B. Gravestock, B. E. McCarry, Acetylenic Bond Participation in Biogenetic-Like Olefinic Cyclizations. II. Synthesis of *dl*-Progesterone. *J. Am. Chem. Soc.* **93**, 4332-4334 (1971).
[6] M. J. Sowden, M. S. Sherburn, Four-Step Total Synthesis of Selaginpulvilin D. *Org. Lett.* **19**, 636-637 (2017).
[7] W. S. Johnson, L. Werthemann, W. R. Bartlett, T. J. Brocksom, T.-T. Li, D. J. Faulkner, M. R. Petersen, A Simple Stereoselective Version of the Claisen Rearrangement Leading to *trans*-Trisubstituted Olefinic Bonds. Synthesis of Squalene. *J. Am. Chem. Soc*. **92**, 741-743 (1970).
[8] O. Diels, K. Alder, Synthesen in der Hydroaromatischen Reihe. *Liebigs Ann*. **460**, 98-122 (1928).
[9] H. Hopf, M. S. Sherburn, Dendralenes Branch Out: Cross-Conjugated Oligoenes Allow the Rapid Generation of Molecular Complexity. *Angew. Chem. Int. Ed*. **51**, 2298-2338 (2012).
[10] (a) A. T. Blomquist, J. A. Verdol, 2-Vinyl-1,3-butadiene. *J. Am. Chem. Soc*. **77**, 81-83 (1955). (b) H. Hopf, The Dendralenes—a Neglected Group of Highly Unsaturated Hydrocarbons. *Angew. Chem. Int. Ed*. **23**, 948-960 (1984).
[11] S. Fielder, D. D. Rowan, M. S. Sherburn, First Synthesis of the Dendralene Family of Fundamental Hydrocarbons. *Angew. Chem. Int. Ed.* **39**, 4331-4333 (2000).
[12] E. G. Mackay, M. S. Sherburn, Demystifying the Dendralenes. *Pure Appl. Chem*. **85**, 1227-1239 (2013).
[13] T. A. Bradford, A. D. Payne, A. C. Willis, M. N. Paddon-Row, M. S. Sherburn, Practical Synthesis and Reactivity of [3]Dendralene. *J. Org. Chem*. **75**, 491-494 (2010).
[14] N. A. Miller, A. C. Willis, M. S. Sherburn, Formal Total Synthesis of Triptolide. *Chem. Commun*., 1226-1228 (2008).
[15] R. M. Wilson, W. S. Jen, D. W. C. MacMillan, Enantioselective Organocatalytic Intramolecular Diels-Alder Reactions. The Asymmetric Synthesis of Solanapyrone D. *J. Am. Chem. Soc*. **127**, 11616-11617 (2005).
[16] (a) H. Nakamura, J. Kobayashi, M. Kobayashi, Y. Ohizumi, Y. Hirata, Xestoquinone. A Novel Cardiotonic Marine Natural Product Isolated from the Okinawan Sea Sponge Xestospongia Sapra. *Chem. Lett*. 713-716 (1985). (b) D. M. Roll, P. J. Scheuer, G. K. Matsumoto, J. Clardy, Halenaquinone, a Pentacyclic Polyketide from a Marine Sponge. *J. Am. Chem. Soc.* **105**, 6177-6178 (1983).
[17] F. J. Schmitz, S. J. Bloor, Xesto- and Halenaquinone Derivatives from a Sponge, Adocia sp., from Truk Lagoon. *J. Org. Chem*. **53**, 3922-3925 (1988).
[18] (a) T. Kubota, Y. Kon, J. I. Kobayashi, Xestosaprol C, a New Pentacyclic Hydroquinone Sulfate from a Marine Sponge Xestospongia sapra. *Heterocycles* **76**, 1571-1575 (2008). (b) J. I. Kobayashi, T. Hirase, H. Shigemori, M. Ishibashi, New Pentacyclic Compounds from the Okinawan Marine Sponge Xestospongia Sapra. *J. Nat. Prod*. **55**, 994-998 (1992). (c) N. Millan-Anguinaga, I. E. Soria-Mercado, P.

Williams, Xestosaprol D and E from the Indonesian Marine Sponge Xestospongia sp. *Tet. Lett*. **51**, 751-753 (2010). (d) J. Dai, A. Sorribas, W. Y. Yoshida, M. Kelly, P. G. Williams, Xestosaprols from the Indonesian Marine Sponge Xestospongia sp. *J. Nat. Prod*. **73**, 1188-1191 (2010). (e) Y.-J. Lee, C.-K. Kim, S.-K. Park, J. S. Kang, J.-S. Lee, H. J. Shin, H.-S. Lee, Halenaquinone Derivatives from Tropical Marine Sponge Xestospongia sp. *Heterocycles* **85**, 895-901 (2012). (f) R. M. Centko, A. Steino, F. I. Rosell, B. O. Patrick, N. de Voogd, A. G. Mauk, R. J. Andersen, Indoleamine 2,3-Dioxygenase Inhibitors Isolated from the Sponge Xestospongia vansoesti: Structure Elucidation, Analogue Synthesis, and Biological Activity. *Org. Lett*. **16**, 6480-6483 (2014). (g) G. P. Concepcion, T. A. Foderaro, G. S. Eldredge, E. Lobkovsky, J. Clardy, L. R. Barrows, C. M. Ireland, Topoisomerase II-Medicated DNA Cleavage by Adocia- and Xestoquinones from the Philippine Spnonge Xestospongia sp. *J. Med. Chem.* **38**, 4503-4507 (1995).

[19] M. Nakamura, T. Kakauda, J. Qi, M. Hirata, T. Shintani, Y. Yoshioka, T. Okamoto, Y. Oba, H. Nakamura, M. Ojika, Novel Relationship Between the Antifungal Activity and Cytotoxicity of Marine-Derived Metabolite Xestoquinone and Its Family. *Biosci. Biotechnol. Biochem*. **69**, 1749-1752 (2005).

[20] D. Laurent, V. Jullian, A. Parenty, M. Knibiehler, D. Dorin, S. Schmitt, O. Lozach, N. Lebouvier, M. Frostin, F. Alby, S. Maurel, C. Doerig, L. Meijer, M. Sauvain, Antimalarial Potential of Xestoquinone, a Protein Kinase Inhibitor Isolated from a Vanuatu Marine Sponge Xestospongia sp. *Bioorg. Med. Chem*. **14**, 4477-4482 (2006).

[21] M. Ito, Y. Hirata, H. Nakamura, Y. Ohizumi, Xestoquinone, Isolated from Sea Sponge, Causes Ca^{2+} Release through Sulfhydryl Modification from Skeletal Muscle Scaroplasmic Reticulum. *J. Pharmacol. Exp. Ther*. **291**, 976-981 (1999).

[22] H. Sakamoto, K. Furukawa, K. Matsunaga, H. Nakamura, Y. Ohizumi, Xestoquinone Activates Skeletal Muscle Actomyosin ATPase by Modification of the Specific Sulfhydryl Group in the Myosin Head Probably Distinct from Sulfhydryl Groups SH1 and SH2. *Biochemistry* **34**, 12570-12575 (1995).

[23] M. Kobayashi, H. Nakamura, J. Kobayashi, Y. Ohizumi, Mechanism of Inotropic Action of Xestoquinone, a Novel Cardiotonic Agent Isolated from a Sea Sponge. *J. Pharmacol. Exp. Ther*. **257**, 82-89 (1991).

[24] (a) K. A. Alvi, J. Rodriguez, M. C. Diaz, R. Moretti, R. S. Wilhelm, R. H. Lee, D. L. Slate, P. Crews, Protein Tyrosine Kinase Inhibitory Properties of Planar Polycyclics Obtained from the Marine Sponge Xestospongia cf. carbonaria and from Total Synthesis. *J. Org. Chem.* **58**, 4871-4880 (1993). (b) R. H. Lee, D. L. Slate, R. Moretti, K. A. Alvi, P. Crews, Marine Sponge Polyketide Inhibitors of Protein Tyrosine Kinase. *Biochem. Biophys. Res. Comm*. **184**, 765-772 (1992).

[25] H. Fujiwara, K. Matsunaga, M. Saito, S. Hagiya, K.-I. Furukawa, H. Nakamura, Y. Ohizumi, Halenaquinone, a Novel Phosphatidylinositol 3-Kinase Inhibitor from a Marine Sponge, Induces Apoptosis in PC12 Cells. *Eur. J. Pharmacol*. **413**, 37-45 (2001).

[26] L. C. Creemer, H. A. Kirst, C. J. Vlahos, R. M. Schultz, Synthesis and in Vitro Evaluation of New Wortmannin Esters: Potent Inhibitors of Phosphatidylinositol 3-Kinase. *J. Med. Chem.* **39**, 5021-5024 (1996).

[27] I. A. Gorshkova, B. A. Gorshkov, S. A. Fedoreev, V. A. Stonik, Halenaquinol, a Natural Cardioactive Pentacyclic Hydroquinone, Interacts with Sulfhydryls on Rat Brain Na^+,K^+-ATPase. *Comparative Biochemistry and Physiology Part C* **128**, 531-540 (2001).

[28] (a) S. Cao, C. Foster, M. Brisson, J. S. Lazo, D. G. Kingston, Halenaquinone and Xestoquinone Derivatives, Inhibitors of Cdc25B Phosphatase from a Xestospongia sp.

Bioorg Med Chem **13**, 999-1003 (2005). (b) M. Nakamura, T. Kakuda, Y. Oba, M. Ojika, H. Nakamura, Synthesis of Biotinylated Xestoquinone that Retains Inhibitory Activity Against Ca^{2+} ATPase of Skeletal Muscle Myosin. *Bioorg. Med. Chem*. **11**, 3077-3082 (2003).

[29] J. Rodriguez, E. Quinoa, R. Riguera, B. M. Peters, L. M. Abrell, P. Crews, The Structures and Stereochemistry of Cytotoxic Sesquiterpene Quinones from Dactylospongia elegans. *Tetrahedron* **48**, 6667-6680 (1992).

[30] (a) W. Fenical, J. J. Sims, D. Squatrito, R. M. Wing, P. Radlick, Marine Natural Products. VII. Zonarol and Isozonarol, Fungitoxic Hydroquinones from the Brown Seaweed Dictyopteris zonarioides. *J. Org. Chem*. **38**, 2383-2386 (1973). (b) *Marine Natural Products. Chemical and Biological Perspectives*. (Academic Press, New York, 1978), vol. 1. (c) M. A. Kienzler, I. Total Synthesis of Smenochromene B and Halenaquinone and II. Studies on the Chemical and Biological Properties of Azobenzene Photoswitches, UC Berkeley, Berkeley (2010).

[31] N. Harada, T. Sugioka, H. Uda, T. Kuriki, M. Kobayashi, I. Kitagawa, Total Synthesis, Absolute Configuration, and Later Isolation of (–)-Prehalenaquinone, a Putative Biosynthetic Precursor to the Marine Natural Products Halenaquinone and Xestoquinone. *J. Org. Chem.* **59**, 6606-6613 (1994).

[32] G. M. Schwarzwalder, C. D. Vanderwal, Strategies for the Synthesis of the Halenaquinol and Xestoquinol Families of Natural Products. *Eur. J. Org. Chem*. **2017**, 1567-1577 (2017).

[33] (a) K. M. Muller, B. A. Keay, Regiospecific Synthesis of the C and D Rings of Viridin. *Synlett*. **8**, 1236-1238 (2008). (b) A. D. Findlay, A. Gebert, I. A. Cade, M. G. Banwell, The Enantiocontrolled Synthesis of a Highly Functionalized Cyclohexenone Related to the A-Ring of the Furanosteroid Viridin. *Aus. J. Chem*. **62**, 1173-1180 (2009). (c) Y. Yamaguchi, K. Hayakawa, K. Kanematsu, An Efficient Furan Ring Transfer Reaction: A Versatile Key Intermediate Leading to the Basic Skeleton of Naturally Occurring Fused Furans. *J. Chem. Soc*., 515-516 (1987). (d) B. H. Norman, J. Paschal, C. J. Vlahos, Synthetic Studies on the Furan Ring of Wortmannin. *Bioorg. Med. Chem. Lett*. **5**, 1183-1186 (1995). (e) R. Carlini, K. Higgs, C. Older, S. Randhawa, R. Rodrigo, Intramolecular Diels-Alder and Cope Reactions of *o*-Quinonoid Monoketals and Their Adducts: Efficient Syntheses of (+/–)-Xestoquinone and Heterocycles Related to Viridin. *J. Org. Chem*. **62**, 2330-2231 (1997). (f) F. E. S. Souza, R. Rodrigo, Progress Towards Viridin: Synthesis of the Pentacyclic Furanosteroid Ring System via *o*-Benzoquinonoid Cycloadditions. *Chem. Commun*., 1947-1948 (1999). (g) E. H. Sessions, R. T. O'Connor, P. A. Jacobi, Furanosteroid Studies. Stereoselective Synthesis of the A,B,E-Ring Core of Wortmannin. *Org. Lett.* **9**, 3221-3224 (2007). (h) S. Honzawa, T. Mizutani, M. Shibasaki, Synthetic Studies on (+)-Wortmannin. An Asymmetric Construction of an Allylic Quaternary Carbon Center by a Heck Reaction. *Tet. Lett*. **40**, 311-314 (1999). (i) C. A. Broka, B. Ruhland, Synthetic Studies on Wortmannin and 1l-Desacetoxywortmannin. *J. Org. Chem*. **57**, 4888-4894 (1992).

[34] P. Wipf, R. J. Halter, Chemistry and Biology of Wortmannin. *Org. Biomol. Chem*. **3**, 2053-2061 (2005).

[35] (a) N. Harada, T. Sugioka, Y. Ando, H. Uda, T. Kuriki, Total Synthesis of (+)-Halenaquinol and (+)-Halenaquinone. Experimental Proof of Their Absolute Stereostructures Theoretically Determined. *J. Am. Chem. Soc*. **110**, 8483-8487 (1988). (b) N. Harada, T. Sugioka, H. Uda, T. Kuriki, Total Synthesis and Absolute Stereochemistry of (+)-Xestoquinone and Xestoquinol. *J. Org. Chem*. **55**, 3158-3163 (1990).

[36] K. Kanematsu, S. Soejima, G. Wang, Formal Total Synthesis of Xestoquinone via Furan Ring Transfer Reaction Strategy. *Tetrahedron Lett*. **32**, 4761-4764 (1991).

[37] H. S. Sutherland, K. C. Higgs, N. J. Taylor, R. Rodrigo, Isobenzofurnas and Ortho-Benzoquinone Monoketals in Syntheses of Xestoquinone and its 9- and 10-Methoxy Derivatives. *Tetrahedron* **57**, 309-317 (2001).

[38] M. A. Kienzler, S. Suseno, D. Trauner, Vinyl Quinones as Diels-Alder Dienes: Concise Synthesis of (–)-Halenaquinone. *J. Am. Chem. Soc*. **130**, 8604-8605 (2008).

[39] S. P. Maddaford, N. G. Andersen, W. A. Cristofoli, B. A. Keay, Total Synthesis of (+)-Xestoquinone Using an Asymmetric Palladium-Catalyzed Polyene Cyclization. *J. Am. Chem. Soc*. **118**, 10766-10773 (1996).

[40] (a) F. Miyazaki, K. Uotsu, M. Shibasaki, Silver Salt Effects on an Asymmetric Heck Reaction. Catalytic Asymmetric Total Synthesis of (+)-Xestoquinone. *Tetrahedron* **54**, 13073-13078 (1998). (b) A. Kojima, T. Takemoto, M. Sodeoka, M. Shibasaki, Catalytic Asymmetric Synthesis of Halenaquinone and Halenaquinol. *J. Org. Chem*. **61**, 4876-4877 (1996). (c) A. Kojima, T. Takemoto, M. Sodeoka, M. Shibasaki, Catalytic Asymmetric Synthesis of Halenaquinone and Halenaquinol. *Synthesis* **1998**, 581-589 (1998). (d) M. Shibasaki, A. Kojima, S. Shimizu, Catalytic Asymmetric Synthesis of Natural Products with Heterocyclic Rings. *J. Heterocyclic Chem.* **35**, 1057-1064 (1998).

[41] S. Goswami, K. Harada, M. F. El-Mansy, R. Lingampally, R. G. Carter, Enantioselective Synthesis of (–)-Halenaquinone. *Angew. Chem. Int. Ed*. **57**, 9117-9121 (2018).

[42] Y. Yamaguchi, N. Tatsuta, S. Soejima, K. Hayakawa, K. Kanematsu, 4,5,6,7-Tetrahydroisobenzofuran-5-one as a Versatile Building Block Leading to the Basic Skeleton of Naturally Occurring Fused Furans. *Heterocycles* **30**, 223-226 (1990).

[43] H. S. Sutherland, F. E. S. Souza, R. G. A. Rodrigo, A Short Synthesis of (±)-Halenaquinone. *J. Org. Chem*. **66**, 3639-3641 (2001).

[44] (a) M. Azadi-Ardakani, T. W. Wallace, 3,6-Dimethoxybenzocyclobutenone: A Reagent for Quinone Synthesis. *Tetrahedron* **44**, 5939-5952 (1988). (b) M. Azadi-Ardakani, R. Hayes, T. W. Wallace, Preparation of Functionalised Anthra[*b*]cyclobutenes from 3,6-Dimethoxybenzocyclobutenone. *Tetrahedron* **46**, 6851-6858 (1990).

[45] (a) C. C. Hughes, J. J. Kennedy-Smith, D. Trauner, Synthetic Studies toward the Guanacastepenes. *Org. Lett.* **5**, 4113-4115 (2003). (b) A. K. Miller, C. C. Hughes, J. J. Kennedy-Smith, S. N. Gradl, D. Trauner, Total Synthesis of (–)-Heptemerone B and (–)-Guanacastepene E. *J. Am. Chem. Soc*. **128**, 17057-17062 (2006).

[46] D. Nasipuri, G. Pyne, D. N. Roy, R. Bhattacharya, P. Dutt, Synthetic Studies in the Diterpene Series. Part VI. Synthesis of Some Hydrophenalene Derivatives. *J. Chem. Soc*., 2146-2150 (1964).

[47] B. Wakefield, R. J. Halter, P. Wipf, Synthesis of (±)-Thiohalenaquinone by Iterative Metalations of Thiophene. *Org. Lett*. **9**, 3121-3124 (2007).

[48] (a) N. Toyooka, H. Nagaoka, H. Kakuda, H. Nemoto, Rapid Access to the Potential Intermediate for the Synthesis of Halenaquinol and Halenaquinone. *Synlett*. **7**, 1123-1124 (2001). (b) N. Toyooka, M. Nagaoka, E. Sasaki, H. Qin, H. Kakuda, H. Nemoto, Model Studies Toward the Total Synthesis of Halenaquinol and Halenaquinone. *Tetrahedron* **58**, 6097-6101 (2002).

[49] C. M. Ahn, H. B. Woo, A Model Study Toward the Synthesis of Xestoquinone. *J. Korean Chem. Soc.* **47**, 354-362 (2003).

[50] N. Harada, T. Sugioka, T. Soutome, N. Hiyoshi, H. Uda, T. Kuriki, Synthesis and Absolute Stereoehemistry of (+)-Adociaquinones A and B. *Tetradehron: Asymmetry* **6**, 375-376 (1995).

[51] T. Sato, K. Tamura, Metal-Catalyzed Organic Photoreactions. Photoreaction of Olefins with 2-Chloroacetophenone in the Presence of Silver Trifluoromethanesulfonate. *Tet. Lett*. **25**, 1821-1824 (1984).

[52] Y. Shi, Y. Ji, K. Xin, S. Gao, Total Synthesis of (–)-Xestosaprol N and O. *Org. Lett*. **20**, 732-735 (2018).

[53] C. L. Arthurs, G. A. Morris, M. Piacenti, R. G. Pritchard, I. J. Stratford, T. Tatic, R. C. Whitehead, K. F. Williams, N. S. Wind, The synthesis of 2-Oxyalkyl-cyclohex-2-enones, Related to the Bioactive Natural Products COTC and Antheminone A, Which Possess Anti-Tumour Properties. *Tetrahedron* **66**, 9049-9060 (2010).

[54] D. Knueppel, J. Yang, B. Cheng, D. Mans, S. F. Martin, Total Synthesis of the Aglycone of IB-00208. *Tetrahedron* **71**, 5741-5757 (2015).

[55] F. Wagner, K. Harms, U. Koert, Hauser−Heck: Efficient Synthesis of γ‑Aryl-β-ketoesters en Route to Substituted Naphthalenes. *Org. Lett*. **17**, 5670-5673 (2015).

[56] S. Sato, M. Nakada, M. Shibasaki, The First Chemical Synthesis of Wortmannin by Starting from Hydrocortisone. *Tet. Lett*. **37**, 6141-6144 (1996).

[57] T. Mizutani, S. Honzawa, S. Tosaki, M. Shibasaki, Total Synthesis of (±)-Wortmannin. *Angew. Chem. Int. Ed*. **41**, 4680-4682 (2002).

[58] (a) A. S. Caselli, D. J. Collins, G. M. Stone, The Structure and Function of Oestrogens. III. 3,17β-Dihydroxy-6-oxaoestra-1,3,5(10),8(9)-tetraen-7-one and Related Steroidal Coumarins. *Aust. J. Chem*. **45**, 799-808 (1982). (b) G. Stork, R. N. Guthikonda, A General Synthesis of Esters of Acryloyl Acetic Acid and Their Homologs. *Tet. Lett*. **13**, 2755-2758 (1972). (c) G. Nomine, G. Amiard, V. Torelli, Catalytic Hydrogenation of Tetrahydroindane Structures Intermediates in Total Synthesis of Steroids *Bull. Soc. Chim. Fr*., 3664 (1968).

[59] Y. Guo, T. Quan, Y. Lu, T. Luo, Enantioselective Total Synthesis of (+)-Wortmannin. *J. Am. Chem. Soc*. **139**, 6815-6818 (2017).

[60] J. L. Frie, C. S. Jeffrey, E. J. Sorensen, A Hypervalent Iodine-Induced Double Annulation Enables a Concise Synthesis of the Pentacyclic Core Structure of the Cortistatins. *Org. Lett*. **11**, 5394-5397 (2009).

[61] (a) G.-X. Li, J. Qu, Friedel–Crafts Alkylation of Arenes with Epoxides Promoted by Fluorinated Alcohols or Water. *Chem. Commun*. **46**, 2653-2655 (2010). (b) Y. Tian, X. Xu, L. Zhang, J. Qu, Tetraphenylphosphonium Tetrafluoroborate/1,1,1,3,3,3-Hexafluoroisopropanol (Ph_4PBF_4/HFIP) Effecting Epoxide-Initiated Cation-Olefin Polycyclizations. *Org. Lett*. **18**, 268-271 (2016).

[62] K. C. Mascall, P. A. Jacobi, Synthetic Studies on Furanosteroids. Functionalisation of Ring A of the Viridin Core. *Heterocycles* **88**, 1527-1538 (2014).

[63] E. A. Anderson, E. J. Alexanian, E. J. Sorensen, Synthesis of the Furanosteroidal Antibiotic Viridin. *Angew. Chem. Int. Ed*. **43**, 1998-2001 (2004).

[64] M. Del Bel, A. R. Abela, J. D. Ng, C. A. Guerrero, Enantioselective Chemical Syntheses of the Furanosteroids (–)-Viridin and (–)-Viridiol. *J. Am. Chem. Soc*. **139**, 6819-6822 (2017).

[65] D. Lucciola, B. A. Keay, Further Developments of an Enantioselective Palladium-Catalyzed Polyene Cyclization: Surprising Solvent and Ligand Effects. *Synlett*. **11**, 1618-1622 (2011).

[66] Y. Ji, Z. Xin, H. He, S. Gao, Total Synthesis of Viridin and Viridiol. *J. Am. Chem. Soc.* **141**, 16208-16212 (2019).

[67] A. Panda, R. G. Biswas, S. Pal, A Unified and Common Intermediate Strategy for the Asymmetric Total Synthesis of 3-Deoxy-neo-inositol and Conduritol E. *Tet. Lett.* **57**, 3625-3628 (2016).

[68] Y. Ji, Z. Xin, Y. Shi, H. He, S. Gao, Asymmetric Total Synthesis of Nodulisporiviridin E. *Org. Chem*. *Front*. **7**, 109-112 (2020).

[69] (a) T. M. Barros, C. D. Maycock, M. R. Ventura, Approaches to the Synthesis of (+)- and (–)-Epibatidine. *J. Chem. Soc., Perkin Trans. 1*, 166-173 (2001). (b) M. T. Barros, C. D. Maycock, M. R. Ventura, The Effect of DMSO on the Borohydride Reduction of a Cyclohexanone: A Formal Enantioselective Synthesis of (+)-Epibatidine. *Tet. Lett*. **40**, 557-560 (1999).

[70] (a) E. H. Sessions, P. A. Jacobi, Studies on the Synthesis of Furanosteroids. I. Viridin Models. *Org. Lett*. **8**, 4125-4128 (2006). (b) E. O. Onyango, P. A. Jacobi, Synthetic Studies on Furanosteroids: Construction of the Viridin Core Structure *via* Diels−Alder/Retro-Diels−Alder and Vinylogous Mukaiyama Aldol-Type Reaction. *J. Org. Chem*. **77**, 7411-7427 (2012).

[71] R. A. Miller, R. M. Smith, S. Karady, R. A. Reamer, A Direct Preparation of Silyl Oxazoles: a Dramatic Chemoselectivity Difference Between R_3SiOTf and R_3SiCl. *Tet. Lett*. **43**, 935-938 (2002).

[72] K. C. Mascall, P. A. Jacobi, Furanosteroid Studies. Improved Synthesis of the A,B,C,E-Ring Core of Viridin. *Tet. Lett.* **53**, 1620-1623 (2012).

[73] (a) B. Thirupathi, S. Breitler, K. Mahender Reddy, E. J. Corey, Acceleration of Enantioselective Cycloadditions Catalyzed by Second-Generation Chiral Oxazaborolidinium Triflimidates by Biscoordinating Lewis Acids. *J. Am. Chem. Soc*. **138**, 10842-10845 (2016). (b) K. Mahender Reddy, E. Bhimireddy, B. Thirupathi, S. Breitler, S. Yu, E. J. Corey, Cationic Chiral Fluorinated Oxazaborolidines. More Potent, Second-Generation Catalysts for Highly Enantioselective Cycloaddition Reactions. *J. Am. Chem. Soc.* **138**, 2443-2453 (2016). (c) S. Mukherjee, J. W. Yang, S. Hoffmann, B. List, Asymmetric Enamine Catalysis. *Chem. Rev*. **107**, 5471-5569 (2007).

[74] E. P. Farney, S. S. Feng, F. Schafers, S. E. Reisman, Total Synthesis of (+)-Pleuromutilin. *J. Am. Chem. Soc.* **140**, 1267-1270 (2018).

[75] I. Kerschgens, A. R. Rovira, R. Sarpong, Total Synthesis of (–)-Xishacorene B from (*R*)-Carvone Using a C−C Activation Strategy. *J. Am. Chem. Soc.* **140**, 9810-9813 (2018).

[76] M. Souweha Santos, A. Arab, M. ApSimon, A. G. Fallis, Diene-Transmissive Cycloadditions: Control of Monocycloaddition by Self-Assembly on a Lewis Acid Template. *Org. Lett.* **9**, 615-618 (2007).

[77] N. J. Green, A. L. Lawrence, G. Bojase, A. C. Willis, M. N. Paddon-Row, M. S. Sherburn, Domino Cycloaddition Organocascades of Dendralenes. *Angew. Chem. Int. Ed*. **52**, 8333-8336 (2013).

[78] J. George, M. S. Sherburn, Diene-Transmissive Enantioselective Diels–Alder Reactions and Sequences Involving Substituted Dendralenes. *J. Org. Chem*. **84**, 14712-14723 (2019).

[79] S. Woo, S. Legoupy, S. Parra, A. G. Fallis, A Diene Transmissive Diels−Alder Strategy for Oxygenated Nor-Steroid and Triterpenoid Skeletons. *Org. Lett.* **1**, 1013-1016 (1999).

[80] N. A. Miller, A. C. Willis, M. N. Paddon-Row, M. S. Sherburn, Chiral Dendralenes for Rapid Access to Enantiomerically Pure Polycycles. *Angew. Chem. Int. Ed.* **46**, 937-940 (2007).

[81] C. G. Newton, S. L. Drew, A. L. Lawrence, A. C. Willis, M. N. Paddon-Row, M. S. Sherburn, Pseudopterosin Synthesis from a Chiral Cross-Conjugated Hydrocarbon Through a Series of Cycloadditions. *Nat Chem* **7**, 82-86 (2015).
[82] J.-P. Tassara, M. Baudoin, in *Eur. Pat. Appl. EP646561*. (1995).
[83] K. M. Cergol, C. G. Newton, A. L. Lawrence, A. C. Willis, M. N. Paddon-Row, M. S. Sherburn, 1,1-Divinylallene. *Angew. Chem. Int. Ed*. **50**, 10425-10428 (2011).
[84] H. Toombs-Ruane, Organometallic Routes to Cross-Conjugated Hydrocarbons, Australian National University, Australia (2013).
[85] J. George, J. S. Ward, M. S. Sherburn, A General Synthesis of Dendralenes. *Chem. Sci*. **10**, 9969-9973 (2019).
[86] (a) U. Ravid, M. Bassat, E. Putievsky, Isolation and Determination of Optically Pure Carvone Enantiomers from Caraway (Carum carvi L.), Dill (Anethum graveolens L.) Spearmint (Mentha spicata L.) and Mentha longifolia (L.) Huds. *Flavour Frag. J*. **2**, 95-97 (1987). (b) *The Merck Index*. (Merck & Co., New Jersey, 1976). (c) *Fenaroli's Handbook of Flavour Ingredients.* (CRC Press, Cleveland Ohio, ed. 2nd, 1975), vol. 2.
[87] (a) L. Friedman, J. G. Miller, Odor Incongruity and Chirality. *Science* **172**, 1044-1046 (1971). (b) G. F. Russell, J. I. Hills, Odor Differences between Enantiomeric Isomers. Science **172**, 1043-1044 (1971). (c) T. J. Leitereg, D. G. Guadagni, J. Harris, T. R. Mon, R. Teranishi, Evidence for the Difference between the Odours of the Optical Isomers (+)- and (−)-Carvone. *Nature* **230**, 455-456 (1971).
[88] (a) E. C. Talenti, H. A. Taher, G. O. Ubiergo, Constituents of the Essential Oil of *Blepharocalyx tweediei*. *J. Nat. Prod*. **47**, 905-906 (1984). (b) A. I. R. Luz, M. G. B. Zoghbi, L. S. Ramos, J. G. S. Maia, M. L. Silva, Essential Oils of Some Amazonian *Zingiberaceae*, 3. Genera *Alpinia* and *Rengalmia*. *J. Nat. Prod*. **47**, 907-908 (1984). (c) A. J. MacLeod, N. M. Pieris, Volatile Aroma Constituents of Sri Lankan Ginger. *Phytochemistry* **23**, 353-359 (1984). (d) G. Fournier, A. Hadjiakhoondi, M. Leboeuf, A. Cave, J. Fourniat, B. Charles, Chemical and Biological Studies of *Xylopia longifolia* A. DC. Essential Oils. *J. Essent. Oil Res*. **5**, 403-410 (1993). (e) H. M. Sirat, L. F. Hong, S. H. Khaw, Chemical Compositions of the Essential Oil of the Fruits of *Amomum testaceum Ridl*. *J. Essent. Oil Res*. **13**, 86-87 (2011).
[89] R. F. Lowe, M. F. Russell, I. A. Southwell, Astartea, a New Source of (+)-(1S,5R)-Myrtenal. *J. Essent. Oil Res*. **17**, 683-685 (2005).
[90] M. Ito, M. Toyoda, G. Honda, Chemical Composition of Essential Oil of Perilla frutescens. *Nat. Med.* **53**, 32-36 (1999).
[91] (a) Y. Tsuchiya, S. Kikuo, Thermal Decomposition Products of Cellulose. *J. Appl. Polym. Sci.* **14**, 2003-2013 (1970). (b) Y. Halpern, R. Riffer, A. Broido, Levoglucosenone (1,6-anhydro-3,4-dideoxy-Δ^3-β-D-Pyranosen-2-one). Major Product of the Acid-Catalyzed Pyrolysis of Cellulose and Related Carbohydrates. *J. Org. Chem*. **38**, 204-209 (1973).
[92] M. B. Comba, Y. Tsai, A. M. Sarotti, M. I. Mangione, A. G. Suarez, R. A. Spanevello, Levoglucosenone and Its New Applications: Valorization of Cellulose Residues. *Eur. J. Org. Chem*. **2018**, 590-604 (2018).
[93] (a) G. R. Clemo, R. D. Haworth, E. Walton, The Constitution of Santonin. Part II. The Synthesis of Racemic demotropoSantonin. *J. Chem. Soc*., 1110-1115 (1930). (b) L. Ruzicka, A. Steiner, Polyterpene und Polyterpenoide LXXXIX. Synthese der Heptan-2,5,6-tricarbonsäure, eines Abbauproduktes des Santonins. *Helv. Chim. Acta* **17**, 614-621 (1934). (c) E. J. Corey, The Stereochemistry of Santonin, β-Santonin and Artemisin. *J. Am. Chem. Soc*. **77**, 1044-1045 (1955). (d) W. Cocker, T. B. H. McMurry, Stereochemical Relationships in the Eudesmane (Selinane) Group of

Sesquiterpenes. *Tetrahedron* **8**, 181-204 (1960). (e) J. D. M. Asher, G. A. Sim, The Stereochemistry of Isophotosantonic Lactone. *Proc. Chem. Soc. London*, 111-112 (1962). (f) J. D. M. Asher, G. A. Sim, The Stereochemistry of α-Santonin. *Proc. Chem. Soc. London* 335 (1962). (g) M. Nakazaki, H. Arakawa, The Absolute Configuration at C11 of Santonin. *Bull. Chem. Soc. Jpn* **37**, 464-467 (1964). (h) P. S. Pregosin, E. W. Randall, ^{13}C Fourier Studies. The Configurational Dependence of the Carbon-13 Chemical Shifts in Santonin Derivatives. *J. Chem. Soc. Perkin Trans*., 299-301 (1972). (i) J. E. Shillinger, Anthelmintic Properties of Santonin. *J. Argic. Res*. **34**, 839-845 (1927).

[94] (a) C. E. Angell, F. Fringuelli, F. Pizzo, B. Porter, A. Taticchi, E. Wenkert, Diels–Alder Reactions of Cycloalkenones. 7. Reactions of Carvone. *J. Org. Chem*. **50**, 4696-4698 (1985). (b) K. Otsubo, J. Inanaga, M. Yamaguchi, Lewis Acid-Promoted [4 + 2] Cycloaddition Reaction of 1-Phenyl-3-trimethylsilyloxy-1,3-butadiene with Cyclohexenones. *Memoirs of the Faculty of Science, Kyushu University, Series C: Chemistry* **17**, 119-122 (1989). (c) A. A. Haaksma, B. J. M. Jansen, A. De Groot, Lewis Acid Catalyzed Diels–Alder Reactions of S-(+)-Carvone with Silyloxy Dienes. Total Synthesis of (+)-α-Cyperone. *Tetrahedron* **48**, 3121-3130 (1992). (d) T. K. M. Shing, H. Y. Lo, T. C. W. Mak, Diels-Alder Reaction of R-(–)-carvone with Isoprene. *Tetrahedron* **55**, 4643-4648 (1999). (e) T. Inokuchi, M. Okano, T. Miyamoto, H. B. Madon, M. Takagi, Lewis Acid Catalyzed Procedure for Selective Conversion of the Carbocyclic Diels-Alder Adducts of Danishefsky's Diene to 2-Cyclohexenones and its Extension to their One-Pot Syntheses. *Synlett*. **11**, 1549-1552 (2000). (f) H. S. P. Rao, R. Murali, A. Taticchi, H. W. Scheeren, High-Pressure-Promoted Diels–Alder Reactions between Cycloalkenones and 3-Methylsulfanylfuran and 3-Phenylsulfanylfuran. *Eur. J. Org. Chem*. **15**, 2869-2876 (2001). (g) S. Dratch, T. Charnikhova, F. C. E. Saraber, B. J. M. Jansen, A. De Groot, A New Approach Toward the Synthesis of C,D-*cis* Coupled Steroid and C,D-*cis* coupled D-Homosteroid Skeletons. *Tetrahedron* **59**, 4287-4295 (2003). (h) T. K. M. Shing, C. M. Lee, H. Y. Lo, A Synthetic Approach Toward Taxol Analogs: Studies on the Construction of the CD Ring. *Tetrahedron* **60**, 9179-9197 (2004). (i) A. R. Angeles, D. C. Dorn, C. A. Kou, M. A. S. Moore, S. J. Danishefsky, Total Synthesis of Peribysin E Necessitates Revision of the Assignment of its Absolute Configuration. *Angew. Chem. Int. Ed*. **46**, 1451-1454 (2007). (j) S. G. Pardeshi, D. E. Ward, Enantiospecific Total Synthesis of Lairdinol A. *J. Org. Chem*. **73**, 1071-1076 (2008). (k) A. R. Angeles, S. P. Waters, S. J. Danishefsky, Total Syntheses of (+)- and (–)-Peribysin E. *J. Am. Chem. Soc*. **130**, 13765-13770 (2008). (l) S. Zhou, E. Sanchez-Larios, M. Gravel, Scalable Synthesis of Highly Reactive 1,3-Diamino Dienes from Vinamidinium Salts and their Use in Diels–Alder Reactions. *J. Org. Chem*. **77**, 3576-3582 (2012). (m) C. Peter, B. Ressault, P. Geoffroy, M. Miesch, Concise Approach to (ent)-14 β-Hydroxysteroids through Highly Diastereo-/Enantioselective Diels–Alder Reactions. *Chem. Eur. J.* **22**, 10808-10812 (2016). (n) B. Yang, K. Lin, Y. Shi, S. Gao, Ti(O*i*-Pr)$_4$-Promoted Photoenolization Diels–Alder reaction to Construct Polycyclic Rings and its Synthetic Applications. *Nat. Commun*. **8**, 1-10 (2017).

[95] I. Fleming, *Frontier Orbitals And Organic Chemical Reactions*. (Wiley, London, 1978).

[96] J. Sane, J. Rius, T. Calvet, M. A. Cuevas-Diarte, Chiral Molecular Alloys: Patterson-Search Structure Determination of L-Carvone and DL-Carvone from X-ray Powder Diffraction Data at 218 K. *Acta Crystallogr., Sect.B: Struct.Sci.* **53**, 702-707 (1997).

[97] W. Zheng, B.-B. Wnag, J.-C. Lai, C.-Z. Wan, X.-R. Lu, C.-H. Li, X.-Z. You, Electrochromic Properties of Novel Octa-Pinene Substituted Double-Decker Ln(III)

(Ln = Eu, Er, Lu) Phthalocyanines with Distinctive Near-IR Absorption. *J. Mater. Chem. C* **3**, 3072-3080 (2015).

[98] C. Chapius, D. Skuy, J.-Y. De Saint Laumer, R. Brauchli, *endo*/*exo* Stereoselectivity in Diels–Alder Reactions of α, β-Dialkylated Conjugated Enals to Cyclic 1,3-Dienes: Intermediates in the Synthesis of (–)-β-Santalol and Its Analogs. *Chemistry and Biodiversity* **11**, 1470-1516 (2014).

[99] K. Tiefenbacher, J. Mulzer, Short Formal Synthesis of (–)-Platencin. *Angew. Chem. Int. Ed.* **47**, 6199-6200 (2008).

[100] D. C. J. Waalboer, M. C. Schaapman, F. L. Van Delft, F. P. J. T. Rutjes, High-Pressure Entry into Platencin. *Angew. Chem. Int. Ed*. **47**, 6576-6578 (2008).

[101] (a) K. Tiefenbacher, J. Mulzer, A Nine-Step Total Synthesis of (–)-Platencin. *J. Org. Chem*. **74**, 2937-2941 (2009). (b) D. C. J. Waalboer, S. H. A. M. Leenders, T. Schulin-Casonato, F. L. Van Delft, F. P. J. T. Rutjes, Total Synthesis and Antibiotic Activity of Dehydrohomoplatencin. *Chem. Eur. J.* **16**, 11233-11236 (2010). (c) K. Mukai, D. Urabe, S. Kasuya, N. Aoki, M. Inoue, A Convergent Total Synthesis of 19-Hydroxysarmentogenin. *Angew. Chem. Int. Ed*. **52**, 5300-5304 (2013). (d) K. Mukai, S. Kasuya, Y. Nakagawa, D. Urabe, M. Inoue, A Convergent Total Synthesis of Ouabagenin. *Chem. Sci*. **6**, 3383-3387 (2015). (e) D. Urabe, Y. Nakagawa, K. Mukai, K. Fukushima, N. Aoki, H. Itoh, M. Nagatomo, M. Inoue, Total Synthesis and Biological Evaluation of 19-Hydroxysarmentogenin-3-O-α-L-rhamnoside, Trewianin, and Their Aglycons. *J. Org. Chem*. **83**, 13888-13910 (2018).

[102] (a) B. B. Snider, K. Yang, Stereo- and Enantiospecific Syntheses of (–)-Reiswigins A and B. Assignment of Absolute and Relative Configuration. *J. Org. Chem*. **55**, 4392-4399 (1990). (b) B. B. Snider, K. Yang, Synthesis of (–)-Reiswigin A. Assignment of Absolute and Relative Configuration. *Tet. Lett*. **30**, 2465-2468 (1989). (c) B. B. Snider, N. H. Vo, S. V. O'Neil, B. M. Foxman, Synthesis of (±)-Allocyathin B2 and (+)-Erinacine A. *J. Am. Chem. Soc*. **118**, 7644-7645 (1996). (d) G. Quinkert, H.-G. Schmalz, E. Walzer, T. Kowalczyk-Przewloka, G. Durner, J. W. Bats, Total Synthesis of the Pseudoguaianolide (+)-Confertin. *Angew. Chem*. **99**, 84-82 (1987). (e) J. D. White, T. C. Somers, Total Synthesis of (±)-2-Desoxystemodinone. A novel Hydroxyl-Assisted, Intramolecular Ene Reaction. *J. Am. Chem. Soc.* **109**, 4424-4426 (1987). (f) N. Kanoh, K. Sakanishi, E. Limori, K. Nishimura, Y. Iwabuchi, Asymmetric Total Synthesis of (–)-Scabronine G *via* Intramolecular Double Michael Reaction and Prins Cyclization. *Org. Lett.* **13**, 2864-2867 (2011). (g) J. Deng, S. Zhou, W. Zhang, J. Li, R. Li, A. Li, Total Synthesis of Taiwaniadducts B, C, and D. *J. Am. Chem. Soc*. **136**, 8185-8188 (2014).

[103] N. Kennedy, T. Cohen, The Stereoselective Reductions of Ketones to the Most Thermodynamically Stable Alcohols Using Lithium and Hydrated Salts of Common Transition Metals. *J. Org. Chem.* **80**, 8134-8141 (2015).

[104] (a) A. T. Stevens, M. R. Caira, J. R. Bull, K. Chibale, Cycloaddition and One-Carbon Homologation Studies in the Synthesis of Advanced Iridoid Precursors. *Org. Biomol. Chem.* **7**, 3527-3536 (2009). (b) G. F. Giri, A. M. Sarotti, R. A. Spanevello, Understanding Reactivity and Regioselectivity in Diels–Alder Reactions of a Sugar-Derived Dienophile Bearing Two Competing EWGs. An Experimental and Computational Study. *Carbohydrate Research* **415**, 54-59 (2015).

[105] M. S. Sherburn, Preparation and Synthetic Value of π-Bond-Rich Branched Hydrocarbons. *Acc. Chem. Res*. **48**, 1961-1970 (2015).

[106] E. G. Mackay, C. G. Newton, H. Toombs-Ruane, E. J. Lindeboom, T. Fallon, A. C. Willis, M. N. Paddon-Row, M. S. Sherburn, [5]Radialene. *J. Am. Chem. Soc*. **137**, 14653-14659 (2015).

[107] D. Liotta, M. Saindane, C. Barnum, Diels-Alder Reactions Involving Cross-Conjugated Dienones. Effects of Substitution on Reactivity. *J. Am. Chem. Soc*. **103**, 3224-3226 (1981).
[108] C. Kitabayashi, Y. Matsuura, N. Tanaka, Y. Katsube, Structure of α-Santonin. *Acta Cryst. Sect. C: Cryst. Struct. Commun* **41**, 1779-1781 (1985).
[109] M. Karthikeyan, R. Kamakshi, V. Sridar, B. S. R. Reddy, Rapid Access to Tricyclic Systems: Highly Endoselective Diels–Alder Reaction of Cycloalkenones with Cyclic Dienes Under Microwave Irradiation. *Synthetic Communications* **33**, 4199-4204 (2003).
[110] A. D. Payne, G. Bojase, M. N. Paddon-Row, M. S. Sherburn, Practical Synthesis of the Dendralene Family Reveals Alternation in Behavior. *Angew. Chem. Int. Ed*. **48**, 4836-4839 (2009).
[111] Sherburn-Group, Unpublished Results, Research School of Chemistry, Canberra.
[112] (a) W. J. Middleton, R. E. Heckert, E. L. Little, C. G. Krespan, Cyanocarbon Chemistry. III. Addition Reactions of Tetracyanoethylene. *J. Am. Chem. Soc*. **80**, 2783-2788 (1958). (b) K. Morimoto, T. P. Le, S. K. Manna, I. N. C. Kiran, S. Tanaka, M. Kitamura, Water, an Essential Element for a ZnII-Catalyzed Asymmetric Quinone Diels-Alder Reaction: Multi-Selective Construction of Highly Functionalized *cis*-Decalins. *Chem. Asian J.* **14**, 3283-3290 (2019). (c) T. Fujiwara, T. Ohsaka, T. Inoue, T. Takeda, The Diels–Alder and Ring Enlargement Reactions of 1-Cyclobutenyl Ketones. Preparation of 1-Acetyl-1,3,5-Cyclooctatrienes. *Tet. Lett*. **29**, 6283-6286 (1988).
[113] (a) T. A. Bradford, A. D. Payne, A. C. Willis, M. N. Paddon-Row, M. S. Sherburn, Cross-Coupling for Cross-Conjugation: Practical Synthesis and Diels–Alder Reactions of [3]Dendralenes. *Org. Lett*. **9**, 4861-4864 (2007). (b) H. Toombs-Ruane, E. L. Pearson, M. N. Paddon-Row, M. S. Sherburn, On the Diels–Alder Dimerisation of Cross-Conjugated Trienes. *Chem. Commun*. **48**, 6639-6641 (2012).
[114] O. Kwon, S. B. Park, S. L. Schreiber, Skeletal Diversity *via* a Branched Pathway: Efficient Synthesis of 29 400 Discrete, Polycyclic Compounds and Their Arraying into Stock Solutions. *J. Am. Chem. Soc*. **124**, 13402-13404 (2002).
[115] H.-J. Liu, Y. Li, E. N. C. Browne, Face-Selective Diels–Alder Reactions of (1R,5R)-3-Formyl-6,6-dimethylbicyclo[3.1.1]hept-3-en-2-one *Can. J. Chem*. **72**, 1883-1893 (1994).
[116] T. Nishimura, A. K. Unni, S. Yokoshima, T. Fukuyama, Concise Total Synthesis of (+)-Lyconadin A. *J. Am. Chem. Soc*. **133**, 418-419 (2010).
[117] (a) N. Waizumi, T. Itoh, T. Fukuyama, Synthetic Studies on CP-225,917 and CP-263,114. *Tet. Lett.* **39**, 6015-6018 (1998). (b) J. Lee, Y. Zhang, S. J. Danishefsky, A Straightforward Route to Functionalized *trans*-Diels-Alder Motifs. *J. Am. Chem. Soc*. **132**, 14330-14333 (2010). (c) Y. Wu, L. Han, X. Zhang, J. Mao, L. Gong, W. Guo, K. Gu, S. Li, Cationic Polymerization of Isobutyl Vinyl Ether in an Imidazole-Based Ionic Liquid: Characteristics and Mechanism. *Polym. Chem*. **6**, 2560-2568 (2015).
[118] (a) S. Masamune, W. Choy, J. S. Petersen, L. R. Sita, Double Asymmetric Synthesis and a New Strategy for Stereochemical Control in Organic Synthesis. *Angew. Chem. Int. Ed*. **24**, 1-76 (1985). (b) E. L. Eliel, S. H. Wilen, L. N. Mander, in *Stereochemistry of Organic Compounds*. (John Wiley & Sons Inc., New York, 1994), Chapter 12: Stereoselective Synthesis.
[119] W. Andrews, N. Magann, M. S. Sherburn, Unpublished Results (Research School of Chemistry, Australian National University, Canberra, 2020).
[120] M. F. Saglam, Investigations into Higher Dendralenes, Australian National University, Canberra, Australia (2016).

[121] C. G. Newton, D. N. Tran, M. D. Wodrich, N. Cramer, One-Step Multigram-Scale Biomimetic Synthesis of Psiguadial B. *Angew. Chem. Int. Ed*. **56**, 13776-13780 (2017).
[122] (a) H.-J. Liu, S. Y. Chew, E. N. C. Browne, Diels–Alder reactions of Chiral 5,5-Dimethyl-4,6-methano-2-methoxycarbonyl-2-cyclohexenone. *Tet. Lett*. **32**, 2005-2008 (1991). (b) H.-J. Liu, S. Y. Chew, E. N. C. Browne, J. B. Kim, Facial selective Diels–Alder Reactions of (1*R*,5*R*)-(+)-3-Carbomethoxy-6,6-dimethylbicyclo[3.1.l]hept-3-en2-one. Unusual Ketalization-Fragmentation Reaction of Adducts *Can. J. Chem*. **72**, 1193-1210 (1994).
[123] A. J. Smaligo, M. Swain, J. C. Quintana, M. F. Tan, D. A. Kim, O. Kwon, Hydrodealkenylative $C(sp^3)$–$C(sp^2)$ Bond Fragmentation. *Science* **364**, 681-685 (2019).
[124] (a) E. Ciganek, in *Organic Reactions*. (John Wiley & Sons, Inc., 1984). (b) A. G. Fallis, The Intramolecular Diels–Alder Reaction: Recent Advances and Synthetic Applications. *Can. J. Chem*. **62**, 183-234 (1984).
[125] A. B. Pangborn, M. A. Giardello, R. H. Grubbs, R. K. Rosen, F. J. Timmers, Safe and Convenient Procedure for Solvent Purification. *Organometallics* **15**, 1518-1520 (1996).
[126] W. L. F. Armarego, C. L. L. Chai, *Purification of Laboratory Chemicals*. (Butterworth-Heineman, Oxford, 7th ed., 2013).
[127] CrysAlisPro Software System (Rigaku Oxford Diffraction, 2018).
[128] F. Peng, M. Dai, A. R. Angeles, S. J. Danishefsky, Permuting Diels–Alder and Robinson Annulation Stereopatterns. *Chemical Science* **3**, 3076-3080 (2012).
[129] J. Barluenga, E. Campos-Gomez, A. Minatti, D. Rodriguez, J. M. Gonzalez, Iodoarylation Reactions of Allenes: Inter- and Intramolecular Processes. *Chem. Eur. J.* **15**, 8946-8950 (2009).
[130] D. Birney, T. K. Lim, J. H. P. Koh, B. R. Pool, J. M. White, Structural Investigations into the Retro-Diels–Alder Reaction. Experimental and Theoretical Studies. *J. Am. Chem. Soc.* **124**, 5091-5099 (2002).

7.2 References for Chapter 2

The following section provides references for Chapter 2.

References

(1) I. Abe, Enzymatic Synthesis Of Cyclic Triterpenes. *Nat. Prod. Rep.* **24**, 1311-1331 (2007).
(2) W. D. Nes, Biosynthesis Of Cholesterol And Other Sterols. *Chem. Rev.* **111**, 6423-6451 (2011).
(3) K. C. Nicolaou, S. A. Snyder, T. Montagnon, G. Vassilikogiannakis, The Diels–Alder Reaction In Total Synthesis. *Angew. Chem. Int. Ed*. **41**, 1668-1698 (2002).
(4) L. Gao, C. Su, X. Du, R. Wang, S. Chen, Y. Zhou, C. Liu, X. Liu, R. Tian, L. Zhang, K. Xie, S. Chen, Q. Guo, L. Guo, Y. Hano, M. Shimazaki, A. Minami, H. Oikawa, N. Huang, K. N. Houk, L. Huang, J. Dai, X. Lei, FAD-Dependent Enzyme-Catalysed Intermolecular [4+2] Cycloaddition In Natural Product Biosynthesis. *Nat. Chem*. **12**, 620-628 (2020).
(5) H. Hopf, M. S. Sherburn, Dendralenes Branch Out: Cross-Conjugated Oligoenes Allow The Rapid Generation Of Molecular Complexity. *Angew. Chem. Int. Ed*. **51**, 2298-2338 (2012).
(*6*) W. G. Dauben, A. P. Kozikowski, Organic reactions at high pressure. Cycloadditions of enamines and dienamines. *J. Am. Chem. Soc.* **96**, 3664-3666 (1974).
(7) I. Fleming, Frontier Orbitals And Organic Chemical Reactions. London: Wiley (1978).
(8) The only previously reported carbocyclic dienophiles in diene-transmissive Diels-Alder reaction sequences are *para*-benzoquinone and benzyne.
(9) H. Lachance, S. Wetzel, K. Kumar, H. Waldmann, Charting, Navigating, And Populating Natural Product Chemical Space For Drug Discovery. *J. Med. Chem.*, **55**, 5989-6001 (2012).
(10) C. J. O'Connor, H. S. G. Beckmann, D. R. Spring, Diversity-Oriented Synthesis: Producing Chemical Tools For Dissecting Biology. *Chem. Soc. Rev.*, **41**, 4444-4456 (2012).
(11) D. M. Roll, P. J. Scheuer, G. K. Matsumoto, J. Clardy, Halenaquinone, A Pentacyclic Polyketide From A Marine Sponge. *J. Am. Chem. Soc.* **105**, 6177-6178 (1983).
(12) H. Nakamura, J. Kobayashi, M. Kobayashi, Y. Ohizumi, Y. Hirata, Xestoquinone. A Novel Cardiotonic Marine Natural Product Isolated From The Okinawan Sea Sponge Xestospongia Sapra. *Chem. Lett*. 713-716 (1985).
(13) F. J. Schmitz, S. J. Bloor, Xesto- And Halenaquinone Derivatives From A Sponge, Adocia Sp., From Truk Lagoon. *J. Org. Chem*. **53**, 3922-3925 (1988).
(14) J. Kobayashi, T. Hirase, H. Shigemori, M. Ishibashi, New Pentacyclic Compounds From The Okinawan Marine Sponge Xestospongia Sapra. *J. Nat. Prod.* **55**, 994-998 (1992).
(15) G. P. Concepcion, T. A. Foderaro, G. S. Eldredge, E. Lobkovsky, J. Clardy, L. R. Barrows, C. M. Ireland, Topoisomerase II-Mediated DNA Cleavage By Adocia- And Xestoquinones From The Philippine Sponge Xestospongia Sp. *J. Med. Chem*. **38**, 4503-4507 (1995).
(16) T. Kubota, Y. Kon, J. Kobayashi, Xestosaprol C, A New Pentacyclic Hydroquinone Sulfate From A Marine Sponge Xestospongia Sapra. *Heterocycles* **76**, 1571-1575 (2008).
(17) N. Millan-Anguinaga, I. E. Soria-Mercado, P. Williams, Xestosaprol D And E From The Indonesian Marine Sponge Xestospongia sp. *Tet. Lett*. **51**, 751-753 (2010).
(18) J. Dai, A. Sorribas, W. Y. Yoshida, M. Kelly, P. G. Williams, Xestosaprols From The Indonesian Marine Sponge Xestospongia sp. *J. Nat. Prod*. **73**, 1188-1191 (2010).
(19) Y.-J. Lee, C.-K. Kim, S.-K. Park, J. S. Kang, J.-S. Lee, H. J. Shin, H.-S. Lee, Halenaquinone Derivatives From Tropical Marine Sponge Xestospongia sp. *Heterocycles* **85**, 895-901 (2012).
(20) R. M. Centko, A. Steino, F. I. Rosell, B. O. Patrick, N. de Voogd, A. G. Mauk, R. J. Andersen, Indoleamine 2,3-Dioxygenase Inhibitors Isolated From The Sponge Xestospongia Vansoesti: Structure Elucidation, Analogue Synthesis, And Biological Activity. *Org. Lett*. **16**, 6480-6483 (2014).
(21) M. Nakamura, T. Kakauda, J. Qi, M. Hirata, T. Shintani, Y. Yoshioka, T. Okamoto, Y. Oba, H. Nakamura, M. Ojika, Novel Relationship Between The Antifungal Activity And Cytotoxicity Of Marine-Derived Metabolite Xestoquinone And Its Family. *Biosci. Biotechnol. Biochem*. **69**, 1749–1752 (2005).
(22) D. Laurent, V. Jullian, A. Parenty, M. Knibiehler, D. Dorin, S. Schmitt, O. Lozach, N. Lebouvier, M. Frostin, F. Alby, S. Maurel, C. Doerig, L. Meijer, M. Sauvain. Antimalarial Potential Of Xestoquinone, A Protein Kinase Inhibitor Isolated From A Vanuatu Marine Sponge Xestospongia sp. *Bioorg. Med. Chem*. **14**, 4477–4482 (2006).

(23) M. Ito, Y. Hirata, H. Nakamura, Y. Ohizumi, Xestoquinone, Isolated From Sea Sponge, Causes Ca^{2+} Release Through Sulfhydryl Modification From Skeletal Muscle Scaroplasmic Reticulum. *J. Pharmacol. Exp. Ther*. **291**, 976-981 (1999).
(24) M. Kobayashi, H. Nakamura, J. Kobayashi, Y. Ohizumi, Mechanism Of Inotropic Action Of Xestoquinone, A Novel Cardiotonic Agent Isolated From A Sea Sponge. *J. Pharmacol. Exp. Ther.* **257**, 82-89 (1991).
(25) M. Nakamura, T. Kakauda, J. Qi, M. Hirata, T. Shintani, Y. Yoshioka, T. Okamoto, Y. Oba, H. Nakamura, M. Ojika, Novel Relationship Between The Antifungal Activity And Cytotoxicity Of Marine-Derived Metabolite Xestoquinone And Its Family. *Biosci. Biotechnol. Biochem*. **69**, 1749–1752 (2005).
(26) G. M. Schwarzwalder, C. D. Vandwerwal, Strategies For The Synthesis Of The Halenaquinol And Xestoquinol Families Of Natural Products. *Eur. J. Org. Chem*. 1567–1577 (2017).
(27) N. Harada, T. Sugioka, H. Uda, T. Kuriki, Total Synthesis And Absolute Stereochemistry Of (+)-Xestoquinone And Xestoquinol. *J. Org. Chem.* **55**, 3158-3163 (1990).
(28) K. Kanematsu, S. Soejima, G. Wang, Formal Total Synthesis Of Xestoquinone Via Furan Ring Transfer Reaction Strategy. *Tetrahedron. Lett.* **32**, 4761-4764 (1991).
(29) R. Carlini, K. Higgs, C. Older, S. Randhawa, Intramolecular Diels-Alder And Cope Reactions Of *Ortho*-Quinonoid Monoketals And Their Adducts: Efficient Syntheses Of (±)-Xestoquinone And Heterocycles Related To Viridin. *J. Org. Chem.* **62**, 2330-2331 (1997).
(30) H. S. Sutherland, K. C. Higgs, N. J. Taylor, R. Rodrigo, Isobenzofurans And *Ortho*-Benzoquinone Monoketals In Syntheses Of Xestoquinone And Its 9- And 10-Methoxy Derivatives. *Tetrahedron* **57**, 309-317 (2001).
(31) S. P. Maddaford, N. G. Andersen, W. A. Cristofoli, B. A. Keay, Total Synthesis Of (+)-Xestoquinone Using An Asymmetric Palladium-Catalysed Polyene Cyclization. *J. Am. Chem. Soc.* **118**, 10766-10773 (1996).
(32) F. Miyazaki, K. Uotsu, M. Shibasaki, Silver Salt Effects On An Asymmetric Heck Reaction. Catalytic Asymmetric Total Synthesis Of (+)-Xestoquinone. *Tetrahedron* **54**, 13073-13078 (1998).
(33) N. Harada, T Sugioka, Y. Ando, H. Uda, T. Kuriki, Total Synthesis Of (+)-Halenaquinol And (+)-Halenaquinone. Experimental Proof Of Their Absolute Stereostructures Theoretically Determined. *J. Am. Chem. Soc.* **110**, 8483-8487 (1988).
(34) H. S. Sutherland, F. E. S. Souza, R. G. A. Rodrigo, A Short Synthesis Of (±)-Halenaquinone. *J. Org. Chem.* **66**, 3639-3641 (2001).
(35) A. Kojima, T. Takemoto, M. Sodeoka, M. Shibasaki, Catalytic Asymmetric Synthesis Of Halenaquinone And Halenaquinol. *J. Org. Chem.* **61**, 4876-4877 (1996).
(36) A. Kojima, T. Takemoto, M. Sodeoka, M. Shibasaki, Catalytic Asymmetric Synthesis Of Halenaquinone And Halenaquinol. *Synthesis* 581-589 (1998).
(37) M. A. Kienzler, S. Suseno, D. Trauner, Vinyl Quinones As Diels-Alder Dienes: Concise Synthesis Of (-)-Halenaquinone. *J. Am. Chem. Soc.* **130**, 8604-8605 (2008).
(38) S. Goswami, K. Harada, M. F. El-Mansy, R. Lingampally, R. G. Carter, Enantioselective Synthesis Of (-)-Halenaquinone. *Angew. Chem. Int. Ed.* **57**, 9117-9121 (2018).
(39) Several syntheses of [3]dendralene have been previously reported (see reference 3) but all involve high temperature eliminations and/or lengthy preparations. The method reported here is much more convenient and scalable.
(40) This diene could also be generated in one step from [3]dendralene via Diels-Alder reaction with a substituted benzyne, generated *in situ* from 3,6-dimethoxy-2-(trimethylsilyl)phenyl trifluoro-methanesulfonate by cesium fluoride. This synthetic route was, however, lower yielding and required a 5 step synthesis of the benzyne precursor (See Supporting Information).
(41) This straightforward removal of the now superfluous carbonyl activating group also confirms the versatility of the cyclic enone dienophiles employed in the methodological section of this project.
(42) C. K. Jana, R. Scopelliti, K. Gademann, Connecting C19 Norditerpenoids To C20 Diterpenes: Total Syntheses Of 6-Hydroxy-5,6-Dehydrosugiol, 6-Hydroxysugiol, And Taiwaniaquinone H, And Formal Synthesis Of Dichroanone. *Synthesis* **2010**, 2223-2232.
(43) The requisite furan functionality could also be installed via a two-step sequence involving: 1) ring opening of the lactol with KHMDS and 2) oxidation of the primary alcohol to the aldehyde by EDC•HCl, followed by cyclisation and dehydration under acidic conditions. See Supporting Information for details.
(44) B. M. Trost, The Atom Economy: A Search For Synthetic Efficiency. *Science*, **254**, 1471-1477 (1991).
(45) N. A. Miller, A. C. Willis, M. S. Sherburn, Formal Total Synthesis Of Triptolide. *Chem. Commun*. 1226- 1228 (2008).

(46) S. V. Pronin, R. A. Shenvi, Synthesis Of A Potent Antimalarial Amphilectene. *J. Am. Chem. Soc.* **134**, 19604-19606 (2012).
(47) C. G. Newton, S. L. Drew, A. L. Lawrence, A. C. Willis, M. N. Paddon-Row, M. S. Sherburn, Pseudopterosin Synthesis From A Chiral Cross-Conjugated Hydrocarbon Through A Series Of Cycloadditions. *Nat. Chem.* **7**, 82–86 (2015).
(48) H.-H. Lu, S. V. Pronin, Y. Antonova-Koch, S. Meister, E. A. Winzeler, R. A. Shenvi, Synthesis Of (+)-7,20-Diisocyanoadociane And Liver-Stage Antiplasmodial Activity Of The Isocyanoterpene Class. *J. Am. Chem. Soc.* **138**, 7268-7271 (2016).

7.3 References for Chapter 5

The following section provides references for Chapter 5.

[1] O. Diels, K. Alder, *Justus Liebigs Ann. Chem.* **1928**, *460*, 98-122.
[2] In more complex examples with several pre-existing rings, for clarity of presentation the blue coloration convention is waived.
[3] A research topic search of SciFinder® conducted in September 2020 produced around 50,000 references containing the concept "Diels-Alder", with >28,000 references since the year 2000. A similar search produced around 5,000 references containing the concept "intramolecular Diels-Alder", with 50% published since the year 2000.
[4] W. Oppolzer, *Angew. Chem. Int. Ed.* **1977**, *16*, 10-23.
[5] G. Brieger, J. N. Bennett, *Chem. Rev.* **1980**, *80*, 63-97.
[6] D. F. Taber, *Intramolecular Diels–Alder and Alder Ene Reactions*, Springer–Verlag, Berlin, **1984**.
[7] E. Ciganek in *Organic Reactions*, Vol. 32 (Ed.: W. G. Dauben) John Wiley & Sons: New York, **1984**, pp 1-374.
[8] G. Fallis, *Can. J. Chem.* **1984**, *62*, 183-234.
[9] D. Craig, *Chem. Soc. Rev.* **1987**, *16*, 187-238.
[10] W. R. Roush in *Advances in Cycloaddition*, Vol. 2 (Ed.: D. P. Curran) JAI Press: Greenwich, CT, **1990**, pp. 91-146.
[11] W. R. Roush in *Comprehensive Organic Synthesis*, Vol. 5 (Eds.: B. M. Trost, I. Fleming) Pergamon Press, Oxford, UK, **1991**, pp 513-550.
[12] K. C. Nicolaou, S. A. Snyder, T. Montagnon, G. Vassilikogiannakis, *Angew. Chem., Int. Ed.* **2002**, *41*, 1668-1698.
[13] B. R. Bear, S. M. Sparks, K. J. Shea, *Angew. Chem., Int. Ed.* **2001**, *40*, 820-849.
[14] E. Marsault, A. Toró, P. Nowak, P. Deslongchamps, *Tetrahedron*, **2001**, *57*, 4243-4260.
[15] K. Takao, R. Munakata, K. Tadano, *Chem. Rev.* **2005**, *105*, 4779-4807.
[16] M. Juhl, D. Tanner, *Chem. Soc. Rev.* **2009**, *38*, 2983-2992.
[17] M. M. Heravi, V. F. Vavsaria, *RSC Adv.* **2015**, *5*, 50890-50912.
[18] D. Tanner, E. Ascic, in *Comprehensive Organic Synthesis (2nd Ed.)*, Vol. 5 (Eds.: P. Knochel, G. A. Molander) Elsevier, **2014**, pp 466-517.
[19] See, for example: (a) C. O. Kappe, S. S. Murphree, A. Padwa, *Tetrahedron* **1997**, *53*, 14179-14233; (b) S. W. Weinreb, *Acc. Chem. Res.* **1985**, *18*, 16-21; (c) V. V. Kouznetsov, *Tetrahedron* **2009**, *65*, 2721-2750; (d) A. Padwa, A. C. Flick, in *Adv. Heterocycl. Chem., Vol. 110*, Elsevier Inc., **2013**, pp. 1-41; (e) P. T. Parvatkar, H. K. Kadam, S. G. Tilve, *Tetrahedron* **2014**, *70*, 2857-2888.
[20] http://publications.iupac.org/pac/2006/pdf/7810x1897.pdf accessed 22 December 2020.
[21] Based upon reaction structure searching on SciFinder®, we estimate that less than 2% of all published IMDA reactions describe type 2 processes and less than 1% are transannular processes. Around 50% of all IMDA examples involve 1,3,9-decatrienes, and 45% describe 1,3,8-nonatrienes.
[22] Many publications erroneously describe the products of a 1,3,9-decatriene IMDA reactions as a "decalin" (a contracted form of decahydronaphthalene). A more correct name is $\Delta^{1,2}$-octalin.
[23] Selected early contributions: (a) F. K. Brown, K. N. Houk, *Tetrahedron Lett.* **1985**, *26*, 2297-2300; (b) F. K. Brown, U. C. Singh, P. A. Kollman, L. Raimondi, K. N. Houk, C. W. Bock, *J. Org. Chem.* **1992**, *57*, 4862-4869; (c) L. Raimondi, F. K. Brown, J. Gonzalez, K. N. Houk, *J. Am. Chem. Soc.* **1992**, *114*, 4796-4804.
[24] Selected examples: (a) M. J. Lilly, M. N. Paddon-Row, M. S. Sherburn, C. I. Turner, *Chem. Commun.* **2000**, 2213-2214; (b) M. N. Paddon-Row, M. S. Sherburn, *Chem. Commun.* **2000**, 2215-2216.
[25] M. K. Diedrich, F.-G. Klaerner, B. R. Beno, K. N. Houk, H. Senderowitz, W. C. Still, *J. Am. Chem. Soc.* **1997**, *119*, 10255-10259.
[26] H. Krenske, E. W. Perry, S. V. Jerome, T. J. Maimone, P. S. Baran, K. N. Houk. *Org. Lett.* **2012**, *14*, 3016-3019.
[27] Y.-T. Lin, K. N. Houk, *Tetrahedron Lett.* **1985**, *26*, 2269-2272.
[28] M. N. Paddon-Row, A. I. Longshaw, A. C. Willis, M. S. Sherburn, *Chem. Asian. J.* **2009**, *4*, 126-134.
[29] M. N. Paddon-Row, D. Moran, G. A. Jones, M. S. Sherburn, *J. Org. Chem.* **2005**, *70*, 10841–10853.
[30] S. Thamapipola, E. P. Kündig, *Org. Biomol. Chem.* **2011**, *9*, 7564-7570.
[31] See, for example, references 61 and 62.
[32] W. R. Roush, H. R. Gillis, A. I. Ko, *J. Am. Chem. Soc.* **1982**, *104*, 2269-2283.
[33] (a) D. A. Smith, K. Sakan, K. H. Houk, *Tetrahedron Lett.* **1986**, *27*, 4877-4880; see also (b) M. E. Jung, K. M. Halweg, *Tetrahedron Lett.* **1981**, *22*, 3929-3932; (c) S. A. Bal, P. Helquist, *Tetrahedron Lett.* **1981**, *22*, 3933-3936.
[34] R. M. Wilson, W. S. Jen, D. W. C. MacMillan, *J. Am. Chem. Soc.* **2005**, *127*, 11616-11617.
[35] For related intermolecular Diels-Alder processes, see: K. A. Ahrendt, C. J. Borths, D. W. C. MacMillan, *J. Am. Chem. Soc.* **2000**, *122*, 4243-4244.
[36] The 2005 MacMillan paper erroneously describes the use of the (*S,S*)-catalyst in the main body of the manuscript. The (*R,R*)-catalyst is given correctly in the SI.
[37] Review: H. Oikawa, *Bull. Chem. Soc. Jpn.* **2005**, *78*, 537-554.
[38] H. Oikawa, K. Katayama, Y. Suzuki, A. Ichihara, *J. Chem. Soc., Chem. Commun.* **1995**, 1321-1322.
[39] K. Kasahara, T. Miyamoto, T. Fujimoto, H. Oguri, T. Tokiwano, H. Oikawa, Y. Ebizuka, I. Fujii, *ChemBioChem* **2010**, *11*, 1245-1252.
[40] For other IMDA studies on solanapyrones, see: (a) A. Ichihara, M. Miki, H. Tazaki, S. Sakamura, *Tetrahedron Lett.* **1987**, *28*, 1175-1178; (b) H. Oikawa, T. Kobayashi, K. Katayama, Y. Suzuki, A. Ichihara, *J. Org. Chem.* **1998**, *63*, 8748-8756; (c) B. Lygo, M. Bhatia, J. W. B. Cooke, D. J. Hirst, *Tetrahedron Lett.* **2003**, *44*, 2529-2532; (b) B. Lygo, D. J. Hirst, *Synthesis* **2005**, 3257-3262.
[41] A. R. Healy, M. Izumikawa, A. M. Z. Slawin, K. Shin-ya, N. J. Westwood, *Angew. Chem., Int. Ed.* **2015**, *54*, 4046-4050.
[42] For the synthesis of JBIR-22 using a late stage IMDA reaction, see A. R. Healy, N. J. Westwood, *Org. Biomol. Chem.* **2015**, *13*, 10527-10531.
[43] For Lewis acid catalyst-controlled enantioselective IMDA reactions of achiral trienes, see: (a) K. Furuta, A. Kanematsu, H. Yamamoto, S. Takaoka, *Tetrahedron Lett.* **1989**, *30*, 7231-7232; (b) N. Iwasawa, J. Sugimori, Y. Kawase, K. Narasaka, *Chem. Lett.* **1989**, 1947-1950; (c) K. Narasaka, M. Saitou, N. Iwasawa, *Tetrahedron: Asymmetry* **1991**, *2*, 1305-1318; (d) K. Ishihara, H. Kurihara, H. Yamamoto, *J. Am. Chem. Soc.* **1996**, *118*, 3049-3050; (e) D. A. Evans, J. S. Johnson, *J. Org. Chem.* **1997**, *62*, 786-787; (f) K. Ishihara, H. Kurihara, M. Matsumoto, H. Yamamoto, *J. Am. Chem. Soc.* **1998**, *120*, 6920-6930; (g) G. Zhou, Q.-Y. Hu, E. J. Corey, *Org. Lett.* **2003**, *5*, 3979-3982; (h) E. P. Balskus, E. N. Jacobsen, *Science* **2007**, *317*, 1736-1740; (i) S. Thamapipol, G. Bernardinelli, C. Besnard, E. P. Kundig, *Org. Lett.* **2010**, *12*, 5604-5607; (j) M. S. Andrae, J. Thiemermann, J. Schnaubelt, D. Lentz, R. Zimmer, H.-U. Reissig, *Eur. J. Org. Chem.* **2017**, *2017*, 124-130.

[44] The Enders group reported only traces of IMDA product in attempts to use the Hayashi-Jørgensen catalyst with an enal dienophile, and instead resorted to Lewis acid catalysis. See: (a) D. Enders, M. R. M. Huettl, J. Runsink, G. Raabe, B. Wendt, *Angew. Chem., Int. Ed.* **2007**, *46*, 467-469; (b) D. Enders, M. R. M. Huettl, G. Raabe, J. W. Bats, *Adv. Synth. Catal.* **2008**, *350*, 267-279.
[45] For chiral Brønsted acid-catalyzed aza-dienophile IMDA reactions (Povarov reactions), see: C. Min, C.-T. Lin, D. Seidel, *Angew. Chem., Int. Ed.* **2015**, *54*, 6608-6612.
[46] (a) L. T. Burke, D. J. Dixon, S. V. Ley, F. Rodriguez, *Org. Lett.* **2000**, *2*, 3611-3613; (b) L. T. Burke, D. J. Dixon, S. V. Ley, F. Rodriguez, *Org. Biomol. Chem.* **2005**, *3*, 274-280.
[47] (a) Original report for intermolecular DA reactions: P. A. Grieco, J. J. Nunes, M. D. Gaul, *J. Am. Chem. Soc.* **1990**, *112*, 4595-4596; first reports of use in IMDA reactions: (b) P. A. Grieco, S. T. Handy, J. P. Beck, *Tetrahedron Lett.* **1994**, *35*, 2663-2666; (c) P. A. Grieco, J. P. Beck, S. T. Handy, N. Saito, J. F. Daeuble, *Tetrahedron Lett.* **1994**, *35*, 6783-6786.
[48] (a) W. G. Dauben, A. P. Kozikowski, *J. Amer. Chem. Soc.* **1974**, *96*, 3664-3666; (b) W. G. Dauben, H. O. Krabbenhoft, *J. Amer. Chem. Soc.* **1976**, *98*, 1992-1993; (c) W. G. Dauben, H. O. Krabbenhoft, *J. Org. Chem.* **1977**, *42*, 282-287.
[49] For a recent review, see: C. L. Hugelshofer, T. Magauer, *Synthesis* **2014**, *46*, 1279-1296.
[50] See, for example: (a) K. Yuki, M. Shindo, K. Shishido, *Tetrahedron Lett.* **2001**, *42*, 2517-2519; (b) J. Xu, E. J. E. Caro-Diaz, M. H. Lacoske, C.-I. Hung, C. Jamora, E. A. Theodorakis, *Chem. Sci.* **2012**, *3*, 3378-3386; (c) J. Yin, C. Wang, L. Kong, S. Cai, S. Gao, *Angew. Chem. Int. Ed.* **2012**, *51*, 7786-7789; (d) J. Deng, B. Zhu, Z. Lu, H. Yu, A. Li, *J. Am. Chem. Soc.* **2012** *134*, 920-923; (e) J. Xu, E. J. E. Caro-Diaz, L. Trzoss, E. A. Theodorakis, *J. Am. Chem. Soc.* **2012**, *134*, 5072-5075; (h) J. Yin, S. Gao, *Synlett* **2014**, *25*, 1-7; (f) J. Yin, C. Wang, L. Kong, S. Cai, S. Gao, *Angew. Chem. Int. Ed.* **2012**, *51*, 7786-7789; (g) J. Yin, L. Kong, C. Wang, Y. Shi, S. Cai, S. Gao, *Chem. Eur. J.* **2013**, *19*, 13040-13046; (h) L. Kong, M. Rao, J. Ou, J. Yin, W. Lu, M. Liu, X. Pang, S. Gao, *Org. Biomol. Chem.* **2014**, *12*, 7591-7597; (i) C. Liu, Z. Zeng, R. Chen, X. Jiang, Y. Wang, Y. Zhang, *Org. Lett.* **2016**, *18*, 624-627; (j) X. Li, Q. Zheng, J. Yin, W. Liu, S. Gao, *Chem. Commun.* **2017**, *53*, 4695-4697.
[51] For a review, see: G. Li, S. Kusari, M. Spiteller, *Nat. Prod. Rep.* **2014**, *31*, 1175-1201.
[52] C. S. Jamieson, M. Ohashi, F. Liu, Y. Tang, K. N. Houk, *Nat. Prod. Rep.* **2019**, *36*, 698-713.
[53] For seminal contributions to tether substituent-based stereocontrol, see: (a) T. Kametani, H. Matsumoto, H. Nemoto, K. Fukumoto, *J. Am. Chem. Soc.* **1978**, *100*, 6218–6220; (b) W. R. Roush, *J. Org. Chem.* **1979**, *44*, 4008–4010; (c) T. Mukaiyama, N. Iwasawa, *Chem. Lett.* **1981**, 29–32; (d) M. P. Edwards, S. V. Ley, S. G. Lister, *Tetrahedron Lett.* **1981**, *22*, 361–364; (e) K. C. Nicolaou, R. L. Magolda, *J. Org. Chem.* **1981**, *46*, 1506–1508; (f) W. R. Roush, A. G. Myers, *J. Org. Chem.* **1981**, *46*, 1509–1511; (g) K. A. Parker, T. Iqbal, *J. Org. Chem.* **1982**, *47*, 337–342; (h) R. K. Boeckman, T. E. Barta, *J. Org. Chem.* **1985**, *50*, 3421–3433; (i) W. R. Roush, M. Kageyama, *Tetrahedron Lett.* **1985**, *26*, 4327–4330.
[54] D. F. Taber, B. P. Gunn, *J. Am. Chem. Soc.* **1979**, *101*, 3992-3993.
[55] The corresponding *chairlike-cis* TSs have less favorable conformations at both ends of the tether: a gauche butene conformation at the diene end and a gauche ethanone conformation at the dienophile end. See J. W. Coe, W. R. Roush. *J. Org. Chem.* **1989**, *54*, 915–930.
[56] For a recent review featuring several such examples, see M. E. Daub, P. C. Roosen, C. D. Vanderwal, *J. Org. Chem.* **2017**, *82*, 4533-4541.
[57] J. E. Golden, J. Aube. *Angew. Chem. Int. Ed.* **2002**, *41*, 4316 – 4318.
[58] C.-Y. Chen, D. J. Hart. *J. Org. Chem.* **1993**, *58*, 3840-3849.
[59] E. M. Stang, M. C. White, *J. Am. Chem. Soc.* **2011**, *133*, 14892-14895.
[60] T. S. Chou, H. H. Tso, L. J. Chang, *J. Chem. Soc., Chem. Commun.* **1985**, 236-237.
[61] (a) W. Oppolzer, R. L. Snowden, *Tetrahedron Lett.* **1976**, 4187-4190; (b) W. Oppolzer, R. L. Snowden, D. P. Simmons, *Helv. Chim. Acta* **1981**, *64*, 2002-2021.
[62] (a) J. L. Gras, M. Bertrand, *Tetrahedron Lett.* **1979**, *19*, 4549-4552; (b) J. L. Gras, *J. Org. Chem.* **1981**, *46*, 3738-3741. This latter paper would have been the second example of a total synthesis featuring an IMDA reaction, had the structure been correct. For the corrected structure, see: (c) M. Tori, T. Hasebe, Y. Asakawa, *J. Chem. Soc., Perkin Trans. 1* **1989**, 1552-1553.
[63] This transformation was exploited in 1,3,9-decatrien-8-one IMDA-based syntheses of the natural product biflora-4,10(19),15-triene, a diterpene from a termite soldier (a) O. P. Vig, M. L. Sharma, S. Kiran, J. Singh, *Indian J. Chem., Sect. B* **1983**, *22B*, 746-748; (b) K. Mori, M. Waku, *Tetrahedron* **1984**, *40*, 305-309; (c) K. A. Parker, J. G. Farmar, *J. Org. Chem.* **1986**, *51*, 4023-4028.
[64] E. J. Corey, P. A. Magriotis, *J. Am. Chem. Soc.* **1987**, *109*, 287-289.
[65] P. Yates, P. Eaton, *J. Am. Chem. Soc.* **1960**, *82*, 4436-4437.
[66] G. I. Fray, R. Robinson, *J. Am. Chem. Soc.* **1961**, *83*, 249.
[67] E. F. Lutz, G. M. Bailey, *J. Am. Chem. Soc.* **1964**, *86*, 3899-3901.
[68] J. Sauer, J. Kredel, *Tetrahedron Lett.* **1966**, *7*, 731-736.
[69] P. A. Grieco, S. T. Handy, J. P. Beck, *Tetrahedron Lett.* **1994**, *35*, 2663-2666.
[70] K. Maruoka, H. Imoto, H. Yamamoto, *J. Am. Chem. Soc.* **1994**, *116*, 12115-12116.
[71] The 2-methyl substituent has a profound influence upon the rate of the thermal reaction: this substrate requires heating at 120 °C for extended periods for the uncatalyzed IMDA reaction to reach completion, whereas the des-methyl analogue undergoes IMDA reaction at ambient temperature.
[72] E. L. Pearson, N. Kanizaj, A. C. Willis, M. N. Paddon-Row, M. S. Sherburn, *Chem. Eur. J.* **2010**, *16*, 8280-8284.
[73] Reference 43j reports moderate enantioselectivities for this challenging transformation.
[74] M. Movassaghi, D. K. Hunt, M. Tjandra, *J. Am. Chem. Soc.* **2006**, *128*, 8126-8127.
[75] M. Movassaghi, M. Tjandra, J. Qi, *J. Am. Chem. Soc.* **2009**, *131*, 9648-9650.
[76] a) N. J. Line, A. C. Burns, S. C. Butler, J. Casbohm, C. J. Forsyth, *Chem. Eur. J.* **2016**, *22*, 17983-17986; (b) S. C. Butler, C. J. Forsyth, *J. Org. Chem.* **2013**, *78*, 3895-3907; (c) A. C. Burns, C. J. Forsyth, *Org. Lett.* **2008**, *10*, 97-100.
[77] O. L. Chapman, M. R. Engel, J. P. Springer, J. C. Clardy, *J. Am. Chem. Soc.* **1971**, *93*, 6696-6698.
[78] Y. Zou, Q. Che, B. B. Snider, *Org. Lett.* **2006**, *8*, 5605-5608.
[79] (a) M. Kita, M. Kondo, T. Koyama, K. Yamada, T. Matsumoto, K.-H. Lee, J.-T. Woo, D. Uemura, *J. Am. Chem. Soc.* **2004**, *126*, 4794-4795; (b) M. Kita, N. Ohishi, K. Washida, M. Kondo, T. Koyama, K. Yamada, D. Uemura, *Bioorg. Med. Chem.* **2005**, *13*, 5253-5258.
[80] G. N. Varseev, M. E. Maier, *Angew. Chem. Int. Ed.* **2006**, *45*, 4767-4771.
[81] J. Kim, R. J. Thomson, *Angew. Chem. Int. Ed.* **2007**, *46*, 3104-3106.
[82] (a) B. B. Snider, Q. Che, *Angew. Chem. Int. Ed.* **2006**, *45*, 932-935; (b) Y. Zou, Q. Che, B. B. Snider, *Org. Lett.* **2006**, *8*, 5605-5608; (c) E. Sakai, K. Araki, H. Takamura, D. Uemura, *Tetrahedron Lett.* **2006**, *47*, 6343-6345.

[83] T. Sammakia, D. M. Johns, G. Kim, M. A. Berliner, *J. Am. Chem. Soc.* **2005**, *127*, 6504-6505.
[84] R. T. Larson, R. P. Pemberton, J. M. Franke, D. J. Tantillo, R. J. Thomson, *J. Am. Chem. Soc.* **2015**, *137*, 11197-11204.
[85] M. Miyashita, M. Sasaki, I. Hattori, M. Sakai, K. Tanino, *Science* **2004**, *305*, 495-499.
[86] The proposed biogenesis involves a twofold Michael addition to form the C ring. See: K. Makoto, H. Koji, Y. Kohji, Y. Mika, T. Tomoko, U. Daisuke, *Bull. Chem. Soc. Jpn*. **1998**, *71*, 771-779.
[87] (a) M. Bueschleb, S. Dorich, S. Hanessian, D. Tao, K. B. Schenthal, L. E. Overman, *Angew. Chem., Int. Ed.* **2016**, *55*, 4156-4186; (b) K. W. Quasdorf, L. E. Overman, *Nature* **2014**, *516*, 181-191; (c) E. A. Peterson, L. E. Overman, *Proc. Natl. Acad. Sci. U. S. A.* **2004**, *101*, 11943-11948.
[88] (a) Y. Murata, D. Yamashita, K. Kitahara, Y. Minasako, A. Nakazaki, S. Kobayashi, *Angew. Chem. Int. Ed.* **2009**, *48*, 1400-1403; (b) D. Yamashita, Y. Murata, N. Hikage, K. Takao, A. Nakazaki, S. Kobayashi, Angew. Chem. Int. Ed. **2009**, *48*, 1404-1406.
[89] (a) E. J. Corey, R. L. Danheiser, S. Chandrasekaran, P. Siret, G. E. Keck, J. L. Gras, *J. Am. Chem. Soc.* **1978**, *100*, 8031-8034; (b) E. J. Corey, R. L. Danheiser, S. Chandrasekaran, G. E. Keck, B. Gopalan, S. D. Larsen, P. Siret, J. L. Gras, *J. Am. Chem. Soc.* **1978**, *100*, 8034-8036.
[90] M. E. Jung, *Synlett* **1990**, 186-190.
[91] A. Saito, H. Yanai, T. Taguchi, *Tetrahedron Lett.* **2004**, *45*, 9439-9442.
[92] H. W. Gschwend, A. O. Lee, H. P. Meier, *J. Org. Chem.* **1973**, *38*, 2169-2175.
[93] G. Stork, N. Saccomano, *Tetrahedron Lett.* **1987**, *28*, 2087-2090.
[94] G. Stork, D. Sherman, *J. Am. Chem. Soc.* **1982**, *104*, 3758-3759.
[95] G. Stork, G. Clark, C. S. Shiner, *J. Am. Chem. Soc.* **1981**, *103*, 4948-4949.
[96] See, for example: (a) Y. Horiguchi, E. Nakamura, I. Kuwajima, *J. Am. Chem. Soc*. **1989**, *111*, 6257-6265. (b) Y. Horiguchi, E. Nakamura, I. Kuwajima, *J. Org. Chem*. **1986**, *51*, 4323-4325.
[97] S. V. Pronin, R. A. Shenvi. *J. Am. Chem. Soc.* **2012**, *134*, 19604-19606.
[98] Reviews: (a) H. Hopf, M. S. Sherburn, *Angew. Chem. Int. Ed.* **2012**, *51*, 2298–2338; (b) M. S. Sherburn, *Acc. Chem. Res.*, **2015**, *48*, 1961–1970.
[99] (a) For the first total synthesis using a dendralene, see: N. A. Miller, A. C. Willis, M. S. Sherburn, *Chem. Commun.* **2008**, 1226-1228; (b) For the first total synthesis efforts involving DTDA sequences of "oxa-dendralenes", see C. Spino, G. Liu, *J. Org. Chem*. **1993**, *58*, 817−819.
[100] S. Kanemasa, H. Sakoh, E. Wada, O. Tsuge, *Bull. Chem. Soc. Jpn*. **1986**, *59*, 1869-1876.
[101] H. H. Lu, S. V. Pronin, Y. Antonovna-Koch, S. Meister, E. A. Winzeler, R. A. Shenvi. *J. Am. Chem. Soc.* **2016**, *138*, 7268-7271.
[102] For recent impressive achievements in cycloamphilectane total synthesis, see: (a) E. E. Robinson, R. J. Thomson, *J. Am. Chem. Soc.* **2018**, *140*, 1956-1965; (b) A. S. Karns, B. D. Ellis, P. C. Roosen, Z. Chahine, K. G. Le Roch, C. D. Vanderwal, *Angew. Chem., Int. Ed.* **2019**, *58*, 13749-13752.
[103] C. A. Reiher, R. A. Shenvi, *J. Am. Chem. Soc.* **2017**, *139*, 3647-3650.
[104] T. J. Maimone, J. Shi, S. Ashida, P. S. Baran. *J. Am. Chem. Soc.* **2009**, *131*, 17066-17067.
[105] Review: C. Draghici, J. T. Njardarson, *Tetrahedron* **2015**, *71,* 3775-3793.
[106] C. M. Grisé, G. Tessier, L. Barriault, *Org. Lett.* **2007**, *9*, 1545-1548.
[107] J. Poulin, C. M. Grisé-Bard, L. Barriault, *Angew. Chem. Int. Ed.* **2012**, *51*, 2111-2114.
[108] For another IMDA-based total synthesis of vinigrol featuring a dearomatization, see: Q. Yang, J. T. Njardarson, C. Draghici, F. Li, *Angew. Chem. Int. Ed.* **2013**, *52*, 8648-8651.
[109] T. J. Maimone, A.-F. Voica, P. S. Baran. *Angew. Chem. Int. Ed.* **2008**, *47*, 3054-3056.
[110] IMDA reactions controlled by H-bonds between dienes and dienophiles had been previously reported: see T. N. Cayzer, M. N. Paddon–Row, M. S. Sherburn, *Eur. J. Org. Chem.* **2003**, 4059-4068.
[111] G. Stork, A. Yamashita, J. Adams, G. R. Schulte, R. Chesworth, Y. Miyazaki, J. J. Farmer. *J. Am. Chem. Soc.* **2009**, *131* 11402-11406.
[112] For IMDA reactions with benzofurans as acceptors see: (a) E. Ciganek. *J. Am. Chem. Soc.* **1981**, *103*, 6261-6262; (b) S. France, J. Boonsombat, C. A. Leverett, A. Padwa. *J. Org. Chem.* **2008**, *73*, 8120-8123.
[113] For intermolecular DA reactions with benzofurans as acceptors see: (a) E. Wenkert, S. R. Piettre. *J. Org. Chem.* **1988**, *53*, 5850-5853; (b) N. Chopin, H. Gerard, I. Cantaigner, S. R. Piettre. *J. Org. Chem.* **2009**, *74*, 1237-1246.
[114] (a) V. Varghese, T. Hudlicky, *Angew. Chem. Int. Ed.* **2014**, *53*, 4355-4358; (b) K. Ho Park, R. Chen, D. Y. K. Chen, *Chem. Sci.* **2017**, *8*, 7031-7037.
[115] M. A. Kienzler, S. Suseno, D. Trauner. *J. Am. Chem. Soc.* **2008**, *130,* 8604-8605.
[116] For related studies involving this diene by the Trauner group, see (a) F. Loebermann, P. Mayer, D. Trauner, *Angew. Chem., Int. Ed.* **2010**, *49*, 6199-6202; (b) F. Loebermann, L. Weisheit, D. Trauner, *Org. Lett.* **2013**, *15*, 4324-4326.
[117] Z.-X. Ma, J. B. Feltenberg, R. P. Hsung. *Org. Lett.* **2012**, *14*, 2742-2745.
[118] W. Oppolzer, K. Keller. *J. Am. Chem. Soc.* **1971**, *93*, 3836-3837.
[119] For a review of recent literature, see: B. Yang, S. Gao, *Chem. Soc. Rev.* **2018**, *47*, 7926-7953.
[120] Funk, R. L.; Vollhardt, K. P. C. *Chem. Soc. Rev.* **1980**, *9*, 41–61.
[121] T. Kametani, H. Nemoto, *Tetrahedron* **1981**, *37*, 3-16.
[122] E. G. Mackay, M. S. Sherburn *Synthesis*, **2015**, *47*, 1–21.
[123] (a) Kametani, T.; Nemoto, H.; Ishikawa, H.; Shiroyama, K.; Fukumoto, K. *J. Am. Chem. Soc.* **1976**, *98*, 3378–3379; (b) Kametani, T.; Nemoto, H.; Ishikawa, H. *J. Am. Chem. Soc.* **1977**, *99*, 3461–3466.
[124] Funk, R. L.; Vollhardt, K. P. C. *J. Am. Chem. Soc.* **1980**, 5253–5261.
[125] Y.-K. Chen, R. K. Peddinti, C.-C. Liao, *Chem. Commun.* **2001**, 1340-1341.
[126] (a) K. C. Nicolaou, Q.-Y. Toh, D. Y. K. Chen, *J. Am. Chem. Soc.* **2008**, *130*, 11292-11293; (b) K. C. Nicolaou, G. S. Tria, D. J. Edmonds, M. Kar, *J. Am. Chem. Soc.* **2009**, *131*, 15909-15917.
[127] a) W. R. Roush, M. Kageyama, R. Riva, B. B. Brown, J. S. Warmus, K. J. Moriarty. *J. Org. Chem.* **1991**, *56*, 1192 – 1210. b) R. K. Boeckman, T. E. Bart. *J. Org. Chem.* **1985**, *50*, 3423–3425.
[128] (a) N. Iwasawa, J. Sugimori, Y. Kawase, K. Narasaka, *Chem. Lett.* **1989**, 1947–1950; (b) K. Furuta, A. Kanematsu, H. Yamamoto, S. Takaoka, *Tetrahedron Lett.* **1989**, *30*, 7231–7232; (c) K. Narasaka, M. Saitou, N. Iwasawa, *Tetrahedron: Asymmetry* **1991**, *2*, 1305–1318; (d) K. Ishihara, H. Kurihara, H. Yamamoto, *J. Am. Chem. Soc.* **1996**, *118,* 3049–1050;(e) K. Ishihara, H. Kurihara, M. Matsumoto, H. Yamamoto, *J. Am. Chem. Soc.* **1998**, *120*, 6920–6930; (f) G. Zhou, Q. Y. Hu, E. Corey, J. *Org. Lett.* **2003**, *5*, 3979–3982.

[129] (a) D. A. Evans, J. S. Johnson, *J. Org. Chem.* **1997**, *62*, 786-787; (b) D. A. Evans, D. M. Barnes, J. S. Johnson, R. Lectka, P. von Matt, S. J. Miller, J. A. Murry, R. D. Norcross, E. A. Shaughnessy, K. R. Campos, *J. Am. Chem. Soc.* **1999**, *121*, 7582–7594.
[130] D. A. Evans, S. J. Miller, T. Lectka, *J. Am. Chem. Soc.* **1993**, *115*, 6460-6461.
[131] Q. Xiao, K. Young, A. Zakarian. *J. Am. Chem. Soc.* **2015**, *137*, 5907-5910.
[132] I. W. Davies, L. Gerena, N. Lu, R. D. Larsen, P. J. Reider. *J. Org. Chem.* **1996**, *61,* 9629-9630.
[133] K. Young, Q. Xiao, A. Zakarian, *Eur. J. Org. Chem.* **2015**, *2015*, 2337-2341.
[134] B. Flores, T. F. Molinski *Org. Lett.* **2011**, *13*, 3932–3935.
[135] Q. Xie, K. Young, A. Zakarian. *Org. Lett.* **2013**, *15*, 3314-3317.
[136] H.-J. Zhang, L. Hu, Z. Ma, R. Li, Z. Zhang, C. Tao, B. Cheng, Y. Li, H. Wang, H. Zhai. *Angew. Chem. Int. Ed.* **2016**, *55*, 11638-11641.
[137] For IMDA with similar structural features see: a) S. Chackalamannil, Y. Xia, W. J. Greenlee, M. Clasby, D. Doller, H. Tsai, T. Asberom, M. Czarniecki, H.-S. Ahn, G. Boykow, C. Foster, J. Agans-Fantuzzi, M. Bryant, J. Lau, M. Chintala. *J. Med. Chem.* **2005**, *48*, 5884-5887. b) S. Chackalamannil, R. J. Davies, T. Asberom, D. Doller, D. Leone. *J. Am. Chem. Soc.* **1996**, *118,* 9812-9813.
[138] (a) G. Stork, T. Y. Chan, G. A. Breault, *J. Am. Chem. Soc.* **1992**, *114*, 7578-7579.
[139] H. Shi, I. N. Michaelides, B. Darses, P. Jakubec, Q. N. N. Nguyen, R. S. Paton, D. J. Dixon, *J. Am. Chem. Soc.* **2017**, *139*, 17755-17758.
[140] A. Padwa, M. Dimitroff, B. Liu. *Org. Lett.* **2000**, *2*, 3233-3235.
[141] K. A. Parker, M. R. Adamchuk. *Tet. Lett.* **1978**, *19*, 1689-1692.
[142] A. Padwa, M. A. Brodney, M. Dimitroff, B. Liu, T. Wu. *J. Org. Chem.* **2001**, *66*, 3119-3128.
[143] a) W. Oppolzer, W. Frosti. *Helv. Chim. Acta* **1975**, *58*, 590-593. b) D. J. Tantillo, K. N. Houk, M. E. Jung. *J. Org. Chem.* **2001**, *66*, 1938-1940.
[144] (a) S. K. Bur, S. M. Lynch, A. Padwa. *Org. Lett.* **2002**, *4*, 473-476; (b) Q. Wang, A. Padwa. *Org. Lett.* **2004**, *6*, 2189-2192.
[145] J. E. Sears, D. L. Boger, *Acc. Chem. Res.* **2016**, *49*, 241-251.
[146] S. R. McCabe, P. Wipf. *Angew. Chem. Int. Ed.* **2017**, *56*, 324–327. For synthesis of (±)-cycloclavine see F. R. Petronijevic, P. Wipf. *J. Am. Chem. Soc.* **2011**, *133*, 7704–7707.
[147] T. Heiner, S. I. Kozhushkov, M. Noltemeyer, T. Haumann, R. Boese, A. de Meijere. *Tetrahedron* **1996**, *52*, 12185-12196.
[148] a) A. Padwa, M. A. Brodney, M. Dimitroff. *J. Org. Chem.* **1998**, *63*, 5304–5305. b) F. Petronijevic, C. Timmons, A. Cuzzupe, P. Wipf. *Chem. Commun.* **2009**, 104–106.
[149] a) S. A. Kozmin, V. H. Rawal, *J. Org. Chem.* **1997**, *62*, 5252-5253. b) S. Danishefsky, T. Kitahara. *J. Am. Chem. Soc.* **1974**, *96*, 7807–7808.
[150] F. Liu, R. S. Paton, S. Kim, Y. Liang, K. N. Houk, *J. Am. Chem. Soc.* **2013**, *135*, 15642-15649.
[151] a) M. T. Crimmins, B. H. Brown, H. R. Plake. *J. Am. Chem. Soc.* **2006**, *128*, 1371– 378. b) M. T. Crimmins, B. H. Brown. *J. Am. Chem. Soc.* **2004**, *126*, 10264-10266.
[152] J. F. Hooper, N. C. James, E. Bozkurt, V. Aviyente, J. M. White, M. C. Holland, R. Gillmour, A. B Holmes, K. N. Houk. *J. Org. Chem.* **2015**, *80*, 12058–12075.
[153] H. Kim, H. Lee, J. Kim, S. Kim, D. Kim. *J. Am. Chem. Soc.* **2006**, *128*, 15851–15855.
[154] J. E. P. Davidson, R. Gilmour, S. Ducki, J. E. Davies, R. Green, J. W. Burton, A. B. Holmes. *Synlett.* **2004**, *8*, 1434–1436.
[155] (a) M. Ladlow, P. M. Cairns, P. Magnus *J. Chem. Soc., Chem. Commun.* **1986**, 1756–1757; (b) K. Cardwell, B. Hewitt, M. Ladlow, P. Magnus, *J. Am. Chem. Soc.* **1988**, *110*, 2242–2248.
[156] (a) K. C. Nicolaou, D. Gray, J. Tae, *Angew. Chem., Int. Ed.* **2001**, *40*, 3675-3678; (b) K. C. Nicolaou, D. Gray, J. Tae, *Angew. Chem., Int. Ed.* **2001**, *40*, 3679-3683; (c) K. C. Nicolaou, D. L. F. Gray, J. Tae, *J. Am. Chem. Soc.* **2004**, *126*, 613-627.
[157] N. C. Yang, C. Rivas, *J. Am. Chem. Soc.* **1961**, *83*, 2213.
[158] (a) G. Quinkert, H. Stark, *Angew. Chem. Int. Ed.* **1983**, *22*, 637-655; (b) J. L. Charlton, K. Koh, G. L. Plourde, *Tetrahedron Lett.* **1989**, *30*, 3279-3282; (c) G. A. Kraus, L. Chen, R. A. Jacobson, *Synth. Commun.* **1993**, *23*, 2041-2049; (d) G. A. Kraus, G. Zhao, *J. Org. Chem.* **1996**, *61*, 2770-2773.
[159] (a) H. S. Sutherland, F. E. S. Souza, R. G. A. Rodrigo, *J. Org. Chem.* **2001**, *66*, 3639-3641; (b) H. S. Sutherland, K. C. Higgs, N. J. Taylor, R. Rodrigo, *Tetrahedron* **2001**, *57*, 309-317.
[160] V. Varghese, T. Hudlicky, *Angew. Chem. Int. Ed.* **2014**, *53*, 4251-4251.
[161] M. Toyota, T. Odashima, T. Wada, M. Ihara, *J. Am. Chem. Soc.* **2000**, *122*, 9036-9037.
[162] L. K. Sydnes, L. Skatteboel, C. B. Chapleo, D. G. Leppard, K. L. Svanholt, A. S. Dreiding, *Helv. Chim. Acta* **1975**, *58*, 2061-2073.
[163] A. S. Burns, S. D. Rychnovsky, *J. Am. Chem. Soc.* **2019**, *141*, 13295-13300.
[164] K. C. Nicolaou, D. Sarlah, T. R. Wu, W. Zhan, *Angew. Chem., Int. Ed.* **2009**, *48*, 6870-6874.
[165] C. Yuan, B. Du, L. Yang, B. Liu, *J. Am. Chem. Soc.* **2013**, *135*, 9291-9294.
[166] K. C. Nicolaou, H. Xu, M. Wartmann, *Angew. Chem., Int. Ed.* **2005**, *44*, 756-761.
[167] A. E. Hayden, H. Xu, K. C. Nicolaou, K. N. Houk, *Org. Lett.* **2006**, *8*, 2989-2992.
[168] J. P. Malerich, D. Trauner, *J. Am. Chem. Soc.* **2003**, *125*, 9554-9555.
[169] J.-P. Lumb, K. C. Choong, D. Trauner, *J. Am. Chem. Soc.* **2008**, *130*, 9230-9231.
[170] H. C. Lam, H. P. Pepper, C. J. Sumby, J. H. George *Angew. Chem., Int. Ed.* **2017**, *56*, 8532-8535.
[171] R. C. Godfrey, N. J. Green, G. S. Nichol, A. L. Lawrence, *Nat. Chem.* **2020**, *12*, 615-619.
[172] A. E. A. Porter, P. G. Sammes, *J. Chem. Soc. D: Chem. Commun.* **1970**, 1103a-1103a.
[173] L. R. Domingo, J. F. Sanz-Cervera, R. M. Williams, M. T. Picher, J. A. Marco, *J. Org. Chem.* **1997**, *62*, 1662-1667.
[174] (a) J. M. Finefield, J. C. Frisvad, D. H. Sherman, R. M. Williams, *J. Nat. Prod.* **2012**, *75*, 812-833; (b) K. A. Miller, R. M. Williams, *Chem. Soc. Rev.* **2009**, *38*, 3160-3174; (c) R. M. Williams, R. J. Cox, *Acc. Chem. Res.* **2003**, *36*, 127-139.
[175] (a) K. Klas, S. Tsukamoto, D. H. Sherman, R. M. Williams, *J. Org. Chem.* **2015**, *80*, 11672-11685; (b) E. M. Stocking, R. M. Williams, *Angew. Chem., Int. Ed.* **2003**, *42*, 3078-3115.
[176] R. Schutte, G. R. Freeman. *J. Am. Chem. Soc.* **1969**, *91*, 3715. b) T. L. Penner, D. G. Whitten, G. S. Hammond. *J. Am. Chem. Soc.* **1979**, *101*, 2861.
[177] N. L. Bauld, D. J. Bellville, B. Harirchian, K. T. Lorenz, P. A. Pabon, D. W. Reynolds, D. D. Wirth, H.-S. Chiou, B. K. Marsh. *Acc. Chem. Res.* **1987**, *20*, 371-378.
[178] a) S. Lin, M. A. Ischay, C. G. Fry, T. P. Yoon. *J. Am. Chem. Soc.* **2011**, *133*, 19350-19353. b) S. Lin, C. E. Padilla, M. A. Ischay, T. P. Yoon. *Tetrahedron Lett.* **2012**, *53*, 3073-3076.

[179] S. L. Drew, A. L. Lawrence, M. S. Sherburn. *Chem. Sci.* **2015**, *6*, 3886-3890.
[180] S. L. Drew, A. L. Lawrence, M. S. Sherburn. *Angew. Chem. Int. Ed.* **2013**, *52*, 4221-4224.
[181] H. N. Lim, K. A. Parker, *Org. Lett.* **2013**, *15*, 398-401.
[182] (a) T. R. Hoye, B. Baire, D. Niu, P. H. Willoughby, B. P. Woods, *Nature* **2012**, *490*, 208-212; (b) T. Wang, R. R. Naredla, S. K. Thompson, T. R. Hoye, *Nature* **2016**, *532*, 484-488; (c) S. P. Ross, T. R. Hoye, *Nat. Chem.* **2017**, *9*, 523-530; (d) X. Xiao, T. R. Hoye, *Nat. Chem.* **2018**, *10*, 838-844.
[183] P. Wessig, G. Mueller, *Chem. Rev.* **2008**, *108*, 2051-2063.
[184] Review: M. B. Andrus, D. I. Saavedra, *Tetrahedron* **2019**, *75*, 2129-2142.
[185] L.H. Klemm, K.W. Gopinath, *Tetrahedron Lett.* **1963**, *4*, 1243-1245.
[186] L. S. Kocsis, K. M. Brummond, *Organic Letters* **2014**, *16*, 4158-4161.
[187] A. E. Morrison, T. T. Hoang, M. Birepinte, G. B. Dudley, *Org. Lett.* **2017**, *19*, 858-861.
[188] Review: O. J. Diamond, T. B. Marder, *Org. Chem. Front.* **2017**, *4*, 891-910.
[189] R. Karmakar, D. Lee, *Org. Lett.* **2016**, *18*, 6105-6107.
[190] P. McGee, G. Bétournay, F. Barabé, L. Barriault, *Angew. Chem. Int. Ed.* **2017**, *56*, 6280-6283.
[191] A. K. Miller, D. Trauner *Synlett* **2006**, 2295-2316.
[192] J. Zsindely, H. Schmid, *Helv. Chim. Acta* **1968**, *51*, 1510-1514.
[193] M. J. R. Richter, M. Schneider, M. Brandstatter, S. Krautwald, E. M. Carreira, *J. Am. Chem. Soc.* **2018**, *140*, 16704-16710.
[194] L. A. Wein, K. Wurst, P. Angyal, L. Weisheit, T. Magauer, *J. Am. Chem. Soc.* **2019**, *141*, 19589-19593.
[195] M. Schneider, M. J. R. Richter, S. Krautwald, E. M. Carreira, *Org. Lett.* **2019**, *21*, 8705-8707.
[196] Recent examples: (a) J. E. Moses, J. E. Baldwin, R. M. Adlington, A. R. Cowley, R. Marquez, *Tetrahedron Lett.* **2003**, *44*, 6625-6627; (b) J. E. Moses, J. E. Baldwin, S. Brueckner, S. J. Eade, R. M. Adlington, *Org. Biomol. Chem.* **2003**, *1*, 3670-3684; (c) S. M. Ng, C. M. Beaudry, D. Trauner, *Org. Lett.* **2003**, *5*, 1701-1704; (d) A. Abad, C. Agullo, A. C. Cunat, I. de Alfonso, I. Navarro, N. Vera, *Molecules* **2004**, *9*, 287-299; (e) J. Dubarle-Offner, J. Marrot, M.-N. Rager, F. Le Bideau, G. Jaouen, *Synlett* **2007**, 800-802; (f) D. Skropeta, R. W. Rickards, *Tetrahedron Lett.* **2007**, *48*, 3281-3284; (g) K. Yamaguchi, M. Eto, Y. Yoshitake, K. Harano, *Chem. Pharm. Bull.* **2009**, *57*, 749-751; (h) S. Zhu, Z. Guo, Z. Huang, H. Jiang, *Chem. - Eur. J.* **2014**, *20*, 2425-2430.
[197] C.-C. Tseng, H. Ding, A. Li, Y. Guan and D. Y.-K. Chen, *Org. Lett.* **2011**, *13*, 4410–4413.
[198] K. S. Khuong, C. M. Beaudry, D. Trauner, K. N. Houk, *J. Am. Chem. Soc.* **2005**, *127*, 3688-3689.
[199] Two studies describe examples of octatriene IMDA processes, with two more recent investigations describing stepwise ways to achieve a similar transformation to an octatriene IMDA process: (a) A. G. Schultz, F. P. Lavieri, T. E. Snead, *J. Org. Chem.* **1985**, *50*, 3086-3091; (b) A. Padwa, Y. S. Kulkarni, L. W. Terry, *J. Org. Chem.* **1990**, *55*, 2478-2486; (c) G. Blond, C. Bour, B. Salem, J. Suffert, *Org. Lett.* **2008**, *10*, 1075-1078; (d) L. Candish, A. Levens, D. W. Lupton, *J. Am. Chem. Soc.* **2014**, *136*, 14397-14400.
[200] (a) S. J. Burrell, A. E. Derome, M. S. Edenborough, L. M. Harwood, S. A. Leeming, N. S. Isaacs, *Tetrahedron Lett.* **1985**, *26*, 2229-2232; (b) L. M. Harwood, G. Jones, J. Pickard, R. M. Thomas, D. Watkin, *J. Chem. Soc., Chem. Commun.* **1990**, 605-607; (c) L. M. Harwood, T. Ishikawa, H. Phillips, D. Watkin, *J. Chem. Soc., Chem. Commun.* **1991**, 527-530; (d) A. C. Brickwood, M. G. B. Drew, L. M. Harwood, T. Ishikawa, P. Marais, V. Morisson, *J. Chem. Soc., Perkin Trans. 1* **1999**, 913-922; (e) M. G. B. Drew, L. M. Harwood, A. J. Macias-Sanchez, R. Scott, R. M. Thomas, D. Uguen, *Angew. Chem., Int. Ed.* **2001**, *40*, 2311-2313.
[201] K. Tanino, M. Takahashi, Y. Tomata, H. Tokura, T. Uehara, T. Narabu, M. Miyashita. *Nature Chem.* **2011**, *3*, 484–488.
[202] I. R. Hunt, C. Rogers, S. Woo, A. Rauk, B. A. Keay, *J. Am. Chem. Soc.* **1995**, *117*, 1049-1056.
[203] For other exploratory synthetic efforts towards natural products using 1,3,10-undecatriene IMDA reactions, see: (a) P. C. B. Page, D. C. Jennens, H. McFarland, *Tetrahedron Lett.* **1997**, *38*, 6913-6916; (b) A. Ishiwata, S. Sakamoto, T. Noda, M. Hirama, *Synlett* **1999**, 692-694; (c) P. C. B. Page, C. M. Hayman, H. L. McFarland, D. J. Willock, N. M. Galea, *Synlett* **2002**, 583-587; (d) B.-C. Hong, F.-L. Chen, S.-H. Chen, J.-H. Liao, G.-H. Lee, *Org. Lett.* **2005**, *7*, 557-560; (e) C.-C. Li, S. Liang, X.-H. Zhang, Z.-X. Xie, J.-H. Chen, Y.-D. Wu, Z. Yang, *Org. Lett.* **2005**, *7*, 3709-3712; (f) G. Liu, J.-C. Han, C.-C. Li, *Tetrahedron* **2017**, *73*, 3629-3635; (g) M. He, J. Yi, G. Zhao, P. Chen, D. Long, X. Hu, H. Li, X. Xie, X. Wang, X. She, *Org. Chem. Front.* **2019**, *6*, 383-387.
[204] (a) M. E. Kuehne, W. G. Bornmann, W. G. Earley, I. Marko, *J. Org. Chem.* **1986**, *51*, 2913-2927; (b) J. G. C. Hamilton, A. M. Hooper, J. A. Pickett, K. Mori, S. Sano, *Chem. Commun. (Cambridge)* **1999**, 355-356; (c) S. Sano, K. Mori, *Eur. J. Org. Chem.* **1999**, 1679-1686; (d) M. Zaghouani, C. Kunz, L. Guedon, F. Blanchard, B. Nay, *Chem. - Eur. J.* **2016**, *22*, 15257-15260; (e) K. Matsunaga, N. Saito, H. Kogen, K. Takatori, *Org. Lett.* **2019**, *21*, 6054-6057; (f) K. Yu, Z.-N. Yang, C.-H. Liu, S.-Q. Wu, X. Hong, X.-L. Zhao, H. Ding, *Angew. Chem., Int. Ed.* **2019**, *58*, 8556-8560.
[205] Y. Nishiyama, Y. Han-ya, S. Yokoshima, T. Fukuyama, *J. Am. Chem. Soc.* **2014**, *136*, 6598-6601.
[206] S. Tooriyama, Y. Mimori, Y. Wu, N. Kogure, M. Kitajima, H. Takayama, *Org. Lett.* **2017**, *19*, 2722-2725.
[207] D. E. Kaelin, Jr., S. M. Sparks, H. R. Plake, S. F. Martin, *J. Am. Chem. Soc.* **2003**, *125*, 12994-12995.
[208] (a) B. M. O'Keefe, D. M. Mans, D. E. Kaelin, S. F. Martin, *J. Am. Chem. Soc.* **2010**, *132*, 15528-15530; (b) B. M. O'Keefe, D. M. Mans, D. E. Kaelin, Jr., S. F. Martin, *Tetrahedron* **2011**, *67*, 6524-6538.
[209] (a) C.-L. Chen, S. M. Sparks, S. F. Martin, *J. Am. Chem. Soc.* **2006**, *128*, 13696-13697; (b) S. M. Sparks, C.-L. Chen, S. F. Martin, *Tetrahedron* **2007**, *63*, 8619-8635.
[210] (a) W. M. Best, D. Wege, *Tetrahedron Lett.* **1981**, *22*, 4877-4880; (b) W. M. Best, D. Wege, *Aust. J. Chem.* **1986**, *39*, 647-666.
[211] (a) J. C. Estevez, R. J. Estevez, E. Guitian, M. C. Villaverde, L. Castedo, *Tetrahedron Lett.* **1989**, *30*, 5785-5786; (b) J. C. Estevez, R. J. Estevez, L. Castedo, *Tetrahedron Lett.* **1992**, *33*, 6883-6884; (c) B. Gomez, E. Guitian, L. Castedo, *Synlett* **1992**, 903-904; (d) J. C. Estevez, R. J. Estevez, L. Castedo, *Tetrahedron* **1995**, *51*, 10801-10810; (e) C. Gonzalez, D. Perez, E. Guitian, L. Castedo, *J. Org. Chem.* **1995**, *60*, 6318-6326; (f) C. Gonzalez, E. Guitian, L. Castedo, *Tetrahedron Lett.* **1996**, *37*, 405-406.
[212] K. R. Buszek, D. L. Bixby *Tetrahedron Lett.* **1995**, *36*, 9129–9132.
[213] (a) P. M. Tadross, B. M. Stoltz, *Chem. Rev.* **2012**, *112*, 3550-3577; (b) H. Takikawa, A. Nishii, T. Sakai, K. Suzuki, *Chem. Soc. Rev.* **2018**, *47*, 8030-8056.
[214] (a) D. A. Smith, K. Sakan, K. N. Houk, *Tetrahedron Lett.* **1986**, *27*, 4877-4880; (b) J. D. Winkler, S. Kim, K. R. Condroski, A. Asensio, K. N. Houk, *J. Org. Chem.* **1994**, *59*, 6879-6881; (c) A. Deagostino, J. Maddaluno, C. Prandi, P. Venturello, *J. Org. Chem.* **1996**, *61*, 7597-7599; (d) J. D. Winkler, S. K. Bhattacharya, R. A. Batey, *Tetrahedron Lett.* **1996**, *37*, 8069-8072; (e) A. Deagostino, J. Maddaluno, M. Mella, C. Prandi, P. Venturello, *J. Chem. Soc., Perkin Trans. 1* **1998**, 881-888; (f) M. Shanmugasundaram, R. Raghunathan, *Tetrahedron Lett.* **1999**, *40*, 4869-4870; (g) S. Manikandan, M. Shanmugasundaram, R. Raghunathan, *Tetrahedron* **2002**, *58*, 597-601; (h) J.-T. Shin, S. Shin, C.-G. Cho, *Tetrahedron Lett.* **2004**, *45*, 5857-5860.

[215] C. Tian, X. Lei, Y. Wang, Z. Dong, G. Liu, Y. Tang. *Angew. Chem. Int. Ed.* **2016**, *55*, 6992-6996.
[216] M. Zaghouani, C. Kunz, L. Guedon, F. Blanchard, B. Nay. *Chem. Eur. J.* **2016**, *22*, 15257-15260.
[217] G. Stork, E. Nakamura, *J. Am. Chem. Soc.* **1983**, *105*, 5510-5512.
[218] S. J. Bailey, E. J. Thomas, W. B. Turner, J. A. J. Jarvis, *J. Chem. Soc., Chem. Commun.* **1978**, 474-475.
[219] (a) *cytochalasan H:* E. J. Thomas, J. W. F. Whitehead, *J. Chem. Soc., Chem. Commun.* **1986**, 724-726; (b) *cytochalasan G:* H. Dyke, R. Sauter, P. Steel, E. J. Thomas, *J. Chem. Soc., Chem. Commun.* **1986**, 1447-1449; (c) *proxiphomin:* S. A. Harkin, R. H. Jones, D. J. Tapolczay, E. J. Thomas, *J. Chem. Soc., Perkin Trans. 1* **1989**, 489-497; (d) *cytochalasan H:* E. J. Thomas, J. W. F. Whitehead, *J. Chem. Soc., Perkin Trans. 1* **1989**, 507-518; (e) *cytochalasan D:* E. Merifield, E. J. Thomas, *J. Chem. Soc., Chem. Commun.* **1990**, 464-466; (d) *Review:* E. J. Thomas, *Acc. Chem. Res.* **1991**, *24*, 229-235.
[220] C. W. Zapf, B. A. Harrison, C. Drahl, E. J. Sorensen, *Angew. Chem. Int. Ed.* **2005**, *44*, 6533-6537.
[221] C. I. Turner, M. N. Paddon–Row, A. C. Willis, M. S. Sherburn, *J. Org. Chem.* **2005**, *70*, 1154–1163.
[222] B. B. Snider, Y. Zou, *Org. Lett.* **2005**, 7, 4939-4941. See also E. A. Couladouros, E. A. Bouzas, A. D. Magos, *Tetrahedron* **2006**, *62*, 5272–5279.
[223] D.-W. Niu and T. R. Hoye, *Org. Lett.* **2012**, *14*, 828–831.
[224] K. Takeda, Y. Igarashi, K. Okazaki, E. Yoshii and K. Yamaguchi, *J. Org. Chem.* **1990**, *55*, 3431–3434.
[225] J. A. McCauley, K. Nagasawa, P. A. Lander, S. G. Mischke, M. A. Semones and Y. Kishi, *J. Am. Chem. Soc.* **1998**, *120*, 7647–7648.
[226] E. J. Corey, M. Petrzilka, *Tetrahedron Lett.* **1975**, *16*, 2537-2540.
[227] S. A. Snyder, E. J. Corey, *J. Am. Chem. Soc.* **2006**, *128*, 740-742.
[228] K. J. Shea, S. Wise, L. D. Burke, P. D. Davis, J. W. Gilman, A. C. Greeley, *J. Am. Chem. Soc.* **1982**, *104*, 5708-5715.
[229] P. A. Peixoto, R. Severin, C.-C. Tseng, D. Y. K. Chen, *Angew. Chem. Int. Ed.* **2011**, *50*, 3013-3016.
[230] M. Dong, B. Cong, S.-H. Yu, F. Saurio, C.-H. Huo, Q.-W. Shi, Y.-C. Gu, L. O. Zamir, H. Kiyota. *Org. Lett.* **2008**, *10*, 701-704.
[231] T. Magauer, J. Mulzer, K. Tiefenbacher. *Org. Lett.* **2009**, *11*, 5306-5309.
[232] K. J. Shea, P. D. Davis, *Angew. Chem., Int. Ed. Engl.* **1983**, *22*, 419-420.
[233] P. A. Brown, P. R. Jenkins, J. Fawcett, D. R. Russell, *J. Chem. Soc., Chem. Commun.* **1984**, 253-255.
[234] S. M. Rubenstein, R. M. Williams, *J. Org. Chem.* **1995**, *60*, 7215–7223.
[235] A. Mendoza, Y. Ishihara, P. S. Baran, *Nature Chem.* **2012**, *4*, 21-25.
[236] P. A. Brown, P. R. Jenkins, *J. Chem. Soc. Perkin. Trans. I.* **1986**, 1303-1309.
[237] S. G. Krasutsky, S. H. Jacobo, S. R. Tweedie, R. Krishnamoorthy, A. S. Filatov, *Org. Process Res. Dev.* **2015**, *19*, 284-289.
[238] Y. Kanda, H. Nakamura, S. Umemiya, R. K. Puthukanoori, V. R. Murthy Appala, G. K. Gaddamanugu, B. R. Paraselli, P. S. Baran, *J. Am. Chem. Soc.* **2020**, *142*, 10526-10533.
[239] The step count range indicates lower and higher limits of hand one-pot transformations and separate reagent additions.
[240] (a) K. C. Nicolaou, M. W. Harter, L. Boulton, B. Jandeleit, *Angew. Chem., Int. Ed. Engl.* **1997**, *36*, 1194-1196; (b) K. C. Nicolaou, P. S. Baran, Y.-L. Zhong, H.-S. Choi, W. H. Yoon, Y. He, K. C. Fong, *Angew. Chem., Int. Ed.* **1999**, *38*, 1669-1675; (c) K. C. Nicolaou, J.-K. Jung, W. H. Yoon, Y. He, Y.-L. Zhong, P. S. Baran, *Angew. Chem., Int. Ed.* **2000**, *39*, 1829-1832; (d) N. Waizumi, T. Itoh, T. Fukuyama, *J. Am. Chem. Soc.* **2000**, *122*, 7825-7826; (e) K. C. Nicolaou, J. Jung, W. H. Yoon, K. C. Fong, H. S. Choi, Y. He, Y. L. Zhong, P. S. Baran, *J. Am. Chem. Soc.* **2002**, *124*, 2183-2189.
[241] S. L. Gwaltney, K. J. Shea, *Tetrahedron Lett.* **1996**, *37*, 949-952.
[242] For a review, see: K.Afarinkia, V. Vinader, T. D. Nelson, G. H. Posner, *Tetrahedron* **1992**, *48*, 9111-9171.
[243] For other examples of pyrone-alkyne IMDA processes in total synthesis, see: (a) D. Perez, G. Bures, E. Guitian, L. Castedo, *J. Org. Chem.* **1996**, *61*, 1650-1654; (b) F. Fan, J. Dong, J. Wang, L. Song, C. Song, J. Chang, *Adv. Synth. Catal.* **2014**, *356*, 1337-1342; (c) P. Gan, M. W. Smith, N. R. Braffman, S. A. Snyder, *Angew. Chem., Int. Ed.* **2016**, *55*, 3625-3630; (d) J.-H. Lee, C.-G. Cho, *Org. Lett.* **2016**, *18*, 5126-5129; (e) M. W. Smith, Z. Zhou, A. X. Gao, T. Shimbayashi, S. A. Snyder, *Org. Lett.* **2017**, *19*, 1004-1007.
[244] (a) P. S. Baran, N. Z. Burns, *J. Am. Chem. Soc.* **2006**, *128*, 3908-3909; (b) N. Z. Burns, P. S. Baran, *Angew. Chem., Int. Ed.* **2008**, *47*, 205-208.
[245] For an earlier report of a kinetically stable designed molecule with non-planar benzene rings, see H. Kawai, T. Suzuki, M. Ohkita, T. Tsuji, *Angew. Chem. Int. Ed.* **1998**, *37*, 817–819; *Angew. Chem.* **1998**, *110*, 827–829.
[246] For a related synthesis of (+)-cavicularin using a type 2 IMDA reaction, see P. Zhao, C. M. Beaudry, *Angew. Chem. Int. Ed.* **2014**, *53*, 10500-10503.
[247] C. D. Dzierba, K. S. Zandi, T. Möllers, K. J. Shea, *J. Am. Chem. Soc.* **1996**, *118*, 4711–4712.
[248] (a) K. C. Nicolaou, Y. Tang, J. Wang, *Angew. Chem., Int. Ed.* **2009**, *48*, 3449-3453; (b) K. C. Nicolaou, J. Wang, Y. Tang, *Angew. Chem., Int. Ed.* **2008**, *47*, 1432-1435.
[249] For a review containing several TADA-based total syntheses, see P. A. Clarke, A. T. Reeder, J. Winn, *Synthesis* **2009**, 691-709.
[250] E. P. Balskus, E. N. Jacobsen, *Science* **2007**, *317*, 1736-1740.
[251] M. N. Paddon-Row, L. C. H. Kwan, A. C. Willis, M. S. Sherburn *Angew. Chem. Int. Ed.* **2008**, *47*, 7013-7017.
[252] T. K. M. Shing, J. Yang, *J. Org. Chem.* **1995**, *60*, 5785-5789.
[253] K. C. Nicolaou, A. A. Shah, H. Korman, T. Khan, L. Shi, W. Worawalai, E. A. Theodorakis, *Angew. Chem., Int. Ed.* **2015**, *54*, 9203-9208.
[254] T. Suzuki, K. Usui, Y. Miyake, M. Namikoshi, M. Nakada, *Org. Lett.* **2004**, *6*, 553-556.
[255] Y.-M. Zhao, T. J. Maimone, *Angew. Chem., Int. Ed.* **2015**, *54*, 1223-1226.
[256] P. Soucy, A. L'Heureux, A. Toro, P. Deslongchamps, *J. Org. Chem.* **2003**, *68*, 9983-9987.
[257] A. Toró, P. Nowak, P. Deslongchamps, *J. Am. Chem. Soc.* **2000**, *122*, 4526–4527.
[258] J. Germain, P. Deslongchamps, *J. Org. Chem.* **2002**, *67*, 5269-5278.
[259] (a) R. Munakata, H. Katakai, T. Ueki, J. Kurosaka, K. Takao, K. Tadano, *J. Am. Chem. Soc.* **2003**, *125*, 14722-14723; (b) R. Munakata, H. Katakai, T. Ueki, J. Kurosaka, K. Takao, K. Tadano, *J. Am. Chem. Soc.* **2004**, *126*, 11254-11267
[260] (a) D. J. Mergott, S. A. Frank, W. R. Roush, *Proc. Natl. Acad. Sci. U. S. A.* **2004**, *101*, 11955-11959; (b) S. M. Winbush, D. J. Mergott, W. R. Roush, *J. Org. Chem.* **2008**, *73*, 1818-1829.
[261] T. A. Dineen, W. R. Roush, *Org. Lett.* **2004**, *6*, 2043-2046.
[262] S. Phoenix, M. S. Reddy, P. Deslongchamps, *J. Am. Chem. Soc.* **2008**, *130*, 13989-13995.
[263] (a) S. P. Cook, A. Polara, S. J. Danishefsky, *J. Am. Chem. Soc.* **2006**, *128*, 16440-16441; (b) A. Polara, S. P. Cook, S. J. Danishefsky, *Tetrahedron Lett.* **2008**, *49*, 5906-5908.
[264] D. J. Cram, G. R. Knox, *J. Am. Chem. Soc.* **1961**, *83*, 2204-2205.

[265] V. H. Rawal, S. Iwasa, *J. Org. Chem.* **1994**, *59*, 2685-2686.
[266] (a) M. E. Layton, C. A. Morales, M. D. Shair, *J. Am. Chem. Soc.* **2002**, *124*, 773-775; (b) C. A. Morales, M. E. Layton, M. D. Shair, *Proc. Natl. Acad. Sci.* **2004**, *101*, 12036-12041.
[267] X. Fu, M. B. Hossain, D. van der Helm, F. J. Schmitz, *J. Am. Chem. Soc.* **1994**, *116*, 12125-12126.
[268] (a) J. A. Porco, F. J. Schoenen, T. J. Stout, J. Clardy, S. L. Schreiber, *J. Am. Chem. Soc.* **1990**, *112*, 7410-7411; (b) D. Elbaum, J. A. Porco, Jr., T. J. Stout, J. Clardy, S. L. Schreiber, *J. Am. Chem. Soc.* **1995**, *117*, 211-225.
[269] (a) D. A. Evans, J. T. Starr, *Angew. Chem., Int. Ed.* **2002**, *41*, 1787-1790; (b) D. A. Evans, J. T. Starr, *J. Am. Chem. Soc.* **2003**, *125*, 13531-13540.
[270] (a) D. A. Vosburg, C. D. Vanderwal, E. J. Sorensen, *J. Am. Chem. Soc.* **2002**, *124*, 4552-4553; (b) C. D. Vanderwal, D. A. Vosburg, S. Weiler, E. J. Sorensen, *J. Am. Chem. Soc.* **2003**, *125*, 5393-5407.
[271] N. Tanaka, T. Suzuki, T. Matsumura, Y. Hosoya, M. Nakada, *Angew. Chem. Int. Ed.* **2009**, *48*, 2580-2583.
[272] X. Yu, L. Xiao, Z. Wang, T. Luo, *J. Am. Chem. Soc.* **2019**, *141*, 3440-3443.
[273] (a) H. J. Kim, M. W. Ruszczycky, S.-h. Choi, Y.-n. Liu, H.-w. Liu, *Nature* **2011**, *473*, 109-112; (b) A. Patel, Z. Chen, Z. Yang, O. Gutiérrez, H.-w. Liu, K. N. Houk, D. A. Singleton, *J. Am. Chem. Soc.* **2016**, *138*, 3631-3634
[274] K. N. Houk, F. Liu, Z. Yang, J. I. Seeman, *Angew. Chem. Int. Ed.* **2020**, 10.1002/anie.202001654
[275] P. Caramella, P. Quadrelli, L. Toma, *J. Am. Chem. Soc.* **2002**, *124*, 1130-1131.
[276] D. H. Ess, S. E. Wheeler, R. G. Iafe, L. Xu, N. Çelebi-Ölçüm, K. N. Houk, *Angew. Chem. Int. Ed.* **2008**, *47*, 7592-7601.